ECSS-E-HB-32-20 Part 7A
20 March 2011

Space engineering

Structural materials handbook - Part 7: Thermal and environmental integrity, manufacturing aspects, in-orbit and health monitoring, soft materials, hybrid materials and nanotechnoligies

NOTE:
This pdf-file does not contain automatic cross-references. To make use of the cross-references please use the MS Word version of this document.

ECSS Secretariat
ESA-ESTEC
Requirements & Standards Division
Noordwijk, The Netherlands

Foreword

This Handbook is one document of the series of ECSS Documents intended to be used as supporting material for ECSS Standards in space projects and applications. ECSS is a cooperative effort of the European Space Agency, national space agencies and European industry associations for the purpose of developing and maintaining common standards.

This handbook has been prepared by the ECSS-E-HB-32-30 Working Group, reviewed by the ECSS Executive Secretariat and approved by the ECSS Technical Authority.

Disclaimer

Published by: ESA Requirements and Standards Division
ESTEC, P.O. Box 299,
2200 AG Noordwijk
The Netherlands

Change log

ECSS-E-HB-32-20 Part 7A 20 March 2011	First issue

Table of contents

Figures

Tables

Introduction

The Structural materials handbook, ECSS-E-HB-32-20, is published in 8 Parts.

A glossary of terms, definitions and abbreviated terms for these handbooks is contained in Part 8.

The parts are as follows:

Part 1	Overview and material properties and applications	Clauses 1 - 9
Part 2	Design calculation methods and general design aspects	Clauses 10 - 22
Part 3	Load transfer and design of joints and design of structures	Clauses 23 - 32
Part 4	Integrity control, verification guidelines and manufacturing	Clauses 33 - 45
Part 5	New advanced materials, advanced metallic materials, general design aspects and load transfer and design of joints	Clauses 46 - 63
Part 6	Fracture and material modelling, case studies and design and integrity control and inspection	Clauses 64 - 81
Part 7	Thermal and environmental integrity, manufacturing aspects, in-orbit and health monitoring, soft materials, hybrid materials and nanotechnoligies	Clauses 82 - 107
Part 8	Glossary	

82
Thermal behaviour

82.1 Introduction

82.1.1 General

The two principal issues in the behaviour of high-temperature materials are the:

- physical response to thermal loads, i.e. thermal cycling and thermal shock.
- physical properties, i.e. thermal conductivity and diffusivity, specific heat capacities, emissivity and surface catalyticity.

82.1.2 Physical response

Information on physical response shows the temperature ranges to which different materials can be applied and the level of microstructural changes that can occur. This is viewed in conjunction with the effects of thermal loads which are likely to be compounded by:

- mechanical loading, [See: Chapter 83], and
- operating environments, [See: Chapter 85].

Any modification to the material's microstructure alters the physical properties.

82.1.3 Physical properties

Physical properties are used to establish the amount of heat energy that a structural design can absorb. Thermal conductivity is a non-linear parameter whose value is temperature dependent.

Thermal cycling is divided into two major regimes:

- Low Range: Cryogenic up to 300°C. For:
  - magnesium,
  - aluminium, and
  - glass composites.
- High Range: Above 300°C. For propulsion system materials and thermo-structural designs, i.e.
  - copper,
  - titanium,

— nickel,
— GCMC,
— CMC, and
— C-C

Where cryogenic LH/LOX fuels are used, thermal cycling can extend from -253°C to +800°C.

The thermal behaviour of materials is influenced by:

- plastic behaviour (MMC),
- thermal strain hysteresis (MMC and CMC),
- microvoidage and fibre-matrix interface damage (MMC),
- porosity (CMC),
- microcracking (CMC).

82.2 MMC: Thermal cycling

82.2.1 General

Thermal cycling damage is more likely to occur with, Ref. [82-4]:

- significant CTE mismatch between reinforcement and matrix,
- high residual stresses within the matrix phase,
- over-extension of upper temperature capabilities of matrix or fibre,
- repeated thermal cycling.

Reinforcement of metals increases the upper service temperature for very short life applications by limiting gross creep. For repeated thermal cycling and longer life requirements, accumulating changes in matrix microstructure inhibit the upper service temperature. Some published work shows that over-extension of the temperature limits causes degradation, e.g. an accumulation of micro-damage associated with the matrix-reinforcement interfaces (microvoids or cracks at the interfaces) often leading to interfacial debonding.

Thermal cycling a MMC under constant mechanical load can cause a ratcheting effect. This shakedown phenomenon results in small increments in permanent strain on each thermal cycle, Ref. [82-1].

Information on gross changes in mechanical performance due to thermal cycling is provided.

[See: Chapter 84 for modifications to CTE behaviour from lower thermal cycling regimes]

82.2.2 Magnesium-carbon fibre composites

Combining magnesium with UHM carbon fibres is attractive for dimensionally stable structures. In these, permanent residual strain is induced on the first thermal cycle, Ref. [82-2], but not subsequently.

Important for designing dimensionally stable mirrors, for example.

Similar residual strains can be induced in aluminium composites with UHM fibres, e.g. P100.

82.2.3 Aluminium-carbon fibre composites

The combination of carbon fibres and aluminium causes a brittle aluminium carbide interface due to chemical reaction between the two. Thermal cycling to 350°C can result in severe losses in mechanical performance, Ref. [82-3]. Special attention should be given to the interface with C/Al composites if they are to retain their integrity.

82.2.4 Aluminium-boron filament composites

Severe damage from thermal cycling was seen in boron fibre-reinforced 6061 aluminium alloy in cycling to 320°C or 420°C, Ref. [82-4]. Gross failure of the fibre-matrix interface occurred throughout the composite.

The unidirectional strength properties reduced significantly, as shown in Figure 82.2.1, Ref. [82-4]. The transverse 90° properties were effectively destroyed giving gross embrittlement. The work showed that the peak temperatures were excessive for prolonged composite use as the composite was losing integrity.

The base alloy is not normally used above 120°C.

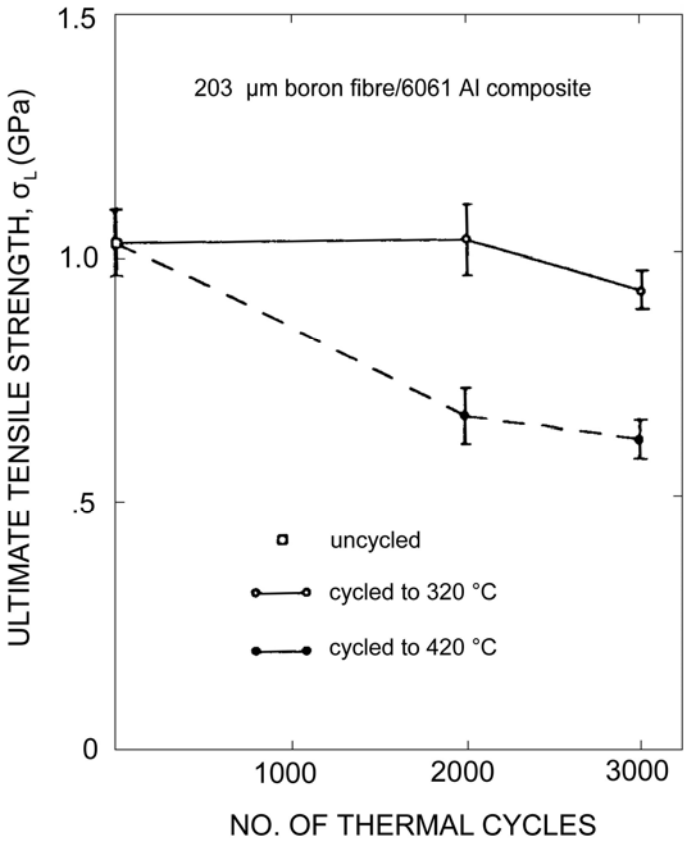

RT UTS of 203µm boron fibre/6061 Al composites.

Thermally cycled between RT and Tmax (320°C and 420°C)

Figure 82.2-1 - MMC thermal cycling: Effect on UTS for boron/Al composite

82.2.5 Titanium-silicon carbide filament composites

Higher performance titanium alloys can be used at temperatures up to 600°C. Prior to replacement by Beta 21S (Timet 21), Ti-15-3-3 was a β-alloy studied widely in the USA, [See also Chapter 47].

Quasi-isotropic SCS6/Ti-15-3-3 composites were exposed to differing thermo-cyclic regimes, i.e.:

- 149°C to 427°C,
- 316°C to 649°C,
- isothermal fatigue at 649°C.

From 149°C to 427°C, the sequence observed was, Ref. [82-5]:

- after 500 cycles, the reaction zone (interface) between fibre and matrix changed in appearance,
- radial cracks grew through the reaction zone,
- at 1500 cycles, cracks initiated on the edge of the specimen,
- edge cracks were arrested at fibres,
- after 16750 cycles, the composite was still intact.

The conclusion was that the damage was very minor and the composite was capable of sustaining many cycles at temperatures up to 427°C.

From 316°C to 649°C, [0/±45/90]s laminates exhibited significant damage after several hundred cycles, Ref. [82-6], such as:

- significant fibre-matrix debonding,
- ply-to-ply separation (delamination) in the 45° and 90° plies,
- contact or close proximity of fibres increased the occurrence of cracking.

82.2.6 Superalloy (FeCrAlY) composites

Thermal cycling tests have been conducted on FP alumina/FeCrAlY and W-ThO_2/FeCrAlY composites, [See: Chapter 48]. The constituents were selected to minimise the CTE mismatch between matrix and reinforcement, Ref. [82-7]. Thermal cycling was taken to 1100°C for up to 200 cycles. Severe microstructural damage occurred, which emphasises the difficulties in producing MMC materials that are expected to sustain large changes in temperature.

82.3 CMC: Thermal cycling

Ceramic composites (CMCs) differ from MMC materials in not having a plastically deformable matrix. Microcracks, created in the matrix on cooling, are the internal stress relief mechanism. Microcracks are tolerated in CMCs as a means of gaining a benign fracture behaviour.

Thermal cycling does not contribute significantly to accumulated internal damage in CMCs, unless the thermal limit of the fibre is exceeded. Thermal cycling involves incremental heating throughout the specimen at a fairly constant rate.

Ceramics are more likely to undergo rapid high temperature excursions with uneven through-thickness heating. Thermal shock is therefore a more severe test for CMCs, particularly as the low overall conductivity gives rise to large temperature gradients, [See: 82.5]

82.4 MMC: Thermal shock

82.4.1 General

Thermal shock occurs in propulsion systems with the ignition of high energy fuels. The high thermal conductivity of metals assists in dissipating heat away from the immediate surface.

82.4.2 Metal alloys

Metallic materials applied to propulsion systems and experiencing thermal shock include:

- copper alloys (including ODS alloys), [See: Chapter 45].
- nickel alloys, [See: Chapter 48].
- refractory metals, e.g. niobium and tantalum, [See: Chapter 50].

All have shown acceptable thermal shock resistance.

For short duration firings, creep can occur in combustion chambers, e.g. Vulcain, showing the combined effects of temperature and pressure to be severe.

82.4.3 MMC

TMC, such as SiC/Ti composites, are destined for gas turbine applications (blisks) and feature significantly in the NASP programme, [See: Chapter 71]. Blisks are integrally-formed turbine blade and disc components.

Actual applications of MMC materials are unknown.

82.4.4 Intermetallics

Titanium aluminides (TiAls) are also under evaluation for gas turbine applications, [See: Chapter 49].

82.5 CMC: Thermal shock

82.5.1 General

Continuous fibre GCMC, CMC and C-C materials have shown a remarkable resistance to severe thermal shock, Ref. [82-8].

These materials do not undergo the single crack, catastrophic mode of failure of monolithic ceramics.

The materials can sustain a high degree of microcracking whilst still retaining their basic integrity.

This is true even when the fibres have undergone severe thermal degradation, as with SiC fibres taken to 1700°C. Their mechanical strengths are lowered by repeated thermal shocks, but continue to perform a thermo-structural function. They are in effect a form of rigidised fibre insulation material.

82.5.2 SiC-SiC composites

As an example of their resistance, SiC-SiC composites have undergone thermal shock conditioning more severe than that seen in the current Space Shuttle Main Engine (SSME) turbopump, Ref. [82-9].

Figure 82.5.1 shows the strength retention of SiC-SiC after exposures to 1900°C, Ref. [82-9].

At 1900°C, material erosion produced a 40% cross-sectional reduction after 25 cycles. Little or no decrease in tensile strength for thermal shock up to 1700°C was seen. The testing comprised of a hydrogen-oxygen rocket engine firing in one second pulses.

Other methods used to demonstrate shock resistance are:

- using a high intensity electron beam, Ref. [82-10], or
- plunging white-hot CMC specimens into water.

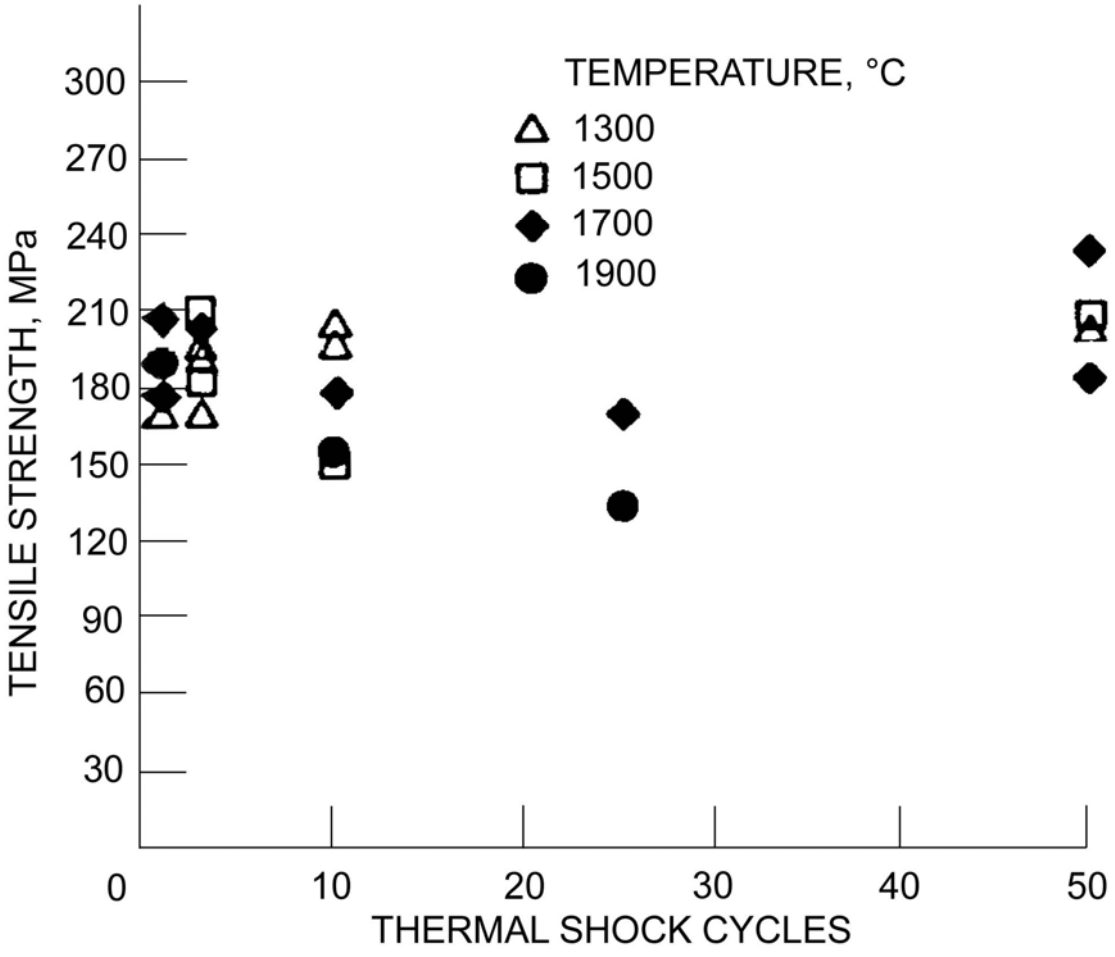

Material: Nicalon/SiC

Figure 82.5-1 - Thermal shock: Retained RT tensile strength for SiC-SiC CMC

82.6 MMC: Thermal conductivity

82.6.1 General

Thermal conductivity of MMC materials varies with temperature.

Thermal diffusivity is the parameter measured directly and thermal conductivity calculated by:

$$\lambda = \alpha \rho C_p \qquad [82.6\text{-}1]$$

where:

λ = *thermal conductivity*

α = *thermal diffusivity*

ρ = *material density*

C_p = *specific heat capacity*

82.6.2 Thermal diffusivity measurement

Accurate measurement of thermal diffusivity is best achieved by a laser flash method, introducing a precisely quantified amount of heat energy, Ref. [82-11]. This said, published data on the diffusivity of structural materials is often inconsistent and ambiguous. With the anisotropic nature of composites, diffusivity is influenced by factors, including:

- reinforcement orientation,
- alloy and reinforcement composition,
- voidage,
- interface materials.

82.6.3 Effect of material composition

82.6.3.1 General

Introducing ceramic reinforcing phases into metallic materials usually lowers thermal conductivity. There are some exceptions, e.g.

- titanium has very low thermal conductivity in comparison with aluminium and copper,
- crystalline silicon carbide and carbon have good conductivities with a reduced lowering effect when compared with alumina,
- highly graphitised reinforcements have excellent conductivity.

Where high thermal conductivity is essential, a number of specialised composites have appeared which retain this characteristic at medium to high temperatures.

Copper has excellent thermal conductivity, but modest strength characteristics and a high density. It is used sparingly in some propulsion systems, e.g. the Vulcain engine for Ariane 5, but copper composites offer better structural capabilities in conjunction with high conductivity, Ref. [82-11].

[See: Chapter 45]

82.6.3.2 Particulate reinforcements

The effect on thermal conductivity of particulate additions to titanium is shown in Figure 82.6.1, Ref. [82-12].

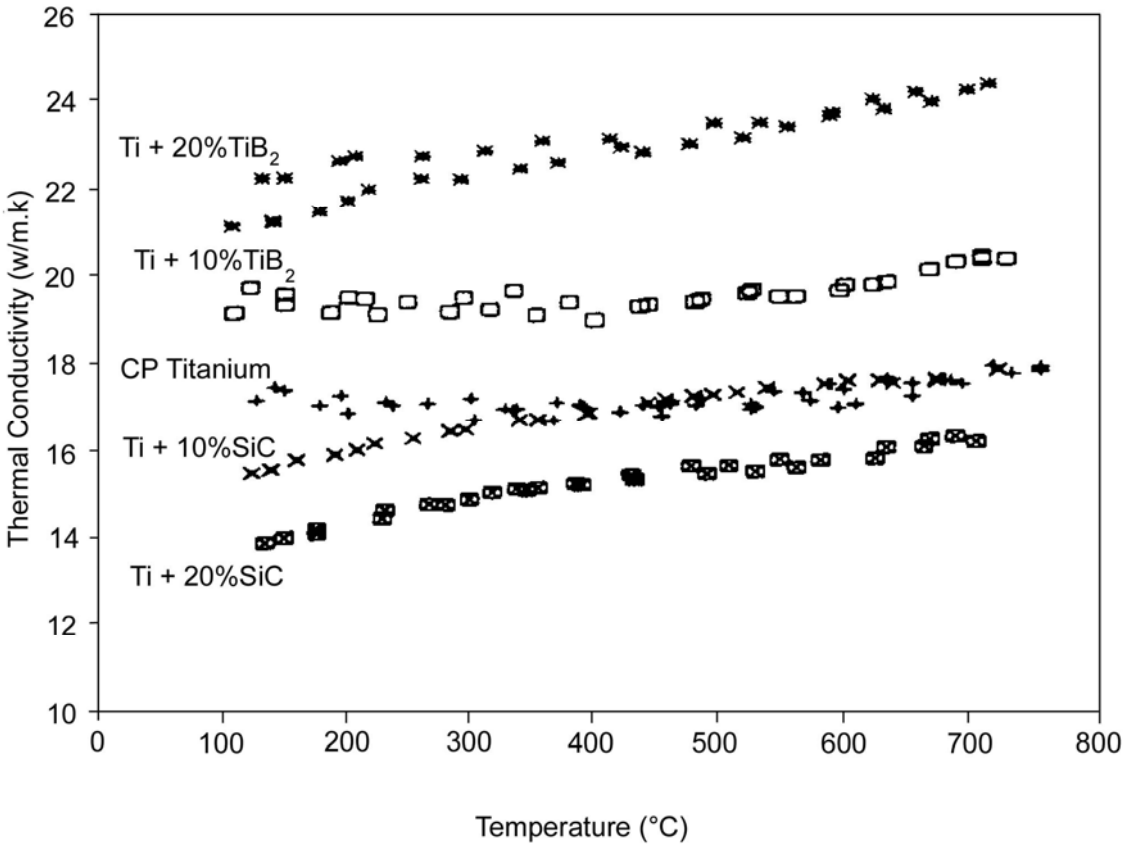

Figure 82.6-1 - Thermal conductivity: Unreinforced titanium compared with Ti-SiC and Ti-TiB2 particulate reinforced composites

82.6.4 Modelling

Prediction of thermal conductivity by various modelling techniques uses the properties of the constituent parts, Ref. [82-4], [82-13].

82.7 CMC: Thermal conductivity

82.7.1 General

The main constituents for CMC composites are shown in Table 82.7.1.

Table 82.7-1 - CMC thermal conductivity: General classification

Composite phase	Conductive	Insulative
Matrix	SiC (CVD) Carbon	Glass-ceramic, e.g. LAS, CAS, MAS.
Fibre reinforcement	Carbon	SiC (Nicalon) Alumina

The conductivity of CMCs is temperature dependent and the temperature range over which they operate can be large. The maximum temperatures quoted are:

- C-C: 2500°C,
- C-SiC: 1900°C,
- SiC-SiC: 1700°C,
- LAS-SiC: 1200°C.

At maximum temperatures, the composites are functioning close to their physical limits and progressive changes in microstructure occur which alters conductivity.

Thermal conductivity of CMC materials is strongly influenced by:

- Fibre type and volume fraction,
- Fibre orientation,
- Matrix microcracking density and porosity.

For bi-directional laminates with C or SiC fibres, the transverse, through-thickness conductivity is appreciably lower than in the fibre directions, Ref. [82-14].

82.7.2 Glass-ceramic matrix composites

The unidirectional thermal conductivity of LAS/Carbon is typically ~2.5W/m/°C.

The measured conductivity of amorphous SiC fibres, along with LAS/SiC composites, is shown in Figure 82.7.1, Ref. [82-15].

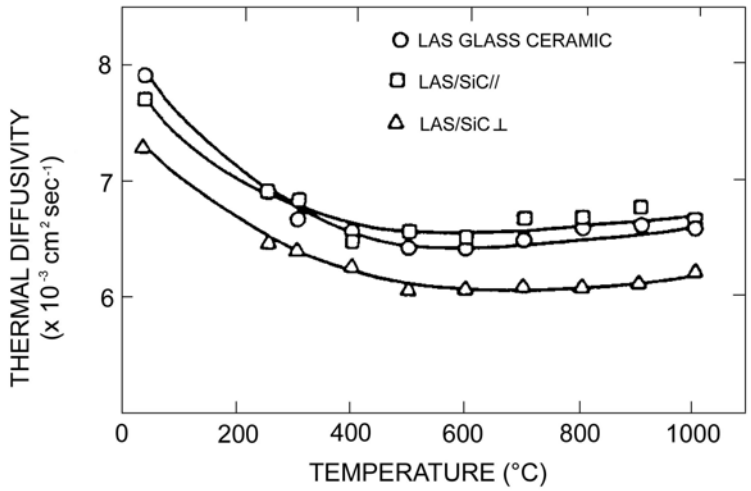

A: Experimental data for thermal diffusivity with temperature for LAS matrix with 0, 48 and 49% SiC fibres parallel and perpendicular to the fibre axis.

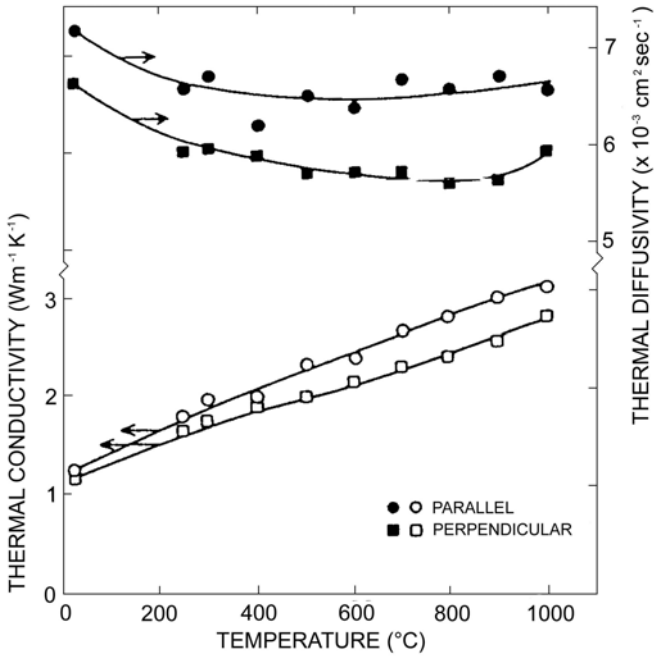

B: Temperature dependence of thermal conductivity and diffusivity of amorphous SiC fibres, calculated from A.

Figure 82.7-1 - Thermal conductivity and diffusivity for LAS/SiC composites

82.7.3 SiC-SiC and C-SiC composites

The properties of some composites are given for, Ref. [82-16]:

- thermal diffusivity:
  - for SiC-SiC - Figure 82.7.2 (perpendicular to fibres); Figure 82.7.3 (parallel and perpendicular to fibres).
  - C-SiC in Figure 82.7.5, Figure 82.7.6 and Figure 82.7.7
- thermal conductivity: CVD SiC matrix, in Figure 82.7.4.

In some cases, the matrix microstructure can change subtly due to heat treatment, which alters the diffusivity, as shown in Figure 82.7.8, Ref. [82-17].

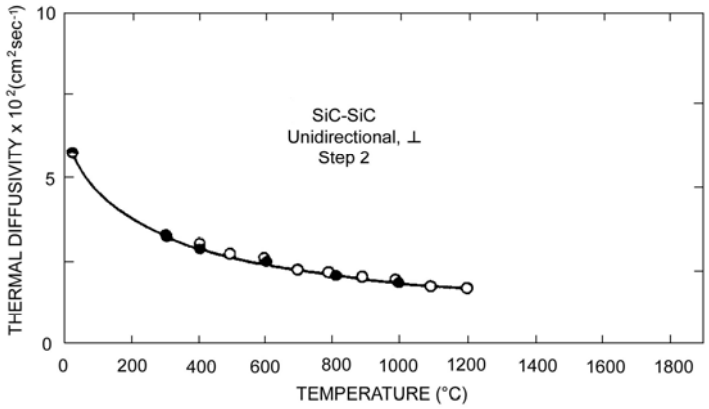

A: Cycled to 1200°C, specimen density: 2.39 g cm^{-3}

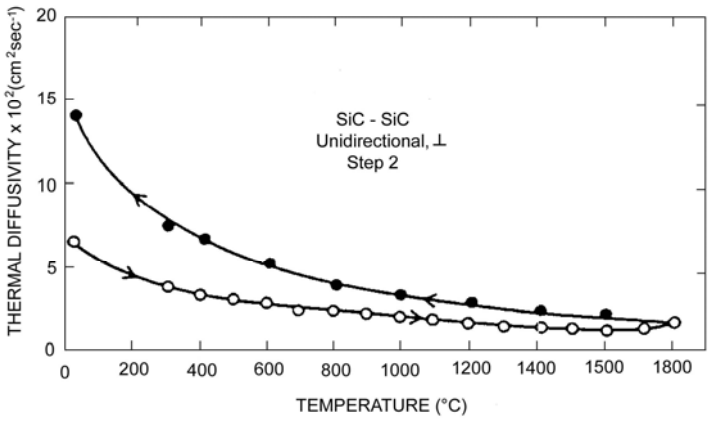

B: Cycled to 1800°C, specimen density: 2.47 g cm^{-3}

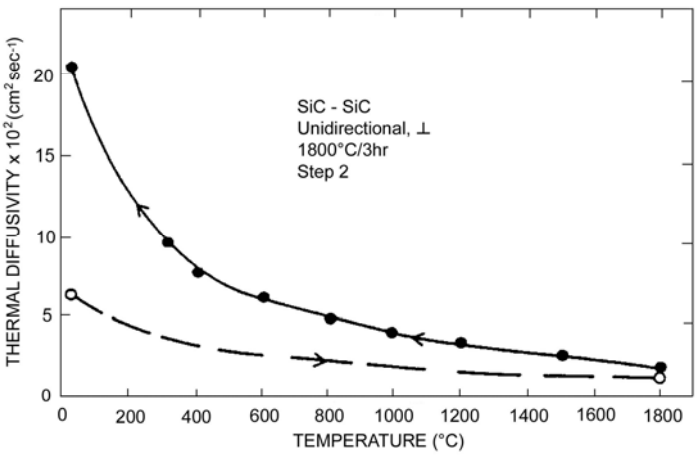

C: Heated rapidly to 1800°C, 3hr hold, cooled at normal rate, specimen density: 2.45 g cm^{-3}

Open symbols = heating; Closed symbols = cooling

Figure 82.7-2 - Thermal diffusivity with temperature for SiC-SiC composite, perpendicular to the fibres

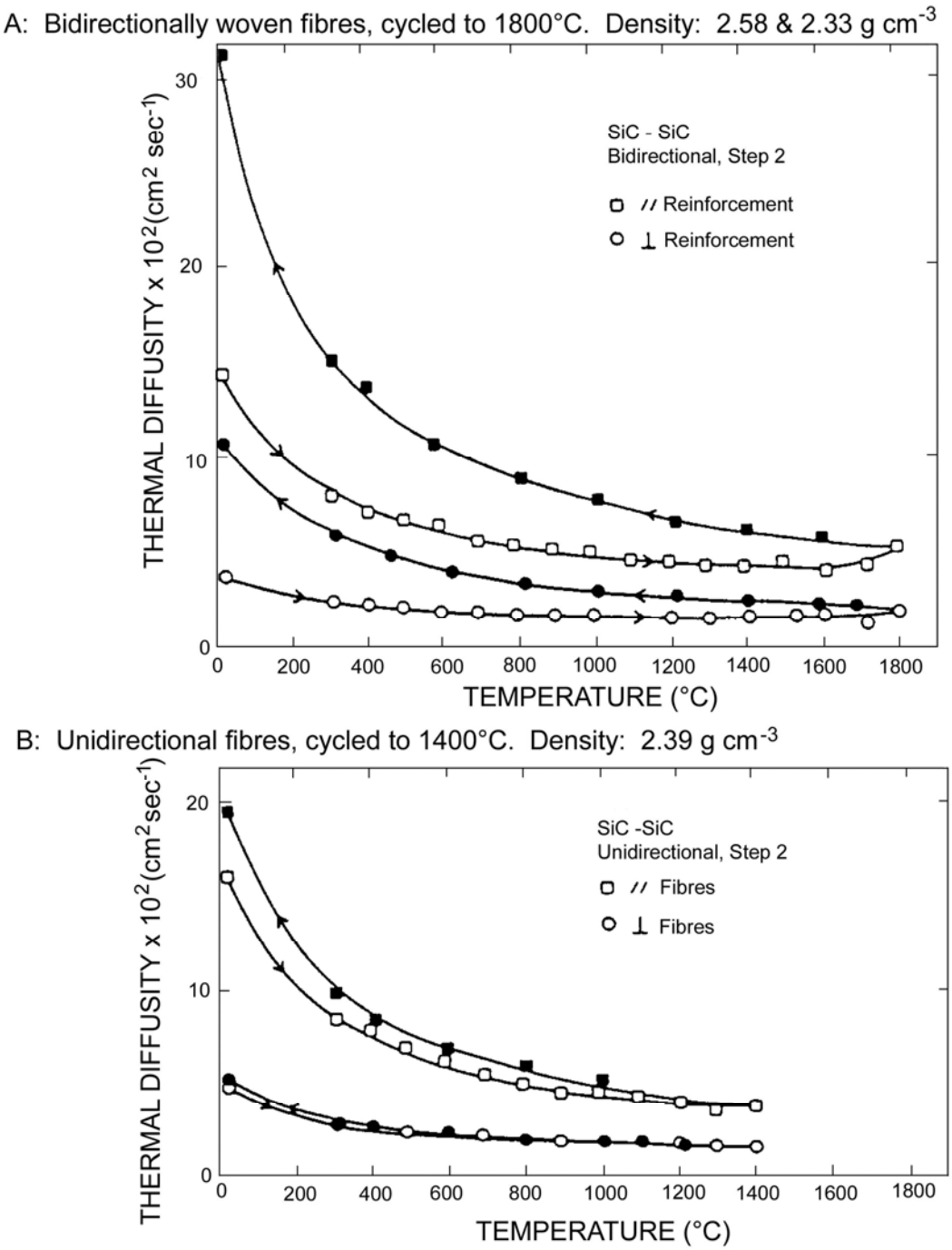

Open symbols = heating; Closed symbols = cooling

Figure 82.7-3 - Thermal diffusivity with temperature for SiC-SiC composite, parallel and perpendicular to the fibres

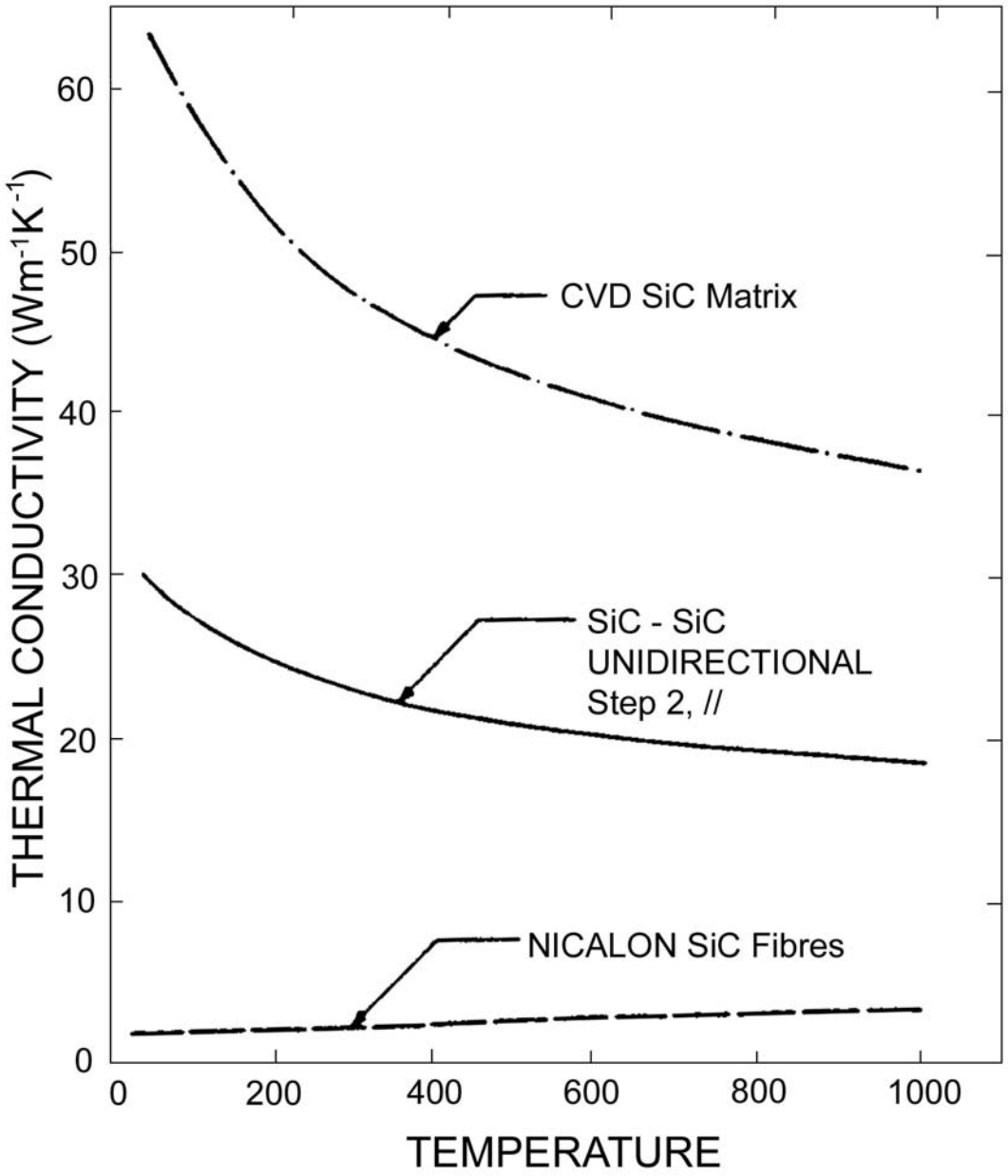

Values determined by composite theory, using the conductivity of Nicalon SiC fibres

Figure 82.7-4 - Thermal conductivity of CVD SiC matrix

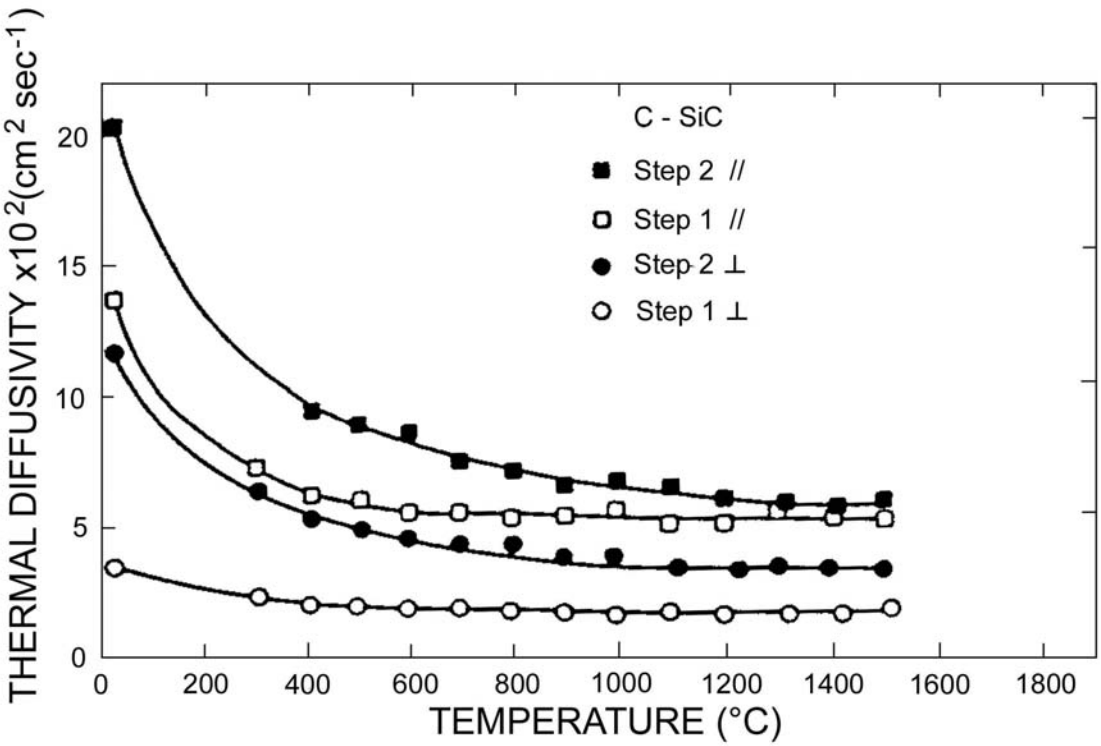

Key: Values perpendicular and parallel to the fibre.
Step 1: Low density, 1660 and 1540 kg m^{-3}.
Step 2: Intermediate density, 2330 and 2130 kg m^{-3}

Figure 82.7-5 - Thermal diffusivity with temperature to 1500°C for C-SiC composites

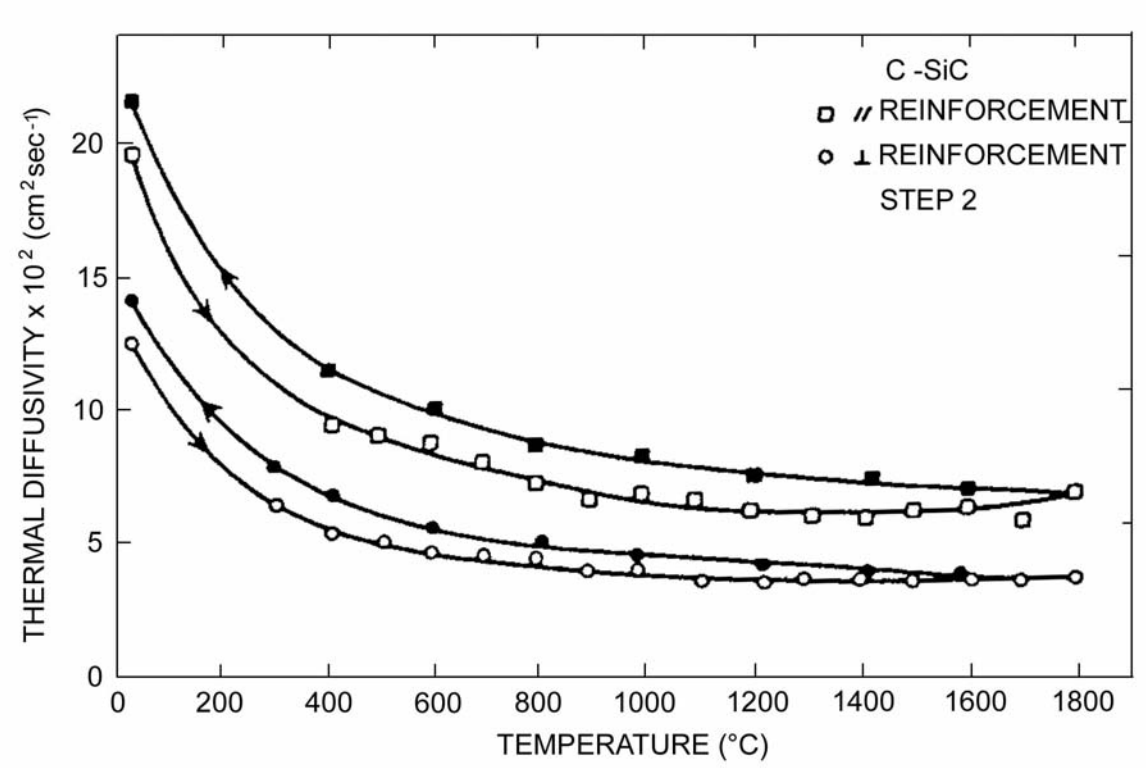

Key: Values parallel and perpendicular to fibre in intermediate density (Step 2) composites, cycled to 1800°C.

Open symbols = heating; Closed symbols = cooling.

Figure 82.7-6 - Thermal diffusivity with temperature for C-SiC composites

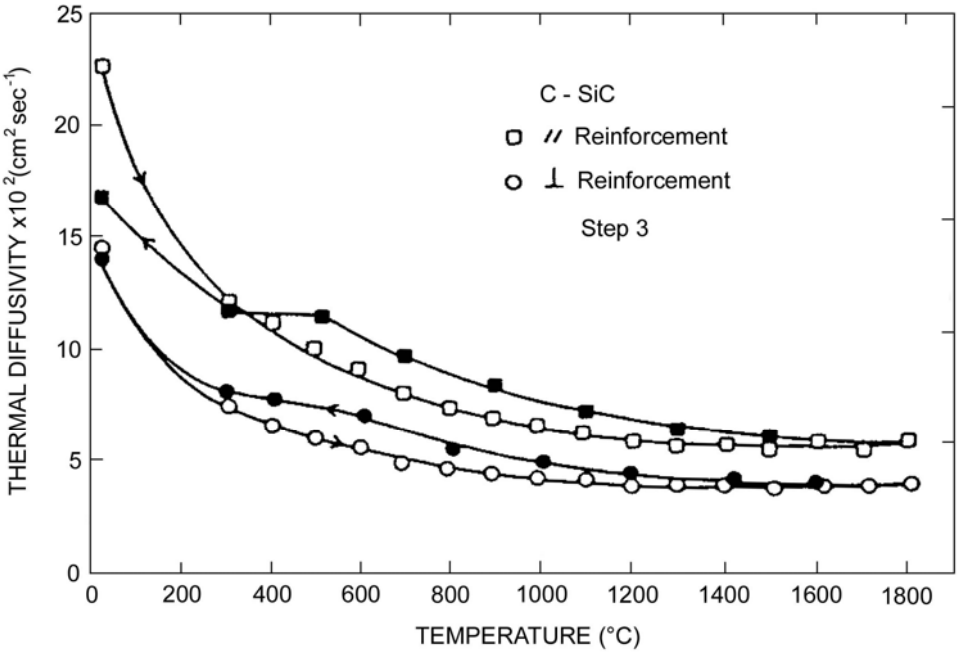

Key: Values parallel and perpendicular to fibre in densified (Step 3) composites, cycled to 1800°C.
Open symbols = heating; Closed symbols = cooling.

Figure 82.7-7 - Thermal diffusivity with temperature for C-SiC composites

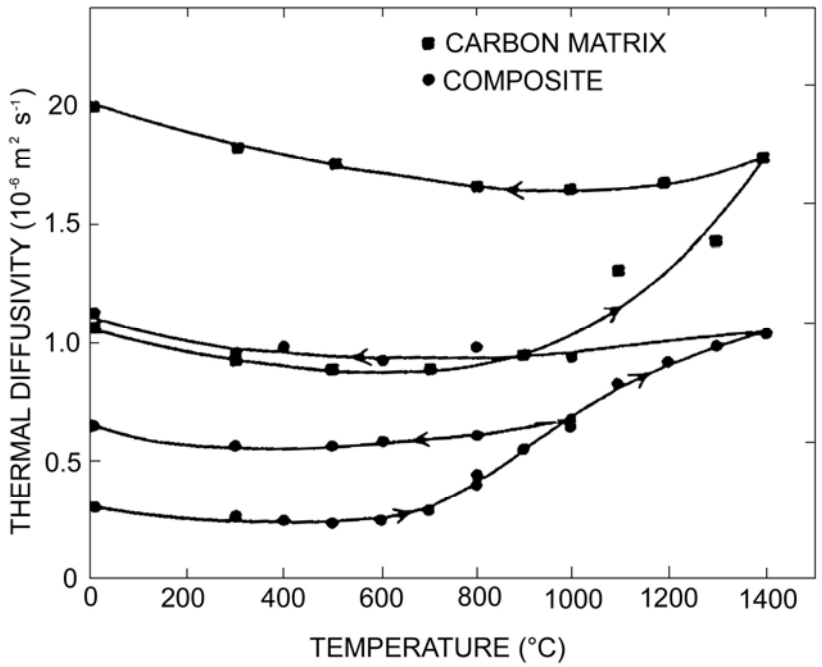

Figure 82.7-8 - Effect of thermal cycling on thermal diffusivity of a carbon matrix and aluminosilicate-carbon composite

The diffusivity of C-C composites is dependent on the overall density, Ref. [82-18]. The diffusivity also falls appreciably as the temperature rises to 2200°C, which is typical of a phonon conductor.

Thermal conductivity for C-C materials can vary between 50W/m/°C and 200W/m/°C, depending on the material characteristics and temperature.

82.8 Specific heat capacity

Knowledge of material heat capacities is important in determining how much heat energy a structural configuration retains in a high heat flux environment.

Heat capacity, like conductivity, changes as temperatures increase. Specific heat capacity values are often available for individual material elements near room temperature but are less common for MMC and CMC materials.

Figure 82.8.1 shows specific heat values for LAS glass-ceramic and amorphous Nicalon SiC fibres, Ref. [82-15].

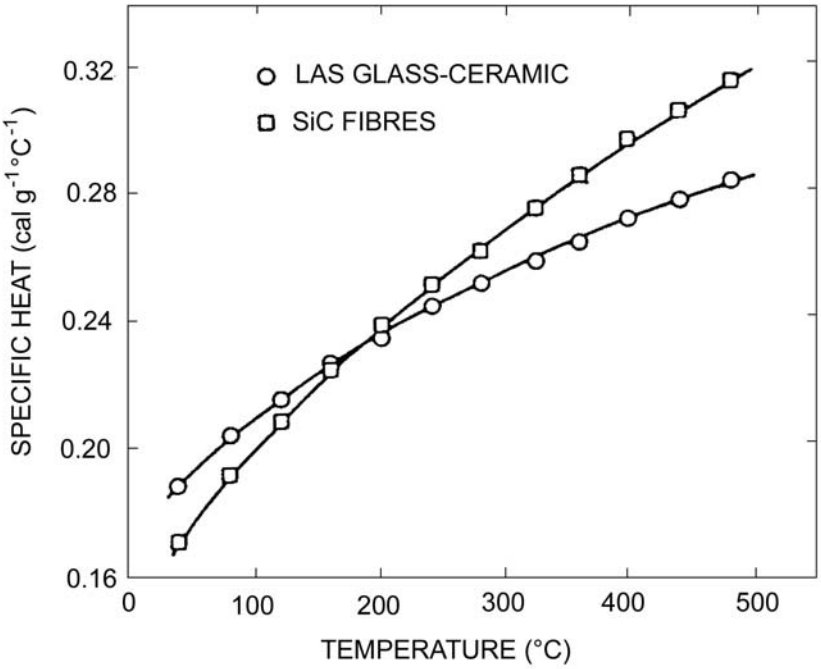

Figure 82.8-1 - Specific heat capacity of LAS glass-ceramic and amorphous SiC fibres

82.9 Surface emissivity

Surface emissivity is an important characteristic for structures experiencing high heat fluxes; such as propulsion units or the leading edges of re-entry vehicles. A high surface emissivity enables heat to be re-radiated, so that heat conducted to underlying structures can be controlled. A desirable emissivity value of 0.85 is often quoted. As an example, Table 82.9.1 shows how the wall temperature of a CMC TPS could vary if the emissivity is low, Ref. [82-19]. This equates to emissions in the 0.4µm to 15µm wavelength band.

Table 82.9-1 - Effect of low surface emissivity on CMC TPS wall temperatures

Total emissivity	Wall temperature (°C)		
0.85	1000	1300	1500
0.80	+ 20	+ 25	+ 30
0.70	+ 60	+ 80	+ 90
0.50	+ 180	+ 220	+ 250

With high temperature materials, emissivity is often governed by the coatings applied for protective purposes or to deliberately change the emissivity to a required value.

82.10 Surface catalyticity

This term relates to the ability of a surface to act as a catalyst in the recombination of reactive chemical species under particular conditions.

The requirement for low surface catalysis is a appropriate to re-entry vehicles and spaceplanes.

A vehicle surface re-entering an atmosphere encounters reactive oxygen and nitrogen radicals. If catalysed, these radicals recombine to form molecules, e.g. O_2, N_2 and $[NO]_X$, with exothermic reactions. The heat of reaction at the surface compounds aerodynamic heating.

Surface catalysis is particularly critical for surfaces experiencing the re-entry shockwave, where gas temperatures of 6000°C can result.

Table 82.10.1 shows how surface emissivity and catalyticity can combine to cause severe heat management problems.

Table 82.10-1 - Emissivity and catalyticity: Combined effects on re-entry surface temperatures

Emissivity	Catalyticity	
	Low	High
0.85	1500°C	+ 100
0.70	+ 90	+ 190
0.50	+ 240	+ 360

If correctly formulated, the glassy outer layers of oxidation protection systems can provide high emissivity and low catalyticity.

82.11 References

82.11.1 General

[82-1] A.C.F. Cocks et al
'Effect of Cyclic Thermal Loading on the Properties of Metal Matrix Composites'
Journal of Thermal Stresses, 15, 1992, p175-184

[82-2] S.S. Tompkins
'Effects of Thermal Cycling on Composite Materials for Space Structures'
NASA/SDIO Workshop on Space Environmental Effects on Materials, June 1989, part 2, p447-470

[82-3] T. Kyono et al
'Effects of Thermal Cycling on Properties of Carbon Fiber/Aluminium Composites'
Transactions of the ASME, Journal of Engineering Materials and Technology, April 1988, Vol.110, p89-95

[82-4] M. Taya & R.J. Arsenault
'Metal Matrix Composites: Thermomechanical Behaviour'
Pergamon Press, ISBN 0-08-036983-9, 1989

[82-5] P.G. Ermer & S. Mall
'Damage Mechanisms in a Unidirectional Metal Matrix Composite During Thermal Cycling'
Proceedings of the 5th Technical Conference on Composite Materials, East Lansing USA, 12-14 June 1990, p528-536

[82-6] G.M. Newaz et al
'Thermal Cycling Response of Quasi-Isotropic Metal Matrix Composites'
Transactions of the ASME, Journal of Engineering Materials and Technology, April 1992, Vol.114, p156-161

[82-7] T. Morimoto & M. Taya
'Thermal Cycling Damage of High Temperature Metal Matrix Composites'
Advances in Fracture Research, 7th International Conference on Fracture, Houston, May 20-24, 1989, Vol. 4, p2987-2996

[82-8] Y.R. Wang & T.W. Chou
'Thermal Shock Resistance of Laminated Ceramic Matrix Composites'
Journal of Materials Science 26 (1991), p2961-2966

[82-9] A.J. Eckel et al
'Thermal Shock Fiber-Reinforced Ceramic Matrix Composites'
Ceram. Eng. Sci. Proc. 12[7-8], p1500-1508 (1991)

[82-10] J.L. Yuen & R.J. Walter
'Thermal Shock and Thermal Fatigue Testing'
Journal of Testing and Evaluation, JTEVA, Vol. 19, No. 5
Sept 1991, p403-407

[82-11] R. Taylor & Y. Qunsheng
'Thermal Transport in Carbon Fibre-Copper and Carbon Fibre/Aluminium Composites'
ICCM 8, Honolulu, 15-19 July, 1991, Paper 18

[82-12] S.P. Turner et al
'Thermal Properties of Ti-SiC and Ti-TiB2 Particulate Reinforced Composites'
ECCM6, Bordeaux, Sept 1993, ISBN 1-85573-142-8, p513-518

[82-13] W.P. Schimmel
'Transient Thermal Conduction in Aerospace Composite Materials: A Simplified Design and Analysis Technique'
Thermal Conductivity 21, 1990, p429-443

[82-14] D.P.H. Hasselman et al
'Heat Conduction Characteristics of a Carbon Fibre-reinforced Lithia-alumino-silicate (LAS) Glass-ceramic'
Journal of Materials Science 22 (1987) p701-709

[82-15] J.J. Brennen et al
'Determination of the Thermal Conductivity and Diffusivity of Thin Fibres by the Composite Method'
Journal of Material Science 17 (1982), p2337-2342

[82-16] H. Tawil et al
'Thermal Diffusivity of Chemically Vapour Deposited Silicon Carbide Reinforced with Silicon Carbide or Carbon Fibres'
Journal of Material Science 20 (1985), p3201-3212

[82-17] H. Tawil et al
'Effect of Heat Treatment on the Thermal Diffusivity of an Aluminosilicate Fiber-Reinforced Carbon Matrix'
Carbon Vol. 22, No.6, 1984, p571-574

[82-18] A.J. Whittaker et al
'Thermal Transport Properties of Carbon-carbon Fibre Composites: I - Thermal Diffusivity Measurements'
Proc. R. soc. Lond .A (1990) 430, p167-181

[82-19] G. Bernhart
'Materials for Hermes Hot Structural Parts: Requirements and Testing'
Proceedings of an International Symposium on Space Applications of Advanced Structural Materials, ESTEC, 21-23 March 1990
ESA SP-303, p411-417

83 Thermo-mechanical fatigue

83.1 Introduction

The behaviour of materials under combined mechanical and thermal load is particularly relevant to:

- spaceplanes, [See also: Chapter 69 and Chapter 71],
- thermostructural designs, [See also: Chapter 70],
- propulsion systems, [See also: Chapter 73].

When the thermal excursions are severe and repeated, a material undergoes thermo-mechanical fatigue (TMF).

For high-temperature materials operating close to their physical limits, this can greatly accelerate degradation mechanisms within the composites.

[See: Chapters 64, 65, 66, 67 and 68]

If oxidative or corrosive environments are also present, the life expectancy of materials can be seriously impaired, [See: Chapter 85].

A thorough understanding of material behaviour is essential for high-temperature materials applied to space programmes where TMF occurs. The degradative processes are highlighted, along with the associated loss of mechanical properties.

High-temperature technology from the gas turbine industry is relevant, as life expectancies are greater than for space applications.

83.2 Phased TMF

High-temperature composites consist of two or more phases with different moduli and coefficients of thermal expansion (CTE). Consequently, composites contain residual stresses, particularly on cooling from the manufacturing temperature. Tensile stresses predominate in the matrix phases, because their thermal expansion characteristics are usually the higher. This has important implications for TMF behaviour depending on whether the thermal and mechanical loads are applied 'in-phase' or 'out-of-phase' with each other. Residual stresses are strongly influenced by the volume fraction of reinforcement and whether it is continuous (fibres) or discontinuous (whiskers and particulates), Ref. [83-1].

Given that residual stress is highest when the composite is cold, any applied mechanical load compounds the stresses. At higher temperatures, residual stresses are lower and applied loads do not normally contribute significantly to approaching the limits of the material. Out-of-phase TMF can, in some cases, provide more arduous conditions for the composite than in-phase TMF.

The intended applications and the sequence in which applied thermal and mechanical loads occur are important considerations.

In-phase and out-of-phase effects of TMF are different for alloys, where:

- out-of-phase (OP TMF) gives maximum strain at minimum temperature,
- in-phase (IP TMF) gives maximum strain at maximum temperature.

83.3 Superalloys

Comprehensive TMF studies have been conducted on the behaviour of superalloys applied to gas turbine engines, Ref. [83-2], [83-3], [83-4], [83-5].

Typical gas turbine and jet engine hot-section components are subjected to severe environments with variable thermal and mechanical loading histories. Nickel-base superalloys are often used because of their superior creep resistance and strength at high temperatures, [See also: Chapter 48].

The most popular predictive models for TMF life are based on the creep-fatigue interactions exhibited by ductile metals and do not explicitly contain an environmental feature, e.g. oxidation effects. These models are viewed as parametric damage approaches, in which the environmental effect is assumed to be incorporated in the time dependence of the formulation, Ref. [83-5]. Creep-fatigue interaction models that exclude environmental effects, or include them only implicitly, are applied cautiously to TMF life prediction, since the mechanistic basis is suspect. Construction of predictive models that include the combined effects of creep and oxidative environments is under way for a range of alloys, Ref. [83-4], [83-5]. The presence or otherwise of protective coatings is also important in determining TMF response, Ref. [83-2]

[See also: 48.9 and Chapter 74 for protective coatings]

Superalloy technology is now approaching the limits of its development in terms of extending the maximum operating temperatures for the advanced alloys over prolonged periods of time. Application temperatures in gas turbine engines are presently about 800°C to 1000°C for Ni-based alloys. Effort placed in improving processing methods and innovative designs for engine components enables superalloys to continue to function in gas turbine applications.

[See also: Chapter 49 for intermetallic materials]

83.4 Aluminium composites

83.4.1 Particulate reinforced composites

The behaviour of Al-SiCp composites under severe TMF conditions has been studied, Ref. [83-6], [83-7], [83-8]. An ALCOA composite (2124 alloy with 15% SiCp and 20% SiCp) evaluated in the temperature range 100°C to 200°C and 100°C to 300°C with OP TMF showed that, Ref. [83-7]:

- reinforcement of 20% SiCp increased OP TMF fatigue lives as much as 5 times compared with the unreinforced alloy,
- in the composites, oxide cracking was noted at temperatures above 200°C,
- cyclic softening of all specimens was noted above 200°C.

Further work on the same materials revealed that, Ref. [83-6]:

- fatigue life of unreinforced alloy was very strain-rate sensitive,
- composite fatigue lives reduced by a factor of 10 when the maximum temperature increased from 200°C to 300°C,
- mechanisms promoting crack growth are:
  - oxidation,
  - intergranular cracking,
  - mean tensile stress, and
  - increased matrix strain fields.

A predictive model to describe the behaviour of these composites was proposed, Ref. [83-8].

83.4.2 Continuous fibre reinforced composites

The behaviour of continuous fibre aluminium composites has been studied with reference to the modes of failure, Ref. [83-9].

83.5 Titanium composites

The behaviour of SiC monofilament reinforced titanium composite is widely studied, Ref. [83-8], [83-10] to [83-17], inc.].

Owing to compatibility problems between the fibre and matrix, a brittle interface usually exists. TMF is a severe test for the interfacial bond. It is useful to know the maximum temperatures for these materials, whilst understanding the failure mechanisms. The behaviour of multidirectional composites is different from that of solely unidirectional construction, mainly owing to the low transverse properties of Ti-based composite materials.

Most published information is for Ti-15V-3Cr-3Al-3Sn alloy matrix with SiC SCS-6 monofilament reinforcement, which has undergone:

- simple RT tensile fatigue, Ref. [83-12],
- isothermal fatigue,
- residual strength evaluation after thermal cycling,
- TMF up to 550°C (both IP and OP).

In the unidirectional composite form, the MMC has good isothermal fatigue resistance at 300°C and 550°C at low cyclic stresses with fatigue cracks initiating from fibre-matrix interfaces, Ref. [83-11].

At high cyclic stresses, stress relaxation in the matrix reduced isothermal composite fatigue resistance at 550°C. Non-isothermal fatigue loading substantially degraded the composite fatigue resistance, Ref. [83-10]. This degradation was produced by a TMF damage mechanism at the fibre-matrix interfaces.

The conclusions drawn from the fatigue cycles are shown in Figure 83.5.1, where applied stress varied between 700MPa and 1200MPa, Ref. [83-10].

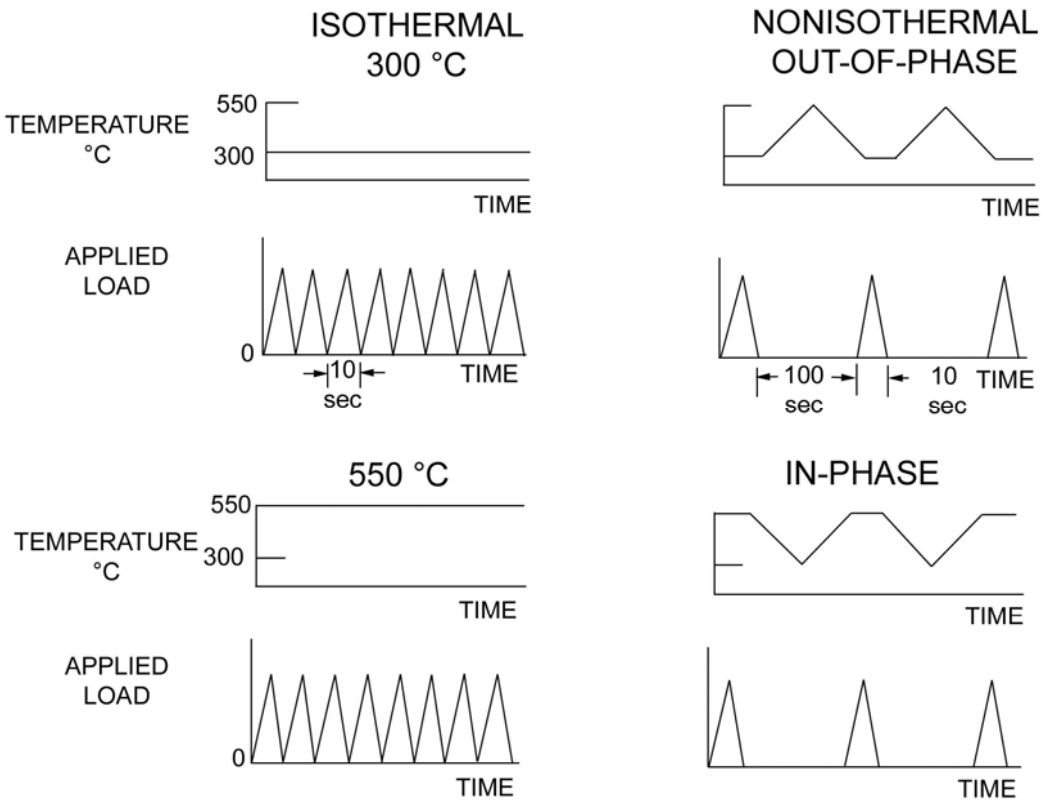

Figure 83.5-1 - TMF of Ti-based composite: Fatigue test cycles

A comparison of the isothermal and OP performances is shown in Figure 83.5.2, Ref. [83-10].

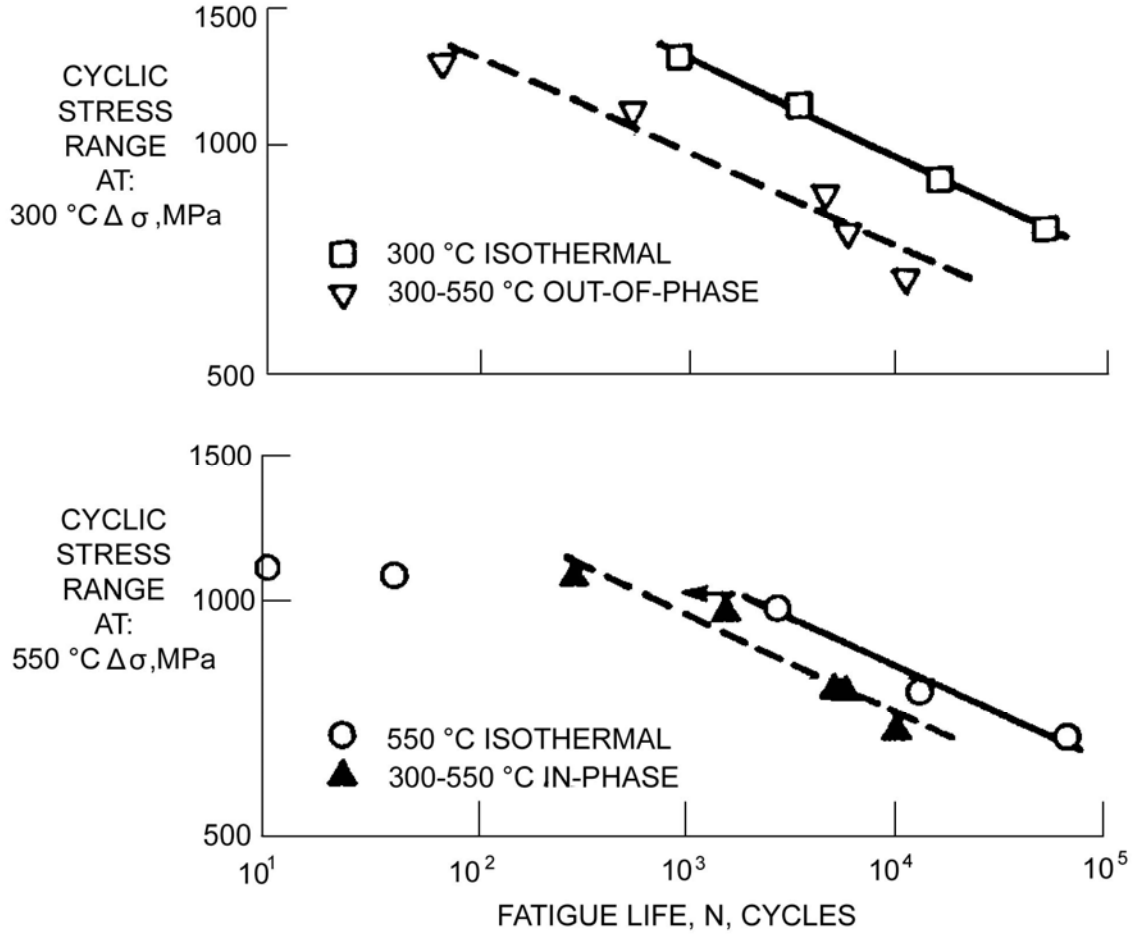

Figure 83.5-2 - TMF of Ti-based composite: Comparison of isothermal and non-isothermal fatigue lives with cyclic stress range

A wider range of laminate configurations were also tested, Ref. [83-14].

[See: 47.7]

Thermal cycling was studied to 427°C for specimens with interface dominated mechanical properties, $[90]_8$, $[\pm30]_{2s}$, $[\pm45]_{2s}$, $[0/90]_{2s}$ and $[90/0]_{2s}$, Ref. [83-14]; showing only small changes in mechanical strength.

If the composite experiences high residual and applied stresses at elevated temperatures, the matrix can begin to creep at a lower temperature than if it were not reinforced. This is particularly true for composites with transverse plies.

A few broad conclusions drawn from work to date include:

- β-alloy TMC laminates are stable to ~425°C in TMF conditions,
- UD composites have good axial fatigue characteristics and high tensile strength, with reasonable TMF capabilities up to 500°C,
- multidirectional laminates contain plies with poor transverse properties that can be significantly degraded by TMF.

The first applications for these materials in gas-turbine engine are blisks; integrally formed blade and disks. A unidirectional winding is used with a single, axial loading mode in the fibre direction, so avoiding poor transverse properties.

83.6 Copper composites

[See also: Chapter 45]

The behaviour of 9 vol.% tungsten fibre-reinforced, oxygen-free, high conductivity copper has been studied, Ref. [83-18].

A strong fibre to matrix bond exists without interfacial reaction products. This type of material has been considered as a candidate combustor liner material where TMF occur. The composite has undergone testing, including Ref. [83-18]:

- isothermal fatigue at 260°C and 560°C.
- TMF, both IP and OP, between 260°C and 560°C.

The results are summarised in Figure 83.6.1, Ref. [83-18].

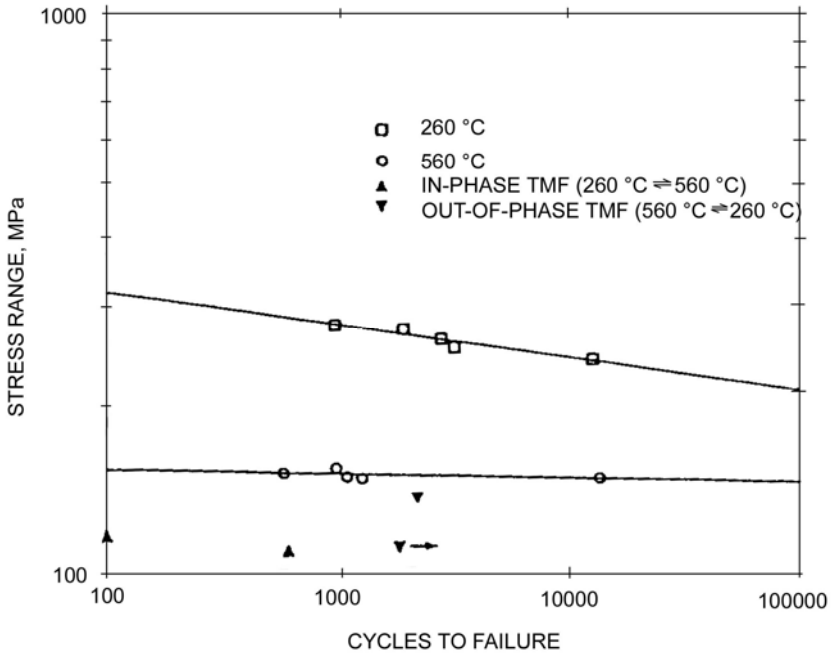

Figure 83.6-1 - TMF: Tungsten/copper composites under various thermal regimes

The conclusions were:

- stress-strain response under all conditions displayed considerable inelasticity,
- strain ratcheting was observed during all fatigue experiments:
  - for isothermal fatigue and IP TMF, ratcheting was always in a tensile direction and continued to failure,
  - for OP TMF, ratcheting shifted to a compressive direction,
- satigue lives were controlled by damage to the copper matrix, principally grain boundary cavitation.

For the intended combustor application the material could be expected to experience temperatures to 560°C. It remains to determine whether the composite performs better than the base metal. In both, the metal phase is in a seriously softened condition.

83.7 Ceramic composites

TMF is difficult to isolate in the overall behaviour of ceramic composites as these composites contain porosity and microcrack populations. Their as-made ultimate mechanical strengths are modest for multidirectional laminates. Localised, progressive microcracking can be induced at low stresses, Ref. [83-19], [83-20], [83-21].

The main degradation mechanisms for ceramic-based composites occur when TMF is compounded with environmental attack, e.g.

- thermal cycling,
- matrix microcracking,
- microstructural changes in the fibre, e.g. SiC Nicalon at temperatures above 1200°C,
- matrix creep,
- coating breakdown and failure,
- oxidation at the fibre-matrix interface,
- diffusion of oxygen into the fibres,
- gross embrittlement.

The applied mechanical loads are normally kept very low in structural applications. This is to offset the large thermal transients that occur and to maintain minimum strain level, e.g. ~0.%1 to 0.2%. The remaining strain capacity of the composite, where progressive microcracking and fibre pull-out occurs, is the safety margin. In the latter stages of load application, the composite is losing effective stiffness.

83.8 Carbon-carbon composites

TMF is not a significant issue with C-C materials. The matrix is stable provided it is graphitised at a temperature higher than that of the intended application.

The fibres are often the first to change their microstructure if the temperature is increased to above 1500°C. However, a highly graphitised fibre can resist such changes to above 2300°C.

Obtaining resistance to oxidation is by far the greatest problem with these materials, [See: 54.4].

The use of 3D reinforcement further reduces the opportunities for interlaminar fracture.

83.9 Predictive methods

TMF is principally a concern for MMCs, where the metal matrix is the main source of failure mechanisms.

Attempts are being made to produce models which can predict the TMF behaviour of MMC materials, Ref. [83-8], [83-22], [83-23], [83-24].

A framework of modelling TMF behaviour has been proposed, Ref. [83-22]. This summarises isothermal fatigue composite data for:

- tungsten-reinforced copper (ductile-ductile system),
- SiC/Ti-15-3-3-3 TMC (brittle-ductile),
- SiC/Ti-24Al-11Nb intermetallic composite (brittle-brittle).

The fatigue behaviour of all these material systems is heavily influenced by the matrix, whose characteristics change as the number of cycles increases. Such matrix changes include:

- mean stress relaxation,
- hardening,
- softening,
- microcrack initiation, and
- microcrack propagation.

83.10 References

83.10.1 General

[83-1] M. Taya & R.J. Arsenault
'Metal Matrix Composites: Thermomechanical Behaviour'
Pergamon Press, ISBN 0-08-036983-9, 1989

[83-2] J. Bressers et al
'Thermo-mechanical Fatigue of a Coated and Uncoated Nickel-based Alloy'
Meeting on Mechanical Behaviour of Materials - VI, Vol.2, Kyoto Japan, 29 July - 2 Aug 1991, p463-468

[83-3] 'Advances in Fatigue Lifetime Predictive Techniques'
ASTM STP 1122, edited by M.R. Mitchell & R.E. Landgraf, 1992

[83-4] H. Sehitoglu
'Thermo-Mechanical Fatigue Life Prediction Methods'
ASTM STP 1122, 1992, p47-76

[83-5] D.L. McDowell et al
'Mechanistic Considerations for TMF Life Prediction of Nickel-based Superalloys'
Nuclear Engineering and Design 133 (1992), p383-399

[83-6] M. Karayaka & H. Sehitoglu
'Thermomechanical Fatigue of Particulate-Reinforced Aluminium 2XXX-T4'
Metallurgical Transactions A, Volume 22a, March 1991, p697-707

[83-7] H. Sehitoglu & M. Karayaka
'Thermo-mechanical Fatigue of Al-SiCp Composites'
Proceedings of the 4th International Conference on Fatigue and Fatigue Thresholds, Fatigue '90, Volume 3, p1693-1698

[83-8] H. Sehitoglu & M. Karayaka
'Prediction of Thermomechanical Fatigue Lives in Metal Matrix Composites'
Metallurgical Transactions A, Volume 23A, July 1992, p1992-2038

[83-9] W.S. Johnson
'Mechanisms Controlling Fatigue Damage Development in Continuous Fiber Reinforced Metal Matrix Composites'
Advances in Fracture Research, Proceedings of the 7th International Conference on Fracture, Houston, 20-24 Mar 1989, Vol.2, p897-905

[83-10] T.P. Gabb et al
'Isothermal and Non isothermal Fatigue Behaviour of a Metal Matrix Composite'
Journal of Composite Materials, Vol. 24, June 1990, p667-686

[83-11] J. Gayda et al
'The Isothermal Fatigue Behaviour of a Unidirectional SiC/Ti Composite and the Ti Alloy Matrix'
Fundamental Relationships Between Microstructure & Mechanical Properties of Metal-Matrix Composites. The Minerals, Metals & Materials Society, 1990, p497-514

[83-12] K.R. Bain & M.L. Gambone
'Fatigue Crack Growth Of SCS-6/Ti-64 Metal Matrix Composites'
Fundamental Relationships Between Microstructure & Mechanical Properties of Metal-Matrix Composites. The Minerals, Metals & Materials Society, 1990, p459-469

[83-13] R.A. Naik & W.S. Johnson
'Observations of Fatigue Crack Initiation and Damage Growth in Notched Titanium Matrix Composites'
ASTM STP 1110, 1991, p753-771

[83-14] J.E. Grady & B.A. Lerch
'Evaluation of Thermal and Mechanical Loading Effects on the Structural Behaviour of a SiC/Titanium Composite'
AIAA-90-1026-CP

[83-15] W. Wei
'High Temperature Low Cycle Fatigue of a SiC/Ti Matrix Composite'
ECCM4, Sept 1990, Stuttgart, ISBN 1-85166-562-5, p319-324

[83-16] F.H. Gordon & T.W. Clyne
'Thermal Cycling Creep of Ti-6Al-4V/SiC Monofilament Composites under Transverse Loading'
Symposium on "Residual Stresses in Composites: Modelling Measurement and Effects on Thermomechanical Properties"
TMS Annual Meeting, Denver, USA, 21-25 Feb 1993

[83-17] J.J. Schubbe & S. Mall
'Damage Mechanisms in a Cross-ply Metal Matrix Composite under Thermal-mechanical Cycling'
ICCM 8, 15-19 July 1991, Paper 20, p20B1-20B9

[83-18] M.J. Verrilli et al
'High Temperature Fatigue Behaviour of Tungsten Copper Composites'
Fundamental Relationships Between Microstructure & Mechanical Properties of Metal-Matrix Composites. Edited by P.K. Liaw and M.N. Gungor, The Minerals, Metals & Materials Society, 1990. p479-495

[83-19] Y. Kim et al
'Thermal Fatigue Behaviour of Ceramic Matrix Composites: A Comparison among Fiber Reinforced, Whisker Reinforced,Particulate Reinforced, and Monolithic Ceramics'
American Society for Composites Technical Conference, 12-14 June 1990, p871-881

[83-20] T Fujii et al
'Are There Fatigue Effects on Ceramics and Ceramic Matrix Composites under Cyclic Loading?'
Metal & Ceramic Matrix Composites: Processing, Modelling & Mechanical Behaviour, The Minerals, Metals & Materials Society, 1990, p253-260

[83-21] L.P. Zawada & R.C. Wetherhold
'The Effects of Thermal Fatigue on a SiC Fibre/aluminosilicate Glass Composite'
Journal of Materials Science 26 (1991), p648-654

[83-22] G.R. Halford et al
'Proposed Framework for Thermomechanical Life Modelling of Metal Matrix Composites'
NASA Technical Paper 3320, 1993

[83-23] G.S. Daehn
'Effects of Environmental and Microstructural Variables on the Plastic Deformation of Metal Matrix Composites Under Changing Temperature Conditions'
In Thermal and Mechanical Behaviour of Metal Matrix Composites ASTM STP 1080, p70-86, 1990

[83-24] C.C. Chamis et al
'Computational Simulation of High-Temperature Metal Matrix Composites Cyclic Behaviour'
In Thermal and Mechanical Behaviour of Metal Matrix Composites ASTM STP 1080, p56-69, 1990

84 Dimensional control

84.1 Introduction

The material characteristics which influence the physical dimensions of a component as it undergoes thermal excursions to high temperatures are considered.

The main factors include:

- material expansion, and
- any permanent changes that can occur, such as creep.

Where available, data is given on the changes in CTE that can occur as temperatures vary, or as material microstructures change.

84.2 Residual stresses

Residual stress levels within high-temperature materials can be very high, particularly for two phase composites.

If stress relief is possible, a change in the dimensions of a component can be expected. Typical mechanisms for stress relief include:

- heat treatments,
- thermal cycling,
- plastic deformation of matrix,
- microcracking,
- slippage at the fibre-matrix interface,
- out-of-plane bending.

Stress relief by heat treatment is preferable before components are assembled.

84.3 Creep: Metallic materials

84.3.1 General

Creep occurs with time at elevated temperature when there is sufficient load applied to induce a measurable permanent strain. Superplasticity is in effect a severe form of creep in alloys where small applied loads induce very high levels of strain, usually at high temperatures. If an alloy is very ductile, plasticity can be induced at low temperatures.

Creep in metal-based composites is considered serious if it induces permanent plastic strains of more than 0.1% in service.

84.3.2 Particulate reinforced aluminium composites

Creep experiments conducted on particulate reinforced aluminium sought to correlate composite behaviour with theory by establishing the levels of residual stress in the matrix, Ref. [84-1], [84-2]. Pure aluminium of low yield strength showed its ductile matrix characteristics in creep tests.

Whilst such composites are of little practical use, the work emphasises the high residual stresses in the matrix. The addition of particles does not automatically improve the creep behaviour of a MMC; it can reduce creep resistance. Low temperature creep can be reduced by an appropriate heat treatment for the MMC.

Some particulate reinforced MMC materials can be superplastically formed. This has been successfully applied to aluminium with AlN and TiC particle reinforcements at 600°C, Ref. [84-5].

84.3.3 Discontinuous fibre reinforced aluminium

Discontinuous Saffil® alumina fibres in high silicon casting alloys are popular engineering MMC materials.

Creep tests on Al-5Si-3Cu-1Mg alloy reinforced with 20% Saffil showed 1.25% strain at 300°C and 75 MPa after 5 hours, Ref. [84-3]. The creep damage sequence was:

- dislocation creep in the matrix,
- slip of both grain boundary and at weak fibre-matrix interfaces,
- fibre rupture and interface debonding, and finally
- matrix free deformation and fracture.

Use of laser interferometry enables accurate measurements of creep at high temperatures, Ref. [84-4]. A short (discontinuous) fibre 10 vol.% carbon fibre-reinforced pure aluminium composite was studied with an accuracy of ±2µm over a gauge length of 10mm. A load of 18MPa was applied continuously during thermal cycling between 138°C and 338°C. The material exhibited reverse creep, i.e. contracted, because the residual stresses in the matrix far exceeded the applied 18MPa. The mechanical properties of the composite are matrix dominated because of the discontinuous fibres.

84.4 Creep: Ceramic composites

84.4.1 General

Some creep studies on continuous fibre GCMC and CMC materials have been conducted, Ref. [84-6] to [84-10].

A comprehensive review of the limited work conducted reveals the temperatures to which a range of composites have been exposed, Ref. [84-9].

84.4.2 Creep mismatch ratio (CMR)

84.4.2.1 General

Creep behaviour and macroscopic creep damage mechanisms can be related to the creep mismatch ratio (CMR). Where CMR is defined as the ratio of the creep rate of the fibres to that of the matrix. The CMR response of various composites is summarised in Table 84.4.1.

84.4.2.2 Conclusions

- For CMR < 1: Microstructural damage during creep involves debonding between fibres and matrix.
- For CMR > 1: Matrix fracture and associated fibre bridging can occur. All composites showed a threshold stress in the 60MPa to 90MPa range for temperatures around 1200°C. Above these stresses, creep is a serious progressive failure mechanism.

Methods have been developed for calculating the residual stresses within C-C/SiC and SiC/C/SiC materials including the presence of the interface material, Ref. [84-7].

Table 84.4-1 - Creep in ceramic composites: Summary of testing of various CMC materials

Composite System	Comments
Creep mismatch ratio (CMR) < 1	
0°/90° (woven) Nicalon SiC/SiC CMC	Creep experiments conducted from 1100 to 1400°C. Stress dependence of apparent steady-state creep rate thresholds: • 60 MPa at 1200°C, • 40MPa at 1300°C. These are the stresses at which the creep rate was below detectable levels.
0° Nicalon SiC/MLAS GCMC	Flexural loading in vacuum from 900 to 1200°C, with stresses in the range 10 to 300MPa, Ref. [84-9], [84-10]. At 1100°C, creep strains after 50 hours: • At 50 MPa: 0.15%, • At 200 MPa: 0.25% • At 300 MPa: 0.37%. Conclusions: • for the lower stresses and temperatures, debonding along the fibre-matrix interface and matrix cracking parallel to the fibres ultimately occurred, • for high stresses and low temperatures, matrix microcracking perpendicular to the fibres occurred. • at high temperatures, the deformation of the composite was governed by creep of the Nicalon fibres.
0° and 0°/90° Nicalon SiC/CAS-II GCMC	0° composite: No creep observed at 60 MPa for 100 hours. At 120 MPa, periodic fibre fracture was found as a fundamental creep damage mode. **(**Transverse fibres in 0°/90° composites can contribute significantly to creep resistance) • Creep strain at 60 MPa was similar for both the unidirectional and bidirectional composites. • 0°/90° composite exhibited more strain recovery during cyclic creep loading.
0° SCS-6 SiC/HPSN CMC (Hot Pressed)	• Evaluated between 1200 and 1350°C and in air. • At 1200°C, a threshold stress for creep deformation was 60MPa. • At all applied stresses the majority of creep occurred in the first 10 hours, whereupon creep slowed significantly.
Creep mismatch ratio (CMR) > 1	
0° SCS-6 SiC/RBSN (Reaction Bonded)	• Contained 24 vol.% fibres and 30% porosity. • Creep testing was conducted at 1300°C, in nitrogen, at 90, 120 and 150 MPa. • At 90MPa for 100 hours: No detectable microstructural damage. • At 120 MPa: Matrix cracking observed.

84.5 Crack densities

Microcracks occur in both MMC and CMC materials, depending on their thermo-mechanical history.

Some microcracking is tolerated in CMC materials for single-cycle, short-life applications; less for reusable components with a reasonable life requirement (a few tens of hours) and corresponding thermal cycles.

A judgement is made as to the tolerable level of microcracking. This is closely associated with the criticality of the component and whether it is a 'Safe-life' or 'Fail-safe' item.

A limitation on the allowable material strain is the best way of controlling the growth of microcracks. Excessive microcracking modifies both mechanical and physical properties, such as thermal conductivity and expansion.

[See also: Chapters 82, 83 and 85]

84.6 CTE: Metallic materials

84.6.1 General

The thermal expansion characteristics of MMC materials are influenced by:

- matrix composition,
- reinforcement material:
  - volume fraction,
  - continuity, and
  - orientation.
- thermal history, e.g. heat treatments,
- presence of secondary phases, e.g.
  - porosity,
  - precipitates,
  - interfaces, and
  - cracks.

84.6.2 Continuous reinforcement

Continuous fibres suppress the high CTE of all metals. Adding high-modulus carbon fibres, with slightly negative CTEs, to aluminium or magnesium reduces the axial composite CTE to almost zero. The transverse CTE values are very high, so multidirectional laminates are used for a low, all round expansion. Through-thickness expansion of 2D laminates is large.

An approximation of CTE can be calculated using the 'Law of Mixtures' based on the properties of the matrix and reinforcement, Ref. [84-11].

CTE values also depend on the temperature range, as shown in Table 84.6.1.

Table 84.6-1 - Thermal expansion: Average values for aluminium-based composites

Material †	Direction	CTE ($x10^{-6}°C^{-1}$)			
		-196 to -129	-129 to +24	+24 to +177	+177 to +371
6061-T6	-	3.70	6.06	8.12	8.39
B/Al	0	0.65	1.17	1.86	1.87
	90	2.78	4.61	5.56	7.37
BORSIC/Al	0	0.81	1.39	1.73	1.85
	90	2.68	4.64	5.04	6.08
BORSIC/Ti/Al	0	0.72	1.16	1.70	2.21
	90	1.61	3.23	3.94	4.20

Key † Al = 6061

84.6.3 Particulate reinforcement

The high expansion of aluminium is reduced by the addition of particulates, Ref. [84-12].

Particulate reinforced MMCs benefit from a high conductivity matrix, which forms the bulk of the composite, with a reduced CTE.

84.7 CTE: Ceramic composites

84.7.1 SiC matrix composites

The thermal expansion of various SiC matrix composites has been studied, Ref. [84-13].

Table 84.7.1 gives calculated CTE values for some composites in the temperature range 25°C to 1000°C, Ref. [84-13]. Figure 84.07.1 shows the thermal expansion and contraction behaviours of these composites, Ref. [84-13].

The data indicate the non-linear expansion and, in one case, a hysteresis effect.

Table 84.7-1 - CTE: Calculated values for CMC SiC matrix composites, with material data

Composition and physical properties of as-received composites				
Fibre	**Weave {1}**	***Vff* {2}**	***Vfm* {3}**	**Density {4} (kg/m^3)**
FP Alumina	4HS	0.26	0.45	2470
Nextel 312	8HS	0.34	0.33	1980
Nicalon	8HS	0.31	0.30	1900

Physical property values (used in calculation of linear CTE)			
Material	***E* (GPa)**	**Density (kg m^{-3})**	**α (x10^{-6}°C^{-1})**
CVI SiC	420	3210	4.45
FP-Alumina	379	3900	8.80
Nextel	186	3050	5.33
Nicalon	190	2550	4.45

Composite thermal expansion coefficients		
Fibre	$\overline{\alpha}_{measured}$* **(x10^{-6}°C^{-1})**	$\overline{\alpha}_{calculated}$* **(x10^{-6}°C^{-1})**
FP Alumina	5.30 ± 0.03	5.86
Nextel 312	4.77 ± 0.04	4.73
Nicalon	4.45 ± 0.07	4.45

Key
{1} Harness Satin (HS)
{2} Fibre volume fraction
{3} Matrix volume fraction
{4} Manufacturers' data
$\overline{\alpha}_{measured}$* Average values from 25°C to 1000°C.
$\overline{\alpha}_{calculated}$* ± values are 95% confidence intervals

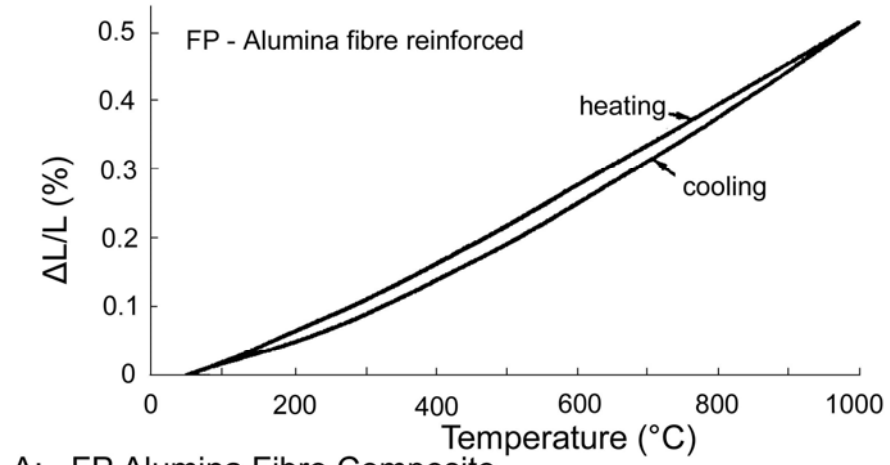

A: FP Alumina Fibre Composite

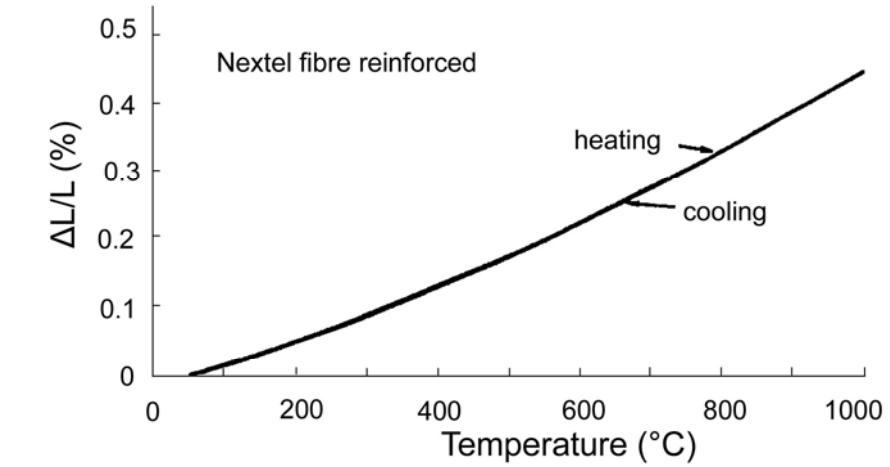

B: Nextel Fibre Composite

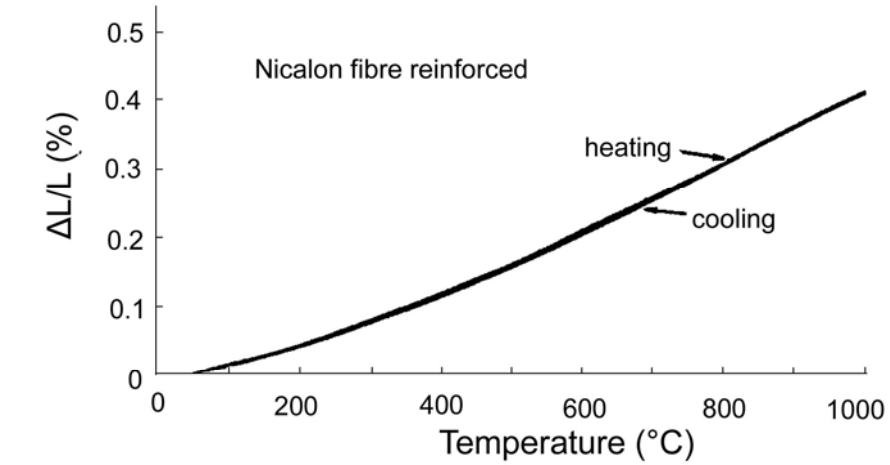

C: Nicalon Fibre Composite

Figure 84.7-1 - Expansion and contraction behaviour of SiC matrix composites with different reinforcing fibres

84.7.2 Glass matrix composites

Combining carbon fibres with a glass matrix can give low CTE composites, because the modulus of the carbon fibres dominates the lower modulus glass; as shown in Table 84.7.2.

Table 84.7-2 - CTE: Carbon fibre-reinforced borosilicate GMC

Graphite fibre reinforced borosilicate matrix composite			
Composite type	**Fibre vol.%**	**CTE at 22°C to 150°C ($x10^{-6}$ °C^{-1})**	
		Longitudinal	**Transverse**
GY-70/7740	60	- 0.29	+ 7.6
HMS/7740	60	- 1.0	+ 3.6
T-300/7740	60	+ 0.38	+ 4.3

Unidirectional graphite fibre reinforced borosilicate matrix composite				
Fibre type	**Fibre elastic modulus (GPa)**	**Fibre vol.%**	**CTE at 22°C ($x10^{-6}$ °C^{-1})**	
			0°	**90°**
Thornel 300	234	54	- 0.10	+ 4.6
HM	350	70	- 0.50	+ 6.5
P-100	654	50	- 1.0	+ 4.4
Celion 6000 (chopped)	234	30	+ 1.7	+ 1.7 (+ 4.2)
Borosilicate glass	-	0	+ 3.25	+ 3.25

84.7.3 Environmental factors

CMC materials are being considered for highly dimensionally stable structures owing to their stability with respect to a wide range of factors, [See also: 52.7]. Such structures are normally made of CFRP, as they do not function at very high temperatures.

Given that CMCs received a pre-assembly heat treatment to stabilise their microstructure, CMCs do not suffer from moisture absorption, moisture expansion, outgassing or LEO degradation as do polymer composites.

84.8 References

84.8.1 General

[84-1] Yong-Ching Chen & G.S. Daehn
'The Thermal Cycling Deformation of a Particle Reinforced Metal Matrix Composite: Comparison Between a Model and Experimental Observations'
Scripta Metallurgica et Materialia, Vol.25, p1543-1548, 1991

[84-2] S.M. Pickard & B. Derby
'The Deformation of Particle Reinforced Metal Matrix Composites during Temperature Cycling'
Acta metall. mater, Vol. 38, No. 12, p2537-2552, 1990

[84-3] X.C. Liu & C. Bathias
'Creep Damage of Al2O3/Al Alloy Composites'
Proceedings of ECCM6, Bordeaux, Sept 1993
ISBN 1-85573-142-8, p525-532

[84-4] J.A.G. Furness & T.W. Clyne
'The Application of Scanning Laser Extensometry to explore Thermal Cycling Creep of Metal Matrix Composites'
Materials Science and Engineering, A141 (1991), p199-207

[84-5] T. Imai et al
'High Strain Rate Superplasticity of AlN and TiC Particulate Reinforced Aluminium Alloys'
Proceedings of ECCM6, Bordeaux, Sept 1993
ISBN 1-85573-142-8, p533-538

[84-6] M. Khobaib & L. Zawada
'Tensile and Creep Behaviour of a Silicon Carbide Fiber-Reinforced Aluminosilicate Composite'
Ceram. Eng. Sci. Proc. 12[7-8], p1537-1555 (1991)

[84-7] J.L. Bobet et al
'Thermal Residual Stress Field on Continuous Fibre-reinforced Ceramic Matrix Composites: Analytical model and Experimental Measurements'
Proceedings of HT-CMC1, Bordeaux, Sept 1993
ISBN 1-85573-143-6, p515-522

[84-8] M. Koenig
'Shape Distortion and Residual Stresses in High Temperature Ceramic Matrix Composite Shells'
Proceedings of HT-CMC1, Bordeaux, Sept 1993
ISBN 1-85573-143-6, p607-614

[84-9] J.W. Holmes & J.l. Chermant
'Creep Behaviour of Fiber-reinforced Ceramic Matrix Composites'
Proceedings of HT-CMC1, Bordeaux, Sept 1993
ISBN 1-85573-143-6, p633-648

[84-10] D. Kervadec & J.L. Chermant
'Visco-elastic Deformation during Creep of 1D-SiC/MLAS Composite'
Proceedings of HT-CMC1, Bordeaux, Sept 1993
ISBN 1-85573-143-6, p649-658

[84-11] M. Taya & R.J. Arsenault
'Metal Matrix Composites: Thermomechanical Behaviour'
Pergamon Press, ISBN 0-08-036983-9, 1989

[84-12] R.K. Everett & P.L. Higby
'Expansivity of Diboride-Particulate Aluminium Composites'
Scripta METALLURGICA et MATERIALIA, Vol.25, p625-630, 1991

[84-13] A.J. Eckel & R.C. Bradt
'Thermal Expansion of Laminated, Woven, Continuous Ceramic Fiber/Chemical-Vapor-Infiltrated Silicon Carbide Matrix Composites'
J. Am. Ceram. Soc., 73 {5} p1334-1338 (1990)

85 High-temperature environmental stability

85.1 Introduction

Most applications of high-temperature materials involve their operation in aggressive environments. The presence of chemically aggressive species can reduce material integrity when operating close to their thermal limits in terms of microstructural stability. Corrosion and oxidation are chemical reactions that affect a material. Some of those deleterious reactions that can occur to materials used in space programmes are described. Important factors relevant to overall environmental stability include:

- residual stresses within materials can promote corrosion and cracking,
- interfaces are areas particularly prone to chemical action, e.g. stress-corrosion cracking at grain boundaries in alloys; attack of the fibre-matrix interface in MMC and CMC materials.
- aggressive species can permeate through materials, e.g. hydrogen and oxygen,
- cracks and porosity provide easy pathways for access by aggressive species,
- aggressive species can be both liquid and gaseous,
- fuel and airborne contaminants at high temperatures can be extremely corrosive, e.g. sodium and sulphur atoms.

Allowances for potential environmental degradation are an essential part of fracture or integrity control evaluations of space structures and assemblies, Ref. [85-1].

85.2 Aqueous corrosion: Metals

85.2.1 General

Although it is not a high-temperature phenomenon, some general comments on the corrosion behaviour of some advanced metallic materials are given, Ref. [85-2], [85-3], [85-4], [85-5], [85-6]. The application conditions determine whether aqueous corrosion is a concern.

85.2.2 Aluminium-based composites

85.2.2.1 General

Corrosion studies have concluded that, Ref. [85-6]:

- various corrosion problems exist associated with:
  - galvanic coupling,
  - interfacial phases of high reactivity,

— micro-crevices,

— voids and porosity.

- potential corrosion problems depend on the reinforcement and the processing route.
- in general, aluminium composites are more susceptible to corrosive attack than the unreinforced matrix alloy, Ref. [85-4], [85-6].
- crevice corrosion is common in composites containing localised porosity or cracking.
- galvanic and 'active' reaction products are particularly acute in SiC and carbon fibre-reinforced composites.
- galvanic effect between carbon fibres and aluminium can be modified by a fibre coating, Ref. [85-3].
- pit density on Al/SiC composites is increased with respect to the base alloy, but pit penetration is less.
- anodising or the use of chemical conversion coatings improves the corrosion resistance of Al-based MMCs by reducing pit density.

85.2.2.2 Stress corrosion cracking

SCC behaviour is a very important factor in the selection of materials for space applications.

[See: ECSS-Q-70-71 for material and process selection]

[See: ECSS-Q-ST-70-36 and ECSS-Q-ST-70-37]

Aluminium alloys containing copper are particularly vulnerable to premature failure, as are certain Al-Li alloys, [See also: 46.7].

If the matrix alloys is known to be prone to SCC, then the MMC is normally treated with caution. Each is considered on its own merits for the intended applications, Ref. [85-5].

85.3 Hot corrosion: Metals

85.3.1 Applications

Hot corrosion is not usually a critical factor in space programmes, unless the vehicle is reusable and encounters conditions, such as:

- fuels containing trace elements, notably metal ions, which are aggressive species in the exhaust gases,
- atmospheres containing trace elements, e.g. salt laden air, which passes through a propulsion system or over hot leading edges.

85.3.2 Causes

Hot corrosion results primarily from the formation of low melting point phases that act as 'solvents' in attacking the base material. The phases are typically mixed oxides that form glasses.

The classic examples are:

- sodium sulphate (Na_2SO_4), and
- sodium chloride (NaCl).

85.3.3 Protection systems

Specific MCrAlY coatings exist for nickel-based alloys to combat hot corrosion, [See: 74.7].

[See also: Chapter 48 for coatings on superalloys]

85.4 Hot corrosion: CMC

85.4.1 Causes

The operating temperatures for ceramic composites are usually in excess of 1000°C. Hot corrosion is more active if aggressive species are present, Ref. [85-2], [85-7], as the range of glassy phases possible increases. Avoiding contaminating ions, such as sodium, is essential.

Factors to be aware of include:

- sodium oxide (Na_2O) reacts with protective SiO_2 enabling active oxidation at the interface between SiO_2 and SiC. This causes surface recession of SiC,
- moisture in hot gases dissolves boric oxide (B_2O_3) glazes, used as sealants in oxidation protection systems.

85.5 Oxidation: Metals

Immediate surface oxidation can, in most instances, be accepted. It can provide a barrier to further oxidation.

Oxidation becomes a significant problem when it breaches the outer layer and begins to penetrate the bulk of the material. This occurs when the outer oxide layer cracks and spalls. If a protective coating or barrier is penetrated, then failure occurs as the protective layer is consumed or broken down.

Stable oxide formation as a barrier to further oxygen ingress is an important aim in material composition and selection. The formation of stable oxides is often a function of secondary alloying additions, Ref. [85-8].

[See also: Chapter 47 for oxidation protection of Ti-alloys; Chapter 48 for Superalloys]

85.6 Oxidation: Ceramics

85.6.1 Carbon-containing materials

All carbon-containing materials require protection from oxidation when used at high temperatures.

85.6.2 SiC-SiC composites

Even supposedly oxidation-resistant materials experience some degradation. This is particularly true of SiC composites, where the microstructure provides access for oxygen through porosity, microcracking and at fibre-matrix interfaces.

If sufficient internal surfaces are converted from SiC to SiO_2 then the composite looses integrity, Ref. [85-9].

The combined effects of oxidation and thermal excursions are shown in Figure 85.6.1 and Figure 85.6.2 for SiC composites with different fibres, Ref. [85-9].

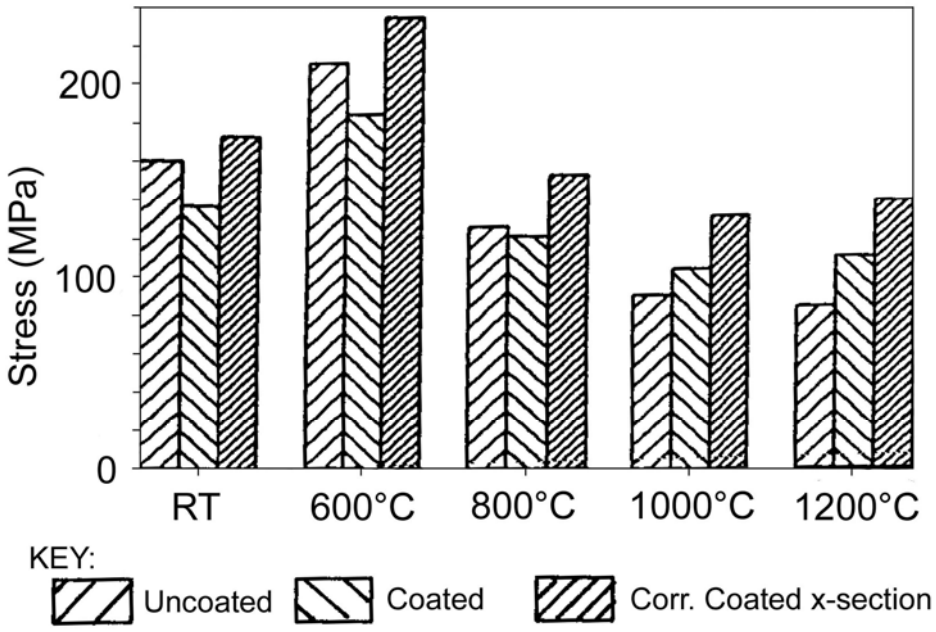

Figure 85.6-1- Oxidation: Effect of test temperature on fracture stress of coated and uncoated SiC-SiC

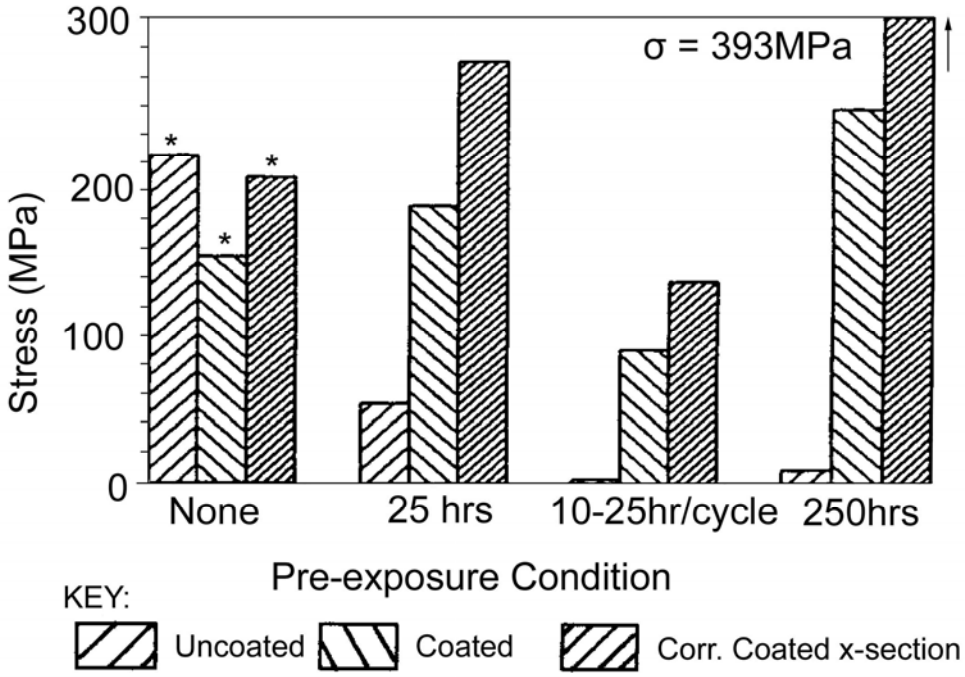

Figure 85.6-2 - Oxidation: Effect of pre-exposure in air at 1000°C on fracture stress of coated and uncoated SiC-SiC

85.6.3 Chemical reactions

The solid-gas reactions that can occur are, Ref. [85-10]:

$$C_{(s)[fibre,\ interface]} + O_{2(g)} \rightarrow CO,\ CO_{2(g)}$$

$$SiC_{(s)[fibre,\ matrix]} + 2O_{2(g)} \rightarrow SiO_{2(s)} + CO_{2(g)}$$

$$SiOxCy_{(s)[fibre]} + (1 + y - 0.5x)O_{2(g)} \rightarrow SiO2_{(s)} + yCO_{2(g)}$$

85.6.4 Effect of conditions

Crack propagation occurs faster with higher oxygen concentrations, Ref. [85-11]. A short preliminary heat treatment in air may be used to establish the initial surface oxide layer, Ref. [85-12], [85-13].

Thin sections are far more vulnerable to oxidation than thicker ones. Any penetration of the outer 50µm to 100µm protective layer has serious consequences for laminates 1mm to 2mm thick compared with 10mm or 20mm sections.

Once the bulk of the composite is attacked, serious strength and integrity reductions occur. That said, provided that the thermal limits of SiC fibres are not exceeded, e.g. 1200°C, a natural sealing mechanism occurs once all the surface SiC is converted to silica and a volumetric change in the material occurs, Ref. [85-9].

85.6.5 Effect of manufacturing route

The oxidation behaviour of composites vary with the manufacturing route used, e.g. C-SiC and SiC-SiC composites made by CVI, resin pyrolysis or liquid siliconising, Ref. [85-15].

85.6.6 Modelling

Oxidation kinetics for ceramic composites have been modelled, with respect to, Ref. [85-14]:

- oxygen partial pressures,
- oxidation rates,
- crack opening,
- crack sealing with formed silica,
- exposure time,
- effects of applied load.

85.7 Hydrogen embrittlement

85.7.1 General

Hydrogen embrittlement is a problem usually encountered by metals working in an environment containing hydrogen, Ref. [85-16].

The different forms of hydrogen embrittlement (HE) are:

- Hydrogen Environment Embrittlement, (HEE),
- Internal Hydrogen Embrittlement, (IHE),
- Hydrogen Reaction Embrittlement, (HRE).

[See also: Chapter 47 for Titanium alloys; Chapter 48 for Superalloys]

85.7.2 Metal-based materials

HEE is primarily encountered in hydrogen-containing, fluid systems, i.e. relevant for vehicles with LH/LOX propulsion systems.

IHE results from the absorption of hydrogen into the metal microstructure.

The use of titanium-based materials is high in spaceplanes concepts, although the greater part of the structure is either storing, conveying or combusting hydrogen, as shown in Figure 85.7.1, Ref. [85-17].

Compatibility of titanium composites and alloys with hydrogen environments is crucial and a sound understanding of material behaviour should be known, Ref. [85-18].

[See also: 85.8 for Ti-based alloys and MMCs; 85.9 for Ti-based intermetallics]

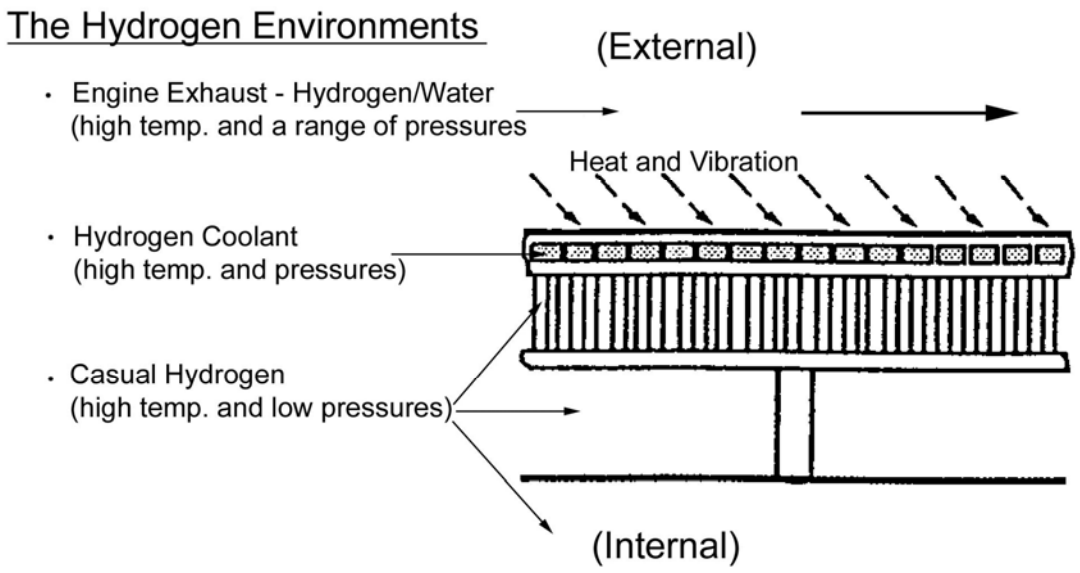

Figure 85.7-1 - Hydrogen on an actively cooled structure

85.7.3 Ceramic-based materials

The effects of hydrogen in high-temperature environments on ceramic composites are not usually studied. However, the evaluation of any possible undesirable reactive effects is necessary for ceramics used in spaceplanes concepts with hydrogen fuels.

HRE is the greatest concern with carbon-containing composites, [See: 85.10].

85.7.4 Precautions

85.7.4.1 General

Precautions can be undertaken to minimise the effects of hydrogen depending on the alloy and environment, Ref. [85-1].

85.7.4.2 Hydrogen environment embrittlement

HEE is applicable to superalloys, Ti-alloys, low-alloy steels and stainless steels.

Restrictions that usually apply include:

- neither low-alloy steels nor titanium alloys are used for the containment of liquid or gaseous hydrogen,
- aluminium alloys are used for hydrogen-containing pressure vessels.

Compatibility of hydrogen with superalloys and stainless steel remains a concern, [See also: 48.7 for superalloys]

85.7.4.3 Internal hydrogen embrittlement

- titanium alloys: IHE can be controlled by stress relieving welds and avoiding local differences in composition in relation to weld material and base alloy.

- low-alloy steels: The risk of IHE is reduced by restricting the strength levels, stress relief and baking after electroplating with aluminium.

85.8 Hydrogen: Titanium materials

85.8.1 General

The effect of hydrogen on titanium-based materials is dependent on, Ref. [85-17]:

- presence and proportions of α and β phases,
- temperature,
- concentration and pressure of hydrogen in the gaseous phase.

[See also: Chapter 47 for titanium alloys; Chapter 49 for intermetallics]

85.8.2 Alloys

Studies in the USA concluded that no titanium-based alloy or aluminide can be used in a hydrogen-containing environment at high temperatures without the potential of a brittle titanium hydride phase forming. The main conclusions were:

- α-phase titanium and the α-2 (Ti_3Al) intermetallic appear the most susceptible to hydride formation, even under low vapour pressures,
- titanium hydride can form in β-phase titanium, but only after significant hydrogen is absorbed into the β lattice.
- single phase, β-alloys rapidly absorb sufficient hydrogen to form brittle titanium hydride in a moderate to high-pressure hydrogen environment at elevated temperatures,
- in low-pressure casual hydrogen environments (~5 Torr), titanium hydride can form, but the hydrogen transport reactions are considerably slower. β-alloys could therefore be used with a hydrogen barrier coating.

Figure 85.8.1 shows the response of β-processed Ti-1100 to a 50Torr hydrogen environment, Ref. [85-17].

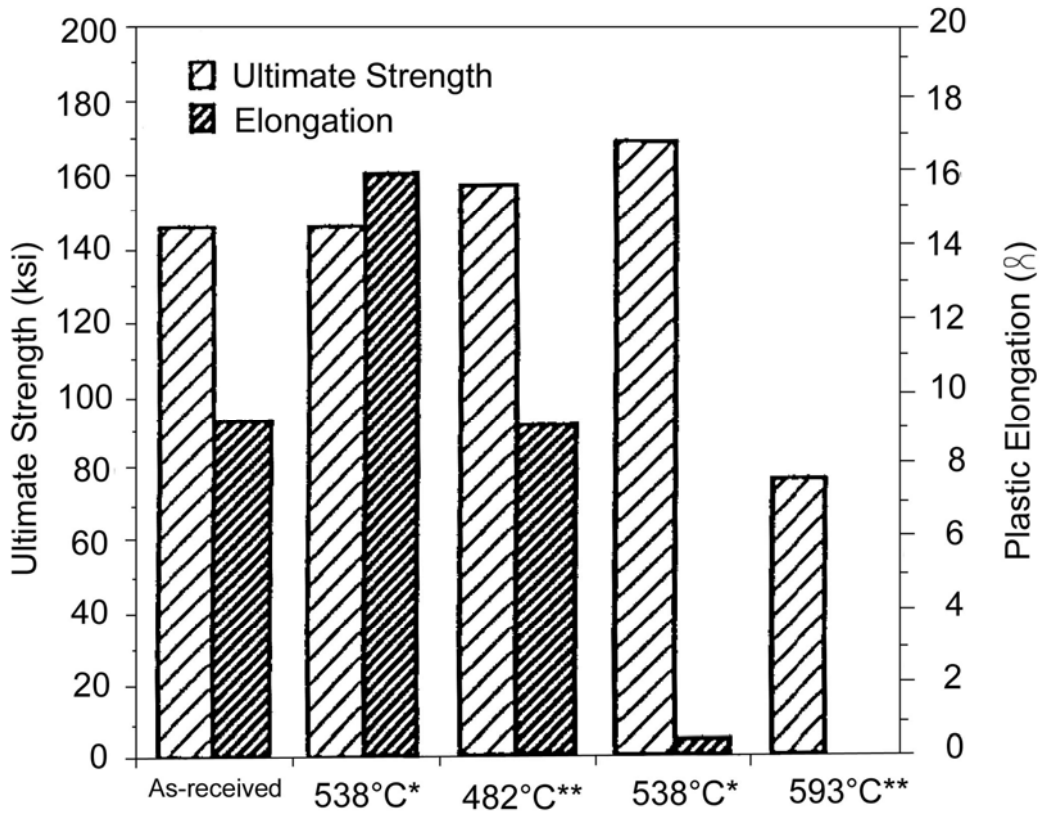

Key ß-processed Ti-110 (Ti-6Al-3Sn-4Zr-0.4Mo-0.4Si) exposed to vacuum and 50 Torr hydrogen environment at various temperatures. Tensile tested at RT, in air.

* Ultra-high vacuum ** 50 Torr Hydrogen

Figure 85.8-1 - Effect of hydrogen on mechanical properties of Ti-alloy Ti-1100

85.8.3 MMC

The β-alloys Ti-15-3-3-3 or TIMETAL® 21S (Beta 21S, Ti-15Mo-3Nb-3Al) used extensively as matrices in TMCs do not perform satisfactorily in hydrogen environments, Ref. [85-19].

[See also: Chapter 47 for titanium alloys; 47.8 for effects of hydrogen]

85.9 Hydrogen: Intermetallic materials

85.9.1 Titanium aluminides

The two basic generic types of TiAls are:

- ordered hexagonal close packed Ti3Al (α2)
- ordered face centred cubic tetragonal TiAl(γ)

The ordered crystal structures confer elevated strength, but reduced low ambient temperature ductility. This can be improved by microalloying with Nb, [See: Chapter 49].

In either alloy or composite form, intermetallics are proposed for NASP, so hydrogen embrittlement is of acute concern, Ref. [48-20], [85-21], [85-22].

Figure 85.9.1 shows the high-temperature, hydrogen activity for some titanium aluminide materials, Ref. [85-22].

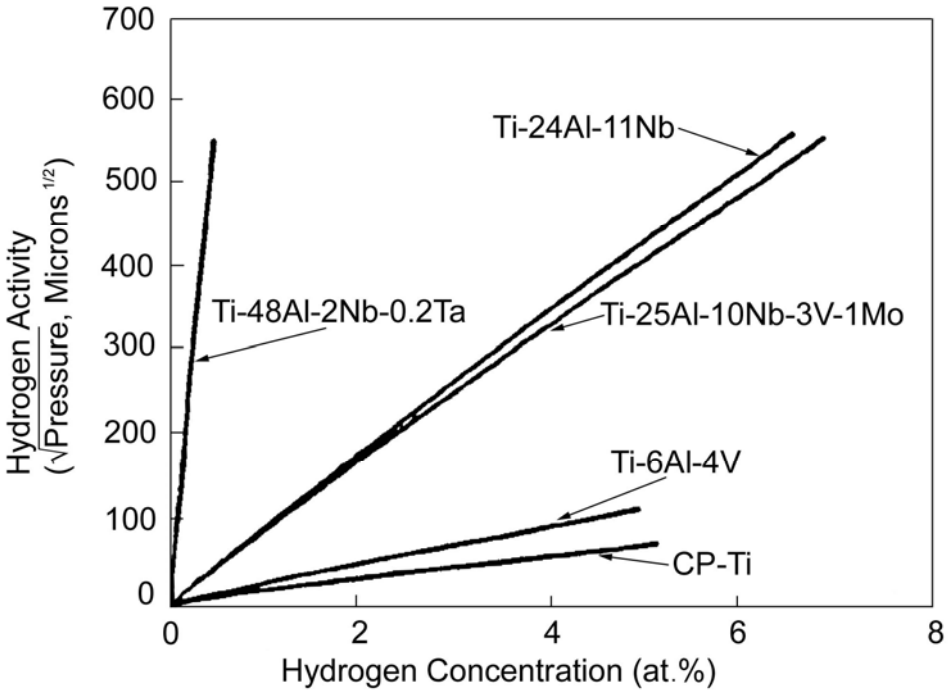

Figure 85.9-1 - Hydrogen activity in certain Ti-alloys at 800°C

Figure 85.9.2 shows that TiAl absorbs less hydrogen than Ti_3Al or the β-phase, Ref. [85-21].

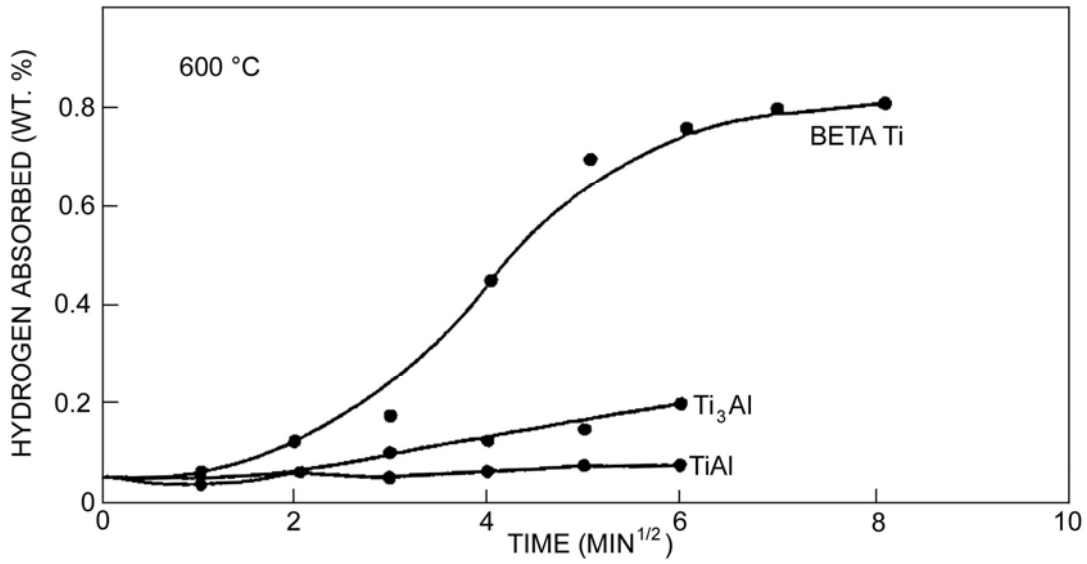

Figure 85.9-2 - Hydrogen absorption in beta titanium alloys and Ti-aluminides

The effect of absorbed hydrogen on intermetallics and their mechanical properties is not yet fully investigated, but some loss of strength and ductility occurs. Typical test conditions are 600°C to 800°C in a hydrogen atmosphere at 13.8MPa to 34.5MPa.

Data suggest that embrittlement is much reduced at 600°C. This however negates the main justification for using aluminides, which are intended to increase operating temperatures into the 800°C to 1000°C range. It remains to be seen whether sufficient confidence can be gained in this class of material to justify its use in high-temperature hydrogen environments.

85.10 Hydrogen: Carbon composites

Under the right conditions, carbon composites can be reduced by hydrogen to form methane and other hydrocarbons, Ref. [85-21].

The effect can be complicated by the presence of oxidation protection coatings and inhibitors.

Serious property reductions can only occur in high pressure, high-temperature hydrogen environments when the chemical reactions are possible.

85.11 References

85.11.1 General

[85-1] R.J.H. Wanhill
'Spacecraft Sustained Load Fracture Control'
Proceedings of International Conference : Spacecraft Structures & Mechanical Testing, ESTEC, 24-26 April 1991, ESA SP-321 Vol.2, p543-549. Also NLR Report TP 89163 U
ESA Contract AO/2-1162 NL/PH

[85-2] R.H. Jones et al
'Overview: Environmental Effects on Advanced Materials'

Journal of Metals, December 1988, p18-30

[85-3] M.A. Buonanno et al
'Corrosion of Graphite Aluminium Metal Matrix Composite'
Environmental Effects on Advanced Materials. The Minerals Metals & Materials Society, 1991, p267-282

[85-4] P.P. Trzaskoma
'Localised Corrosion of Metal Matrix Composites'
Environmental Effects on Advanced Materials. The Minerals Metals & Materials Society, 1991, p249-265

[85-5] R.H. Jones
'Stress Corrosion Cracking of Metal Matrix Composites'
Environmental Effects on Advanced Materials. The Minerals Metals & Materials Society, 1991, p283-296

[85-6] A. Turnball
'Review of Corrosion Studies on Aluminium Metal Matrix Composites'
British Corrosion Journal, Vol.27, No.1, p27-35

[85-7] V. Scott et al
'High Temperature Corrosion of Glass-ceramic Composites'
Proceedings of HT-CMC1, Bordeaux, Sept 1993
ISBN 1-85573-143-6, p691-698

[85-8] 'Oxidation Characteristics of Ti-25Al-10Nb-3V-1Mo Intermetallic Alloy'
NASA Technical Paper 3044, December 1990

[85-9] D.A. Woodford et al
'Effect of Test Temperature, Oxygen Attack, Thermal Transients and Protective Coatings on Tensile Strength of Silicon Carbide Matrix Composites'
Ceramic Engineering and Science Proceedings, Sept-Oct, 1992 Vol 13, No.9-10, p752-759

[85-10] C. Vix-Guterl et al
'Reactivity in Oxygen of a Thermostructural Composite'
Proceedings of HT-CMC1, Bordeaux, Sept 1993
ISBN 1-85573-143-6, p725-734

[85-11] R. Jones & C. Henager
'Effects of Oxygen on the Sub critical Crack Growth of SiC/SiC Composites'
Proceedings of HT-CMC1, Bordeaux, Sept 1993
ISBN 1-85573-143-6, p667-674

[85-12] P. Pluvinage et al
'High Temperature Behaviour of 2D and 3D Braided SiC/SiC Composites'
Proceedings of HT-CMC1, Bordeaux, Sept 1993
ISBN 1-85573-143-6, p675-682

[85-13] M. Li & F. Guiu
'Effect of Heat Treatment on Mechanical Properties and Microstructure of a Glass-coated SiC/SiC Composite'
Proceedings of HT-CMC1, Bordeaux, Sept 1993
ISBN 1-85573-143-6, p683-690

[85-14] J.M. Jouin et al
'Oxidation Kinetics Modelling of a 2D Woven Carbon Fibre Silicon Carbide Matrix Composite'
Proceedings of HT-CMC1, Bordeaux, Sept 1993

ISBN 1-85573-143-6, p707-714

[85-15] P. Schanz & W. Krenkel
'Description of the Mechanical and Thermal Behaviour of Liquid Siliconised C/C'
Proceedings of HT-CMC1, Bordeaux, Sept 1993
ISBN 1-85573-143-6, p715-724

[85-16] H.G. Nelson
'Hydrogen and Advanced Aerospace Materials'
SAMPE Quarterly, Volume 20, No. 1, Oct 1988, p20-23

[85-17] H.G. Nelson
'Hydrogen Environment Effects on Advanced Alloys and Composites in Aerospace Structures'
Proceedings of the 1st Thermal Structures and Materials for High-Speed Flight, 13-15 Nov 1990, p383-399

[85-18] L.G. Fritzmeier et al
'Hydrogen Embrittlement Research: A Rocketdyne Overview'
Hydrogen Effects on Material Behaviour. The Minerals, Metals & Materials Society, 1990, p941-954

[85-19] G.A. Young Jr & J.R. Scully
'Effects of Hydrogen on the Mechanical Properties of a Ti-Mo-Nb-Al Alloy'
Scripta METALLURGICA et MATERIALIA, Vol. 28, p507-512, 1993

[85-20] D. Eliezer et al
'The Effects of Hydrogen on Titanium Aluminides'
JoM, 43, (3), p59-62, Mar 1991

[85-21] R.D. Kane et al
'Evaluation of Titanium Aluminide and Carbon Carbon Composite Materials for Hydrogen Gas Service'
Environmental Effects on Advanced Materials. The Minerals Metals & Materials Society, 1991, p35-46

[85-22] D. Eliezer et al
'Effect of Hydrogen on Behaviour of the Intermetallic Titanium-Aluminides'
SAMPE Quarterly, Vol. 22, No. 4, July 1991, p29-35

86 High-temperature test facilities

86.1 Introduction

It is necessary to test a design under the expected service conditions. This presents additional problems for structures made of high-temperature materials, because reproducing the operating conditions can be both technically complicated and very costly.

The test facility and instrumentation should withstand high temperatures and provide data on the behaviour of the test structure. For spaceplanes, such as Hermes, re-entry conditions comprising of high heat fluxes are needed to generate re-entry surface temperatures of 1800°C.

Some of the more difficult test conditions to generate and control are:

- high gas temperatures,
- high heat fluxes, which can reach 10MW/m^2,
- oxidising conditions,
- high gas velocities,
- acoustic loading, up to 168dB.

In some cases it is not possible to fully reproduce all the operating conditions simultaneously; a series of partial tests are carried out to gain confidence on specific factors relating to structural integrity.

The heat energy source used in test facilities is important, as it determines the size of test structure and how representative the test is of the application. Heat sources include:

- gas burners, for large areas, Ref. [86-1],
- quartz lamps, for medium sized areas, Ref.[86-2], [86-3], [86-4], [86-5],
- high intensity infra-red (IR) heaters, Ref.[85-6],
- lasers, for small areas, Ref.[85-7],
- arc jets, Ref.[85-8], [85-9], [85-10],
- arc lamps, Ref.[85-11],
- graphite heaters, Ref. [85-11].

Facilities with high electrical power consumption are often more expensive than testing by fuel-burning.

Quartz lamps are popular for inducing surface temperatures up to 1000°C with good control of heating parameters. They are less durable when high-velocity gases or acoustic loadings are involved. The use of gas fuels prevails for temperatures beyond 1000°C and larger test panels. For very high heat fluxes, arc jets are appropriate. Such facilities are very expensive if large areas are tested.

Emphasis is placed on European organisations with expertise in high temperature testing, [See: Chapter 89] and some of their test facilities are described.

86.2 Thermo-mechanical loading

86.2.1 General

The combined effects of applied mechanical and thermal loads are more serious than the loads applied singly or in sequence, [See: Chapter 83].

It is usual for a design to go through a sequence of evaluations, culminating in a limited number of tests that are designed to provide the final level of confidence in the structure, Ref. [86-2] to [86-6], [86-9] to [85-17].

86.2.2 Spaceplane verification

86.2.2.1 General

A suitable sequence for a verification programme on spaceplane designs is described.

86.2.2.2 Material allowable

Residual properties after representative periods of thermal exposure require:

- isothermal strength data,
- mechanical fatigue life data,
- TMF data,
- performance in oxidative environments.

86.2.2.3 Component performance

- Acoustic fatigue resistance,
- Isothermal static loading,
- thermal shock.

86.2.2.4 Verification of structural design

- thermo-acoustic testing, with or without applied mechanical load, [See also: 86.3].
- thermo-mechanical loading at a constant temperature enables the evaluation of a single component or subassembly and comparison with the performance predicted. Of particular interest are:
  - deflections under load,
  - failure or fracture events,
  - expansion behaviour.

86.2.3 Test facilities

IABG (Germany) have a range of hot structure testing facilities based on IR-heater systems, Ref. [86-6]. These can typically generate flux intensities of 1MW/m² and surface temperatures up to 1700°C. The facilities are designed to test specific structural configurations, i.e. TPS shingles, wing-leading edges and winglet box-sections. The largest facility has a diameter of 4m and a length of 5m; capable of handling the Hermes Winglet Box (4000 mm x 600 mm x 200 mm).

DLR (Stuttgart) and Aerospatiale (Aquitaine), Ref. [86-14], have facilities capable of thermo-mechanical loading of panel sections.

86.3 Thermo-acoustic testing

86.3.1 General

Exposed surfaces and panels on all spaceplane configurations undergo high energy thermo-acoustic fatigue, particularly on aerodynamic leading surfaces and in the vicinity of propulsion units, Ref. [86-17].

The test facilities provide thermal and acoustic loadings simultaneously. This can be achieved by generating dynamic pressure fluctuations in a high-temperature gas flow, Ref. [86-1].

86.3.2 Test facilities

The Thermal Acoustic Fatigue Apparatus (TAFA) at NASA Langley Research Center has been used for testing 300mm x 300mm panels up to 650°C. The total power input from 12 quartz lamps is 30kW, Ref. [86-17].

IABG (Ottobrunn, Germany) has a combined thermal-mechanical loading facility using a methane-oxygen flame to heat a 1m x 1m area located in a progressive wave tube. This is suitable for testing TPS sections.

86.4 Plasma arc jet tests

86.4.1 General

Plasma arc-jets are used to reproduce a range of high temperatures and various oxygen partial pressures, Ref. [86-18].

86.4.2 Test facilities

- IRS (University of Stuttgart): 1200°C to 1700°C at 60 to 200mb oxygen.
- SIMOUN (Aerospatiale, Aquitaine): 800°C to 1200°C at 5 to 30mb oxygen. Test panels: 300mm x 300mm, Ref. [86-8].

  Capable of reproducing conditions representative of the Hermes nose cap at stagnation point.
- NASA Ames (USA): 60MW arc jet facility.

86.5 Electric arc jet tests

86.5.1 General

Electric arc heating in wind tunnels has been applied to the assessment of TPS for the Buran vehicle, Ref. [86-9].

86.5.2 Test facilities

At various ex-Soviet facilities, sections up to 800mm x 800mm x 800mm can be tested in air or nitrogen for up to 2000 seconds. New equipment uses a high-frequency plasmatron to inductively heat the gas, Ref. [86-9], [86-10].

Supersonic gas velocities, to Mach 2.5, can be achieved for up to 100 minutes. Power consumption is 1 MW.

86.6 Oxygen-hydrogen combustors

For advanced propulsion systems using mixtures of hydrogen and oxygen fuel, test facility design can incorporate evaluation of materials as part of a combuster, Ref. [86-13].

The materials can be retained in the hot gas stream and tested for a selected period of firing.

Other fuels can also be substituted, as appropriate, Ref. [86-13].

86.7 European facilities

86.7.1 General

European facilities are summarised for the testing of materials, components or structures at high temperatures.

86.7.2 France

86.7.2.1 Aerospatiale Aquitaine (Bordeaux)

With expertise in CMC and C-C composites technology, their test facilities include:

- SIMOUN plasma jet test facility,
- isothermal test facility for loaded panels,
- high-temperature mechanical testing for characterising ceramic composites,
- non-destructive test techniques for high-temperature composites.

86.7.2.2 ONERA

- BLOX laser enhanced oxidation facility for material characterisation.

86.7.2.3 SEP

- High-temperature mechanical testing for characterising ceramic-based composites.

86.7.2.4 SNECMA

- High-temperature mechanical testing for characterising ceramic-based composites.

86.7.3 Germany

86.7.3.1 IABG (Ottobrunn)

IABG have expertise and facilities in structural testing, including, Ref. [86-1], [86-6]:

- high-temperature acoustic test facility for panels,
- dedicated isothermal facilities for loaded structural elements, e.g.
  - TPS shingles,
  - wing leading edges,
  - box sections,
  - winglets, and
  - ailerons.

86.7.3.2 DLR (Stuttgart)

Specialists in the application of high-temperature materials, including:

- high-temperature mechanical testing for characterising ceramic-based composites,
- isothermal test facility for loaded panels.

86.7.3.3 IRS (University of Stuttgart)

High-temperature plasma facility for evaluating materials.

86.7.3.4 MAN Technologie GmbH (Munich)

High-temperature mechanical testing for characterising ceramic-based composites.

86.7.4 Switzerland

86.7.4.1 Battelle Europe (Geneva)

Contract organisation with facilities for testing materials, including, Ref. [86-15]:

- hot graphite source for high-heat-flux testing of materials,
- mechanical testing of titanium materials

86.7.5 Austria

86.7.5.1 ÖFS/ARC (Seibersdorf)

Austrian Research Centre with materials testing capabilities for, Ref. [86-16]:

- measurement of thermal diffusivity and conductivity with specific heat capacity for high-temperature materials,
- low cycle fatigue and mechanical property measurement up to 1100°C.

86.7.6 UK

86.7.6.1 Rolls Royce (Bristol)

A gas turbine engine manufacturer, with high-temperature mechanical testing for characterising ceramic composites.

86.7.7 The Netherlands

86.7.7.1 JRC Petten

CEC research centre has facilities for characterising high-temperature materials, including:

- high-temperature mechanical testing for superalloys, ceramics and ceramic-based composites.

86.7.7.2 Stork Product Engineering (Amsterdam)

Test firing of propulsion system components, Ref. [86-13].

86.7.8 Belgium

86.7.8.1 University of Leuven

Measurement of surface catalyticity for high-temperature materials.

86.7.9 Russia

86.7.9.1 Tsniimash (Kaliningrad)

Central Research Institute of Machine-Building (Moscow Region). Development of high-temperature test facilities as part of Russian space programmes, including:

- arc-jet wind tunnels,
- high-frequency plasmatrons.

86.8 References

86.8.1 General

[86-1] G. Bayerdörfer
'Development of a Thermoacoustic Test Facility'
Proceedings of the International Conference: 'Spacecraft Structures and Mechanical Testing', ESTEC, 19-21 October 1988. ESA SP-289, p407-412

[86-2] J.V. Anselmo & L.O. Kretz
'Hypervelocity Technology Carbon-Carbon Testing'
Seventh SEM Conference on Structural Testing Technology at High Temperatures, p38-45

[86-3] R.C. Thompson & W.L. Richards
'Thermal-Structural Panel Buckling Tests'
Seventh SEM Conference on Structural Testing Technology at High Temperatures, p46

[86-4] D. Hart
'Thermal Life-Cycle Testing of a Titanium Matrix Composite'
Seventh SEM Conference on Structural Testing Technology at High Temperatures, p47-49

[86-5] W.L. Richards & R.C. Thompson
'Titanium Honeycomb Panel Testing'
Seventh SEM Conference on Structural Testing Technology at High Temperatures, p50

[86-6] K.K.O. Bär & W.W. Jarzab: IABG
'Qualification Testing of Thermal Protection Systems Test Technologies and their Applications'
First ESA/ESTEC Workshop on Thermal Protection Systems ESTEC, Noordwijk, 5-7 May 1993, ESA-WPP-053 (August 1993) p356-362

[86-7] C.M. Banas
'Laser Thermal Simulation puts Jet Engines to the Test'
Photonics Spectra, April 1992, p88-92

[86-8] P. Charpentier
'SIMOUN - un nouveau moyen d'essais pour le developpement des protections thermiques d'Hermes'
ESA Symposium on Space Applications of Advanced Structural Materials, March 1990, ESA SP-303, p419-425

[86-9] N.A. Anfimov & V.B. Knotko: Tsniimash
'Testing and Verification of Re-entry Vehicle Thermal Protection'
First ESA/ESTEC Workshop on Thermal Protection Systems ESTEC, Noordwijk, 5-7 May 1993, ESA-WPP-053 (August 1993) p350-355

[86-10] A.N. Gordeev, A.F. Kolesnikov & M.I. Yakushin
'An Induction Plasma Application to Buran's Heat Protection Tiles Ground Tests: Part I'
SAMPE Journal Vol.28, No.3, May/June 1992, p29-33

[86-11] T.P. Sikora & K.B. Lefer
'Simulation of High Heat Flux Levels with Graphite Heating and Arc Lamps'
Seventh SEM Conference on Structural Testing Technology at High Temperatures, p3-8

[86-12] A. Ajarrista & C. Petiau: Dassault Aviation
'Verification and Acceptance of Thermal Protection Systems'
First ESA/ESTEC Workshop on Thermal Protection Systems, ESTEC, Noordwijk, 5-7 May 1993, ESA-WPP-053 (August 1993) p341-349

[86-13] S.R. Birjimohan et al: Stork Product Engineering
'Verification on a High Temperature Vitiator'
First ESA/ESTEC Workshop on Thermal Protection Systems ESTEC, Noordwijk, 5-7 May 1993, ESA-WPP-053 (August 1993) p363-368

[86-14] J.M. Bouilly & D. Guerrir: Aerospatiale
'Entry Testing of AQ60 for Huygens'
First ESA/ESTEC Workshop on Thermal Protection Systems ESTEC, Noordwijk, 5-7 May 1993, ESA-WPP-053 (August 1993) p369-381

[86-15] M. Kornmann & D. Richon: Battelle Europe
'A Simple Rig for Thermal Tests of TPS in Realistic Atmosphere'

First ESA/ESTEC Workshop on Thermal Protection Systems ESTEC, Noordwijk, 5-7 May 1993,
ESA-WPP-053 (August 1993), p388-391

[86-16] E. Semerad et al: ÖFS/ARC
'Programme of Material Assessment Relevant for Thermal Protection Systems'
First ESA/ESTEC Workshop on Thermal Protection Systems ESTEC, Noordwijk, 5-7 May 1993,.
ESA-WPP-053 (August 1993), p392-398

[86-17] J.D. Leatherwood et al: NASA Langley
'Acoustic Testing of High Temperature Panels'
AIAA-90-3939-CP

[86-18] G. Bernhardt
'Materials for Hermes Hot Structural Parts: Requirements and Testing'
ESA Symposium on Space Applications of Advanced Structural Materials, March 1990,
ESA SP-303, p411-418

87 Integrated manufacturing

87.1 Introduction

New manufacturing techniques were developed with the advent of advanced metallic and ceramic-based materials. Many of these aim to produce near-net shape items to avoid the obvious problems of machining and finishing inherently complex materials containing hard, brittle phases.

As manufacturing methods significantly influence the final material properties, an integrated material and process development programme is necessary.

87.2 Process development

87.2.1 Techniques

Some manufacturing techniques have evolved from those used in more traditional metal or ceramic processing, including:

- powder metallurgy techniques, [See: 88.3].
- diffusion bonding, [See: 88.8].
- hot pressing, [See: 88.9].
- hot isostatic pressing (HIP), [See: 88.5].
- sintering, [See: 88.4].
- slip (slurry) casting, [See: 88.17].

Others are adapted from polymer composite technology, notably those associated with, [See also: Chapter 38]:

- fibre placement, and
- lay-up.

87.2.2 Status

Some manufacturing techniques have reached commercial use, e.g. for motor vehicles. Others have been optimised and used to produce demonstration aerospace parts for evaluation. Many have shown feasibility in the laboratory, but require further development to be scaled up for production, [See: Chapter 88].

87.2.3 Expertise

Many of the processes used are capital intensive and can be slow, e.g. matrix deposition and infiltration processes, when compared with traditional processing methods.

As a consequence, centres of expertise have evolved across the world. These companies tend to offer a complete service from design to the supply of the finished items.

A listing of the expertise of some major European organisations is included for guidance, [See: Chapter 89].

87.3 Stages in manufacture

87.3.1 Process techniques

In general, composite manufacturing techniques can be considered in the four stages summarised in Figure 87.3.1.

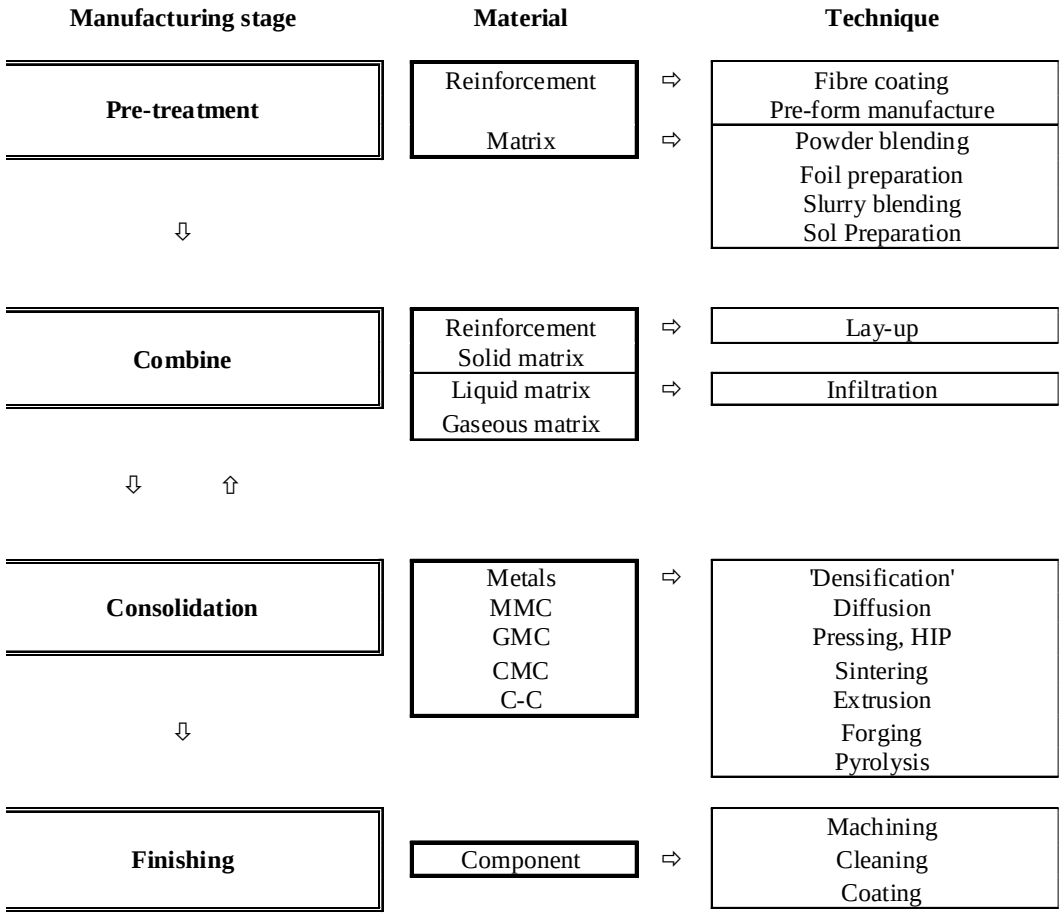

Figure 87.3-1 - Typical manufacturing sequence for advanced metal and ceramic-based materials

In order to achieve acceptable materials in terms of both mechanical and environmental resistance characteristics, it can be necessary to repeat the 'Combine' and 'Consolidation' steps. 'Infiltration' processes are often repeated.

87.3.2 Finishing

On completion of the manufacture, the component can require minor machining operations. These are minimised wherever possible, and are not always necessary for net-shape parts.

[See: 56.7 for guidance on machining]

87.3.3 Surface protection and coatings

Depending on the intended use, modification of the components' surface by additional chemical, physical or coating processes can be necessary.

Certain metals and carbon-based (C-C) composites require coatings to enable them to resist the intended aggressive service environments. The materials used can be metallic or ceramic, or mixtures and multi-layers of both.

[See: Chapter 74 - Protective coatings]

88 Manufacturing techniques

88.1 Introduction

This chapter provides a basic description of the manufacturing techniques used in the production of metal and ceramic-based composite materials and coatings applied to them. In many cases more than one process method is used. This is especially true of components made to near-net shape.

Techniques evolved from the more traditional material processing industries but were adapted to limit undesirable chemical reactions reducing composite properties. Publications tend to describe modifications to the basic methods. There are numerous techniques applied to composites.

88.2 Composite manufacture

88.2.1 Matrix phase

88.2.1.1 General

Table 88.02.1 summarises the various manufacturing techniques developed to produce acceptable quality, advanced metallic and ceramic-based materials. They can be broadly grouped by the state of the matrix phase for processing, i.e.:

- solid,
- liquid (viscous), or
- gaseous.

88.2.1.2 Solid matrix

Several techniques are available for combining a solid matrix with a reinforcing phase. The advantages of using a solid matrix are that it:

- avoids the need to melt very high temperature materials,
- can be used for materials otherwise impossible to process,
- can reduce the degradation of the reinforcement by a molten matrix.

88.2.1.3 Liquid matrix

Numerous, well-established, methods exist to process materials in a liquid or viscous state. Most are described in detail in many publications, and are not repeated here. Within this chapter emphasis is placed on composite manufacture.

For composites manufacture, the matrix liquid may be either a:

- melt,
- colloidal dispersion (slurry), or
- solution (Sol-Gel).

Table 88.2-1 - Typical manufacturing techniques for advanced metallic and ceramic-based materials

Matrix state	Technique	Material systems							
		Metal	Composites					Coatings	
			MMC	GMC	GCMC	CMC	C-C	Metal	Ceramic
Solid	Powder processing	✪	✪	✪	✪	✪		✪	✪
	Sintering	✪	✪	✪	✪	✪		✪	✪
	Hot isostatic pressing (HIP)	✪	✪	✪	✪	✪		✪	✪
	Foil and fibre consolidation		✪						
	Superplastic forming (SPF)	✪	✪						
	Diffusion bonding	✪	✪						
	Diffusion coatings							✪	✪
	Reaction bonding		✪	✪	✪	✪			
Liquid	Polymer/pitch infiltration and pyrolysis					✪	✪		
	Melt infiltration: • Squeeze casting • Pressure infiltration casting • Liquid pressure forming • Matrix transfer moulding		✪ ✪ ✪ ✪	✪ ✪	✪ ✪	✪			
	Sol-gel			✪	✪	✪			
	Slurry infiltration		✪	✪	✪	✪			
	In-situ oxidation: • Lanxide™ process		✪			✪ ✪	✪		✪
	In-situ siliconising					✪	✪		
	Investment casting	✪	✪						
	Plasma spraying	✪	✪					✪	✪
Gaseous	Physical vapour deposition (PVD)		✪					✪	✪
	Chemical vapour deposition (CVD)			✪	✪	✪	✪	✪	✪
	Chemical vapour infiltration (CVI)		✪			✪	✪		

The objective for slurry and sol-gel processes is to reduce detrimental reinforcement and matrix interactions, possible when using materials in the reactive molten state. They also avoid the need to process at the high-melting point of ceramics.

Some methods allow (near) net-shape component manufacture in one process, whereas others require a densification process after combining matrix and reinforcement. In some cases, further infiltration is needed prior to final consolidation. The complexity of the process depends largely on which materials are being combined, together with the geometry and size of the required component.

88.2.1.4 Gaseous matrix

Deposition of materials from the vapour phase has long been a part of coating technology, where a component acts as the deposition substrate. Depending on the substrate material, a subsequent heat-treatment is often required to recover the properties after high-temperature coating deposition.

For near-net shape composite manufacture, a porous preform of reinforcement acts as the receptor; allowing the gradual build-up of matrix material in the interstices. In general, all vapour phase processes are conducted at elevated temperature and are slow in comparison with solid or liquid phase processing routes. Chemical Vapour Infiltration (CVI) is an established technique for the manufacture of Carbon and SiC-based composite components, [See: Chapter 89 for European centres of expertise].

With the aim of reducing the long process times of vapour-phase processing, modified techniques using thermal gradients and forced gas-flow are possible for thicker-section components. Vapour-phase processing may also be combined with other methods of manufacture; e.g. fibre preforms initially rigidised by CVI and subsequently melt infiltrated.

88.2.2 Reinforcement

88.2.2.1 General

The reinforcing phases can be either:

- particulate,
- short fibre (whisker), or
- continuous fibres or filaments.

88.2.2.2 Pretreatment

In general, pretreatment of reinforcements should be performed prior to combining with the matrix; e.g. coatings, preform manufacture.

88.2.3 Processing

A single technique can be appropriate for a part or all of the manufacture of one or a number of material types, although the precise process conditions vary for each.

For composites, the manufacturing process aims to minimise those reactions between matrix and reinforcement that are detrimental to overall composite properties. In general, these are accelerated at high processing temperatures and protracted processing times. Likewise, processes using high pressures, or excessive mechanical working, can damage reinforcements. Processing parameters require thorough optimisation to reduce all these property-reducing effects.

It is not uncommon for more than one technique to be used to manufacture an acceptable material or component; e.g. slurry infiltration followed by reaction bonding or hot pressing, initial CVI of preform followed by liquid matrix infiltration. Combining methods is intended to increase production rates without adverse affect on material performance.

88.3 Powder processing

88.3.1 Metals

The preparation of metals by powder metallurgy techniques is well established and has become part of the standard processing of temperature-resistant alloys, including:

- superalloys,
- oxide dispersion strengthened (ODS) alloys, and
- intermetallics, e.g. aluminides.

Figure 88.3.1 summarises the processing routes available by powder metallurgy, Ref. [88-1].

Consolidation of materials prepared by the powder route are numerous, and include many traditional material processing techniques, e.g. extrusion, forging.

88.3.2 MMC

The powder route is appropriate for particle and short fibre reinforcements in metal matrices, where they are added at the powder blending stage. However, the process is limited in that only low volume fractions of reinforcements are possible.

Damage to reinforcements, notably short fibres, can be caused by the mechanical working involved. In general, alignment of short reinforcement fibres is possible only during consolidation by extrusion, forging or rolling processes.

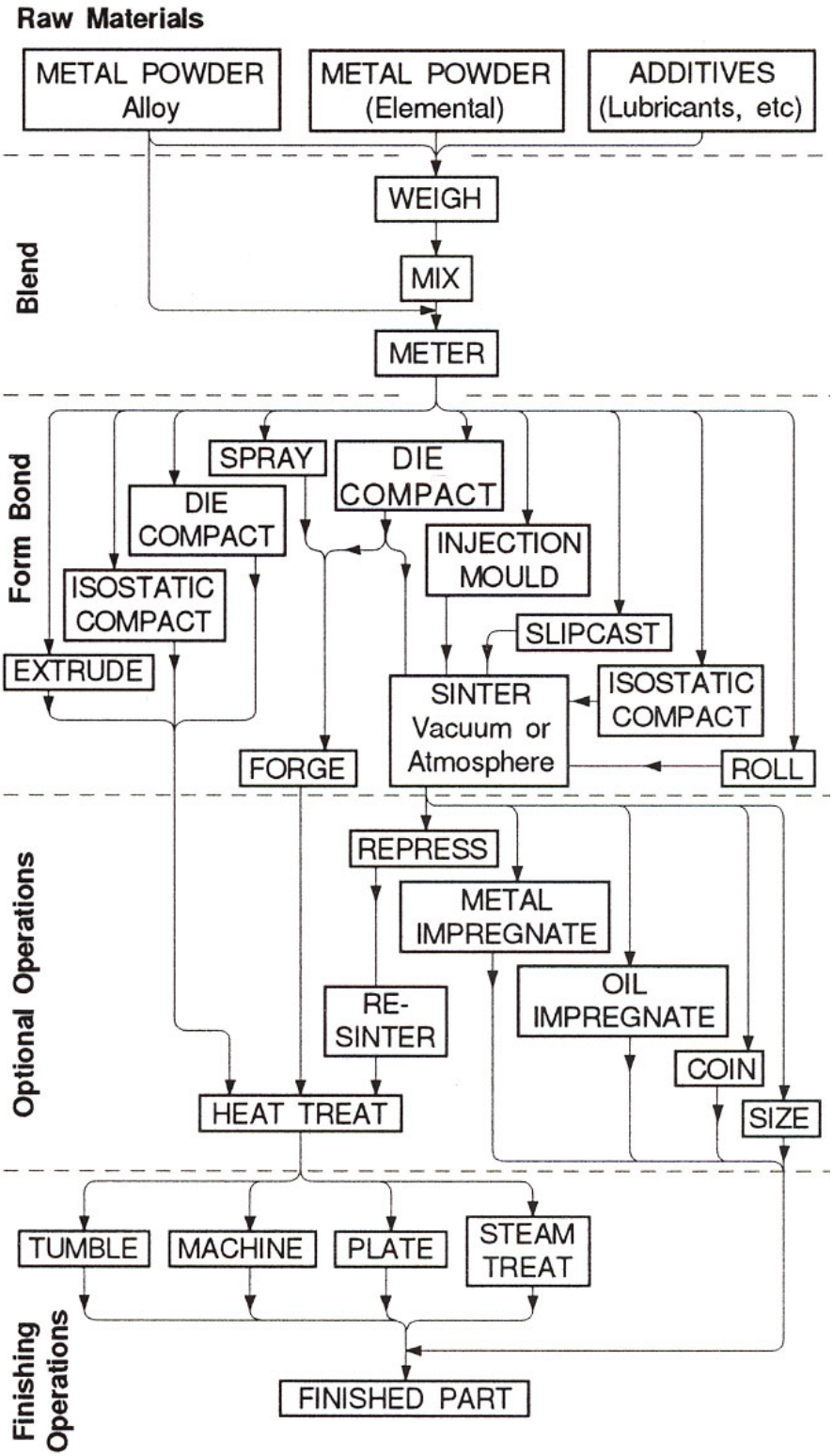

Figure 88.3-1 - Powder metallurgy processing methods

88.4 Sintering

This is a recognised technique for the consolidation of both metal and ceramic-based materials prepared by a powder route.

It relies on a 'low melting point' constituent (relative to the others) which, when heated, melts and reacts with the adjacent material. No pressure is required, although the furnace atmosphere is often controlled to be non-oxidising.

The resulting consolidated material can approach full theoretical density, although it can also be used to deliberately produce less dense materials, e.g. bearings, where the porous structure can subsequently be infiltrated with a lubricant.

88.5 Hot isostatic pressing (HIP)

HIP is now an established method for the consolidation of a variety of materials, both metal and ceramic, either as part of the manufacture (consolidation) or as a corrective measure to close porosity or other undesirable features in components produced by non-powder routes; e.g. castings.

Materials are processed at very high pressures at the selected process temperature in the HIP pressure vessel - a limiting factor on the size of components. The resulting consolidated materials reach full theoretical density.

Materials which benefit from mechanical working to improve their microstructure, and hence final material properties, do not always reach the optimum when processed by HIP. The lack of mechanical working, however, does mean that damage to particulate or whisker reinforcements is limited.

88.6 Foil and fibre consolidation

88.6.1 General

This technique is appropriate for the manufacture of both sheet materials and complex components, as shown in Figure 88.6.1, Ref. [88-3].

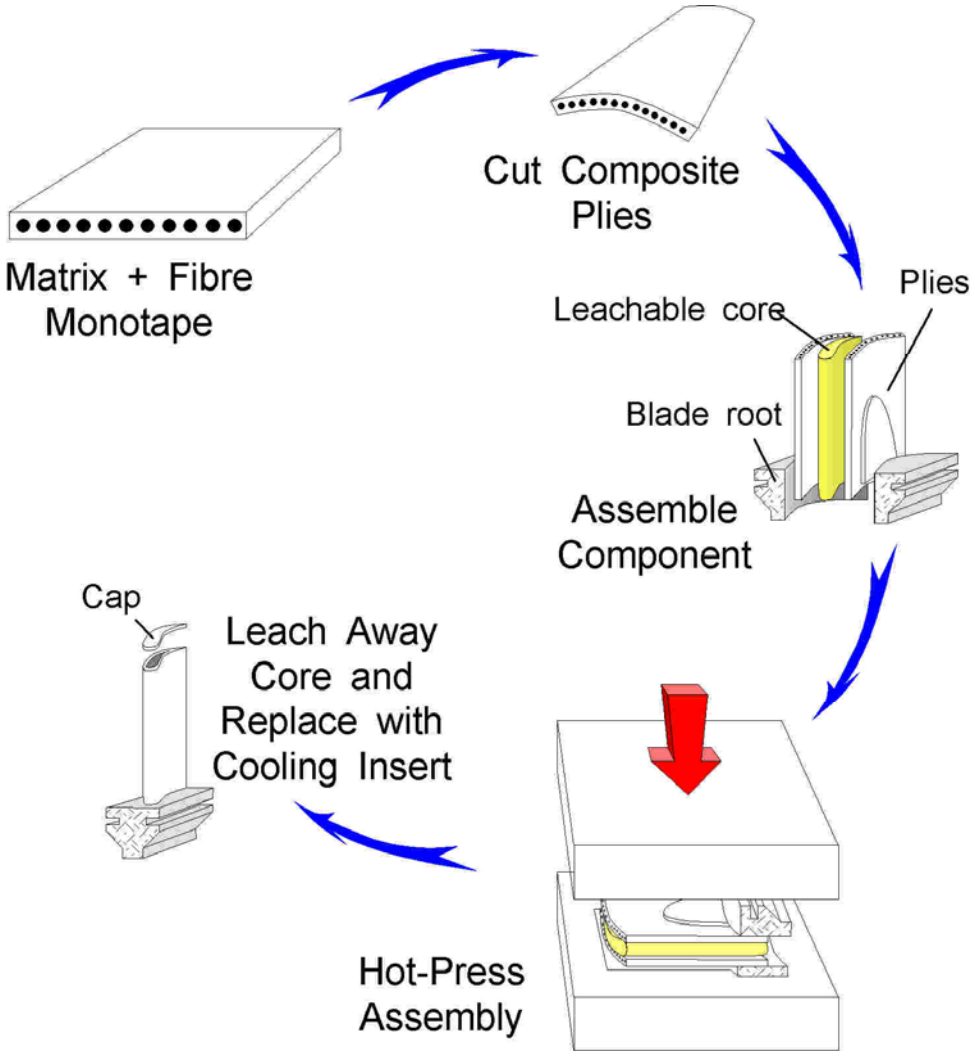

Figure 88.6-1 - Metal foil and fibre compaction

88.6.2 Metal foils

Unidirectional fibres, often pre-coated, are laid-up in the required orientation between thin sheets of metal (matrix). The matrix is usually in the form of thin rolled foils (several microns thick).

88.6.3 Powder cloth

For metals which cannot be rolled successfully, e.g. intermetallics, then 'Powder Cloths' can be considered, Ref. [88-3].

The process, shown in Figure 88.6.2, was developed by NASA for aluminide powders. The completed lay-up is consolidated by hot pressing, during which the matrix softens and diffusion bonding occurs.

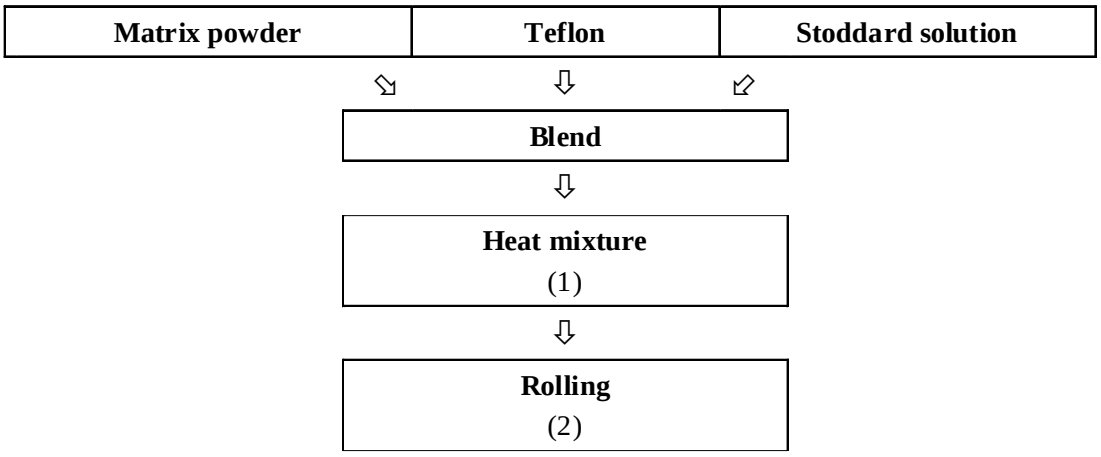

Key: **(1)** To remove excess Stoddard solution
(2) To required thickness

Figure 88.6-2 - Powder cloth manufacture

88.7 Superplastic forming (SPF)

88.7.1 Metal characteristics

Metals are said to be superplastic when they are capable of plastic deformations in the range of 100% to 1500% without fracture, whilst under relatively low forming stresses. Superplastic implies that a material has certain characteristics and is processed in a particular way, i.e.:

- correct metal microstructure: Grain size 1 to 5 mm, stable at the temperature of deformation.
- forming temperature at least 50 % of the absolute melting temperature (K).
- slow strain rate, e.g. 0.01/min.

Several groups of metal alloys are capable of a superplastic response. The commercially available alloys, include Ref. [88-1]:

- Al-alloys, [See: Chapter 46]: 8090 Al-Li alloy, Ref. [88-4].
- Ti-alloys, [See: Chapter 47 and 47.4]:
  - Ti 1100
  - IMI 829, Ref. [88-4].

[See also: Chapter 72 for SPF/DB titanium designs]

88.7.2 Techniques

Examples of SPF techniques are summarised in Table 88.7.1, Ref. [88-1].

Table 88.7-1 - Superplastic forming processes

Process	Method	Advantages	Applications
Sheet thermo-forming	Clamped, heated sheet is forced into contact with a male or female mould by differential pneumatic pressure.	Lower tooling costs than pressing or stamping. 3-D curved with or without re-entrant forms.	Dished cups and box shapes. Corrugated and Waffle shapes.
Blow moulding	A heated hollow material (cup or tube) is subjected to an internal pressure which forces the material in contact with the mould.	Intricate shapes with thin walls.	Hollow shapes. Vacuum chambers and pressure vessels.
Die-less drawing	Bar, tube or section is passed through an induction coil. Tension applied causes 'necking down' in the hot region. Coil is then moved along material to reduce zones successively.	Materials difficult to deform are reduced by this method.	Reduced sections.
Forging : Gatorizing (1)	Conventional forming, but using superplastic material. Lower ram speeds.	Materials difficult to work. Reduced machining costs. Powder metals used.	Complex functional and structural components, e.g. integral blade & turbine discs.

Key: (1) Developed by Pratt & Whitney

A combined SPF/DB blow moulding process for a three-layer sandwich, aerospace structural panel is shown in Figure 88.7.1, Ref. [88-4].

[See also: Chapter 72 for SPF/DB titanium designs]

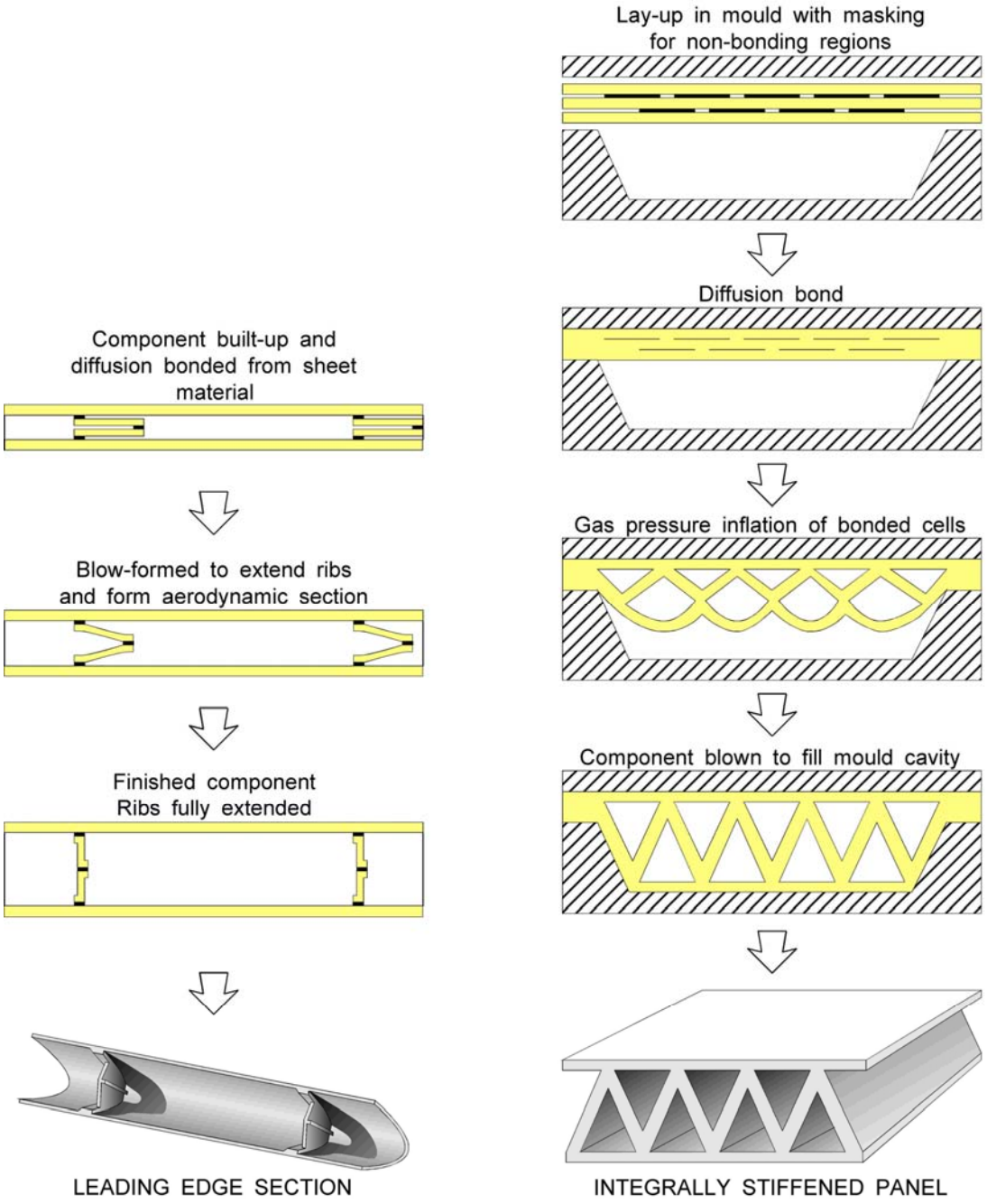

Figure 88.7-1 - SPF/DB blow moulding process

88.8 Diffusion bonding (DB)

Two, or more, materials are placed in intimate contact, heated to below the melting temperature and pressure applied for a pre-determined time. Diffusion occurs across the boundary forming an 'integral' joint. An intermediate layer (interlayer) of a different material can be required. [See: Chapter 60 - Fusion Joints].

Diffusion bonding is used in the 'Hot pressing' consolidation of MMCs and is often combined with superplastic forming techniques. This allows complex metal structures to be formed and joined in one operation, [See: Chapter 72 - SPF/DB Titanium designs].

A successful bond relies on:

- contacting surfaces: clean and in good contact,
- control of temperature: below the lowest melting point constituent,
- control of pressure: to maintain contacting surfaces, but without excessively deforming the softened materials or damaging the reinforcement phase,
- control of time: based on diffusion kinetics between the various materials.

For complex structures made by SPF/DB techniques, 'stopping-off' compounds are applied to some areas to prevent diffusion bonding occurring and forming unwanted joints. Such areas can then form expanded cells by superplastic pressurisation.

[See also: Figure 72.2.1, Figure 72.2.2 and Figure 72.2.3]

88.9 Hot pressing

88.9.1 MMC

[See: 88.8 Diffusion bonding]

88.9.2 Glass and ceramic-based composites

The matrix phase is in a viscous state during hot pressing. Process temperature varies for the particular matrix, but is generally in the range 1000°C to 1400°C. Typically, pressures of 3.5 to 14 MPa are applied to ensure proper consolidation, i.e. approaching 100% dense structures, Ref. [88-5].

Process parameters are selected to minimise detrimental reactions at the fibre-matrix interface.

88.10 Diffusion coatings

88.10.1 General

The basic principle is that described for diffusion bonding, [See: 88.8].

Several methods are available to improve the oxidation and corrosion resistance of alloys for high-temperature applications, e.g. the Superalloy family, [See: 48.10]. These aim to produce a coherent protective layer on the exposed surfaces of components.

Coatings are generally stable oxides or aluminides capable of resisting the service temperatures for a given period of use. Pack cementation is a recognised and widely used process for aero engine turbine blade assemblies, [See also: Chapter 74 - Protective coatings]

88.10.2 Pack cementation

The general principles of pack cementation are described in Table 88.10.1, Ref. [88-6].

Table 88.10-1 - General principles of pack cementation

Process principle	Comments
Components to be coated are buried in a pack in a sealed retort. Pack consists of: • Donor alloy • Halide activator • Inert oxide dilutent	Releases solute at known rate (Pack activity). Dissociates and transports solute material to avoid pack sintering.
Retort heated to process temperature.	900°C to 1050°C, typically, depending on desired coating.
Oxidation prevented by: • Inert gas • Hydrogen	Hydrogen used to reduce surface of carbon-containing alloys.
Two distinct process steps: 1. Solute elements transported by halide activator and brought into contact with component. 2. Solute diffuses into component surface forming a surface alloy or compound of different composition to substrate.	
Post-process heat treatment.	To recover component mechanical properties if pack cementation temperature degrades component condition (heat treatment).

88.10.3 Chromising

Process details of chromising is given in Table 88.10.2, Ref. [88-6].

Table 88.10-2 - Summary of chromising coating process

Process	Details	Comments
Typical pack composition	48Cr - 48 Al_2O_3 - 4NH_4Cl	-
Process temperature	850°C to 1050°C	-
Process gases	Dry Hydrogen Cracked Ammonia	Reduce chromium oxides formed. More uniform coatings result.
Process chemistry (1)	One of four reaction routes: $Fe(s) + CrX_2(g) \rightarrow FeX_2(g) + Cr(s)$ $CrX_2(g) \rightarrow X_2(g) + Cr(s)$ $CrX_2(g) + H_2(g) \rightarrow 2HX + Cr(s)$ $3CrX_2(g) \rightarrow 2CrX_3(g) + Cr(s)$	Interchange Thermal dissociation Reduction Disproportionation
Coating thickness	Initial period, then $Time^{½}$ dependency.	
Coating type	Surface rich in Cr which decreases with increasing depth to substrate alloy levels.	Typical coating on Fe-based alloy, Cr diffusion zone ~ 200µm.
Key: (1) X is a halide (activator)		

88.10.4 Aluminising

Process details of aluminising are given in Table 88.10.3, Ref. [88-6].

Table 88.10-3 - Summary of aluminising coating process

Process	High activity pack	Low activity pack
Typical pack composition	Bal Al_2O_3 - 1.2 to 2.7Al - 0.8 to 1.2 NaF	-
Time/ temperature	900°C/7hrs, typically.	1050°C/16hrs, typically.
Chemistry	$9AlX(g) + 4Ni(s) \rightarrow 2Ni_2Al_3(s) + 3AlX_3(g)$ + Al, in pack.	$3AlX(g) + 2Ni(s) \rightarrow 2NiAl(s) + AlX_3(g)$
Coating thickness (1)	30 to 100µm, typically.	30 to 100µm, typically.
Coating type	Three layer structure (2): Outer: Second phase particles (carbides). Middle: Dense precipitate free NiAl zone. Inner: Transition zone from substrate to NiAl layer.	Two layer structure (3): Outer: NiAl zone. Inner: Transition zone from substrate to NiAl layer.

Key:
(1) Deposition rate: $Time^{1/2}$ relationship.
(2) Depends on aluminide formed. Deposits evenly on free surfaces. For areas with reduced gas access - pulse carrier gas.
Inward diffusion of aluminium, giving outer layer of Ni_2Al_3. Requires heat treatment to convert to NiAl.
(3) Outward diffusion of Ni. External layer may have entrapped particles from the pack.

88.10.5 Selective oxidation

This process relies on the substrate alloy containing sufficient levels of Cr and Al to produce a stable oxide scale containing chromia or alumina when placed in an oxidising atmosphere. Cr and Al contents should be >16% and 10% respectively.

Factors associated with processing are summarised in Table 88.10.4, Ref. [88-6].

Table 88.10-4 - Factors associated with selective oxidation

Process details	Comments
Select oxidising atmosphere to promote formation of: Al_2O_3 Cr_2O_3	Refer to Ellingham-Richardson diagrams. Correct selection will inhibit formation of other oxides, providing Yttrium is not present in substrate for Al_2O_3 exclusive formation. Mn, Si and Ti oxides usually accompany Cr_2O_3 on commercial alloys (owing to their presence in the alloys at levels of 0.5% typically). This may affect the protective nature of the resulting oxide.
Pre-oxidising treatments, in: Air Other atmosphere	Oxide is less adherent unless Y is present to promote adhesion. Limit thermal cycling.
Oxidising temperature: > Service temp.	Temperature chosen also to promote rapid formation of layer.
Coating thickness:	1 to 5 μm, typically.

88.10.6 Modified native oxides

This process involves exposing the alloy substrate to the service environment after altering its surface composition, or by adding trace amounts of materials to the oxidising atmosphere. The resulting coating consists of scales modified to a more resistant type.

Process variables depend upon:

- substrate alloy composition,
- trace additions made,
- service environment.

Each combination of alloy and service environment are assessed on its own merits.

88.11 Reaction bonding

This process is very similar to sintering of powder materials, [See: 88.4].

The principle difference is that a 'reactive' elemental powder or a gas, is used in place of a low melting point constituent, e.g. the nitriding of Si to form Si_3N_4, Ref. [88-7], [88-8]. At the process temperature, the elements react to form a compound bridging adjacent constituents.

The technique is appropriate for metals and ceramics, but excessive porosity is possible when applied to ceramics with reinforcements present. In composite manufacture, it can be used in conjunction with other manufacturing processes, e.g. after slurry infiltration of a preform (RBSN), or aluminium metal infiltration to form an aluminide matrix, Ref. [88-9].

88.12 Polymer or pitch infiltration and pyrolysis

A standard CFRP composite or infiltrated preform is pyrolysed, under controlled conditions, to create a composite. 3-D or complex geometry shapes are possible.

Figure 88.12.1 illustrates the process when a standard CFRP precursor is used, Ref. [88-10]. The process is essentially the same when there is (repeated) infiltration and pyrolysis of a preform with polymer or pitch.

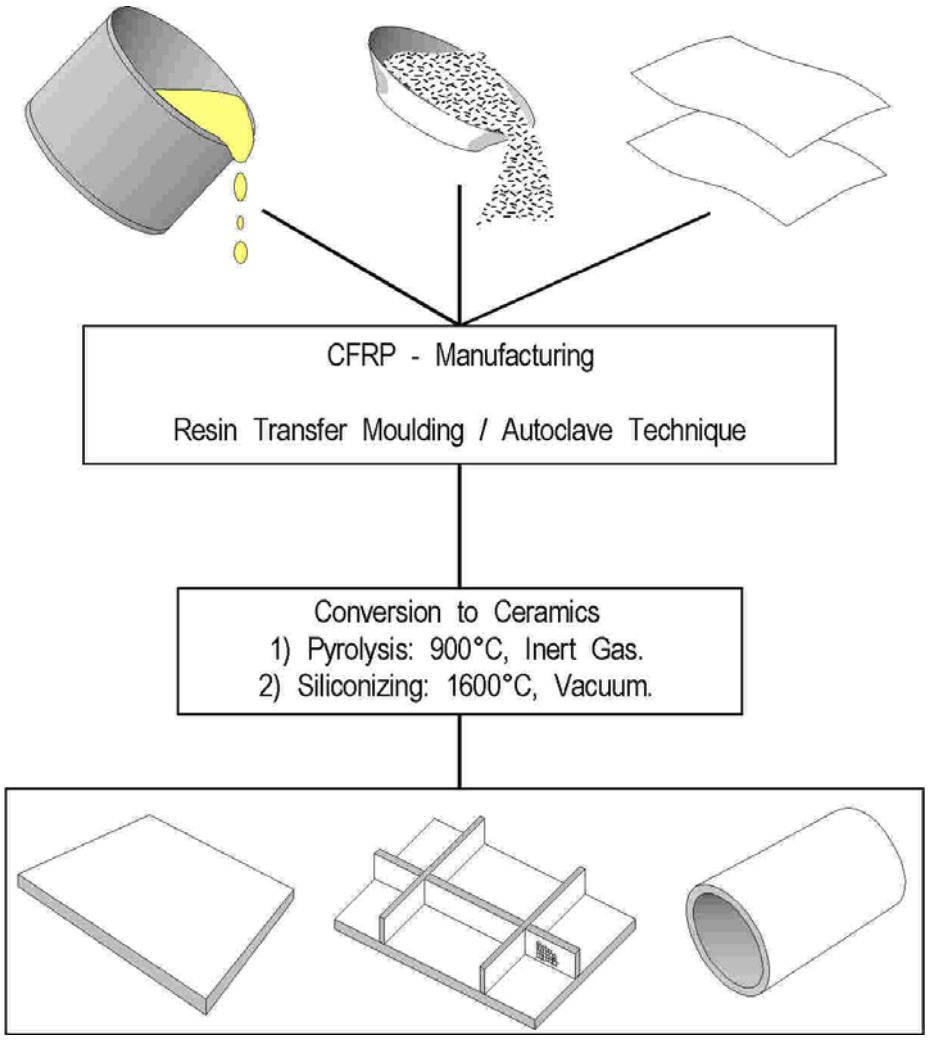

Figure 88.12-1 - Polymer infiltration and pyrolysis

The polymer can be a resin solution or in molten form for the infiltration stages. It can also contain additives, e.g. for oxidation protection. Infiltration and pyrolysis is normally repeated two or more times.

The matrix yield and type depends on the polymer formulation and the processing used. For C-C composites, phenolic, furfurylester, furan and epoxy resins are common. Siliconising treatments may be used to convert C to SiC, [See: 88.14].

The repeated infiltration and firing can reduce porosity to an acceptable level and fill shrinkage cracks or other undesirable features.

It is appropriate for the manufacture of thick-section components where vapour-phase techniques have limitations, [See: 88.22].

88.13 Melt infiltration

88.13.1 General

A molten matrix material is drawn into a reinforcement preform of either continuous or short fibres (whiskers) by capillary action. For some fibre-matrix combinations this is not possible without causing excessive degradation of the reinforcing phase, e.g. very reactive matrix or high temperatures to obtain acceptable matrix fluidity. However, it does allow more complex geometry or near-net shape parts to be manufactured, compared with those made by hot-pressing prepreg; it can require repeated infiltration and densification steps to ensure the resulting composite does not contain excessive porosity or cracks.

Numerous techniques have been developed to aid infiltration, by either positive pressure or vacuum.

88.13.2 Metal matrix

88.13.2.1 General

A very wide range of techniques have been developed to produce MMCs using liquid matrices; many are Patented. Figure 88.13.1 summarises some of the techniques, Ref. [88-11]. Most techniques have been applied to Al-alloys, with various types of reinforcements.

The primary objective is to obtain satisfactory densification of the preform without serious degradation to the reinforcement by the liquid metal. Reducing the melt temperature and process time factors can reduce infiltration, so, often, pressure or vacuum systems are added to assist.

88.13.2.2 Squeeze casting

This was the first method developed to produce near-net shape components. To avoid damage to the reinforcement by the high pressures used (70MPa, typically), variants based on the same principle were developed.

88.13.2.3 Pressure infiltration casting

There are several variants of this process which are conducted in a pressure vessel with the aim of increasing production rates, Ref. [88-12].

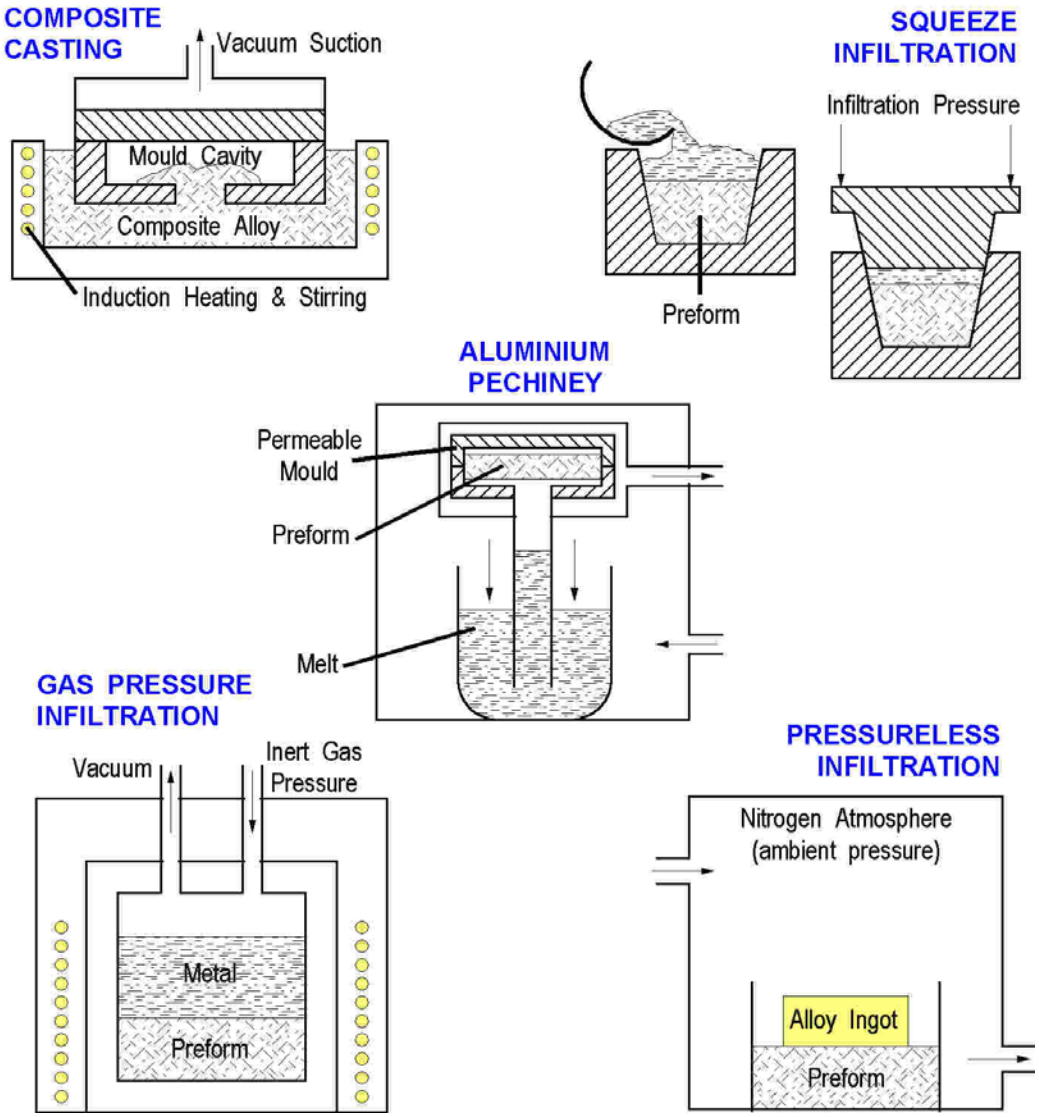

Figure 88.13-1 - MMC melt infiltration techniques

88.13.2.4 Liquid pressure forming

A development of low-pressure die casting, also conducted inside a pressure vessel. The various stages are shown in Figure 88.13.2, Ref. [88-13]. A means of restraining the reinforcement preform should be performed while the liquid metal enters the die. Process temperatures are selected depending on the:

- matrix alloy,
- reinforcement material, and
- preform type, e.g. particulate, short or continuous fibres.

Both preforms and die are pre-heated.

For aluminium alloys typical process conditions are:

- Matrix alloy temperature: 100°C to 200°C above melting,
- Pressure: 8MPa (80 bar), Ref. [88-13].

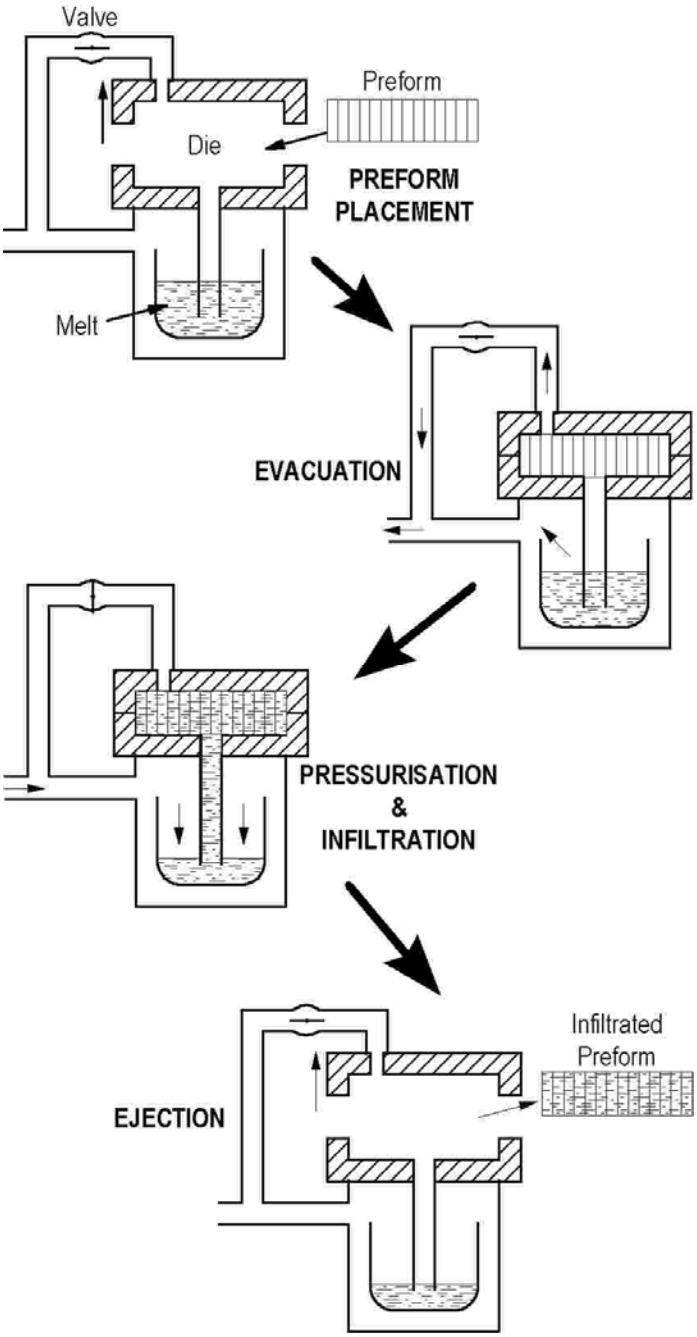

Figure 88.13-2 - Liquid pressure forming

88.13.3 Glass matrix

Molten glass is transferred to a mould containing a reinforcement preform. This technique is also known as 'Matrix Transfer Moulding'.

The major problem is that to achieve acceptable fluidity, the process temperature is substantially higher than that for hot pressing, so excessive fibre-matrix reactions can occur.

88.13.4 Ceramic matrix

It is an appropriate process for ceramics with a modest melting temperature. Process conditions aim to minimise periods at high temperature, which allow unacceptable levels of reinforcement degradation.

Table 88.13.1 gives examples of composites produced successfully by this method.

Table 88.13-1 - Ceramic melt infiltration

Matrix	Melting point (°C)	Reinforcement (fibre and whisker)
Si (amorphous)	1420	C SiC
$SrSiO_3$	1580	SiC
$CaSiO_3$	1540	SiC

88.14 In-situ siliconising

88.14.1 Molten

Molten silicon infiltrates a pre-heated, porous C-C material containing continuous fibres. At the process temperature, typically 1600°C in vacuum, the Si reacts with the carbon to form SiC.

The resultant material consists of a cracked carbon matrix protected by SiC interfaces with carbon fibre-reinforcement, Ref. [88-14]. The composite contains approximately one third SiC, which acts as an internal oxidation barrier in addition to any external coatings used.

Si infiltration is very rapid; several minutes typically. It is only one stage of the manufacturing process, but has demonstrated that, compared with gaseous infiltration techniques, it is faster for production of whole components, Ref. [88-14], [88-15].

88.14.2 Particulate

Other, similar, processes use a particulate SiC preform with added carbon to create SiC-SiC materials, Ref. [88-16] or carbon fibres which react with the Si melt to form SiC. This latter, whilst retaining a fibre-reinforced appearance under the microscope, has mechanical properties comparable to those of particle-reinforced material, Ref. [88-16].

Such materials are of interest only in high-temperature, modestly loaded, applications.

88.15 In-situ oxidation

88.15.1 MMC to ceramic oxide matrix

In-situ oxidisation starts with molten metal infiltration of a fibre preform. The molten matrix is then oxidised, creating a composite with a ceramic oxide matrix. It is most commonly applied to

aluminium. The resultant matrix phase is metallo-ceramic with free metal present. Severe reservations have been expressed in the use of such a material at high service temperatures.

The Lanxide™ process is an example of this technique and is shown schematically in Figure 88.15.1, Ref. [88-5].

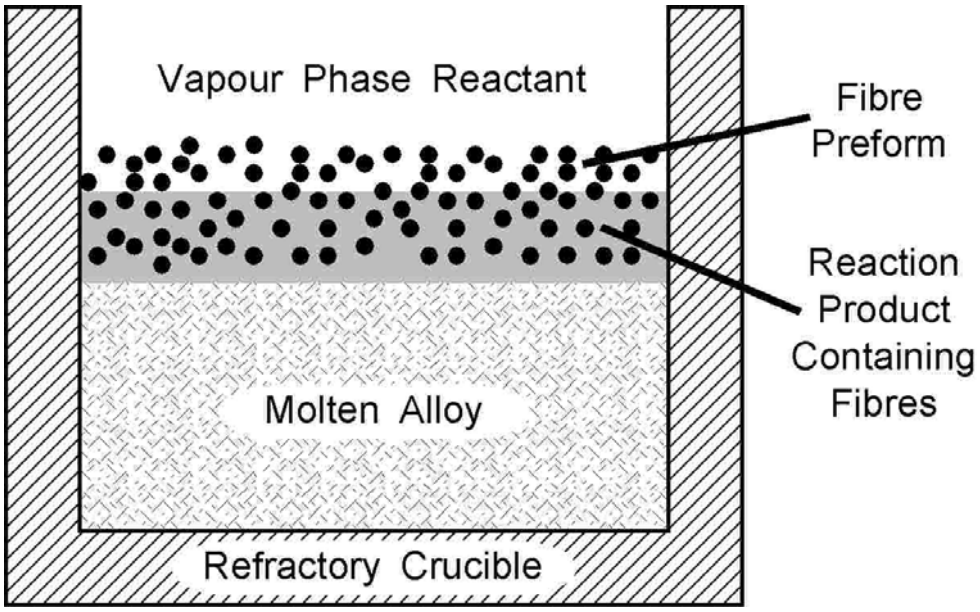

Figure 88.15-1 - In-situ oxidation: Lanxide™ process

Success relies on creating the proper surface energy balances to maintain a network of liquid phase within the reaction product to feed the outward growing interface. There are critical temperature ranges and alloy compositions which optimise the kinetics of oxide growth. Again, metal residue within the ceramic matrix is possible, but techniques for its removal have been developed, Ref. [88-5].

88.15.2 Oxide coatings on metals

[See: 88.10 - Diffusion coatings; Chapter 74 – Protective coatings]

88.15.3 Oxide coatings on ceramics

[See: 88.21 - Chemical vapour deposition; Chapter 74 – Protective coatings]

88.16 Sol-gel

Initially developed for unreinforced oxides, 'sol-gel' has also been applied to the manufacture of composites.

A chemical solution is formed, which can be converted into a gelled state. The solutions contain various:

- alkoxide compounds,
- catalysts,
- dissolved salts, and
- other additives.

A gel is formed from the solution by further hydrolysis and subsequent dehydration and polymerisation.

Table 88.16.1 summarises some 'sol-gel' chemistry for single and mixed oxides, Ref. [88-5].

Table 88.16-1 - Examples of sol-gel chemistry

Matrix	Precursor	Gelling process
SiO_2	Tetraethoxysilane (TEOS)	HCl catalyst in ethanolic solution.
TiO_2-SiO_2	TEOS + $Ti(OC_2H_5)_4$	Simultaneous hydrolysis HCl catalysed in ethanolic solution.
GeO_2-SiO_2	TEOS + tetraethoxygermane (TEOG)	HCl catalyst in ethanolic solution.
	TEOS + $GeCl_4$	Ethanolic solution without catalyst.
B_2O_3-SiO_2	TEOS + B_2O_3 hydr.	HCl catalyst in ethanolic solution.
Al_2O_3-SiO_2	TEOS + Al(sec-OC_4H_9)	Aqueous ethanolic solution.
Al_2O_3	Al (iso-C_3H_7)$_3$	HCl catalyst in ethanolic solution.
	Al(sec-OC_4H_8)$_3$	Two-step (NH_4OH/HCl) catalyst.
ZrO_2-SiO_2	TEOS + $ZrCl_4$	Ethanolic solution without catalyst.

The gel is infiltrated into a fibre or preform and dried. Firing at high temperature (>600°C) creates a ceramic matrix. It is similar to slurry or colloidal infiltration, [See: 88.17].

Figure 88.16.1 shows various developments for sol-gel impregnation of fibres, Ref. [88-25].

Dip coating process

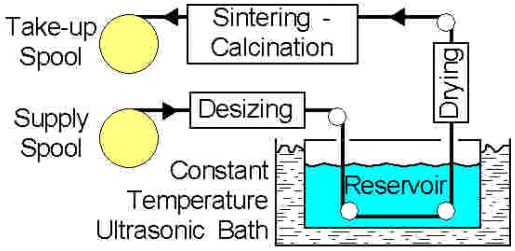

Reservoir: Metal Alkaloid Sol
Drying: $nM_i(OR)_j$(alchohol) + Fibre ➔ $nMO_i(OR)_j$· Fibre
Calcination: $MO_i(OH)_j$· Fibre ➔ MO_k· Fibre + H_2O + CO_2(g)

In-situ curing process

Reservoir: Metal Salt Solution

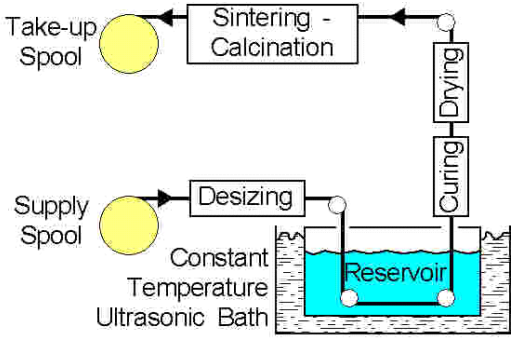

Curing: M(i)+(aq) + H_2O + OH- ➔ $MO_i(OH)_k$(aq)
$MO_i(OH)_j$(aq) + Fibre ➔ $MO_i(OH)_j$· Fibre
Drying: Remove H_2O solvent
Calcination: $MO_i(OH)_j$· Fibre ➔ MO_k· Fibre + H_2O(g)

Reaction bonding process

Reservoir: $M(OR)_i$(alchohol) + $M_jO_k(OH)_l$· Fibre ➔ $M_{j+l}O_{k+l}(OR)_{(i+l)l}$· Fibre + ROH
Curing: $M_iO_j(OR)_k$· Fibre + H_2O ➔ $M_iO_j(OH)_k$· Fibre + ROH

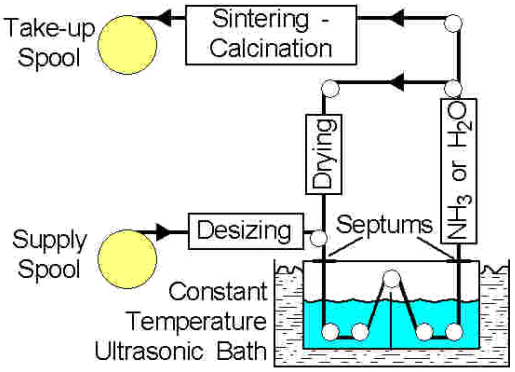

Drying: Remove H_2O solvent
Calcination: $MO_i(OH)_i$· Fibre ➔ MO_k· Fibre + H_2O(g)

Figure 88.16-1 - Sol-gel: Fibre infiltration processes

The sol-gel process enables good control of matrix composition and fairly easy impregnation of continuous tows with a lower densification temperature than hot pressing powder.

The major disadvantages are the low matrix yield and the significant shrinkage which occurs when fusing. Consequently, repeated infiltration and densification stages are necessary. A final high temperature hot pressing can be necessary to ensure full consolidation.

88.17 Slurry infiltration

Also known as 'Slip casting' for conventional ceramics, this process is applied to prepreg manufacture or preform infiltration.

The slurry consists of a:

- matrix phase: In its final form or with an elemental powder for reaction bonding, e.g. RBSN, [See: 88.11]
- binder,
- solvent or water,
- wetting agent(s), as required.

For prepreg, the continuous fibres are drawn through the slurry bath and wrapped on a mandrel to create a sheet for subsequent processing, as shown in Figure 88.17.1, Ref. [88-17], [88-18].

Slurry infiltration of preforms is similar to other liquid matrix infiltration processes; with a dry-out stage to remove all additives prior to consolidation by hot pressing' or reaction bonding.

Figure 88.17.2 shows a combined infiltration and reaction bonding process, Ref. [88-8].

The dry-out and final firing temperature depends on the specific matrix materials. For RBSN, nitriding at 1350°C for 3 hours is typical, although by use of ZrO_2, Y_2O_3 or Al_2O_3 additives, both times and temperatures can be reduced. This is beneficial in reducing chemical and thermal damage to reinforcements, Ref. [88-8].

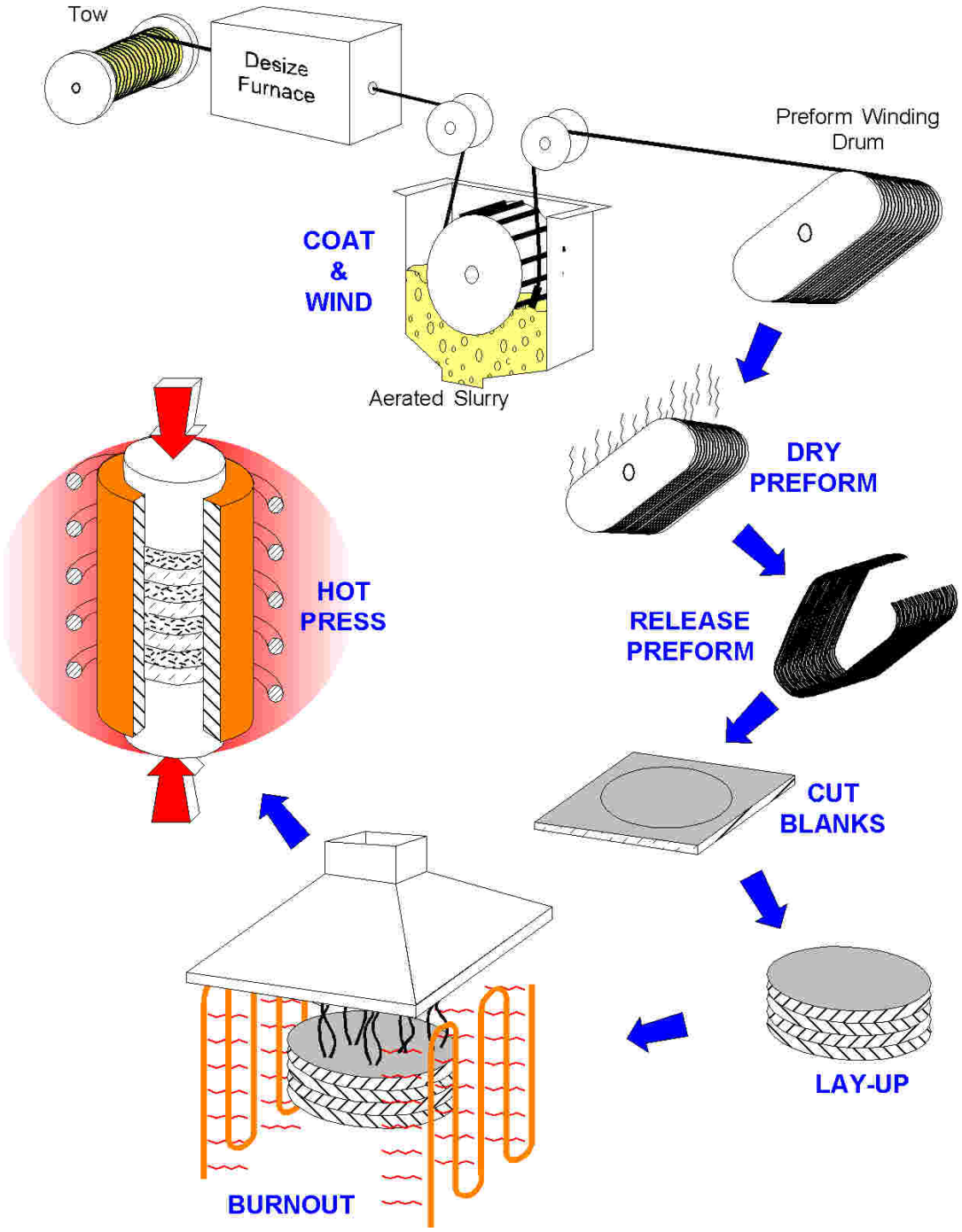

Figure 88.17-1 - Slurry infiltration process

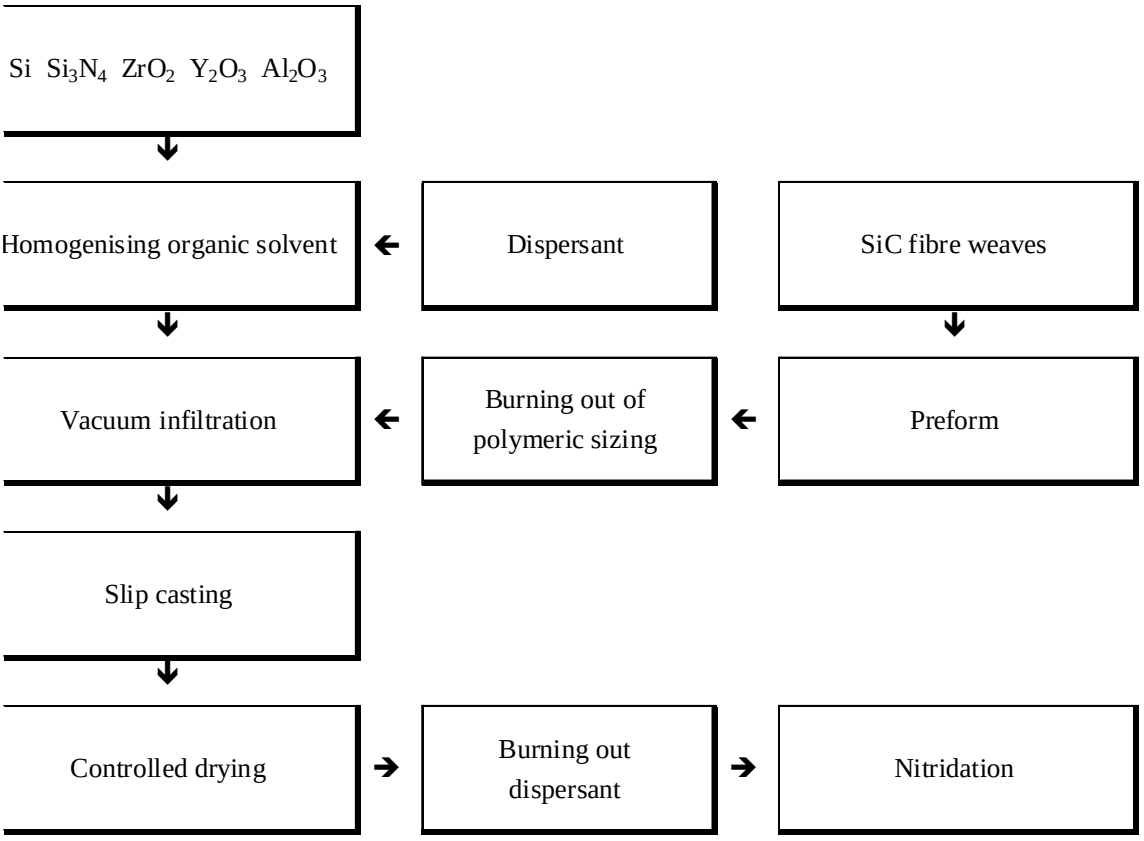

Figure 88.17-2 - Slurry infiltration and reaction bonding

88.18 Investment casting

Investment casting is an established production technique for many high-temperature alloys. The basic manufacturing process is shown schematically in Figure 88.18.1

By control of the cooling stage, the microstructure of the final component can be altered, i.e. directionality can be introduced.

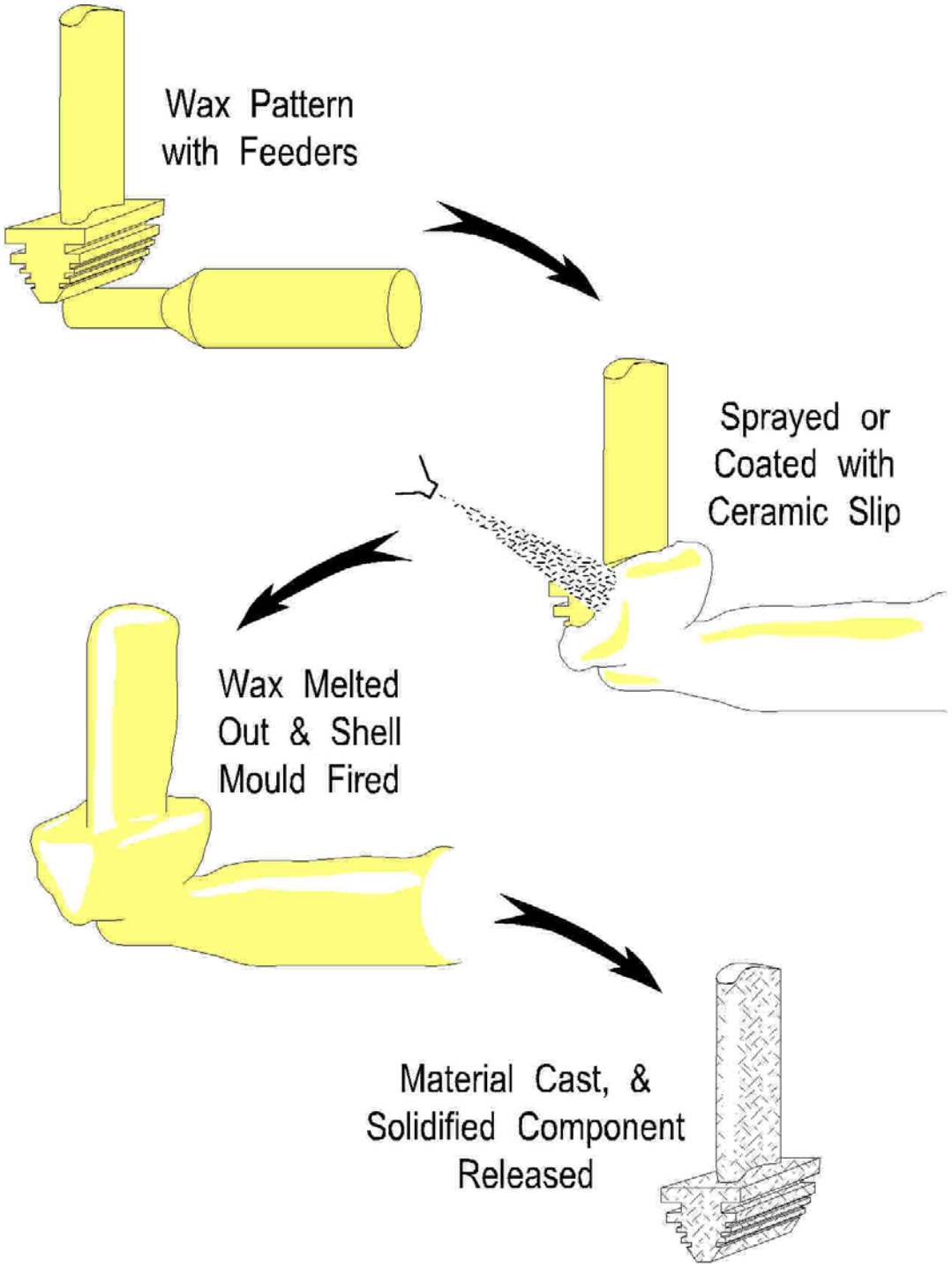

Figure 88.18-1 - Investment casting

88.19 Spray techniques

88.19.1 Atomisation

Figure 88.19.1 shows a schematic of the atomisation process, Ref. [88-19], [88-20]. The alloy is induction-melted in a pressurised crucible. The melt is then forced through a nozzle to be atomised by the high-velocity, inert-gas stream. The semi-solid metal droplets are collected on a substrate.

This is the principle of the OSPREY® process, Ref. [88-19]. A further development is co-deposition of particulate ceramics and metals Ref. [88-20]; described as COSPRAY® by Alcan UK, Ref. [88-19].

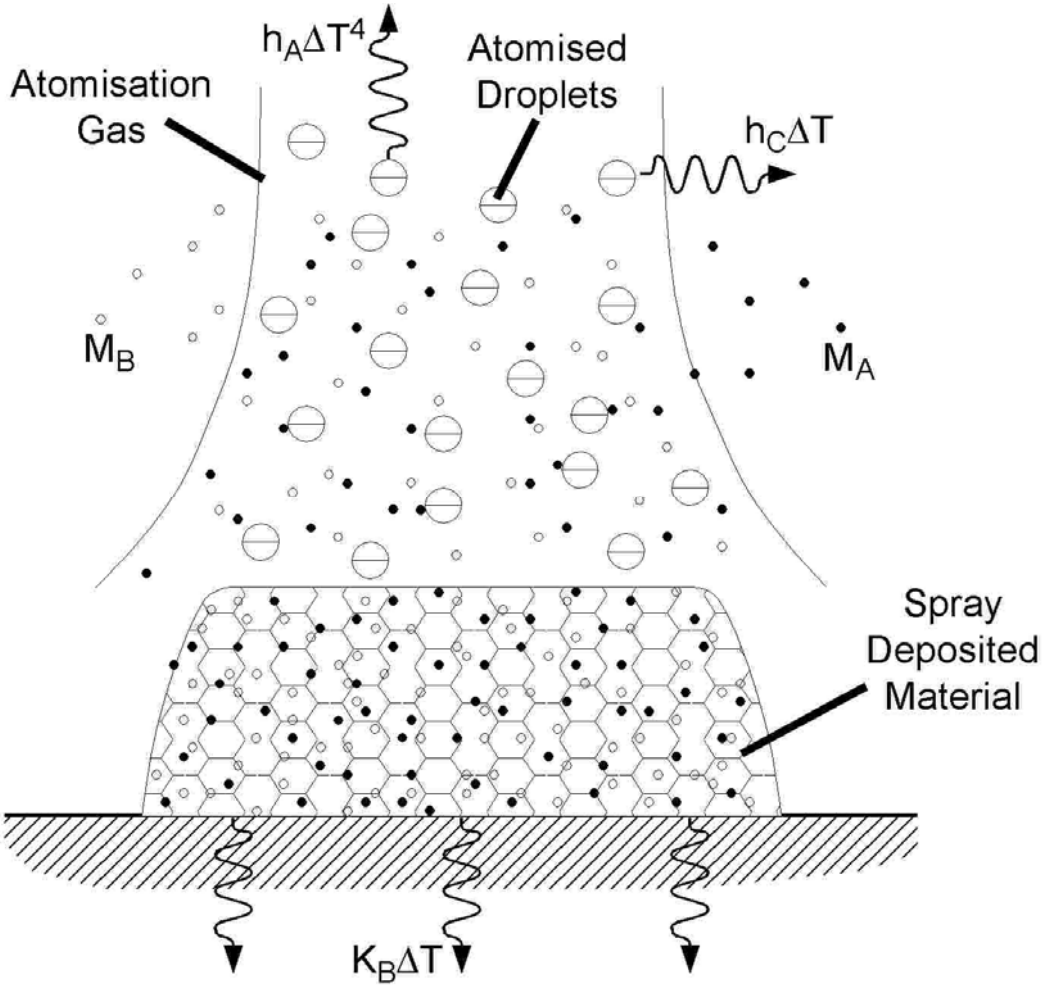

Figure 88.19-1 - Atomisation

88.19.2 Plasma spraying

88.19.2.1 General

Several techniques exist to deposit metals, ceramics, or mixtures of the two, onto substrates. The feed stock is in powder or wire form.

The deposited material normally has a fine grain structure but is porous. For co-sprayed metal and particulate, porosity is usually higher than for metal alone. Therefore a consolidation treatment should be performed; especially for coatings, Ref. [88-6].

[See also: Chapter 74 - Protective Coatings]

88.19.2.2 Uses

Figure 88.19.2 shows some uses for plasma spraying, Ref. [88-21], [88-22], [88-23]:

- depositing coatings onto components, [See: Figure 88.19.2(A)],
- pre-treatment stage of reinforcement fibres to form reinforcement containing foils for further processing, [See: Figure 88.19.2(B)]; [See also: 88.6],
- matrix foils alone. Sprayed either onto a foil-wrapped drum or directly onto the drum, [See also: 88.6].
- particulate reinforced MMC, where the reinforcement is injected into the plasma.

Given the correct selection of process conditions, no significant compositional changes occur during spraying despite differences in vapour pressures between elements.

For co-spraying of particles and metal, the temperature is below that of the melting point of the reinforcing phase.

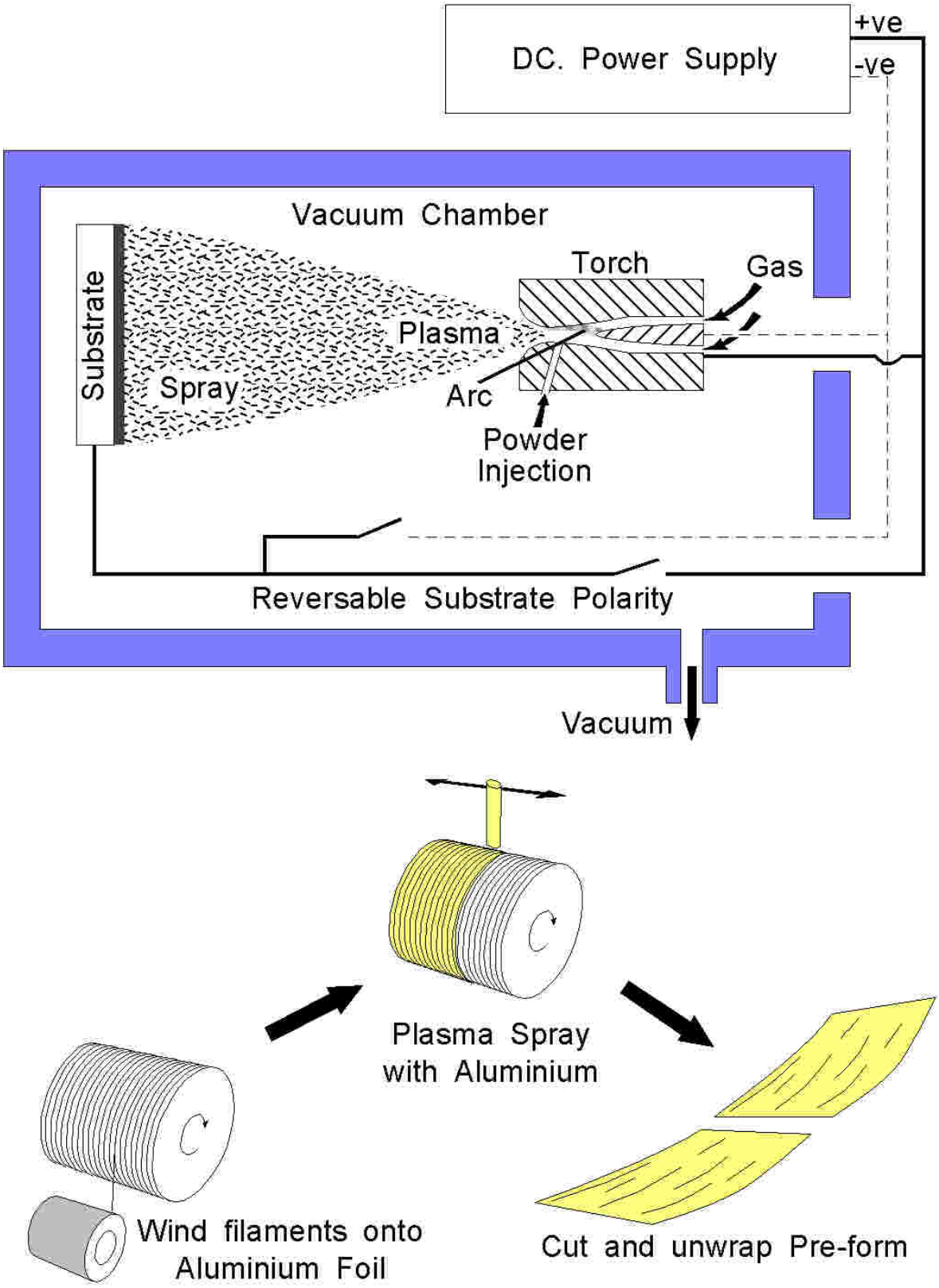

Figure 88.19-2 - Plasma spraying

88.19.2.3 Low pressure plasma spraying (LPPS)

Reactive elements may oxidise if sprayed in air. This is avoided by using a protective atmosphere or by reducing the pressure and controlling the atmosphere.

88.19.2.4 RF induction plasma spraying

This process avoids the use of electrodes. It can deposit larger particles for MMC production and can be used for materials sensitive to contamination, Ref. [88-24].

88.19.2.5 Vacuum plasma spraying

This process can be used for the spraying of titanium which is difficult because of its high reactivity in nitrogen and hydrogen atmospheres, Ref. [88-22].

88.20 Physical vapour deposition (PVD)

88.20.1 Coatings

This term is used to describe a number of techniques, including:

- electron beam (EB-PVD),
- sputtering,
- ion plating,
- sputter ion plating (SIP).

All of these techniques are used to produce coatings and consist of the transfer of metal atoms or ions from a donor material to a substrate under vacuum. The chamber size is a limiting factor on the component dimensions and production numbers.

Techniques can be combined in order to achieve the correct coating composition. Some post-processing treatments are normally required to optimise coating characteristics, or to recover the condition of the substrate after exposure to high temperature.

Table 88.20.1 summarises process details for various PVD techniques, of which EB-PVD is the most commercially advanced for deposition of coatings, Ref. [88-6].

[See also: Chapter 74 - Protective coatings]

Table 88.20-1 - Physical vapour deposition (PVD) techniques for coatings

Typical process details	Electron beam PVD (1)	Sputtering	Ion plating	Sputter ion plating (SIP)
Vacuum (Pa)	10^{-2} to 10^{-4}	10 to 10^{-1}	10 to 10^{-1}	10 to 10^{-1}
Deposition rates (3)	25µm/min	10 to 50µm/hr (2)	10 to 20 µm/min	10µm/hr
Temperature (°C)	800 - 1100 (4)	Low	-	300
Post-processing (5)	Heat treatment	Glass bead peening Heat treatment	-	Glass bead peening Heat treatment

Key:
(1) For Cr containing coatings, vapour phase composition varies to feed stock due to volatility.
(2) Depend on particular equipment, e.g. Diode or Planar Magnetron systems.
(3) Components rotated to give uniform coating.
(4) High temperature promotes some diffusion (adhesion), reduces formation of 'leader' defects.
(5) Peening/heat treatment closes 'leader' defects. Heat treatment to recover substrate condition.

88.21 Chemical vapour deposition (CVD)

A schematic diagram of CVD equipment is shown in Figure 88.21.1, Ref. [88-29].

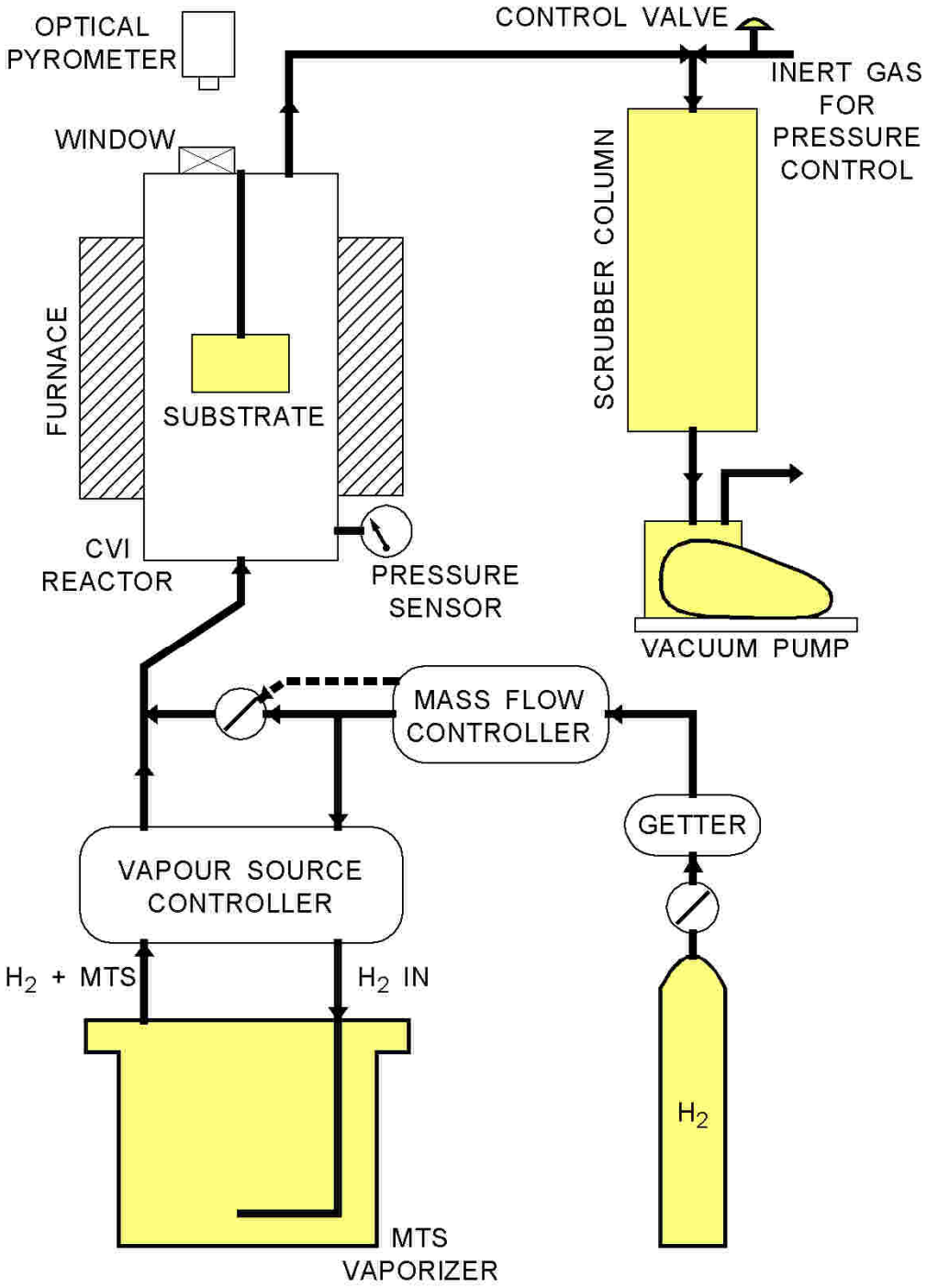

Figure 88.21-1 - Chemical vapour deposition: Process equipment

The basic process relies on the decomposition of a pre-cursor gas rich in the element to be deposited, under a controlled environment (temperature, pressure, gas mixture) within a reaction vessel; a limiting factor on the size or number of components.

It is appropriate for the deposition of metals and ceramics, with ceramics being the most common. Deposition rates are slow, but can be comparable to PVD rates. The speed largely depends on the process conditions for the particular deposited material.

Laser-CVD can enhance deposition rates, where a laser is used as the heat source (pyrolytic activation) or for heating the substrate to promote the CVD reaction (photolysis activation).

For Si-based ceramics, Al_2O_3 and AlN, Laser-CVD general deposition rates between 1 to 5 nm/min, and up to 100 nm/min, have been achieved, Ref. [88-6].

The process is usually used for coatings or for the manufacture of thin-walled, simple shape components; where material is deposited onto a mandrel and then removed after cooling.

88.22 Chemical vapour infiltration (CVI)

The basic principle is the same as CVD, [See: 88.21].

The term CVI is used where the material is deposited on to the fibres within a preform. Again, it is possible to deposit a wide variety of matrix materials but is most commonly used to manufacture SiC-SiC, C-SiC and C-C composites.

Table 88.22.1 gives representative reactions for CVI processing, Ref. [88-26], [88-5].

Table 88.22-1 - CVI chemistry for certain matrix materials

Matrix material	Gaseous precursors	Chemical reaction (from gas phase)	Process temp. (°C)
C	CH_4 C_3H_8 C_2H_2 C_6H_6	Methane or Ethane → Pyrolytic Carbon	1000 to 2200 (2000+°C for full graphitisation)
SiC	CH_3SiCl_3-H_2 $(CH_3)2SiCl_2$-H_2	$CH_3SiCl_3 + H_2 \rightarrow SiC + 3HCl + xH_2$	1200
	$SiCl_4$-CH_4-H_2	$HSiCl_3 + CH_4 \rightarrow SiC + 3HCl + H_2$	1000
Si_3N_4	Si-Cl_4-NH_3 SiF_4-NH_3	$3SiCl_4 + xH_2 + 4NH_3 \rightarrow Si_3N_4 + xH_2 + 12HCl$	1200
B_4C	BCl_3-CH_4-H_2 BBr_3-CH_4-H_2	$4BCl_3 + CH_4 + 4H_2 \rightarrow B_4C + 12HCl$	1200 to 1400
TiC ZrC	(M)Cl_4-CH_4-H_2 [(M) = Ti, Zr]	$TiCl_4 + CH_4 + xH_2 \rightarrow TiC + 4HCl + xH_2$	600 to 1000
TiB_2 ZrB_2	(M)Cl_4-BCl_3-H_2 [(M) = Ti, Zr]	$TiCl_4 + 2BCl_3 + 5H_2 \rightarrow TiB_2 + 10HCl$	1000 to 1100
BN	BCl_3-NH_3-H_2 BF_3-NH_3	$BCl_3 + NH_3 \rightarrow BN + 3HCl$ $BF_3 + NH_3 \rightarrow BN + 3HF$	1300 to 1800
ZrO_2	$ZrCl_4$-H_2-CO_2	$ZrCl_4 + 2H_2 + 2CO_2 \rightarrow ZrO_2 + 2CO + 4HCl$	1000
Al_2O_3	$AlCl_3$-H_2-CO_2	Sequence: $3H_2 + 3CO_2 \rightarrow 3H_2O + 3CO$ $2AlCl_3 + H_2O \rightarrow Al_2O_3 + 6HCl$	
		$2AlCl_3 + 3H_2 + 3CO_2 \rightarrow Al_2O_3 + 3CO + 6HCl$	1200

The gas mixtures are very dilute and the deposition rates low; to ensure even through-thickness filling and reduce the porosity.

Total process times can exceed 100 hours, depending on the precise component. This can be reduced by process modifications, such as forced gas-flow and temperature gradients within the component. Such methods enable the infiltration of thicker sections (>10mm, typically), which previously proved difficult, Ref. [88-27], [88-30], [88-31].

Figure 88.22.1 shows the basic classes of CVI techniques, Ref. [88-27]. Their applications are described in Table 88.22.2, Ref. [88-27], [88-28], [88-29].

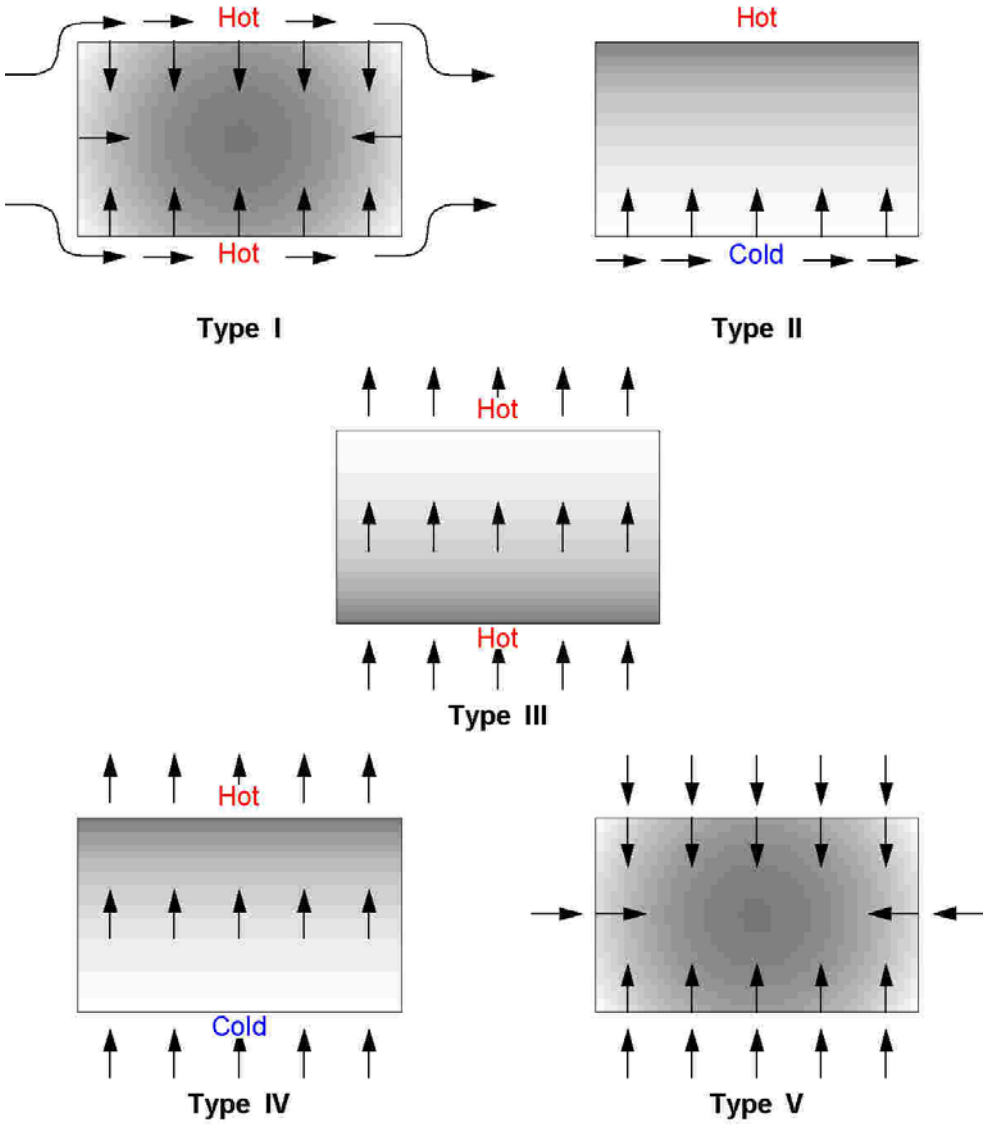

Figure 88.22-1 - Basic classes of CVI techniques

Table 88.22-2 - CVI process types

CVI process type See: Figure 88.22.1	Description	Comments
I : Isothermal. (ICVI)	Reagents surround the preform and transport to the interior via diffusion alone.	Most widely used commercial process. Generally operated at reduced pressure (1 to 10 kPa) for deposition rate control. Initial fixturing of preform required. Density gradients minimised by low reaction temperature, but deposition is often adequate to seal the outer surface before full densification has occurred. Therefore the process is interrupted and the surface sealing layer is removed before continuing infiltration.
II : Thermal gradients	Reagents contact cold surface and also transport by diffusion.	Not widely used. Relatively slow as it is a diffusion process. Sealing of the surface is avoided by maintaining a low surface temperature. As densification nears completion, the surface temperature rises (greater conductivity of dense region) causing infiltration of entire volume.
III : Isothermal forced flow	Reagents flow through preform.	Not widely used. Suffers from density gradients and sealing of the entry surface.
IV : Thermal gradient forced flow. (FCVI)	Reagents flow through preform from cold to hot surface.	Developed at ORNL. Overcomes problems of slow diffusion and surface sealing. It can produce fully densified thick-section parts in several hours.
V : Pulsed flow	Reagents flow in and out of preform because of cyclical evacuation and back filling.	Not widely investigated technique. Theoretically, it can offer significant faster infiltration rates compared to ICVI.

The advantages of CVI are the ability to process a variety of fibre and matrix combinations and to form large, complex shapes.

The limitations are the size of component(s) able to be placed in the reaction vessel (2 to 3m vessels are available), and the need to aid infiltration into thick sections by forced-flow or the use of thermal gradients if production times are to be reduced.

88.23 References

88.23.1 General

[88-1] J. Wilson & D.P. Bashford: RJ Technical Consultants/BNF-Fulmer, (UK)
'Structural Materials and Space Engineering'
R1176/SMaSE. September 1992;
ESTEC Contract No. 7090/87/NL/PP

[88-2] R. Warren: Chalmers University of Technology Göteborg, (S)
'Metal Matrix Composites'
'Research & Development of High Temperature Materials for Industry'. Published by Elseveir, 1989, p269-277

[88-3] S. Nourbakhsh & H. Margolin: Polytechnic University Brooklyn, (USA)
'Fabrication of High Temperature Fibre-reinforced Intermetallic Matrix Composites'
Proceedings of International Conference 'Metal & Ceramic Matrix Composites: Processing Modelling & Mechanical behaviour' Anaheim, USA, 19th-22nd February 1990, p75-89

[88-4] G. Broden: Dornier Fuftfahrt GmbH, (D)
'SPF/DB - A Manufacturing Technique for Lightweight Structures'
Proceedings of International Symposium 'Advanced Materials for Lightweight Structures'. ESTEC, NL, 25th-27th March 1992
ESA SP-336 (October 1992), p149-153

[88-5] J.R. Strife et at.: United Technologies Research Centre, (USA)
'Status of Continuous Fibre-reinforced Ceramic Matrix Composites Processing Technology'
Ceram. Eng. Sci. Proc. 11 [7-8], 1990, p871-919

[88-6] J. Wilson & D.P. Bashford: RJ Technical Consultants/BNF-Fulmer, (UK)
'High Temperature Materials for Space Propulsion Units'
R1176/D13/October 1990. ESTEC Contract No. 7090/87/NL/PP

[88-7] R. Lundberg et al.: Volvo Flugmotor/Tixon AB, (S)
'Chemical Vapour Infiltration (CVI) of SiC Fibre Preforms'
Journal de Physique IV, Colloque C2, Supplementaire au Journal de Physique II, Vol. 1, septembre 1991, C2:491-495

[88-8] J. Brandt et al.: Swedish Ceramic Institute, Göteborg, (S)
'SiC Continuous Fibre-reinforced Si3Ni4 by Infiltration and Reaction Bonding'
Proceedings of 16th Annual Conference 'Composites & Advanced Ceramic Materials', Cocoa Beach, 1992, p623-631
ISSN 01 96-6219

[88-9] I. Horsfall & S.J. Cundy: Cranfield Institute of Technology, (UK)
'A Process for the Fabrication of Ceramic Fibre-reinforced Titanium Aluminide'
Proceedings of 16th Annual Conference 'Composites & Advanced Ceramic Materials', Cocoa Beach, 1992, p605-613
ISSN 01 96-6219

[88-10] W. Krenkel & P. Schanz: DLR, (D)
'Fibre Ceramic Structures based on Liquid Impregnation Technique'
Acta Astronautica, Vol.28, 1992, p159-169

[88-11] J.A. Clegg: Loughborough University of Technology, (UK)
'Cast Metal Matrix Composites'
The Foundryman Aug./Sept. 1991, p312-319

[88-12] A.J. Cook & P.S. Wiener: PCast Corporation, (USA)
'Pressure Infiltration Casting of Metal Matrix Composites'
Materials Science & Engineering, A144 (1991), p189-206

[88-13] N. Mykura: Advanced Material Systems Ltd., (UK)
'Casting Metal Matrix Composites by Liquid Pressure Forming'
Metals & Materials, Vol.7, No. 1, Jan 1991, p7-11

[88-14] Prof. R. Kochendörfer: DLR, (D)
'High Temperature Materials for Hypersonic Transport'
Proceedings of International Symposium 'Advanced Materials for Lightweight Structures', ESTEC, NL, 25th-27th March 1992
ESA SP-336 (October 1992), p7-13

[88-15] H. Hald et al: DLR, (D)
'Development and Real Test of a Ramjet Nozzle made of Liquid Silicon Infiltrated C/SiC'
Proceedings of ESA Symposium 'Space Applications of Advanced Structural Materials', ESTEC, NL, 21-23rd March 1990
ESA SP-303 (June 1990), p283-289

[88-16] J. Willig
'Melt Infiltration Process for making Ceramic Matrix Composites'
Journal of Fibre Reinforced Ceramic Composites, 1990,p260-277

[88-17] A. Moguez: Aerospatiale, (F)
'Glass Matrix Composites, Manufacture and Performance Data'
Looking Ahead for Materials and Processes. Published by Elsevier, 1987, p.9-17

[88-18] D.M. Dawson et al.: Harwell Lab., (UK)
'Fabrication and Materials Evaluation of High Performance Aligned Ceramic Fibre-reinforced Glass Matrix Composite'
Ceram. Eng. Sci. Proc. 8[7-8], 1987, p815-821

[88-19] I. Parker
'Droplets of Density'
Aerospace Composites & Materials

[88-20] E.J. Lavernia: University of California, (USA)
'Synthesis of Particulate Reinforced Metal Matrix Composites using Spray Atomisation and Co-deposition'
SAMPE Quarterly, Jan. 1991, p2-12

[88-21] S. Dallaire: Industrial Material Institute, Canada
'Thermal Spraying of Reactive Materials to form Wear-resistant Composite Coatings'
Journal of Thermal Spray Technology, Vol.1(1) Mar. 1992, p41-47

[88-22] P.A Dearnley & K.A. Roberts: University of Auckland, (NZ) / University of Cambridge, (UK)
'Titanium Matrix Composites via Vacuum Plasma Spraying. Part I: Optimising Process Parameters'
Powder Metallurgy 34 (1), 1991, p23-32

[88-23] O. Betsalel et al.: Israel Institute of Metals/Israel Aircraft Industries
'Manufacture of Fibre-reinforced Metal Matrix Monolayer Composites by Plasma Spraying'
Israel Journal of Technology, Vol.24, 1988, p425-432

[88-24] M. Boulos: University of Sherbrooke, Canada
'R.F. Induction Plasma Spraying State of the Art Review'
Journal of Thermal Spray Technology, Vol.1(1), Mar 1992, p33-40

[88-25] D.A. Hazelbeck et al: General Atomics, (USA)
'Novel Sol-Gel Coating Techniques for Ceramic Tows: In-situ Curing & Reaction Bonding'
Ceramic Eng. Sci. Proc. 12 [7-8] 1991,p1075-1085

[88-26] D.P. Bashford & J. Wilson: Fulmer Research Ltd., (UK)
'Ceramic Matrix Composites & Carbon-Carbon Composites for High Temperature Space Applications'
R1176/D7/2 February 1990.
ESTEC Contract No. 7090/97/NL/PP

[88-27] T.S. Besmann et al: ORNL - Oak Ridge National Lab., (USA)
'Vapour-phase Fabrication and Properties of Continuous Filament Ceramic Composites'
Science, Vol. 253, 6 September 1991, p1104-1109

[88-28] W.J. Lackey: Georgia Institute of Technology, (USA)
'Review, Status and Future of CVI Process for Fabrication of Fibre-reinforced Ceramic Composites'
Ceram. Eng. Sci. Proc 10 [7-8] 1989, p577-584

[88-29] D.P. Stinton et al: ORNL - Oak Ridge National Lab., (USA)
'Advanced Ceramics by CVD Techniques'
Ceramic Bulletin, Vol. 67, No. 2, 1988, p350-355

[88-30] A. Mülratzer et al: MAN Technologie AG, (D)
'New Processes for Lightweight Ceramic Matrix Composites'
Proceedings of International Symposium 'Advanced Materials for Lightweight Structures'. ESTEC, NL. 25th-27th March 1992.
ESA SP-336, October 1992, p249-254

[88-31] D. Sygulla et al: MAN Technologie AG, (D)
'Integrated Approach in Modelling, Testing and Design of Gradient-CVI derived CMC Components'
AGARD Workshop 'Introduction of Ceramics into Aerospace Structural Composites', 21 - 22 April 1993, Antalya, Turkey

89 European sources of expertise

89.1 Introduction

Certain manufacturing processes require considerable investment in plant and equipment, e.g. 3-D fibre placement, Chemical Vapour processing equipment (CVD and CVI). This has therefore been a restraining factor on the number of organisations prepared to commit extensive capital to set-up and run a manufacturing plant; especially where the components to be manufactured are large with small production runs.

Where investment has been made, each organisation tends to offer a complete service, i.e. from design to supply of a finished item.

There are centres of expertise in both Europe and the USA, with the leaders in a particular technology licensing it to others.

Table 89.1.1 gives a summary of major European organisations with appropriate expertise in manufacturing of metal and ceramic-based materials.

Table 89.1-1 - Major European organisations with expertise in manufacture with advanced metallic and ceramic-based materials

Major European organisation (1)	Metal (2)	MMC	GMC/ GCMC	CMC	C-C
France					
Aerospatiale	✪	✪	✪	✪	✪(B)
SEP	✪			✪(A)	✪
ONERA	✪			✪	
Le Carbone					✪
Dassault Aviation	✪			✪	
SNECMA	✪			✪	
Germany					
Dornier Luftfahrt	✪				
Dornier Deutche Aerospace				✪	✪
MAN Technologie	✪			✪	
Sigri	✪				✪
MBB (DASA)	✪	✪		✪	
MTU	✪	✪			
Sintec Keramik					✪
DLR	✪	✪	✪	✪	
UK					
BAe	✪				
Rolls Royce	✪	✪	✪	✪	
Dunlop Aviation					✪

Major European organisation (1)	Metal (2)	MMC	GMC/ GCMC	CMC	C-C
BP Composites Ltd		✪(C)			
British Alcan	✪	✪			
Magnesium Electron Ltd	✪	✪			
DRA Farnborough	✪	✪			
AEA Technology (Harwell)	✪	✪	✪	✪	
Norway					
Raufoss A/S	✪	✪			
Netherlands					
Stork Product Engineering	✪				
Sweden					
Volvo Flugmotor	✪				
Switzerland					
Battelle	✪			✪	

Key: (1) Excluding research facilities within various universities.
(2) [See: 46.8 for Al-Li, 51.3 for Be].
(A) SEPCARBINOX™ : C-SiC, CERASEP™ : SiC-SiC.
(B) NOVELTEX™ : C-C
(C) SIGMA SiC monofilaments

89.2 Company specialisation

89.2.1 General

This is a summary of European expertise in advanced structural materials. It does not detail all of the activities of the companies mentioned.

89.2.2 Aerospatiale

Aerospatiale is a major aerospace company with manufacturing capabilities for:

- aircraft,
- missiles,
- ARIANE Launchers,
- spacecraft, and
- satellites.

Les Mureaux has expertise in metallic materials, whereas CMC and C-C facilities are located at St. Médard-en-Jalles, Aquitaine.

89.2.3 Societe Européene de Propulsion (SEP)

Located at Suresnes and St. Médard-en-Jalles, SEP specialise in the construction of:

- missile motors,
- rocket engines,
- boosters, and
- ARIANE propulsion systems.

With extensive use of high-temperature nickel alloys, they are also a. world leader in the use of CVI for preparing SiC-SiC, C-SiC and C-C components for advanced propulsion systems and TPS concepts.

89.2.4 ONERA : L'Office National d'Etudes et de Recherches Aerospatiale

ONERA is a National research and development organisation which supports aerospace requirements and undertakes material development and evaluation.

89.2.5 Le Carbone

Le Carbone specialise in the production of C-C composite components for braking systems and aerospace engineering requirements.

89.2.6 SNECMA

SNECMA is a major aero-engine manufacturer with extensive manufacturing capabilities in titanium and nickel alloys. They undertake evaluation of high-temperature MMC and CMC materials for new gas turbine engines designs and have expertise in high-temperature coatings.

89.2.7 Dassault Aviation

Dassault is a major aerospace company undertaking civil and military aircraft construction. They participated in the Hermes development programme and have manufacturing capabilities for SPF/DB of titanium components.

89.2.8 Dornier Luftfahrt GmbH

Dornier Luftfahrt construct civil aircraft. They have manufacturing capabilities in SPF/DB of titanium.

89.2.9 Dornier Deutche Aerospace

Dornier are part of the larger Deutche Aerospace (DA) group. Located at Freidrichshafen, S. Germany, they are a prime contractor for space programmes with specialist microgravity facilities. They are also active in developing low-cost manufacturing routes for ceramic matrix composites, e.g. C-SiC and SiC-SiC.

89.2.10 MAN Technologie AG

Located at Munich, MAN is a development and manufacturing organisation for aerospace programmes, including the manufacturing facilities for Ariane 5 boosters. They are active in developing rapid CVI process for the manufacture of SiC-SiC and C-SiC components. They also have advanced metal forming technology.

89.2.11 SIGRI

SIGRI are a supplier of carbon fibre products and components in C-C composites.

89.2.12 MBB (DASA)

The central laboratories of MBB, located at Munich, undertake materials development. They have a long history of developing advanced metallic and ceramic material processing techniques.

89.2.13 MTU Motoren und Turbinen Union GmbH

MTU are located at Munich and manufacture gas turbine engine assemblies. With extensive use of Ni alloys, they are also evaluating titanium matrix composites (TMC) for future designs.

89.2.14 Sintec Keramik

Sintec are a specialist manufacturer of advanced ceramics, CMC and C-C materials. They supply components and demonstrators to space programmes.

89.2.15 Deutche Forschunganstalt fur Luft und Raumfahrt (DLR)

Located at Stuttgart, DLR are a research and technical organisation undertaking high-temperature materials and process development.

89.2.16 British Aerospace (BAe)

BAe sites located at Cranfield-Filton manufacture aircraft components by SPF/DB of titanium.

89.2.17 Rolls Royce

Located at Derby, Rolls Royce is a major aero-engine manufacturer. They are evaluating titanium composites (TMC), GCMC and SiC-SiC materials for future gas turbine engine designs.

89.2.18 Dunlop Aviation

Dunlop manufactures C-C composite components by CVI for aerospace applications.

89.2.19 BP Metal Composites Ltd

Located at Sunbury, BP Composites manufactures SIGMA silicon carbide monofilaments by CVD and have expertise in preparing titanium matrix composites. The facility at Farnborough for manufacturing particle reinforced aluminium composites closed in 1993.

89.2.20 British Alcan

Located at Banbury, British Alcan is a primary aluminium alloy producer. As part of an international company, they sell Duralcan particle reinforced aluminium composites and appropriate processing technology. The COSPRAY business for atomisation and consolidation of advanced MMC materials closed in 1993.

89.2.21 AEA Technology (Harwell)

AEA is a contract research and technical organisation. They have processing facilities for MMC and CMC materials including PVD, CVD and CVI.

89.2.22 Magnesium Elektron Ltd

A primary producer of magnesium alloys. They have process technology for particulate reinforced magnesium composites.

89.2.23 Defence Research Agency (DRA)

Located at Farnborough, DRA is a National research body for aerospace. They undertake material process development, including Al-Li alloys, Al-Li MMC and Ti MMC.

89.2.24 Stork Product Engineering BV

Located in Amsterdam, Stork manufacture aerospace components in advanced metals and fibre metal laminates (FMLs).

89.2.25 Volvo Flygmotor AB

Volvo manufactures gas turbine engine assemblies and participates in the Vulcain engine development and production.

89.2.26 Raufoss A/S

Raufoss has extensive manufacturing capabilities for aluminium alloy products, including process facilities for ODS aluminium alloys.

89.2.27 Battelle

Battelle is an international contract and technical organisation with pilot manufacturing facilities.

89.2.28 Saab Ericsson Space

Saab Ericsson Space, Sweden, is a supplier to the space industry. Manufactured components include spacecraft structures, adapters and separation systems, computer systems, electronics and antennas.

90 Smart technologies

90.1 Introduction

90.1.1 Smart materials, technologies and systems

‘Smart’ is increasingly used to describe certain materials, devices, systems and structures to imply a level of 'intelligence', Ref. [90-1], [90-2], [90-3], [90-4]. However, there is no single accepted definition of the term ‘smart’, and this can lead to misunderstanding of the true capabilities of any particular technology.

'Intelligence' is implied where manual recognition or response is replaced by a level of automation, e.g. by computer-based systems programmed to recognise anomalies and instigate responsive actions.

Within this handbook, ‘smart’ is used to describe, [See: 90.2]:

- materials, which posses an inherent characteristic, e.g. piezoelectric or shape memory effect, that can be exploited to act as a sensor or actuator and become a constituent part of a ‘smart’ system, [See: Chapter 91],
- technologies: e.g. associated with the use of sensors, actuators and their monitoring or control equipment. These are constituent parts of ‘smart' systems, [See: Chapter 91],
- systems: comprising of one or more ‘smart’ technologies, [See: 90.4 and 91.8]. Some of these can have a level of intelligence.

Once integrated into a structure, some of the more complex smart systems are known as ‘adaptive’ or ‘intelligent structures’, [See: 92.7].

90.1.2 European space structures

90.1.2.1 Smart materials

Smart materials have been investigated for many years and tested in some flight experiments and missions, e.g.

- shape correction in Hubble-COSTAR, using electrostrictors,
- launch locking in CLEMENTINE or STRV-2 , using shape memory alloy (SMA Frangibolt),
- vibration control in STRV-1b, CFIE or ACTEX, using piezoceramics.

Future space applications rely largely on the development of a next-generation of advanced transducer materials; often called intelligent materials, e.g. piezoceramic patches and stacks; electrostrictives and shape memory alloys, Ref. [90-7], [90-8]. For integration into deployable or inflatable structures, such as JWST or Solar sail, flexible intelligent materials are necessary, e.g. anisotropic piezo-fibre-based or electro-active polymer components, Ref. [90-7], [90-8].

90.1.2.2 Smart structures

Within this handbook, smart systems applied to structures are grouped by complexity and functionality levels, i.e. solely sensory; solely reactive-actuator based or full smart system, [See: 90.2].

Level 1 and level 2 structures are more or less well-established technologies for space applications. Level 3, which are known as smart, adaptive or intelligent structures are of primary interest for the ultra-lightweight design of future space large structures.

Smart technologies and systems which have potential value in European space structures (satellites, spacecraft, space planes and space stations) are described in:

- Chapter 90 - Smart technologies
- Chapter 91 - Smart system constituents
- Chapter 92 - Potential space applications
- Chapter 93 - Limitations of smart technologies
- Chapter 94 - European capabilities in smart technologies

Some 'smart' technologies have been integrated into future RLV programmes, [See: 92.3].

Adaptive- or intelligent-structure technology is being considered for some very large space structures that need some means of adjusting their shape, dynamic stability or accuracy once deployed in space, [See: 92.7].

90.1.2.3 Adaptive structures

The focus of work on adaptive structures is usually summarised to be on active, continuous, ideally, broadband vibration and shape control. Level 3 structures integrate intelligent material systems with actuator and sensor functions linked to adequate controllers, which enable the structure to sense its structural condition and adapt its structural parameters to the current need.

To efficiently design a level 3 structure, it is very important to consider a number of interrelated factors, including:

- attachment or integration of intelligent 'active' components within a 'passive' host structure,
- electromechanical effects, including signal conditioning and electronics, software and control,
- structural mechanics, especially structural dynamics when considering lightweight structures.

Consequently, a highly interdisciplinary approach is needed to achieve such structures, [See: 92.7 for some examples of concepts].

Advanced transducer materials are an essential factor in the development of adaptive structures. These are often called intelligent materials.

Depending on the application, these intelligent materials need to be either rigid or flexible. In developing the design for the active system, the stiffness of the actuator materials needs to be taken into account,

90.1.3 Condition and health monitoring

The long-term durability of load-bearing structures is of prime concern for the safe operation of vehicles, equipment and plant in a variety of industries.

Many industry sectors are now faced with ageing infrastructure (e.g. civilian and military aircraft fleets, bridges, roads, offshore and power generation), and the ability to ensure continued safe operation has become increasingly important.

Maintenance costs continue to rise as structures age further. These concerns have provoked a large number of studies within Europe and the USA, Ref. [90-5].

Numerous 'smart' solutions have been proposed for monitoring the structural condition or health of:

- existing structures, where monitoring systems are retrofitted
- new structures, where the monitoring system is built-in at the time of construction.

Some of these smart technologies have potential in space applications, benefiting from the development and reliability studies conducted by other industry sectors.

90.2 Smart terminology

90.2.1 General

The term 'smart' has many interpretations for the academics and engineers working in different industrial sectors.

Within this handbook the term smart is used to describe applications in space programmes where the principal requirements are for smart systems with a self-inspection (or sensory) capability, with or without an inherent adaptive response. Such systems can only impose minimal additional mass and energy consumption on any project.

A truly smart system is one where both sensory and adaptive capabilities are combined with an intelligent control loop to give immediate responses to the operating environment. These are commonly known as adaptive or intellegent structures.

90.2.2 Smart system levels

90.2.2.1 General

The smart systems described are grouped into these three levels:

- Level 1: solely sensory,
- Level 2: solely reactive actuator based,
- Level 3: full smart system.

90.2.2.2 Level 1 - Solely sensory

A structure with a distribution of sensors to measure a physical parameter (measurand), e.g. temperature, pressure or strain.

The outputs from the sensors are logged or interpreted for their significance.

Strain gauges and thermocouples are classical sensors. Fibre optics are a more recent type of sensor offering a wider range of responses

[See: 91.4]

90.2.2.3 Level 2 - Solely reactive actuator based

Actuators are incorporated into the structure to give a direct response to an external stimulating signal, e.g. for deployment or as release mechanisms.

These can be simple mechanical actuators or incorporate more elaborate smart technologies using shape memory alloys (SMAs) or piezoelectric materials.

[See: 91.5]

90.2.2.4 Level 3 - Full smart system

Sensors are linked to a control loop, which in turn initiates movement from actuators to achieve the desired real-time response by the structure, [See: 92.5, 92.7].

The key demand is to provide the necessary level of integration for the desired adaptive capabilities; which are frequency dependent.

90.2.3 Application

Historically, Level 1 and 2 systems are already used in space structures. The complexity of the systems increases with successive developments.

In Level 3 systems, smartness can give significant opportunities for advancement, given realistic initial specifications. Some examples of concepts and developments for adaptive space structures are described, [See: 92.7].

90.3 Space requirements for smart systems

90.3.1 General

In general, for structural configurations the three main areas of interest for the use of smart technologies are:

- damage detection and self-diagnosis,
- vibration damping,
- active compensation and alignment,

90.3.2 Damage detection and self-diagnostics

90.3.2.1 General

RLVs with smart monitoring systems can be maintained on the ground using data gathered in-flight, whereas long-term deployed structures cannot. The capture, maintenance and repair of these is an expensive operation.

[See: Chapter 92]

90.3.2.2 Long-life deployed structures

For long-life deployed structures such as satellites and space stations, there is a need to monitor the integrity of structural elements in service. These elements may be made from composites or metal alloys.

Various types of structural damage may occur, including:

- impact damage,
- debris,
- micrometeorite impact,
- delaminations,
- crack initiation,
- crack propagation.

In some structural configurations, manual inspection is not feasible over the operating life of the structure. In these cases, in-situ, self-diagnostic inspection systems could provide the necessary level of confidence in the structure's condition at any point in its life.

This is a health (condition) monitoring system of some complexity, i.e. a Level 1 Smart System, [See: 90.2 for terminology].

The interest in developing such systems is centred on manned vehicles with life expectancies up to 30 years. The areas receiving the most attention include:

- damage initiation and propagation in composite components and structural elements (FRP, CFRP),
- crack propagation in metal pressurised vessel and fuselage configurations,
- micrometeorite and debris impacts to orbiting vehicles.

90.3.2.3 Reusable launch vehicles (RLV)

Both US and European future RLV programmes have identified the need for an integrated approach to monitoring vehicle health during operational life, e.g. 30 years, Ref. [90-6].

The overall aims are to ensure safety, reduce turn-round times between flights, focus maintenance operations to reduce costs, and allow reusability.

An integrated heath monitoring approach involves both, Ref. [90-5]:

- in-flight, real time monitoring: using experience from the aircraft industry or that evolved from smart technologies to monitor the structural health, e.g. Level 1 Smart System, [See: 92.3],
- on-ground verification: using inspection methods mainly based on those applied within the aircraft industry, [See also: Chapter 34 - polymer composites]. Additional techniques or modifications to existing methods are used for specific structures within space-vehicles, e.g. TPS. [See also: Chapter 80 - new advanced materials].

The main areas of future RLV concepts targeted for health monitoring, include, Ref. [90-5], [90-6]:

- thermal protection systems (TPS): especially those regions experiencing severe thermal loads during re-entry, e.g. nose cone on X-38.
- tanks: e.g. LH2 tank on DC-XA, X-33, X-38 and Clipper-Graham
- structural regions under high mechanical loads: e.g. X-38 aft section.

[See: 92.3]

90.3.3 Vibration damping

Many satellite structures require high dimensional stability to provide a stable platform for communications signals and imaging systems. Vibration in orbiting structures arising from movement of structural elements causes loss in stability. Such structures could benefit from active damping systems to counter the vibrations. Level 3 smart systems, [See: 90.2], could be applied to quantify the vibration levels and provide counter impulses to damp out low energy vibrations or low frequency oscillations.

90.3.4 Active compensation and alignment

The dimensional tolerance requirements for future large antenna designs may not be achievable by material selection and design alone. Whilst CFRP possesses a controllable near zero CTE, it is still susceptible to small dimensional changes in space conditions. It may therefore be appropriate to use a Level 3 smart system, [See: 90.2], to achieve active compensation and realignment when the shape of the antenna changes under cyclic thermal conditions.

Other reasons for adopting active compensation include:

- compensation to take account of variable signal frequencies.
- in-orbit as opposed to on-earth calibration or optimisation.

90.4 Elements of a smart system

90.4.1 General

The permutations of the constituents parts of a smart system are numerous. In some cases, an element of the system can be a material which displays a unique physical phenomenon, e.g.:

- piezoelectric [See: 91.3],
- shape memory [See: 91.5],
- electrostrictive [See: 91.5],
- magnetostrictive [See: 91.5].

Unfortunately, these physical phenomena are promoted as 'smart materials' in their own right, without reference to the necessary interpretation and control systems.

The material characteristics can be used for measurement (sensor), [See: 91.2], or responses (actuator), [See: 91.5].

Figure 90.4.1 illustrates the interactions between the component elements of a Level 3 smart system, Ref. [90-1]. These in turn can be broken down into constituent parts, [See: Chapter 91].

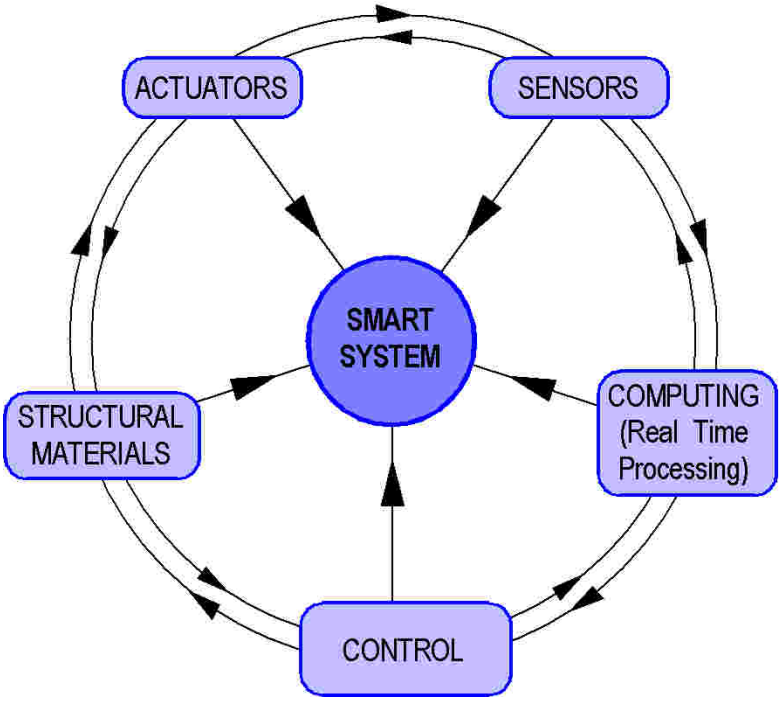

Figure 90.4-1 - Smart system: Schematic diagram showing interactions between component elements

90.4.2 Sensors

90.4.2.1 General

A network of sensors is embedded or bonded onto the structure, [See: 91.2]. These can measure physical conditions (the stimuli for a responsive smart system) such as:

- stress,
- strain,
- temperature,
- electrical properties,
- magnetic properties, or
- another measurand.

90.4.2.2 Options

- strain gauges,
- thermocouples,
- accelerometers,
- transducers,
- optical fibres,
- piezoelectric materials.

[See: 91.2]

90.4.3 Actuators

90.4.3.1 General

A network of actuators incorporated within the structure enables it to respond to the stimulus via instructions from the control loop, [See: 91.5].

90.4.3.2 Options

- mechanical devices,
- shape memory alloys,
- piezoelectric materials,
- electrostrictive materials, and
- magnetostrictive materials.

[See: 91.5]

90.4.4 Control mechanism

Closed loop control determines the relationship between the stimulus and the response. It can be deterministic, but can also result from an intelligent choice made from several alternative responses. This is where the 'intelligence' lies and is achieved with microprocessors (computers). For very complex interactions, the selected use of artificial intelligence, neural networks and nanotechnology is proposed for advanced systems, [See: 91.7].

90.4.5 Immediacy

The reaction to the stimulus should be immediate, i.e. capable of reacting at the same rate as the stimulus is received. Consequently, this requires real-time computational analysis for the control algorithms.

90.4.6 Structural materials

Structural materials are normally made of either FRP composite or metal alloy. The options for applying smart technologies to these materials are:

- composites: Embed sensors or actuators within the material or mount them on the surface.
- metallic structures: Surface mounting of sensors is the more realistic option.

Sensors or actuators cannot adversely affect the function or integrity of the material.

90.4.7 Structures

Structural elements are made of one or more materials, e.g. composite skinned metal honeycomb panels.

Assembled structures are a complex mixture of different materials, each selected to perform a particular function, e.g. metal, composite, insulation layers for cryotanks, [See: 92.3]; CMCs, insulation layers and metals for TPS, [See: 92.3].

Sensors or actuators can be surface mounted at key positions on structural elements. These can have limited access in assembled structures, so are considered to be embedded within the structure. Sensors or actuators cannot adversely affect the function or integrity of the structure.

90.5 Key issues for success

Factors important to establish a successful smart system include:

- does the sensor accurately measure or quantify the measurand?
- is there need for a reference sensor?
- is there sufficient redundancy to compensate for failed sensors?
- is the sensor reliable over the intended life of the structure?
- what is the frequency of events requiring an active response?
- can the sensors and actuators respond within the required time interval?
- is there sufficient redundancy in the control loop to compensate for electronic failures?
- can the actuators provide enough force and displacement for the active compensation required? Again frequency of response is important.
- does the sensor or actuator's response change with repeated operation over the intended life of the structure?
- how can the smart system (sensors, actuators and control systems) be integrated into the structure?
- does the smart system provide sufficient benefit for its overall mass and power consumption?

90.6 References

90.6.1 General

[90-1] N.D.R. Goddard et al
'Smart Materials : A Review of the Four Key Technologies and Their Likely Industrial Impact'
ERA Technology Report 92-0246R, November 1992

[90-2] M.V. Gandhi & B.S. Thompson
'Smart Materials and Structures'
Chapman & Hall, ISBN 0 412 37010 7, 1992

[90-3] B. Culshaw, P.T. Gardner & A. McDonach (Editors)
First European Conference on Smart Structures and Materials
Held in Glasgow, 12-14 May 1992. Proceedings co-published by IoP Publishing and EOS/SPIE EUROPTO Series SPIE 1777, ISBN: 0-7503-0222-4

[90-4] 'Smart Structures for Aircraft and Spacecraft'
75th Meeting of the AGARD Structures and Materials PanelLindau, Germany, 5th-7th October 1992
AGARD Conference Proceedings AGARD-CP-531, 31 papers
ISBN 92-835-0701-X, 1993

[90-5] J. Wilson & R.J. Hussey: RJ Technical Consultants, (F)
'Structural Health Monitoring Techniques & Potential Application to RLV Composite Primary Structures & Cryogenic Tanks'
Report No. RJTC-046-SHM (September 1999)
ESA Contract 10983/94/NL/PP - Work Order No. 16

[90-6] Dr. R. Graue & A. Reutlinger: Kayser-Threade, (D)
'Structural Health Monitoring for Future Launchers: Results from Breadboarding and Prototype Development'
Proceedings of the 3rd European Conference on Launcher Technology, Strasbourg. 11th – 14th December 2001, p755-766

[90-7] T. Melz
Adaptronik in der Raumfahrt, Bedarf und Potential
Adaptronics in space applications
DLR-IB 131-2000-19, July 2000, Braunschweig

[90-8] T. Melz
Entwicklung und Qualifikation modularer Satellitensubsysteme zur adaptiven Vibrationskompensation an mechanischen Kryokühlern
PHD thesis, Darmstadt, 2002

91 Smart system constituents

91.1 Overview

91.1.1 Introduction

Over the years, developments in smart technology have investigated numerous materials with potentially usable sensory or actuator effects. Some are well-known and have been successfully exploited in sensors and actuators within devices and mechanisms in space, whereas some other materials are more recent innovations.

91.1.2 Application classes for sensors and actuators

For the selection of suitable smart materials for smart structures, some of the main considerations can be summarised as:

- capabilities of the material itself, e.g. stress-strain, force, energy-related characteristics,
- forms of materials, e.g. liquid, solid (rigid or flexible), films or sheets, fibre-forms,
- status, i.e. availability of materials or devices; proven or development,
- function, which covers:
  - application, e.g. measurement (sensors); deployment, shape-control, vibration control.
  - use, e.g. sensor, actuator or a combined sensor-actuator is necessary.
- structure, e.g. applied or integrated into a conventional space structure made of metal or composite; ultra lightweight structures made from a variety of thin, flexible materials, where mass is a prime design driver.
- integration into, or onto, a structure, including: mass, power demands for sensors and actuators, control equipment, calibration, testing, maintenance and long-term reliability.

Actuators and sensors are used widely in every spacecraft for a variety of different applications. A major characteristic of an actuator or sensor system is the force (or stress) versus displacement (or strain) ratio.

Figure 91.1.1 provides a general classification scheme in which examples of space applications are shown in relation to the necessary force-displacement ratio.

Other means of classifying the performance of such systems can be used, e.g.:

- ratio of energy versus frequency,
- shape control (quasi-static) versus vibration control (damping),
- structural health-related aspects for the integrity of structures.

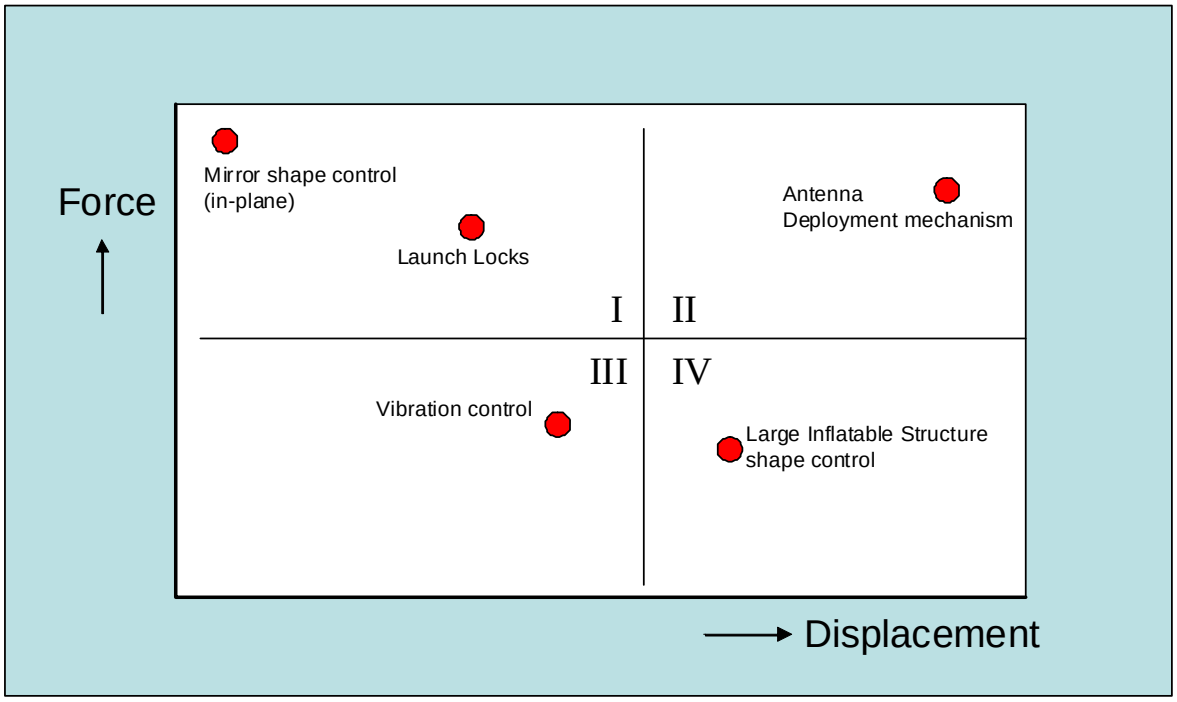

Figure 91.1-1 – Smart materials: General classification of sensor and actuator capabilities for types of structures

91.1.3 Types of smart materials

91.1.3.1 General

A very wide range of different material types are described as 'smart' because they exhibit particular characteristics, e.g.:

- shape memory (metals and polymers)
- piezoelectric (ceramics and polymers),

Excluding materials used in conventional devices, e.g. thermocouples and strain gauges, Table 91.1.1 lists various materials that have been considered, to some extent, over the years for use in smart technologies, either as sensors, as actuators or as both.

Table 91.1-1 – Smart materials: Summary materials and possible uses

Material	Type	Applications
Silicon	Semiconductor	microsensors (pressure, vibration, acceleration)
PZT lead-zirconate-titanate	Piezoelectric ceramics (wafers or fibres), [See: 91.3]	wafers: sensors (acceleration, acoustic emission) actuators. Fibres: sensors, actuators
PVdF	Piezoelectric polymers, [See: 91.3]	sensors
Glasses	Fibre optics, [See: 91.4]	sensors (temperature, strain, hydrogen, crack and damage detection)
NiTi-alloys; C-based alloys (Cu-Zn-Al; Cu-Al-Ni)	Shape memory alloys, [See: 91.5]	actuators
PMN – lead-magnesium-niobate (ceramic)	Electrostrictive, [See: 91.5]	actuators
Terbium-iron alloys	Magnetostrictive, [See: 91.5]	actuators
Various combinations of fine dispersed particles in non-conducting liquids	ER electrorheological fluids, [See: 91.5]:	actuators (damping; coupling)
Various polymers and elastomers	EAP electroactive polymers, [See: 91.9]: Ionic; Electronic	actuators

91.1.3.2 Development status

Table 91.1.2 summarises the basic performance characteristics and development status for a range of smart materials, Ref. [91-24].

Table 91.1-2 – Smart materials: Summary of performance and development status

Smart Material	Energy-density	Specific Power-Density	Force	Strain	Response	Efficiency	State of the art
Piezoelectric	low	high	large	small	quick	high	Batch Production (Material & Systems)
Magnetostrictive	low	medium	large	small	quick	medium	Military Applications
Shape Memory Alloys	high	medium	large	medium	slow	low	Batch Production (Material)
Shape Memory Polymers	medium	medium	medium	large	slow	low	Early Development stage
Electrostrictive Polymers	medium	high	large	medium	quick	high	Early Development stage
Dielectric Elastomers	medium	medium	medium	large	quick	high	Sophisticated Prototype stage
Conducting Polymers	high	medium	large	medium	slow	low	Lab Scale Prototypes
Responding Gel/ Ionic Polymer Metal Composite	low	low	small	large	slow	medium	Lab Scale Prototypes
Carbon Nanotubes	medium	high	medium	medium	medium	medium	Early Development stage

For actuators, in recent years, interest has focussed on:

- piezoceramic materials; mainly PZT lead-zirconate-titanate, [See: 91.5]
- shape memory alloys; nickel-titanium alloy 'Nitinol', [See: 91.5]
- magnetostrictive materials, [See: 91.5; 91.9]

These materials all generate strong actuator forces, but with very low displacements, e.g. about 0.1% for magnetostrictive and piezoceramics. SMA shape memory alloys exhibit a switching effect not a continuous displacement. In general, the technology of these ceramic and metallic materials is relatively mature with various products commercially-available. A problem for adaptive structures is their mass and rigidity.

For composites, some alternative materials are also of interest, e.g.

- piezoceramic fibres, comprising of parallel arrangements of PZT piezo fibres embedded in a polymer matrix to form a composite. These materials, of which there are several variants, can be used as sensors or actuators. An advantage of piezo fibre composites for use in space applications is that the stiffness and mass are lower than conventional piezoceramic materials, [See: 91.5].
- EAP (electroactive polymers), which refers to a very large number of comparatively flexible and lightweight materials. A common classification for EAPs is related to the electrochemical processes that occur during use, i.e. ionic and electronic. Some thermally-responsive variants also exist, [See: 91.9].

91.1.3.3 Performance capabilities

Figure 91.1.2 summarises the performance capabilities of some smart materials commonly considered for sensors and actuators, compared with respect to:

- energy density (from stress-strain),

- specific power density (from specific energy density v. frequency).

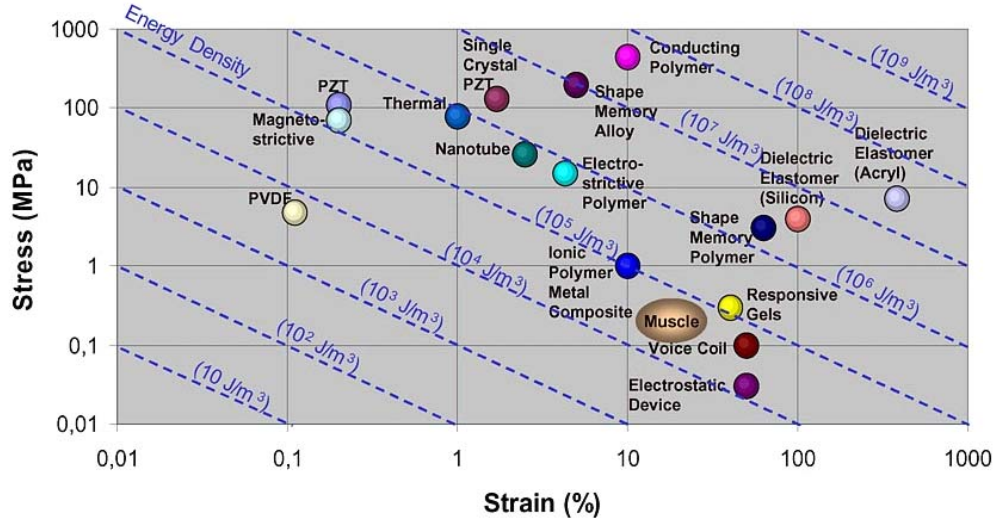

Energy density property diagram for sensor and actuator smart materials; stress-strain

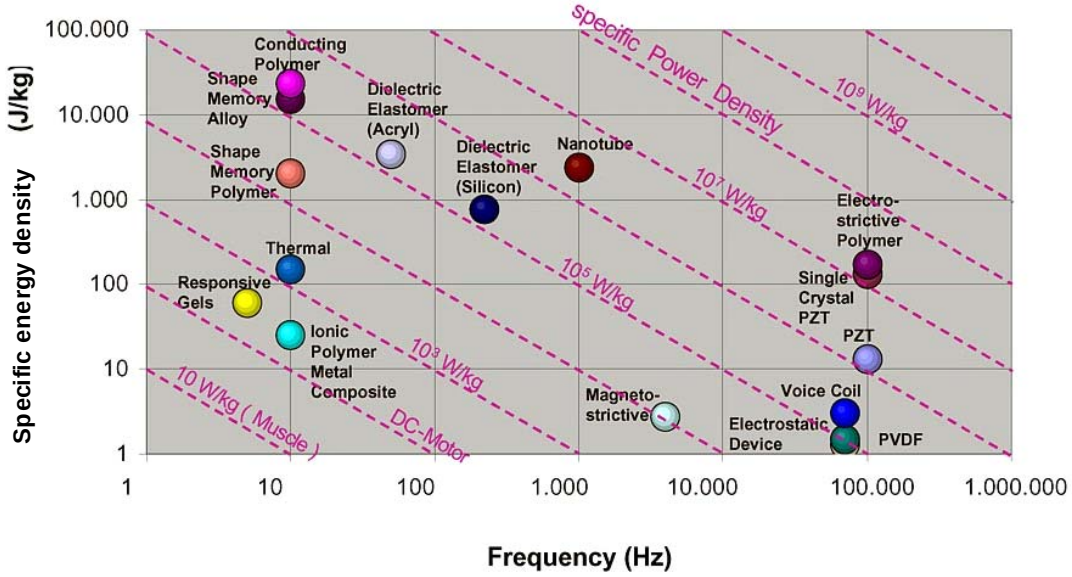

Specific power density property diagram for sensor and actuator smart materials; specific energy density v frequency

Figure 91.1-2 – Smart materials: Summary of performance capabilities

91.2 Sensors

91.2.1 General

A sensor is a device which provides a signal for either detecting or measuring a physical property to which it responds, Ref. [91-3].

The sensor responds by:

- transmitting the information,
- initiating change, or
- operating controls.

This is a similar definition to that of a transducer, e.g.:

- pressure transducers, which convert pressure into a voltage output.
- linear variable differential transformers (LVDT).

Sensors and transducers are terms which have a different emphasis depending on who is applying the technology. The terms detector, gauge and pickup have similar definitions.

91.2.2 Strain gauges

Mechanical strain gauges have been used for many years to accurately measure strains in materials and components. Surface bonded gauges have become miniaturised and micro-directional rosettes are commonly used.

Strain gauges rely on a thin film of metal being stretched elastically such a way that its electrical resistance changes linearly with strain. A direct conversion of resistance to strain can be easily calculated. Compensation for temperature variations is usually needed, with an unstrained gauge used as a reference.

Considerations for the use of strain gauges includes:

- the presence of strain gauges on structures provides confidence that the actual strains incurred are comparable with those anticipated at the design stage.
- strain gauges require hard wiring with two wires per gauge. This limits the number of gauges (and associated wiring) which can be realistically added to the structure.
- strain gauges only measure the strain at the immediate point of connection and in the planar direction of their orientation.
- they provide useful reference points for comparison with other less proven sensors, such as fibre optics.

91.2.3 Thermocouples

Thermocouples measure temperature at the immediate point of placement. The use of a metal couple produces an electrical voltage which is dependent on the temperature at the coupling point. The interrogation of a thermocouple is simple and accurate, provided the necessary calibration is undertaken before installation.

Thermocouples are best used under equilibrium temperature conditions. Where temperature fluctuations occur in and around a structure a single thermocouple cannot provide sufficient information. Also the thermal inertia of a thermocouple can differ from the structural material it is embedded in, hence a temperature lag can exist between the two in non-equilibrium conditions.

Conventional thermocouples have limitations in responding to dynamic conditions and the associated electrical circuitry is bulky. Again, their presence can provide a proven reference point for comparison with new, unfamiliar sensors.

91.2.4 Accelerometers

Measurable vibration effects can be grouped as, Ref. [91-3]:

- displacement,
- acceleration, and
- velocity.

Vibration is measured in terms of:

- frequency,
- amplitude,
- phase angle,
- form, and
- shape.

Acceleration is the rate of change of velocity. Both velocity and acceleration are vector quantities, having magnitude and direction. An accelerometer is a transducer that responds to this acceleration in one or more axes.

Popular variable resistance type accelerometers that rely on an electromechanical response are:

- slide-wire potentiometer,
- strain gauge, or
- piezoelectric element.

Piezoelectric devices rely on an inertial mass to impose a fluctuating force on a piezoelectric crystal. The voltage generated by the is proportional to the acceleration over a broad frequency range. The system has no moving parts and is less prone to damage than earlier accelerometers that relied on spring and damping mechanisms.

Accelerometers can providing useful data on events causing vibration in space structures, and in defining a vibration frequency spectrum.

91.2.5 Microsensors

This term has appeared in recent years to describe a group of devices produced by the micro-machining of silicon. This is also known as 'microengineering'.

As an extension of advanced integrated circuit (IC) technologies, it is feasible to fabricate millimetre-sized, three-dimensional mechanical devices with micron-sized features.

The ability to preferentially etch specific planes in the silicon microstructure can incorporate features such as diaphragms or resonant beams.

Sensors can be made to measure:

- pressure,
- vibration, and
- acceleration.

Such devices have greatly reduced mass and volume, compared with more obtrusive traditional sensors.

The technology can be taken a step further to provide an integrated device with all the necessary interconnections to relays and the overall interpretative or control systems.

The use of such sensors in space programmes is attractive, as multiple dispersed units avoid significant weight penalties, whilst offering options for comprehensive monitoring of complex structures. Embedding microsensors in composites has also been proposed.

91.3 Piezoelectric sensors

91.3.1 Features

Piezoelectric materials produce, Ref. [93-1], [93-2]:

- an electric field if mechanically strained, or conversely
- elastic deformation if an electric field is applied.

They therefore possess both sensory and actuating attributes.

[See: 91.8 for piezo-based actuators]

91.3.2 Materials

The most common piezoelectric materials are:

- single crystals of lithium niobate ($LiNbO_3$).
- single crystals of quartz (SiO_2).
- polycrystalline ferroelectric ceramics:
  - Barium titanate ($BaTiO_3$)
  - PZT (lead zirconate titanate).
- polyvinylidene fluoride (PVDF) polymer.

The piezoceramics (inorganic materials) are normally processed from powders and can be readily moulded and pressed into shape.

PVDF is usually prepared as thin, flexible, films, which are then metallised to provide electrical connections.

91.3.3 Terminology

Common terms associated with piezoelectricity include:

- Ferroelectricity: Defined as the reversibility in the dielectric dipole of a polar crystal by means of an applied field.
- Pyroelectricity: Development of electric polarisation in special classes of crystals when subjected to a temperature change.

- Electrostriction: A weaker effect than piezoelectricity, where the induced strain deformation is dependent on even powers of the applied electric field and is independent of field polarity. All dielectrics exhibit this behaviour.
- Electric poling: The action of applying a strong electric field to orientate the dipoles within a ferroelectric ceramic as it is cooled through the ferroelectric transformation point. A similar process is applied to PVDF film as it cools.
- Curie point: The temperature at which a material begins to lose its piezoelectric characteristics. Once lost the process is irreversible, though the material can be recoverable by re-poling.

91.3.4 Manufacture

The manufacture of commercial piezoelectric materials involves taking the material to elevated or high temperatures while imposing a high-intensity electric field in a desired direction, i.e. the process of poling.

91.3.5 Properties

91.3.5.1 General

Piezoelectric materials are electrically and mechanically anisotropic, hence their responses are directional.

Data for different types of piezoelectric materials are shown in Table 91.3.1 for piezoceramics and Table 91.3.2 for PVDF, Ref. [91-2].

Commercial sources for piezoceramics and property data are given in Ref. [91-23].

Table 91.3-1 - Ceramic piezoelectric materials: Indicative properties

Property		Ceramic piezoelectric material		
		PVDF	PZT	$BaTiO_3$
Density	(kg/m^3)	1780	7500	5700
Relative permittivity	($\varepsilon/\varepsilon_0$)	12	1200	1700
d_{31} constant	(10^{-12} m/V)	23	110	78
g_{31} constant	(10^{-3} Vm/N)	216	10	5
k_{31} constant	(% at 1kHz)	12	30	21
E, Young's modulus	(GPa)	2 to 3	63	-
Temperature range	(°C)	-40 to +90	<190	-
Max. electric field	(10^6 V/m)	40	0.6	-
Curie point	(°C)	100	190	-

Key: Crystallographic axes determine the piezoelectric operation modes:
1: X-axis 2: Y-axis 3: Z-axis
d = strain/applied field or piezoelectric strain constant
g = field/applied stress or piezoelectric stress constant
Suffixes:
1 - applied stress, or induced strain in the 1 direction.
3 - indicates that the electrodes are perpendicular to the 3-axis.

Table 91.3-2 - Piezoelectric PVDF: Typical properties

Property		PVDF
Compressive strength	(MPa)	60
Tensile strength: MD	(MPa)	160 to 300
TD	(MPa)	30 to 35
Water absorption	(% water)	0.02
Max. operating voltage	(V/μm)	30
Breakdown voltage	(V/μm)	100
C Capacitance	(pF/cm^2)	380 †
c_v Speed of sound	(10^3 m/s)	1.5 to 2.2 ‡
d_{33} Piezoelectric strain constant	(10^{-12} m/V)	-33
g_{33} Piezoelectric stress constant	(10^{-3} Vm/N)	-339
k_{33} Electromagnetic coupling factor	(% at 1 kHz)	19
t thickness	(μm)	9, 28, 52, 110, 220, 800
ε Permitivity	(10^{12} F/m)	106 to 113
Pe Volume resistivity	(Ωm)	10^{13}
tan δ_e Loss tangent	(at 10^1 to 10^4 Hz)	0.015 to 0.2

Ke †: for 28μm film, $\varepsilon/\varepsilon_o = 12$

‡: transverse thickness

91.3.5.2 Characteristics

A number of points can be highlighted, including:

- PVDF films are robust and flexible but of low modulus. In comparison, the piezoelectric ceramics are rigid and brittle, but less durable with higher densities.
- Piezoelectric characteristics are only shown at temperatures below the Curie point. For PVDF, this limits the potential applications to below 90°C.
- PVDF and PZT develop an electrical charge proportional to the change in mechanical loading, i.e. they are dynamic materials. PVDF can respond at higher frequencies than PZT.
- The high rigidity of ceramic elements ensures that electrical energy is efficiently converted into mechanical energy which ensures good actuation capabilities.
- PVDF has a low charge characteristic, implying weak electro-mechanical performance compared with the ceramics in low frequency applications and near resonant frequencies.
- PVDF elements are more sensitive to mechanical loads over a wider range of loading conditions than piezoceramics. Consequently they are good candidates for sensor applications. The pressure sensitivity can range from micro-torr to mega-bar.
- PVDF films have wide-band, frequency-dependent characteristics (Hz to GHz), depending on film thickness. A 28μm sheet has a fundamental resonant frequency near 40MHz; very thin films resonate in the GHz range.

- The relative dielectric permittivity of PVDF is typically of the order of 12, while piezoceramics are 1200 or higher. Consequently, the piezoelectric stress constant (g_{31}) is typically 20 times greater than that for the piezoceramics.
- Having a high dielectric strength (40000 V/µm) compared with piezoceramics (2 V/µm), PVDF can be exposed to much higher electric fields than the ceramics.
- The low modulus of PVDF (2 GPa) renders it ineffective for electromechanical actuators at low frequencies.
- PVDF is appropriate for sensors, whilst PZT is attractive for actuating materials.

[See also: 91.8 for piezo actuators; 91.9 for PVDF]

91.4 Fibre optic sensors (FOS)

91.4.1 Features

Fibre optic sensors (FOS) have better capabilities for the interrogation of structures than conventional single-point sensors, such as thermocouples or strain gauges, Ref. [91-1], [91-2], [91-4].

The advantages include, Ref. [91-18]:

- small size and low mass, including the connectors.
- intrinsically safe and chemically inert.
- high sensitivity, large bandwidth, high resolution.
- installation-related:
  - flexibility; continuous fibres can be looped around a structure.
- signal-related:
  - ease of remote transmission.
  - multiplexing capability: multiplexing several positions along one fibre optic can significantly reduce the front-end electronics and harness needed.

Fibre optics are immune to interference from electromagnetic radiation, which is useful in integrated structures such as aircraft and spacecraft.

Some of the disadvantages of FOS and their systems are, Ref. [91-18]:

- difficulty in replacing or repairing failed sensors, especially embedded sensors where it is almost impossible.
- joining requirements for large arrays.
- more complex signal processing techniques required, compared with purely electronic systems.
- material properties and long-term characteristics: any effects should be evaluated for sensors embedded in composite materials.
- durability and reliability: for sensors integrated into structures during their manufacture and assembly. Some redundancy should be designed-in from the start.

Given these application-based complications, the attractions of FOS-based systems either:

- serial arrays of fibres: Each monitoring a single point, connected by a single fibre optic sensor bus to give a quasi-distributed sensor, or
- fully distributed sensor: With several monitoring points along a single length of optical fibre that can be interrogated individually. This enables the monitoring of any changes in the measurand along the fibre optic path.

A distributed sensor is attractive in using a single telemetry channel carrying signals which can be resolved to describe many (hundreds) of points along the fibre. Systems based on such sensors are under development for health monitoring systems, Ref. [91-18], [91-19]. Terminology associated with the science and technology of fibre optics is given in Ref. [91-22].

91.4.2 Types of fibre optic sensors (FOS)

91.4.2.1 General

In fibre optic sensors, the magnitude of the measurand is gauged by the size of its influence on some property of the light propagating along the fibre, e.g.:

- amplitude,
- phase,
- polarisation,
- frequency.

Sensors are either 'extrinsic' or 'intrinsic'. Their basic characteristics are summarised in Table 91.4.1.

Table 91.4-1 - Fibre optic sensors: Basic characteristics of types

Intrinsic: Fibre as sensing element
• Propagation delay • Transmission: - Intensity - Spectrum - Modal power distribution • Backscatter (OTDR) † • Polarisation • Light generation in fibre
Extrinsic: Fibre-compatible sensors
• Light collecting • Intensity modulation • Reflective • Light scattering • Spectral filtering • Energy transition • Polarisation
Evanescent field sensors
• Unclad fibre • Reactive fibre cladding • Polished half coupler • Integrated optics • Plasmon resonance
Key: † Optical time domain reflectometry

A schematic diagram of each of the basic types of FOS is given in Figure 91.4.1.

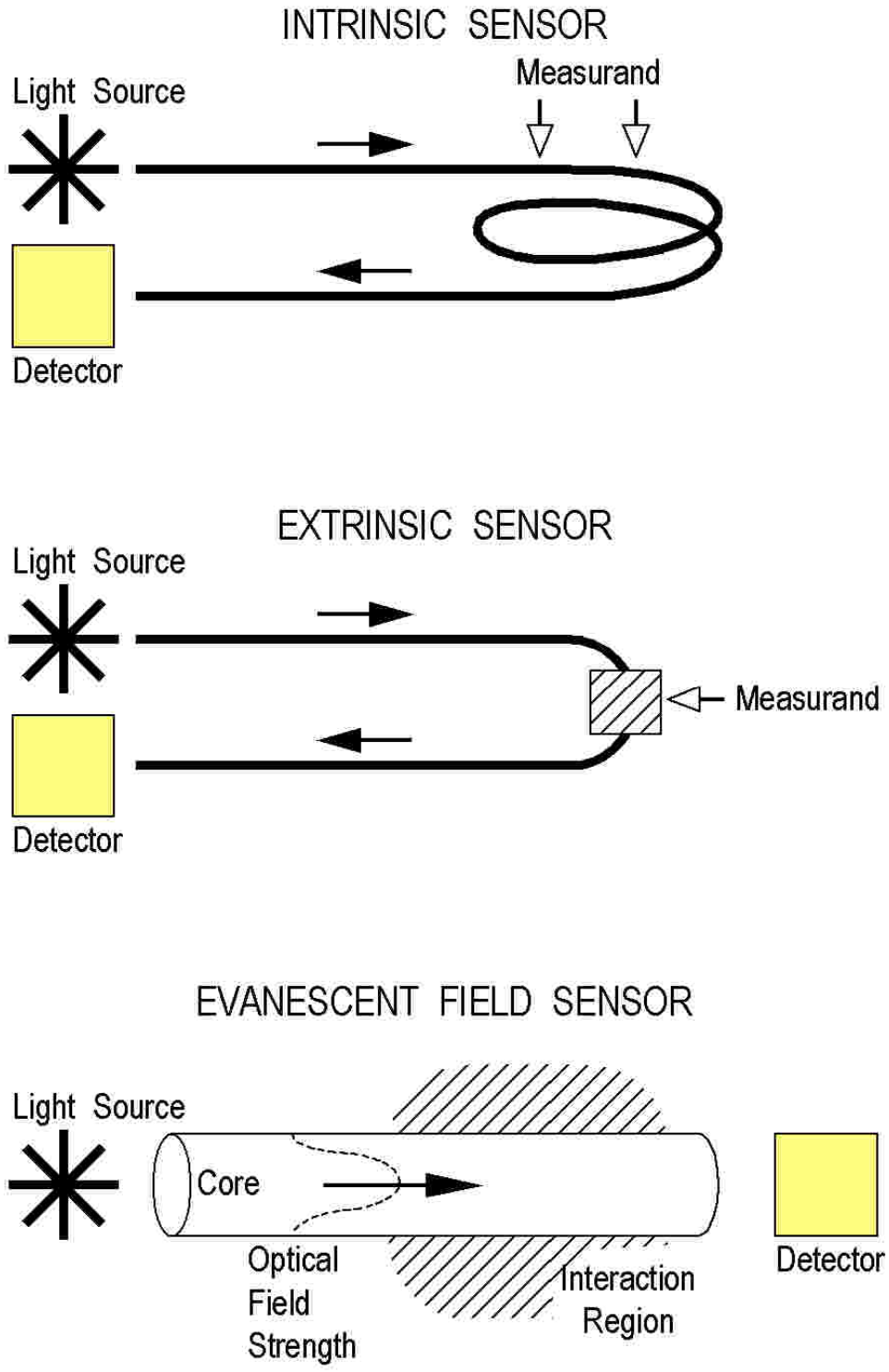

Figure 91.4-1 - Fibre optic sensors: Basic types

91.4.2.2 Extrinsic sensors

The light leaves one fibre, experiences the measurand externally, and then enters another (or re-enters the same) fibre for transmission to the diagnostic instrumentation, [See: Figure 91.4.1].

91.4.2.3 Intrinsic sensors

Of more immediate use are 'intrinsic' sensors, where interaction between the light and the measurand takes place within the fibre itself. Of necessity, distributed fibre optic sensors should be intrinsic devices, [See: Figure 91.4.1].

91.4.2.4 Evanescent field sensor

These types of sensor [See: Figure 91.4.1] detect changes in the evanescent field that occurs outside the fibre, but which is generated and coupled to some component of the light travelling within the fibre core, Ref. [91-22]. In communications applications, evanescent waves can be transferred from one unclad fibre optic to an adjacent, but not physically connected, one.

91.4.2.5 Data gathering and transmission

There are two main methods by which a distributed sensor is able to determine spatial information concerning the measurand:

- time domain: propagation times are measured directly,
- frequency domain: detected by a frequency modulated continuous wave.

Both rely on differences in propagation time for light reaching different locations.

91.4.3 Technical background

91.4.3.1 Light transmission

Optical fibres work on the principle of total internal reflection, according to Snell's Law.

Figure 91.4.2 illustrates this effect using a simple ray-path model, Ref. [91-1].

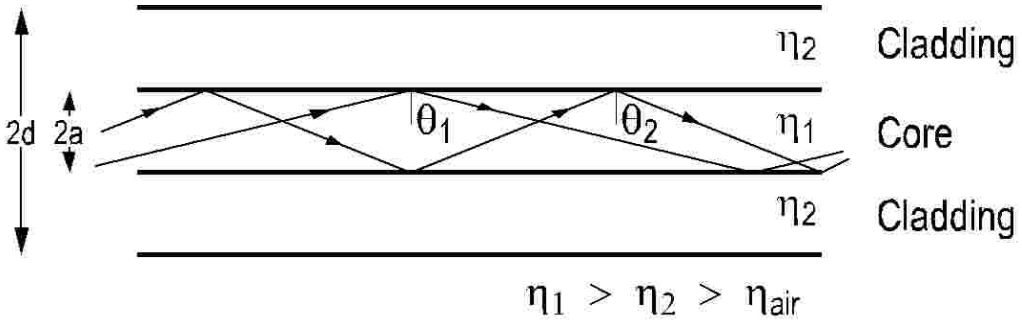

Figure 91.4-2 - Multi-mode optical fibre: Principle of wave guidance by total internal reflection

The ray model indicates that light propagates along the fibre by multiple reflections from the core-cladding interface. The ray represents the direction of a plane wave front and it is essential that on each reflection the wave fronts remain in phase. This defines a discrete set of paths (modes) along which the light can travel.

Different wave modes passing along the same fibre, are distinguished by different angles of incidence at the core-cladding interface. The number of modes transmitted is limited. The most effective way to reduce the number of allowable modes is to reduce the core diameter until it approaches the same order of magnitude as the wavelength of the light transmitted.

91.4.3.2 Fibre optic construction

The two main types of fibre optics are:

- single or mono-mode fibres: Commercially available fibre typically has a core diameter of 5µm to 10µm, surrounded by cladding with an external diameter of about 150µm.
- multi-mode fibres: With a much larger core, usually in the range 50µm to 100µm, with cladding thickness adjusted accordingly.

In most practical applications, the core and cladding layers are surrounded by a protective outer polymeric coating up to 100µm in thickness. For sensing applications the overall 'optical fibre' diameter ranges from 250µm to 500µm.

Figure 91.4.3 shows light transmission in single and multi-mode fibres.

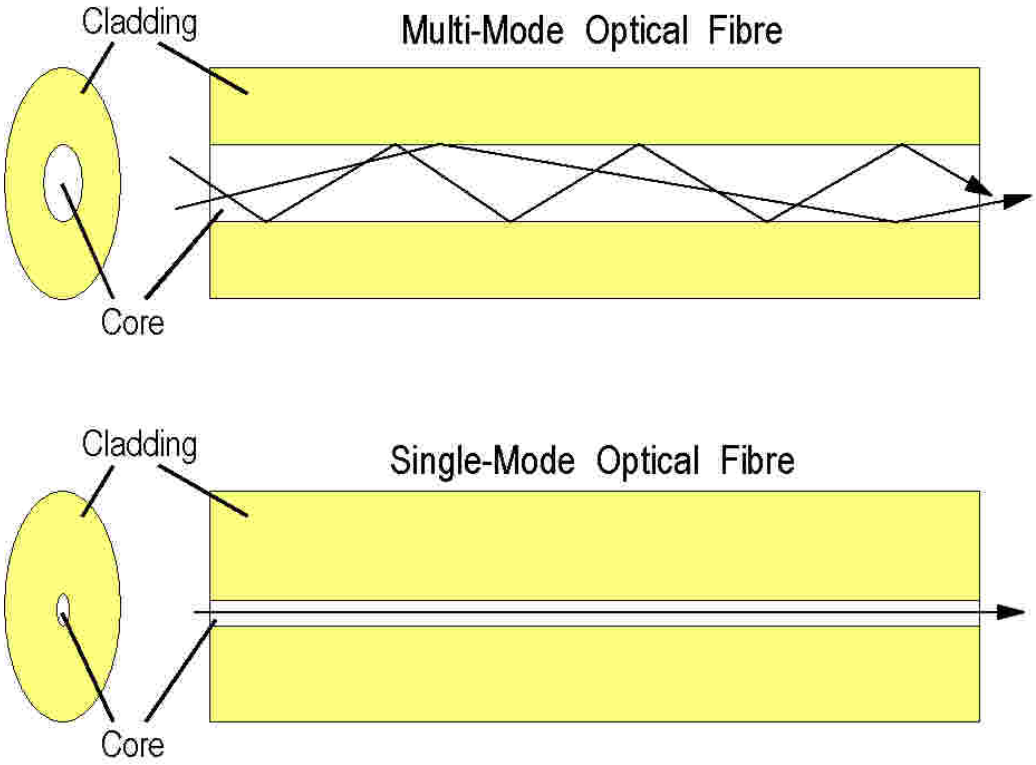

Figure 91.4-3 - Single and multi-mode fibre optics: Light transmission

The overall fibre optic diameter is similar in thickness to that of fabric or UD fibre-reinforced plastic (FRP) plies, e.g. usually 125µm to 300µm. There is at least an order of magnitude difference compared with carbon (8µm) and glass (13µm) fibre reinforcements.

91.4.3.3 Signal mode and transmission

By careful arrangement of equipment, it is possible to direct well defined polarised light into an optical fibre as either:

- pulses, or
- continuous wave.

For multi-mode and standard single-mode fibres, the optical signal emerge after transmission with a polarisation state which is both undefined and variable. However, specially configured single-mode fibres can be produced which propagate light while maintaining two orthogonal polarisation states. Since these two polarisations travel with different velocities, the fibre is said to be birefringent.

91.4.3.4 Birefringence

Birefringence is defined by the beat length, which is the length of fibre over which the two polarisation modes slip relative phase by 2π radians, i.e. a shift of 1 wavelength. Beat lengths >1mm are common.

There are two principal ways of producing highly birefringent, or 'HiBi' fibres:

- elliptical, rather than circular, core cross-section. Two transmission modes then exist with their planes of polarisation parallel to the long and short axes of the elliptical fibre.
- axially non-symmetric stresses in the core during manufacture. All polarisation maintaining optical fibres have very small cores, typically less than 3µm in diameter. Such fibres can be used in two-lead or single-ended polarimetric configurations, as shown in Figure 91.4.4.

  Method used by York Fibres & Sensors, Southampton (UK)

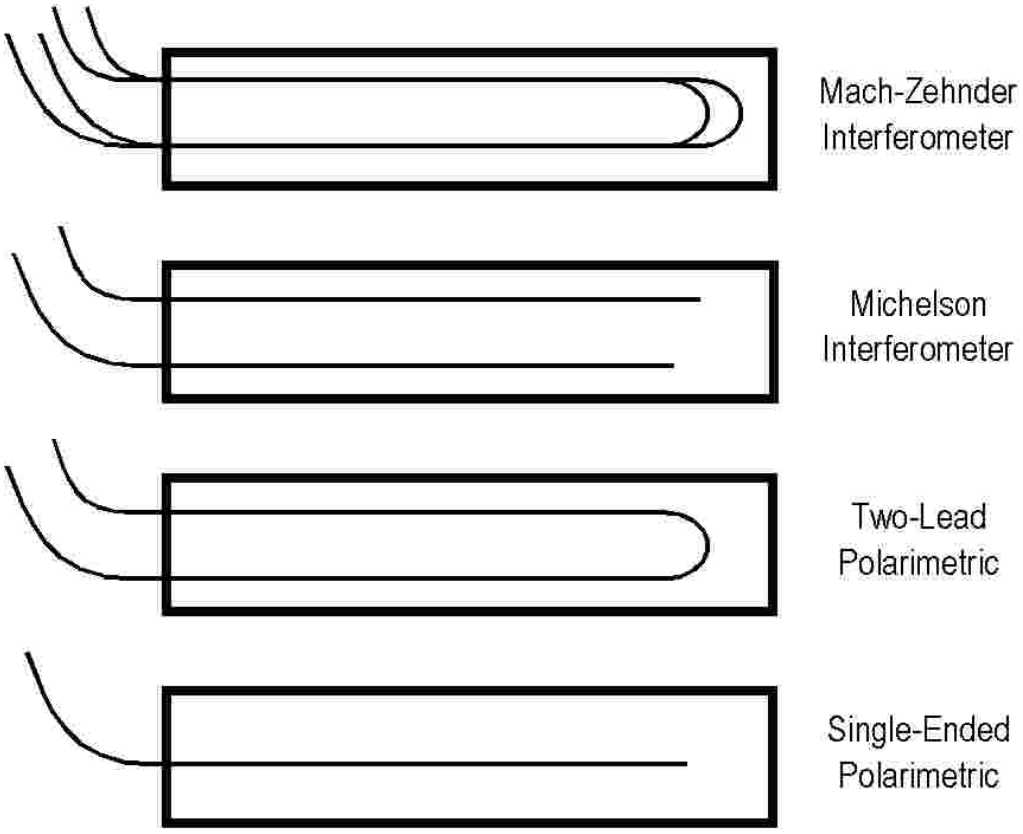

Figure 91.4-4 - Fibre optic sensors: Configurations

91.4.3.5 Interference

If two coherent sources of light are combined, interference patterns will result. The best way to produce two coherent waves is to split the output from a single laser source. This is the approach taken in devices known as interferometers. The paths travelled from the point of splitting to the

point of recombination are the two 'arms' of the interferometer. If one light path is kept fixed as a 'reference' arm and the other light path is subject to some form of change, such as length, then changes can be detected from the effect that they have on the re-combined interference pattern.

91.4.4 Interferometers

Interferometers are useful practical tools in the application of 'conventional', i.e. unguided optics. Several different configurations have been devised of which the most common types are:

- Mach-Zehnder,
- Michelson,
- Fabry-Pérot.

The generic layouts for all of the fibre optic versions produced are shown in Figure 91.4.5, Figure 91.4.6 and Figure 91.4.7, respectively, Ref. [91-1].

Each diagram shows the basic sensors, but does not convey all the complexities of forming a system, e.g. including light source (laser), couplers, connectors, signal conversion units and output displays.

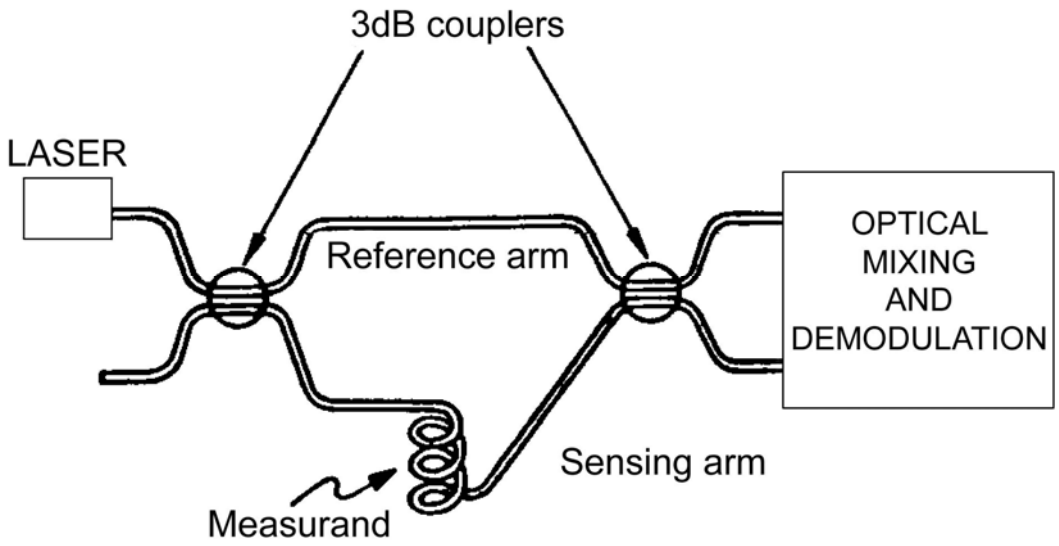

Figure 91.4-5 - Fibre optic interferometers: Generic configuration of Mach-Zehnder type

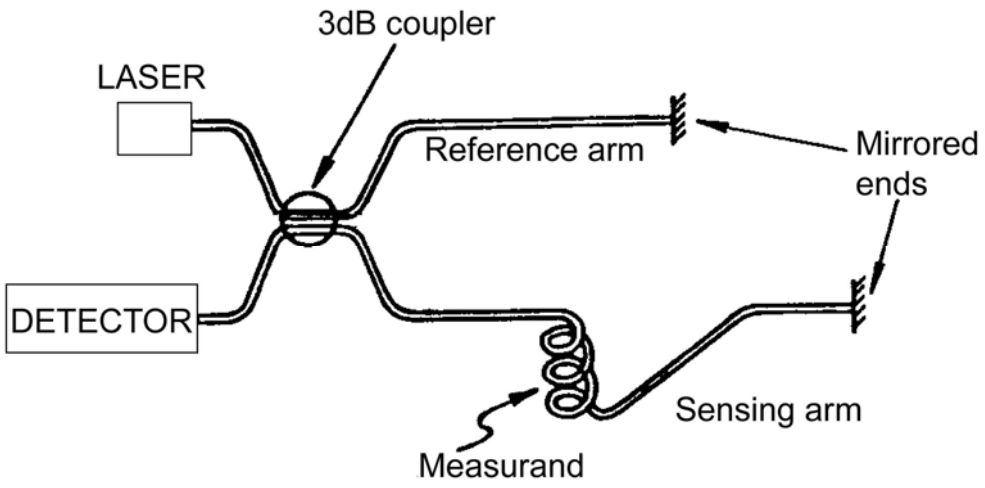

Figure 91.4-6 - Fibre optic interferometers: Generic configuration of Michelson type

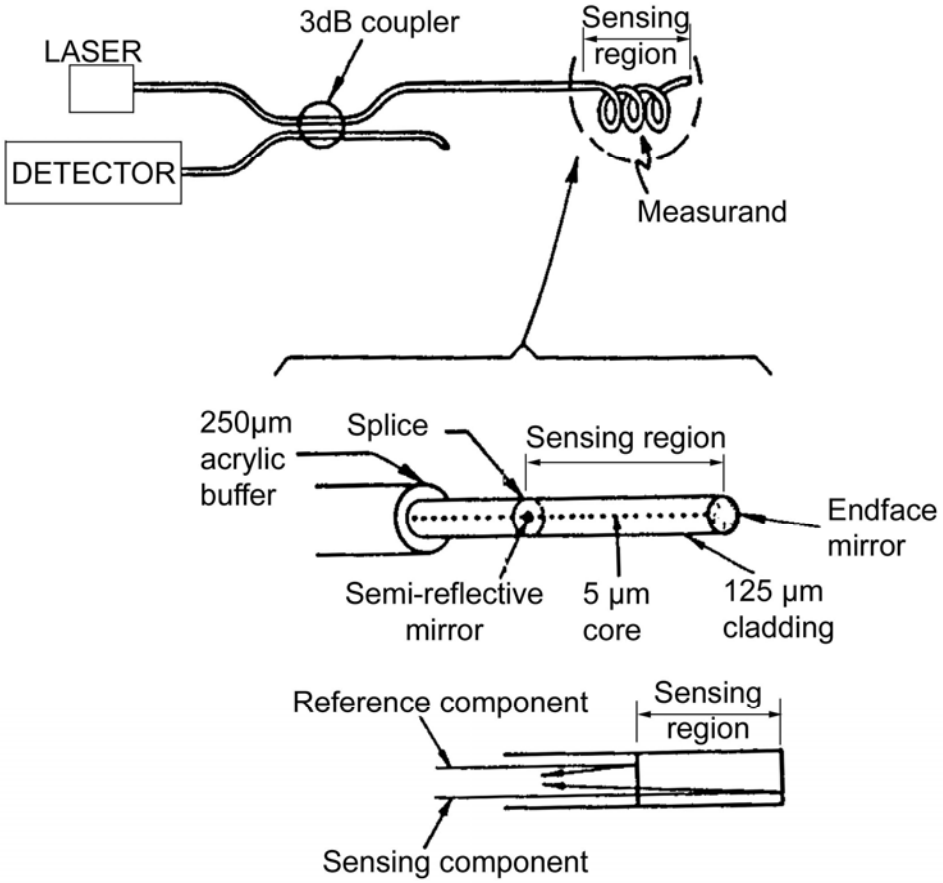

Figure 91.4-7 - Fibre optic interferometers: Generic configuration of Fabry-Pérot type

The advantage of fibre optic interferometers is their compact size, and that the two arms need no longer consist of straight light paths, but can be routed to whatever geometry desired. It is even possible to produce fibre optic interferometers in which the two arms are formed from two modes passing along the same fibre.

Interferometry is a very important technique in the development of fibre optic sensors (FOS). In such devices the magnitude of a measurand is detected from the effect that it has on one arm of a fibre optic interferometer. In classical interferometers, the effect detected is almost always a simple change in arm length, and it is true that fibre optic sensors based on interferometers are most often used to measure strain. However, the physical requirement for an interferometric effect is merely that a change in phase be introduced into one arm, and with fibre optics this can be achieved by a variety of interactions in addition to strain along the fibre axis. Fibre optic interferometers can therefore be used to detect a range of different measurands.

91.4.5 Bragg grating

91.4.5.1 General

A sensor employing a Bragg grating can also be used for distributed sensing. A section of fibre is illuminated by converging UV light beams to achieve a photo-refractive effect, this gives a periodic variation in refractive index along the core of the fibre. The grating structure reflects a narrow band of light having a peak reflective wavelength corresponding to the Bragg equation. This is the condition where reflection from each small refractive index perturbation adds coherently with that reflected from its neighbours, such that all reflected waves reinforce. The peak wavelength of reflection varies with strain, due both to the physical extension of the grating and the changes in refractive index of the glass due to the elasto-optic effect, i.e. the strain induced change in the effective wavelength of light within the optical waveguide.

91.4.5.2 Strain measurement

These types of fibre optic sensors (FOS) are generally described as OFBG 'Optical fibre bragg grating' or IFBG 'In-fibre Bragg grating'.

The length of a photo-imprinted grating can vary from 1mm to several cm. The gauge lengths for these sensors can be either long (cm to m lengths) or short (mm to cm lengths). A large number of gratings may be present within one fibre optic sensor to allow distributed, single-point strain measurements, e.g. 50 gratings in 7m length, Ref. [91-18].

91.4.5.3 Hydrogen presence

Bragg gratings can be used to monitor the presence of hydrogen. Here, the Bragg grating is bonded to palladium. The reversible absorption of hydrogen by the palladium, to form a hydride, produces a deformation, or strain, measured by the grating, Ref. [91-18].

91.4.6 Backscattering

91.4.6.1 Rayleigh

When light passes along an optical fibre, at any given point the majority of the signal propagates 'forward' (away from the launch point), but a small proportion is scattered 'backward' (towards the launch point). This is known as the 'Rayleigh Backscattered Signal', and has an intensity approximately 10-5 times (50dB) less than the signal in the forward direction.

91.4.6.2 Raman

Most of the backscattered signal returns at the same frequency as the light originally launched. However, some of the light exchanges energy with atoms in the fibre core during backscattering, and therefore returns with a frequency shift.

The shifted frequencies lie equidistant from the launch frequency, forming two bands centred on the 'Raman' frequencies. These have an intensity approximately 30dB less than the Rayleigh backscattered signal. The lower frequencies are the 'Stokes' band and the higher frequencies the 'Anti-Stokes' band.

The difference between the Raman and launch frequencies depends on the material properties of the fibre core, whereas the ratio between the intensities of the Stokes and Anti-Stokes bands is temperature dependent. This principle is used for FOS distributed temperature measurements, Ref. [91-18].

91.4.7 Optical time domain reflectometry (OTDR)

91.4.7.1 General

A narrow pulse of light is launched into an optical fibre and the backscattered signal monitored over a period of time. The backscattered signal, at a given moment, is characteristic of the backscattering process at some particular point along the length of the fibre.

If the propagation velocity of the pulse is known, the correlation between different portions of the backscattered signal-time characteristic and different positions along the fibre can be established quantitatively. This is the principle underlying a technique known as OTDR - optical time domain reflectometry. This technique was first developed as a method of locating breaks or damage in optical fibre communications networks, i.e. unacceptable signal attenuation

91.4.7.2 Crack detection

Early OTDR-based sensors used the break in an optical fibre, caused by cracking of the structure, to locate the crack position, e.g. by measuring the time-of-flight of the returning signal.

A further development of the technique measures the signal loss in an intact optical fibre due to localised microbending caused by a crack occurring or opening in a structure, as summarised in Figure 91.4.8 for a development civil engineering application, Ref. [91-18].

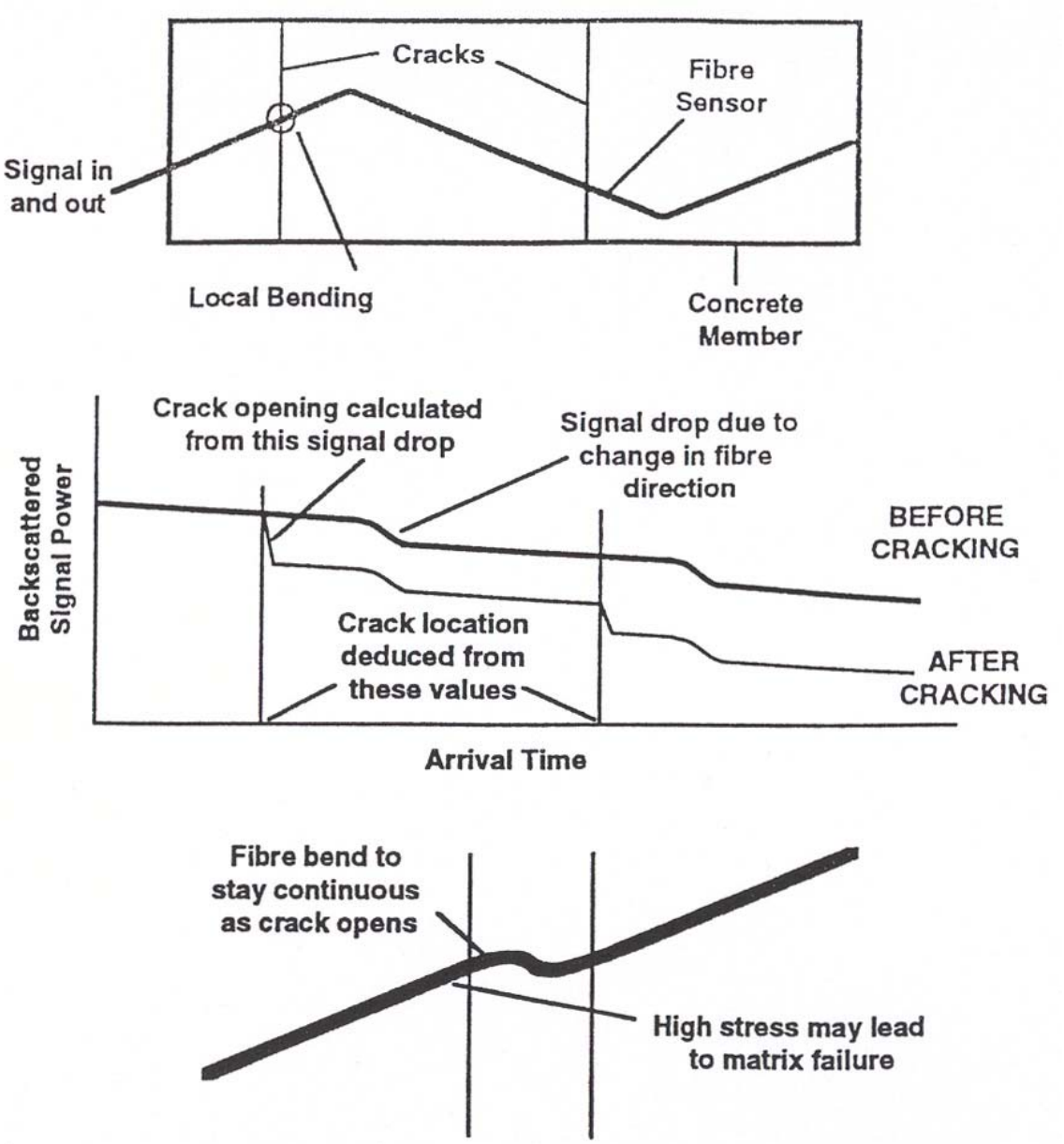

Figure 91.4-8 - Fibre optic sensors: Optical time domain reflectometry (OTDR) – Crack detection

Here, the FOS are surface mounted or embedded in the structure. They are orientated in different directions so as to bridge any cracks (existing or new). The signal loss can be related to time-of-flight and so indicate position. Likewise, given calibration of crack-opening with signal loss, the crack dimensions can also be determined.

91.4.8 Uses for fibre optics

91.4.8.1 General

Various parameters of direct relevance to space structures can be measured using fibre optic sensors:

- temperature,
- strain,

- hydrogen sensing,
- crack and damage detection.

These may be obtained from both single and multiple (quasi- or fully distributed) points along the fibre optic sensor using appropriate signal analysis and interpretation techniques.

FOS-based systems proposed for structural applications often combine one or more sensing techniques, e.g. different types of interferometers and Bragg gratings, Ref. [91-18].

[See: 92.3]

91.4.8.2 Temperature

The basic techniques available are:

- differential absorption distributed thermometry (DADT): With an extrinsic sensor.
- optical coherence domain polarimetry (OCDP): With polarised coherent light projected down a HiBi fibre.
- distributed anti-Stokes ratio thermometry (DART).
- distributed temperature sensing (DTS): based on the Raman principle. A commercial system can measure temperature along a 4km long optical fibre with a spatial resolution of 1m and a temperature accuracy of 1°C, Ref. [91-18].

A DTS system is being applied for X-33 cryogenic tank health monitoring, [See: 92.3].

91.4.8.3 Strain

Distributed strain measurement relies on ensuring proper strain-coupling between the sensor and the locally varying strain field it is measuring:

- coupling between sensor and measurand is a generic problem for strain sensors.
- the rate of change of strain may be much more rapid than that of thermal changes, e.g. vibration-related loads, impacts. Frequency is therefore critical.

A number of techniques are available, including:

- Optical time domain reflectometry (OTDR): Techniques based on the detection of a reflected or backscattered signal to locate positions where signals are either lost or reduced due to a break or deformation of the fibre optic, [See also: 'Crack and damage detection'].
- Interferometry: Using twin arms, the measuring arm of the interferometer is arranged so that it experiences the same strain as the body being monitored, while the reference arm follows as far as possible the same routing as the measuring arm, but is maintained in a stress-free state. Any temperature effects are then cancelled out. Twin-armed Fabry-Pérot and Mach-Zehnder type interferometers are commonly used, [See: Figure 91.4.5 and Figure 91.4.7]. Protecting the reference arm from stray influences can be difficult. Suggested solutions include forming the interferometer arms from two polarisations in a HiBi fibre, two modes in a dual-mode fibre or fibre with twin cores.
- Fabry-Pérot and Mach-Zehnder type interferometers, along with Bragg grating sensors are proposed for a combined strain, temperature and vibration monitoring system, Ref. [91-18].
- Bragg gratings: The ability to produce numerous diffraction gratings, of different lengths, along the entire length of a continuous fibre optic provides a very flexible means of creating

a distributed sensor system. This is the basis for the DSS 'Distributed Strain Sensor' system proposed for X-33 cryogenic tanks, Ref. [91-18].

- Frequency-modulated continuous wave (FMCW) differs fundamentally from the OTDR-based methods. This technique obtains spatial information by resolving in the frequency, rather than the time, domain. A frequency ramped continuous wave is launched exclusively into one mode of a two mode fibre. If at some point along the fibre, strain causes a component of the light to couple into the second mode, then the two signals sharing a common frequency travel with different group velocities, eventually arriving at the detector separated by a time delay. As a result, beat patterns are observed, the frequency of which are proportional to the time delay between the original mode coupling and subsequent signal recombination. This provides information on the spatial distribution of the measurand.

91.4.8.4 Hydrogen sensing

Optical fibres with Bragg gratings, bonded to a hydrogen-sensitive media (palladium) at various positions along the length, are the basis for the DHS 'distributed hydrogen sensing' system proposed for X-33 cryogenic tanks, Ref. [91-18]. The hydrogen concentration is inferred from the measured strain.

91.4.8.5 Crack sensing and damage detection

Fibre optics are candidates for applications where inaccessible or sub-surface locations require monitoring for the development of cracks, delaminations and debonding. Monitoring systems based on OTDR techniques, including 'Micro-bending Loss,' have been proposed for gross damage, such as crack detection or opening, [See: Figure 91.4.8].

More subtle forms of damage, such as delaminations in composite materials or debonding at interfaces between different materials, can be more difficult to quantify.

Systems that indicate that a defect is present could be sufficient for structures that are maintained on the ground. Another sensing technique could be combined with FOS-based systems to provide additional evidence, e.g. acoustic emission monitoring, [See: 92.3].

Impact detection, using FOS-based systems, requires that, Ref. [91-18]:

- sensors survive any impacts throughout their service life, or can be easily replaced, i.e. accessible; surface mounted rather than embedded,
- useful data regarding the impact can be obtained, e.g. measurement of strain-transients and impact site position.

Work conducted on impact detection generally considers impacts likely to occur on composite aircraft structures, rather than micrometeoroid and debris impact of interest for deployed space structures.

Some observations on the performance of FOS embedded in CFRP can be summarised as Ref. [91-18]:

- sensor survivability has been related to the fibre optic coating, proximity to the impact, impact energy (25 to 55J) and position within a (32-ply) laminate,
- impact strain measurements and strain-transients have been made using a Bragg grating technique. The measurements compared well with those made by conventional strain gauges.

91.5 Actuators

91.5.1 Introduction

91.5.1.1 Material groups

The main groups of materials considered for actuators can be summarised as:

- SMA shape memory alloys.
- Piezoelectric ceramics.
- Electrostrictive.
- Magnetostrictive.
- ER electrorheological fluids.

Any material found to change shape to some extent under the application of electrical, magnetic or thermal energy is of potential interest for actuator applications.

91.5.1.2 Space structures

With continued research and development, the number of material options were reduced to those likely to provide useful displacements in realistic structures for a reasonable energy input. A further consideration was the material's stability in the space environment. For space use, piezoceramics and shape memory alloys emerged as the most suitable options.

Although ER and magnetorheological fluids can exhibit very large changes in viscosity, they are often abrasive and chemically unstable. Whilst the response of shape memory alloys is now too slow for many advanced applications, active damping of vibrations is a possible application. This is also a suitable application for some magnetorestrictive materials.

91.5.1.3 Large, ultra-lightweight structures

With the development of very large, ultra-lightweight space structures, actuators could perform several functions, e.g. deployment, pointing, vibration and shape control.

SMAs and conventional piezoceramics are considered too heavy. Further research to find suitable low density, flexible materials with fast enough response times, has seen the emergence of a group of materials known as electroactive polymers (EAP), [See: 91.9].

91.5.2 Shape memory alloys (SMA)

91.5.2.1 General

Shape memory alloys can give large, controllable deformations in response to temperature change, by means of metallurgical phase transformations. When first developed, the alloys were applied in a 'one-way' mode, i.e. material previously deformed at low temperature regains its original shape when heated above a critical temperature.

Further development produced more complex alloys with partial 'two-way', or in some cases 'all-round' effects. In these, a reversible condition is exploited by cycling between critical temperatures to switch the material between shape states. The process is not necessarily fully reproducible on successive cycles, as hysteresis can occur in two-way alloys, Ref. [91-1], [91-2].

The process of shape change is associated with a reverse transformation of the martensitic phase to the higher temperature austenitic phase with an accompanying volumetric change. Commercial SMA products are usually:

- Nickel-titanium (NiTi) based compositions, or
- Copper-based ternary alloys.

The NiTi alloys offer higher displacement forces than equivalent sections made from the lower cost copper alloys.

The shape memory effect (SME) can be applied in engineering applications provided that the temperature change needed to induce a change of state is permissible. For an actuator within a smart system, where the process needs to be reversible and repeatable, the system should provide more complex heating and cooling cycles.

91.5.2.2 Transformation process

The SME transformation processes are shown in Figure 91.5.1, where electrical resistivity is used to monitor the material, Ref. [91-1].

In SMAs the hysteresis is typically in the 5 to 30°C range.

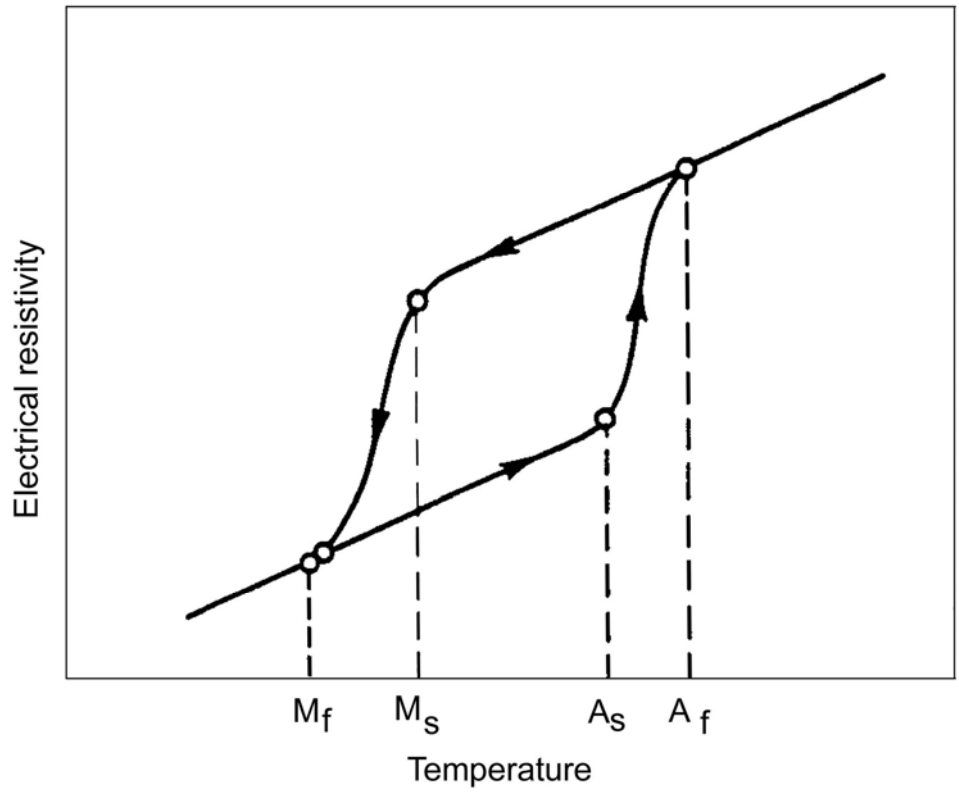

Key: M_s – martensite start; M_f – martensite finish; A_s – austenite start; A_f – austenite finish

Figure 91.5-1 - Shape memory alloy: Resistivity curve for a typical martensitic phase transformation

The curve shows the material changes related to the four relevant temperature points. As temperature decreases, the 'martensite start' (Ms) is reached, at which the new phase begins to

form within the high temperature parent phase. The transformation is complete when the lower ‘martensite finish’ (Mf) temperature is reached.

On re-heating the martensitic phase begins to transform back to the parent phase at the ‘austenite start’ (As) temperature and the reverse transformation is complete at the higher ‘austenite finish’ (Af) temperature.

91.5.2.3 'One-way' effect: Simple single cycle

The SME process is summarised in Figure 91.5.2. The difference between the 'deformation temperature' and the 'transformation temperature' is usually of the order of 100 to 200°C. By modification of the alloy metallurgy, the temperatures can be customised to speed up the response and reduce the power consumption.

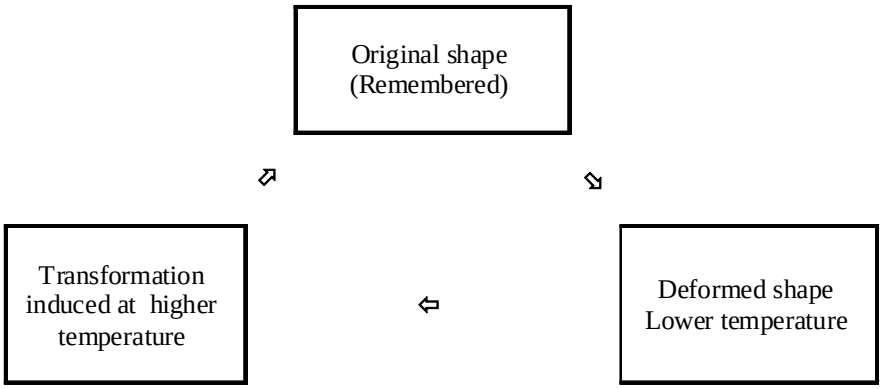

Figure 91.5-2 - Shape memory effect cycle

91.5.2.4 'Two-way' effect

This is produced by having two SME components in the same alloy, but triggered at different temperatures. A two-way SMA component behaves in a similar manner to a one-way component when heated, in that both deform to adapt to some ‘remembered’ shape. Whereas a one-way component retains that shape on subsequent cooling, for a two-way component the deformation reverses as the temperature decreases.

For two-way alloys the 'forward' (heating) cycle is generally more geometrically accurate than the 'reverse' (cooling) cycle, so that components made from two-way SMAs do not necessarily remain unchanged by an excursion above the transformation temperature.

91.5.2.5 'All-round' effect

Under carefully controlled processing, a near-perfect two-way SME can be produced, but only under certain conditions.

The all-round effect is similar to that exhibited by a bimetallic strip. The difference is that SMAs undergo far greater deflection once triggered, as seen in Figure 91.5.3, Ref. [91-1]. SMAs are able to apply forces equivalent to stresses of 200 to 800MPa generated within the material.

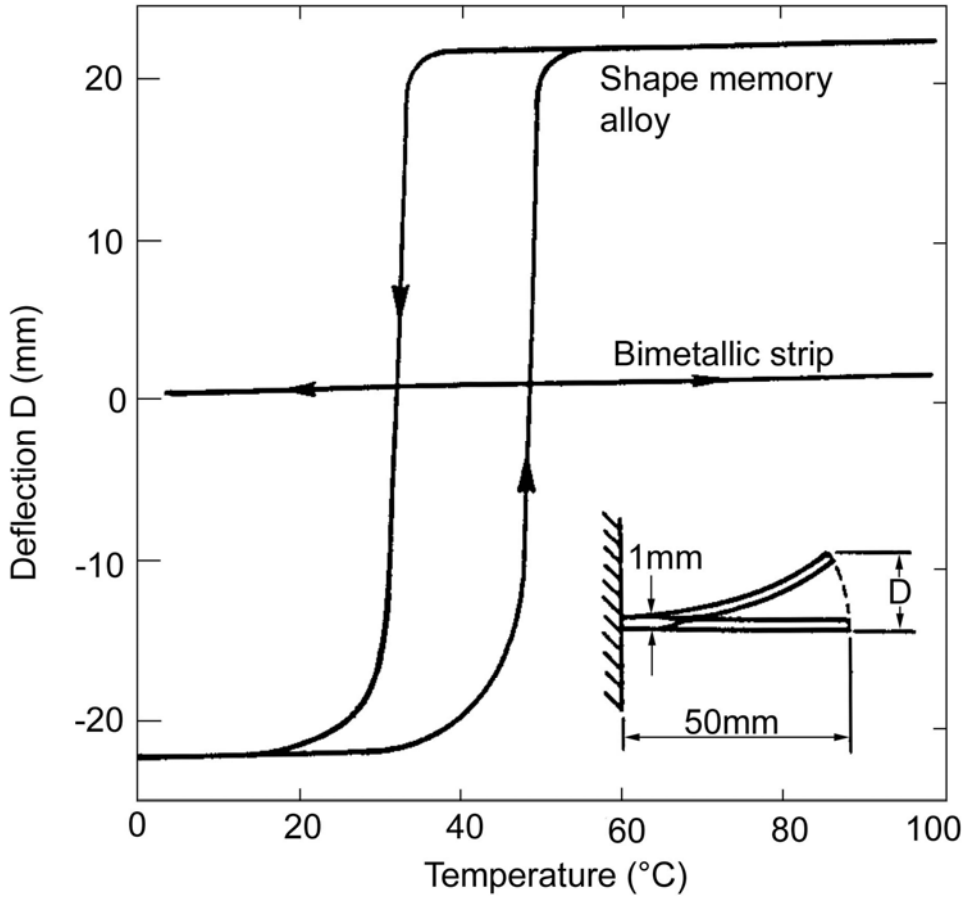

Figure 91.5-3 - Shape memory alloys: Comparison of properties with a bimetallic strip

91.5.3 SMA materials

91.5.3.1 General

The martensitic transformation depends on alloy composition and microstructure. Transformation temperatures can be 'customised' by changing the alloying parameters. Transformations can be 'non thermo-elastic' or 'thermo-elastic', Ref. [91-2].

There are more than ten basic systems which exhibit SME, to which alloying additions can be made. However, in terms of commercial availability for engineering applications the choice comes down to:

- NiTi (called Nitinol), and
- CuZnAl.

For space applications, NiTi-based alloys are preferred, Ref. [91-2], [91-5].

91.5.3.2 Nickel-titanium-based alloys

Table 91.5.1 compares NiTi with CuZnAl alloys, Ref. [91-1].

Table 91.5.2 provides data on NiTi Nitinol alloy.

Table 91.5-1 - Shape memory alloys: Comparison of properties for NiTi and CuZnAl materials

Property	NiTi alloy	CuZnAl alloy
Density (kgm^{-3})	6500	8000
Melting point (°C)	1310	970
CTE ($x10^{-6}°C^{-1}$)	7 to 15	18 to 19
Recovery strain (%)	8 Max.	4 Max.
Recovery stress (MPa)	400 Max.	200 Max.
Repetition life: • ε = 0.02% (2%) • ε = 0.005% (0.5%)	 10^5 10^7	 10^2 10^5
Corrosion resistance	Good	Problematic, especially stress corrosion cracking
Workability	Poor	Fair
Shape memory processing	Comparatively easy	Fairly difficult
Material cost	Expensive	Moderate

Table 91.5-2 - Shape memory alloys: Typical properties of NITINOL

Property		Value
Transition temperature	(°C)	100 †
Anneal temperature for permanent damage	(°C)	320
Shear modulus: • Martensitic • Austenitic	(GPa)	 7.5 22.0
Yield stress: • Martensitic • Austenitic	(MPa)	 80 620
Expansion coefficient: • Martensitic • Austenitic	($x10^{-6}°C^{-1}$)	 10 6.6

Key: † Can be tailored depending on composition.

The important features of NiTi alloys are:

- the transformation temperature can fall in the range -50°C to +100°C. Fine tuning of an alloy can be achieved by ternary alloying additions e.g. V, Cr or Mn replacing Ti, or Fe and Co replacing Ni.
- further adjustments can be made by altering the 50:50 stoichiometry of NiTi. This is more of a disadvantage than a positive feature, because the transformation temperature is very sensitive to variations. A 0.5 wt.% change in each alloy constituent may alter the transformation temperature by 50°C.
- copper can be added (up to 30%) to replace nickel. The effect is more subtle as the transformation temperature changes little but the yield strength can be modified. Also the

difference between Af and Mf temperatures can be kept small, so allowing reversible cycles over a limited temperature range.

- NiTi alloys are sensitive to interstitial contaminants such as carbon and oxygen which show a preference for the titanium. The precipitation of titanium carbides is not as problematical as oxide formation.
- metallurgical ageing of two-way Ti49Ni51 SMAs under shape constraint can induce transformation temperatures in the useful 0°C to +100°C range, while promoting a two-way SME. The ageing process is critical, while the imposed shape restraint should be associated with a strain less than about 1.5%. Indicative behaviour is shown in Figure 91.5.4, Ref. [91-1].

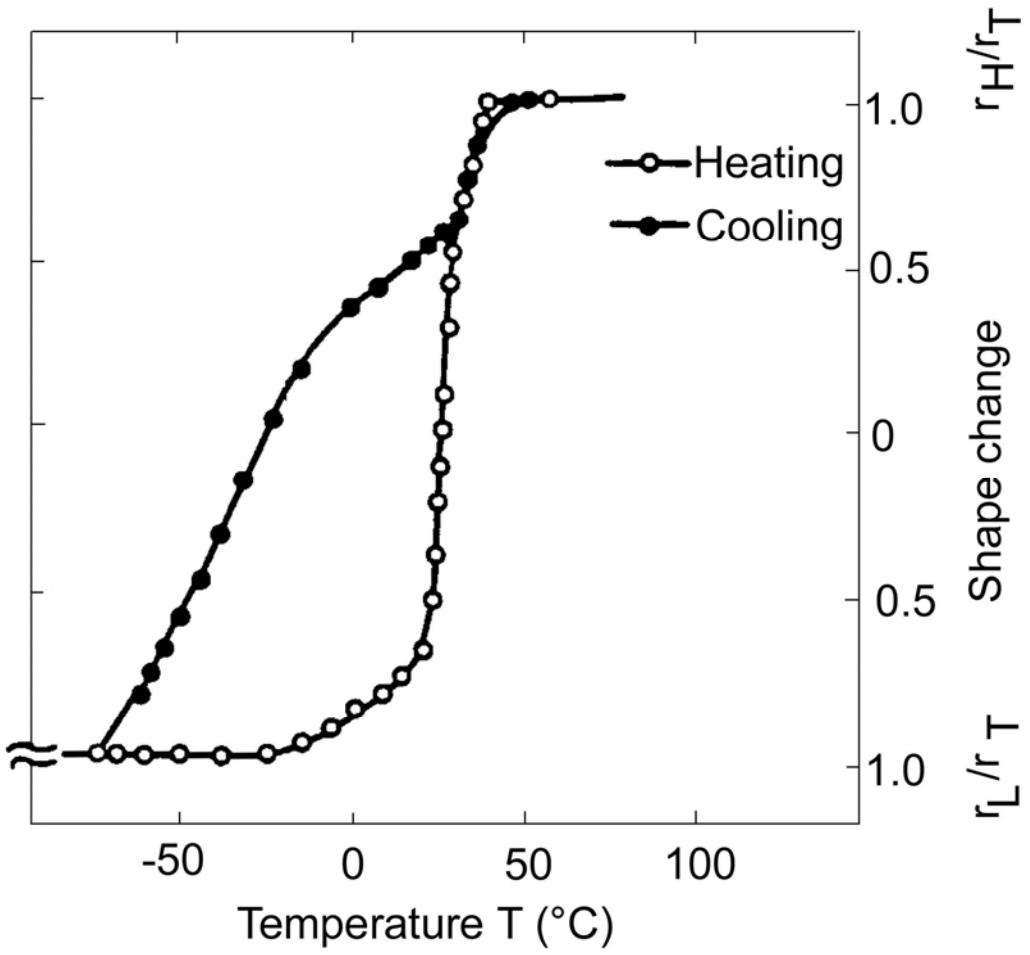

Figure 91.5-4 - Shape memory alloy (Ti49Ni51): Shape change during thermal cycling

Figure 91.5.5 shows the change in mechanical properties on either side of the transformation temperature, Ref. [91-2].

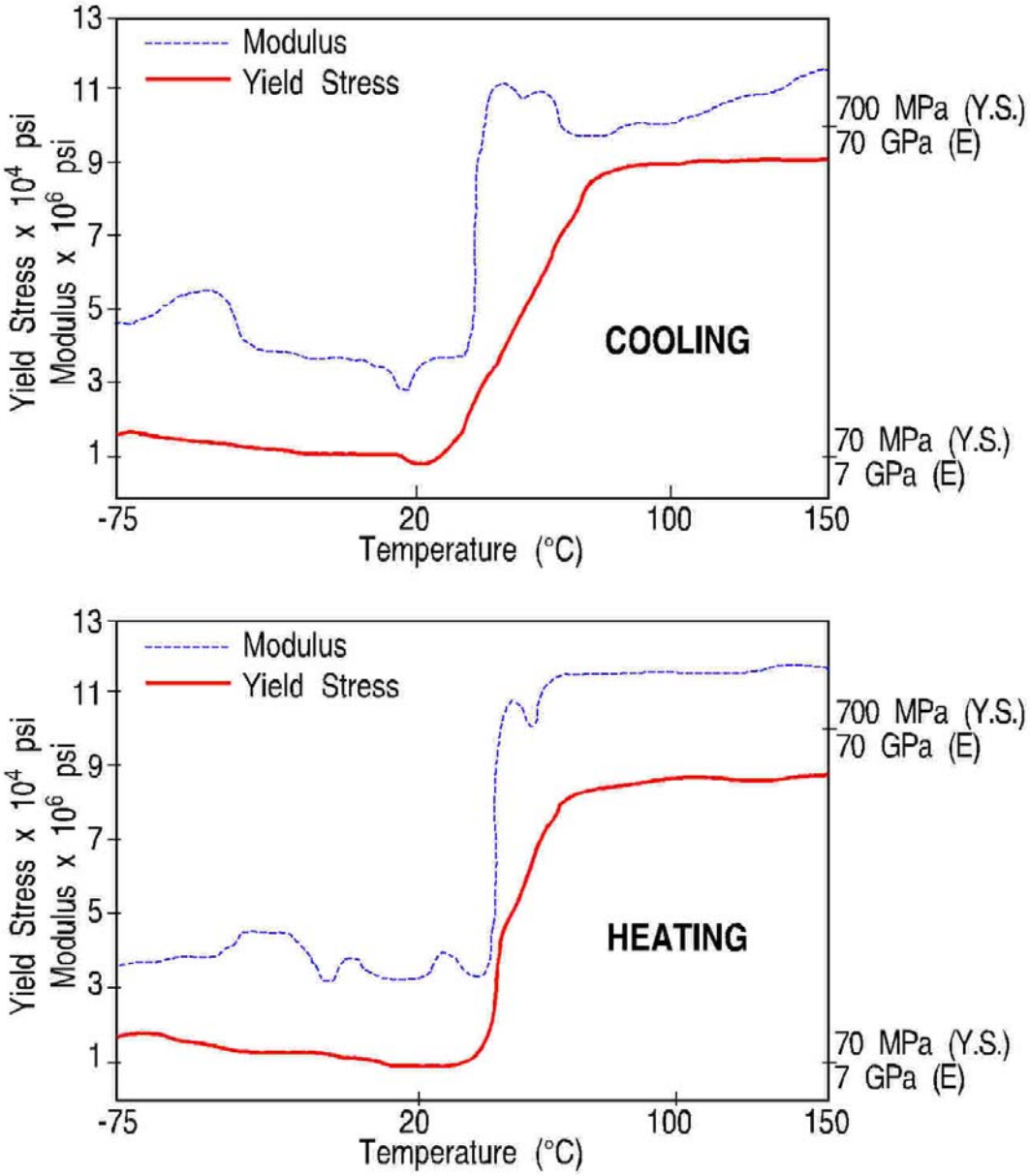

Figure 91.5-5 - Shape memory alloy (NITINOL): Typical materials characteristics

91.5.3.3 Copper-based alloys

The main features of CuZnAl and CuAlNi-based alloys include:

- Both groups are produced by solution treating an appropriate ternary alloy composition at high temperature, and then quenching to produce a phase with a superlattice structure. This constitutes the parent phase, from which further quenching produces a thermo-elastic martensitic phase.

  Typical compositions are:

  — Cu-25Zn-6Al (wt%), and

  — (Cu3Al)Ni, with ~4%Ni.

- for practical purposes, their use is limited to temperatures below 100°C, whereas NiTi approaches 250°C.

- the Cu-alloys also experience induced 'ageing' by repeated thermal cycles. Mf and As tend to decrease, but usually stabilises after about 10 cycles; shifts are in the order of a few degrees.
- repeated mechanical cycling is more likely to induce degradation, with the development of fatigue cracks. Degradation is directly linked to the stresses induced, which, if around 200MPa, are clearly high for any copper alloy to sustain repeatedly. The NiTi alloys have a greater strength and strain capacity.
- the CuAlNi systems offer improvements not least in better fracture behaviours, but are underdeveloped compared with CuZnAl.
- the copper systems are an order of magnitude cheaper, i.e. 10% compared with NiTi, but the superior capabilities of the latter are more appropriate for repetitive actuating applications.

91.5.3.4 Product forms

SMAs can be prepared in forms similar to other metals, e.g.

- sheet,
- rod,
- tube,
- wire.

These can be machined to the desired shape before manipulation and deformation to the final configuration. Items to consider include:

- fine wires (down to 25µm diameter) woven into meshes and fabrics. These can be incorporated into polymer composite laminates such that the mesh 'transforms' the stiffness or shape of the laminate when triggered by heat.
- simple tubular sleeves of SMA can be used for pipe couplings.
- displacements achieved by SMA components are comparable to electromagnetic solenoids or hydraulic cylinders. Their mass, however, is considerably less.

  An SMA component was used in a boom latch mechanism developed by ESTEC in the late 1970's.
- shapes possible for SMA components include:
  - springs,
  - coils,
  - levers,
  - fasteners,
  - fuses,
  - linkages, and
  - release mechanisms.

  However, the means of predicting performance for design purposes is lacking, indicating a trial and error path for achieving practical designs, Ref. [91-6], [91-7].
- Joining an SMA component to another material requires care. Under normal service conditions, other components, be they metal or composite, do not have the capability to elastically strain beyond approximately 0.5%. SMAs can greatly exceed this, so any permanent connection, e.g. welded, brazed or bonded, should avoid inducing unsustainable strains in the substrate.

91.5.4 Piezoelectric ceramics

Both ceramic and polymer piezoelectric materials are used for sensors, [See: 91.2; 91.3]. Piezoceramics are more appropriate than PVDF polymers for actuators, [See also: 91.9].

Although not producing the high forces of shape memory alloys, piezoelectric ceramics expand and contract quickly when a voltage is applied. This makes them suitable for precise, high-speed, actuator applications, Ref. [91-24].

Piezoceramics, are classed as functional technical ceramics, Ref. [91-23]. Some application examples include:

- device actuators,
- sensors and transducers, e.g. in accelerometer, pressure, sonar or ultrasonic-based systems,
- microphones and high-frequency speakers,
- optical-tracking devices,
- computer peripheral components, e.g. magnetic heads, dot-matrix printers, keyboards,
- igniters.

Of the range of material options commercially-available, the most common piezoelectric ceramic is lead–zirconate-titanate (PZT).

The main problems associated with piezoceramics for actuators in smart structures can be summarised as, Ref. [91-24]:

- thin in-plane actuators tend to be brittle and somewhat heavy, especially for ultra-lightweight structural concepts, [See: 92.7],
- loss of piezoelectric effect above a material-dependent temperature threshold; Curie temperature,
- difficult to scale to larger applications because of their limited stroke or displacement,
- practical aspects of their use, i.e. soldering, cracking owing to their brittle nature, and electrical insulation. These problems can be overcome by encapsulating the brittle piezoceramic wafers before processing, which provides mechanical stabilization, electrical insulation and electrical contacts.

Encapsulation, although adding a manufacturing step, is usually necessary. The slight reduction in actuator strain due to the relatively soft encapsulating material is generally considered acceptable.

91.5.5 Piezoceramic actuators

91.5.5.1 Concepts

There are several ways in which piezoceramics can be used as actuators, Ref. [91-24]:

- PZT wafers, the simplest design, comprises conductive layers which are in electrical contact with the electrodes. Additional surrounding layers provide mechanical support and electrical insulation. Applying an electrical voltage causes a homogeneous electrical field normal to the wafer, which is polarized in the same direction. This set-up activates the longitudinal effect in the polarization direction and the transverse effect in the wafer plane. In thin wafers, the effect in the normal direction is negligible, so the actuator basically operates in-plane (d31). A great amount of experience has been gained with this type of actuator, and there are many, reasonably-priced, commercially-available, products.

- IDE inter-digitised electrodes, which are also wafers but have the appearance of interlaced comb-like structures. This is a more complex configuration, but benefits from the higher longitudinal piezoelectric effect (d33).
- PZT fibre-based actuators, which consist of a large number of aligned PZT-fibres (100µm to 250µm diameter, typically) and embedded in a polymer resin. This configuration aims to overcome the known problems of brittle wafers.

Table 91.5.3 summarises the overall advantages and disadvantages of the piezoceramic concepts described, Ref. [91-24].

Table 91.5-3 – Piezoceramic actuators: Comparison between different in-plane actuator concepts

Actuator design	PZT volume fraction	Piezoelectric effect used	Orientated actuation	Cost	Damage characteristic
Patch	●	d31	⊗	●	⊗ / ●
Patch IDE	●	d33	○	○	⊗
Ribbon IDE	○	d33	●	○	○
Fibre IDE	⊗	d33	●	⊗	●
Key:	Relative benchmark:	● good	○ average	⊗ poor	

91.5.5.2 Wafer-based 'patch' actuators

Figure 91.5.6 shows examples of wafer-based actuators using the transverse (d31) and longitudinal (d33) piezoelectric effects, Ref. [91-24].

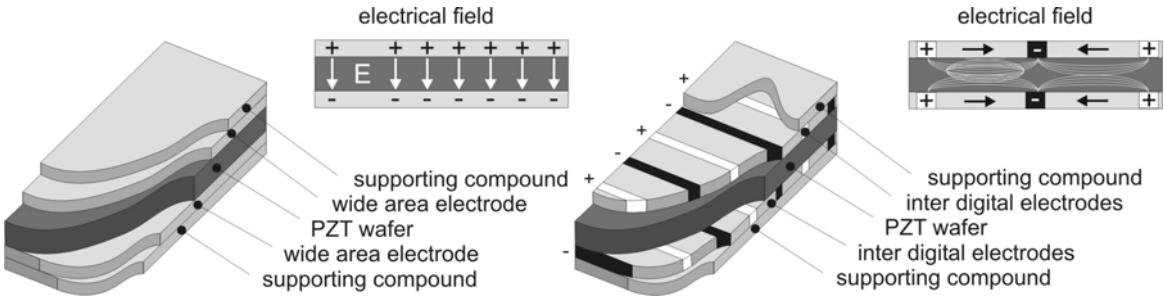

Transverse, d31 effect **Longitudinal, d33 effect**

Figure 91.5-6 - Piezoceramic actuators: Wafer-based concepts

Quickpack®, available from MIDE (formerly ACX), are encapsulated patches that utilise the d31 piezoelectric effect. The encapsulation is a foil coating (polyimide) with copper stripes to contact the electrodes. These actuators have been applied successfully for controlling vibration on the vertical tail of an F/A-18 airframe. NASA's 'Flex-patch' is a comparable approach, Ref. [91-26].

DLR developed flexible structures, which are based on copper mesh to provide a large contact with the electrodes to improve the reliability and damage tolerance of the actuators, Ref. [91-27].

Typical free strain values for d31 in-plane actuators are 400µm/m to 500µm/m, which are obtained with a peak-to-peak voltage of 400V.

IDE inter digitised electrodes are used in order to exploit the higher longitudinal piezoelectric effect (d33). The design utilises two interlaced comb-like electrodes symmetrically arranged on each side. Actuators of this design are available commercially from ACX and MIDE. Polarization of the PZT electrode material occurs when high voltages are applied to the electrode fingers. The resulting electrical field is inhomogeneous, with most of the field lines in the wafer plane. The advantage compared with conventional actuators is the higher performance due to the longitudinal effect. A disadvantage is the more complex architecture and the inhomogeneous electrical field. The strong electrical field gradients in the electrode fingers cause high mechanical stresses in the actuator material (ageing). A minimum thickness for the electrode fingers is necessary otherwise the mechanical stress is too high. Thin electrodes are also desirable because the area below the electrodes does not contribute to the active performance.

Since the distance between the electrode fingers is relatively large, high driving voltages are necessary, e.g. 3000V for a typical electrode distance of 1mm and a 200µm thick wafer.

The electrode distance is largely determined by the thickness of the PZT-wafer and is a compromise between the voltage, field inhomogeneity and thickness of the electrode fingers.

Both of the actuators described are based on PZT wafers. In this shape the PZT-material is, even within a reinforcing compound, relatively fragile. If damaged, cracks propagate easily across the monolithic wafer.

91.5.5.3 PZT 'ribbon and fibre' actuators

Figure 91.5.7 shows examples of ribbon and fibre actuators, Ref. [91-24].

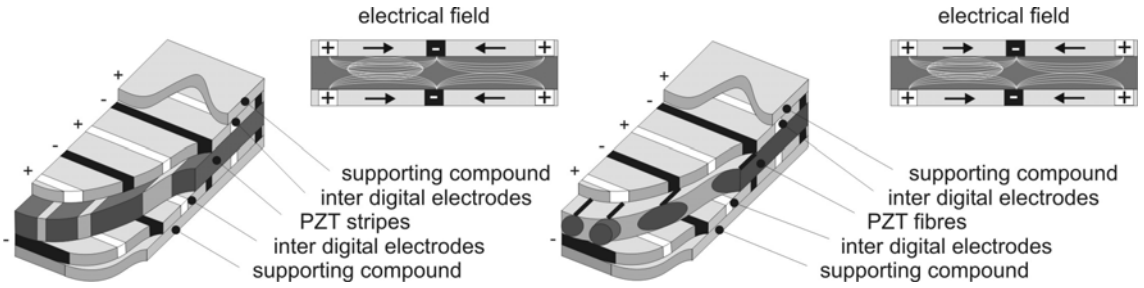

Figure 91.5-7 - Piezoceramic actuators: Fibre and ribbon-based concepts

Large numbers of PZT-fibres (100µm to 250µm diameter) are aligned side by side and embedded in an epoxy resin, Ref. [91-28]. IDE-electrodes are used to apply the electric field.

The interfaces between fibres and resin act as crack-stoppers, so the mechanical properties are better than monolithic 'patch' type actuators. Owing to the improved crack-resistance, higher electrical fields can be applied, giving better actuating performance compared with patch actuators with the same type of electrode. The disadvantages are the reduced PZT volume fraction and high driving voltages.

Instead of fibres, with a circular cross section, PZT ribbons have a rectangular cross section that increases the PZT volume fraction and also the contact area between PZT material and electrodes. PZT ribbons have better performance because dielectric loss is reduced. These types of actuators were developed by MIT and are available commercially from Continuum Control Corp. or Material System Inc.

The manufacturing process is very labour intensive, hence expensive. The PZT fibres need to be accurately positioned by hand. This can cause quality-related problems and inconsistencies in actuator characteristics. The sintering process for PZT fibres and ribbons is also expensive.

An alternative automated manufacturing process uses commercially-available PZT-wafers that are cut into ribbons. The wafer is placed on a tacky film and cut using a wafer saw similar to that used for silicon chip manufacture. The ribbons are precicely aligned in parallel and the gaps between the ribbons are filled with resin and polyimid films. IDE-electrodes are then bonded on the top and the bottom of the assembly. This approach, known as 'Macro Fiber Composite', was developed by NASA, Ref. [91-30], and is available commercially from Smart Materials Corp., Ref. [91-31].

Typical free strain values for d33 in-plane actuators are 1400µm/m to 1800 µm/m when a peak-to-peak voltage of 2000V to 3000V is applied.

91.5.5.4 Composite-layering technology

A recent innovation is a 'Stripe actuator' from APC International (USA), which uses composite-layering technology. The 'stripe actuator' claims to achieve about 20% more displacement compared with conventional bimorph elements, e.g. 1.1mm to 2.8mm; 0.1N to 0.95 N blocking force.

91.5.5.5 Commercial sources

There are many sources of piezo ceramic elements, available in standard or bespoke shapes and sizes, including, Ref. [91-23]:

- CeramTec-Hoeschst (D)
- Ferroperm (DK)
- MEC Morgan ElectroCeramics, previously Morgan Matroc, (UK)
- Sensor Technology Ltd. (Canada)
- Toshiba Ceramics (Japan)

Some examples of sources of PZT actuators, include:

- APCI - APC International Ltd., (USA)
- Continuum Control Corp., (USA)
- Material System Inc. (USA)
- MIDE, formerly ACX Inc. (USA)
- Piezo Systems Inc., (USA)
- Sensor Technology Ltd., (Canada)
- Smart Materials Corp, (USA)

91.5.5.6 International standards

Piezoelectric materials usually appear in international standards for electrical and electronic components. In Europe, the CENLEC (EN), IEC and IEEE series of standards are usually applied, Ref. [91-64].

91.5.6 Electrostrictive

Electrostrictive materials develop mechanical deformations when subjected to an external electrical field, Ref. [91-2].

The electrostrictive phenomenon is attributed to the rotation of small electrical domains in the material when an electrical field is imposed on them. In the absence of this field, the domains are randomly oriented. The alignment of these electrical domains parallel to the electrical field results in the development of a deformation field.

The ceramic compound lead-magnesium-niobate (PMN) exhibits a thermo-electrostrictive effect and the quadratic electrostrictive phenomenon is dependent upon the ambient temperature. This type of material, while exhibiting less hysteresis loss than piezoceramics, has a non-linear constitutive relationship requiring some biasing in practice to achieve a nominally linear relationship over a limited range of excitation, [See also: 91.9].

91.5.7 Magnetostrictive

Magnetostrictive materials are solids which typically develop large mechanical deformations when subjected to a magnetic field, Ref. [91-2].

The magnetostriction phenomenon is attributed to the rotations of small magnetic domains in the material, which are randomly-oriented when the material is not exposed to a magnetic field.

Orienting the small domains by the imposition of the magnetic field results in the development of a strain field. As the intensity of the magnetic field is increased, more and more magnetic domains orientate themselves so that their principle axes of anisotropy are co-linear with the magnetic field in each region until saturation.

Terbium-iron alloys are typical magnetostrictive materials capable of strains up to 0.2%. This class of mechano-magnetic material suffers from some disadvantages which should be carefully considered when developing smart systems. These include:

- delivering a controlled magnetic field to a magnetostrictive actuator embedded within a host structural material.
- materials generate a much greater response when subjected to compressive loads.
- power requirements for this class of actuator are greater than those for piezoelectric materials.

[See also: 91.9]

91.5.8 ER electrorheological fluids

91.5.8.1 General

ER fluids are a class of colloidal dispersion which exhibit large reversible changes in their rheological behaviour when subjected to external fields, Ref. [91-1], [91-2]. The change is typically a dramatic increase in flow resistance or apparent 'viscosity'. An ER fluid often has Newtonian characteristics in the absence of an external electric field, which become non-Newtonian when the electric field is imposed upon the fluid domain. Information is provided here only to present a complete picture on smart technologies, rather than in any expectation that ER fluids can be used in space.

ER fluids consist of evenly dispersed fine solid particles (dispersed phase) in a continuous non-conducting liquid phase; examples are given in Table 91.5.3, Ref. [91-2].

The level of viscosity change achieved by the application of a strong electric field is dependent on the:

- volume fraction of the dispersed phase, and
- third phase additions.

[See also: 91.9]

Table 91.5-4 - Electrorheological fluids: Typical ingredients

Solvent	Solute	Additive
Kerosene	Silica	Water and detergents
Silicone oils	Sodium carboxymethylcellulose	Water
Olive oil	Gelatine	None
Mineral oil	Aluminium dihydrogen	Water
Transformer oil	Carbon	Water
Dibutyl sebacate	Iron oxide	Water and surfactant
Mineral oil	Lime	None
P-xylene	Piezoceramic	Water and glycerol oleates
Silicone oil	Copper phthalocyanine	None
Transformer oil	Starch	None
Polychlorinated biphenyls	Sulphopropyl dextran	Water and sorbitan
Hydrocarbon oil	Zeolite	None

The fundamental characteristics of an idealised ER fluid are shown in Figure 91.5.8, Ref. [91-2] and Figure 91.5.9, Ref. [91-1].

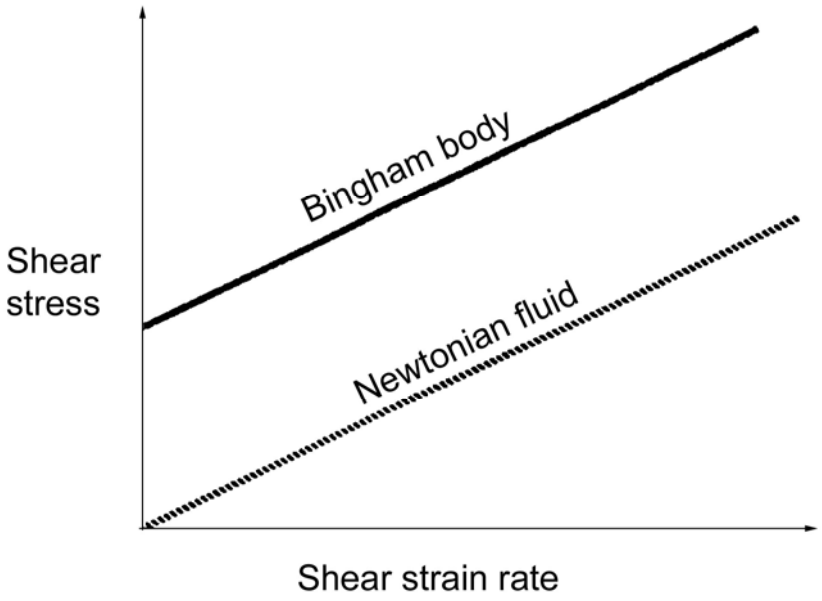

Figure 91.5-8 - Electrorheological fluids: Bingham-body model for isothermal constitutive typical behaviour

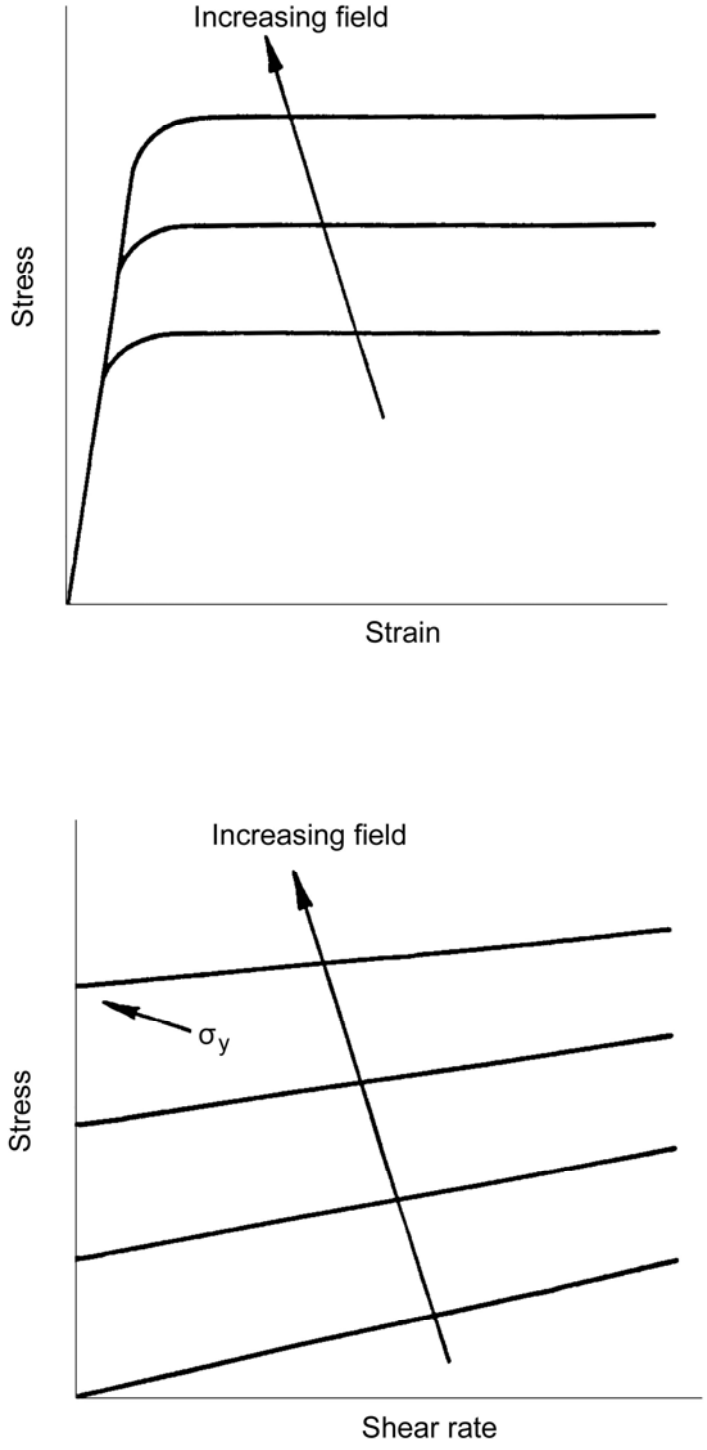

Figure 91.5-9 - Electrorheological fluids: Idealised shear-stress and stress-shear rate behaviour

With the application of an electrical field the fluid rheology moves from Newtonian to a Bingham plastic. The ER phenomenon is represented by Figure 91.5.10, Ref. [91-2].

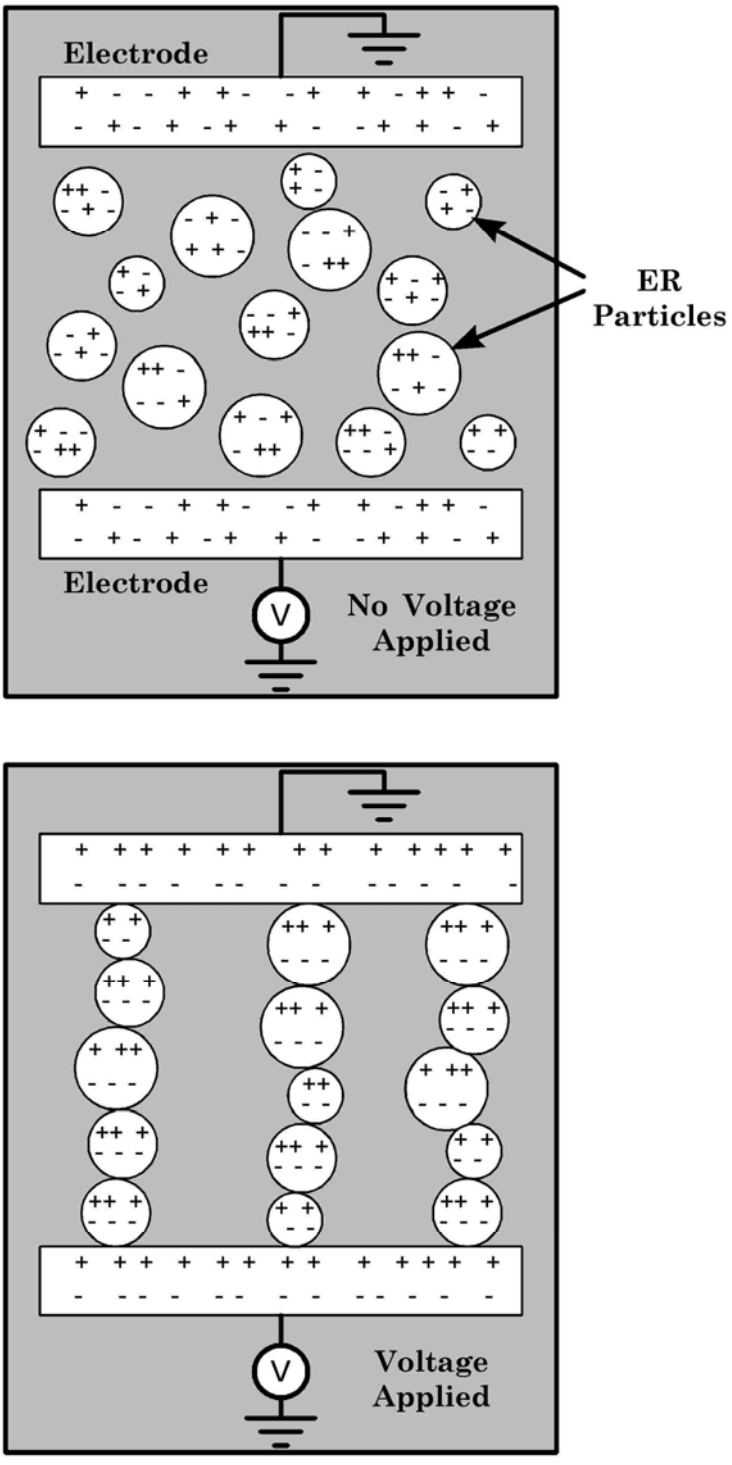

Figure 91.5-10 - Electrorheological phenomenon

Further points to be made about ER fluids include:

- application of an electric field induces 'chain-like' alignment of dispersed particles between the charged surfaces, [See: Figure 91.5.8]. Particle sizes are usually 5 to 30µm.

- electric field intensities are usually in the range 1 to 5kV/mm with viscosity changes between 10 and 1000+ Pa. The viscosity is strain-rate dependent, but electrically controllable shear stresses in the range 1 to 3kPa are typical.
- some of the fluids listed in Table 91.5.1 are corrosive to some metals.
- it is proposed that ER fluids located in structural cavities could be used to control damping behaviour by modifying the overall stiffness and hence natural frequency. This has been tried with very limited success on CFRP panels. However, it is considered to be impracticable for most applications.
- four basic models describe ER fluids. These are:
  - Winslow fluids.
  - Strangroom's fluids.
  - Block's fluids.
  - Filisko fluids.
- A high voltage supply is necessary.

91.5.8.2 Applications

The potential applications of ER fluids fall into the general areas of:

- damping, and
- coupling.

The prospects for industrial uses are:

- coupling devices, e.g. clutches for mechanical power transmission,
- damping components, e.g. shock absorbers.

It is not easy to envisage the use of liquid media in space programmes, even when retained within sealed, leak-proof, mechanisms.

91.6 System complexity

91.6.1 General

The expectations placed on individual smart systems and the necessary components of such systems are described.

91.6.2 Passive sensory smart materials and structures (Level 1)

91.6.2.1 General

These include applications where only a sensory function is provided, i.e. a monitoring role. They have existed for many years using strain gauges and thermocouples. Although these systems do not include response mechanisms, the two more recent developments are said to justify their inclusion under smart technologies are:

- the advent of miniature sensors and compact computer processing power enables more detailed data to be gathered on the state of a structure, e.g. temperature and strain distributions, damage detection and location, and vibration levels. The available computing power enables multiple sensors to be addressed whilst providing real-time output on the significance of the data collected.
- comprehensive sensing systems provide confidence in proceeding to fully smart systems with integrated actuators and an intelligent control loop.

91.6.2.2 Condition or health monitoring

These use passive sensory systems, Ref. [91-8], [91-9], [91-10] and [91-11]. For space structures, the newer sensors are based on, [See also: 91.2]:

- fibre optics, [See: 91.4],
- piezoelectric elements, [See: 91.3]
- accelerometers.

These can be used in conjunction with both, [See: 91.2]:

- strain gauges,
- thermocouples.

Embedding fibre optics and piezoelectric elements in composites (FRP) has some attractions. Surface-bonded sensors remain important because aluminium alloys continue to be used for many structural elements.

The likely applications for passive sensing are, [See also: 91.8; 92.3]:

- vibration monitoring: Orbiting satellites and space stations for diagnostic purposes in interpreting the health of the structure and its mechanisms.
- thermal monitoring:
  - mapping of temperature variations on long-life and reusable structures.
  - enables the prediction of thermally-induced, dimensional changes and residual stresses.
- impact location:
  - orbiting space stations, e.g. micrometeorites, or
  - RLVs: In-service impacts on Earth or in orbit.

  Knowledge of impact location and severity is a useful aid for targeting inspection procedures.
- inaccessible structures: self-monitoring and diagnosis of, e.g.:
  - crack detection and propagation in metal structures, or
  - delamination in composite structures.

Damage propagation in spaceplanes is a particular concern due to their complex flight.

[See: 92.7]

91.6.3 Smart skins (Level 1)

The term 'smart skin' was originally used to describe concepts in which arrays of sensors were integrated into the external surfaces of aircraft, Ref. [91-12] to [91-16].

The concepts centred on sensors embedded in composite skins, i.e. aerodynamic and control surfaces. In theory, this is applicable to any skinned structure.

Fibre optics are attractive as they can be moulded into the prepreg plies during consolidation and curing. The use of narrow pitch arrays, with fibres in multiple directions, was proposed as a means of detecting and locating defects caused by impact or fatigue.

On-board monitoring then provides a continuous means of diagnosing the integrity of the aircraft. If on-board monitoring is not appropriate, data outlet points could be used during the regular service intervals to download information.

A comprehensive strain monitoring capability can also provide a means of comparing actual in-service behaviour with that predicted by design. This could:

- provide greater confidence for producing more highly stressed and more efficient structures.
- allow aircraft to be operated in flight modes closer to their structural limits and, if necessary, warning to reduce the severity of the manoeuvring.

91.6.4 Reactive actuator-based smart structures (Level 2)

91.6.4.1 General

As with Level 1, true intelligence is not really being shown. A reactive actuator-based system relies on simple command signals triggering a single response, e.g. open or close. This can be repeated cyclically, but at low frequencies and more usually on an infrequent basis.

91.6.4.2 Shape memory alloys

The transformation of shape memory alloys initiates a command signal from the control system, e.g. to heat the SMA. It is unlikely that there will be a real-time return signal (from sensors) to modify the SMA behaviour.

91.6.4.3 Piezoelectric materials

A good frequency response is possible with piezoelectric materials. Therefore, piezoelectric actuators can be activated to resonate at a desired frequency.

The frequency can be pre-selected to counter, i.e. damp, previously known vibrations in a structure.

Such a system would be reactive to single predetermined events. No intelligence is needed nor possible to balance frequency changes, random vibrations or energy levels.

91.6.4.4 Applications

Likely space uses can be summarised as:

- deployment of structures and antennas from a folded position to fully extended using SMAs. Retraction requires a controllable means of heating and cooling the SMA.
- re-orientation and compensation of antennae to predetermined positions.
- vibration damping of predetermined events.

These are all seen as first stage achievements towards true active sensing and reactive smart structures.

91.6.5 Active sensing and reactive smart structures (Level 3)

These systems would typically feature:

- host structure,
- network of sensors,
- data links,
- data-processing capabilities and algorithms: Programmed into microprocessors to operate the actuators,
- network of actuators,
- power supply and conditioning.

The system is autonomous and responds to environmental changes and unpredictable events over a considerable life-span.

It is possible to envisage the need for these in transport systems with variable modes of operation, e.g. aircraft, helicopters, ships or automobiles.

Classical examples include:

- active suspension in racing cars and road transport vehicles.
- vibration suppression; variable spectrums in helicopter blades and airframes.
- aeroelastic tailoring of aircraft aerodynamic or control surfaces.

Operating conditions are more predictable for orbiting space structures and for repetitive cycles, therefore response times are less demanding.

For space programmes, active compensation seems to be the main opportunity for a fully smart system.

91.6.6 Active compensation (Level 3)

Some factors that drive the development of active compensation systems for orbiting space stations and satellites are:

- service life: Orbiting structures with extended operational lives, e.g. 25+ years.
- dimensional stability: Subtle changes in dimensionally stable structural materials can occur over long time spans e.g. CFRP.
- dimensional tolerances: Large antenna concepts (between 4 to 10+ m) with very close dimensional tolerance requirements (tens of microns).
- antenna alignment and frequency response: Operational changes once in-service, i.e. at any time in the 25 years.

These combined factors imply designing structures where there are:

- sensory functions; describing the physical state of the structure,
- active components; enabling adjustment to a desired configuration.

[See: 92.6]

91.7 Data manipulation, simulation and control systems

91.7.1 General

The term 'smart' has been likened to 'intelligence'. Smart materials in themselves cannot provide a useful function unless connected to a control system.

The complexity and sophistication of the control system determines what can be expected of a smart system in terms of output or response. A control system can have multiple functions depending on the expectations placed on the smart system.

91.7.2 Complexity levels

The progression of increasing levels of complexity are:

- on/off switching of a single stroke actuator.
- data-logging from a single channel (sensor) e.g. thermocouple or strain gauge.
- data-logging from multiple channels.
- signal interpretation from fibre optic sensors to quantify measurands from multiple locations.
- defining the significance of a sensor output against pre-defined limits.
- implementing control algorithms in real-time to achieve an actuator response to sensory output.
- implementing simultaneous multiple actuator responses to multiple sensory outputs.
- ensuring balance in the system in closing the loop to achieve the desired overall effect.

Although the details of smart system electronic packages are not described in detail, their role is as crucial as that of the sensors and actuators.

Similarities exist between the electronic packages needed for radar and acoustic signal recognition and display, and those necessary for truly smart systems.

91.7.3 System development and integration

To achieve a successful smart system, integrated into a structure requires an interdisciplinary approach between:

- engineers,
- designers,
- material specialists,
- sensor and actuator technologists, and
- electronic systems designers.

Work on 'smart technologies' has seen the development of specialist disciplines, notably in materials and sensors.

A fully integrated approach has yet to be tackled in earnest to produce 'smart systems'. A central issue is confidence that a smart system is capable of interpreting and quantifying what is occurring.

Structural designers and engineers understand the basic physical parameters, including:

- stresses (MPa),
- strains (% or micro-strain),
- stiffness (GPa),
- loads (N),
- displacement (mm),
- CTE.

However, sensor technology relies largely on theoretical equations and assumptions based on signal characteristics, e.g.:

- frequency (Hz),
- attenuation (dB),
- wavelength (nm),
- phase change,
- modulation, etc.

These effects can be related directly to the physical parameters using electronic systems and computing. System complexity is largely dependent on the number and frequency of inputs and outputs occurring in the smart system.

91.7.4 Simulation

91.7.4.1 General

Designing smart structures with strong interactions between the various components relies to a great extent on an interdisciplinary system simulation process. The interactions to be considered within an intelligent structural system are mainly those between structural components, actuators, sensors, signal conditioning, electronics, control architecture, software algorithms and power management.

System simulation enables an efficient, concurrent, 'active-passive' system design. This means that both passive and active parts, and their interactions within the system, can be evaluated numerically and the performance of the whole system can be predicted.

The interdisciplinary simulation enables an assessment of smart material performance together with system modification and optimisation. It should consider both the passive and active behaviour of an intelligent system, in order to assess failure and the modification of characteristics of components or subsystems. The simulation assumes linear structural mechanics characteristics and electro-mechanical intelligent material behaviour, Ref. [91-24].

91.7.4.2 Integrated approach

The design and simulation development systematically cross-links the standard engineering tools, combining all essential information into an 'integrated simulation environment'. The main focus is on combining CAD, FEA, MBS and CACE (controller development, via 'Computer Aided Control Engineering') with rapid prototyping system implementation and assessment, Ref. [91-24].

91.7.4.3 Software environments and packages

Current research work indicates that Matlab/Simulink (M/S) environment has good potential in professional CACSD (Computer Aided Control System Design) for simulating interactive, intelligent structural systems; especially where the focus is on active, dynamic control of structures, e.g. vibration control, Ref. [91-24].

For integrated design and simulation systems, M/S has the benefit that it is a well-established standard tool and is widely used in industry, public and educational R&D institutions. Other potential packages, such as SciLAB and Octave (freeware) or the commercial MatrixX or Easy5 are not as widely used in the same sectors. As a result, M/S code and its associated toolboxes are frequently validated and upgraded. The ability to combine it with established rapid prototyping control software and hardware, e.g. dSpace, is validated and robust. Although dSpace is widely used, M/S is considering the use of lower-cost controller hardware, Ref. [91-24].

91.7.4.4 Simulation process example

Figure 91.7.1 shows an example of an integrated simulation process, Ref. [91-24].

CAD data can be used to perform FEA simulations, e.g. with ANSYS or NASTRAN, for the analysis of the elastic structural characteristics of 'passive' components. For example, only the passive host structure or this structure with the attached/integrated active, but not activated, structural components are numerically analysed, Ref. [91-24].

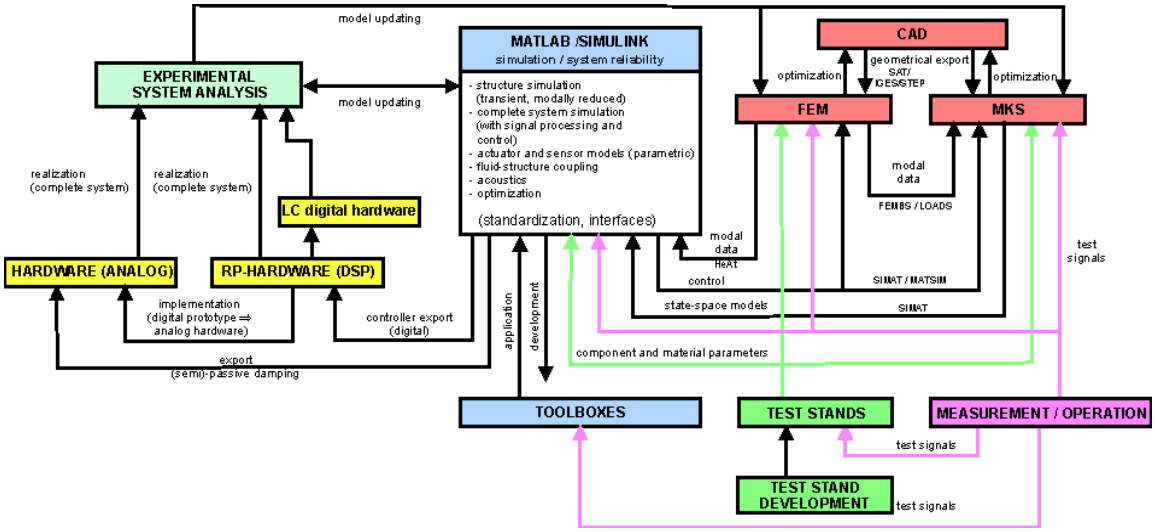

Figure 91.7-1 – Simulation: Example of integrated simulation process for smart materials design

It is assumed that deformations are small and mechanical characteristics can be considered to be linear. The focus is on linear active material models that, if feasible technically, could be extended.

Apart from FEA deformation and strength analyses, a numerical modal analysis is performed which can be validated by experimental modal analysis when the hardware is available. This then enables an updated FE model, Ref. [91-24].

Reduced modal data is used to describe the structure as a state space model within M/S. Within M/S the positioning of smart materials can be optimised, Ref. [91-24].

The electro-mechanical characteristics of the smart materials are integrated into M/S, then signal conditioning, such as filters or other electronics, are added. Having completed these actions the controller is developed, compiled and finally transferred to the control hardware, Ref. [91-24].

The most commonly-used control hardware environment is dSpace, which enables controller optimisations to be done while working with the manufactured and commissioned systems hardware. This describes the CAD-FEA-M/S-dSpace line, Ref. [91-24].

There is often a need to consider multibody simulations (MBS), e.g. using Simpack, and to establish a CAD-FEA-MBS-M/S-dSpace line for this. In this situation it is usual to crosslink FEA and MBS in order to determine the elastic structural behaviour of components within FEA and then include this for kinematic consideration of the active system within MBS. Again, the controller development is done within M/S, but the controlled system can simulate within the MBS environment, within M/S or in a co-simulation of both, Ref. [91-24].

91.7.5 Emerging technologies

91.7.5.1 General

The descriptions of 'smart systems' can go as far as discussing structures in similar terms to those used for biological entities. Examples of various emerging future technologies with bio-simulation slant are:

- artificial intelligence (AI),
- neural networks,
- nanotechnology, and
- biomimetics.

91.7.5.2 Artificial Intelligence (AI)

AI is a field of computer science focused upon the development of systems that can be programmed to act intelligently and possibly learn from experience. The development of continuous, logical and symbolic systems aim to simulate human intelligence in a computer.

91.7.5.3 Neural networks

Artificial neural networks are an attempt to build computing systems analogous to biological nervous systems, Ref. [91-17]. Their main features are:

- trainable, removing the need for explicit programming of functions.
- massively parallel, offering high-speed computation which is fault tolerant and capable of coping with progressive degradation, Ref. [91-17].

91.7.5.4 Nanotechnology

In the field of smart structure development, nanotechnologies can refer to:

- materials, e.g. carbon nanotube actuators, [See: 91.9],
- use of molecular-scale objects as components for molecular machines, i.e. the next scale down from microdevices (microsensors) with nanometre (nm) dimensions as opposed to micrometre (μm).

91.7.5.5 Biomimetics

The mimicking in engineering of biological materials for selected features and characteristics, where evolution has produced highly-efficient solutions at a molecular level, e.g. muscle, bone, ligaments, tendons, skin or nerve systems, Ref. [91-64].

91.8 Integrated systems

91.8.1 Overview

The development of 'smart' technologies is closely linked to the rapid evolution in various sectors of the electronics industry. In particular these are:

- optical fibres.
- high-speed communications.
- fast computer-based signal and data processing.

Initially, much of the development work was conducted in separate industry sectors to meet their own particular demands. Consequently the overall 'smart' picture was somewhat fragmented, and the terminology confusing, [See: 90.2].

The situation has improved greatly following the pan-industry effort to identify the practical attributes of 'smart' technologies. This has led to a more applications-based approach to prove the various technologies.

In addition to the aerospace industries (civil and military aircraft fleets; space structures), industry sectors considering the use of 'smart' technologies are, Ref. [91-18]:

- ground-based transportation.
- civil engineering (bridges, buildings, road and rail infrastructure).
- process plant and offshore structures.
- energy (conventional and alternative, e.g. wind turbines).

The common interest in all of these is the safety and reliability of structures which are difficult to inspect and therefore costly to maintain. Many of these structures are old, with the aim being to safely extend their useful life beyond the original design. For new designs the driving forces are very similar to those for the introduction of 'smart' technologies into aerospace structures.

91.8.2 Health monitoring

Amongst the 'smart' technologies, those which continuously monitor structures have attracted the widest interest. Numerous USA- and European-funded programmes have aided the development of systems for integration into structures to provide useful, interpretable, information, Ref. [91-18].

The long-term degradation of structures is associated with the combined effects of:

- operational conditions: including temperature, pressure, vibration, loading and contact with process materials.
- environment: including corrosion, temperature, accidental damage and overloads.

These largely dictate what needs to be measured, the data to be interpreted and the resulting actions; either manually or, for fully smart systems, automatically.

It is rare that one sensor or sensing technique can measure all of the required characteristics. This is true for conventional ground-based non-destructive inspection techniques and is equally true for continuous monitoring systems. The smart sensors can themselves be developments of conventional NDI methods. Fibre optic sensors (FOS) are of interest because they allow both strain and temperature measurement.

Integrated systems commonly combine a number of different types of sensor, e.g. fibre optics for strain measurement, using one or more of the available techniques; acoustic emission and acousto-ultrasonics for corrosion and damage detection; fibre optics or conventional thermocouples for temperature measurement; vibration sensors for local or global assessments.

The associated signal capture equipment should cope with large amounts of data arriving continuously. Signal analysis therefore should be extremely fast with large memory capacities. This can now be provided by 'standard' computers and is often within the capabilities of PCs rather than dedicated specialist computers.

The algorithms used for data interpretation and spatial resolution should be proven against known defect types at known positions in complex structures made from a variety of materials. This needs considerable initial input from conventional NDI evaluation of materials and structural components. Data interpretation has also to be linked to the original design parameters in order to assess the implications of the presence, location and criticality of defects on structural integrity.

The resulting signal analysis has then to be transmitted to a controlling authority; remote integrated systems require telemetry to transmit processed or raw data. This 'output' can then be used to schedule maintenance operations when they are required (for ground-based structures or equipment), instead of the conventional system of routine maintenance at specified intervals. This is viewed as one of the major advantages of continuous monitoring systems, reducing maintenance costs without compromising reliability or safety.

For space applications targeted maintenance is important, although for some of the proposed applications, the practical intervals are dictated by returns to Earth, e.g. RLV.

Another advantage of the continuous monitoring of structures under actual conditions in-service is that the data gathered can be applied in the design, or modification, of similar future applications.

A number of integrated systems are in an advanced stage of development. Some of these have been included in the designs for future space vehicle structures, [See: 92.3]. Figure 91.8.1 shows a schematic layout for a health monitoring system for airframes in military aircraft, Ref. [91-18]. Developed under the US ASIP 'Aircraft Structural Integrity Programme', the system is modular for ease of integration, modification or replacement. The main elements are:

- sensors: monitoring strain, acceleration, temperature, corrosive environment, structural damage.
- local pre-processors: associated with sensor groups in zones, providing sensor management, supervision, polling and acoustic emission data analysis.
- software: maintenance, logistics and decision-making.

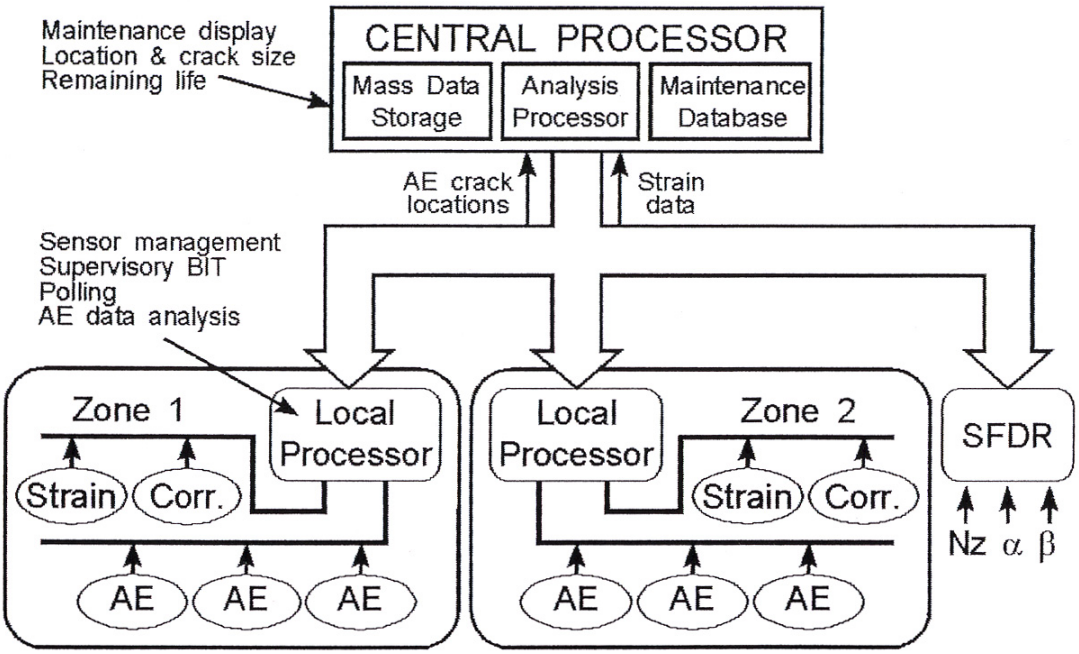

Figure 91.8-1 – Structural health monitoring: Example of an integrated system for military aircraft

91.9 EAP electroactive polymers

91.9.1 Introduction

91.9.1.1 Types of EAPs

The term EAP covers a large number of comparatively flexible and lightweight materials that exhibit a change in shape when subjected to electrical energy. A common classification method distinguishes between materials based on chemical nature and the functional mechanism, Ref. [91-35]:

- ionic or ‘wet’ because they often use an aqueous component,
- electronic or ‘dry’.

Grouping is related to electro-chemical processes occurring during their use. Displacements occur by mass transport processes where ions and solvent molecules are redistributed. Applying an electric field drives electric materials, such as dielectric elastomer actuators and electrostrictive polymers, in much the same way as piezoceramic ceramics. Liquid crystalline elastomers are driven by thermally-induced phase changes. The energy can be supplied through 'Joule heating', in the same way as shape memory alloys. Other polymer materials can change shape or volume when heated, Ref. [91-36].

91.9.1.2 Potential applications

All EAPs are under investigation as potential actuators for both industrial and medical uses, e.g. synthetic muscle. The materials exhibit interesting characteristics and some have been developed as demonstrators. However, turning these phenomena into reliable, functional devices suitable for long-term use in space is a subject for intensive research and development, [See: 92.7].

91.9.1.3 Development status

Research on polymer-based actuators is relatively immature. The first work was conducted in the 1950s, Ref. [91-37]. Work on volume-responsive gels began in the 1980s, leading to EAPs in the 1990s. Activity has increased rapidly since then, e.g. from 20 groups active worldwide in 1996 to more than 60 groups as of 2005, Ref. [91-62], [91-63].

Table 91.9.1 summarises the main types of EAP described in published literature, Ref. [91-64].

Table 91.9-1 – Electroactive polymers: Summary of development of types of materials for actuators

	Materials	Type (1)	Reference
Ionic EAP	Gels:	Ionic	
	- Volume-responsive gels	Ionic	Ref. [91-38], [91-39], [91-41]
	- PVA gels	Ionic	Ref. [91-59], [91-60], [91-61]
	IPMC ionic polymer metal composite	Ionic	Ref [91-51], [91-52]
	Conductive polymers	Ionic	Ref. [91-42], [91-43], [91-44], [91-45]
	Carbon nanotubes	Ionic (partly electronic)	Ref. [91-53]
Electronic EAP	Ferroelectric (piezoelectric) polymers, [See also: 91.3 - sensors; 91.4 - actuators]	Electronic	Ref. [91-46], [91-47]
	Dielectric elastomers	Electronic	Ref. [91-50]
	Electrostrictive polymers, [See also: 91.5]	Electronic	Ref. [91-48], [91-49]
Other EAPs (2)	ER electrorheological, [See also: 91.5]	(electronic)	
	MR magnetorheological, [See also: 91.5]	Magnetic	
	PVME gels.	Thermal	Ref. [91-41]
	Liquid crystal elastomers	Thermal phase change (electronic)	Ref. [91-54], [91-55], [91-56]

Key: (1) Main classes of polymer actuators, Ref. [91-35]; (2) materials that cannot be attributed unambiguously to another group, Ref. [91-64].

91.9.2 Ionic EAPs

91.9.2.1 General

Ionic EAPs, of which several types are described, are generally wet materials as they need an electrolyte to transport ions.

The electrolyte is usually water-based, although some early experiments with non-aqueous electrolytes were performed. The presence of volatile liquids presents a severe problem in applications for materials used in vacuum, such as in space.

An advantage of ionic EAPs is that they operate at low voltages, e.g. 1V to 5V. The response is generally relatively slow (fractions of a second). With the exception of piezo-actuators, they cannot be purchased in standard forms, so they should be developed and adapted for each particular application.

91.9.2.2 Ionic gels

Ionic gels consist of a soft polymer network which is filled with an electrolyte. An increase or decrease in pH changes the electrolyte concentration and generates a swelling or shrinking of the gel. In order to serve as an electromechanical actuator the gel is in contact with two electrodes. The application of a voltage makes the gel swell at one electrode and shrink at the other. The gel body then bends to one side or the other, depending on the polarity of the voltage.

An example of an ionic gel which has been extensively investigated is PVA, which functions by solvent exchange between water and acetone. PVME is a thermally responsive gel with a faster reaction time than PVA, Ref. [91-41].

Gels have been made that respond directly to an electric field, and their behaviour can be precisely modelled, Ref. [91-59]. A composite system, PAMPS (poly 2-acrylamido-2-methylpropanesulfonic acid), consists of a membrane with surfactant molecules, which, when subjected to an applied electric field, gives an overall bending of the membrane.

Recently, various patterning techniques including photolithography have been used to create the microstructures needed to facilitate rapid responses in gels. Such techniques are considered to have promise for microfluid and sensor systems, Ref. [91-61].

91.9.2.3 IPMC ionomeric polymer-metal composites

The actuator properties of IPMCs were first demonstrated in the early 1990s, Ref. [91-51]. These materials have been subject to further extensive development, Ref. [91-52].

IPMC are polymer strips, about 200μm thick, sandwiched between two metal electrodes. Generally the base material is a commercially-available, perfluorinated ionomeric polymer. The anionic polyelectrolyte matrix in a hydrated state is neutralised with cations, balancing the charge fixed to the anionic polymer.

A voltage between the electrodes forces the mobile cations in the polymer to move to the negative electrode. As a result, the composite undergoes a bending deformation toward the anode. The properties of the actuator depend on the polymer, along with the type and concentration of the cations.

IPCM ion exchange membranes made from perfluoronated polysulphonic acids, such as Nafion® polymer (DuPont), have been used in composite actuators and ICPF ionic conducting polymer gel film, Ref. [91-51], [91-52].

91.9.2.4 CP conductive polymers

Conductive polymers were proposed as actuators in 1990, Ref. [91-42], [91-43], [91-44]. Subsequently, bending CP actuators were developed and characterised, resulting in CP micro-actuators, Ref. [91-45].

Conductive polymers can be electro-chemically oxidised or reduced by the application of a voltage. In an electrolyte, this leads to the absorbtion or expulsion of ions and solvent giving a volume change.

Laminating a conductive polymer sheet with another sheet, which does not change in volume, generates a bending moment in the composite. A structure with two conductive conductive polymer sheets has also been used, in which one sheet expands and the other shrinks due to different electric potentials.

91.9.2.5 Carbon nanotube actuators

Carbon nanotube actuators, developed in 1999, Ref. [91-53], are basically fabrics of single- or multi-wall carbon nanotubes in contact with an electrolyte. The length of the nanometre-diameter tubes depends on the applied electrical potential. This arises from changes in the carbon-carbon bond length. The electrolyte is needed in order to form double layers at the surface of the nanotubes. Since the synthesis of carbon nanotubes is a sophisticated process, the availability of pure raw material is limited.

[See also: 43.10 for carbon nanotube materials]

91.9.3 Electronic EAPs

91.9.3.1 General

Several types of Electronic EAP are described. These are known as 'dry EAP' because they do not need an electrolyte, being based on other functional mechanisms. In general, they respond to an electric field, but do not depend on the mobility of ions.

91.9.3.2 Ferroelectric polymers

Ferroelectric polymers exhibit piezoelectric effects and are, in some cases, an alternative to piezoceramics, [See also: 91.3; 91.5].

The most widely-known piezo-polymer material, PVDF (poly-vinylidene fluoride), was discovered in the late-1960s, Ref. [91-46]. Commercially-available piezoelectric polymers are based on PVDF and co-polymers, Ref. [91-47], and these are used in some products, [See also: 91.3].

PVDF has a low expansion in the electric field and a lower coupling coefficient, d33, than the piezoceramic material PZT. The low strain and energy output means that their potential as actuators is somewhat limited. A main application is as high-frequency sensors, e.g. sonic and ultrasonic transducers.

In an attempt to improve energy density, some modifications have been introduced:

- electron radiation of a co-polymer of PVDF with trifluorethylene (P(VDF-TrFE)) has increased the strain up to 5%, but needs very high field strengths.
- electrostrictive co-polymers of PVDF, which have significantly increased the energy density, Ref. [91-48], [91-49].

91.9.3.3 Dielectric elastomer actuators

Dielectric elastomer actuators consist of a thin stretchable polymer film, about 50µm thick, with electrodes on both sides. It can be stretched in the same way as the polymer film and maintain the electric contact under these conditions. Polymer materials that have been used already are silicone and acrylic elastomers.

The actuator effect is based on electrostatic attraction of the electrodes, which compresses the elastomer film perpendicular to its surface and stretches it parallel to the surface. These materials offer the largest elongations of all EAPs (some up to 10%), Ref. [91-50].

91.9.3.4 Electrostrictive graft elastomers

Electrostrictive graft elastomers are polymer materials that comprise two components: a flexible backbone macromolecule and a grafted polymer that can form crystals.

These materials have relatively high electromechanical power densities and offer strains up to 4%.

In combination with P(VDF-TrFE), it can be operated both as a piezoelectric sensor and as an electrostrictive actuator.

91.9.4 Others

91.9.4.1 General

Several other smart materials cannot be unambiguously attributed to other classes of materials. Some of these have attracted much attention and are approaching commercial availability.

91.9.4.2 ER electrorheological materials

Within this group, there are two main types:

- ER fluids, which are suspensions of electrically polarisable particles in a carrier liquid. They exhibit drastic changes of their viscosity in electric fields, [See also: 91.5]. Owing to their controllable viscosity, ER fluids are very promising for adaptive vibration damping and hydraulic applications. Although sometimes grouped under ionic EAP, there are some differences between ER fluids and ionic EAPs.
- ER elastomers, which are the solid analogue of ER fluids. The polarisable particles are distributed in an elastomer matrix instead of a carrier liquid, avoiding problems of sedimentation.

91.9.4.3 MR magnetorheological materials

MR materials exhibit a change in consistency in the presence of a magnetic field.

- MR fluids are analogous to ER fluids.
- MR elastomers contain magnetically polarisable particles, e.g. iron particles in an elastomer matrix.

As with ER materials, MR materials have potential for adaptive vibration damping.

91.9.4.4 Liquid crystal elastomers

First developed in 1980, Ref. [91-54], these materials exhibit a thermal response. Further work has investigated their use as actuators, Ref. [91-55], [91-56].

91.10 References

91.10.1 General

[91-1] N.D.R. Goddard et al
'Smart Materials : A Review of the Four Key Technologies and Their Likely Industrial Impact'
ERA Technology Report 92-0246R, November 1992

[91-2] M.V. Gandhi & B.S. Thompson
'Smart Materials and Structures'
Chapman & Hall, ISBN 0 412 37010 7, 1992

[91-3] R.G. Seippel
'Transducers, Sensors and Detectors'

Reston Publishing Co, Inc. ISBN 0-8359-7797-8, 1983

[91-4] B. Culshaw & J.P. Dakin (Editors)
'Optical Fibre Sensors'
Vol. 1: Principles & Components (ISBN 0-89006-317-6, 1988)
Vol. 2: Systems & Applications (ISBN 0-089006-376-1, 1989)
Published by Artech House, Inc

[91-5] L. McDonald Schetky
'Shape Memory Alloy Applications in Space Systems'
Materials & Design Vol.12 No.1 February 1991, p29-32

[91-6] C.M. Friend
'The Stability of Strain in Shape-Memory Actuators'
SPIE 1777, p181-184

[91-7] L.C. Brinson
'One Dimensional Constitutive Behaviour of Shape Memory Alloys: Thermomechanical Derivation with Non-Constant Material Functions and Redefined Martensite Internal Variable'
Journal of Intelligent Material Systems and Structures, 1993

[91-8] B. Culshaw, P.T. Gardner & A. McDonach (Editors)
First European Conference on Smart Structures and Materials
Glasgow, 12-14 May 1992. Proceedings copublished by IoP Publishing & EOS/SPIE EUROPTO Series SPIE 1777
ISBN: 0-7503-0222-4

[91-9] C. Boller et al
'Technological Challenges with Smart Structures in German Aircraft Industry'
SPIE 1777, p289-292

[91-10] 'Smart Structures for Aircraft and Spacecraft'
75th Meeting of the AGARD Structures and Materials Panel, Lindau, Germany, 5th-7th October 1992
AGARD Conference Proceedings AGARD-CP-531
31 papers, ISBN 92-835-0701-X, 1993

[91-11] P.A. Tutton & F.M. Underwood
'Structural Health Monitoring using Embedded Fibre Optic Sensors'
AGARD Conference Proceedings AGARD-CP-531, Paper No 18, ISBN 92-835-0701-X, 1993

[91-12] P.J. Erbland
'Fiber Optics for the National Aero-Space Plane'
SPIE Vol. 1370 Fiber Optic Smart Structures and Skins III (1990) p29-44

[91-13] R.M. Measures et al.
'Structurally Integrated Fiber Optic Damage Assessment System for Composite Materials'
SPIE Vol. 986 Fiber Optic Smart Structures and Skins I (1988) p120-129

[91-14] G.A. Hickman et al
'Application of Smart Structures to Aircraft Health Monitoring'
J. of Intell. Mater. Syst. and Struct., Vol.2 - July 1991, p411-430

[91-15] P. Sansonetti et al
'Intelligent Composites Containing Measuring Fibre Optic Networks for Continuous Self Diagnosis - I'
Fibre Optic Smart Structures and Skins II, Boston, Sept 1989, SPIE Vol.1170

[91-16] P. Sansonetti et al
'Intelligent Composites Containing Measuring Fibre Optic Networks for Continuous Self Diagnosis - II'
Fibre Optic Smart Structures and Skins IV, Boston, Sept 1991, SPIE Vol.1588

[91-17] L. Bjorkegren et al
'Applications for Artificial Neural Networks'
ERA Technology Report 92-0871R. December 1992

[91-18] J. Wilson & R.J. Hussey: RJ Technical Consultants, (F)
'Structural Health Monitoring Techniques & Potential Application to RLV Composite Primary Structures & Cryogenic Tanks'
Report No. RJTC-046-SHM (September 1999)
ESA Contract 10983/94/NL/PP - Work Order No. 16

[91-19] Dr. R. Graue & A. Reutlinger: Kayser-Threade, (D)
'Structural Health Monitoring for Future Launchers: Results from Breadboarding and Prototype Development'
Proceedings of the 3rd European Conference on Launcher Technology, Strasbourg. 11th – 14th December 2001, p755-766.

[91-20] L. Melvin et al: NASA/Lockheed Martin, (USA)
'Integrated Vehicle Health Monitoring (IVHM) for Aerospace Vehicles'
Proceedings of Structural Health Monitoring: Current Status & Perspectives, Stanford (September 1997). p705. Technomic Publishing ISBN 1-56676-605-2.

[91-21] M.H. Weik
'Fibre Optics Standard Dictionary'
Chapman & Hall. 3rd Edition (1997). ISBN 0-412-12241-3

[91-22] R.J.. Hussey & J. Wilson: RJ Technical Consultants, (F)
'Advanced Technical Ceramics – Directory and Databook'
Chapman & Hall. (1998). ISBN 0-412-80310-0

[91-23] H.G. Wulz & K. Rohwer: EADS-Astrium GmbH/DLR, (D)
'Smart Materials'
ESTEC Contract No. 15865/NL/MV/ CCN3 (September 2004)

[91-24] MIDE Corporation (USA), website: http//www.mide.com

[91-25] G. Horner
Smart Actuator Research, AC2001, Berlin, 2001

[91-26] Wierach, D. Sachau,
'Design and Manufacturing of Complex Adaptive Structures with Piezoceramic Patch Actuators'
International Mechanical Engineering Congress and Exposition, New York, November 2001

[91-27] Bent, A. A., Hagood, N.W., and Rodgers, J.P.,
'Anisotropic Actuation with Piezoelectric Fiber Composites',
Journal of Intelligent Materials Systems and Structures, Vol. 6, May 1995

[91-28] MSI Materials Systems Inc., (USA)
website: http://www.matsysinc.com

[91-29] Wilkie, W et al
'Low Cost Piezocomposite Actuator for Structural Control Applications',
Proceedings SPIE's 7th International Symposium on Structures and Materials, California, March 5-9, 2000

[91-30] Smart Material Corp., (USA)
website: http//www.smart-material.com

[91-31] J.K. Dürr et al
'Smart Composites for Adaptive Satellite Mirrors', AC 2000

[91-32] Melz, T
'Adaptronics in space applications - Adaptronik in der Raumfahrt, Bedarf und Potential,
DLR-IB 131-2000-19, July 2000, Braunschweig

[91-33] Melz, T.
‚Entwicklung und Qualifikation modularer Satellitensubsysteme zur adaptiven Vibrationskompensation an mechanischen Kryokühlern'; PHD thesis, Darmstadt, 2002

[91-34] Y. Bar-Cohen (Editor):
'Electroactive polymer (EAP) actuators as artificial muscles'
SPIE Press (2001)
Y. Bar-Cohen, Jet Propulsion Laboratories, also maintains the World Wide EAP Web hub: http://eap.jpl.nasa.gov/

[91-35] H. Tobushi, S. Hayashi, & S. Kojima,
'Mechanical Properties of Shape Memory Polymer of Polyurethane Series',
JSME International Journal. I, 35:3, 1992.

[91-36] W. Kuhn, B.Hargtay, A.Katchalsky & H.Eisenberg,
Nature 165:514, (1950).

[91-37] T. Tanaka, I. Nishio, S.-T. Sun, and S.Ueno-Nisio,
Science 218, p. 467 (1982).

[91-38] D.W. Urry,
Journal of Protein Chemistry 7 (1988), 1- 34;
Scientific American, 272, Jan. pp. 64-69 (1995).

[91-39] D. De Rossi,
Artificial Organs 12, 3, pp. 259- 260 (1988).

[91-40] Y. Osada, H. Okuzaki, & H. Hori, Nature 355, pp. 242-244 (1992); M. Suzuki and O. Hirasa, Advances in polymer, Science 110, pp. 241-261 (1993).

[91-41] R. H. Baughman et al
'Conjugated Polymeric Materials: Opportunities in Electronics' Optoelectronics and Molecular Electronics, Editors. J. L. Bredas & R. R. Chance, Kluwer Academic Publishers, NL,.pp. 559-582 (1990); R.H. Baughman, Synthetic Metals 78, pp. 339-353 (1996).

[91-42] T. F. Otero et al
Journal of Electroanalytical Chemistry 341, pp. 369-375 (1995).

[91-43] D. De Rossi & P. Chiarelli
'Biomimetic macromolecular actuators',
ACS Symp. Ser. 548, pp. 517-530 (1994); P. Chiarelli, D. De Rossi, A. Della Santa, and A. Mazzoldi, Polymer Gels and Networks, 2, pp. 289-297 (1994)

[91-44] Q. Pei & O. Inganäs, Adv. Mater. 4, pp. 277-278 (1992); E. Smela, O. Inganäs, and I. Lundstrom, Science 268, pp. 1735-1738 (1995); E. Smela, O. Inganäs, Q.B. Pei, and I. Lundstrom, Adv. Mater. 5, pp. 630-632 (1993).

[91-45] H. Kawai,
The Piezoelectricity of Poly(vinylidene Fluoride),
Jpn. J. Appl. Phys., 8, pp. 975-976 (1969).

[91-46] Measurement Specialties Inc., Fairfield, New Jersey, USA.

[91-47] M. Zhenyi, J. Scheinbeim, J. Lee, and B. Newman,
J. Pol. Sci. B : Pol. Phys. 32, pp. 2721- 2731 (1994).

[91-48] Q. M. Zhang, V. Bharti, and X. Zhao, Science 280, pp. 2101-2104 (1998); Z. Cheng, H. Cohen; Proc. SPIE, 4329, pp. 106–116 (2001).

[91-49] R. Kornbluh, R. Pelrine & J. Joseph
Proceedings of 3rd IASTED International Conference on Robotics and Manufacturing, Cancun, Mexico, pp. 1–6 (1995).

[91-50] K. Oguro, Y. Kawami & H. Takenaka,
J. Micromachine Soc 5, pp. 27-30 (1992).

[91-51] M. Shahinpoor et al
Smart Mat. Struct. 7, R15-R30 (1998).

[91-52] R.H. Baughman et al
Science 284, pp. 1340-1344 (1999).

[91-53] H. Finkelmann, & G. Rehage, Macromol. Chem. Rapid Commun. 1, pp. 31-34; ibid. pp. 733-740 (1980); H. Finkelmann, H.J. Koch, and G. Rehage, Macromol. Chem. Rapid Commun. 2, pp. 317-322 (1981).

[91-54] P.-G. De Gennes,
C. R. Acad. Sci. Paris, Ser. II, 324, pp. 343-348 (1997).

[91-55] D.L. Thomsen III et al
Macromolecules 34, pp. 5868-5875 (2001).

[91-56] D. Brock et al
Intelligent Material Systems and Structures 5, pp 764-771 (1994)

[91-57] H.B. Schreyer et al
Biomacromolecules 1, pp 642-647, (2000).

[91-58] T. Wallmersperger, B. Kröplin & R.W. Gülch
'Electroactive polymer (EAP) actuators as artificial muscles'
Editor Y. Bar-Cohen, SPIE Press, pp. 285-308 (2001)

[91-59] Osada, Y., Okuzaki, H & Hori H.
'A polymer gel with electrically driven motility'
Nature 355 (6357), pp. 242-244 (1992).

[91-60] Ito, Y.
'Photolithographic synthesis of intelligent microgels,
J Intelligent Material Systems and Structures 10 (7), pp. 541-547 (1999); Hu, Z.B et al: Polymer gels with engineered environmentally responsive surface patterns, Nature 393 (6681), pp. 149-152 (1998).

[91-61] P. Sommer-Larsen: The Danish Polymer Centre
Risø National Laboratory, Denmark

[91-62] R. Kornbluh
SRI International, Menlo Park, Califonia, USA

[91-63] NPL – National Physical Laboratory, (UK)
http://www.npl.co.uk/materials/functional/standards.html

[91-64] 'Biomimetics – a new approach for space system design'
ESA Bulletin, No. 125, February 2006
ESA ACT Advanced Concepts Group:
http://www.esa.int/gsp/ACT/biomimetics/testcases_research_CM.htm

92 Potential space applications

92.1 Introduction

Over the years, many imaginative ideas have been put forward for smart systems to enhance the capabilities of structures, Ref. [92-1]. Although some smart technologies are relatively new, they are maturing rapidly, [See: 91.8]. This chapter concentrates on those which have realistic prospects of achieving useful functions in aerospace structural configurations. Improvements in aircraft design have been a prime motivator. Some examples are discussed briefly, Greater attention is given to technologies which may be of use in space, [See: 93.3].

Space applications can be broadly grouped as:

- long-term deployed structures.
- reusable launch vehicles (RLVs).

A particular smart technology or system can be appropriate for both application groups. Under the European FESTIP and FLTP programmes, the technologies investigated for future reusable launch vehicles (RLVs) indicated a number of structures that could benefit from 'smart' systems. A similar approach has been taken in the US X-vehicle programmes and TETRA in Germany.

[See: 93.3]

92.2 Perceptions of aerospace requirements

92.2.1 Aircraft smart skin configurations

92.2.1.1 General

The concept of 'smart skins' came from the idea that most aircraft external surfaces would be moulded fibre-reinforced plastics, and that composites are an adaptable medium for containing a network of sensors, Ref. [92-2] to [92-15].

Significant benefits are claimed for these ideas, including:

- networks of sensors could detect surface impacts and indicate the presence of damage, e.g. BVID.
- actual strains induced by flight manoeuvres could be recorded and any overloads indicated.
- damage detection could be extended to monitoring crack growth and fatigue damage propagation.

The overall benefit would be a comprehensive health and condition monitoring system avoiding regular manual inspection. This would save inspection costs and give consistent diagnosis independent of human interpretation.

92.2.1.2 Damage

Composite damage and its significance to structural integrity is important. Composites on the whole are tolerant of impact damage and delaminations because total failure by a single crack propagation mode is not possible. Composite structures presently in service confirm this. A partial explanation is that structures are designed to meet both stiffness and strength criteria and that applied composites are under-utilised from a strength perspective. The low strain and stress levels experienced in service coupled with the good fatigue performance of composites, mean few problems arise unless gross damage is experienced.

Composites are increasingly being applied to primary, as well as secondary structures. As loads increase, so does the available elastic energy for damage propagation. It could be argued that integrated monitoring is becoming essential, not least because of the inaccessibility to traditional inspection techniques.

The reasons for use of smart skin configurations requires closer examination. Composites have been used successfully for many years without smart systems. Addition of these can only be justified if they perform necessary functions. Indicating a selective process to identify critical areas for integrated monitoring of, for example:

- high risk of impact damage.
- high, uncertain localised loads with repetitive cycling.

92.2.2 Helicopter rotor blades

Helicopters have been likened to flying fatigue machines. The level of mechanical fatigue in rotor blades is high, where high cyclic loads are experienced with rotation and various flight modes. High noise and vibration levels are present in the fuselage, which is both a physical discomfort to the occupants and a fatigue concern for the structure. The incentives to reduce vibration levels by active control are therefore present, not least as passive damping techniques have reached their limitations, Ref. [92-16].

Current rotor blade technology relies on a reinforced plastic composite with the blade design optimised for fatigue strength, stiffness and natural frequency. The blade core is suggested as a possible location for actuating media, communicating by fibre optic sensors (FOS) embedded in the laminar composite construction. All of the known 'smart' actuating materials have been proposed as having a potential role in:

- vibration damping, and
- modifying the aerodynamics of blade sections.

No data has been identified to quantify the weight or volume of actuating medium needed to achieve the desired effects.

It is proposed that Individual Blade Control (IBC) can be achieved by PZT sensor-actuators, Ref. [92-17], [92-18]. A closed-loop subsystem could be used to control the blade modes that are recognised to have low damping ratio in the vicinity of the fundamental resonance frequency of the rotor.

92.2.3 Detection of ice build-up (Location detector)

Ice build-up on wing leading edges affects the aerodynamics of fixed wing aircraft. A similar phenomenon is experienced with helicopters.

The presence of ice is not critical until sufficient build-up is present. Human judgement usually determines whether or not the deposition is at a critical level. This is subjective, and mistakes have been made with consequent loss of aircraft.

Adding sensors to the leading edge can quantify the build-up. This has been successfully demonstrated with PVDF piezoelectric point sensors acting as locating sensors, which indicate additional loads on the structure.

Similar point sensors could be used to monitor load distribution within an orbiting space-station, for example.

92.2.4 Composite cure monitoring

Integration of fibre optic sensors (FOS) into composite laminates is widely described for structural integrity monitoring. A further possible benefit lies in the use of the fibre optics to monitor the cure cycle of composites.

Interrogating light pulses in the fibre optics can determine the temperature distribution and residual stresses during pressure consolidation.

The monitoring outputs could then be used to:

- provide assurance that a reproducible consolidation had occurred in comparison with previous mouldings, i.e. quality control.
- more ambitiously, the fibre optic response could be looped into the moulding facilities providing 'active compensation' for cure cycle conditions.

Both ideas appear tenuous because:

- composites are already adequately moulded without resorting to fibre optic monitoring.
- un unwelcome additional complexity and cost in instrumenting the fibre optics during the manufacturing cycle.

The need or use of fibre optics for 'cure monitoring' is unproven. It is considered a possible application, without any current justification.

92.2.5 Composite structure embedded communications networks

92.2.5.1 General

A smart skin need not only contain a network of sensors, but could be expected to have embedded elements capable of performing other functions, such as:

- fibre optic communication links.
- electro-magnetic functions: Radio communications by in-skin arrays, avoiding the weight and aerodynamic inefficiency of a protruding aerial.
- radar: A look-up and look-down facility produced by elements distributed in the wing upper and lower surfaces.

Embedding any media in composites requires consideration of:

- complication of the moulding process.
- reduction in the integrity of the composite.

92.2.5.2 Embedded actuators

Embedding actuators in structural sections has been proposed, particularly within composite sections. An actuator filled cavity within metal sections is another concept.

Surface bonded actuators are less exciting for 'smart material' concepts, but pose fewer problems in guaranteeing the integrity of a structural section.

92.2.5.3 Effect on structural integrity

Most aerospace composites are laminar constructions based on fabric or UD plies. Their integrity depends on bonding between adjacent plies, as characterised by interlaminar shear strength (ILSS).

The presence of a third phase between the plies begins to compromise laminate shear integrity. An embedded actuator material can be likened to inclusions or porosity.

The integrity of the composite can impaired in a number of actuator concepts, these include:

- sandwiching of complete layers of PVDF film between prepreg plies; adhesion between prepreg and PVDF is poor.
- incorporating heavy meshes of SMA, e.g. woven wires, between prepreg plies without additional adhesive. The co-weaving of SMA wires with reinforcing fibres would be far better.
- incorporating large areas of piezoceramic which is brittle and has insufficient strain capacity to flex with the composite.

These points do not preclude the development of embedded actuator technology, provided that it is thoroughly considered.

Further factors are:

- thin sheets of SMA may be incorporated between prepreg plies with additional film adhesive giving a laminated material similar to FML.
- design rules for creating balanced laminates apply, unless controlled distortion is designed for. An SMA incorporated into a planar composite could induce transverse stressing when triggered. Such stressing should be accommodated without causing delamination.
- overall actuator mass is a controlling factor and actuators are unlikely to contribute significantly to the overall strength and stiffness of a composite section. They could therefore be a liability in mass-management.

Justification for using embedded actuators causing a mass penalty of more than 10 to 20% is unlikely.

92.3 Level 1: Condition and health monitoring

92.3.1 General

The term ‘condition monitoring’ generally describes monitoring systems applied to machinery and plant, whereas ‘health monitoring’ is a term applied to assembled structures.

Condition monitoring is widely applied to various spacecraft subsystems. Structural health monitoring (SHM) is of growing interest for long-term deployed structures, particularly in future RLV concepts.

All health monitoring systems are classed as ‘Level 1’ smart systems, [See: 90.2].

[See also: 94 – European capabilities]

92.3.2 Objectives

Structural health monitoring (SHM) provides evidence on the safety and reliability of a structure throughout its intended service life (with a required level of confidence). An additional aim when considering RLVs is to reduce between-flight maintenance and turn-round times by targeting the on-ground inspection and maintenance procedures, Ref. [92-35], [92-36].

SHM is a supplementary technology that can provide additional confidence in structural performance under real operational conditions over extended periods of time. It cannot replace, even in part, the stringent design analysis, testing and on-ground verification exercises used to produce safe, reliable structures.

92.3.3 Approach

92.3.3.1 General

Figure 92.3.1 shows a logical approach applied to developing a health monitoring system, Ref. [92-35]. Although this was developed for cryogenic tank structures, it can also be applied to other types of structures. However, the details will vary with each application, e.g. identification stage, operational parameters, etc.

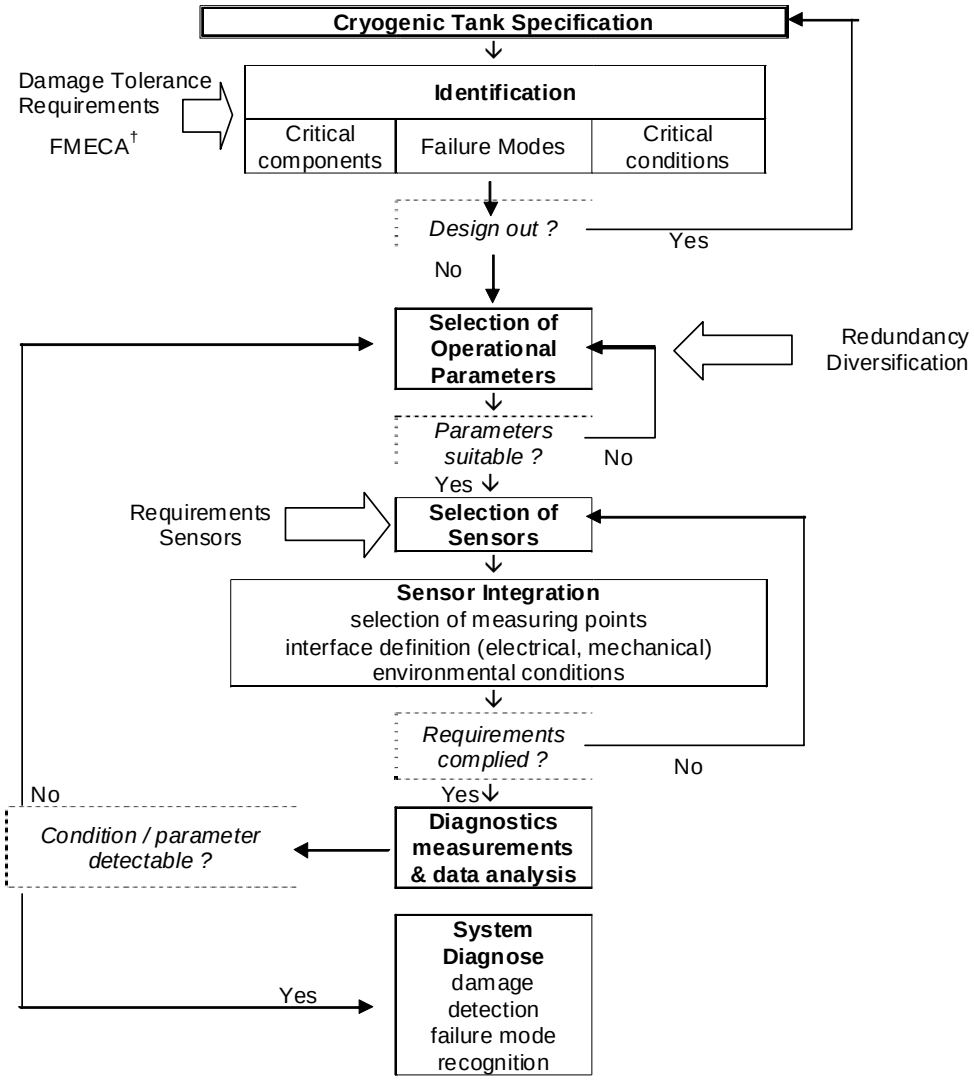

Key: † - FMECA - Failure mode effects and criticality analysis

Figure 92.3-1 – Structural health monitoring: Logic chart for RLV cryogenic tank structures

92.3.3.2 Potential failure modes

The definition and identification of potential structural defects and failure modes is supported by analytical methods, e.g. FMECA, which examines all conceivable failures and their effects on the structure.

92.3.3.3 Operational parameters

This stage identifies which detection principles and techniques are suitable for the potential failure modes and defects. It also establishes a set of measurands (properties and characteristics of the structure) to be monitored.

Independent sensors are used to measure the required properties of any given failure mode (diversification), so allowing a more accurate assessment. The effect of defects (or damage) on the overall assembled structure dictates the level of redundancy in the design. All assessments of the structural integrity resulting from damage/defects should be in accordance with the damage tolerance design principles applied, i.e. each damaged area should be determined, localised and

monitored. In-flight monitoring measures the various flight parameters and determines whether they are within the defined operational range.

92.3.3.4 Sensor selection

The selection of appropriate sensor technologies is very important as are the choices in automation or remote sensing. Technologies should be sufficiently mature and the overall system should be robust in order to survive repeated excursions in the service environment, e.g. extreme temperatures, loads.

92.3.3.5 Sensor integration

The ease of integration of the system into the structure is important. There may be requirements to monitor large areas such as tanks, or discrete points with limited access, e.g. within cryogenic insulation, TPS stand-offs, composite structures.

Ideally the mass and power requirements of the system should be minimised, and be within the overall defined project budgets. This includes not only the sensors but all of the supporting data capture, analysis and telemetry equipment.

92.3.3.6 Diagnostics

Requirements for the 'measurement and data analysis' and the 'system' diagnostic stages are similar to those applied in on-ground NDE, [See also: Chapter 34; Chapter 80]. These two stages effectively determine whether the system is producing accurate, reliable data that has been interpreted correctly to give damage detection, progression and failure mode recognition.

92.3.4 Applications

European studies FESTIP, FLTP and TETRA (D), along with US X-vehicle programmes, identified the RLV structures that could benefit from structural health monitoring as, Ref. [92-35], [92-36]:

- cryogenic tanks.
- airframe components, made of composite materials.
- hot structures.
- thermal protection systems components, e.g. nose cone, nose skirt.
- highly-loaded regions.

Considerable effort has been placed on developing monitoring systems that can be applied to these structures, [See: 92.3].

SHM is only one part of the overall integrity control approach to reusable space structures. It is combined with proven design analysis techniques and on-ground NDI and NDE of the materials used in structural configurations.

92.3.5 Techniques

The techniques for SHM systems have developed from:

- conventional NDE techniques that are applied to the same structures on the ground, e.g. acoustic emission.
- smart technologies, e.g. fibre optics, piezoelectrics.

Only a few conventional NDI techniques are readily adaptable for in-flight use, e.g. those not requiring specialist facilities (clean-room, vibration-free).

Some in-flight sensors can be embedded in the materials themselves, whereas others are surface mounted, albeit within an assembled structure and not always easily accessible.

Table 92.3.1 summarises some developments in fibre optic strain measurement techniques.

Table 92.3-1 – Structural health monitoring: Fibre optic - Example developments for strain measurement

Type of system	How applied	Achievement/claims
Double polarisation Michelson interferometer	Surface bonded (CFRP)	Point strain measurement comparable with conventional resistive strain gauge, Ref. [92-5]
White light quasi-distributed polarimetric sensing with Hi-Bi pig-tailed SLD, with multi-thickness Michelson mirror	Embedded/surface bonded (GRP)	Accurate and linear measurement with temperature compensation (in development), Ref. [92-19]
Novel OTDR system with local inhomogeneities (Bragg grating)	Embedded (CFRP)	For multiple point strain measurement of strain and temperature (in development), Ref. [92-4], [92-20], [92-21]
Time division multiplexing (TDM) of in-line coupled Fabry-Perot interferometers with Bragg gratings as weak reflectors. Two core fibre.	For embedding in composite	Simultaneous and separate measurement of strain and temperature (in development), Ref. [92-22]
Interfero-polarimetric measurements with Hi-Bi 'Bow Tie' and side-hole birefringent 'FASE' fibre.	Embedded/surface bonded (Woven ARP)	Developed for impact detection, Ref. [92-6]
Intrinsic Fabry-Perot fibre optic strain gauges with single modulated laser diode	Surface bonded	Measurement of static and dynamic (vibration) strain. Good agreement with metal foil strain gauges, Ref. [92-23]
Silica mono-mode fibre with Fabry-Perot resonator end termination. λ=783 nm wavelength laser diode	Embedded (CFRP sandwich panel face skins)	Linear response (point sensing). Compensation required to match foil strain gauges, Ref. [92-13]

The potential techniques considered for health monitoring of space structural applications are summarised in Table 92.3.2 for both on-ground and in-flight use, Ref. [92-35], [92-36].

The selection process has taken into account the various requirements established during the stages in the SHM design approach, [See: Figure 92.3.1 (bold text)].

Table 92.3-2 – Structural health monitoring: Potential techniques for space structures

Application	Technique(s)	Use
DC-XA Delta Clipper: LH2 tank	Acoustic emission	In-flight
X-33: Propulsion tanks	Distributed fibre optic sensor network (Bragg grating; Raman) Acoustic emission	In-flight
X-38: Cryogenic tank structures	Distributed fibre optic sensors Acoustic emission	In-flight
X-38: Thermal protection system (1)	Acoustic emission	In-flight
	Vibrometry	
	Laser shearography	On-ground
	Infra red thermography	
Clipper-Graham: LH2 tank	Fibre optic sensors (Bragg grating) (2)	In-flight
Solar sail	Fibre optic sensors	In-flight

Key: (1) Comparison with conventional, high-temperature strain gauges.
(2) Patented and licensed technology (Boeing Co.)

92.3.6 Cryogenic tanks

92.3.6.1 Potential failure modes

In the SHM approach outlined, [See: Figure 92.3.1], the potential failure modes that can cause degradation in a tank structure are identified as, Ref. [92-35]:

- metallic tank wall: cracks, corrosion, stress-corrosion cracking.
- composite tank walls: delaminations, voids, inclusions.
- joint failures and disbonds: between various parts of the tank, e.g. cryogenic insulation to tank wall, liner-to-composite skin.
- cryogenic fuel leaks.

92.3.6.2 Sensor selection and integration

Table 92.3.3 summarises the techniques considered for the various potential failure modes and defects identified in cryogenic tank subsystems, Ref. [92-35]. This shows that acoustic emission and fibre optic-based technologies have the most potential for in-flight use because they are capable of detecting a large number of defect types.

Table 92.3-3 – Structural health monitoring: Potential techniques for RLV cryogenic tanks

Cryotank subsystem	Failure/Damage	Technologies	Use
TPS panels, hot insulation, oxidation protection coatings	Surface and impact damage, cracks and other defects.	Visual inspection IR Thermography Ultrasonic	On-ground
		Acoustic emission	In-flight
Tank wall (metal)	Through-thickness cracks	Ultrasonics Optical interferometry	On-ground
		Acoustic emission	In-flight
Tank wall (composite)	Delamination Fibre and/or matrix cracking	Fibre optic sensors (strain, temperature) Acoustic emission	In-flight
		Laser shearography Electronic speckle pattern interferometry	On-ground
Debonding	Cryoinsulation-to-tank wall Insulation core splices CFRP skin-to-insulation core	Laser shearography Ultrasonic S-scan IR thermography Holography Tele-robotic systems	On-ground
	Internal insulation (composite tank)	Acoustic emission	In-flight
TPS/Tank wall	Hot joint failure	Laser-based ultrasonics	On-ground
		Acoustic emission	In-flight
Cryoinsulation/Tank wall	Hydrogen Leak	Hydrogen sensors	In-flight
		Fibre optic H_2 sensors	

92.3.6.3 X-33 cryotank structural health monitoring system

This SHM system provides a global strain and temperature map for monitoring the health of the X-33 tank structure, cryo-insulation and TPS. Hydrogen sensors, sited along the multi-lobe tank joint, monitor leaks.

It relies on a network of distributed fibre optic sensors (FOS) consisting of:

- Optical fibres, [See: 91.4]:
  - Bragg Grating: measuring strain and hydrogen (16 single mode optical fibres with 20 to 25 Bragg gratings per fibre on the LH2 tank).
  - Raman: measuring temperature (2 multi-mode FOS on each of the 3 tanks).
- Acoustic sensors: to locate cracks and monitor their growth (4 sensors on LH2 tank).

The FOS 'Distributed Strain Sensor' (DSS) system was applied to the composite substructure at both bolted joint locations and along the barrels. Biaxial strain was monitored from FOS placed in hoop and axial directions.

The FOS 'Distributed Temperature Sensor' (DTS) system was installed on top of the foam in a repeated loop pattern to allow a thermal profile of the foam insulation. Special techniques were developed for installing optical fibres onto tankage, e.g. curved ramps, protective tubing. Conventional strain gauges and thermocouples were mounted on the structure for comparison purposes.

The associated electronics and instrumentation were mounted in the avionics bay and optical fibres routed from the chassis to the tank structures.

Initial trials on a 70% scale dual-lobed composite LH2 tank used over 180m of DSS and DTS and underwent 30 cryo-cycles up to 0.7MPa (100 psi).

92.3.6.4 DC-XA cryotank structural health monitoring system

The DC-XA LH2 tank is a CFRP (IM7/epoxy) cylindrical structure with elliptical domed ends. Thermal insulation is bonded to the inside of the composite tank structure.

Boeing developed an acoustic emission (AE) based SHM system, known as AEFIS 'Acoustic Emission Flight Instrumentation System'. This consists of 4 sets of 3 different types of AE sensors which were adhesively bonded at a tank-skirt joint. During trials, both traditional AE and waveform data was recorded in the AEFIS instrumentation and downloaded to a PC after the test.

Waveform analysis combined with real-time filtering was necessary to discriminate 'real' features or events from the in-flight background noise, which reached ~170dB with rocket engine noise and aeroshell vibration.

The results of 3 completed flight trials showed AE events that could be correlated with flight processes (launch, ascent and descent, acceleration and deceleration, landing). Other AE events were related to thermal stresses at cryogenic temperatures, pressurisation and flight-induced loads. These were considered to originate from non-detrimental levels of microcracking in the composite and within insulation constructions. A fourth flight trial was aborted when the AE event hit rate was significantly higher than that seen previously.

From triangulation of the sensors, the spatial resolution indicated a significant event had occurred at the top of the tank and appeared to be progressing along it. Post-flight inspection confirmed debonding of the internal thermal insulation.

92.3.7 Thermal protection systems (TPS)

92.3.7.1 General

Within the X-38/TETRA programme, critical areas were identified as those under the highest thermal and mechanical loads during re-entry, e.g.:

- hot structures: leading edges, body flaps.
- TPS: stand-offs, seals, CMC panels (C-SiC)
- structural components: spars and ribs.

The aim of the SHM system was to identify large defects that are then targeted for on-ground inspection and maintenance.

92.3.7.2 X-38 nose skirt

Acoustic emission (AE) sensors are mounted inside the structure, with a waveguide (titanium wire) connected to the CMC nose skirt panel. Advanced data processing and analysis (FFT, pattern recognition, filtering) is applied to the received signals in order to discriminate real events from the background noise. This system, coupled with on-ground IR thermography, has demonstrated the feasibility of detecting critical defects, such as delaminations, impacts and cracks.

92.3.8 Structural components

92.3.8.1 X-38 aft structure

Mechanical load analysis showed that Frame 3 (7075 aluminium alloy with anti-oxidation protective coating) in the aft structure experiences two peak loads on the deployment of drogue chutes and the firing of the propulsion system.

FOS loop sensors each containing 6 Bragg Gratings (4 strain; 2 temperature) are surface mounted on Frame 3 to monitor predetermined positions. Each FOS is looped to position the gratings orthogonal to each other. Figure 92.03.2 is a schematic of the installed system, Ref. [92-35], [92-36].

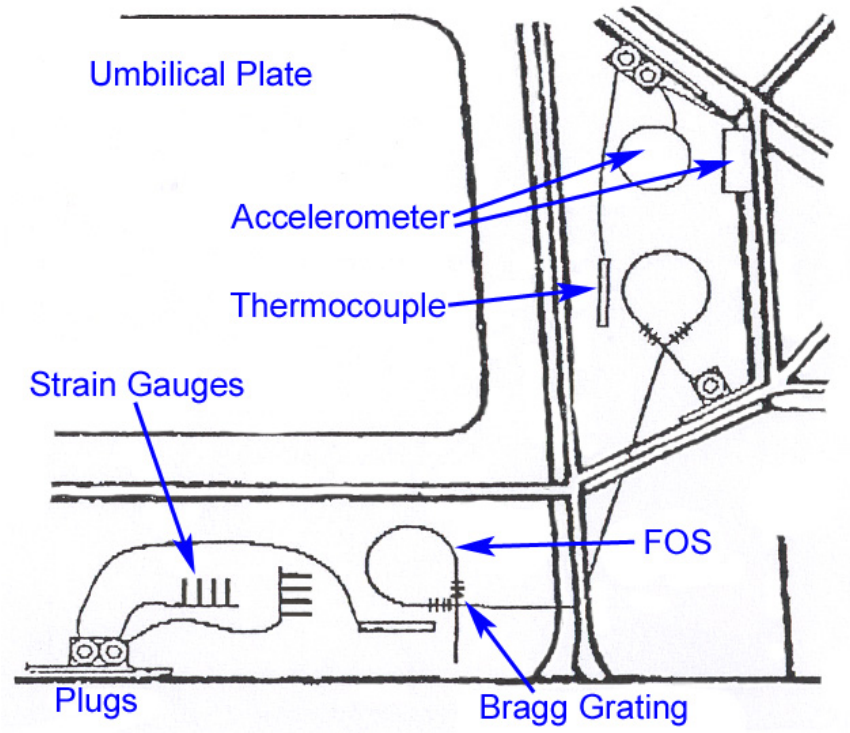

Figure 92.3-2 – Structural health monitoring: X-38 aft structure

92.3.8.2 X-33 composite wing box

High-temperature capability, carbon fibre-based composites are being considered for primary airframe components in order to meet mass budgets on future RLVs.

Destructive testing of a full-scale composite (carbon/bismaleimide) wing segment was also used to evaluate the applied SHM system that measured deflection, strain and temperature. No further details have been openly published.

92.3.9 Long-term deployed structures

92.3.9.1 General

Likely degradation mechanisms of long-term deployed structures are:

- environment-related: exposure to space (thermally-, vacuum- and radiation induced, atomic oxygen), particle and debris impacts,
- accidental damage: either during or post assembly; docking with visiting vehicles.

Such structures have an additional complication in that all preventative or corrective maintenance is conducted in space. Apart from the technical difficulties, this is an expensive option, particularly if it requires a special mission. Consequently the ability to continually monitor structures and make an early and accurate assessment of degradation or damage is important for reducing costs.

Manned structures, such as ISS, have additional stringent safety requirements.

92.3.9.2 Solar sail

Owing to their low mass, fibre optic sensors have been investigated for measurement of boom bending during the operation of a solar sail concept, Ref. [92-36].

92.4 Level 2: Deployment

92.4.1 Requirements

As antenna structures become larger, then deployment techniques are necessary for unfolding stacked payloads. The projected use of extensive truss structures also increases the need for joints to connect structural sections. In the context of 'smart materials', this provides opportunities for shape memory alloys (SMA).

92.4.2 Shape memory alloys

92.4.2.1 General

The majority of applications only need a single deployment action which can be achieved with one-way SMAs. More complex two-way systems would be justified if structure retrieval or dismantling were in the mission specification.

92.4.2.2 Mass and power efficiency

The arguments for considering SMAs for actuators centre on their efficiency in terms of mass and power consumption given the forces and displacements provided by them. In some cases this is better than that achieved with electromechanical or hydraulic actuators.

92.4.2.3 Temperature ranges

Heating is essential to trigger the shape memory phenomenon. If the operational environment for the actuator was, for example, -100°C to +150°C, then the transformation temperatures of the alloy needs to be below and above these temperatures to avoid mis-operations.

Local heating above 150°C, for triggering, requires sufficient electrical power. A narrower operational temperature range, through careful alloy selection, lowers the power consumption. Quantifying thermal losses is also important.

92.4.2.4 Concepts

Some concepts for SMA applied to deployment mechanisms and structural connections are given in Figure 92.4.1, Figure 92.4.2, Figure 92.4.3 and Figure 92.4.4, Ref. [92-24].

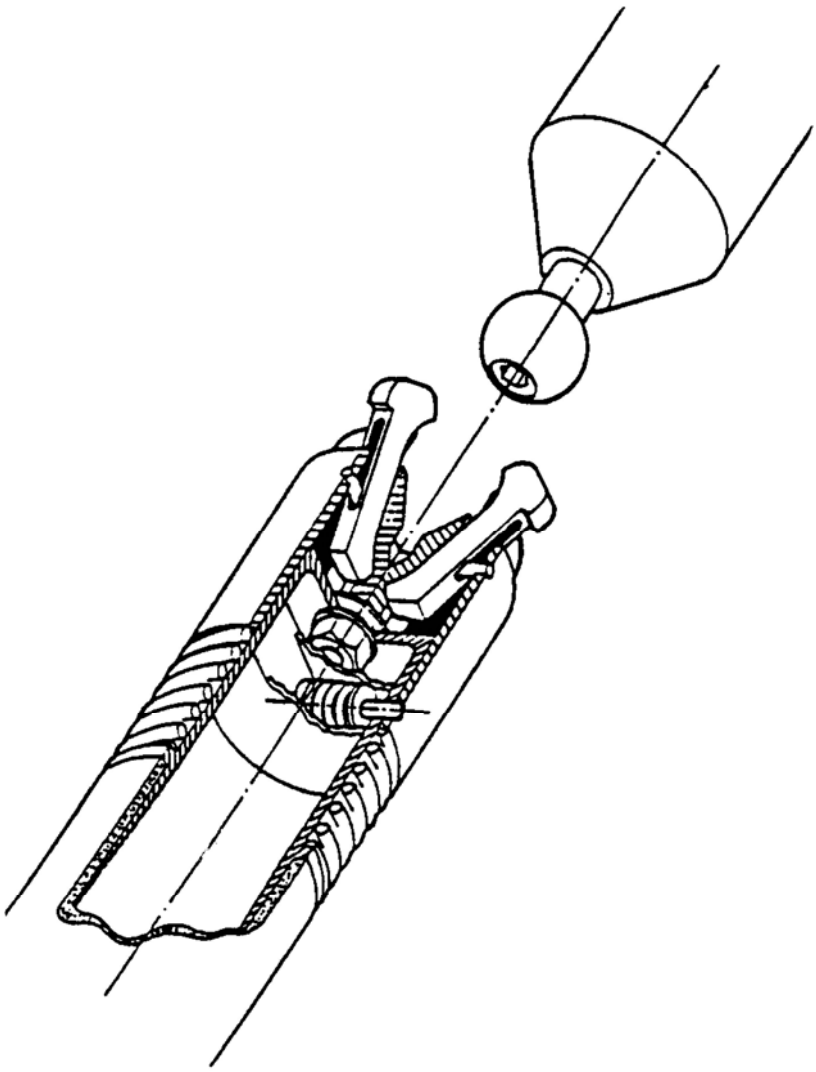

Figure 92.4-1 - Shape memory alloy concepts: Ball and socket for assembling composite tubing

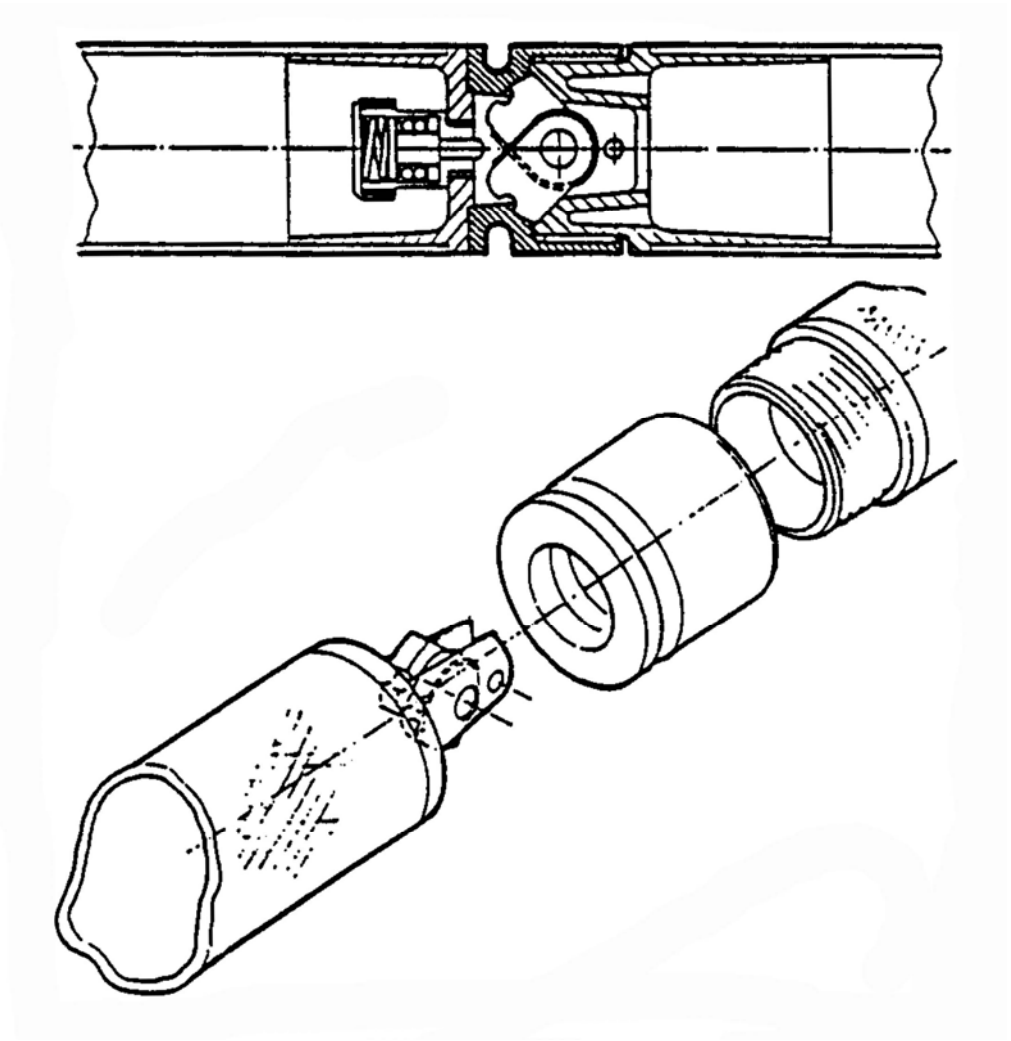

Figure 92.4-2 - Shape memory alloy concepts: Sprag-type coupling for assembling composite tubing

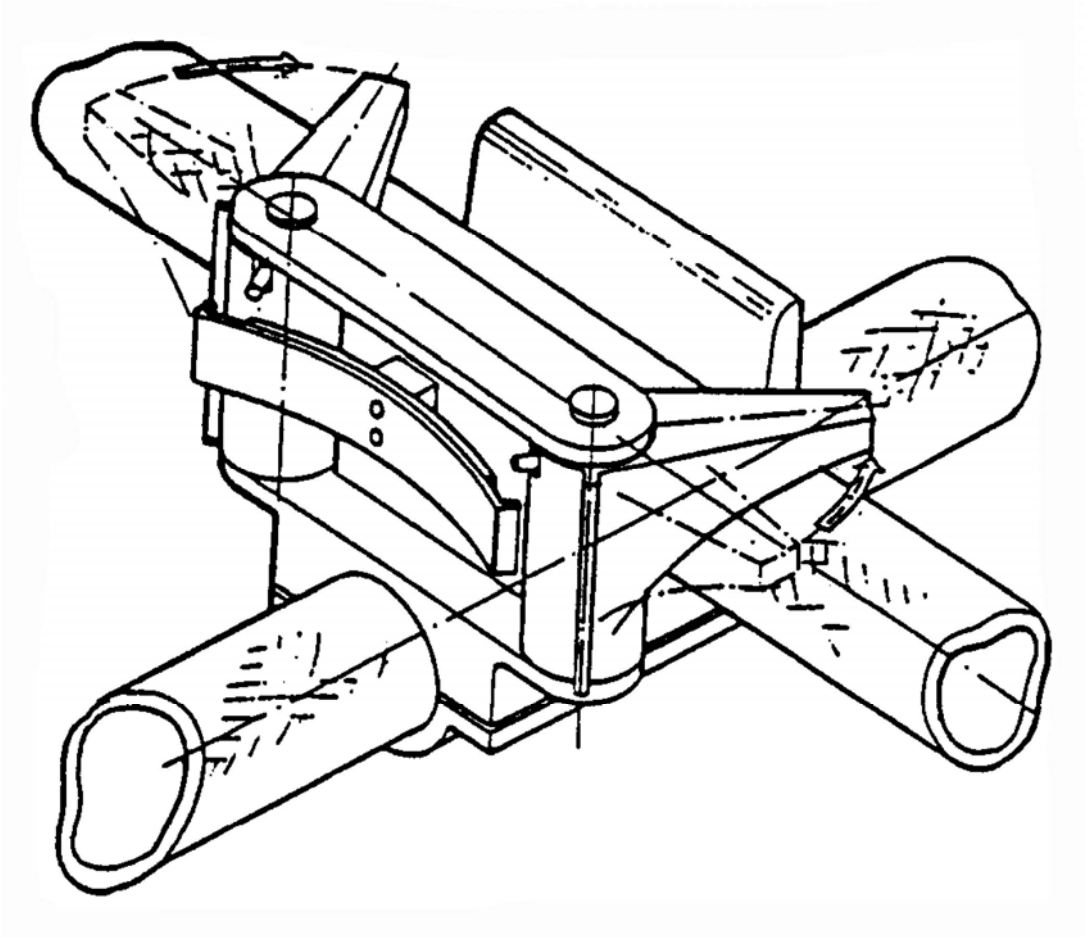

Figure 92.4-3 - Shape memory alloy concepts: Latching system for assembling cross-type composite tubing structure

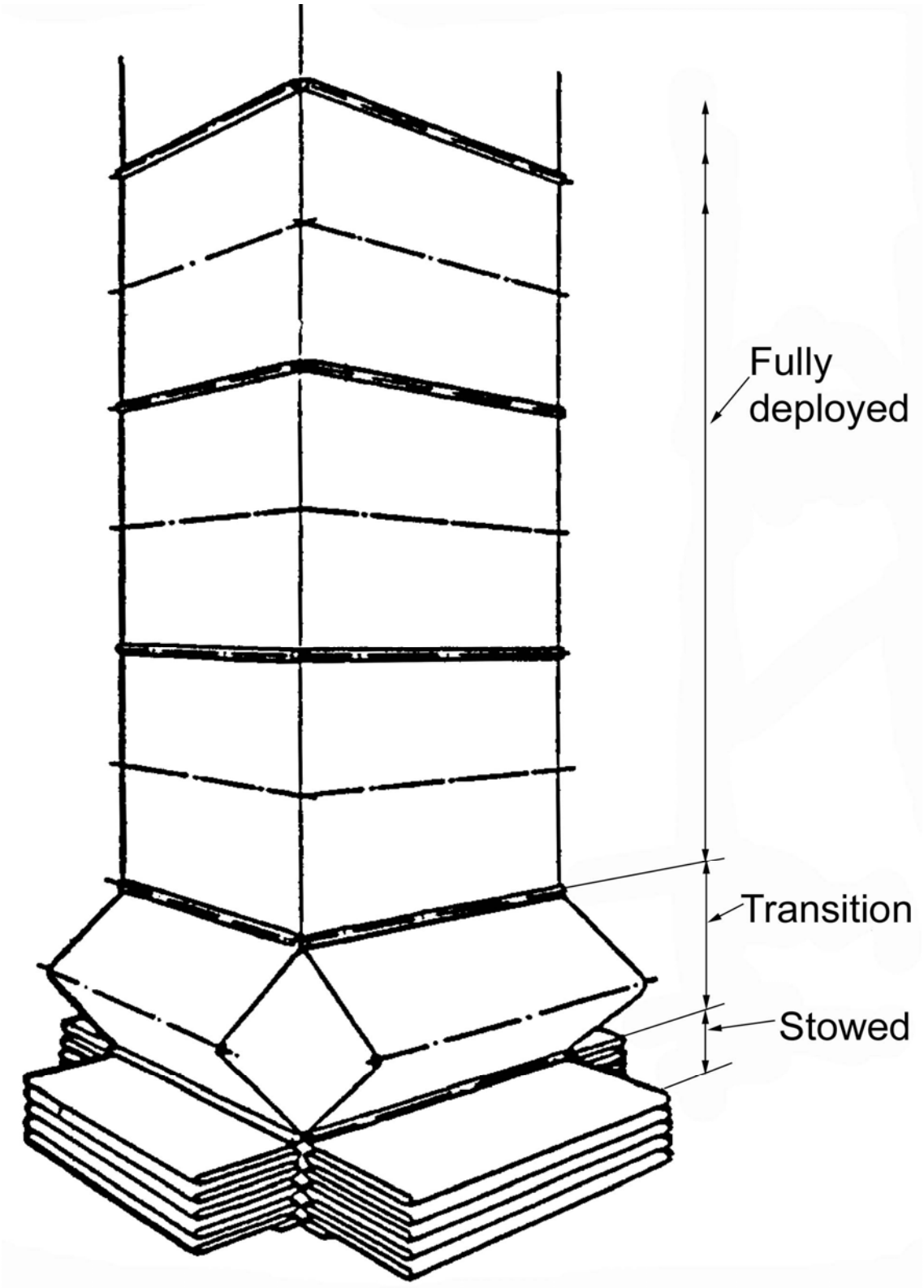

Figure 92.4-4 - Shape memory alloy concepts: Folding box protective shell erected by SMA actuator

92.4.2.5 Developments

A lack of material characterisation has been proposed as a limiting factor for greater utilisation of SMAs. Whilst high theoretical recovery stresses over large strains can be attractive on paper, a very good understanding of the transformation characteristics of the alloy is needed to design engineering components.

SMA wires in development studies are popular because:

- wire is readily available.
- thermo-mechanical treatment is relatively simple.
- use of the wires as resistive heating elements is simple.

Table 92.4.1 shows the characteristics of a development actuator, Ref. [92-25].

Table 92.4-1 - Shape memory alloy: Development actuator characteristics

Actuator length (mm)	280
Operational stroke (mm)	± 3 (push/pull)
Force applied (N)	± 1000
Material: NiTi alloy, with two-way function	

The actuator consisted of twenty-four wires, each 0.5mm in diameter. The total cross-sectional area of SMA material was 4.7mm2. The maximum achieved force was 4000N, implying a recovery stress of 850MPa.

To produce a balanced push-pull (two-way) capability, the design was limited to a maximum of 1000N each way or 2000N for a single 'one-way' stroke. A length of 280mm provided the option of gradient heating to allow some positional control over the ± 3mm stroke.

The control over heating and cooling rates was dependent on heat dissipation. Typical cyclic rates of operation were 0.01Hz to 0.05Hz, i.e. 100 to 20 seconds per cycle, in air.

Optimistic claims suggested improvements could be made to achieve 0.2Hz in air and 0.005Hz (once every 200 seconds) in vacuum.

92.4.2.6 Summary of SMA actuators

The justification for SMA actuators lies largely in the assembly and disassembly of large complex space platforms, e.g. truss structures made up of numerous structural elements.

In addition, they can provide:

- tensioning and compressive functions to rigidise structures.
- repeatable function, indicating simple deployment actions.

SMA actuators are unlikely to replace pyrotechnic release devices.

92.5 Level 3: Vibration damping

92.5.1 Requirements

92.5.1.1 General

In the context of this handbook, vibration damping refers to orbiting structures where the energy transmitted through the structure is modest. Micro-vibrations, flutter and low frequency oscillations are included. These effects can be caused by:

- reaction wheels,
- motors,
- cryocoolers,
- thermal ratcheting,
- docking manoeuvres.

92.5.1.2 Development active systems

Active systems are presently being conceived to reduce instabilities in highly dimensionally critical structures, e.g. telescopes, trusses and high frequency antennas.

Systems intended for active noise and vibration control for launchers are at a very early stage of development. The high energy levels experienced on launch are a challenge, if they are to be countered by an active system.

Possible active damping options for consideration are:

- piezoceramic transducers, providing out-of-phase output to counter structural vibrations, by either:
  - surface mounting, or
  - embedded in a polymer composite.
- SMA wires embedded in a composite, when triggered change the overall stiffness (modulus), hence natural frequency of the composite. Vibration is suppressed by modal change in natural frequency.
- surface layers of PVDF film applied to the structure. PVDF provides passive damping without an electric field and active damping when energised. It provides both a change in natural frequency for the structure and a means of providing an 'out-of-phase' energy input to counter vibrations.
- embedded optic fibres coated in electro-strictive material, which sense and 'counter' strain energy produced by vibrations. This is a speculative option.

A review of published papers on vibration damping concluded that:

- total elimination of vibration could be an unreasonable expectation, unless vibration energies are very low.
- present systems are not yet optimised making it difficult to determine their relative merits and efficiencies.

92.5.2 Active damping with piezoceramic actuators

92.5.2.1 General

The information presented covers piezoceramic actuators generally, whether surface bonded or embedded. Currently there is insufficient information to examine the relative merits or otherwise of how these actuators are integrated into real structures. In the first instance all means are assumed worth exploring.

92.5.2.2 Basic system development

A basic system consists of:

- a sensor (presumably piezoceramic) which measures vibration levels and provides an output to a controller.
- a controller which generates the necessary input for the actuator,
- an actuator, to counter the original vibration with out-of-phase vibration energy.

92.5.2.3 Beam demonstrator

A simple beam demonstrator is often used for gaining experience on developing smart technologies. The addition of a sensor and piezoceramic actuator shows that some damping can be achieved, Ref. [92-26], [92-27]. Real structures are a different proposition.

92.5.2.4 Truss structures

Truss structures have been put forward as potential recipients of active damping systems, Ref. [92-28], [92-29]. Individual truss members are candidates for actuators, but not all members need actuators for an optimised system. The use of finite element analysis and so-called 'Independent Modal Space Control' is appropriate to identify the optimum placement of actuators, Ref. [92-28]. By this means, the mass and complexity of the smart system can be controlled.

92.5.2.5 Temperature stability

A further concern on using piezoelectric ceramics is their behavioural instabilities over the temperature range anticipated on orbiting structures. Compensation should be added to the control system to counter the temperature of the piezoceramic at any one time.

If piezoceramics are embedded in composites, they should be able to withstand the moulding temperatures without losing polarity. Temperatures are typically 130° to 190°C for epoxy or cyanate ester resins and 300° to 380°C for thermoplastics.

92.5.2.6 Advanced control technology experiment (ACTEX)

The US ACTEX demonstrator programme (1994) evaluated piezoceramics embedded in CFRP 'smart struts', Ref. [92-30].

The test structure consisted of a cantilevered tripod of struts (600mm x 300mm x 250mm). The unit is mounted on the payload deck of a host satellite and exposed unprotected to the space environment for the intended orbital life of 2 to 3 years.

The structure is monitored with accelerometers and thermistors in order to determine the dynamics of the structure and evaluate the performance of the control system over a wide range of orbital environments.

92.5.2.7 Vibration suppression 'smart patches'

A programme (started in 1993) in the USA aimed to produce 'smart patches' which can be placed at appropriate points on structures, Ref. [92-30].

The modular units contain sensor, actuator and control electronics. The patch is intended to consume low levels of power (28V, 10W) and provide vibration suppression. The intention is to reduce control system weight and volume by 90% over current technology.

The smart patch work is a continuation of the previous Advanced Composites with Embedded Sensors and Actuator (ACESA) programme and the ASTREX (Advanced Space Structure Technology Research Experiments) test bed.

ASTREX produced composite tubes 5.18 metres long and 125mm in diameter with embedded actuators. A degree of modal overdamping occurred with this construction, hence the encouragement to use patches.

92.5.2.8 Summary of piezoceramic technology

Damping with piezoceramic elements seems feasible in orbiting space structures because the vibrational energies involved are small and can be countered with small actuators.

92.5.3 SMA wires embedded in composites

92.5.3.1 General

For completeness, information is given on concepts using SMA materials embedded in composites to provide vibration damping.

In hindsight, these were largely inappropriate because the efficiency of the SMA phases to induce damping was low when the additional weight they imposed was considered.

The concepts rely on small diameter (~30µm) SMA wires. These can be handled in a similar manner to reinforcing fibres in preparing composites. The composites can have:

- a low volume fraction of SMA replacing some reinforcing fibres in, for example, a fabric.
- plies solely made of SMA wires and bonded with resin.

NiTi SMAs have a high density of 6500 kg/m^3 so are not weight efficient.

92.5.3.2 Active modal control

Steady state vibration control can be seen with SMA reinforced composites by 'Active Modal Control'.

The modal response of a structure can be tuned by heating the SMA fibres to change the stiffness of all or portions of the structure.

For example, when NiTi is heated to cause the material transformation from the martensitic phase to the austenitic phase, the Young's modulus of NiTi is increased by a factor of four. The yield strength in turn increases by a factor of ten, [See: Figure 91.5.5].

Changes in the material properties are due to a phase transformation. They do not result in the generation of any appreciable force nor do they need to be initiated by any plastic deformation.

92.5.3.3 Active strain energy tuning

The SMA wires are constrained in such a way that the structure is placed in a residual state of strain but with no deflection. The resulting stored strain energy changes the energy balance in the structures and modifies the elasto-dynamic response.

Both concepts rely on a thorough understanding of specific structural designs and where best to locate SMA units to achieve the optimum effect.

92.5.3.4 NiTi/epoxy composites

Some very dramatic changes have been reported in composites entirely made with NiTi reinforcement with epoxy resins.

For example, a [+45°,-45°,0°,90°]s laminate with 50 volume% NiTi reinforcement, Ref. [92-31]:

- activating 45° plies alone: 40% increase in the overall flexural modulus.
- activating all fibres: 90% modulus increase.

NiTi in the martensitic phase has a modulus of ~24GPa compared with 83GPa when triggered to the austenitic state. Depending on the grade, these are low in comparison to carbon fibres with moduli of 230 to 500+GPa. NiTi has a significant density disadvantage.

Table 92.5.1 lists the characteristics of hypothetical laminates.

The data indicates the effect of NiTi additions on stiffness, and stiffness-to-weight analysis when compared with CFRP and aluminium:

- composite B: Triggering the SMA only changed the 'modulus' by 5% (Martensitic → Austenitic transformation) but with a 31% mass penalty; compared with Composite A.
- composite C: Higher proportions of SMA increase the relative differences between moduli (Martensitic → Austenitic transformation) with a very appreciable mass penalty.

The percentage changes in stiffness and density would be identical if all fibres were oriented in a single direction, as in a single UD composite.

Table 92.5-1 - Shape memory alloy: Composite characteristics

Composite				
A	**B**		**C**	
50% Resin 50% C fibres	50% Resin 40% C fibres 10% NiTi		50% Resin † 0% C fibres 50% NiTi	
	Martensitic	Austenitic	Martensitic	Austenitic
Modulus *E* (GPa)				
36.76	30 (-18%)	31.5 (-14%)	3.0 (-92%)	10.4 (-72%)

Density ρ (kg m^{-3})		
1500	1970 (+31%)	3850 (+257%)

Key † : Resin density: 1200 kg/m^3

Material: Carbon T800 fibre (***E*** = 294GPa; ρ = 1800 kg/m^3)
Laminate: $[+45/-45,0,90]_s$

It is unlikely that SMA wires would be suitable for efficient structures because of their poor stiffness-to-density characteristics. Equally, to achieve a significant change in structural natural frequencies by switching transformation states incurs a substantial weight penalty. If proven to have the desired effect on a structure, only very localised use of SMA reinforcement are justified.

92.5.3.5 Summary of shape memory technology

SMA materials undergo a phase transformation which significantly changes their modulus and natural frequency. The high density and modest modulus of NiTi (compared with recognised structural materials) restricts their wide-scale use on real mass-efficient structures.

SMAs need to be used sparingly and in optimised locations to achieve the desired property changes.

To maintain a specific transformed state in a two-way SMA requires continuous power to be available to heat the material.

92.5.4 Application of PVDF layers to structures

92.5.4.1 General

Attempts have been made to apply PVDF as a damping medium.

Information provided is for completeness of the subject of vibrational damping. It is, however, accepted that PVDF is not mass efficient for most lightweight structures.

92.5.4.2 Developments

One study has considered the possibility of applying thin PVDF films, e.g. 9µm or 25µm, to the surface of composite panels representative of those in satellite reflectors, Ref. [92-32].

Tests were undertaken on simple beam configurations with the construction shown in Figure 92.5.1, Ref. [92-32].

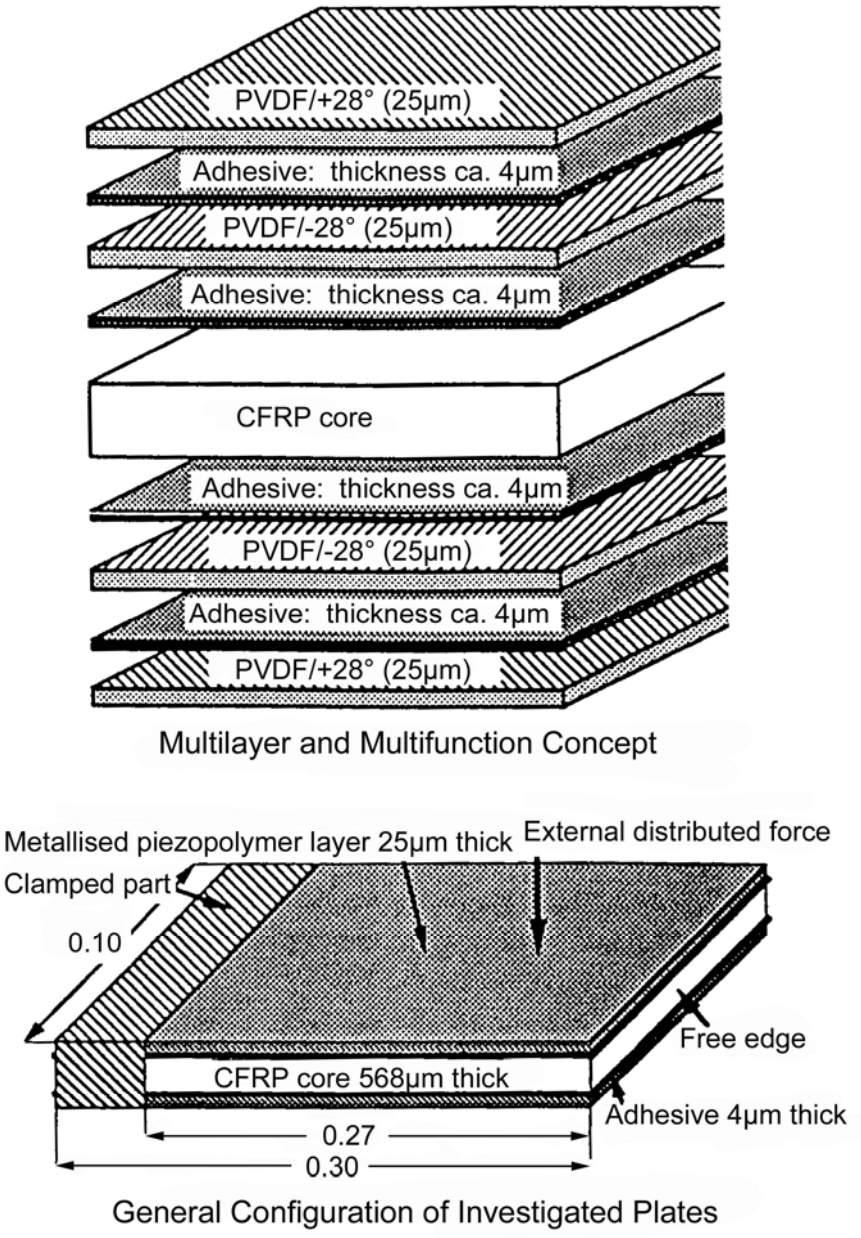

Figure 92.5-1 - Piezoelectric PVDF layers: Example material constructions for CFRP face skins

The thin CFRP plates are representative of face skins used on sandwich panels. The plates were end clamped and the free end allowed to resonate.

The experimental set-ups used are shown in Figure 92.5.2 and Figure 92.5.3, Ref. [92-32].

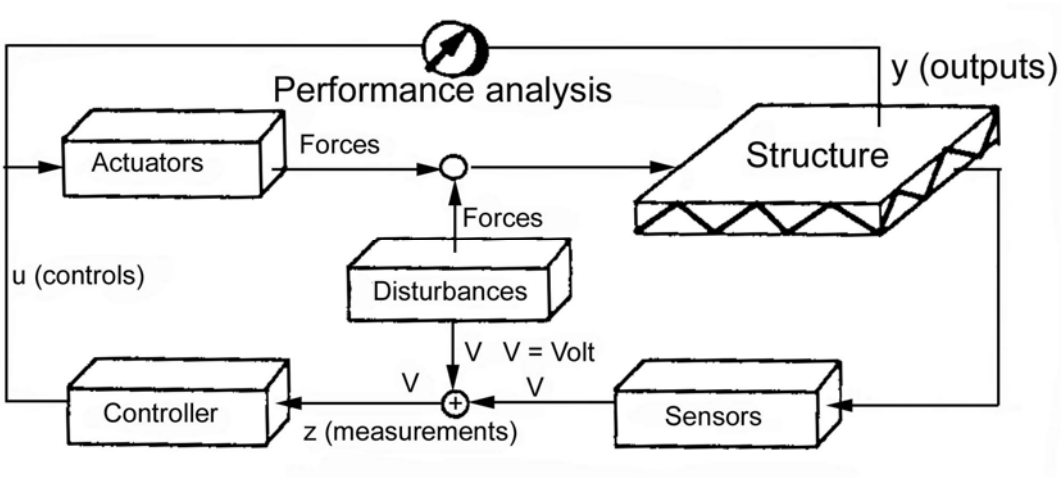

Figure 92.5-2 - Piezoelectric PVDF layers: Principle of active control of structure

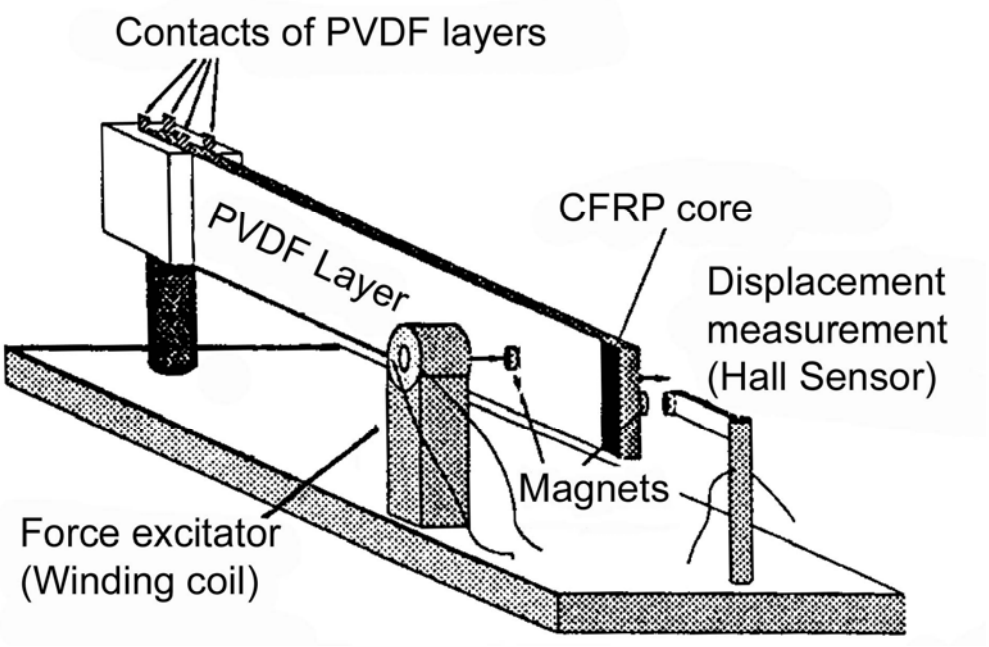

Figure 92.5-3 - Piezoelectric PVDF layers: Test set-up without associated electronics

The preliminary work showed that a level of damping was achieved, but it was not in anyway quantified.

A cursory examination of the specimens tested shows that the PVDF film (and adhesive) increased the mass of the CFRP plates by 22%. This figure would be lower if the PVDF were applied to the intended sandwich panels. However, the damping and resonant characteristics would also be different.

Although at an early stage, this work raises two issues:

- PVDF film has a high positive CTE where as CFRP is low or negative. What is the significance of this over the temperature range anticipated in space? PVDF begins to lose its polarity at around 100°C.
- what is the efficiency of PVDF in terms of damping capacity and mass added to the structure?

92.5.5 Actuator material coated fibre optic sensors

92.5.5.1 Developments

Figure 92.5.4 shows a proposed integrated sensor-actuator fibre optic, Ref. [92-4].

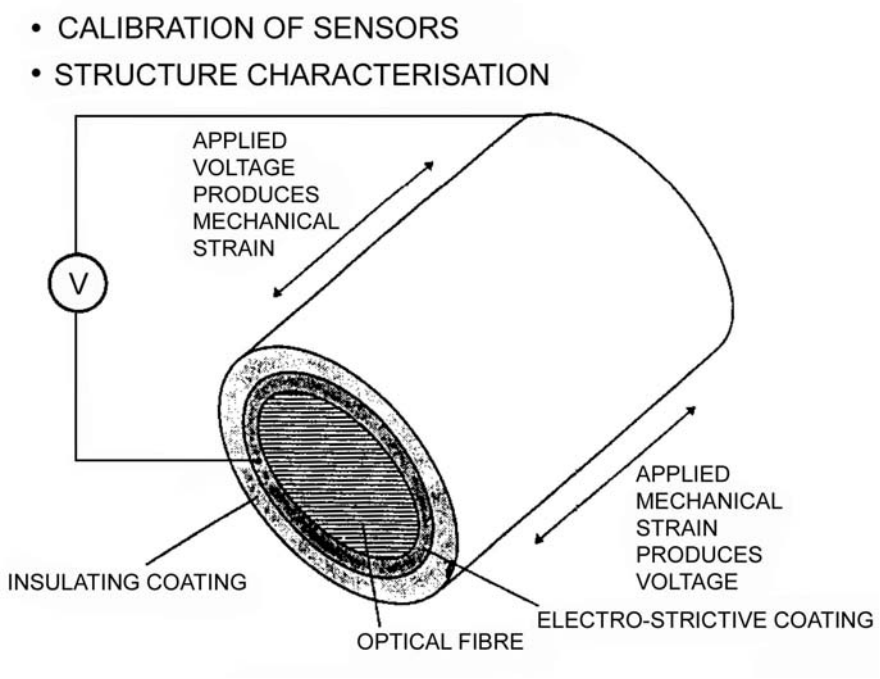

Figure 92.5-4 - Fibre optic: Integrated sensor and actuator

In the actuator mode, a control voltage applied across the coating produces strain in the fibre optic and in the surrounding host composite. By combining actuators the behaviour of the host structure can be modified.

Alternatively, the electro-strictive material can be used to energise the fibre optic as a means of calibrating the sensor. Any subsequent change in the host material results in a different response.

Whilst an elegant concept, doubts exist on the ability of the electro-strictive coating (actuator) to achieve an effect comparable with the host material around it.

The volume fraction of optical fibres necessary to achieve a noticeable actuating effect is significant (10, 20 or even 30%) and cannot be achieved even from hundreds of fibres optic (virtually zero volume fraction). The combination has merit as a sensor system.

92.6 Level 3: Active compensation and alignment

92.6.1 Objectives

92.6.1.1 General

Within the general theme of adaptive structures, this applies particularly to:

- large, truss-based assemblies, or
- unfurlable designs for antennas and arrays.

Such applications can be considered for active control, e.g.:

- realigning,
- reconfiguring, or
- restoring the overall structure.

92.6.1.2 SDI studies

Work in the USA associated with the SDI programme resulted in a range of technology packages and demonstrators, Ref. [92-30], [92-33], [92-34].

A review of SDI activities demonstrates the need to be very selective in the location of smart systems on assembled structures, with a view to maximising efficiency. A thorough understanding of the overall characteristics of the structure is essential. Selected elements of the structure can then be targeted for incorporation of an actuator.

92.6.1.3 Dimensional stability

For highly dimensionally stable structures, the most likely sources of non-linearities are:

- loose or mis-aligned joints.
- material modification, e.g. changes in CTE through outgassing, thermal fatigue and creep.
- thermal gradients.

92.6.1.4 Shape control

An important issue for static or shape control is the determination of the shape of the 'deformed' structure. The expectation is that it is different from that seen during pre-calibration on earth. Shape determination in space is difficult and can require an on-board metrology system.

92.6.1.5 Large truss structures and antenna concepts

Open publications consistently describe truss structures and antenna concepts with assembled dimensions of 5, 10 or 20m or even greater. The overall shape tolerances of a few tens of microns (or less) are stipulated as essential. Large truss structures are regarded as 'flexible' once assembled and can be prone to low frequency oscillations that would need to be suppressed by actuators.

The idea of pre-loaded joints has been put forward to increase the overall rigidity of the structure after assembly. This incorporates the concept of joints dedicated to deployment whereas others are loaded to 'lock' the structure.

To provide active compensation, two concepts are:

- truss element: containing an actuator, or actuators.
- antenna or mirror surface: with an embedded or surface mounted actuators.

92.6.1.6 Shape memory alloy and piezoceramic actuator developments

SMAs and piezoceramics are the popular choices for actuator mechanisms. Piezoceramics are more adaptable as they are more responsive in the 0 to 60Hz range, whilst being capable of both vibration damping and static displacements, [See also: Chapter 91 for the limitations of SMAs and piezoceramics].

In the USA, piezoceramic actuators were applied to a 1m hexagonal CFRP sandwich panel. The radius of curvature was 7.6m and the focal length was changed by up to 30mm. Astigmatism and coma could also be corrected, Ref. [92-34].

Examples of demonstrator 'active' structural members (actuator motors) using different piezoceramics are shown in Table 92.6.1, Ref. [92-34].

Table 92.6-1 - Piezoceramic actuator developments

Piezoceramic	Force (N)	Displacement (µm)	Applied voltage (V)
PZT	500	63	1000
	635	45	150
PMN †	455	39	300

Key: † Lead-Magnesium-Niobate

No information was given on the weight or length of these second generation actuators. However, 63µm displacement, at 0.2% strain, corresponds to a PZT crystal 31.5mm in length.

The embedding of SMAs in composite sections was proposed for achieving compensation (changes) in structural shape. The selective triggering of the SMA imposes internal stresses in the composite, so giving out-of-plane distortion.

Controlling the phenomenon in antennas, for example, has yet to be demonstrated.

92.6.1.7 Summary of technology

Piezoceramics and SMAs can exert useful forces. However, only specific application requirements can provide conclusions as to whether they are useful.

Initial studies on both vibration damping and shape compensation, indicate that each structural configuration should be considered on its own merits. Then, the selective location of sensors and actuators to achieve a desired effect can be determined.

92.7 Application examples

92.7.1 General

Adaptive or intelligent structures could be used in future space missions needing very large adjustable structures, Ref. [92-37]:

- sun shields: shape control, membrane flatness,
- solar sails: shape control, membrane flatness,
- large inflatable structures: shape control of during unfolding,
- unfoldable beams: vibration control and damping of large structures for dynamic control (shift of eigen-frequencies and damping),
- antenna membranes for RF applications: shaping for language beam orientation, contour control for Ku-band or higher frequencies,
- solar generators: vibration control and damping of large structures: dynamic control (shift of eigen-frequencies and damping),
- ultra lightweight large mirrors: shape control, contour accuracy

- release mechanisms,
- launch lock devices: reliable function, minimum mass,
- mechanisms for thermal control (louvers, mobile MLI for thermal tuning): reliable function, minimum mass,
- mechanisms (hinges, shutters, cleaners, wipers, robotics, life supports): reliable function, minimum mass.

With such large structures, dynamic stability control is critical and new active structural material concepts need to be explored. This is even more important for structures where shape stability or pointing accuracy requirements are imposed.

Some examples of spacecraft applications are described, Ref. [92-37].

92.7.2 Sunshields

92.7.2.1 General

Sunshields have requirements which are similar to solar sails except that the flatness specification is generally more severe. For instance a highly stable environment is required for the GAIA mission.

92.7.2.2 GAIA sunshield

The GAIA project is designed to provide very accurate positional and radial velocity measurements of about one billion stars in our galaxy. The collected data will give valuable information about the way the Milky Way was formed and assembled.

During the "GAIA concept and technology study" performed for ESA in 1998, the need for a sunshield was identified to provide the specified stability. This would prevent direct impingement of sunlight on the payload during the mission with a shadow area of about 11m diameter. The internal diameter is 3.8m, with the arrangement shown in Figure 92.7.1.

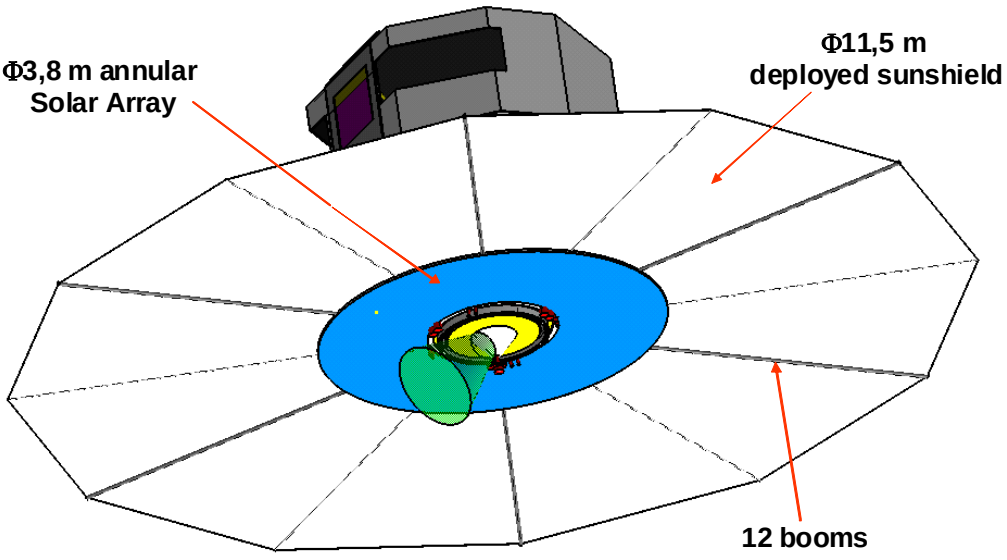

Figure 92.7-1 - GAIA sunshield

Owing to its large size relative to the launcher fairing it is necessary to fold the sunshield for launch. Deployment then occurs at the start of the mission, before the release of GAIA.

The simple structural architecture relies on radial booms supporting trapezoidal (MLI) membranes. More complex concepts could include an outer ring to provide radial tension of the membranes. The bending stiffness of the sunshield is such that it meets a 0.1 Hz requirement.

The maximum acceptable misalignment is about 1° in order to provide a uniform thermal environment. Hence out-of-plane distortion is to be kept below 10 mm. Bending of the radial beams and membrane wrinkling should be strictly controlled.

Deployment devices form part of the sunshield subsystem. In orbit, the geometry and thermal characteristics of the sunshield should provide a very stable thermal environment for the satellite, and in particular for the payload, where temperature stability is very important.

A number of methods are under discussion for providing shape control of the deployed sunshield. The application of smart structures would be an appropriate solution for this.

EAP actuators could reduce membrane wrinkles. Stiffener orientation control could be implemented at the spacecraft interface using controlled hinges. However it remains to be seen whether the actuators can meet the stiffness requirements.

92.7.3 Solar sails

92.7.3.1 General

Solar sails are composed of large flat smooth sheets of very thin film, supported by ultra-lightweight structures. The material used for solar sails can be very thin plastic film (a few microns thick), aluminised by vapour deposition under vacuum on one or both faces.

92.7.3.2 Spin stabilisation

Spin-stabilized sails derive their stability and rigidity from the outward forces generated by the spinning action. No structural booms are needed for stiffness or support. The centripetal force field provides tension in the sail film holding it in the required, near-planar, shape.

92.7.3.3 Truss structures

Another approach provides a truss support structure with tension devices to stretch the thin sail film and eliminate wrinkles. In this case no spin system is necessary. Figure 92.7.2 shows an ESA/DLR solar sail concept based on foldable CFRP booms. In this case EAP actuator devices could provide sail tension. The low sail membrane stiffness would need very low force, but large deformation, devices. Piezoelectric in-plane actuators have already been used to demonstrate the feasibility of active vibration control of a solar sail. In this application permanent DC voltage is needed to retain tension in the sail.

Figure 92.7-2 – Solar sail: CFRP deployable boom

92.7.4 Inflatable structures

Inflatable structures could be a useful approach for the design of very large appended items (e.g. antenna reflectors or solar arrays) on future missions, [See also: 27.7].

An interesting solution uses composites made from fibreglass with a UV-curing resin which cure in orbit with sun UV radiation. Just after deployment the central mast composite skin is in an uncured state and stiffness is provided by an inflated bladder, (polymer film or cloth). At this stage it is possible to use EAP actuators to modify the geometry (e.g. straightness) and improve the shape. In general, shaping actuators could be implemented on any inflatable structure to 'tune' the shape before rigidization has completed.

A potential application for EAP actuators is a tension device for thin membranes. Membranes are a major component of structures or appendages like solar sails, flexible solar arrays, reflector surfaces (SAR), thermal control.

Figure 92.7.3, shows a solar array with an inflatable central mast and two cell-supporting membranes 0.75m × 3m. The film material may be 100µ thick Kapton. After deployment and mast rigidization, longitudinal tension is applied to the membranes to get natural frequencies above a minimum requirement, usually about 1 Hz, sometimes lower for very large solar arrays. To meet this requirement, the overall tension should be between 50 N and 100 N.

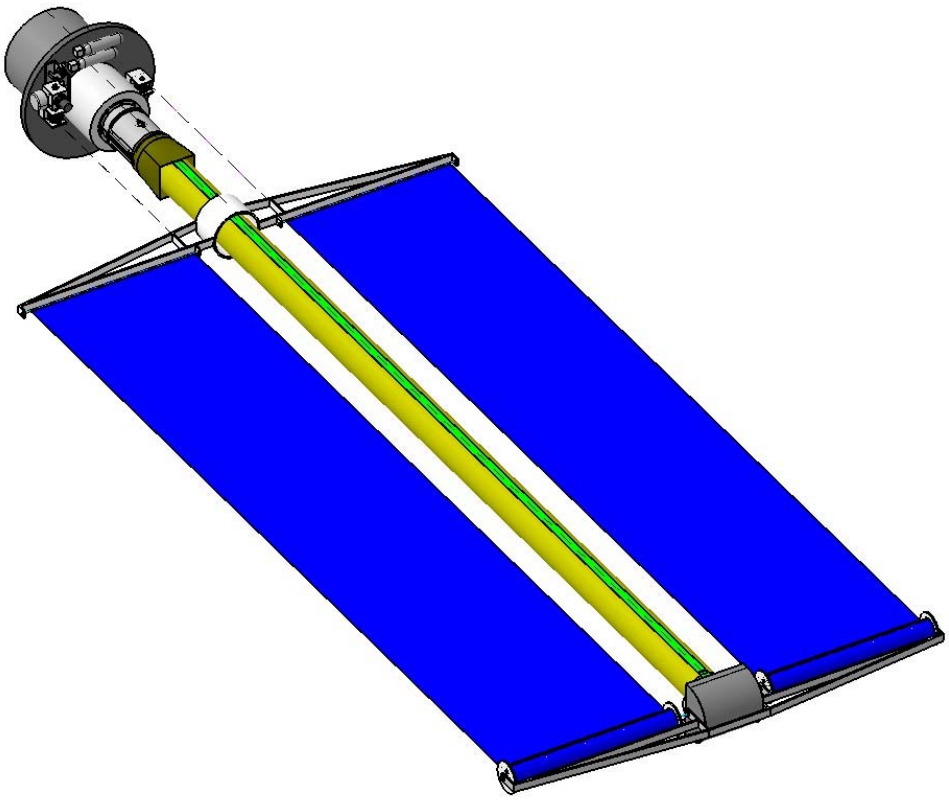

Figure 92.7-3 - Tension device breadboard

92.7.5 Dynamic control

Another possible application for EAP sensors/actuators is the shape control of membranes. Figure 92.7.4 shows a schematic cross-section through a torus-supported membrane reflector.

This could include dynamic load cases since the material response is quite fast (milliseconds). As the lower modes of (large) preloaded membranes are only about 1 Hz, the application looks feasible. There are two ways in which the control could be implemented:

- using out-of-plane tension devices,
- directly through the use of bending properties.

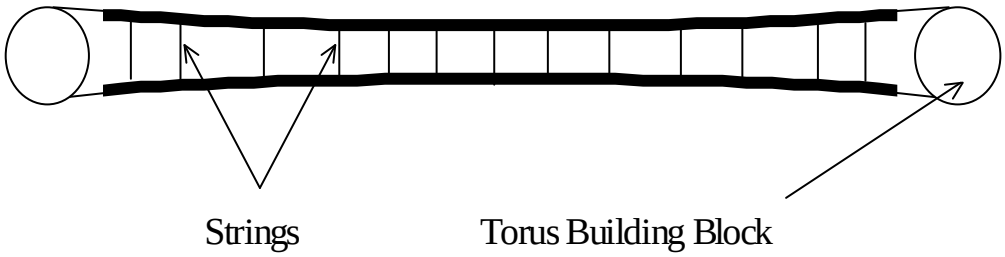

Figure 92.7-4 - Shape control of membranes using EAP sensors/actuators

92.7.6 Antenna membranes for RF applications

There are many applications where the reflector surface is a very thin membrane. The SAR array shown in Figure 92.7.5 was built by L'Garde under contract to NASA.

Figure 92.7-5 - Synthetic aperture radar array

Again tensioning devices are needed, as for solar sails and sunshields; these are generally implemented in the form of straps or strings. For high accuracy reflectors, distributed EAP films could be considered, attached to the reflector surfaces and using an active control system.

92.7.7 Solar arrays and solar generators

92.7.7.1 General

The main task is to provide vibration control or damping of large structures, for example dynamic control (shift of eigenfrequencies and damping) of solar generators.

Standard solar array designs are based on sandwich structures which are too stiff for EAP devices. Nor can they compete with current SADM solutions because of their limited capability. However there are new solar array concepts that make use of thin solar cells mounted on flexible membranes, which could be appropriate for EAP devices.

92.7.7.2 COMED

COMED, a technology program carried out by DLR (D), was successfully completed at the beginning of 2004. The aim was the design, manufacture and testing of a solar array prototype. Testing included functional behaviour, vibration testing and thermal vacuum characteristics.

The COMED prototype, shown in Figure 92.7.6 and Figure 92.7.7, has overall dimensions of 12m × 3.2m, but for final flight hardware, dimensions of 16m × 4m are planned. Hence COMED is designed specifically for larger applications.

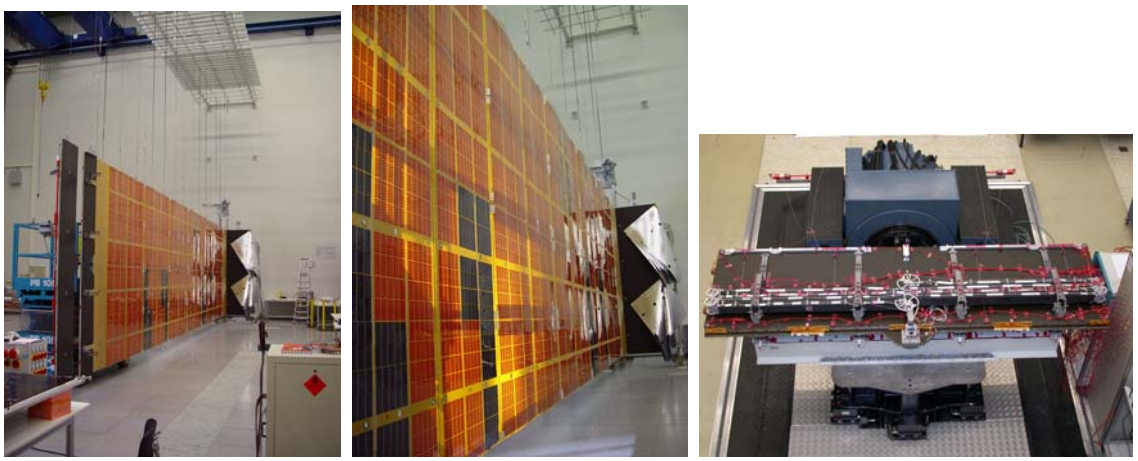

Figure 92.7-6 - COMED prototype, 12m x 3.2m

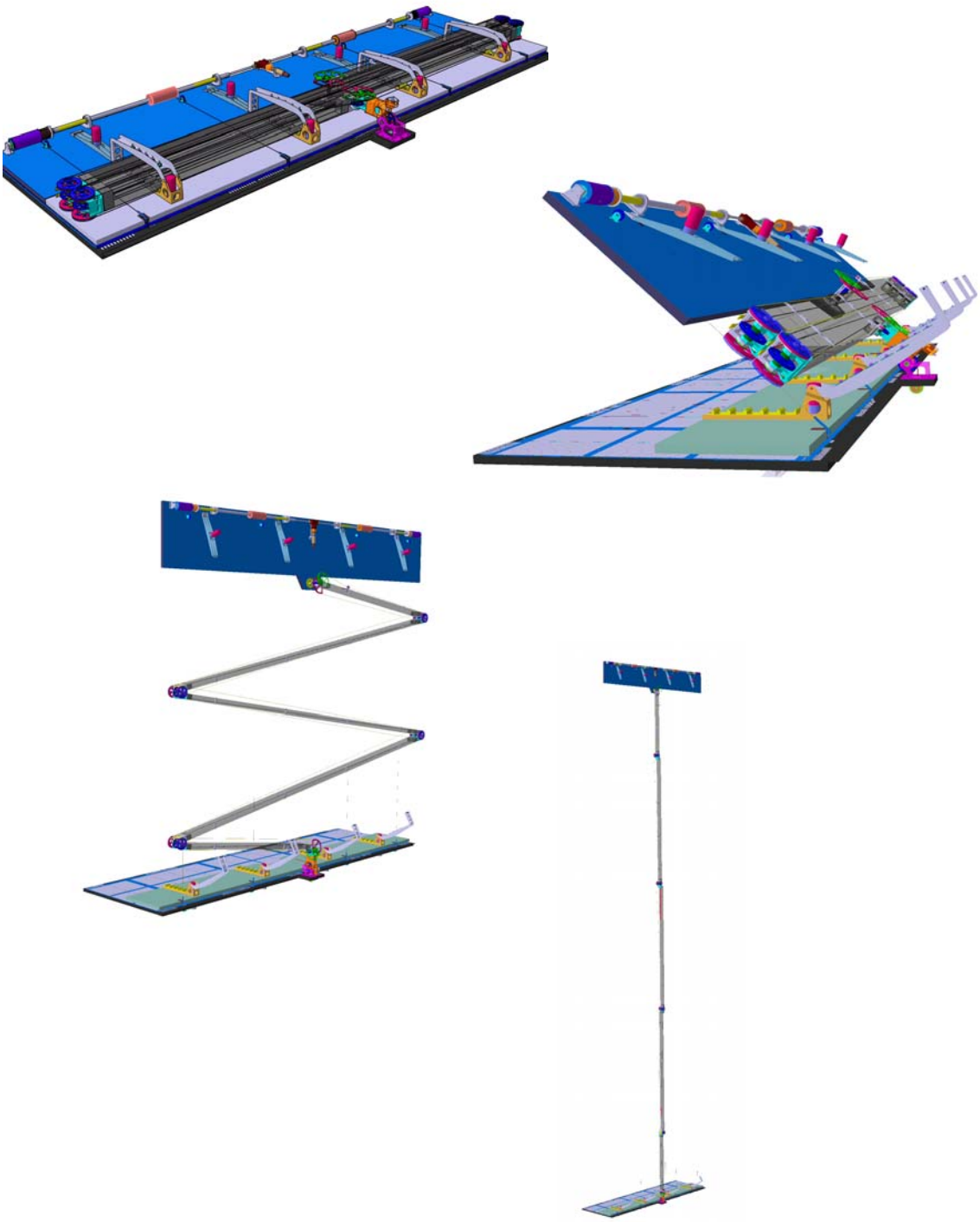

Figure 92.7-7 - COMED prototype: Deployment

92.7.7.3 Pantograph advanced solar array study

Pantograph is an ESA study on the structural design of an advanced solar array concept for small satellites; as shown in Figure 92.7.8. The dimensions are much smaller than those of COMED. The aim of the project is the design and manufacture of a concept model and its verification by testing. Particular emphasis is placed on the functioning of the deployment mechanism.

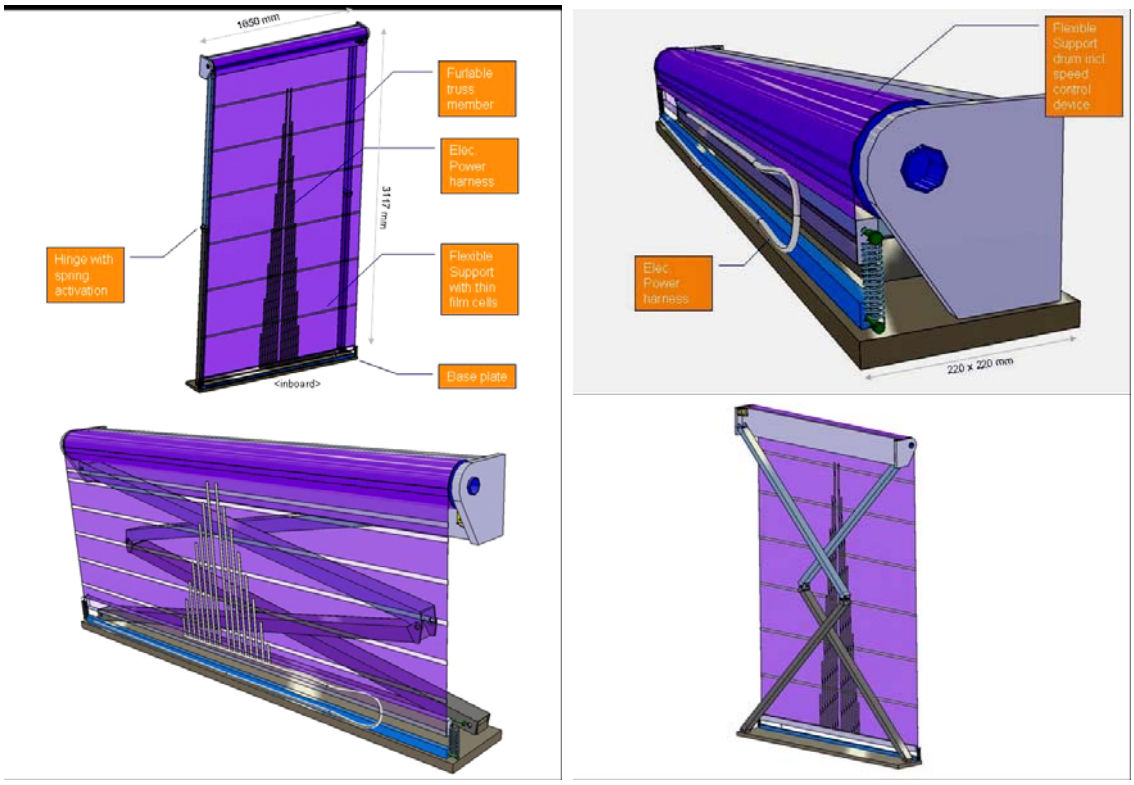

Figure 92.7-8 - Pantograph deployable advanced solar array concept

92.7.8 Shape control of ultra-light-weight mirrors

92.7.8.1 Adaptive lightweight mirror for space applications

Based on an evaluation of different piezo-active concepts, an adaptive light-weight satellite mirror has been developed. The mirror, shown in Figure 92.7.9, is primarily made from CFRP with embedded piezo-ceramic actuators for shape control and a bonded ULE optical layer. To meet the demanding requirements, special in-plane actuators were developed by DLR. This research formed part of the German industrial research project ADAPTRONIK.

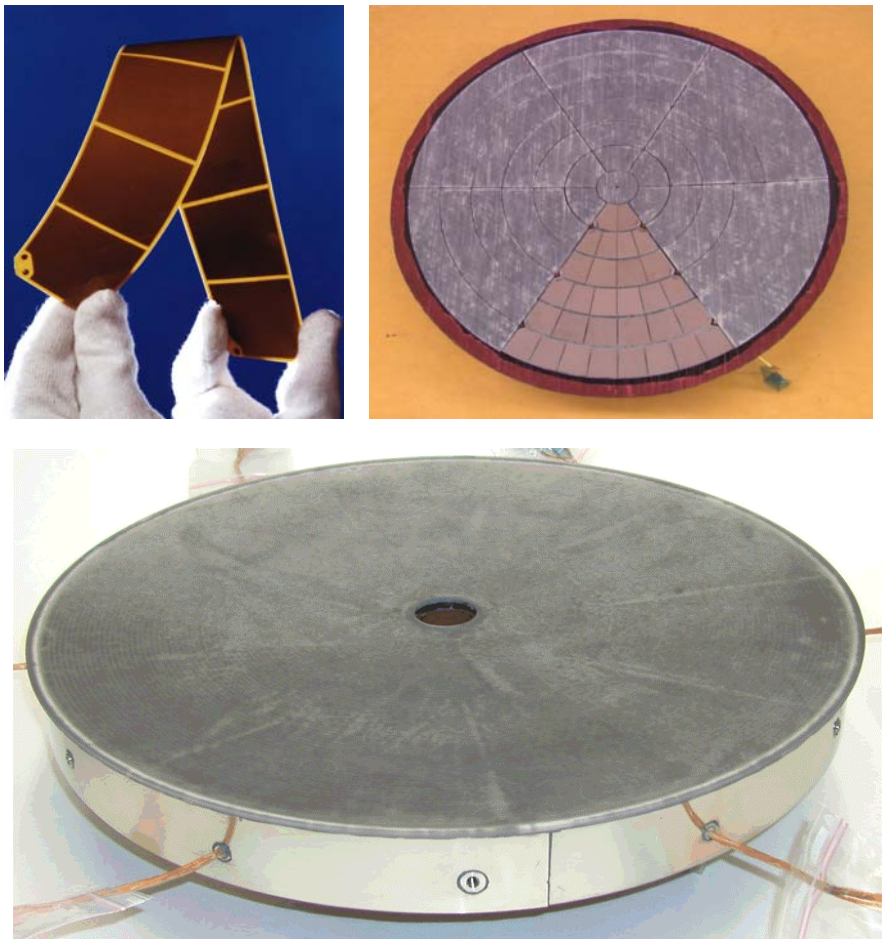

Figure 92.7-9 - Adaptive lightweight satellite mirror

92.7.9 Shutters for optical and thermal applications

Under the DARPA 'Electroactive polymers program, MCNC Research Institute (USA) developed EAP which they call artificial eyelid actuators; as shown in Figure 92.7.10 and Figure 92.7.11. These are curled, thin-film, electrostatic actuators for use as optical shutters to protect sensors against damaging radiation.

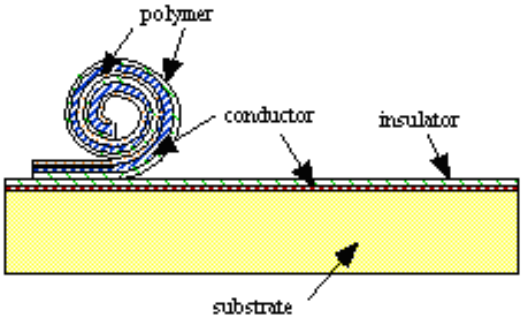

Figure 92.7-10 - Artificial eyelid actuator

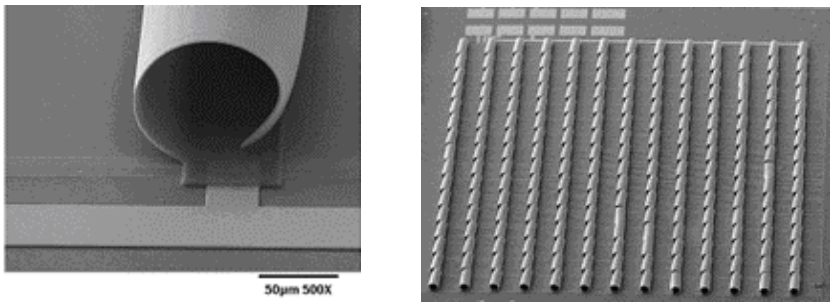

Figure 92.7-11 - Array of artificial eyelid actuators (right) and a single artificial eyelid actuator (left)

The eyelid actuator consists of alternating polymer and metal layers, which form a curled film, anchored to a substrate. The device also contains a fixed conductor deposited on the substrate. Electrostatic actuation is achieved by applying an electric field between the metal electrode in the flexible curled film stack and the fixed substrate conductor. This unrolls the flexible film over the substrate surface. The curl in the device is caused by thermal expansion differences between the metal and polymer layers in the thin film stack and can be varied by changing the thin film layer thickness.

The actuators need a rather large voltage, typically in the 100V to 200V range, depending on degree of curl. They can be operated at frequencies up to 5kHz to 10kHz, although this feature is not particularly useful for most optical protection or thermal control applications.

Other applications being developed for the device include RF and optical shutters and choppers for IR detectors. They could also be used to provide thermal louvers.

92.7.10 Membrane components

92.7.10.1 Diaphragm pumps

EAP materials can be useful for devices where large membrane deformations are needed. For instance, EAMEX proposes pumps based upon this principle; as shown in Figure 92.7.12. The advantages of such a device in this type of application are:

- low drive voltage (1.5V),
- small number of parts,
- low cost,
- small size,
- ability to cope with the presence of bubbles in the liquid.

Use as a fluid pump for deployable radiators or other thermal fluid applications is envisaged, however, one potential limitation is that long life is needed.

Another possible application is for the membrane in propellant tanks, which also require very large deformations. The main issue in this case is device reliability in the presence of highly corrosive fluids such as hydrazine.

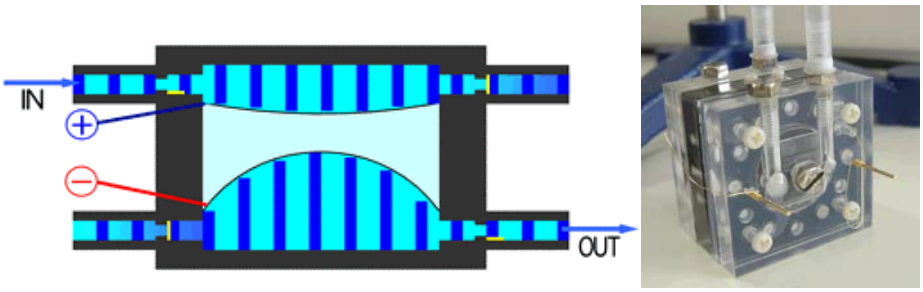

Figure 92.7-12 - EAP membranes for pumps

92.7.11 Active surface control and sensor applications

ERI (USA) has developed a very cheap sensor using perfluorinated polymers; as shown in Figure 92.7.13. When it is bent, flexed or squeezed, the device generates a signal of several millivolts. It can also be used as an actuator in air with a tip motion in cantilever mode of about 3 mm/V to 5 mm/V.

Static or dynamic sensors can be made using EAP materials, in particular for membrane vibration monitoring. Hence they could be used in the verification process for large membranes subject to stability requirements. They could also provide a combination of sensor and actuator, if coupled with an active control system.

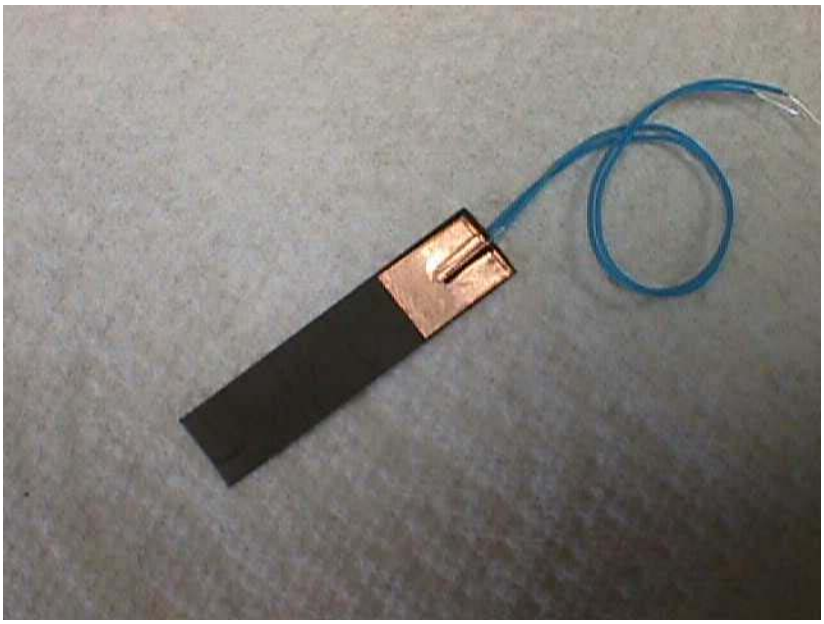

Figure 92.7-13 - EAP sensor from ERI (USA)

92.8 References

92.8.1 General

[92-1] B. Culshaw, P.T. Gardner & A. McDonach (Editors)
First European Conference on Smart Structures and Materials
Glasgow, 12-14 May 1992. Proceedings copublished by IoP Publishing
and EOS/SPIE EUROPTO Series, SPIE 1777. ISBN: 0-7503-0222-4

[92-2] P.J. Erbland
'Fiber Optics for the National Aero-Space Plane'
SPIE Vol. 1370 Fiber Optic Smart Structures and Skins III (1990) p29-44

[92-3] R.M. Measures et al
'Structurally Integrated Fiber Optic Damage Assessment System for Composite Materials'
SPIE Vol. 986 Fiber Optic Smart Structures and Skins I (1988) p120-129

[92-4] N.C. Eaton et al
'Factors Affecting The Embedding of Optical Fibre Sensors in Advanced Composite Structures'
Paper 20, AGARD Conference Proceedings 531 on Smart Structures for Aircraft and Spacecraft. Lindau, Oct 1992

[92-5] N. Furstenau et al
'Composite Strain Sensing with a Combined Interferometric and Polarmetric Fibre-Optic Strain Gauge'
SPIE 1777, p81-84

[92-6] M. Turpin et al
'Process-Induced Birefringence Variations in Fiber Optic Embedded in Composite Materials'; SPIE 1777, p93-96

[92-7] C. Boller et al
'Technological Challenges with Smart Structures in German Aircraft Industry'; SPIE 1777, p289-292

[92-8] G.A. Hickman et al
'Application of Smart Structures to Aircraft Health Monitoring'
J. of Intell. Mater. Syst. and Struct., Vol.2 - July 1991, p411-430

[92-9] B. Culshaw & C. Mitchie
'Fibre Optic Strain and Temperature Measurement in Composite Materials: A Review of the OSTIC Programme'
ESA SP-336. International Symposium on Advanced Materials for Lightweight Structures, ESTEC, March 1992, p393-398

[92-10] B. Fornari et al
'Strain Measurement of Carbon/Epoxy Composite with Fibre Optics White Light Quasi Distributed Polarimetric Sensor'
Paper 12, AGARD Conference Proceedings 531 on Smart Structures for Aircraft and Spacecraft. Lindau, Oct 1992

[92-11] P. Sansonetti et al
'Intelligent Composites Containing Measuring Fibre Optic Networks for Continuous Self Diagnosis - I'
Fibre Optic Smart Structures and Skins II, Boston, Sept 1989, SPIE Vol.1170

[92-12] P. Sansonetti et al
'Intelligent Composites Containing Measuring Fibre Optic Networks for Continuous Self Diagnosis - II'
Fibre Optic Smart Structures and Skins IV, Boston, Sept 1991, SPIE Vol.1588

[92-13] R. Sippel
'A Test Sample with Embedded Fibre Optic Sensors for High Accuracy Strain Measurement'
Dornier GmbH Report, September 1992
Work Order No 23 of ESTEC Contract 7090/87/NL/PP

[92-14] 'Smart Structures for Aircraft and Spacecraft'
75th Meeting of the AGARD Structures and Materials Panel Lindau, Germany, 5th-7th October 1992
AGARD Conference Proceedings AGARD-CP-531
Thirty-one papers, ISBN 92-835-0701-X, 1993

[92-15] P.A. Tutton & F.M. Underwood
'Structural Health Monitoring using Embedded Fibre Optic Sensors'
AGARD Conference Proceedings AGARD-CP-531
Paper 18, ISBN 92-835-0701-X, 1993

[92-16] H. Strehlow & H. Rapp
'Smart Materials for Helicopter Active Control'
AGARD Conference Proceedings AGARD-CP-531, Paper 5
ISBN 92-835-0701-X, 1993

[92-17] F. Nitzsche & E. Breitbach
'The Smart Structures Technology in the Vibration Control of Helicopter Blades in Forward Flight'
SPIE 1777, p321-324

[92-18] F. Nitzsche & E. Breitbach
'A Study of the Feasibility of Using Adaptive Structures in the Attenuation of Vibration Characteristics of Rotary Wings'
Proc. of the AIAA 33rd Structures, Structural Dynamics and Materials Conference, Dallas, April 1992

[92-19] P. Sansonetti et al
'Unidirectional Glass Reinforced Plastic Composite Monitoring with White Light Quasi Distributed Polarimetric Sensing Network'
SPIE 1777, p77-80

[92-20] N.C. Eaton
'Fibre Optic Bragg Grating Sensor Measurements in Composite Materials'
ECCM 6 Conference, Bordeaux, 20-24 September 1993

[92-21] J.P. Dakin
'Optical Fibre Pressure and Strain Sensors for Smart Structures'
ECCM 6 Conference, Bordeaux, 20-24 September 1993

[92-22] L. Wosinki et al
'Quasi-Distributed Fibre-Optic Sensor for Simultaneous Absolute Measurement of Strain and Temperature'
SPIE 1777, p53-56

[92-23] B. Mason et al
'Fiber Optic Strain Sensing for Smart Adaptive Structures'
SPIE 1777, p135-138

[92-24] L. McDonald Schetky
'Shape Memory Alloy Applications in Space Systems'
Materials & Design Vol.12 No.1 February 1991, p29-32

[92-25] B.J. Maclean et al
'Development of a Shape Memory Material Actuator for Adaptive Truss Applications'
J. of Intell. Mater. Syst. and Struct., Vol.2 - July 1991, p261-280

[92-26] S. Hanagud et al
'Optimal Vibration Control by the Use of Piezoceramic Sensors and Actuators'
Journal of Guidance, Control and Dynamics, Vol.15, No.5, Sep - Oct 1992, p1199-1206

[92-27] C.T. Maidment & N.C. Eaton
'Development of Intelligent Structures'
Westland Aerospace Report RD/FO/008, April 1991
ESTEC Contract No. 8521/89/NL/TB

[92-28] R. Lammering
'Optimal Placement of Piezoelectric Actuators in Adaptive Truss Structures'; SPIE 1777, p317-320

[92-29] R. Lammering et al
'Optimal Placement of Piezo-Electric Actuators in Adaptive Truss Structures'; Journal of Sound and Vibration, 166, No.3, 1993

[92-30] A. Das, G. Ormbrek & M. Obal
'Adaptive Structures for Spacecraft: A USAF Perspective'
AGARD Conference Proceedings AGARD-CP-531, Paper 3
ISBN 92-835-0701-X, 1993

[92-31] C.A. Rogers.
'Novel Design Concepts Utilising Shape Memory Alloy Reinforced Composites'
Proceedings of the 3rd Technical Conference on Integrated Composites Technology, Seattle, Sept 1988, p719-731

[92-32] W. Charon et al
'Smart Structures with Piezopolymers for Space Applications'
SPIE 1777, p329-332

[92-33] M.S. Misra et al
'Adaptive Structure Design Employing Shape Memory Actuators'
AGARD Conference Proceedings AGARD-CP-531, Paper 15 ISBN 92-835-0701-X, 1993

[92-34] B.K. Wada & J.A. Garba
'Advances in Adaptive Structures at Jet Propulsion Laboratory'
AGARD Conference Proceedings AGARD-CP-531, Paper 28 ISBN 92-835-0701-X, 1993

[92-35] J. Wilson & R.J. Hussey: RJ Technical Consultants, (F)
'Structural Health Monitoring Techniques & Potential Application to RLV Composite Primary Structures & Cryogenic Tanks'
Report No. RJTC-046-SHM (September 1999)
ESA Contract 10983/94/NL/PP - Work Order No. 16

[92-36] Dr. R. Graue & A. Reutlinger: Kayser-Threade, (D)
'Structural Health Monitoring for Future Launchers: Results from Breadboarding and Prototype Development'
Proceedings of the 3rd European Conference on Launcher Technology, Strasbourg. 11th - 14th December 2001, p755-766.

[92-37] H.G. Wulz & K. Rohwer: EADS-Astrium GmbH/DLR, (D)
'Smart Materials'
ESTEC Contract No. 15865/NL/MV/ CCN3 (September 2004)

93 Limitations of smart technologies

93.1 Introduction

Smart technologies are very much dominated by examples of fundamental physical effects which have potential for use in real applications. Most materials currently described as 'smart' are in effect 'solutions looking for problems'.

The majority of published work describes enhancements to the 'solutions', but do not address the issue of whether they are truly needed. Nor is appreciation shown of the environments in which they can be applied.

In respect of space structures, the possible fields of application are:

- vibrational damping and control.
- active compensation of dimensionally critical structures.
- damage detection.

These come under the general theme of health (condition) monitoring and control.

As few truly smart systems have been applied to aerospace structures, this chapter aims to identify areas where issues need to be resolved. Systems can then be produced which provide justifiable benefits for their adoption in real structures.

An appreciable amount of information on smart technologies is retained within active organisations for commercial-in-confidence or strategic reasons. Open publications do not necessarily describe the real status of the respective technologies.

Most of the unanswered questions relate to the suitability of sensors and actuators for real long-life applications. Some key issues are highlighted.

93.2 Smart system development

93.2.1 Sensors

Do sensors describe accurately what is occurring in quantifying a measurand? Sensors can measure:

- strain,
- temperature, and
- vibration levels.

Truly smart systems envisage the use of distributed sensors to provide multiple point measurement.

- Point measurement of a measurand can be accomplished with any of the appropriate sensors provided precalibration and reference sensors are applied. This applies to:
  - strain gauges,
  - thermocouples,
  - fibre optics, and
  - accelerometers.
- Validity of distributed sensors, particularly fibre optics (FOS), for multiple (tens/hundreds) point measurement is not yet proven. Theory indicates it is viable, but signal processing is very complex.
- Accurate measurement of dynamic strain is dependent on:
  - sensor sensitivity, and
  - frequency of signal change.

  High accuracy and frequent strain variations can be incompatible if complex signals are produced by the sensor which cannot be processed in real-time. Overly sensitive fibre optic devices show this problem if cyclic strain rates are above 10Hz, for example.
- Some sensors are temperature sensitive. With a possible operating temperature range in space of -100°C to +150°C, some sensors will be inappropriate if exposed to extreme temperature fluctuations. The issue of sensitivity to temperature is application and location dependent. The response by PVDF and piezoceramic materials at different temperatures needs to be quantified and allowance made in monitoring systems.

Does the presence of sensors affect the material (structure) in any deleterious manner?

- embedding fibre optics in composites is popular. There is little evidence to suggest that fibre optics will seriously impair the mechanical integrity of composites (>1.0mm thick) with fibre optics at wide (25 to 50mm) spatial intervals. Very thin CFRP sandwich panel face skins may be less amenable, where fibre optic diameter is comparable to, or greater than, the laminate thickness.
- surface mounting sensors by adhesive bonding poses few problems to the host material as all sensors are being miniaturised. The durability of adhesive bonds, and the exposed sensors, is of greater concern.

A few studies have measured the mechanical performance of composites containing fibre optics, Ref. [93-1], [93-2].

Preliminary work with 2mm CFRP laminates of 54% carbon fibre volume fraction and 0/90° construction shows little evidence of composite performance reduction. A 125/155 polyimide-coated, optical fibre (York Hi-Bi fibre of 125µm diameter with 15µm coating) was embedded parallel with the 90° reinforcement. The strength of the composite was dominated by the presence of the 0° carbon fibres. The fibre optic, being of lower modulus than carbon fibres, did not alter the overall composite strength.

Placing fibre optics within a balanced composite requires consideration. Directly embedding a fibre optic parallel to the fibres in a specific UD ply would seem beneficial compared to the direct sandwiching between two plies but at an adjacent orientation. Equally, the sandwiching of a fibre optic between two plies of fabric will introduce uncertainties as to the path of the fibre optic. When consolidated, the fibre optic may deform to the surface profile of the fabric.

In panels, fibre optics will give a different response depending on whether it is embedded near the surface, neutral axis (centre) or back-face of the composite.

93.2.2 Actuators

Will the presence of actuators affect the host structure in any deleterious manner?

This is an uncertain issue as it relates to vibration damping and active compensation where mechanical forces and elastic energy will be introduced into the host material in response to other events:

- embedding actuator materials (SMA and piezoceramics) in composites is being studied. Thought has not been given to the possible interlaminar stresses induced when attempting to achieve a desired compensatory effect.
- presence of actuators may alter the fracture behaviour of materials. If embedded in sufficient quantities, they will change the thermal expansion characteristics.

93.2.3 Control systems

Can monitoring and control systems interpret complex signals from multiple points (sensors or actuators)?

The majority of sensors and actuators do not give linear responses under varying thermal conditions. Any monitoring or control system should therefore have a means of compensating for orbital position:

- smart systems may need multiplexing to achieve a useful response. There are few proven examples of lightweight multiple sensors and actuators being synchronised on orbiting structures, and none with so-called 'smart materials'.
- where multiplexing occurs, the need for true strain measurement is clarified as:
  - direct condition monitoring of damage and fatigue crack growth: Sensor output will need to be converted to true strain to allow a judgement to be made on the integrity of the structure. This level of correlation will be sought by structural design engineers.
  - active compensation, either for vibration or dimensional control: True strain measurement may not be necessary if a reactive loop is created between sensor and actuator. The control loop seeks to retain a desired state and need not quantify precisely the magnitude of all events.
- much work is needed on the integration of smart systems. A commonly quoted example is the unavailability of a universal connector for fibre optics and the signal processor. The issue of connectors is important if fibre optics are being used in a diagnostic role where a data collection unit is connected to fibre optics either singularly or in parallel. Where fibre optics are embedded in composites, the trailing optic fibres will need to be protected and retained by a connector before the composite component is integrated in the structure.

93.3 Durability and longevity

93.3.1 Sensors

93.3.1.1 General

Given that future orbiting space structures will have greater life expectations (~25 years): Can sensors and actuators continue to function satisfactorily and repeatably over this life span? With the miniaturisation of sensors, they could be considered less robust.

Sensor integrity depends on their location and exposure to space environments. Uncertainty exists because there is little evidence of 'smart' materials, e.g. fibre optics (FOS), SMAs, PVDF, piezoceramics and others, having been exposed to LEO, atomic oxygen, irradiation, outgassing, thermal cycling and the like.

The effect of space environments can be different for materials depending on whether they are embedded in a host material or surface mounted.

93.3.1.2 Embedded or surface mounted

Advantages of surface bonding include:

- sensors can be retro-fitted,
- sensors can be replaced or repaired,
- characteristics of structural material are not altered locally,
- basic fabrication route is not altered,
- input and output of the signals from the structure is easier,
- electrical insulation from the structure is easier

Possible disadvantages are that:

- sensors are exposed and may be easily damaged
- no internal information can be obtained during the material lifetime.

Manufacturing of integrated structures is problematical. Fibre optics are brittle and prone to fracture if mishandled. Embedding fibre optics in composites and the subsequent autoclave moulding and machining present acute problems, Ref. [93-3], [93-4].

What happens if an fibre optic is broken during certification of an assembled structure?

93.3.2 Actuators

Smart actuating materials, such as SMAs and piezoelectric materials, will age; notably from repeated actuation and thermal cycling. These materials are very adaptable, depending on the application, and for this reason are also poorly characterised with respect to design and performance data.

93.4 Redundancy to guaranteed operational life

93.4.1 General

Smart systems can only be applied to space structures if they perform a useful function in a reproducible and repeatable manner. The retrofitting of an integrated system on an orbiting structure is an unlikely proposition.

93.4.2 Sensors and actuators

On the assumption that multiple sensors and actuators are installed: How many redundant units are needed to compensate for failed units over a twenty-five year life?

93.4.3 Control systems

The same question applies to the control system, where failure could render the whole smart system inoperative. This in turn could devalue the orbiting structure.

93.5 System mass and efficiency

93.5.1 General

There is no evidence of mass budgets being quantified for smart systems within open publications on the prospects of smart systems for lightweight structures (space or aircraft), Equally, the electrical power consumption is not identified.

Are the smart system's total mass and costs acceptable in respect of the benefits gained?

The main contributors to mass are:

- control circuitry.
- actuators.

93.5.2 Actuators

Actuators will be sized by:

- their location(s), which is application dependent.
- mechanical efficiency.
- energy requirements, e.g. to counter vibrational energies.

Some actuators, e.g. SMAs, can require continual activation and therefore consume electrical power for heating.

93.6 Smart system development for European space programmes

93.6.1 Background

Interest initially focused on the availability of smart materials and smart technologies. In most instances the developments were not application-driven and the technology was a collection of possible solutions seeking applications.

Later some demonstrator components were produced which showed promise, principally composite beams with sensors and actuators. However, simple beams are very limited in comparison with assembled structures. At that time, the functions identified that could benefit future orbiting space structures (antennas and satellites) were:

- vibration damping and control, and
- active compensation and alignment.

Key issues were identified as:

- defining some basic requirements of smart systems which would justify their use.
- using these requirements to prioritise the selection of appropriate sensor and actuator technologies.
- developing systems which would demonstrate the basic requirements through the integration of control functions, sensors and actuators.
- lack of integration with the demonstrator programmes was a major criticism of smart philosophies.
- determining the suitability of selected technologies for prolonged use in space environments.

A critical issue was the sensitivity of the sensors and actuators to a thermo-cyclic environment.

Much of the sensor and actuator technology is theory based on physical phenomena and aspects of materials science. A much closer correlation to quantified physical parameters had to be demonstrated, e.g. strain and temperature measurement and actuating energies (load, displacement, frequency.).

93.6.2 On-going programmes

European and US studies have resulted in the development of prototype systems which have been integrated into real RLV complex structures (sometimes scaled-down demonstrators) and are undergoing evaluation trials.

The main areas of interest are cryotanks, TPS elements and highly-loaded structural components, [See: 92.3 for various application examples].

The smart systems proposed are for monitoring in-flight conditions only, coupled with on-ground inspection and verification. None of the prototype-level developments have any reactive functions built in because the potential applications identified do not require them.

SHM evaluation trials aim to establish not only the validity of the data and its interpretation, but also aspects of the durability of such systems when exposed to simulated or real operational conditions. This gives an indication of their long-term durability.

Whether these systems are actually deployed depends on both the technology proving itself during testing and the continuation of the currently proposed future RLV concepts.

93.7 References

93.7.1 General

[93-1] R. Davidson & S.S.J. Roberts
'Finite Element Analysis of Composite Laminates Containing Transversely Embedded Optical Fiber Sensors'
SPIE 1777, p115-122

[93-2] S.S.J. Roberts & R. Davidson
'Short Term Fatigue Behaviour of Composite Materials Containing Embedded Fibre Optic Sensors and Actuators'
SPIE 1777, p255-262

[93-3] N.C. Eaton et al
'Factors Affecting The Embedding of Optical Fibre Sensors in Advanced Composite Structures'

Paper 20 AGARD Conference Proceedings 531 on Smart Structures for Aircraft and Spacecraft. Lindau, Oct 1992

[93-4] N.C. Eaton et al
'Fibre Optic Bragg Grating Sensor Measurements in Composite Materials'
ECCM 6 Conference, Bordeaux, 20-24 September 1993

94 European capabilities in smart technologies

94.1 Introduction

This chapter provides a resumé of a survey conducted in mid-1993 regarding European activities within 'smart technologies'.

Also included is a summary of European expertise from a review (in 1999), Ref. [94-61]. This covered the applications-based activities in ‘Structural Health Monitoring’ across a wide number of industry sectors. The objective was to establish whether activities conducted elsewhere could have potential for future RLV structures.

94.2 Smart technology survey

A questionnaire was sent in mid-1993 to all known organisations active in the field. The results are given in Table 94.02.1 and Table 94.02.2.

Table 94.2-1 - Smart technology survey: Sensors and actuators

European organisation	Q?	Sensors						Actuators			Ref.
		T/C or SG	Fibre optics	Piezo ceramic	PVDF	Micro-sensors	Acceler-ometers	SMA	Piezo-ceramic	PVDF	
University of Strathclyde (Smart Structures Research Institute)	✓	-	H	H	-	-	-	-	-	-	1 - 4
Matra Marconi Space UK Ltd	✓	-	-	D	-	-	-	-	D	-	-
AEA Technology, Harwell	✓	-	D	-	-	-	-	D	D	-	4 - 12
Westland Aerospace	✓	H	H		-	-	H	-	D	-	13 - 15
ISVR. University of Southampton	✓	-	-	H	H	-	H	-	H	-	16
ORC. University of Southampton	✓	-	H	-	-	-	-	-	-	-	3,13,15, 17,18,25
ERA Technology Ltd.	✓	H	H	-	-	D	-	-	-	-	19,20
DRA, Farnborough (Space Dept. & Materials/Structures Dept.)	V	-	D	D	-	-	-	-	D	-	-
Cranfield Institute of Technology	O	-	-	-	-	-	-	H	-	-	21,22
British Aerospace, SRC	?	?	?	?	?	?	?	?	?	?	-
BAe Military Aircraft Ltd.	O	H	PS	-	-	-	-	-	-	-	23
BAe Space Systems Ltd.	?	?	?	?	?	?	?	?	?	?	-
SAIC UK Ltd.	✓	D	-	D	-	-	D	-	D	-	24
Dornier GmbH	✓	H	H	H	H	-	-	PS	H	H	26 - 35
DASA (MBB GmbH), Munich, Aircraft Div.	O	-	-	-	-	-	-	-	-	-	36
DLR, Institute of Aeroelasticity & DLR, ISM, Braunschweig	✓	H	H	H	H	-	H	H	H	H	37 - 50
University of Hamburg-Hamburg	O	-	-	-	-	-	-	D	-	-	51
CNES	?	?	?	?	?	?	?	?	?	?	-
Aerospatiale, SSSD, Cannes	?	?	?	?	?	?	?	?	?	?	-
Aerospatiale, Suresnes	✓	H	-	H	-	-	-	H	H	-	-

European Organisation	Q?	Sensors						Actuators			Ref.
		T/C or SG	Fibre optics	Piezo ceramic	PVDF	Micro-sensors	Acceler-ometers	SMA	Piezo-ceramic	PVDF	
Thompson-CSF LCR	O	-	H	-	-	-	-	-	-	-	52
Bertin et Cie	O	-	-	-	-	-	-	-	-	-	7,53 - 55
Metravib RDS	✓	-	-	H	H	H	H	-	D	D	-
Alcatel-Espace	?	?	?	?	?	?	?	?	?	?	-
Matra Marconi Space	?	?	?	?	?	?	?	?	?	?	-
CISE Technologic Innovative Spa	✓	-	H	-	-	-	D	-	-	-	56,57
University of Naples	O	-	D	-	-	-	-	-	-	-	58
Alenia Spazio SpA	✓	-	H	-	-	-	-	-	-	-	7,54,55
CASA (Space Division)	✓	H	D	D	-	-	H	-	D	-	-
Institute of Optical Research, Sweden	O	-	D	-	-	-	-	-	-	-	59
Swiss Federal Institute of Technology	O	-	-	-	-	-	-	D	-	-	60

Key:

Q	Received questionnaire on capabilities	**?**	No information provided as yet
?			
✓	Replied to questionnaire	**H**	Has specific hardware technologies to offer which are relevant to space use
O	Capabilities deduced from open publications	**D**	Has technology under development
V	Verbal description of capabilities	**PS**	Is conducting preliminary studies on this topic

Column two of Table 94.02.1 indicates whether the information was obtained from:

- questionnaire reply,
- open literature, or
- no information provided.

Table 94.02.1 covers selected sensory and actuator technologies.

Table 94.2-2 - Smart technology survey: Applications

European organisation	Vibration damping	Fibre optics in composites	Active compensation and alignment	Comments	Ref.
University of Strathclyde (SMART Structures Research Institute)	PS	D	-	Participation in OSTIC and OSMOS BRITE EURAM programmes	1 - 4
Matra Marconi Space UK Ltd.	PS/D	-	PS	Interested in vibration damping for orbiting structures	-
AEA Technology, Harwell	PS	D/H	-	Application of sensors and actuators to composites	4 - 12
Westland Aerospace	H/D	D/H	-	See statement on specialisations	13 - 15
ISVR, University of Southampton	PS, D		-	Specialisation in vibration control	16
ORC, University of Southampton	-	D	-	Work in conjunction with Westland Aerospace	3,13,15, 17,18,25
ERA Technology Ltd.	-	D	PS	Specialisation- Development of sensor technologies and their application to antennas and composites	19,20
DRA, Farnborough (Space Dept. & Materials/Structures Dept.)	PS	PS	PS	Preliminary studies on aircraft structural integrity and Smart systems for space structures	-
Cranfield Institute of Technology	-	-	-	Development of SMAs for actuating requirements	21,22
British Aerospace, SRC	?	?	?	-	-
BAe Military Aircraft Ltd.	-	PS	-	In-flight strain monitoring	23
BAe Space Systems Ltd.	?	?	?		-
SAIC UK Ltd.	PS/D	-	-	Noise and vibration suppression	24
Dornier GmbH	D	D	PS	See statement on specialisations	26 - 35
DASA, Munich, Aircraft Div.	PS	PS	-	Health monitoring and lower costs	36
DLR, Inst. of Aeroelasticity, and DLR, ISM, Braunschweig	D	D/H	-	See statement on specialisations	37 - 50
University of Hamburg-Hamburg	-	-	PS		51
CNES	?	?	?	-	-
Aerospatiale, SSSD, Cannes	-	-	-	-	-
Aerospatiale, Suresnes	-	D	-	Embedding of piezoelectrics in composites	-
Thompson-CSF LCR	-	D	-	-	52
Bertin et Cie	-	D	-	-	7,53 - 55

Metravib RDS	H	-	D	Capabilities in active and passive vibration control	-
Alcatel - Espace	?	?	?	-	-
Matra Marconi Space (France)	PS	?	?	-	-
CISE Technologie Innovative SpA	-	D	-	Specialisation: Development of multiplexed coherent optical fibre sensor systems	56,57
European Organisation	**Vibration Damping**	**Fibre Optics in Composites**	**Active Compensation & Alignment**	**Comments**	**Ref.**
University of Naples	-	D	-	Optical Fibre developments	58
Alenia Spazio SpA	-	D	-	Participation in BRITE "OSTIC" programme	7,54,55
CASA (Space Division)	-	PS	PS	Embedded piezoelectrics in composites. See statement	-
Institute of Optical Research, Sweden	-	-	-		-
Swiss Federal Institute of Technology	FS	-	-		-

Key:

Q	Received questionnaire on capabilities	**?**	No information provided as yet
?			
✓	Replied to questionnaire	**H**	Has specific hardware technologies to offer which are relevant to space use
O	Capabilities deduced from open publications	**D**	Has technology under development
V	Verbal description of capabilities	**PS**	Is conducting preliminary studies on this topic

Table 94.02.2 indicates involvement in applying smart technologies to:

- vibration damping.
- fibre optics in composites (for damage detection).
- active compensation and alignment.

These fields are most relevant to space structures, and do not address any other commercial or industrial uses.

94.3 European expertise

94.3.1 Smart technologies

94.3.1.1 General

A Europe-wide survey conducted in mid-1993 highlighted the principal organisations active in smart technologies. A summary of their activities at that time is given for:

- UK – Westlands Aerospace.
- D – Dornier (now part of EADS); DLR.
- E – CASA (now part of EADS).

94.3.1.2 Germany

In 2005, a list of research centres and industrial centres of competence for smart materials was provided for Germany, Ref. [94-63]:

- DLR Institute of Structural Mechanics, (Braunschweig).
- EADS Astrium GmbH - Structures and Mechanisms, (Friedrichshafen)
- ISC - Fraunhofer Institute für Silicatforschung, (Würzburg)
- LBF - Fraunhofer Institute für Betriebsfestigkeit, (Darmstadt)
- Neue Materialien Würzburg GmbH, (Würzburg)

94.3.1.3 Westland Aerospace Ltd. (UK)

Westland Aerospace, with Westland Helicopters, are one of the largest European manufacturers of composite structures. Two specialisations of note are:

- embedding fibre optic sensors in composites, and
- suppression of airframe vibration in helicopters.

Westland's have worked is in conjunction with:

- United Technologies, USA (twin core optical fibres).
- Optoelectronics Research Centre, University of Southampton (optical fibres with Bragg gratings).

Optic fibres have been applied to thermosetting and thermoplastic composites, and embedding has been integrated with the manufacturing cycle. The principle motivation is composite structure health monitoring of induced stresses, fatigue and damage.

Current developments are aimed at:

- high multiplexing capability,
- ruggedness and reliability,
- effects of embedded sensors on host laminate properties,
- embedding techniques,
- micro-mechanical modelling,
- full-scale demonstrators.

94.3.1.4 Dornier GmbH (G)

Dornier are a substantial aerospace company, active in both aircraft and space structure development. Their skills in sensor and actuator technology are widespread and encompass smart materials, as summarised in Table 94.3.1. They have undertaken a number of demonstrator programmes of direct relevance to space structures:

- fibre optic sensors embedded in composites for strain measurement.
- application of PVDF films to composites for sensing and damping.
- integration of piezo-ceramic films into CFRP.
- study of SMAs.
- active suppression of vibration in solar arrays.
- hierarchical procedures for designing active structures.

Table 94.3-1 - Smart technology: Active structures development with Dornier Product Div. for satellite and application systems

Technologies	Applications					
	Satellite compartment of transport systems	High precision structures for science, earth observation and communication			Interfaces to solar arrays	Other applications
		Appendages (sciences)	Reflectors antennas	Telescope optical system		
Smart materials and structures	X	X	X	X	X	X
Shape control			X	X		X
Design methodology for active structure with numerous actuators		X	X	X		X
Active interfaces • vibration damping • pointing stab. • Isolation		X	X	X	X	X
Active interfaces for testing substructures		X	X	X		
Active noise reduction	X					X
Subsystem engineering	X	Active system Interface	Active system Interface	Active system Interface Isolation	Interface	X
Special developments	• Health monitoring • Robots with elastic arms • Active pre-stressing in bridges					

94.3.1.5 DLR (G)

Comprising the Institute of Aeroelasticity (Gottingen), and Institute of Structural Mechanics (Braunschweig). The combined experience of both institutes is comprehensive in the field of sensors and actuators. Specific themes include:

- in-flight strain measurement with fibre optic interferometric strain gauges.
- real time controllers on digital signal processors with adaptive digital filters.
- damage detection on the basis of measured modal properties of the structure.
- vibration isolation and damping in automobiles, satellites, engines and helicopters.
- constitutive equations of smart materials and their implementation into finite element codes. With particular reference to optimum sensor and actuator placement.

The use of structural modelling techniques to define the locations for smart system integration is a strong feature of their work. The concept of Independent Modal Space Control allows the optimum placement of sensors/actuators for vibration damping.

94.3.1.6 CASA: Space Division (S)

CASA are participating in a number of system development programmes which combine sensors and actuators in conjunction with thermal control techniques. Specific topics include:

- Optical Measurement System (OMS) using optical interferometry for distortion measurement in space structures.
- Application of piezoelectric materials in sensors and actuators.
- Adaptive System with embedded piezoelectrics in CFRP.
- MEDEA (Active Structure Study with Modelling and Development) on active control of space telescope optical planes.
- SISCO BRITE programme on Structurally Integrated System for comprehensive evaluation of Composites.

94.3.2 Structural health monitoring

94.3.2.1 General

A list of European organisations identified as active in smart technologies for health and condition monitoring are provided, Ref. [94-61]. The list was compiled in 1999 using openly published literature and from replies from individual organisations. The summary provided gives an indicative of what is available and from where. It is not a definitive list of all organisations active in this area of technology.

94.3.2.2 Germany

Experience	Company / Organisation
Approach to SHM in aircraft (review); piezoelectric sensing.	Daimler-Benz
Application of Neural Networks for the analysis of data from health monitoring systems (acoustic emission, Lamb wave and vibration-based methods).	Daimler-Benz Research & Technology DLR
NDT by Alternating Current Magnetic measurements (for surface condition of structural steel elements used in civil engineering).	Fraunhofer Institute fur Zerstorungfreie Prufverfahren University of Saarland
Application of integrated health monitoring systems for X-38/TETRA space structures, Ref. [94-62].	Kayser-Threde GmbH
Photorefractive holography for real-time vibration analysis.	Labor Dr Steinbichler [EU project prime contractor]
Application of acoustic emission, data analysis for the removal of geometry-related features in AE traces.	University of Stuttgart

94.3.2.3 Spain

Experience	Company / Organisation
Condition monitoring of wear in machinery.	Asociacion de Investgacion Tekniker [EU project prime contractor]
Expert system development for rotating machinery.	Comp. Internat. de Plantas Papeleras SA [EU project prime contractor]
Modelling and damage detection in high-safety, high-cost structures.	Construcciones Aeronáuticas SA [EU project prime contractor]
Smart materials for space applications (review). MACOIN: Fibre optic sensors embedded in CFRP aeronautical structures.	INSAMET
Fibre optic sensors in machine tools.	Trimek SA [EU project prime contractor]
Embedded fibre optic sensors in composite wind turbine blades.	Universidad Politécnica de Madrid [EU project prime contractor]
Embedded self-sensing piezoelectric (PZT) actuator-sensors.	Universidad Politecnicca de Madrid

94.3.2.4 Switzerland

Experience	Company / Organisation
Embedded fibre optic sensors in CFRP.	Contraves

94.3.2.5 France

Experience	Company / Organisation
'Smart' processing of composite materials.	Aerospatiale
Structural health monitoring.	Aerospatiale
Fibre optic sensors applied to aircraft composite structures and for civil engineering applications (strain, damage initiation, temperature).	Bertin & Cie [EU project prime contractor]
Integrated system for damage mapping and structural integrity of composites.	Bertin & Cie [EU project prime contractor]
Electrical methods for in-situ damage detection in CFRP.	CNRS
Health monitoring of gas turbines.	Metravib RDS [EU project prime contractor]
Acoustic emission for on-line monitoring of chemical industry plant for stress corrosion cracking.	Rhone-Poulenc Industrialisation [EU project prime contractor]

94.3.2.6 Italy

Experience	Company / Organisation
Acoustic emission for on-line monitoring of high-temperature power plant.	CISE SPA [EU project prime contractor]

94.3.2.7 Portugal

Experience	Company / Organisation
On-line erosion, corrosion and temperature monitoring of boiler tubing.	Electricidade de Portugal [EU project prime contractor]

94.3.2.8 Eire

Experience	Company / Organisation
Condition monitoring of plastics industry machinery.	GEM Plastics Ltd. [EU project prime contractor]

94.3.2.9 United Kingdom

Experience	Company / Organisation
Simultaneous strain, temperature and vibration measurement (fibre optic sensors). Noise rejection approach to fibre optic sensor systems. Temperature referenced quasi-static strain measurement, by fibre optic sensors, for concrete bridges. Current transformer evaluation by fibre optic sensors (power distribution industry).	Applied Optics Group (University of Kent) Photonics Research Group (Aston University)
On-line integrated technologies for operational reliability (aircraft).	British Aerospace Defence Ltd [EU project prime contractor]
Embedded Bragg grating fibre optic sensors in composite aerospace structures.	Cranfield University [EU project prime contractor]
Cure monitoring of composite materials by embedded fibre optic sensors. Embedded Bragg grating fibre optic sensors in CFRP under impact testing.	Cranfield University
Structural monitoring development covering: strain measurement (optical fibre & silicon-based devices) and damage detection, principally delamination in composites (optical fibres, Lamb waves, electrical potential methods). Optical fibre sensors (patented method for separation of temperature and strain; vector strain). Silicon strain sensors, with integrated processing and communications. Active structures, incl. aerodynamic & hydrodynamic manoeuvre control; control of vibration and radiated sound. Research and development, including trials on aerospace components, e.g. wingbox structure, full-size wound components, adhesive bonds in CFRP structure.	DERA (Farnborough); now QinetiQ
Development of commercial optical fibre, sensor-based systems for composites, defence and civil engineering structures, etc.	EM Technology Ltd.
Remote monitoring strain in high temperature plant using Surface Acoustic Wave (SAW) based technique.	ERA Technology Ltd. [EU project prime contractor]
Scanning Laser Doppler Vibrometry.	Imperial College [EU project prime contractor]
Lamb wave testing for large structures (quick inspection method).	Imperial College, London TWI [EC THERMIE programme]
Fatigue behaviour of composites with embedded optical fibres. Predicted strain in embedded optical fibres in CFRP.	ISVR (University of Southampton)
Composites performance and design programme (CPD), covering: Structural response & integrity, Life assessment & prediction, Interface characteristics & behaviour, Manufacture, safety & design: specific issues, Dissemination, standardisation & reviews.	National Physical Laboratory (NPL) [UK DTI Programme Co-ordinators]
Optical fibre strain monitoring of large civil engineering structures.	Protodel International Ltd [EU project prime contractor]
Intelligent sensors for plant monitoring/process control & maintenance decision making.	WM Engineering Ltd. [EU project prime contractor]

94.4 References

94.4.1 General

[94-1] B. Culshaw, P.T. Gardner & A. McDonach (Editors)
First European Conference on Smart Structures and Materials
Glasgow, 12-14 May 1992. Proceedings copublished by IoP Publishing and EOS/SPIE EUROPTO Series SPIE 1777
ISBN: 0-7503-0222-4

[94-2] B. Culshaw & C. Mitchie
'Fibre Optic Strain and Temperature Measurement in Composite Materials: A Review of the OSTIC Programme'
ESA SP-336. International Symposium on Advanced Materials for Lightweight Structures, ESTEC, March 1992, p393-398

[94-3] B. Culshaw & J.P. Dakin (Editors)
'Optical Fibre Sensors'
Vol. 1: Principles and Components, ISBN 0-89006-317-6 (1988)
Vol. 2: Systems and Applications, ISBN 0-089006-376-1 (1989)
Published by Artech House, Inc.

[94-4] B. Michie et al
'Fibre Optic Technique for Simultaneous Measurement of Strain and Temperature Variations in Composite Materials'
Fibre Optic Smart Structures and Skins IV, Boston, September 1991, SPIE Vol.1588

[94-5] R. Davidson & S.S.J. Roberts
'Finite Element Analysis of Composite Laminates Containing Transversely Embedded Optical Fiber Sensors'
SPIE 1777, p115-122

[94-6] S.S.J. Roberts & R. Davidson
'Short Term Fatigue Behaviour of Composite Materials Containing Embedded Fibre Optic Sensors and Actuators'
SPIE 1777, p255-262

[94-7] P. Sansonetti et al
'Intelligent Composites Containing Measuring Fibre Optic Networks for Continuous Self Diagnosis - II'
Fibre Optic Smart Structures and Skins IV, Boston, Sept 1991 SPIE Vol.1588

[94-8] R. Davidson et al
'Composite Materials Monitoring Through Embedded Fibre Optics'
Fibre Optics '89, 7th Int Conf Fibre Optics and Optoelectronics
London, Apr 1989, SPIE Vol 1120 p152-160

[94-9] R. Davidson et al
'Composite Material Monitoring Through Embedded Fibre Optics'
International Journal of Optoelectronics, 1990, vol.5, p397-404

[94-10] S.S.J. Roberts & R. Davidson
'Mechanical Properties of Composite Materials Containing Embedded Fibre Optic Sensors'
Fibre Optic Smart Structures and Skins IV, Boston, September 1991, SPIE Vol.1588

[94-11] R. Davidson et al
'Fabrication Monitoring of APC-2 using Embedded Fibre Optic Sensors'
ECCM 5, p441-446, Bordeaux, April 1992

[94-12] R. Davidson et al
'Vibration Reduction in Composite Structures'
ECCM 6: Smart Composites Workshop, Bordeaux,
September 1993, p89-94.
ISBN 1-85573-144-4

[94-13] N.C. Eaton et al.
'Factors Affecting The Embedding of Optical Fibre Sensors in Advanced Composite Structures'
Paper 20 AGARD Conference Proceedings 531 on Smart Structures for Aircraft and Spacecraft. Lindau, Oct 1992

[94-14] C.T. Maidment & N.C. Eaton
'Development of Intelligent Structures'
Westland Aerospace Report RD/FO/008, April 1991
ESTEC Contract No. 8521/89/NL/TB

[94-15] N.C. Eaton et al
'Fibre Optic Bragg Grating Sensor Measurements in Composite Materials'
ECCM 6: Smart Composites Workshop, Bordeaux,
September 1993, p47-58.
ISBN 1-85573-144-4

[94-16] S.J. Elliott & P.A. Nelson
'The Active Control of Sound'
Electronic and Communications Engineering Journal,
August 1990, p127-136

[94-17] J.P. Dakin
'Optical Fibre Pressure and Strain Sensors for Smart Structures'
ECCM 6: Smart Composites Workshop, Bordeaux,
September 1993, p39-46.
ISBN 1-85573-144-4

[94-18] J.P. Dakin
'Multiplexed and distributed optical fibre sensors'
ESA SP-336. International Symposium on Advanced Materials for Lightweight Structures., ESTEC, March 1992, p385-392

[94-19] N.D.R. Goddard et al
'Smart Materials: A Review of the Four Key Technologies and their Likely Industrial Impact'
ERA Technology Report 92-0246R, November 1992

[94-20] L. Bjorkegren et al
'Applications for Artificial Neural Networks'
ERA Technology Report 92-0871R. December 1992

[94-21] C.M. Friend
'The stability of Strain in Shape-Memory Actuators'
SPIE 1777, p181-184

[94-22] C.M. Friend
'The Performance Characteristics of 'Smart' Laminates Containing Shape-Memory Alloy Actuators'
ECCM 6: Smart Composites Workshop, Bordeaux,
September 1993, (withdrawn).

ISBN 1-85573-144-4

[94-23] P.A. Tutton & F.M. Underwood
'Structural Health Monitoring using Embedded Fibre Optic Sensors'
AGARD Conference Proceedings AGARD-CP-531, Paper 18 ISBN 92-835-0701-X, 1993

[94-24] C. Dorling et al
'A Demonstration of Active Noise Reduction in an Aircraft Cabin'
Journal of Sound and Vibration, (1989) 128 (2), p358-360

[94-25] M.G. Xu & J.P. Dakin
'Optical Fibre Sensors for Space Applications'
ORC, University of Southampton Report
Work Order No 24: ESTEC Contract 7090/87/NL/PP, July 1993

[94-26] W. Charon et al
'Smart Structures with Piezopolymers for Space Applications'
SPIE 1777, p329-332

[94-27] W. Charon
'Structural Design of Active Precision Structures'
SPIE 1777, p337-340

[94-28] W. Charon et al
'On Structural Design of Active Structures'
Int. Conf. on Dynamics of Flexible Structures in Space, Cranfield May 1990

[94-29] H. Baier et al
'Deployment Analysis and In-Orbit Control of Large Reflectors'
Int. Conf. on Spacecraft Structures and Mechanical Testing
Noordwijk, April 1991

[94-30] H. Buler
'On Shape Control of Precision Structures: Concepts, Analysis and Technology'
Proc. of the Int. Forum on Aeroelasticity and Structural Dynamics
Aachen, June 1991, DGLR Paper No.91-138

[94-31] W. Charon
'Actuator Positioning within the Mechanical Design of Active Structures'
Proc. of the Int. Forum on Aeroelasticity and Structural Dynamics
Aachen, June 1991, DGLR Paper No.91-143

[94-32] D. Maurer & W. Charon
'Active Structures: Verification of Dynamic Performance after Mechanical Design'
Proc. of the Int. Forum on Aeroelasticity and Structural Dynamics,
Aachen, June 1991, DGLR Paper No.91-140

[94-33] J. Bals et al
'Flows between Structural and Control Designs by example of the Extendible and Retractable Mast'
Int. Conf. on Active Materials and Adaptive Structures, Alexandria VA, Nov 1991

[94-34] G. Lindner et al
'Piezoelectric Polymer Actuator for Vibration Control of Plate Structures'
ACTUATOR 92, 3rd Int. Conf. on New Actuators, Bremen
June 1992

[94-35] R. Sippel
'A Test Sample with Embedded Fibre Optic Sensors for High Accuracy Strain Measurement'
Dornier GmbH Report, September 1992
Work Order No 23: ESTEC Contract 7090/87/NL/PP

[94-36] C. Boller et al
'Technological Challenges with Smart Structures in German Aircraft Industry'
SPIE 1777, p289-292

[94-37] N. Furstenau et al
'Composite Strain Sensing with a Combined Interferometric and Polarimetric Fibre-Optic Strain Gauge'
SPIE 1777, p81-84

[94-38] R. Lammering
'Optimal Placement of Piezoelectric Actuators in Adaptive Truss Structures'
SPIE 1777, p317-320

[94-39] F. Nitzsche & E. Breitbach
'The Smart Structures Technology in the Vibration Control of Helicopter Blades in Forward Flight'
SPIE 1777, p321-324

[94-40] E. Breitbach
'Research Status on Adaptive Structures in Europe'
Proc. of the 2nd Joint/U.S. Conference on Adaptive Structures
Nagoya, Japan, Nov 1991

[94-41] J. Melcher
'Adaptive On-line System Identification of Aerospace Structures using MX Filters'
IFAC Symposium on Aerospace Control, Munich/Ottobrunn
Sept, 1992, Paper No 96

[94-42] E. Breitbach & L.F. Campanile
'Damage Detection in Structural Systems: A Modal Approach'
Proc. of the Int Forum on Aeroelasticity and Structural Dynamics
Strasbourg, May 1993

[94-43] L.C. Brinson
'One Dimensional Constitutive Behaviour of Shape Memory Alloys: Thermomechanical Derivation with Non-Constant Material Functions and Redefined Martensite Internal Variable'
Journal of Intelligent Material Systems and Structures, 1993

[94-44] R. Lammering
'The Application of a Finite Shell Element for Composites Containing Piezo-Electric Polymers in Vibration Control'
Computers & Structures, 41, p1101-1109, 1991

[94-45] R. Lammering et al
'Optimal Placement of Piezo-Electric Actuators in Adaptive Truss Structures'
Journal of Sound and Vibration, 166, No.3, 1993

[94-46] R. Lammering
'A Finite Shell Element for Composites with Integrated Piezoelectric Polymers'
Zeitschrift fur angewandte Mathematrik and Mechanik, 72
pT216-T220, 1992

[94-47] J. Melcher & R. Wimmel
'Modern Adaptive Real-Time Controllers for Actively Reacting Flexible Structures'
To be published in: Journal of Intelligent Material Systems and Structures

[94-48] R. Wimmel
'Adaptive Digital Filters for Modal Control of Adaptive Structures'
Proc. of the Int. Forum on Aeroelasticity and Structural Dynamics
Aachen, June 1991, DGLR Paper No.91-139

[94-49] J. Melcher
'Active Vibration Isolation Using Multifunctional Interfaces and Adaptive Digital Controllers'
Proc. of the Third Int. Conference on Adaptive Structures
San Diego, Nov 1992

[94-50] F. Nitzsche & E. Breitbach
'A Study of the Feasibility of Using Adaptive Structures in the Attenuation of Vibration Characteristics of Rotary Wings'
Proc. of the AIAA 33rd Structures, Structural Dynamics and Materials Conference, Dallas, April 1992

[94-51] K. Schulte
'Development of Active Deformable Composite Structures due to Thermal Residual Stresses and incorporating Shape Memory Alloys'
ECCM 6: Smart Composites Workshop, Bordeaux,
September 1993, p115-120.
ISBN 1-85573-144-4

[94-52] M. Turpin et al
'Process-Induced Birefringence Variations in Fiber Optic Embedded in Composite Materials'
SPIE 1777, p93-96

[94-53] P. Sansonetti et al
'Unidirectional Glass Reinforced Plastic Composite Monitoring with White Light Quasi Distributed Polarimetric Sensing Network'
SPIE 1777, p77-80

[94-54] B. Fornari et al
'Strain Measurement of Carbon/Epoxy Composite with Fibre Optics White Light Quasi Distributed Polarimetric Sensor'
Paper 12 AGARD Conference Proceedings 531 on Smart Structures for Aircraft and Spacecraft. Lindau, Oct 1992

[94-55] P. Sansonetti et al
'Intelligent Composites Containing Measuring Fibre Optic Networks for Continuous Self Diagnosis - I'
Fibre Optic Smart Structures and Skins II, Boston, Sept 1989 SPIE Vol.1170

[94-56] A. Barberis et al
'Elastic Curve Recovery by a Quasi-Distributed Polarimetric Fibre Optic Sensor'
SPIE 1777, p35-38

[94-57] P. Vavassori & M. Martinelli
'Material Processing Diagnostic by Optical Interferometry'
SPIE 1777, p395-398

[94-58] I. Crivelli Visconti
'Technical Characterisation of a New Optical Fibre Sensor for Smart Composites'
ECCM 6: Smart Composites Workshop, Bordeaux,
September 1993, p59-68.
ISBN 1-85573-144-4

[94-59] L. Wosinski et al
'Quasi-Distributed Fiber-Optic Sensor for Simultaneous Absolute Measurement of Strain and Temperature'
SPIE 1777, p53-56

[94-60] A. Venkatesh et al
'Active Vibration Control of Flexible Linkage Mechanisms using Shape Memory Alloy Fibre-Reinforced Composites'
SPIE 1777, p185-188

[94-61] J. Wilson & R.J. Hussey: RJ Technical Consultants, (F)
'Structural Health Monitoring Techniques & Potential Application to RLV Composite Primary Structures & Cryogenic Tanks'
Report No. RJTC-046-SHM (September 1999)
ESA Contract 10983/94/NL/PP - Work Order No. 16

[94-62] Dr. R. Graue & A. Reutlinger: Kayser-Threade, (D)
'Structural Health Monitoring for Future Launchers: Results from Breadboarding and Prototype Development'
Proceedings of the 3rd European Conference on Launcher Technology, Strasbourg. 11th – 14th December 2001, p755-766.

[94-63] H.G. Wulz & K. Rohwer: EADS-Astrium GmbH/DLR, (D)
'Smart Materials'
ESTEC Contract No. 15865/NL/MV/ CCN3
September 2004

95 Textiles

95.1 Introduction

95.1.1 General

Textiles can be considered to be a form of composite material. They are increasingly used in many industrial applications. High performance fibres are available, based on minerals, ceramics and polymers, together with improved coating technologies for fibres and fabrics. Using these, with the advances in computerised knitting, weaving and braiding techniques, the design and production can be optimised to produce highly efficient textiles, Ref. [95-1].

This chapter describes the use of technical textiles in space applications, defines the nomenclature and gives guidelines for their procurement and assessment. In current space applications, textiles are used more often in multi-functional protection, e.g. TPS and spacesuits, than in structural applications.

[See: Chapter 96 – textile testing; Chapter 97 – textile applications]

The scope here is restricted to the use of textiles as materials in their own right, hence this does not include their use as reinforcements in composites.

[See: Chapter 2 and Chapter 3 for the use of fabrics and fibres as composite reinforcement]

95.1.2 Fibre types and combinations

High-performance fabrics made of various woven yarns have a range of space applications. Depending on the specific component, different methods and fibre materials are used in the textile manufacture.

Some examples of fibre combinations with useful properties are:

- Kevlar, Nomex, PTFE textiles for space suits and possible micrometeoroid and debris protection systems.
- Silica (SiO_2) and glass textiles for thermal protection systems under moderate loads.
- Silicon carbide (SiC) and alumino-boro-silicate (ABS) textiles for combined high thermal and structural loads.

95.1.3 Fibre properties

The basic properties of the constituent fibre types used in textiles are summarised in Table 95.1.1.

Table 95.1-1 - Properties of fibre constituents for space textiles

Fibre type	Diameter [μm]	Density [kg/m³]	Strength [MPa]	Young's modulus [GPa]	Service temp. [°C]
Silica	9	2200	3450	70	1000
ABS	10	2700 - 3100	1400 - 2100	200 - 240	1400
SiC	10 - 15	2500	2900	186	1200
Aramid (Kevlar)	12	1450	2800 - 3600	125	230
Aramid (Nomex)	12	1400	700 - 800	25	230

The fibres differ widely in strength, density and their range of service temperatures but all have the potential for processing by weaving and knitting techniques.

By combining different fibres and varying their weave patterns during processing, the properties of the resultant textile component can be tailored for specific requirements.

95.1.4 Textiles in spacecraft

95.1.4.1 General

In general, textiles in space applications are either used structurally in pure tension, or are anchored to a substrate to act as a thermal or mechanical barrier. In some cases these functions may be combined.

[See: 71.5 for examples of fabrics in thermal barrier applications for Space Shuttle Orbiter]

For thermal insulation case studies, [See: 97.3].

Some examples of their varied uses in space programmes are:

- thermal protection, [See: 97.3]:
  - Flexible External Insulation (FEI): Thermal protection of launchers and re-entry vehicles, [See also: 71.11].
  - thermal shields and blankets: Insulation of hot or cold components, e.g. rocket motors, cryogenic tanks.
- micrometeoroid and debris protection:
  - protection for astronauts and vehicles against high energy impacts.
- space EVA suits, [See: 97.2]:
  - flexible space suit structures, i.e. atmosphere containment.
  - protection against mechanical hazard, e.g. low energy impact, abrasion.
  - solar radiation protection (Outer Fabric for a European Space Suit - OFFES).
- parachutes, [See: 97.4]:
  - parachutes for planetary probes.

— earth re-entry capsules.

— braking systems for reusable space vehicles.

- restraint or storage:
  - storage and compartments in manned space stations or cargo applications.
  - general purpose restraining straps.

95.1.4.2 Flexible external insulation

The requirements for FEI and other similar thermal barrier applications are:

- good insulation behaviour.
- good structural behaviour under acoustic and dynamic loads.
- good high temperature strength of components.
- low weight.
- easy processability.

[See: 71.10 - Internal multiscreen insulation (IMI); 71.11 - Flexible external insulation (FEI); 71.23 - High temperature insulation (HTI)]

95.1.4.3 Impact protection

Impact protection is an integral part of the requirements for the outer layers of EVA suits, as exemplified by the OFFES technology study, [See: 97.2].

95.1.4.4 OFFES

The OFFES applications require materials of:

- high strength.
- good impact resistance.
- chemical stability, resistance to degradation.
- specified, stable thermo-optical properties.
- good micrometeoroid and debris protection.

95.1.4.5 Parachutes

Parachute applications require materials with, Ref. [95-2]:

- high melting point.
- good hot-air degradation resistance.
- good resistance to radiation.
- good tensile properties.
- predictable air porosity (permeability).
- known electrical properties and low tribological charging, e.g. to avoid disruption of spacecraft communications.

[See: 97.4 - Planetary entry parachute, case study]

95.1.4.6 Restraints and storage systems

[See: ESA PSS-03-70 - Human factors for the general requirements]

95.1.5 Testing of textiles

All of the requirements for a technical textile for space use are verified by appropriate testing. Some of the more common test methods for textiles are described in Chapter 96 and summarised in 96.17.

The test procedures are based on international and national specifications, as well as practical experience, Ref. [96-1].

95.2 Terminology

95.2.1 Textile terms

95.2.1.1 General

The meaning of the terms used for technical textiles can vary from those same terms applied to composite reinforcements, [See also: Glossary].

95.2.1.2 Fibre

A general term for filamentary materials with a finite length at least 100 times their diameter. Also known as Filament or Spin Fibre.

95.2.1.3 Filament

The smallest unit of a fibrous material. The basic unit formed by drawing and spinning.

95.2.1.4 Strand

Usually an untwisted bundle of continuous filaments used as a unit. Occasionally a single fibre or filament is referred to as a strand.

95.2.1.5 Yarn

A continuous assembly of twisted filaments, fibres or strands (natural or artificial), suitable for processing, e.g. weaving or knitting, to form a textile.

95.2.1.6 Roving

A number of yarns, strands or tows collected into a parallel bundle with little or no twist.

95.2.1.7 Folded yarn

The term folding is synonymous with plying. Folded yarn then denotes a yarn made by twisting together two or more single yarns.

95.2.1.8 Fleece

Fibrous webs (felts, non-woven fabrics, wadding) produced from twisted single textile fibres.

95.2.1.9 Mat

Fibrous material consisting of randomly oriented chopped filaments, short fibres or swirled filaments, loosely held together with a binder.

95.2.1.10 Flock

Short chopped fibres.

95.2.1.11 Textile

These may be woven (or knitted, braided) or non-woven products.

95.2.1.12 Woven textiles

These are fabrics constructed from visually identifiable, compacted bundles of fibres known as yarns. The yarns may consist of:

- continuous (infinitely long) filaments (such as silk or extruded manmade fibres), or
- relatively short, staple fibres, such as cotton, wool, ceramics or cut lengths of manmade fibre.

In the case of short (staple) fibres, a cohesive structure is obtained by twisting the fibres together to form a yarn, Ref. [95-1], [95-3].

95.2.1.13 Non-woven textiles

These felts, fleeces, etc. are fibrous sheet-materials such as those used as the core of a flexible external insulation (FEI) system.

95.3 Textile fibres

95.3.1 General

Textile fabrics, Ref. [95-4], [95-5], can be produced from either natural or artificial (chemical) fibres.

95.3.2 Natural fibres

These have various lengths and diameters depending on their growth pattern. Apart from silk fibres, with lengths up to more than 1000 m, natural fibres are usually of limited length, Ref. [95-4].

95.3.3 Chemical fibres

95.3.3.1 General

These can be produced in many different forms, where the length, cross-section, surface and twist can be individually adapted for a particular application, Ref. [95-4]. The usual product forms are:

- filaments (continuous fibres).

- monofilaments (diameters > 0.1 mm).
- cables (multiple filaments with or without twist).
- filament yarns (smooth, textured, twisted).
- spin fibres (limited length).
- spin ribbons.
- flock (short fibres).

95.3.3.2 Types of chemical fibre

Chemical fibres may be produced from natural or synthetic polymers or from inorganic materials and include, Ref. [95-4]:

- Natural polymers:
  - cellulose fibres,
  - alginates,
  - dienes.
- Synthetic polymers:
  - elastomers,
  - fluorofibre,
  - acrylic,
  - polyamide,
  - chlorofibre,
  - polyester,
  - polyolefin,
  - vinyl.
- Inorganic fibres:
  - glass,
  - ceramic,
  - carbon,
  - metal.

95.4 Yarns

95.4.1 General

Yarn designations give, in a condensed form, details of the yarn components, including the linear density, direction and amount of twist, number of folds, Ref. [95-6]. The actual values of these for the finished yarn are subject to tolerances, which depend greatly on the production process.

There are two methods of yarn notation used in international standards:

- beginning with the details of the components making-up the finished yarn, termed 'single-to-fold' notation.

- beginning with the details of the resultant yarn and breaking this down to the component level, termed 'fold-to-single' notation.

95.4.2 Yarn types

95.4.2.1 General

In general, spun yarn produces fabrics with better flexibility than those of filament yarns. But filament yarns usually have better energy absorption characteristics.

95.4.2.2 Single yarns

Single yarns are composed of either:

- spun yarn: a number of discontinuous fibres held together by twist.
- filament yarn: one or more continuous filaments, with or without twist.
- monofilament yarn: a single filament.
- multifilament yarn: two or more filaments.

95.4.2.3 Multiple wound yarn

Two or more yarns wound, but not twisted, together.

95.4.2.4 Folded yarn

Two or more yarns twisted together.

95.4.2.5 Cabled yarn

Two or more folded yarns twisted together.

95.4.3 Yarn notation

This gives a condensed technical description of the yarn, Ref. [95-6]:

- linear density, i.e. mass per unit length, tex or titer (DIN 53 830).
- twist (direction and number of turns per metre),
- R - resultant linear density in tex or dtex (decitex). Tex gives the mass in grams of one kilometre of yarn, Ref. [95-7].
- f - number of filaments,
- t_n - number of twists per metre, (t_0 = zero twist).

95.5 Yarn characteristics

95.5.1 General

There are many commercially available yarns produced by a large number of manufacturers and production processes. Those most commonly used in spacecraft and shielding applications are:

- "Nomex Delta A" (DuPont): a permanent antistatic fibre (used in US lift-off suit), which solves the charging-discharging problems.
- "Nomex Delta T" rip-stop fabric (special 2-D combination of Nomex and Kevlar).
- Vitreous silica (SiO_2) threads with high temperature resistance, from a number of sources, e.g. Enka, Quartz & Silice, Hexcel, Brochier, 3M, Clark-Schwebel, Gevetex comp.

95.5.2 Nomex and Kevlar

95.5.2.1 General

Nomex and Kevlar (which are both produced in a dry jet - wet spinning process, but with different shear gradients and crystallisation rates) exhibit property profiles which appear to be complementary to each other. The Kevlar fibre has high strength and modulus whilst retaining a certain degree of deformability. The Nomex fibre has a high elongation to break. A combination of both types of thread results in a system with high strength and flexibility and has good impact behaviour.

Aramid-based fibres generally exhibit:

- high glass transition temperatures.
- good high temperature strength.
- excellent fire protection capabilities.
- low shrinkage.
- good impact protection behaviour.
- good processability by weaving and knitting techniques.

Both Nomex and Kevlar are sensitive to UV radiation and require a UV-protective surface layer. This is usually achieved by incorporating an integrally-woven PTFE thread, providing outer surface protection against:

- UV radiation induced alteration of the aramid chemistry,
- operationally induced wear and abrasion,
- contact with chemicals during operation.

95.5.2.2 Nomex

Nomex is part of the nylon fibre family. Its natural colour is white, but this can be changed by spin-forming. The final yarn treatment can be used to vary the properties. Features of Nomex include:

- Developed to have specific properties for certain applications:
  - high temperature resistance,
  - good form stability,
  - textile covers,
  - electrical isolation,
  - tubes,
  - tyres.
- Product forms:

— continuous filament yarn,
— pile fibres,
— spun cables,
— paper.

- Typical physical properties at 20°C:
  — tensile strength at 65% RH.: 5.3 g/den, wet: 4.1 g/den,
  — density: 1380 kg/m^3,
  — thermal capacity: 0.29 cal/g/°C,
  — thermal conductivity: 0.31 kcal.cm/sec/cm^2/°C,
  — poor UV resistance (shielding required),
  — good chemical resistance.

95.5.3 Insulative fibres

95.5.3.1 General

Table 95.5.1 summarises a number of yarns, frequently used in applications where there are high thermal and structural loads, e.g. thermal insulation blankets.

Table 95.5-1 - Typical yarns for high structural and thermal load applications

Designation	Supplier	Material	ρ [kg/m^3]	Diameter [mm]	Tex [g/km]	Thread density [kg/m^3]
AstroquiII, Q-18	J.P. Stevens	SiO_2	2200	0.43	250	1720
AstroquiII, Q-24	J.P. Stevens	SiO_2	2200	0.51	330	1670
Nex 312, AT21	3M	Al_2O_3 - SiO_2 - B_2O_3	2700	0.53	331	1500
Nex 312, AT28	3M	Al_2O_3 - SiO_2 - B_2O_3	2700	0.71	452	1140
FCO 30 PTFE	J.P. Stevens	glass - 18% PTFE	2500	0.45	333	2100
OAK R 751-18	OAK Corp.	glass - 18 % PTFE	1500	0.48	239	1300

95.5.3.2 Silica yarn

This term covers all vitreous silica (SiO_2) thread formed by assembly of separate continuous filaments. The production technique consists of drawing hundreds of separate filaments (~9 µm in diameter) from molten silica and applying a coating of binder. This oiling operation binds the filaments together and covers them with a lubricating film which facilitates flexing of the yarn and increases its abrasion resistance. It also eases later manufacturing operations such as weaving of stranded spun thread.

The product forms available (from Enka, Quartz & Silice, Hexcel, Brochier, 3M, Clark-Schwebel and Gevetex comp.) include:

- weaving thread.
- rovings.
- prepreg fabrics.

95.5.3.3 E-Glass

This material is a special silicate mixture. The typical chemical compositions are within the range of:

- SiO_2: 52% to 56%
- CaO: 16% to 25%
- Al_2O_3: 12% to 16%
- B_2O_3: 8% to 13%

An example of a typical E-Glass notation is CE934Z * 2S 150, where:

E = E-glass.

C = continuous fibre.

9 = filament diameter in microns.

34 = yarn weight in tex (g per 1000 m).

Z = protection spin.

2 = number of spun yarns.

S = protection spin.

150 = twist per metre.

95.5.3.4 Alumino-boro-silicate

Alumino-boro-silicate (ABS) fibres, usually with diameters in the range of 10 to 12µm, are a new generation of fibre materials for high-temperature applications.

The typical chemical composition ranges are:

- Al_2O_3: 62% to 70%
- SiO_2: 24% to 28%
- B_2O_3: 2% to 14%

The fibres can be fabricated as thread, fabric components or bulk fleece material with good insulation properties. They exhibit good high temperature strength and are therefore suitable for structural uses at elevated temperatures.

95.5.3.5 Dyneema thread

Dyneema is a new type of a high-performance fibre, manufactured by DSM (NL), based on high modulus polyethylene. In testing, it had some disadvantages, i.e.:

- significant mechanical strength loss at test temperatures >130°C. This was attributed to the relatively low melting temperature (143°C) of the polyethylene thread.
- failure of the sample in the flammability test, because polyethylene is not self extinguishing.

These two shortcomings, particularly the latter, restrict its usefulness as an insulation material.

95.5.4 Yarn properties

Table 95.5.2 compares the properties of several types of fibre, extensively used in technical fabrics.

Table 95.5-2 - Properties of fibres used in textiles for space

Characteristic	Aramid (Kevlar †)	Silica	E-Glass	Alumino-Boro-Silicate
Tensile strength: Dry	3450 MPa	50 - 270 MPa	1500 MPa	1700 - 2070 MPa
Elongation at fracture	2.5%	1.0 %	3.3%	1.1 - 2.1%
Young's modulus	58 - 146 GPa	48 - 72 GPa	50 GPa	138 - 186 GPa
Density	1440 kg/m^3	2200 kg/m^3	2200 kg/m^3	2700 - 3050 kg/m^3
CTE	-2 x 10^{-6} K^{-1}	0.54 x 10^{-6} K^{-1}	5 x 10^{-6} K^{-1}	3 - 5 x 10^{-6} K^{-1}
Temperature resistance	Good	V. Good, >1000 °C	V. Good, >500 °C	1200 - 1370 °C
UV resistance	Shielding recommended	-	-	-
Chemical resistance	Good	Good	Good	Good
Product forms	Continuous filament yarn Rovings Prepreg fabrics	Weaving thread Rovings Prepreg fabrics		Fibre diameter: 10 - 12 µm
Comments	Mechanical properties almost constant between -40 °C and +130 °C.			Short term temperature: 1370°C - 1650°C Melting point: 1800°C

† - Trademark of E.I. DuPont de Nemours.

95.6 Fabrics

95.6.1 Fabric definitions

95.6.1.1 Fleeces

Fleeces are produced from single twisted textile fibres, Ref. [95-8].

95.6.1.2 Fabrics

Fabrics consist of interwoven fibres (warp and weft) of one or more fibre type, Ref. [95-9]. In the finished fabric, the Warp direction is the longitudinal thread direction, and the Weft direction is the transverse thread direction. Fabrics are defined by:

- fibre type,
- yarn type,

- knitting or weaving technique,
- weave style,
- fibre density,
- fabric texture,
- pattern type,
- fabric condition,
- fabric length, width, density and thickness.

95.6.2 Fabrics for flexible thermal insulation systems

Some of the common fabrics used in flexible thermal insulation systems are summarised in Table 95.6.1.

Table 95.6-1 - Textiles: Typical fabrics used in flexible thermal insulation systems

Designation	Supplier	Material	Density [kg/m³]	d [mm]	w [g/m²]	Weave style	Fabric density [kg/m³]
Hex 593	Hexcel	SiO_2	2200	0.24	270	5H Satin	1125
Hex 1125	Hexcel	SiO_2	2200	0.47	530	5H Satin	1128
JPS 581	J.P. Stevens	SiO_2	2200	0.28	285	8H Satin	1020
JPS 570	J.P. Stevens	SiO_2	2200	0.68	660	5H Satin	970
Nex AF 14	3M	Al_2O_3, SiO_2, B_2O_3	2700	0.36	288	Plain	800
Nex AF 30	3M	Al_2O_3, SiO_2, B_2O_3	2700	0.76	583	Crowfoot satin	770
POR 116	Porcher	Glass	2500	0.10	107	-	1070

95.7 Knitting and weaving techniques

95.7.1 General

These are the two basic categories of technique for converting fibrous products into textiles. Each category contains many variants and many of the techniques are now automated or computer controlled.

95.7.2 Knitting

In knitting techniques, a continuous yarn is looped into the advancing edge of the fabric. This in turn forms the edge for the next pass of the yarn. A knitted textile is thus created from a single piece of yarn. This leads to one of the major disadvantages of these materials; damage causing a single break in the yarn may compromise the whole fabric component.

Since knitted fabrics consist essentially of a series of interlocking yarn loops, they generally have good elasticity and greater bulk than woven ones. This tends to be a disadvantage in structural applications, but may be important where insulation properties or flexibility are required.

Variations in technique can greatly alter the elasticity characteristics in each of the two principal directions, and the thickness, or bulking, of the finished fabric.

95.7.3 Weaving

In weaving techniques a series of parallel warp yarns are laid out and weft yarns are then interwoven with them. Hence the paths of individual yarns in a woven fabric are much closer to a straight line than those in knitted materials. This produces a textile with generally lower elasticity and with mechanical properties more directly related to those of the component yarns. The mechanical properties of woven fabrics vary greatly with the test direction relative to that of the warp and weft.

Again, a great number of process variables enable tailoring of the properties of the finished fabric. Also, since the fabric is not created from a single continuous yarn, yarn types can be varied in different directions and at different points, and the fabric is less susceptible to damage from a single yarn failure.

95.7.4 Comparison of techniques

Table 95.7.1 shows the characteristics of fabrics produced by different 3-D weaving or knitting techniques.

Table 95.7-1 - Characteristics of fabrics produced by 3-D weaving and knitting techniques

Technique	Flexibility	Rip-stop	Puncture resistance	Micrometeoroid/ Debris protection
3-D weaving	low	good	good	good
Interlock weaving	good	low	low	low
3-X weaving	low	good	good	good
3-D Knitting	high	low	good	-

95.8 Textile component properties

95.8.1 General

The final properties of a textile component are strongly dependent on the fibre materials and production processes used to create it.

95.8.2 Thread parameters

Starting with the thread components, major parameters, such as filament length and diameter, twist and protective sizing, are carefully adjusted because they can greatly affect the final mechanical properties and processibility.

As an example, the influence of the thread twist on the strength of a thread is shown in Figure 95.8.1.

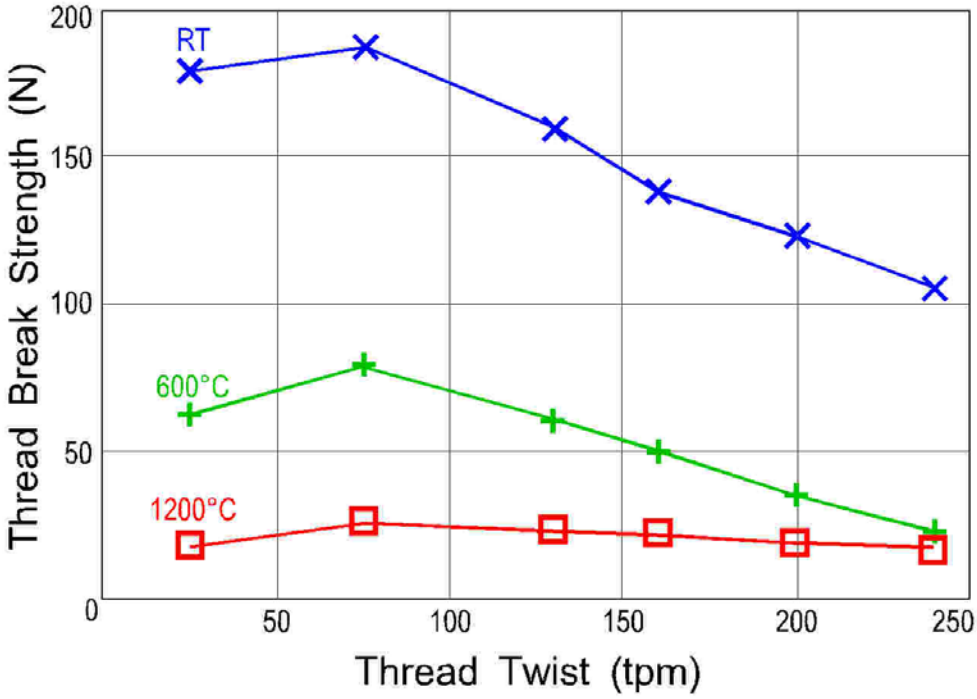

Figure 95.8-1 - Variation of thread strength with twist

The degree of twisting is a sensitive parameter in determining thread strength but requires careful adjustment because the twist which produces optimum strength is not necessarily that leading to optimum processibility.

95.8.3 Effects of temperature on textiles

95.8.3.1 Strength retention

For textile components used at elevated temperatures, the strength behaviour upon annealing is important.

Figure 95.8.2 shows the temperature-to-strength relationship of fabrics manufactured from several threads commonly used in thermal protection systems. This shows that the fabric strength reduces slightly in the temperature range up to 300°C, followed by a steep decrease between 400°C and 550°C.

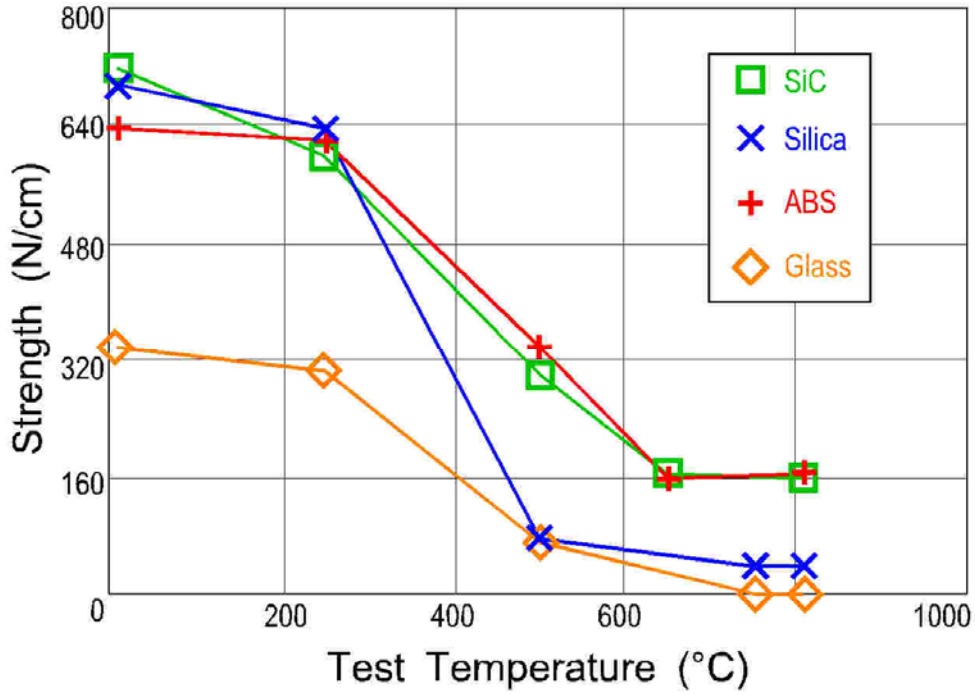

Figure 95.8-2 - Fabric strength as a function of temperature

Figure 95.8.3 shows the high temperature strength retention of threads after sewing. The dramatic strength reduction is attributed to the complete decomposition and removal of the protective sizing at higher temperatures, leading to filament damage and failure during mechanical loading.

The fabric strength in the high temperature regime up to 800°C remains fairly constant showing differences between the amorphous silica and the crystalline alumino-boro-silicate (ABS).

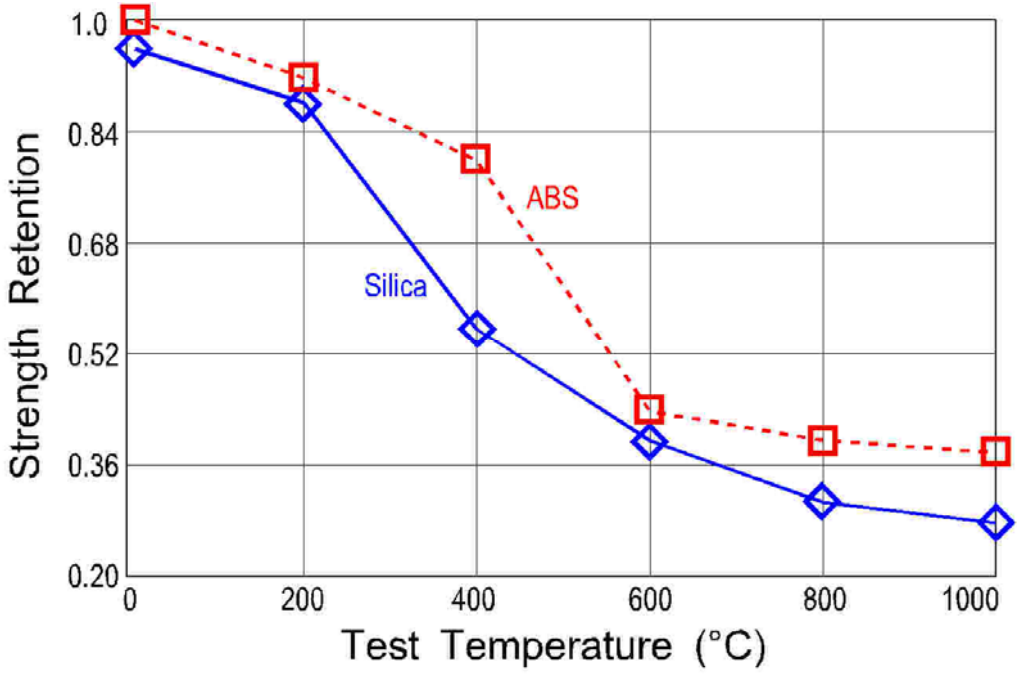

Figure 95.8-3 - Strength retention of threads after sewing

95.8.3.2 Thermal conductivity

Thermal conductivity is one of the key properties of a thermal protection system design and is considered for the entire temperature range.

The thermal conductivities of silica and ABS components are shown in Figure 95.08.4. As expected, the silica material has a lower thermal conductivity than the alumino-boro-silicate ceramic; however, the strength retention of the latter is greater.

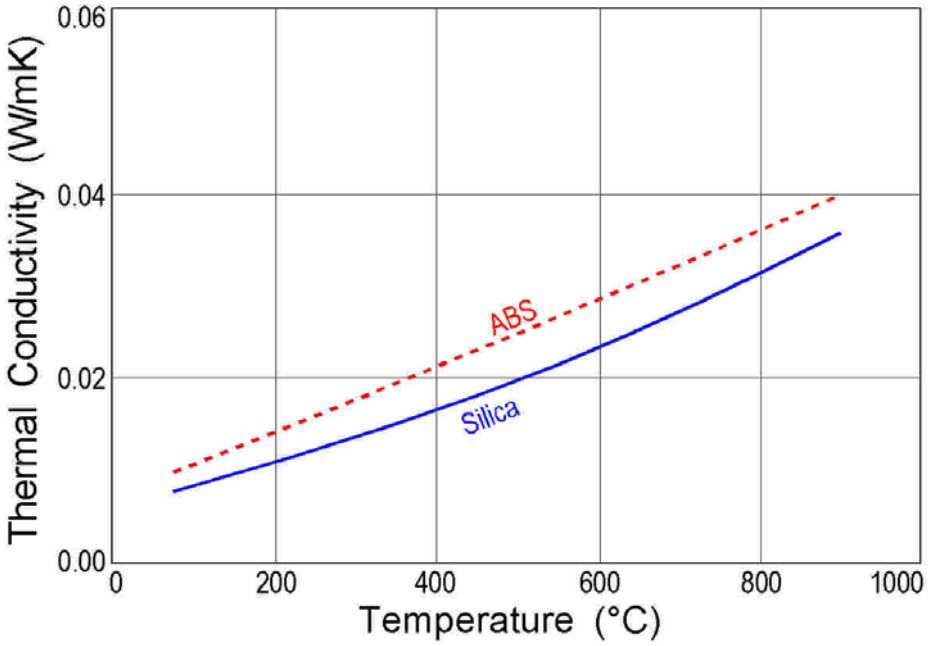

Figure 95.8-4 - Thermal conductivity of Silica and ABS components

95.9 Seam types

Textile seam types consist of a series of stitches or different stitch types, applied to one or more thicknesses of fabric, Ref. [95-10].

Stitched seams are divided into 8 classes according to the number of components within the seam.

Each stitched seam is identified by a numerical designation composed of five digits:

- first digit: class 1 to 8
- second and third digit: numbered 01 to 99 to indicate differences in material configuration
- fourth and fifth digit: numbered 01 to 99 to indicate the location of needle penetrations of the material.

For illustrations of seam types and conventions, see Ref. [95-10].

95.10 Procurement specification

95.10.1 General

A procurement specification defines the procurement requirements for components, and specifies fabrics, i.e. 3-D fabrics woven and knitted. It contains information on:

- yarns for fabric production,
- design configurations required for manufacturing,
- quality assurance activities.

The required properties of a 3-D fabric are stated in DIN 50049-3.1B. A delivered material complies with all of the stated technical and QA requirements.

95.10.2 Applicable standards and documents

All of the applicable documents form part of the specification, and are adhered to. The latest version of any document is always used.

- ASTM-D-2256 - Standard Test method for Tensile Properties of Yarns by Single-Strand-Method,
- other Testing Specifications [See: Chapter 96],
- quality Assurance Specifications,
- documentation Specifications.

95.10.3 Quality assurance

95.10.3.1 Sampling and inspection

- sampling is performed on representative areas of each lot.
- each procured item is supplied with its:
  - identification number.
  - lot number.
  - date of manufacture.
  - certificate regarding yarn size and yarn material.
  - fabric thickness, d ±5 %.
  - fabric mass, m ±1%.
- The manufacturer performs a visual inspection of the fabric; both the front and rear side. The fabric is not released for procurement if any of the defects are detected:
  - voids: >2mm.
  - holes: >2mm.
  - scratches: >5mm.
  - pores: >2mm.
  - loose loops: >3mm.
  - irregular arrangement of warp and fill threads.

The given defect sizes are estimates

95.10.3.2 Inspection test matrix

Table 95.10.1 shows an example of an inspection test matrix for material inspection and acceptance testing.

Table 95.10-1 - Textiles: Example of an inspection test matrix

Inspection stage	Mass	Thickness	Loop tensile strength	Fabric strength	Defects
Material incoming inspection	✓	✓	✓		
Fabric acceptance test	✓	✓		✓	✓
Fabric incoming inspection	✓	✓		✓	✓

95.10.4 Deliverable documents

The documents to be delivered by the manufacturer are:

- certificates comprising all results of required Acceptance Tests.
- certificates of conformance regarding all specified requirements.

95.10.5 Delivery

95.10.5.1 Packing

All materials (yarn, wires, foils) are packed in sealed nylon bags and stored in rigid cartons in order to minimise all potential sources of degradation.

Manufactured fabrics are stored as rolls with a protective wrapping.

95.10.5.2 Marking

All materials and manufactured fabrics are visibly marked stating, at least, the:

- lot number.
- identification number.
- manufacturing date.
- name of manufacturer, supplier.

95.10.6 Storage

The basic storage conditions are:

- temperature, 23°C ± 2°C,
- relative humidity, 60% ± 10%,
- no direct exposure to sunlight,

- storage area to be free of contaminants:
  - dust.
  - chemical vapours.
  - oil, grease and fluids.

95.11 References

95.11.1 General

[95-1] U. Rieck & D. Müller-Weisner: ERNO Raumfahrttechnik GmbH
'Technical Textiles in Space Applications'
Proc. International Symposium on Advanced Materials for Lightweight Structures, ESA-ESTEC, Noordwijk, NL, March 1994.
ESA WPP-070, p589-595

[95-2] A. Peachey: Irvin GB Ltd.
'Planetary Entry Study Theme 3 - Parachute Material Selection'
Irvin Tech. Note RD.413
Dornier Contract No. KAA-DOR 12020 AO 3516

[95-3] 'Textiles: Structures and Processes'
In 'Encyclopaedia of Material Science and Engineering'
Pergamon Press, Oxford. 1986

[95-4] DIN 60 001
Textile Faserstoffe (Textile Fabrics)

[95-5] ISO 8159
Textiles: Morphology of Fibres and Yarns

[95-6] ISO 1139 (or DIN 60 900)
Textiles: Designation of Yarns

[95-7] ISO 1144
Textiles: Universal System for Designating Linear Density

[95-8] DIN 61 210
Vliese, Verfestigte Vliese und Vliesverbundstoffe
(Fleeces, Strengthened Fleeces and Fleece Composites)

[95-9] DIN 61 100 & DIN 61 101
Fabrics and Seam Types (Gewebe und Gewebe-Bindungen)

[95-10] ISO 4916
Textiles: Seam Types Classification

96 Textile testing

96.1 Introduction

96.1.1 Textile industry testing

96.1.1.1 General

The range of tests applied to textiles can be broadly grouped as:

- Fibre Production Tests: quality control tests carried out by the staple fibre manufacturer.
- Fibre Property and Characterisation Tests: carried out by the manufacturer to meet the user requirements.
- Textile Production Tests: carried out by the weaver.
- Textile Property and Characterisation Tests: carried out by the weaver to meet the end-user requirements.
- Incoming and Acceptance Tests: conducted by the end-user to confirm the properties quoted by the fibre manufacturer or weaver.
- Mechanical and Physical Property Testing: to determine:
  - design values (with appropriate confidence levels) for fibres and textile forms. The results aid the specification of fibres and textile products.
  - the characteristics of finished textile products.

96.1.1.2 Test standards and procedures

Numerous sampling, testing procedures and methods have been formulated to ensure that the quality of manufacturers' products is acceptable to the user, Ref. [96-19].

These fall into the three broad categories of:

- internationally accepted standards, e.g. ASTM, ISO.
- national standards, e.g. DIN, NF, BS.
- recommended and approved by the various textile industry organisations, e.g. International Bureau for Standardisation of Man-made Fibres (BISFA).

Many of the methods are appropriate only to natural fibres, Ref. [96-19]. The quality of man-made fibres largely depends on the monitoring and control applied to the manufacturing processes and equipment used, whereas natural fibres are affected by a host of naturally occurring, uncontrollable, changes, e.g. climate.

Given that adequate process control is applied, the basic properties of a man-made fibre can be more or less guaranteed for a process lot.

Errors in the formulation of the starting materials, e.g. monomers, or undetected, machine-induced, faults can produce unacceptable fibre. These can produce variations in fibre

characteristics at different stages of the production process, i.e. direct from the converter, after combing.

96.1.1.3 Tests on staple fibre

The aim of all of these tests is to monitor the quality of the man-made fibre produced, so that it remains within the specification.

Details supplied by manufacturers to users, with respect to the properties of the staple fibre, typically include:

- linear density,
- fibre lengths,
- cross-sectional shape,
- breaking force,
- force-extension curves,
- tenacity,
- extension to break,
- material density,
- viscoelastic and recovery properties,
- crimp,
- lustre,
- electrical resistance,
- dielectric constant,
- specific heat, and
- softening temperature.

[See: 95.2 for terminology specific to textiles]

96.1.1.4 Tests on yarns and textile products

Fibre users aim to ensure that the incoming product (yarns or fabrics) is acceptable.

After further processing, other tests are used to prove that the finished textile product conform to the relevant specification. These tests are normally more application dependent and, although often based on an appropriate recognised standard, may have modified parameters, e.g. loading rate, test temperature.

In general, textiles and yarns present special problems in terms of their mechanical testing. Great care should be taken to achieve representative loading of samples, avoiding edge effects and failures associated with gripping mechanisms.

The properties of textile materials are often strongly influenced by their environment. ISO 139-1973 E states the 'standard atmosphere' conditions for the testing of textiles, Ref. [96-1]:

- test temperature: 20° ± 2°C (RT).
- relative humidity: 65% ± 2%.

This is normally applied to testing of staple fibre as well as yarns and textiles.

Some of the standard test methods used for measuring the properties of textiles and textile components, e.g. fibres and yarns, are described, [See: 96].

The tests described are primarily those used for testing of textiles for space suit development, [See: 97.2 - European EVA space suit], but are in broad agreement with procedures used in parachute development, [See: 97.4 - Planetary entry parachute].

Other textile space applications require additional or different tests, e.g. thermal properties of flexible insulation, tribocharging of parachutes. Such application-specific tests are not currently described.

96.2 Loop tensile test

96.2.1 Test objective

The test identifies properties of single yarns and yarn combinations.

[See: 95.2 for terminology specific to textiles]

It simulates the tensile interaction of linked fibres and therefore gives an indication of the likely success of the weaving or knitting process and the achievable fabric properties, Ref. [96-2].

[See also: DIN 53 834, 53 842 and 53 843 for knots]

96.2.2 Test set up

The procedure is largely in accordance with ASTM-D-2256, Ref. [96-3], (DIN 53 857, Ref. [96-4]), but with a lower crosshead speed.

The crosshead speed of 300 mm/min, as stated in ASTM-D-2256, is regarded as too high for yarn testing.

Consequently, the recommended parameters are:

- crosshead speed: 50 mm/min,
- gauge length: 300 ± 3 mm.

96.2.3 Specimen size

Five loop tensile test specimens, i.e. 10 pieces of yarn, are prepared from the test bobbin. The connecting point of the yarns is located in the middle of the gauge length.

96.2.4 Test results

The test report items include:

- breaking tenacity (mN/dtex).
- strain at break (%).

96.2.5 Success criteria

A specific success criteria is not defined owing to the preliminary nature of the loop tensile test.

96.3 Textile glass yarns: Tensile test

96.3.1 Test objective

Textile glass yarns, including single, folded, cabled, strands, rovings, with a diameter less than 2 mm or a linear density lower than 2000 tex are tested as per ISO 3341-1984, Ref. [96-5].

[See: 95.2 for terminology specific to textiles]

96.3.2 Test set up

The tensile testing machine has a pair of suitable clamps to grip the specimen, without causing slippage and without damaging the specimens. The break point should not occur within 10 mm of the jaws.

96.3.3 Specimen size

Ten tensile test specimens are prepared for the test. Each test specimen has a length of at least 600 mm.

96.3.4 Test results

The test report includes the:

- detailed description of the yarn and its production condition.
- breaking force (N).
- linear density of the bulk sample (tex).

96.4 Mass properties and thickness

96.4.1 Test objective

The tests identify the general fabric characteristics, such as mass per area and thickness, Ref. [96-6].

[See: 95.2 for terminology specific to textiles]

96.4.2 Test set up

The basic set up is that according to:

- ISO 6348 and ISO 2286 to determine coating characteristics, Ref. [96-7].

- ISO 3374 for textile glass mats, Ref. [96-8].

Depending on the test to be conducted, additional equipment can be required as part of the set up, e.g.:

- general test set-up:
  - test temperature: RT.
  - relative Humidity: 65%.
- moisture reduction set-up:
  - for a moisture content >0.2% (ISO 3344), a drying oven and desiccator (glass mats).
- mass determination test set-up:
  - weighing device: accurate to full scale deflection = 0.10%.
  - balance: accurate to 0.005g.
  - number of measurements: 3 per specimen at different locations.
- thickness determination test set-up:
  - presser foot: 25 mm diameter.
  - pressure: 2 kPa.

In each case, 3 measurements are made at different locations.

96.4.3 Specimen size

According to ISO 2286, one specimen with a = 100 cm^2 for mass and thickness determination, Ref. [96-7].

For glass mats a square of 316 mm x 316 mm is recommended, Ref. [96-8].

96.4.4 Test report

The test report includes:

- weight per area ratio of the tested specimen.
- fabric thickness of the tested specimen.

96.5 Textile glass products: Moisture content determination

96.5.1 Test objective

The purpose of the test is to determine the moisture content of textile glass products, such as continuous filament yarns, staple fibre yarns, rovings, chopped strands, mats, glass fabrics and other textile glass reinforcements.

[See: 95.2 for terminology specific to textiles]

96.5.2 Test set up

In accordance with ISO 3344-1977, Ref. [96-10], a ventilated drying oven is used:

- with an air exchange rate of 20 to 50 times per hour,
- capable of maintaining a temperature of 105°C ±2°C, or 80°C ±2°C, or,
- a desiccator containing a suitable drying agent.

A balance with a weighing accuracy of 1 mg.

96.5.3 Specimen size

- yarn, chopped strands or milled fibre with a length that corresponds to 5g.
- glass fabrics specimen sizes: 150 mm x 80 mm.
- glass mats: 316 mm square of at least 5g.

At least five specimens are tested.

96.5.4 Test report

The test report includes the:

- moisture content of each specimen.
- complete reference and dimensions of the tested specimen.
- standard temperature of the weighing room.
- temperature of drying.

96.6 Determination of fibre diameter

96.6.1 General

In DIN 53 811, the measurement of fibre diameters from longitudinal view by microscope projection is a recommended practice for quality assurance.

The average fibre diameter and scatter, as well as the smoothness of the fibres are examined at all production stages.

[See: 95.2 for terminology specific to textiles]

96.6.2 Test set up

- Embedding agents with refractive indexes between 1.53 and 1.43.
- Projection microscope: 500 times magnification.

96.6.3 Specimen size

- single cut and embedded fibres of 0.5 to 1 mm length.
- multiple measurements are recommended to exclude and minimise measurement deviations.

96.6.4 Test report

The test report includes the:

- complete description of the fibre type and its condition.
- average fibre diameter (95% probability and 99% confidence level).
- coefficient of variation.

96.7 Tensile strength and elongation

96.7.1 Test objective

The tensile strength and elongation test identifies the main mechanical properties at different stages of manufacture. It also allows evaluation of any change in mechanical properties caused by coatings or treatments.

[See: 95.2 for terminology specific to textiles]

96.7.2 Test set up

The test set up is performed in accordance with the ISO 142, Ref. [96-11], rather than that within DIN 53 815, i.e.:

- crosshead speed: 10 mm/min.
- test temperature: RT and at elevated temperature.
- gauge length:
  - 100 mm (RT).
  - 450 mm (elevated temperature).

The confirmation of the ISO test set-up (compared with that of DIN 53 815) is provided from the extensive experience of testing fabric by DASA/ERNO.

96.7.3 Specimen size

Five specimens per test temperature and direction (weft and warp) are prepared.

The ends of the specimens are fixed with a polymer.

- specimen dimensions:
  - 150 x 20 mm^2 rectangular specimens (RT).
  - 500 x 30 mm^2 rectangular specimens (elevated temperature).

96.7.4 Test results

The tests report includes:

- breaking strength at RT and elevated temperature in weft and warp direction (N/cm).
- elongation and strain at break (%).
- elongation and strain at 400 N/cm (%), if available.

96.7.5 Success criteria

- the minimum breaking strength in weft and warp direction is >600 N/cm.
- strain at 400 N/cm is <5%.
- no severe degradation of the main mechanical properties at the elevated test temperature.
- no severe degradation occurs in the case of any pretreatment, e.g. by UV-light or J-Fluids. Acceptable values are defined during the test programme.

96.8 Bursting strength and bursting distension: Diaphragm method

96.8.1 Test objective

A pure tensile test can be unsuitable for certain fabrics, e.g. knitted materials.

The measurement of bursting strength provides an alternative criterion of strength, Ref. [96-12]. In this test, the specimen fails across the direction with the least extensibility. Owing to biaxial stressing, the tensile strength cannot directly be calculated from tensile fibre strength.

[See: 95.2 for terminology specific to textiles]

96.8.2 Test set up

The test set up is performed in accordance with the ISO 2960, Ref. [96-12], using a bursting facility of about 140 mm diameter, covered by a flat diaphragm of rubber or similar material.

The operating fluid can be a liquid or a gas.

96.8.3 Specimen size

The diameters of test specimens are 30 mm or 113 mm (10000 mm^2).

The smaller specimens tend to burst at higher stress levels. From this a correlation of $p \times D\alpha$ was found to be fairly constant, i.e. a factor of about 5 was found between the test sizes, when using α = 1.1 to 1.3.

96.8.4 Test results

The test report includes the:

- breaking pressure at RT and elevated temperature in weft and warp directions (kN/m^2).

- diameter(s) of test pieces.
- correlation of $p \times D\alpha$.
- weakest bursting direction (warp or weft).
- test machine parameters.

96.9 Tensile breaking force of textile glass mats

96.9.1 Test objective

The ISO 3342 test method was established for chopped-strand mat but it is equally applicable to certain types of continuous filament mat intended for pultrusion, Ref. [96-13].

The principle is the measurement of a pre-conditioned test-specimen in a tensile test continued to rupture.

[See: 95.2 for terminology specific to textiles]

96.9.2 Test set up

The test set up is performed in accordance with ISO 3342, Ref. [96-13], using a tensile testing machine. A pair of suitable clamps, e.g. 160mm wide and a minimum depth of 25mm, are used to grip the specimen.

96.9.3 Specimen size

At least 5 test specimens are tested. Each specimen is 150 mm wide and 316 mm long.

96.9.4 Test results

The tests report includes the:

- details of the mat tested.
- environmental conditions.
- type of machine used.
- breaking force (longitudinal and transverse direction).
- standard deviation.

96.10 Abrasion resistance

96.10.1 Test objective

The test identifies the textile's behaviour when in contact with an abrasive material, such as grinding paper.

The abrasive loads can be applied by one of three different methods:

- point-like abrasive attack.

- line-like abrasive attack.
- area-like abrasive attack.

The point-like abrasion is the recommended method, using a rotating wheel. The abrasion resistance test simulates a fabric lifetime of 15 years, in steps of 5 years.

[See: 95.2 for terminology specific to textiles]

96.10.2 Test set up

The test is performed according to DIN 53863 T2, Ref. [96-14], i.e.:

- maximum time interval between manufacture and test: 1 month.
- test temperature: RT.
- total number of abrasive cycles (required): 30000 (15 years).
- number of test specimens: 5.
- the test specimens are clean and free from dust, loose particles and moisture.
- the number of abrasive cycles is specified by material pre-testing.

96.10.3 Specimen size

The specimen size is in accordance to DIN 53863 T2, Ref. [96-14]:

- Two test pieces of approximately 114 mm in diameter with a 6mm hole in the centre of the test piece.

96.10.4 Test results

The test report includes the:

- number of abrasive cycles applied to each fabric type.
- visual inspection report for the tested fabrics, including a photocopy of each step of the test (every 1000 cycles).
- weight loss of the test specimens (to 1 mg accuracy).

96.10.5 Success criteria

To pass the abrasion resistance test, the fabric exhibits no significant mass loss after a simulated lifetime of 15 years.

96.11 Wear, wear resistance and mechanical flexing

96.11.1 Test objective

The wear, wear resistance and mechanical flexing test simulates complex mechanical loading by crumpling and rotor-flexing. It is used to simulate a wide spectrum of wear and mechanical conditions. For example, the test simulates the behaviour of a spacesuit elbow. A 15 year life, in

steps of 5 years, was recommended to simulate the life of the outer fabric for the European space suit, [See also: 97.2].

[See: 95.2 for terminology specific to textiles]

96.11.2 Test set up

The test is set up according to TGL 50555, Ref. [96-15], i.e.:

- crumpling length: to be verified at the beginning of the test.
- torsion angle: ±40° (total: 80°).
- test speed: 100 wear cycles per minute.
- wear cycles: 30000 cycles (15 years).
- mechanical cycles: 30000 cycles (6.7 years).

96.11.3 Specimen size

- the specimen dimensions are:
  - length: 200 mm,
  - width: 100 mm,
  - number of specimens: 2 per version.
- the specimen is clamped in the test equipment in such a way that it forms a cylindrical shape.
- this tube is then crumpled in compression. Air permeability measurements are made before and after the test.

96.11.4 Test report

The test report includes the:

- torsion angle,
- crumpling length,
- test speed,
- wear and mechanical cycles,
- pre- and post-test permeability measurement,
- photograph, at x200 magnification, of the specimen before and after the test.

96.11.5 Success criteria

The test is passed successfully if the final permeability measurement shows no degradation.

96.12 Tear and tear resistance

96.12.1 Test objective

Tear resistance is the ability of the fabric to withstand a cut under nominal loads.

The test determines the coated-fabric tear resistance by using the A2 Method of ISO 4674, Ref. [96-18].

[See: 95.2 for terminology specific to textiles]

96.12.2 Test set up

The test is performed in accordance with ISO 4674, Ref. [96-18]:

- general set up:
  - Test temperature: RT.
  - Relative humidity: 65%.
- method A2 test set up:
  - crosshead speed: 2 mm/min at a constant tear rate.
  - the test piece has a longitudinal slit of about 80 mm in the middle of its width. One tongue is placed in each jaw, kept parallel with the tear direction.

96.12.3 Specimen size

The test piece is a rectangular strip (225 mm x 75 mm ±0.5 mm).

5 specimens are tested.

96.12.4 Test report

The test report gives the measured strength values (N) of the 5 tests.

96.12.5 Success criteria

The slit in the fabric should not propagate under a load of 600 N.

96.13 Tear resistance of woven fabrics: Falling pendulum method

96.13.1 Test objective

The ISO 9290 (1990) test gives the force required to propagate a tear, through a specified distance, from a specified slit in the fabric, under specified loading conditions, Ref. [96-17].

[See: 95.2 for terminology specific to textiles]

96.13.2 Test set up

The test frame is mounted on a rigid base, carrying the low friction pendulum and pointer assembly. A pair of jaws, 16 mm deep x 37 mm wide, 2.8 mm apart clamp the sample perpendicular to the plane of the pendulum oscillation. The adjustable pointer stop records the highest point reached by the swing of pendulum.

96.13.3 Specimen size

The specimen dimensions conform to ISO 9290 (approximately 100 mm x 75 mm), containing a slit of 20 mm. A minimum of 5 specimens are tested in both the weft and warp directions.

96.13.4 Test report

This gives the average force (N) to tear the test specimens into two parts.

96.14 Cutting resistance

96.14.1 Test objective

This test shows the capability of fabrics to withstand a defined load across a sharp edge.

[See: 95.2 for terminology specific to textiles]

96.14.2 Test set up

- diameter of knife edge: 0.6 mm.
- mass applied to the knife: 100 kg.
- velocity: 1.5 m/s.

96.14.3 Specimen size

Defined at the beginning of the test.

96.14.4 Test report

The test report includes:

- a photocopy of each specimen, showing the cutting length.
- the mass applied to the fabric.
- velocity and sample pressure.

96.14.5 Success criteria

The fabric should resist cutting.

96.15 Puncture resistance

96.15.1 Test objective

The objective of the puncture resistance test is to determine the ability of a fabric to withstand a protrusion of a certain diameter. This measures the resistance to puncture by a sharp edge or needle.

[See: 95.2 for terminology specific to textiles]

96.15.2 Test set-up

In accordance to ISO 3303, Method A, Ref. [96-18]:

- test temperature: RT.
- crosshead speed: 300 mm/min.
- protrusion diameter: 3 mm.

96.15.3 Specimen size

The test piece has an exposed diameter of 45 mm, with a external diameter of 55 mm to allow for clamping. One specimen is tested per fabric.

96.15.4 Test results

The test report includes:

- a photograph taken at x40 magnification.
- the force needed to penetrate the fabric.

96.15.5 Success criteria

The fabric resists penetration at the given load.

96.16 Quality control tests

96.16.1 Supplier tests

Tests are agreed upon between the customer and supplier, [See: 96.17]. Test certificates are supplied with the textiles.

[See: 95.2 for terminology specific to textiles]

The test methods used are application dependent, therefore additional tests can be selected.

96.16.2 Incoming tests

Normally, incoming inspections of fibre and yarns, as well as supplier certificates, should be done. Depending on the production quantity, lot-to-lot variations are also documented.

[See also: 95.10 - Procurement specification]

The customer can also request intermediate and final quality tests.

96.17 Summary of test standards

96.17.1 General

Test methods applied to textiles are listed by their controlling bodies.

[See: 95.2 for terminology specific to textiles]

96.17.2 ASTM

- ASTM-D-2256: Standard Test Method for Tensile Properties of Yarns by Single-strand Method.

96.17.3 ISO

- ISO 1139 (or DIN 60 900): Textiles - Designation of Yarns.
- ISO 2286: Rubber or plastic-coated fabrics: Determination of roll characteristics.
- ISO 1421: Fabrics coated with rubber or plastic: Determination of breaking strength & elongation at break.
- ISO 4674 Method A2: Fabrics coated with rubber or plastics: Determination of tear resistance.
- ISO 3303: Rubber or Plastic-coated Fabrics: Bursting Strength.
- ISO 4916: Textiles - Seam Types - Classification & Terminology.
- ISO 8159: Textiles - Morphology of fibres and yarns.
- ISO 6348: Textiles - Determination of mass.
- ISO 1144: Textiles - Universal system for designating linear density.
- ISO 139: Textiles - Standard atmospheres for conditioning & testing.
- ISO 1130-1975E: Textile fibres: Some methods of sampling for testing.
- ISO 2960: Textiles: Determination of bursting strength and bursting distension - Diaphragm method.
- ISO 3341-1984: Textile Glass Yarns: Determination of Breaking Force and Breaking Elongation.
- ISO 3342-1987: Textile Glass Mats: Tensile Breaking Force.
- ISO 3344-1977: Textile Glass Products: Moisture Content.

- ISO 3374-1990: Glass Mats: Determination of Mass per Unit Area.
- ISO 9290-1990: Textiles - Woven Fabrics - Determination of Tear Resistance by the Falling Pendulum Method.

96.17.4 DIN

- DIN 53 863 T2: Testing of Textiles - Abrasion Test Methods for Textile Fabrics - Rotary Abrasion Test (Scheuerprüfungen von textilen Flächengebilden).
- DIN 61 100 (and DIN 61 101): Fabrics & Seam Types (Gewebe and Gewebe-Bindungen).
- DIN 60 001: Textile Faserstoffe (Textile Fabrics).
- DIN 61 210: Vliese, verfestigte Vliese und Vliesverbundstoffe (Fleeces, strengthened fleeces and fleece composites).
- DIN 53 857: Einfacher Streifen-Zugversuch an textilen Flächengebilden (Strip Tensile Test on Fabrics).

96.17.5 Others

- TGL 50555: Textile Testing: Determination of the Permanent Wear & Wear Resistance of the Coating of Textile Sheets.
- BS F.100: Procedures for inspection & testing of textiles for aerospace purposes (test methods, acceptance limits, etc.)

NOTE Used in Huygens parachute textile testing, [See: 97.4].

96.18 References

96.18.1 General

[96-1] ISO 139
Textiles - Standard atmospheres for conditioning and testing

[96-2] ISO 1130-1975E
Textile Fibres - Some Methods of Sampling for Testing

[96-3] ASTM-D-2256
Standard Test Method for Tensile Properties of yarns by Single-Strand Method

[96-4] DIN 53 857
Einfacher Streifen-Zugversuch an textilen Flächengebilden
(Strip Tensile Test on Fabrics)

[96-5] ISO 3341-1984
Textile glass - Yarns - Determination of breaking force and breaking elongation

[96-6] ISO 6348
Textiles - Determination of mass

[96-7] ISO 2286
Rubber- or plastic-coated fabrics - Determination of roll characteristics

[96-8] ISO 3374-1990
Textile Glass Mats - Determination of mass per unit area

[96-9] ISO 9862 - 1990
Geotextiles - Sampling and Preparation of Test Specimens

[96-10] ISO 3344-1977
Textile Glass Products - Determination of Moisture Content

[96-11] ISO 1421
Fabrics coated with rubber or plastic - Determination of breaking strength and elongation at break

[96-12] ISO 2960
Textiles - Determination of bursting strength and bursting distension - Diaphragm method

[96-13] ISO 3342-1987
Textile Glass - Mats - Determination of Tensile Breaking Force

[96-14] DIN 53863 T2
Testing of Textiles - Abrasion Test Methods for textile Fabrics - Rotary Abrasion Test
(Scheuerprüfungen von textilen Flächengebilden)

[96-15] TGL 50555
Textile Testing - Determination of the permanent Wear and Wear Resistance of the Coating of Textile Sheets

[96-16] ISO 4674-Method A2
Fabrics coated with rubber or plastics - Determination of tear resistance

[96-17] ISO 9290 - 1990
Textiles - Woven Fabrics - Determination of Tear Resistance by the Falling Pendulum Method

[96-18] ISO 3303
Rubber - or Plastics - coated Fabrics - Determination of bursting Strength

[96-19] S.L. Anderson: The Textile Institute, UK
'Textile Fibres: Testing and Quality Control'
Manual of Textile Technology: Quality Control & Assessment Series.
ISBN 0 900739 50 9

97 Textile applications

97.1 Introduction

This chapter illustrates some of the uses for textiles in space applications. These case studies include a brief description of the requirements, based on the application and operational conditions, and show how these affect the material selection process. The examples described are:

- european space suit development: based on work conducted initially under the Hermes programme and expanded upon in the current EVA 2000 joint European-Russian project, [See: 97.2]
- flexible thermal insulation: developed as part of the Hermes programme, [See: 97.3].
- parachutes for space probes: Study of materials and design aspects for extra-terrestrial space probes, e.g. Huygens planned mission to land on Titan in 2004., [See: 97.4]

97.2 European EVA space suit

97.2.1 General

The European EVA space suit system provides environmental protection, mobility, life support and communications between astronauts working in Low Earth Orbit (LEO) and the attendant space vehicle, e.g. for external servicing of the Columbus Free Flyer. The current EVA 2000 project is a development of earlier work conducted as part of the Hermes programme. It is a joint study between European and Russian space organisations, Ref. [96-4]. The suit design requirements include:

- duration: work outside the air-lock, and autonomous capability.
- operating environment: external conditions and those controlled within the suit.
- dimensions: mass and size restrictions.
- operational life: in years or number of excursions.

97.2.2 EVA suit system concept

97.2.2.1 General

The autonomous EVA suit concept consists of three major subsystems. These are the:

- Suit enclosure subsystem (SES): which provides:
  - protection against the environment,
  - retains oxygen pressure for breathing and ventilation,
  - adequate dexterity, mobility and visibility for working.
- Backpack subsystem (BPS): which provides life support functions and warning of hazardous situations.

- Chest pack subsystem (CPS): which provides communications between the astronaut and the space vehicle, data handling and monitoring.

In addition there is a support and interface subsystem (SIS) located in the space vehicle which interfaces with the suit operator, and facilities for storage of the suit, and all ancillary equipment required for EVA, when not in use.

Only the Suit Enclosure Subsystem is described in this chapter. For further information on this, and other space suit subsystems, see Ref. [96-2], [96-3].

97.2.2.2 Suit enclosure subsystem (SES)

The basic functional requirement is to protect the suit wearer against the environment whilst providing proper mobility, dexterity and visibility. The constituent parts of the suit enclosure are shown in Figure 97.2.1, Ref. [96-2].

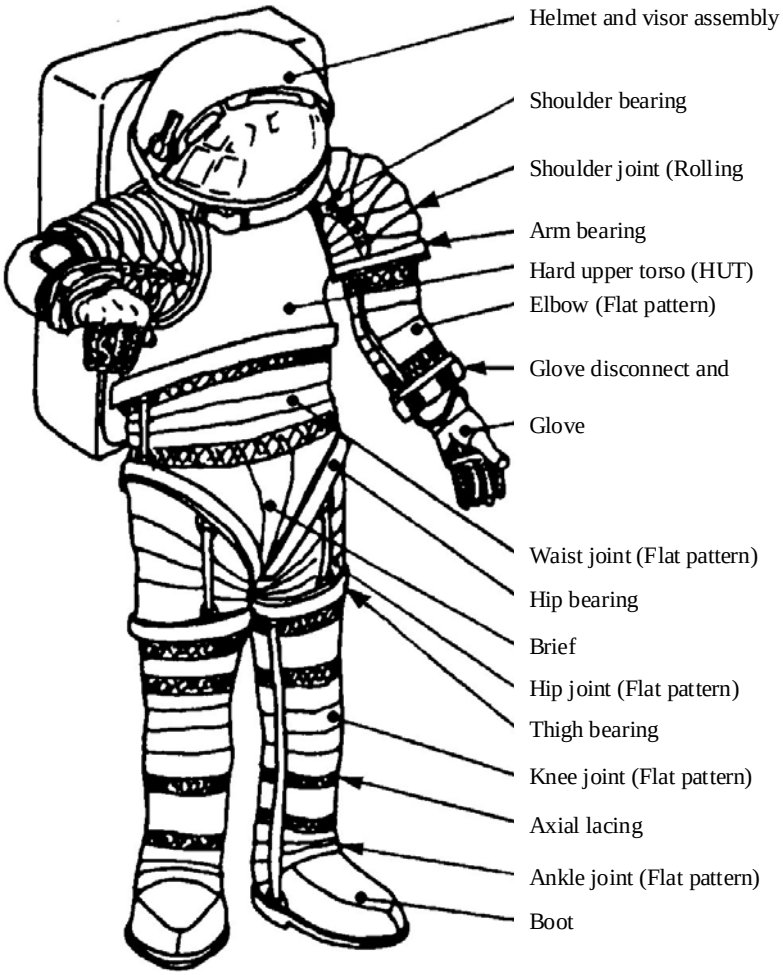

Figure 97.2-1 - European EVA space suit: Suit enclosure subsystem concept

The various parts of the suit are connected by a number of different types of joints, either soft or articulated, depending on the mobility and degrees of freedom necessary. In addition to the

shoulder joint, the gloves are considered of fundamental importance to suit design as these directly affect the dexterity and tactile performance. Three gloves are worn, one on top of another:

- First (inner) Glove: for gas retention.
- Second Glove: A restraint for pressure retention consisting of a fabric restraint and axial restraint provided by stitching for optimised load transfer, e.g. at palm or wrist.
- Third (outer) Glove: Thermal protection consisting of multilayer insulation (MLI) constructed from layers of felt and rubber.

Passive thermal protection of the astronaut is provided by the suit acting as classical multilayer insulation. Material selection includes allowances for flexibility (bending of wearer) and other factors applicable to astronaut activities.

97.2.3 Textile types

97.2.3.1 General

For space suit applications, fabrics are created using combinations of Kevlar, Nomex and PTFE fibres. The aramid materials exhibit good flexibility and strength whilst the PTFE threads, placed at the fabric surface, provide protection against UV radiation and abrasion, and assure constant thermo-optical properties.

97.2.3.2 Textile properties

A summary of the basic fabric properties is given in Table 97.2.1. This shows that the property profile depends on the specific production process used. Woven fabrics are lightweight and very strong while the knitted fabric versions have good flexibility and superior impact behaviour, [See also: 95.6].

97.2.4 Space suit outer layer fabric requirements

97.2.4.1 General

Of major importance is the protection of astronauts in EVA against:

- mechanical hazards,
- micrometeorites and debris, and
- solar radiation.

Table 97.2-1 - Textile materials: Comparison between basic properties

Fabric	Thickness [mm]	Areal mass [g/m²]	Tensile [N/cm]		Puncture resistance [N]	Abrasion [g]	Tear resistance [N]	Out-gassing TML [%]	Flammability	Thermal cycle α/ε
			RT	+130°C						
Variant 1	0.74	498	W 1500 F 1342	340 477	112.5	0.14	Test not possible	1.17	-	0.568
Variant 2 Coated	0.70	556	W 1000 F 2610	850 2096	441	0.143	544/408	1.78	+	0.409
Variant 3 Coated	1.27	1104	W 503 F 956	401 663	962	0.377	576	1.97	+	0.455
Variant 4 Coated	1.61	1718	W 465 F 1248	445 896	1027	0.278	688	2.04	+	
Key: (1) - ISO 4674: Ref. [96-1]										

97.2.4.2 Outer fabric for European space suit (OFFES)

The outermost fabric layer in the external protection is the most important element. It has to serve as the mechanical protection of the pressure retention bladder and, due to its thermo-optical properties, to balance the thermal control of the space suit. The outermost layer protects against:

- atomic oxygen,
- high energy radiation (UV and particle),
- frequent thermal cycling, and
- micrometeoroid and debris (M/D) impact.

The new weaving and knitting technologies permit the fabrication of advanced 3-D fabrics, with interconnected layers and local variation of properties, in a single manufacturing step. These 3-D fabrics have generally good impact properties, so interconnected fabric layers are used to provide micrometeoroid and debris protection. Lightweight woven, and especially knitted, aramid yarn systems have potential in many M/D protection applications for structures used in orbit.

In addition, specially designed outer layers resist mechanical, chemical and tribological (wear) attack, resulting from:

- UV radiation,
- multiple bending,
- abrasion, and
- tear and puncture loads.

97.2.5 Textile specifications

97.2.5.1 General

The yarn and fabric materials selected for the OFFES application are described.

97.2.5.2 Yarns

Examples of deliverable yarns are:

- PTFE yarn:
  - Supplier: Lenzing AG, Austria
  - PTFE white filament yarn
  - Titer: 420 dtex
  - Twist: 230 tpm
  - Pre-treatment: none
- Nomex "Delta A" yarn:
  - Supplier: DuPont de Nemours, Germany
  - Nomex "Delta A" spun yarn
  - Titer: 440 dtex
  - Twist: none
  - Pre-treatment: none
- Kevlar 29 yarn. Delivery example:
  - Supplier: DuPont de Nemours, Germany
  - Kevlar 29 multifilament yarn
  - Titer: 440 dtex
  - Twist: none
  - Pre-treatment: none

97.2.5.3 Woven 3-D fabrics

Examples of deliverable fabrics and assembly specifications are:

- 3-D fabric with PTFE surface protection layer (Typical design)
  - Outer layer: PTFE yarns, 420 dtex, white filament yarn, Twist: 230 t/m, Pre-treatment: none, Supplier: Lenzing AG, Austria.
  - Middle layer, 80% Kevlar 29 + 20% Nomex 'Delta A':
    - Kevlar 29 multifilament yarn, 220 dtex, Twist: none; Pre-treatment: none, Supplier: DuPont, Switzerland,
    - Nomex "Delta A" spun yarn, 440 dtex, Twist: none; Pre-treatment: none, Supplier: DuPont, Switzerland.
  - Inner layer: Material: Not Stated; Twist: none; Pre-treatment: none. Supplier: DuPont.

97.2.5.4 Knitted 3-D fabric

The assembly specification for the deliverable fabric was:

- 3-D knitted fabric with FEP (fluorinated ethylene propylene) surface protection system (Typical design):
  - FEP foil, white coloured with 1% TiO^2 outer foil, Thickness: 25 mm Supplier: DuPont (CH)

— Transparent FEP foil, Thickness: 25 mm, inner foil,

— Supplier: DuPont (CH)

— Kevlar 29, 220 dtex filament yarn

— Kevlar 29, 220 dtex filament yarn Nomex "Delta A" spun yarn 440 dtex

— Kevlar 29, 220 dtex filament yarn

97.2.6 Comparison between US and Russian EVA suits

97.2.6.1 General

In 1995, some Space Shuttle missions involve the approach and docking with MIR. This is a forerunner to the intended construction of an international space station (ISS) starting in 1998. As part of the programme, comparison studies have been conducted between the EVA suits used by astronauts and cosmonauts. This is because it is possible that suits, tools and equipment will be shared during the construction phases. The common design requirements for the US and ex-USSR included the need for life support functions and astronaut protection from the environment, i.e. the basic requirements of all EVA suit design, whereas some specifics of the suit design were different.

The functional requirements are influenced by the types of EVA activities needed, number of crew, mission duration, features of spacecraft and payload design, Ref. [96-10].

97.2.6.2 Suit constructions

Table 97.2.2 describes aspects of the construction materials for each type of EVA suit, Ref. [96-10].

Table 97.2-2 - US and Russian EVA suits: Comparison of materials

NASA Space Shuttle Extra Vehicular Mobility Unit †	ORLAN-DMA Space Suit ‡
Nominal maximum mission duration (hours)	
7	6
Suit Assembly	
• Pressure bladder: Urethane-coated nylon • Orthofabric & aluminised Mylar thermal/meteoroid garment • Fibreglass hard upper torso • Ball-bearing joints • Liquid cooling/ventilation undergarment • Polycarbonate helmet & visor • Modular components • Donning: 15 mins (with assistance)	• Pressure bladder: Semi-rigid with latex rubber (dual in arms & legs) • Dual layer helmet • Dual seal bearings (shoulder & wrist) • Liquid cooling undergarment • Rear-entry suit design • On-orbit limb sizing • Self-donning, rapid
Weight (kg)	
~117	~105
Design life	
Up to 30 years, with maintenance	4 years/10 missions
Key †: United Technologies Hamilton Standard (USA) ‡: Zvede Research Development & Production Enterprise (Russia)	

97.3 Thermal insulation

97.3.1 General

Textile-based thermal protection blankets were developed as part of the Hermes (Flexible External Insulation - FEI) and Ariane 5 programmes.

97.3.2 Hermes flexible external insulation blankets

The FEI-blankets were proposed for the thermal protection of regions on Hermes' external surfaces experiencing temperatures during ascent and re-entry up to 650°C. In addition, propellant tanks and cryogenic fluid containments requiring insulation against the thermal loads generated by exhaust gases, were to be protected by thermal blankets.

97.3.3 FEI construction

In general, the insulation elements consist of a silica microfibre core, held between silica, or alumino-boro-silicate (ABS), fabrics and sewn together with silica or ABS threads. The insulation

performance is dominated by the design of the microfibre core. This can be designed with different thicknesses, and degrees of pre-tensioning, to suit the thermal and structural environment.

97.3.4 Thermal and structural loading

Examples of combining different textile components to suit different thermal and structural load profiles are shown in Table 97.3.1.

Higher-temperature demands can be met using newly developed ceramic fibres. The low thermal conductance of these, combined with low densities (typically 2200 kg/m^3), generally give the lightest and most efficient blankets. Silica components have good specific strengths (ratio of strength to density). However, the initial high strength reduces gradually above 500°C as the temperature increases.

Table 97.3-1 - Textile material combinations for different thermal and structural load profiles

Thermal/Structural Loading	Component		
	Core	Thread	Fabric
650°C	silica microfibre	light silica	light silica
1000°C	silica/alumina hybrid	light ABS	light ABS
1300°C	alumina microfibre fleece	light ABS (advanced)	light ABS (advanced)
High loading	silica fleece, pretensioned.	heavy ABS	heavy ABS

At temperatures above 800°C and in contaminated environments, ceramic materials are a better choice. Ceramic products are basically composed of alumina (Al_2O_3) and silica (SiO_2) with minor additions of boron oxide (ABS), zirconium oxide or chromium oxide. As a general rule, the temperature resistance increases with increasing alumina content. These ceramic materials are generally used in the form of microfibres as fleeces or felts.

At temperatures below 500°C, higher structural or aerodynamic loads can be tolerated. If temperatures are low to moderate, aramid or glass felts are used. The advantages of these, compared with those of inorganic fibres, are:

- better elasticity.
- lower density.
- higher specific strength.

Combinations of fibrous insulation using either normal or metallised (e.g. nickel or platinum) fibres, together with reflective screens, allows a higher thermal heat transfer.

[See: 71.11 - Flexible External Insulation (FEI)]

[See also: Chapters 69, 70, 71 for a general discussion of high temperature structures and thermal protection systems]

97.4 Planetary entry parachute

97.4.1 General

Parachute assemblies for spacecraft consist of two main elements. These are the:

- canopy: fabric portion of a parachute which provides drag, or drag and lift, when inflated.
- rigging line: any cord or tape attached to the canopy which transmits the forces on the parachute canopy to the suspended load via lift webs or strops.

The main parachute canopy can be deployed by means of a drogue parachute. These are relatively smaller than the main parachute, but may also be used to control, decelerate or stabilise the load.

Parachute terminology is described fully in Ref. [97-8].

97.4.2 Applications

97.4.2.1 General

Parachute systems are used in the terrestrial atmosphere to provide deceleration of recoverable space structures, e.g. rocket-booster cases and manned return capsules.

Space probes landing on other planets also use parachutes to reduce impact loads and damage on landing.

The space and atmospheric environment encountered during a planetary mission imposes additional materials selection factors, over and above those for purely terrestrial designs. The details of these factors depends greatly on the planetary environment and the nature of the mission and spacecraft.

This Topic presents information obtained from studies conducted for ESA programmes by Irvin (GB) concerning materials selection and design methods for planetary probe parachutes, Ref. [97-5], [97-6].

97.4.2.2 Huygens

The Huygens probe landed on Titan in January 2005. Its descent is shown schematically in Figure 97.4.1, Ref. [97-7].

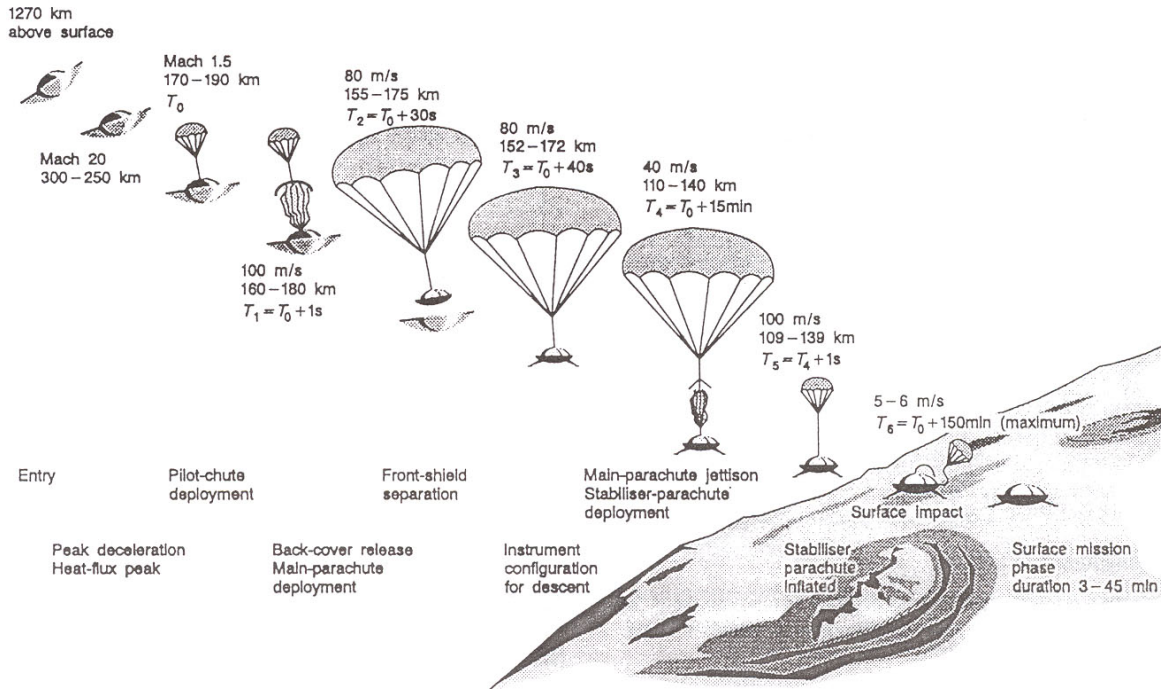

Figure 97.4-1 - Schematic diagram of the parachute system for Huygens probe landing on Titan

During most of its descent, the probe is suspended beneath a stabilising drogue parachute (a nylon canopy-Kevlar disk-gap-band type with a reference diameter of 2.45 m). The terminal velocity of the probe (with parachute) at the surface of Titan was calculated at 5.2 m/s. This is about half the impact velocity of the Apollo capsules and the Pioneer Venus spacecraft, Ref. [97-7].

Originally, a polyester yarn was to be used. Technical problems and the non-availability of a suitable polyester fabric, resulted in a change to nylon. This has been made possible by the use of inert sterilisation and the projected radiation dosage coupled with the overall suitability of nylon for the mission, Ref. [97-9].

[See also: Materials selection]

97.4.3 Property requirements

Materials selected for extraterrestrial parachute applications should have acceptable mechanical, physical and electrical characteristics under the imposed environmental conditions.

Electrical properties need careful consideration to avoid disturbance of the electromagnetic environment of the spacecraft which can interfere with communications links.

The key properties of materials to be considered include:

- mechanical:
  - tensile strength.
  - tensile Modulus.
  - elongation.
- physical:
  - density of fibres and their textile forms.

— vacuum resistance.

— radiation resistance.

— melting point.

— low temperature effects.

— hot air degradation: either at 165°C in air or nitrogen. This gives an indication of the effects on material performance of heat-sterilisation (manufacture) or aerodynamic heating during use.

- electrical:

  — resistance for various relative humidities (% RH),

  — RF loss for given frequencies,

  — potential developed after tribocharging (similar and dissimilar fabrics).

In addition to these technical factors, the commercial availability of products and their specification should be fully considered.

Yarns and textiles used in previous space missions and applications can have undergone further development, either chemically or by using new processing methods. Consequently their properties can be different. For example, the resistance of nylon to hot air degradation has been improved significantly in recent years, so that it now approaches that of polyester.

The benefits obtained by applying additives to textile products can be reduced after scouring treatments.

97.4.4 Materials selection

97.4.4.1 General

Nylon 66, polyester (Dacron and Diolen) and para-aramid (Kevlar and Twaron) textiles are widely used for terrestrial parachute elements. Whilst the cryogenic performance is adequate, nylon is normally rejected for use in space on the grounds of insufficient resistance to hot air and ionising radiation. Oxidation is only one consideration during the material selection process. The selection factors used are mission specific. Hot air degradation may be improved by the use of an inert gas sterilisation treatment, to reduce oxidation effects. Radiation resistance is normally adequate for that encountered in most space missions. In practice, only polyester and para-aramid have been used extensively in space. Polyester fabric is used for the canopy and para-aramid for cords and tapes. Meta-aramid (Nomex) - an established material - and newer materials, such as high-modulus polyethylene (Dyneema and Spectra), E-glass and PTFE (Teflon) have been compared with the primary material types, Ref. [97-5].

Applicable data on the newer materials and the required textile forms is, to date, limited. Other possible materials have also been promoted, such as metals, carbon, ceramics and other polymers. No details are currently available on their benefits or disadvantages.

97.4.4.2 Textile forms

The types of textile forms used in parachute systems are, Ref. [97-7]:

- woven broadloom for the canopy,
- braided cord,
- woven narrow fabric tapes (or ribbons).

97.4.4.3 Textile properties

Table 97.4.1 gives known characteristics of various textile broadloom fabric materials for parachute canopy use, Ref. [97-7].

Table 97.4-1 - Parachute systems: Textile characteristics for canopy space applications

Material: Trade names	**Melting point** [ºC]	**Saturated vapour pressure** [Pa at 25ºC]	**Radiation strength loss †** [%]	**% Strength loss in air** [165ºC/50 hr]	**RF loss at 2.1 GHz** [dB max]	**Resistance at 500V ‡** [ohms min]	**Tribocharging average potential *f*** [V]	**Joint efficiency ††** [%]	**Deployment at 93K**	
									Relative force to deploy	Relative force to uncrease
Nylon: Nylon 66	255	1.3×10^{-7}	3 / 12	10	0.2	2×10^{14} /2×10^{14}	-1600 / 3500	80 / 66	1	1
Polyester: Dacron, Diolen	260	1.3×10^{-5}	1 / 3	8	0.1	2×10^{14} /2×10^{14}	5600 / 3500	80 / 66	2.4	1.6
Para-aramid: Kevlar, Twaron	+500	-	- / -	3	0.2	2×10^{14} /2×10^{14}	290 / 480	30 / 30	1.4	1
Meta-aramid: Nomex	+371	-	- / -	-	-	-	- / -	60 / 60	1.3	1.5
PTFE: Teflon	+327	1.3×10^{-5}	10 / 50	<3	-	-	- / -	- / -	-	-
Polyolefin: Dyneema, Spectra	150	4×10^{-6}	- / -	melts	0.1	7.5×10^{10} /2×10^{13}	-30 / -50	- / -	3.8	1.9
Glass: E-glass	825	-	- / -	-	-	-	- / -	- / -	-	-

Key
+ Decomposes / chars
† 1×10^5 Rads / 1×10^6 Rads
‡ 34% RH / 15% RH
f Against same material: 31% RH / 15% RH
†† Fabric: Lightest/heaviest weight (normal usage)

97.4.4.4 Joint efficiency

Joint efficiency is the strength of a stitched joint as a percentage of that of the bulk broadloom fabric. Joint strength can vary with fabric weight.

97.4.4.5 Deployment characteristics

The deployment characteristics are a ratio of the material compared with nylon (taken to be 1) for:

- force to deploy fan folded fabric, and
- force to remove raised creases (folds).

97.4.5 Design aspects

The general factors to be considered in the design of parachute systems include:

- parachute type.
- design force.
- design factor.
- materials available.
- number of rigging lines.
- line length ratio.
- material safety factors:
  - canopy joint efficiency
  - ageing factors
  - temperature factors
  - rigging line joint efficiency
  - bollard joint efficiency
- nominal area.

[See Ref. [97-8] for definitions of terminology]

Other factors include those associated with:

- cruciforms.
- solids-ribbons.
- disc-gap bands.
- parachute components:
  - tension,
  - materials,
  - masses,
  - reserve factors.
- packing:

— mass.

— specific volume.

— packing density.

Design criteria may be examined using PASDA parachute geometry and stress analysis software developed by Irvin (GB) Ltd., Ref. [97-6].

97.5 References

97.5.1 General

[97-1] ISO 4674-Method A2
Fabrics coated with rubber or plastics - Determination of tear resistance

[97-2] A. Ingemar Skoog: Dornier GmbH
'The EVA Space Suit Development in Europe'
Acta Astronautica Vol. 32, No. 1, p25-38, 1994

[97-3] Guy I Severin: MEE Zvedda (Russia)
'Design to safety: Experience and Plans of the Russian Space Suit Programme'
Acta Astronautica Vol. 32, No. 1, p15-23, 1994

[97-4] 'The European Manned Space Transportation Programme (MSTP)'
ESA Publication 'Reaching for the Skies', No. 11, May 1994

[97-5] A. Peachey: Irvin (GB) Ltd
'Planetary Entry Study Theme 3: Parachute Material Selection'
Irvin Tech. Note RD 413, Aug. 1993.
Dornier Contract No. KAA-DOR 12020 AO 3516

[97-6] M. Martin & D. Brundle: Irvin (GB) Ltd
'PASDA Geometry Module and Stress Analysis Module Definitions'
Irvin Tech. Note RD 373, June. 1991.

[97-7] R.D. Lorenz: University of Kent (UK)
'Huygens Probe Impact Dynamics'
ESA Journal 1994, Vol. 18, p93-117

[97-8] British Standards Institute (UK)
BS F140 (1991) - Glossary of Parachute Terms

[97-9] Irvin (GB) Ltd: Correspondence

[97-10] James R. Asker: Windsor Locks (USA)
'US, Russian Suit Serves Diverse EVA Goals'
Aviation Week & Space Technology (Jan 16 1995), p40-47

98 Elastomers

98.1 Introduction

98.1.1 General

The term elastomer is used to describe a large range of polymeric-type materials that include both natural and synthetic rubbers, [See: 75.3].

Not all types of elastomers are suitable for use in space, [See: ECSS-Q-70-71].

98.1.2 Applications

Whilst elastomers cannot be considered as structural materials, they possess some unique characteristics that, in conjunction with other materials, make them attractive for use in a number of load-bearing space applications, e.g.

- vibration control and damping, [See: 30.14].
- seals, [See: 75.7].

99 Thermal insulation

99.1 Introduction

99.1.1 General

Thermal insulation is widely used in many types of space structure and contributes to the overall spacecraft thermal management and control, [See: ECSS-E-HB-31-01].

In general, thermal insulation applied to structures can be grouped by its main protection function, e.g.:

- protect a structure from thermal cycling experienced in service, e.g. LEO.
- protect a structure from extreme high temperatures, e.g.
  - experienced during re-entry into Earth's atmosphere.
  - experienced during entry into other planetary atmospheres.
  - near to sources of high temperatures, such as propulsion systems and motors.
- protect a structure from low temperatures, such as those experienced during deep space missions.
- prevent, or reduce, the effect of temperature on the contents of a structure such as cryogenic liquids in tanks; particularly liquid hydrogen propellant in launcher cryotanks.

Within some applications, thermal insulation forms an integral part of the thermal protection system used on the external surfaces of a structure, e.g. layers of insulation placed between the primary structure and the external, extreme high-temperature resistant 'shell'.

99.1.2 Materials

Thermal insulation can be made from a wide range of materials and combinations thereof to create complex protection systems for structures.

Material selection for insulation systems is influenced by whether the structure is 'single shot' or reusable. A large amount of the development work for thermal insulation originates from reusable space plane concepts and future reusable launcher studies.

Depending on the application, some thermal insulation materials need to carry significant loads whereas others do not.

Within this handbook, thermal insulation materials are described in context with their application; often by example, i.e.:

- thermo-structural designs, [See: Chapter 70], provides examples of load-bearing carbon-carbon, C-C, composites and ceramic matrix composites, CMC, within reusable space plane concepts.
- thermal protection systems, [See: Chapter 71], provides examples of the use of materials in reusable space plane concepts. Some materials carry significant loads whereas others do not, e.g.:

- C-C carbon-carbon composites, [See : 71.7]
- CMC ceramic matrix composites, [See: 71.12]
- Metallic materials, e.g. beryllium, [See 71.15]; titanium-based, [See: 71.9; 71.8]; superalloy-based, [See: 71.8].
- IMI internal multiscreen insulation comprising metallised ceramic screens combined with fibrous ceramic materials, [See: 71.10].
- FEI flexible external insulation based on fibrous ceramic materials, [See: 71.11].

- reusable cryogenic tank concepts provide examples of:
  - C-SiC for TPS panels, [See: 71.19].
  - Polymer-based insulation foams, also known as 'cryo foams', [See: 71.19 – concepts; 71.22 - materials].

100 Fibre metal laminates

100.1 Introduction

100.1.1 General

Fibre metal laminates are hybrid material constructions comprising of metal sheets interleaved with layers of composite.

Although the various combinations of metals and composites are endless, initial development work concentrated on hybrid materials aimed at aircraft applications, i.e. fatigue-critical structures made of thin-gauge sheet. Consequently, material combinations tended to include aircraft-grade aluminium alloys. Developed in the late 1970s at Delft University of Technology, NL, in collaboration with Fokker, several standard types are available commercially. FML is manufactured and marketed by Structural Laminates Company. Some grades of FMLs are used for commercial and military aircraft applications.

As the performance demands of aircraft increase, especially in the military sector, the use of aluminium alloys becomes questionable because the expected temperatures on aircraft structures exceed the capability of conventional aluminium alloys. As a result, more recent development work has considered the use of titanium alloys within the basic hybrid sheet construction, [See: Chapter 101].

100.1.2 Construction

FMLs are bonded arrangements of thin metal sheets with alternating plies of strong fibres (aramid, glass or carbon) impregnated with a thermoset (epoxy) or thermoplastic adhesive, as shown in Figure 100.1.1, Ref. [100-14].

100.1.3 Characteristics

FMLs have mixed characteristics. Under some conditions they are similar to metals but in others offer the characteristics of composites. They combine the advantages of high-strength isotropic metal sheet with the fatigue resistance of composite materials.
There are three groups of materials, commonly-known by their commercial tradenames:

- ARALL®
- GLARE®
- CARE®

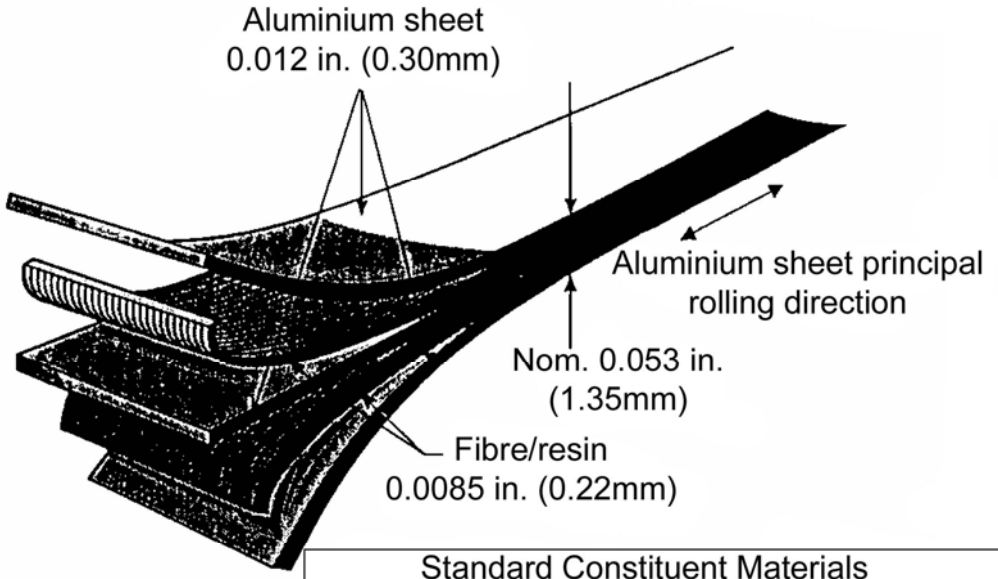

Standard Constituent Materials	
Aluminium sheet alloy	2024-T3 or 7475-T761
Fibre	Aramid or glass
Prepreg	Unidirectional or crossply

Figure 100.1-1 – FML fibre metal laminate: Schematic of a typical 3/2 laminate

Several grades of FML are available commercially, Ref. [100-21]:

- ARALL 2: 2024-T6/UD aramid/epoxy,
- ARALL 3: 7475-T76/UD aramid/epoxy
- GLARE 1 to 6.

GLARE grades use various alloys with a glass fibre-reinforcement, either as UD or cross-ply, within an epoxy adhesive, [See also: Table 100.2.1].

Design allowables for ARALL are given in Ref. [100-1].

100.1.4 ARALL®

ARALL, aramid-reinforced aluminium laminate is the best known of the FML family. It has been used in design studies for the lower wing of a Fokker-50 prototype commercial transport aircraft and the A330/A340 fuselage floor section. It is operational in the McDonnell Douglas C-17 cargo door and intended for the Boeing 777 bulk cargo floor.

100.1.5 GLARE®

GLARE, glass-reinforced aluminium laminate, offers good fatigue performance and a high failure strain provided by the glass fibres. It is intended for use in biaxially loaded elements, such as fuselage panels and beam shear panels.

Within the Airbus A380 construction, GLARE is used for fuselage sections and parts of the leading edges on the tail; as shown in Figure 100.1.2, Ref. [100-22].

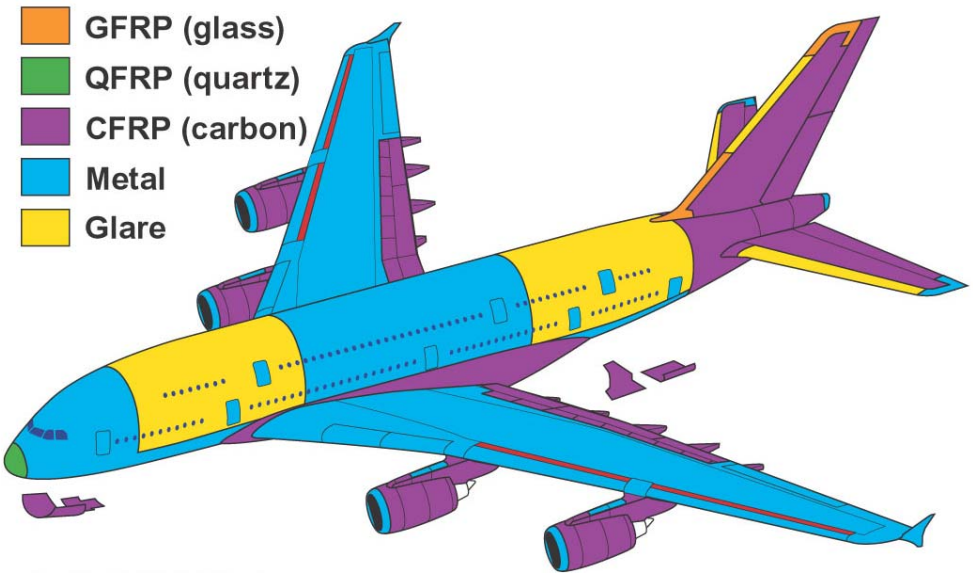

Figure 100.1-2 – GLARE fibre metal laminate: Use on Airbus A380

100.1.6 CARE®

CARE, carbon fibre reinforced metal laminate, is under development. The intended product range uses high-modulus carbon fibres combined with aluminium or titanium alloy sheets, [See also: Chapter 101].

100.2 Constituent materials

100.2.1 Properties

100.2.1.1 General

The properties of FMLs are highly dependent on the constituent materials, so can be tailored for different applications by varying constituent parameters, e.g.:

- fibre and resin system,
- metal alloy,
- fibre orientations.

100.2.1.2 ARALL

ARALL grades consist of a 50% fibre volume adhesive prepreg with (high modulus) aramid fibres.

100.2.1.3 GLARE

GLARE grades comprise an adhesive prepreg with a fibre volume fraction of 60% (V_f = 60%) of unidirectional or cross-ply *R*-glass fibres.

100.2.1.4 CARE

Several grades are the subject of development. They consist of titanium or aluminium sheets combined with unidirectional carbon fibres, Ref. [100-2].

100.2.2 Commercially-available grades

100.2.2.1 Description

Table 100.2.1 gives data for different commercially-available grades of ARALL and GLARE.

ARALL 1 is not available commercially. ARALL 4 is specially designed for higher temperature applications. CARE grades are experimental.

Table 100.2-1 - Fibre metal laminates: Description of commercially-available laminates

Type	Prepreg Type	Orientation	Metal	Comments
ARALL 2	aramid/epoxy	UD	2024-T3	Non-stretched
ARALL 3	aramid/epoxy	UD	7475-T76	0.4% Post-stretched
GLARE 1	R-glass/epoxy	UD	7475-T76	Post-stretched
GLARE 2	R-glass/epoxy	UD	2024-T3	Non-stretched
GLARE 3	R-glass/epoxy	cross-ply	2024-T3	Non-stretched
GLARE 4	R-glass/epoxy	cross-ply + UD	2024-T3	Non-stretched
GLARE 5	R-glass/epoxy	cross-ply	2024-T3	-
GLARE 5-F1	R-glass/epoxy	cross-ply	5052-H34 (outer) 7075-T6 (inner)	For aircraft cargo area
GLARE 5-F2	R-glass/epoxy	cross-ply	2024-T3	For aircraft cargo area
GLARE 5-FW	R-glass/epoxy	cross-ply	5052-H34	For aircraft fire-wall liner (FAR approved)
GLARE 6	R-glass/epoxy	cross-ply	2024-T3	-

100.2.2.2 Designation system

Given that FMLs can consist of a different numbers of interleaved metal alloy and composite reinforced layers, the product designations used are in the form:

Name Grade Metal layers/Composite layers Metal sheet thickness

For example, ARALL 2 3/2 0.2 stands for:

- ARALL 2 grade (2024-T3, non-stretched) with:
  - 3 sheets of aluminium (0.2 mm thickness), and
  - 2 plies of UD aramid-epoxy prepreg.

100.2.2.3 Development grades

Table 46.18.2 summarises the development status for various FML grades, [See also: Chapter 101 for titanium variants under development by DLR].

Table 100.2-2 - Fibre metal laminates: Development status

Trade name	Material			Technology developed	Main characteristics determined	Commercial availability
	Alloy	Matrix	Fibre			
ARALL:						
ARALL 1	7075-T6	Epoxy	Aramid UD	√	√	x
ARALL 2	2024-T3	Epoxy	Aramid UD	√ (1)	√	√
ARALL 3	7475-T76	Epoxy	Aramid UD	√ (1)	√	√
ARALL 4	2024-T8	Epoxy	Aramid UD	√	√	x
GLARE:						
GLARE 1	7475-T76	Epoxy	R-glass UD	√	√	√
GLARE 2	2024-T3	Epoxy	R-glass UD	√	√	√
GLARE 3	2024-T3	Epoxy	R-glass UD	√	√	√
GLARE 4	2024-T3	Epoxy	R-glass UD/CP	√	√	√
GLARE 5	2024-T3	Epoxy	R-glass UD/CP	√	√	√
GLARE 5-F1	5052-H34 (outer) 7075-T3 (inner)	Epoxy	R-glass CP	√	√	√
GLARE 5-F2	2024-T3	Epoxy	R-glass CP	√	√	√
GLARE 5-FW	5052-H34	Epoxy	R-glass CP	√	√	√
GLARE 6	2024-T3	Epoxy	R-glass CP	√	√	√
CARE:						
CARE	Ti-6Al-4V	PEEK	Carbon UD	x	x	x
	Ti (CP)	PEEK	Carbon UD	x	x	x
	Al	Epoxy	Carbon UD	x	x	x
OTHER:						
2A3	2,090	Epoxy	Aramid UD	x	x	x
2C3	2,090	Epoxy	Carbon UD	x	x	x
2AC7	2,090	Epoxy	A/C/A UD	x	x	x
8C3	2,090	Epoxy	Carbon	x	x	x
8G3	2,090	Epoxy	Glass	x	x	x
8MMCC3	8090MMC	Epoxy	Carbon	x	x	x
8MMCG3	8090MMC	Epoxy	Glass	x	x	x

Key : UD: Unidirectional; CP: Cross Ply; A: Aramid; C: Carbon; √: Yes; (1) Certified; x: No

100.2.3 Manufacturing of FML

100.2.3.1 Metal surface preparation

Prior to lay-up and cure, the bare, unclad aluminium surfaces are anodised and primed. This provides good bond integrity and inhibits aluminium bondline corrosion in the event of moisture ingress. A chromic acid or phosphoric acid anodising treatment is used. For added corrosion protection, cladding can be applied to the outer aluminium faces of the FML.

100.2.3.2 Post-cure residual stresses

During cure, residual stresses develop as a result of differences in the coefficients of thermal expansion (CTE) of the constituents. These are tensile in the metal sheets and compressive in the fibre layers. This is called the 'as-cured' condition.

The direction of the residual stresses can be reversed to improve the composite properties by plastically deforming the material after curing. This is called 'post stretching' and is used in laminates based on the 7XXX-series aluminium, i.e. grades known as ARALL 1, ARALL 3 and GLARE 1.

The compressive stresses then produced in the aluminium improve the fatigue properties of post-stretched material over those of the as-cured.

100.3 Mechanical properties

100.3.1 Basic properties

The basic properties of FML material depend on the:

- relative proportions of reinforcement and metal (usually aluminium), and
- bond efficiency.

100.3.2 Typical mechanical properties

100.3.2.1 ARALL

Typical mechanical property data are given in Table 100.3.1 for ARALL, Ref. [100-9].

ARALL S-basis data are given in Ref. [100-1].

100.3.2.2 GLARE

Table 100.3.2 gives typical mechanical properties for GLARE, Ref. [100-9], [100-19].

Table 100.3-1 - ARALL FML: Typical mechanical properties

Property	Direction	ARALL 1 3/2	ARALL 2(1) 3/2	ARALL 3(1) 3/2	ARALL 4 3/2
Density (kg/m^3)		2290	2290	-	-
UTS	L	800	717	821	731
(MPa)	LT	386	317	379	338
Tensile YS	L	641	365	607	373
(MPa)	LT	331	228	324	317
Tensile Modulus	L	68	66	68	61
(GPa)	LT	48	53	49	49
Tensile Elongation	L	0.7	1.4	1	1.4
(%)	LT	7.1	12	-	3.9
Ultimate Strain	L	1.9	2.5	2.2	2.6
(%)	LT	7.9	12.7	8.8	4.6
Poisson's Ratio	L	0.33	0.32	-	-
(tension)	LT	0.25	0.26	-	-
Compressive YS	L	372	255	345	-
(MPa)	LT	393	234	365	-
Compressive Modulus	L	70	65	66	-
(GPa)	LT	52	53	50	-
0.2% Shear Yield	L	-	-	-	-
Strength (MPa)	LT	-	-	-	-
Shear Modulus	L	17	17	-	-
(GPa)	LT	-	16	-	-

Key: (1) See: Ref. [100-9]; UTS: Ultimate tensile strength; YS: Yield strength

Table 100.3-2 - GLARE FML: Typical mechanical properties

Property	Direction	GLARE 1		GLARE 2		GLARE 3		GLARE 4	
		2/1	3/2	2/1	3/2	2/1	3/2	2/1	3/2
Density (kg/m^3)		-	2520	-	2520	-	2520	-	2450
Thickness (mm)		0.89	1.47	0.83	1.34	0.82	1.38	0.95	1.59
UTS	L	1077	1282	992	1214	662	717	843	1027
(MPa)	LT	436	352	331	317	653	716	554	607
Tensile YS	L	525	545	347	360	315	305	321	352
(MPa)	LT	342	333	244	228	287	283	250	255
Tensile Modulus	L	66	65	67	65	60	58	60	57
(GPa)	LT	54	50	55	50	60	58	54	50
Ultimate Strain	L	4.2	4.2	4.7	4.7	4.7	4.7	4.7	4.7
(%)	LT	7.7	7.7	10.8	10.8	4.7	4.7	4.7	4.7
Compressive YS	L	546	546	389	420	319	314	349	370
(MPa)	LT	400	375	252	241	318	316	299	291
Compressive	L	66	65	69	68	62	59	62	59
Modulus (GPa)	LT	54	51	56	53	61	59	61	59
Key: UTS: Ultimate tensile strength; YS: Yield strength									

100.3.3 Metal fraction approach

Since the qualification procedure for new materials demands a vast amount of testing, an initial evaluation uses a rule-of-mixtures type theory. This is called the 'metal fraction approach'. Although it gives promising results, further investigation is needed, Ref. [100-3].

Figure 100.3.1 shows the metal fraction approach applied to GLARE 4, together with the 95% confidence interval, Ref. [100-3].

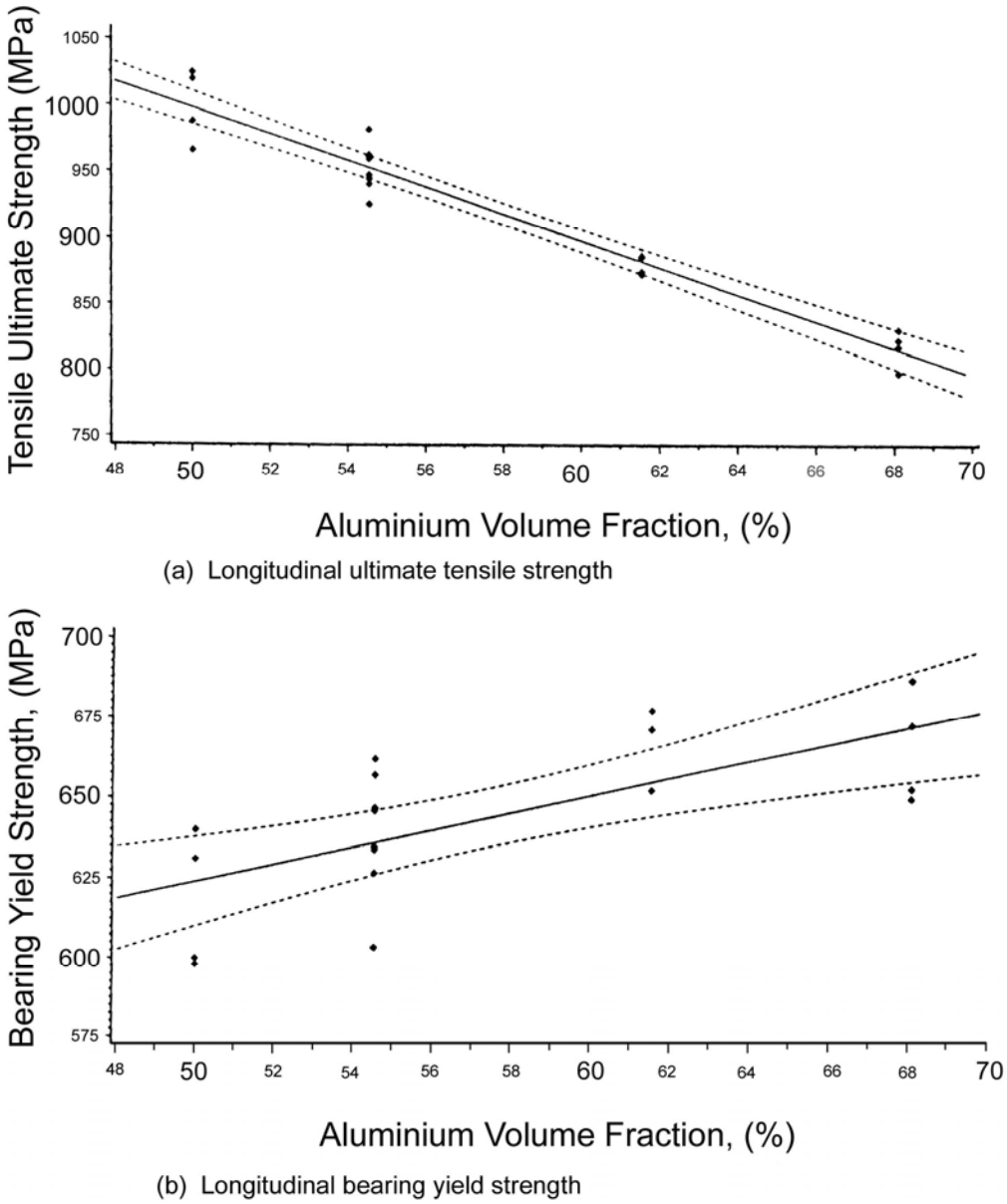

Figure 100.3-1 - GLARE 4 FML: 95% confidence intervals with aluminium volume fraction

100.3.4 Stress-strain response

100.3.4.1 ARALL

Figure 100.03.2 shows the typical stress-strain behaviour of ARALL 3 laminates.

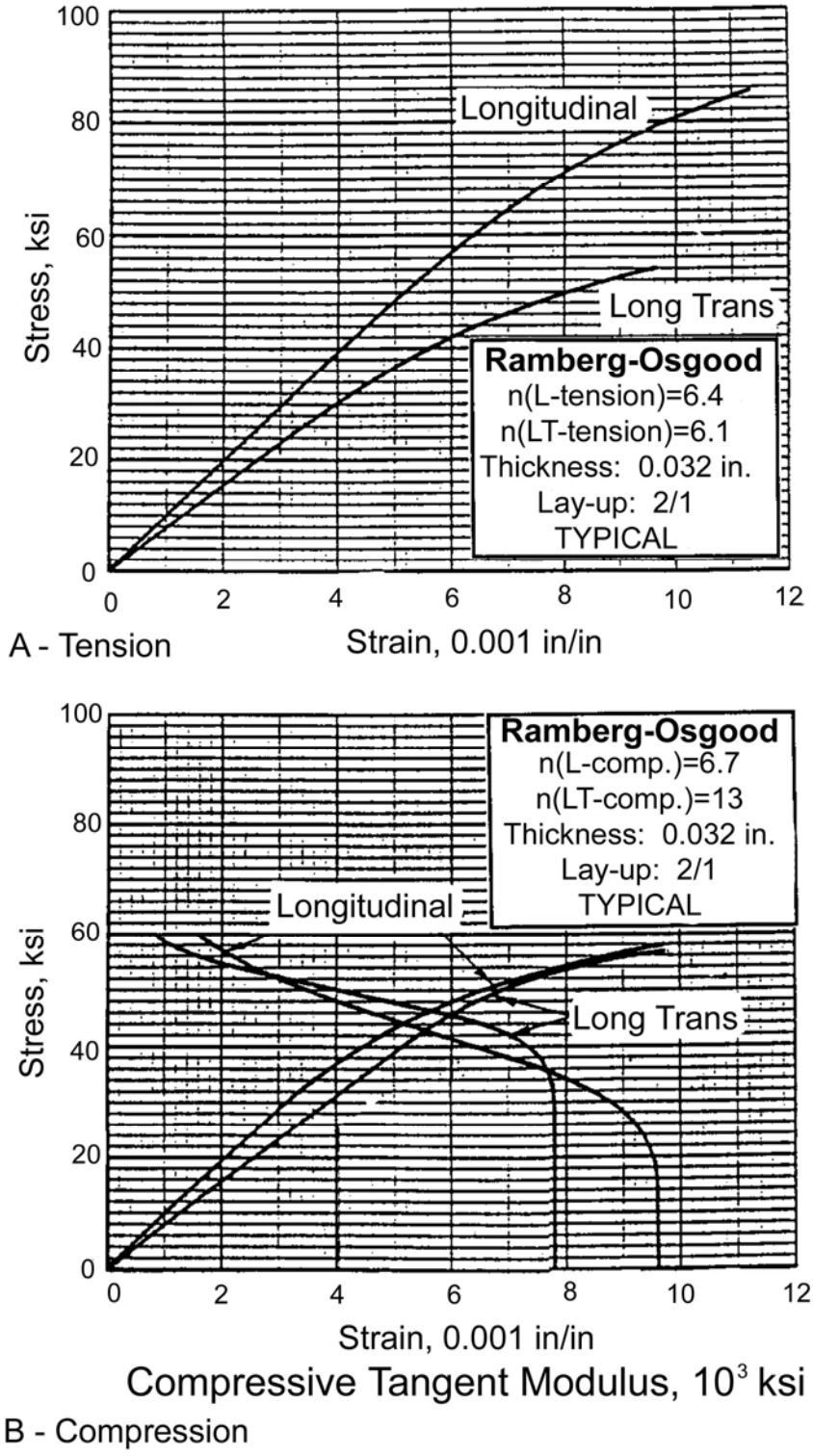

ARALL 3, 2/1 sheet laminate

Figure 100.3-2 - ARALL 3 FML: Typical stress-strain response

100.3.4.2 CARE – aluminium variants

CARE, when available, is possibly the best FML for space applications because of the high specific strength and stiffness, Ref. [100-4]. Although galvanic corrosion is normally a problem for carbon-aluminium combinations, it can be tackled by isolating the fibres; although this can impair the mechanical properties.

100.3.4.3 CARE – titanium variants

A preliminary investigation has been carried out into titanium (Ti-6Al-4V) based CARE, Ref. [100-2], because of the expected good behaviour at high temperatures (250°C). The results were promising, moreover this grade has high strength and stiffness with very good static blunt notch and fatigue properties.

[See also: Chapter 101 for DLR titanium hybrid material]

100.3.5 Effect of temperature

100.3.5.1 General

For ARALL the effects of temperature have been investigated only in tension, but temperature effects are greater on the compression or shear properties.

100.3.5.2 ARALL

Laminates of ARALL grades 1 to 4 were tested in tension at temperatures ranging from -184°C to +204°C and then at room temperature after exposure, Ref. [100-5].

No degradation of ultimate strength, yield strength or moduli were found for either the longitudinal or transverse directions after short-time exposure (five minutes), or when testing at cryogenic temperatures.

Figure 100.3.3 shows the minimal effects of short-time low temperature exposure on the mechanical properties of ARALL 1, 2 and 3, Ref. [100-5].

When tested at higher temperatures, the properties worsen with increasing temperature. Figure 100.3.4 shows this effect for ARALL 4, which is the best suited for elevated temperatures.

For transverse specimens, in the higher temperature range of 230°C, fibre-matrix interface debonding is the dominant cause of property degradation.

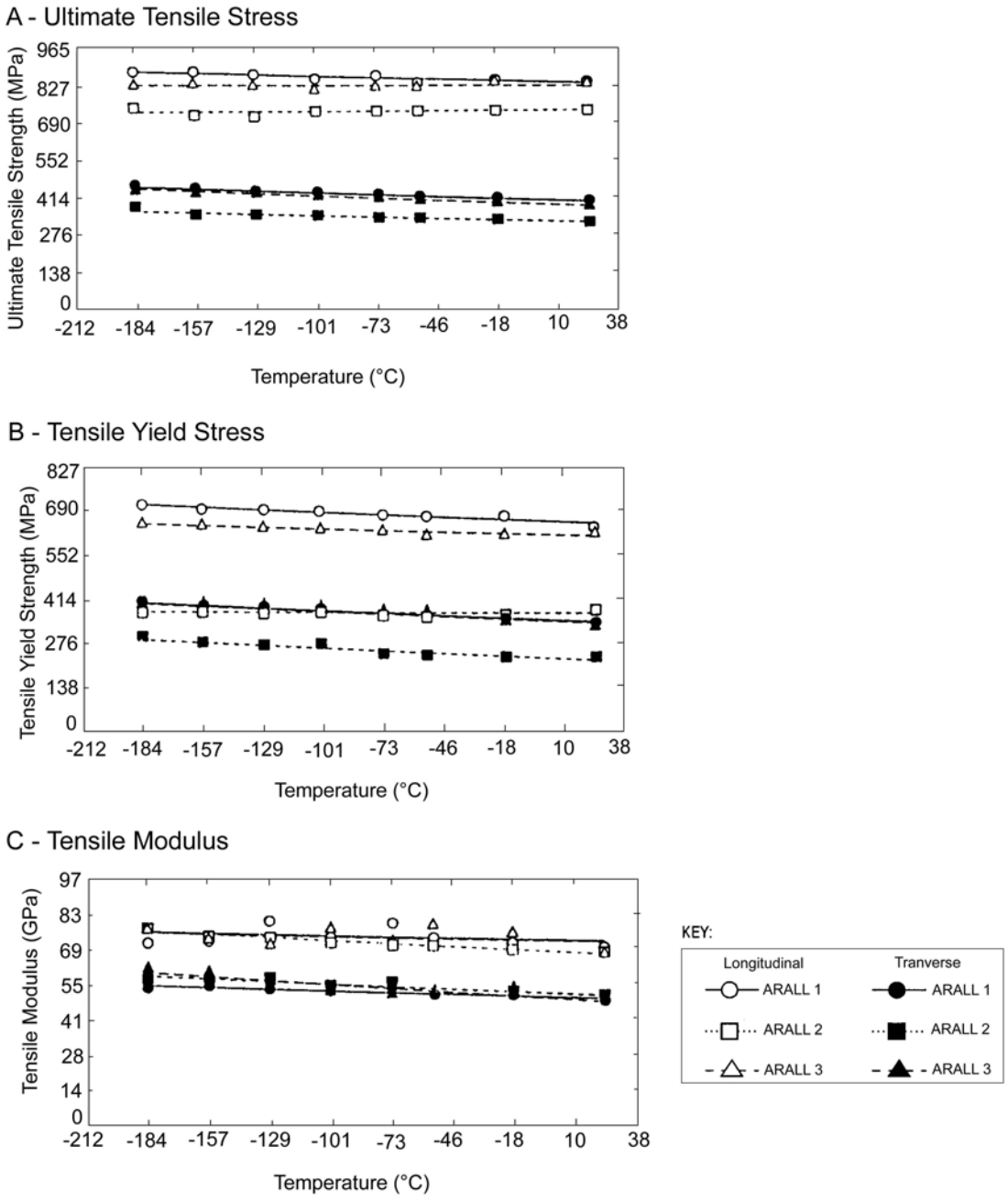

Tested after short-term low temperature exposure

Figure 100.3-3 – FML: Effect of temperature on mechanical properties of various ARALL laminates

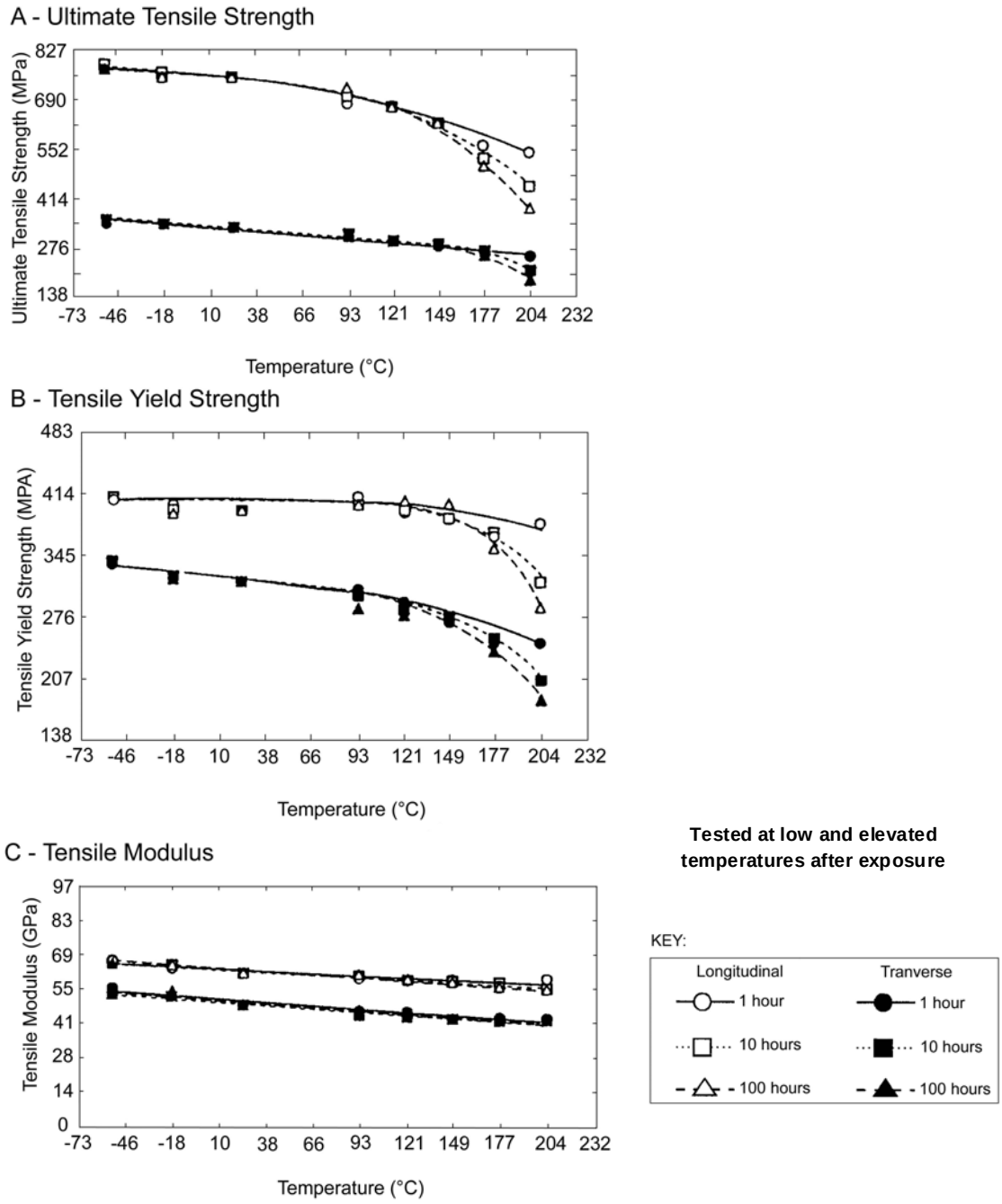

Figure 100.3-4 –FML: Effect of time and temperature on mechanical properties of ARALL 4 laminates

The combined effects of strain rate and temperature were studied for ARALL 1, Ref. [100-6]. The effect of strain rate on tensile strength, strain or modulus is low, except at high temperatures (121°C). In conclusion, the effect of strain rate is less significant than that of temperature. Temperature changes alter the residual stress in the laminate because of differences in CTE of the constituents. This effect should be taken account of in the case of fatigue loading since it can lower the (beneficial) compressive stress in the aluminium layers.

100.3.6 Moisture ingress

The external faces of FML are metal sheets, consequently moisture uptake is limited to the cut edges. Prolonged exposure in aggressive environments, often under cyclic loading, has demonstrated the good durability of ARALL. Even after exposure of more than 60 weeks, only low-level degradation in strength or stiffness was found (approximately 5%), Ref. [100-7].

Salt-fog exposure of ARALL 4 at high stress levels led to moisture absorption at the laminar interfaces causing delamination and destroying the load-carrying ability of the composite, Ref. [100-8].

Cut edges which expose the reinforcement plies need sealing to prevent moisture ingress affecting the epoxy adhesive, around fibres or bondline. Sealing of the cut edges with RTV room temperature vulcanising silicone-based sealant had no influence on the flexural fatigue behaviour of ARALL 4 3/2 in the longitudinal direction, Ref. [100-8].

100.3.7 Corrosion

Providing that the edges are sealed correctly, corrosion of the aluminium is limited to the external surface only because the reinforcement ply acts as a barrier.

100.3.8 Influence of stress concentrations

The effects of stress concentrations on material properties can be summarised as, Ref. [100-4], [100-9]:

- the fracture toughness of ARALL containing saw cuts is worse than monolithic aluminium whereas GLARE and CARE are much better; as shown in Figure 100.3.5, Ref. [100-4].
- after fatigue testing, the fracture toughness of ARALL is better than monolithic aluminium because of unbroken fibres remaining in the wake of the crack. This is particularly important for multi-hole specimens where fatigue cracks grow from one rivet hole to the next.
- the notched strength of ARALL in the L-direction is typically 50% (sharp notch) to 60% (blunt notch) of the ultimate strength, Ref. [100-9].
- GLARE, as shown in Figure 100.3.5, retains 50% to 70% of ultimate strength, which is important in cases of accidental damage. This fraction is higher in the LT-direction.

For ARALL materials, the practical range for the notch factor used for design purposes is 2.5 to 3.5, Ref. [100-7]. This is lower for GLARE.

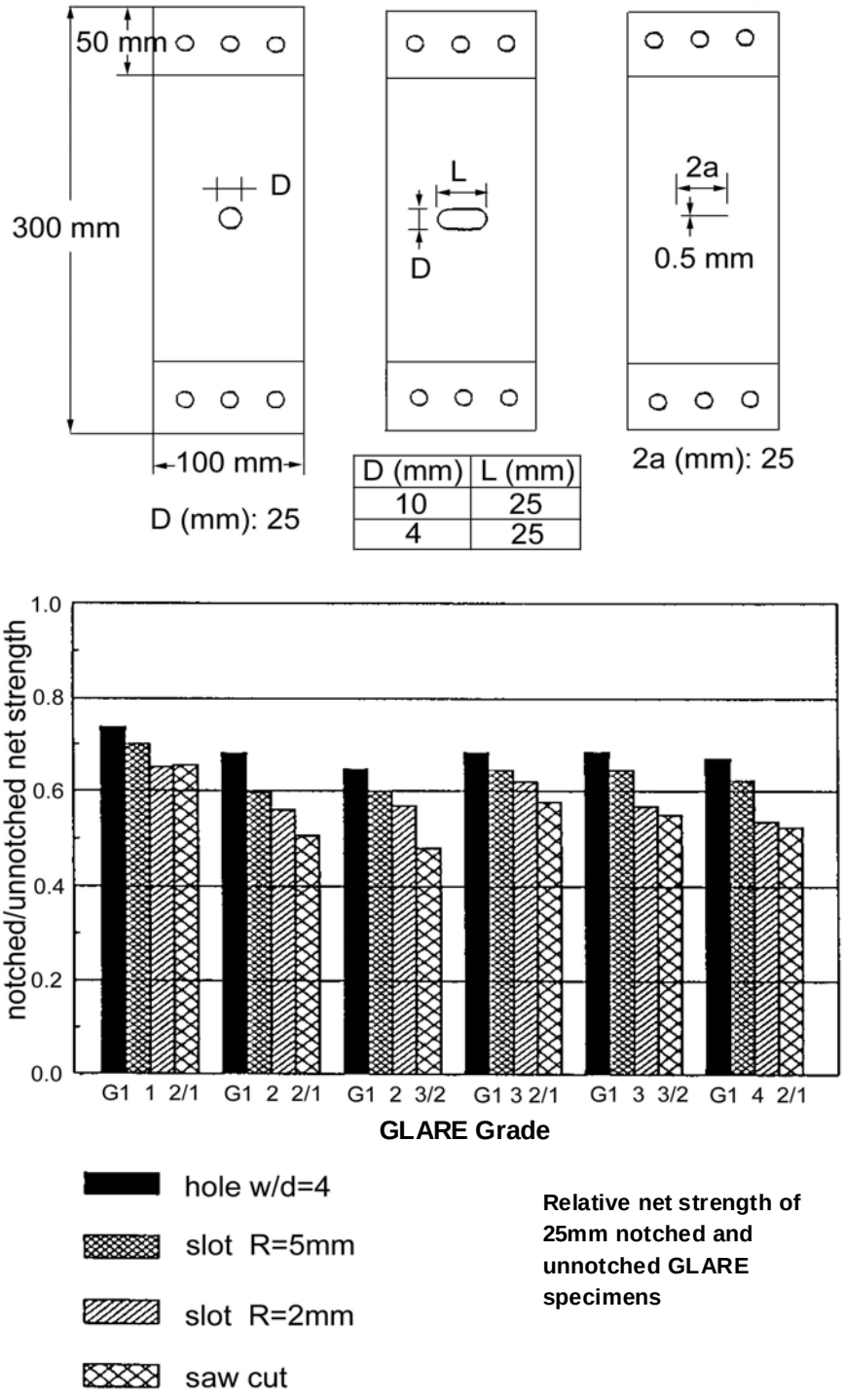

Figure 100.3-5 –FML: Effect of stress concentrations on strength

100.3.9 Effect of fatigue loading

100.3.9.1 Characteristics

ARALL was developed as a sheet material with good fatigue strength, compared with monolithic aluminium, in which any cracks grow very slowly.

The good fatigue properties of FML derive from the crack-bridging function of the fibres. The transverse fatigue properties are largely dictated by the aluminium layers. The efficiency of the crack bridging depends upon the design parameters of the hybrid material.

Comparing the different fibres used in the prepreg, the important factors are:

- stiffness and fibre failure strength and strain,
- good adhesion between fibre, metal and adhesive.

100.3.9.2 Effect of fibres

Aramid fibres are stiffer than R-glass, but show poor adhesion properties which limits the prepreg fibre volume content to 50% and so reduces the bridging efficiency for as-cured ARALL.

Post-stretching the material improves the fatigue properties, as shown in Figure 100.3.6.

Fatigue studies concentrate on tension-tension fatigue because of the poor compressive properties of aramid fibres.

R-glass fibres are very strong with a high failure strain compared with that of aramid and carbon fibres. The fibre content is higher than that of ARALL offering comparable fatigue properties in tension-tension fatigue. The compression-tension fatigue behaviour is superior to ARALL. Carbon fibres are by far the stiffest, giving the highest efficiency.

Crack growth curves are shown in Figure 100.03.7 for a T800/924C based CARE; a 2/1 grade composed of aluminium 2024-T3 with 0° oriented prepreg of T800 fibres with a 180°C cure Fibredux 924C resin.

Figure 100.3.8 shows the fatigue behaviour of various FML materials compared with 2024-T3.

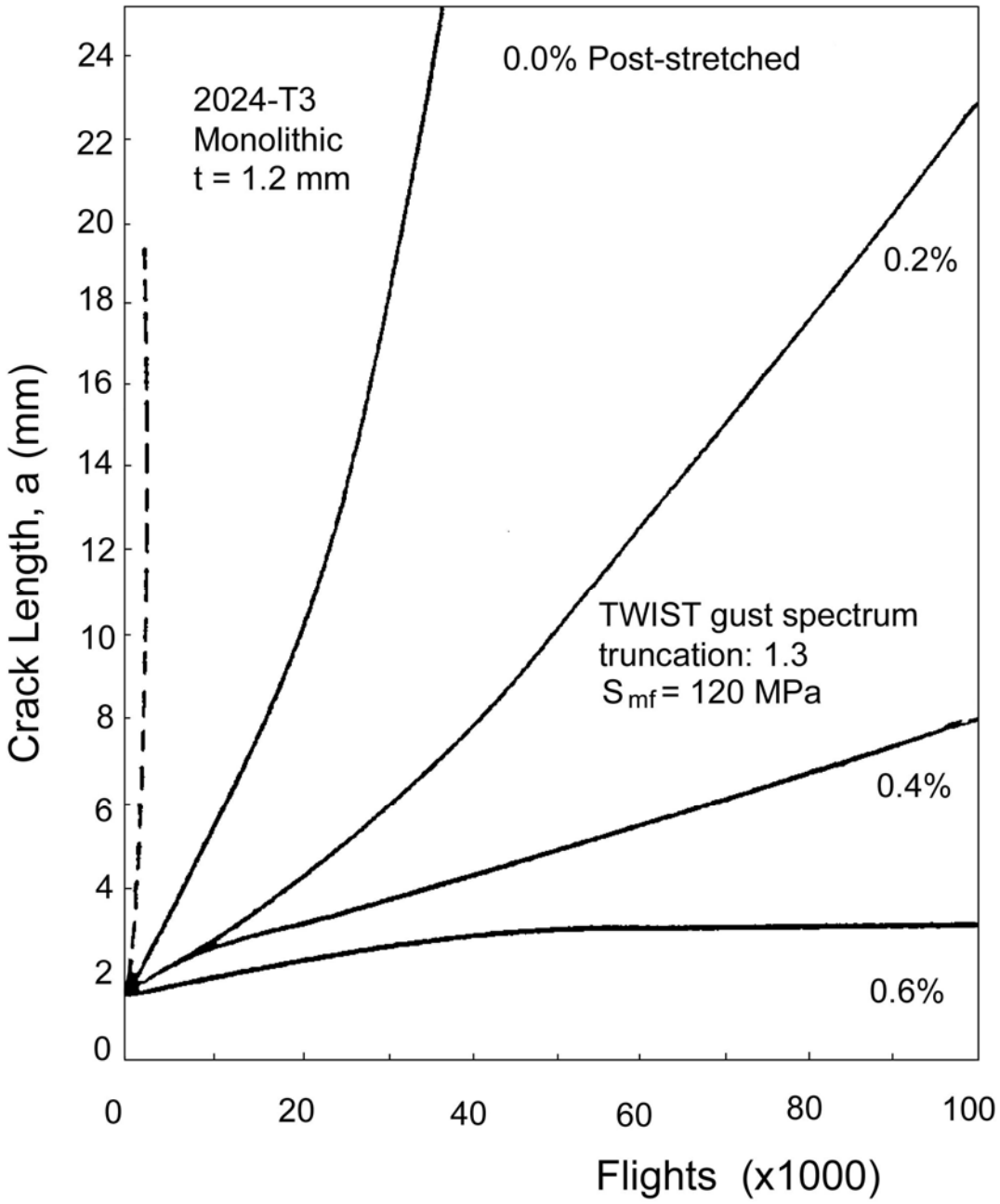

Figure 100.3-6 - FML: Influence of 'post-stretching' process on the fatigue behaviour of ARALL 1

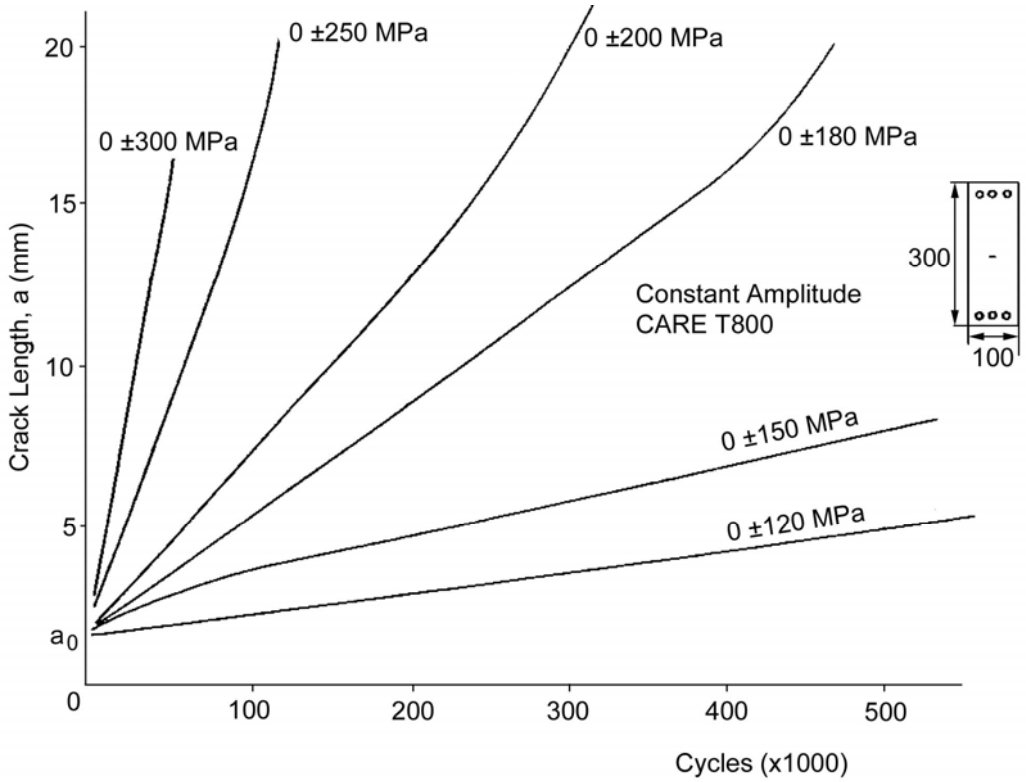

Figure 100.3-7 - FML: Constant amplitude fatigue curves for CARE T800/924 with 2024-T3

Figure 100.3.8 shows the fatigue behaviour of various FML materials compared with 2024-T3.

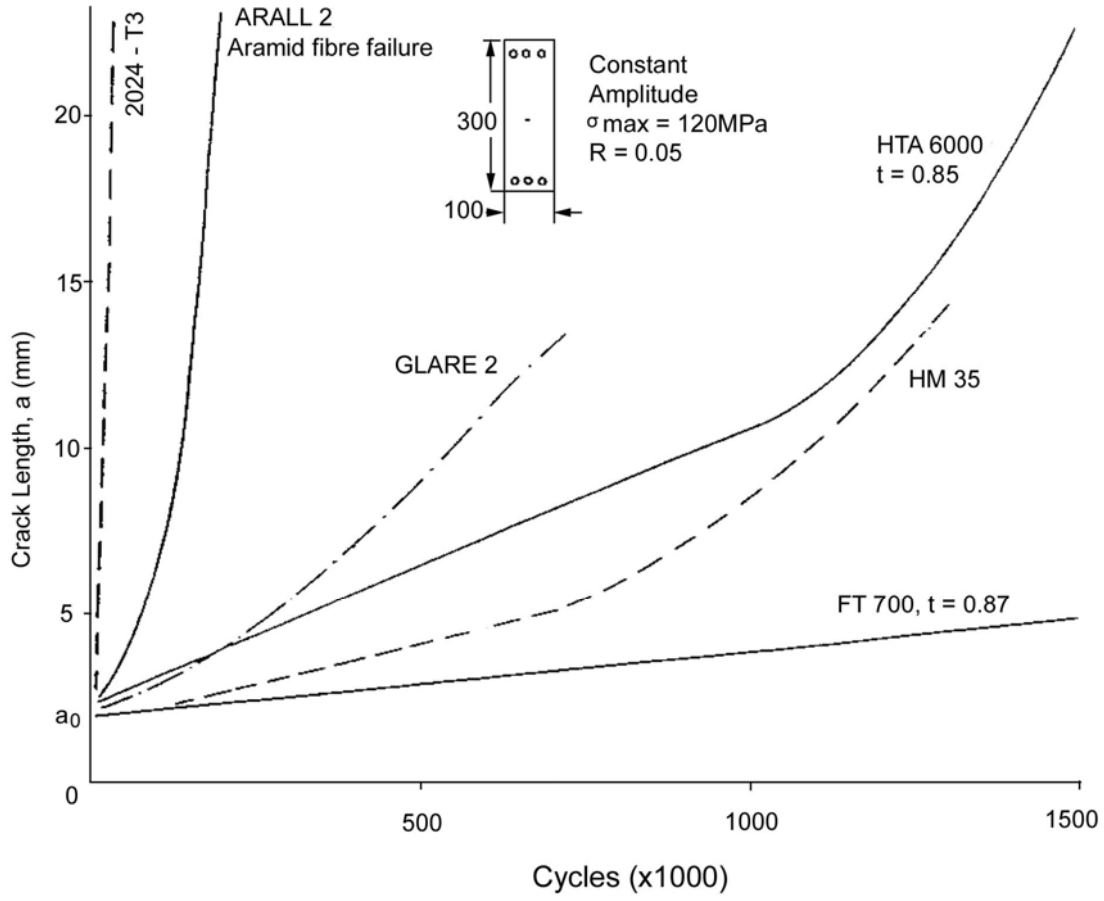

Key: HTA: Tenax fibres; HM35: Tenax fibres; FT700 Tonen fibres.

Figure 100.3-8 - FML: Fatigue properties for 2024-T3 compared with ARALL 2, GLARE 2 and CARE materials

The as-cured ARALL performs rather poorly in the $R = 0.05$ test cycle compared with GLARE and CARE. The fatigue sensitivity of CARE decreases with increasing fibre modulus; the Tonen FT700 based CARE ($E = 700$GPa) is almost fatigue insensitive. The flexural fatigue behaviour of ARALL 4 in the L-direction is superior to 2024, in the LT-direction the properties are comparable, Ref. [100-8].

Fatigue testing of ARALL 3 post-stretched material at higher temperatures showed an improvement compared with the room temperature properties, Ref. [100-10]. The residual strength after fatigue testing at $R = 0.1$, 93°C was only slightly lower (~5%) than the static panel.

A carbon fibre-PEEK-titanium grade laminate was fatigue tested at room temperature and at 250°C, Ref. [100-2]. At high temperature, the crack growth levelled off to a very low level after some initial cracking.

Figure 100.3.9 shows that, in all cases, FML has much better fatigue properties compared with 2024 aluminium alloy. These results are for constant amplitude fatigue tests and flight simulation 'mini-twist' fatigue tests on riveted and bolted-joint specimens.

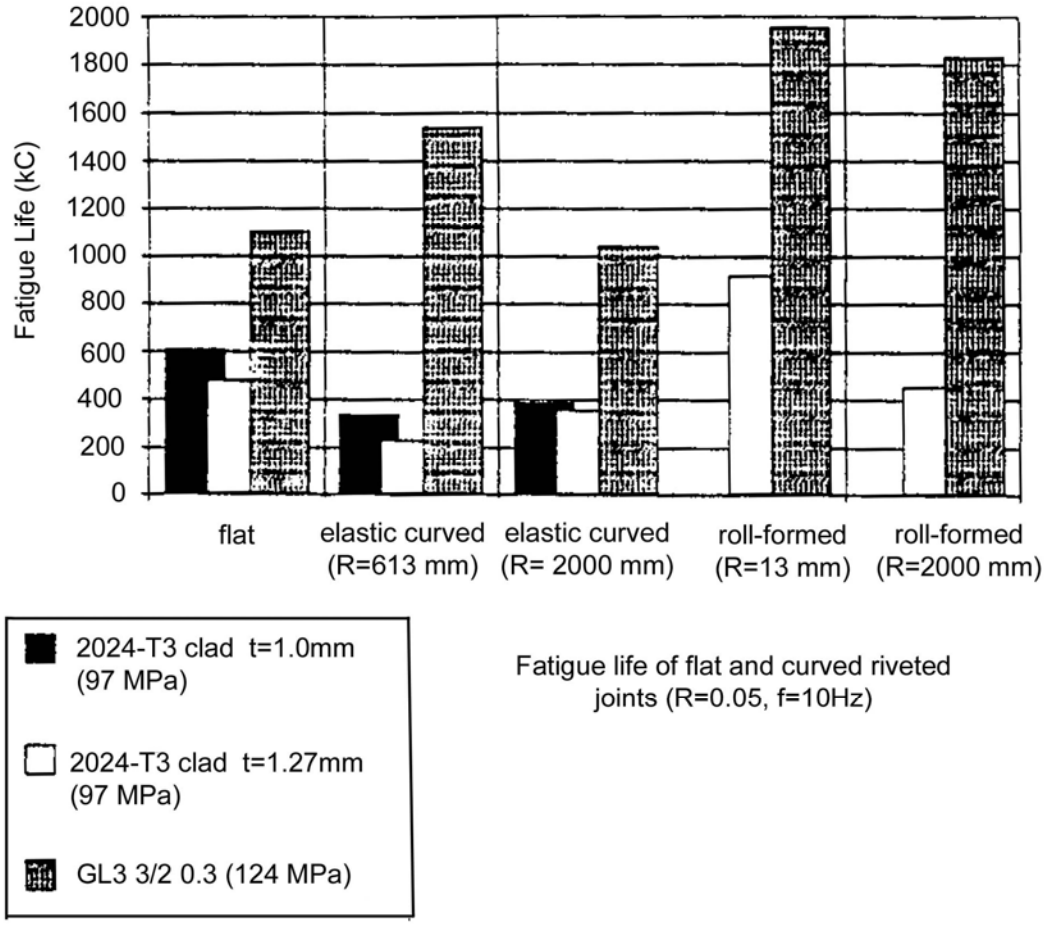

Figure 100.3-9 - FML: Fatigue of joints compared with 2024 alloy

100.4 Specialist properties

100.4.1 Damping

Damping characteristics of FMLs in the range 1Hz to 1kHz show two to three-times better damping than that of monolithic aluminium, with a 30% greater damping parallel to the fibres than in the transverse direction, Ref. [100-11].

100.4.2 Lightning strike

FML materials are reported to show resistance to zone II lightning strike, Ref. [100-11]. Whilst the external aluminium layer is damaged, the composite ply acts as an insulator preventing melting or puncture of the internal layers.

100.4.3 Fire resistance

GLARE laminates have excellent fire resistance characteristics. The fibre layers prevent flame penetration and panel decomposition, even when extensive damage (melting) of the aluminium sheet occurs at the exposed side.

Almost all GLARE 3 grades meet the FAA fire resistance regulations, i.e. materials capable of sustaining a flame of 1100°C for a period of 15 minutes without flame penetration.

Various GLARE 5 grades are for use in aircraft cargo areas. Of which, GLARE 5-FW for 'aircraft fire-wall liners' meets FAR 25.855.

GLARE 3 samples have successfully passed NASA flammability and offgassing tests, with ratings of 'A' and 'K', respectively. Owing to the 'K' rating, GLARE 3 is approved for use in the Space Shuttle manned areas, up to 45.5kg.

100.4.4 Impact properties

100.4.4.1 Impact characteristics

In ARALL and GLARE 3 the outer fibre layer, opposite to the impact side, fails first, immediately followed by failure of the aluminium layers. In GLARE, with unidirectional fibres, the outer aluminium layer, opposite to the point of impact, fail creating a crack in the fibre direction; the fibres remain intact, significantly improving the damage resistance.

Low- (<10 m/s) and high-velocity (<100 m/s) impact tests have been used to compare FML with monolithic aluminium alloys and carbon/thermoplastic composites, Ref.[12].

The damage resistance of GLARE 3 to low-velocity and high-velocity impact is superior to the base alloy 2024-T3 and carbon/PEEK, when expressed as the minimum cracking energy; as shown in Figure 100.4.1. This arises from the influence of strain rate on the strength of the glass fibre.

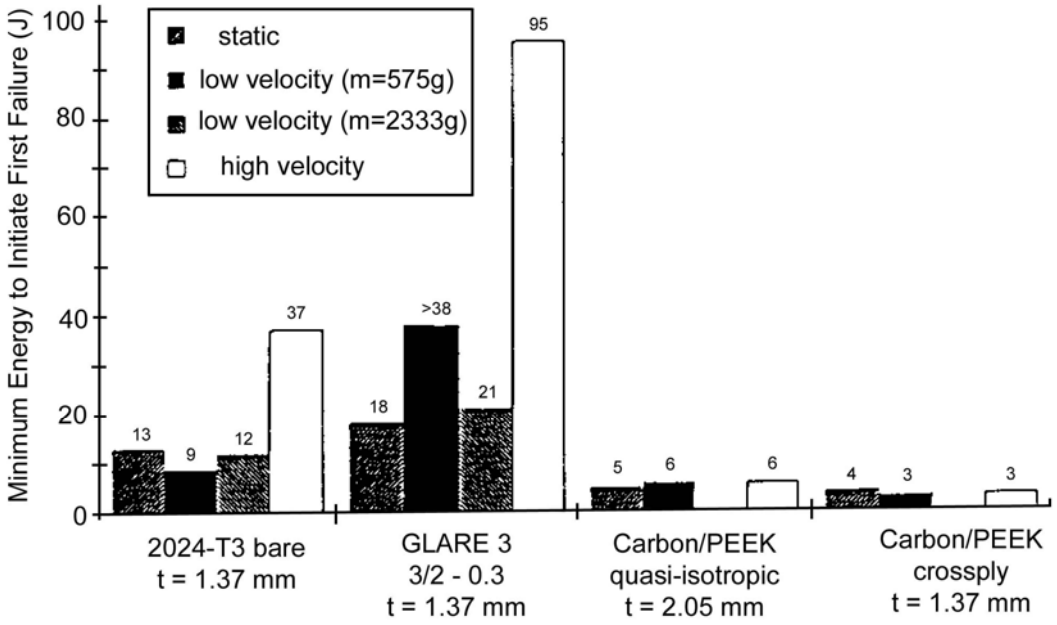

Figure 100.4-1 - FML: Low- and high-velocity impact resistance of GLARE 3 compared with 2024 alloy and CFRP

100.4.4.2 Low-velocity impact resistance

The main features of FML resistance to low-velocity impacts can be ummarised as, Ref. [100-12]:

- ARALL 2: The residual strength of the FML after low-velocity impact and fatigue is higher than the blunt notch strength, providing that no through-crack is present; as shown in Figure 100.4.2, Ref. [100-12].
- ARALL 3: Cracks which were caused by impact did not propagate during fatigue cycling.
- GLARE 3 3/2: Cracks were oriented parallel to the metal rolling direction. Crack propagation occurred only in the surface layer, as shown in Figure 100.4.3.

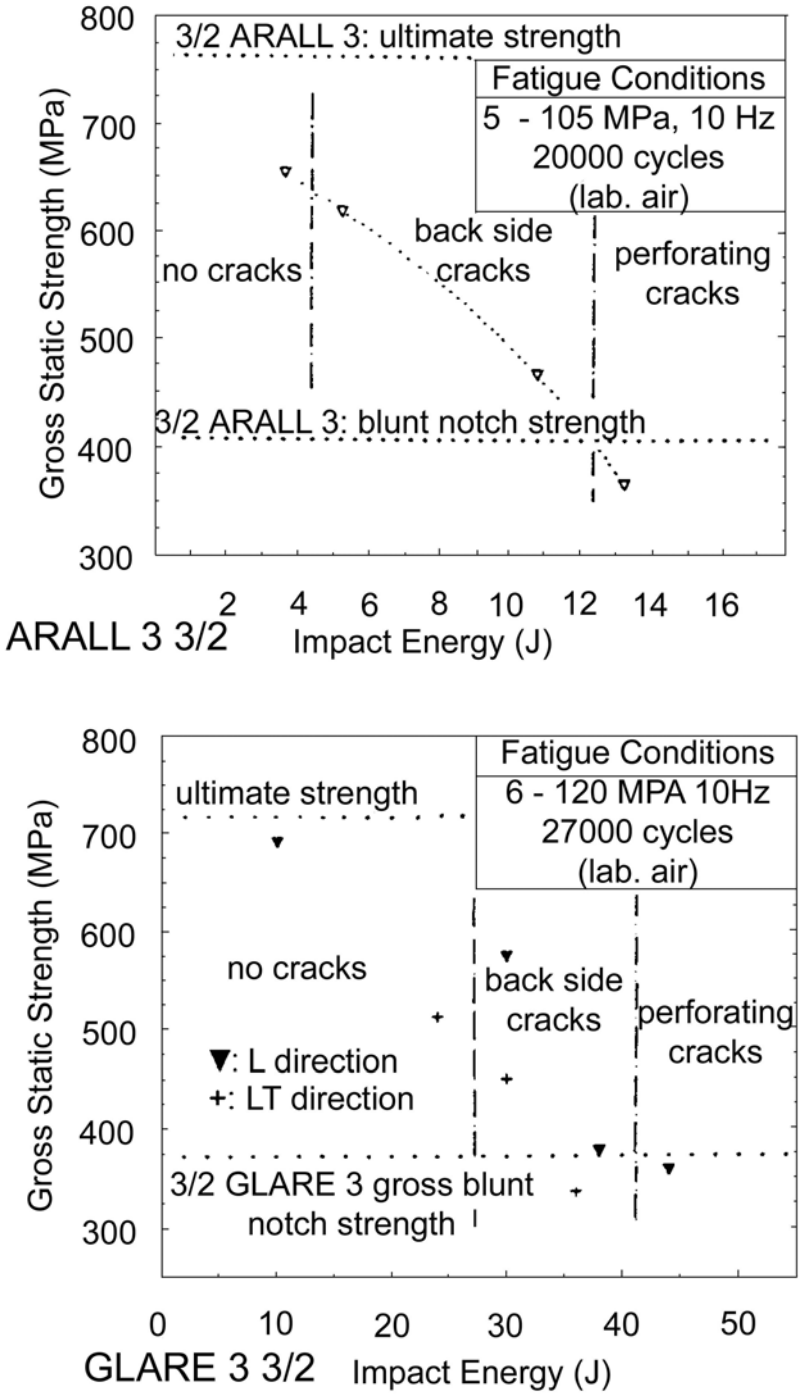

Figure 100.4-2 - FML: Residual strength after low-velocity impact and fatigue

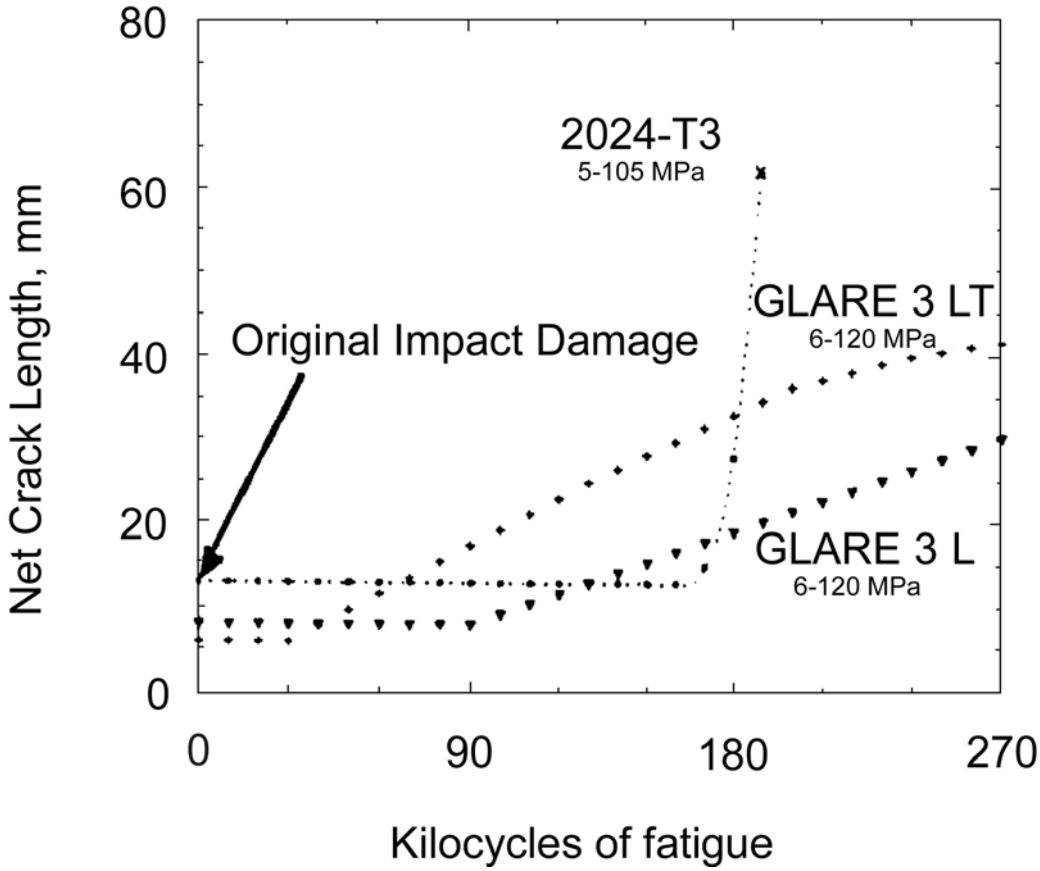

Figure 100.4-3 - FML: GLARE 3 3/2 crack growth during fatigue after low-velocity impact

100.4.4.3 Hyper-velocity impact resistance

Hyper-velocity impact tests, at speeds of 2.5km/s and 7km/s, on GLARE materials gave similar results to those for monolithic aluminium.

FMLs show less delamination after impact, compared with pure composites. Impact damage can be easily detected because of the dent in the outer aluminium layer.

100.5 Load transfer and design of joints

100.5.1 Bonded joints

100.5.1.1 ARALL

The static strength of adhesively bonded ARALL 1 single- and double-lap joints have been evaluated, Ref. [100-13]. Two ARALL 1 configurations were studied with various overlap lengths; 3/2 and 5/4 with laminate thicknesses of 1.35mm and 2.4mm, respectively. The results were compared with finite element and shear lag (based on failure of the adhesive) analyses.

The failure loads for ARALL 1 3/2 for both single-lap and double-lap joints were predicted accurately with the shear lag analysis; as shown in Figure 100.5.1, Ref. [100-13].

The predicted failure loads for the ARALL 1 5/4 single-lap joints, shown in Figure 100.5.2, were considerably higher than the experimental results. This premature failure is attributed to interlaminar tensile stresses within the prepreg layer closest to the bondline.

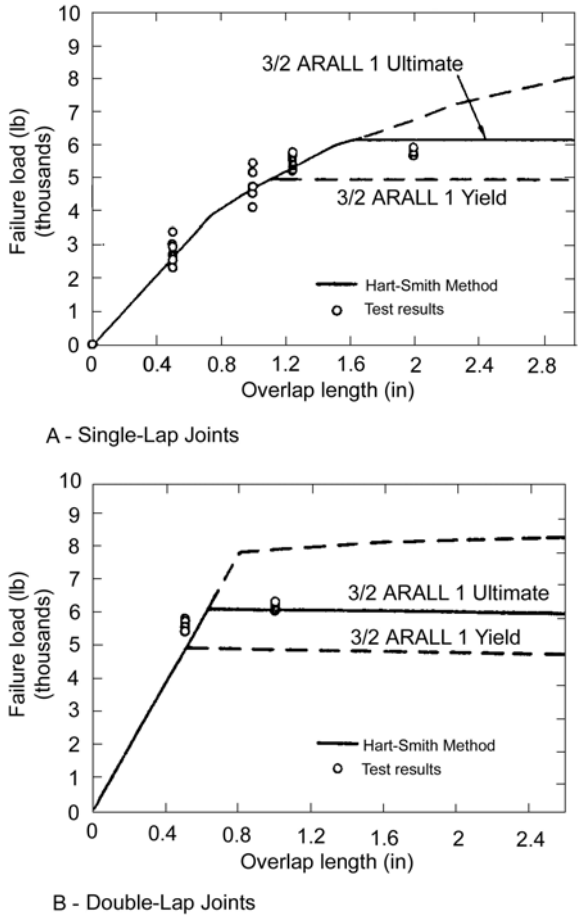

Figure 100.5-1 - FML: ARALL 1 3/2 bonded joint failure loads – Experimental results compared with shear lag analysis prediction

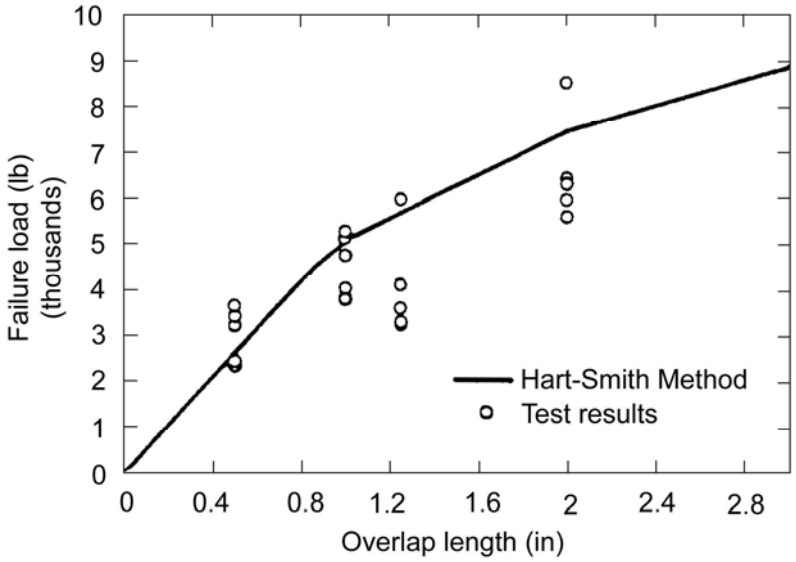

Figure 100.5-2 - FML: ARALL 1 5/4 bonded joint failure loads – Experimental results compared with shear lag analysis prediction

100.5.2 Mechanically fastened joints

100.5.2.1 General

As with composite materials, the bearing strengths of FML depend on a variety of parameters concerning the:

- material,
- fastener, and
- design.

100.5.2.2 Bearing strength

Parametric studies, Ref. [100-14], with analyses, Ref. [100-15], have been carried out. A bolt-type joint gives a bearing strength 20% higher than that of a pin-loaded joint when the full bearing strength is developed.

A minimum edge distance ratio (e/D) of 3, and width ratio (W/D) of 4, is needed to develop the full bearing strength.

Table 100.5.1 gives joint strengths for various FML grades.

Table 100.5-1 - FML: Typical mechanical joint strengths

FML Grade	Lay-up	Pin-type bearing	Bolt-type bearing	
		BUS (1) (MPa)	BUS(1) (MPa)	BUS(1) (MPa)
ARALL 2	3/2	563	492	727
ARALL 3	2/1	593	716	946
	3/2	556	615	825
GLARE 2	3/2 (0.3)	549	530	709
GLARE 3	2/1 (0.3)	-	-	856
	3/2 (0.3)	537	546	789
GLARE 4	3/2	510	518	658

Key: (1) BUS: Bearing ultimate strength

In Figure 100.5.3 the bearing strength of a 3/2 GLARE 2 laminate is given for various edge diameter ratios, e/D, and width diameter, W/D, ratios.

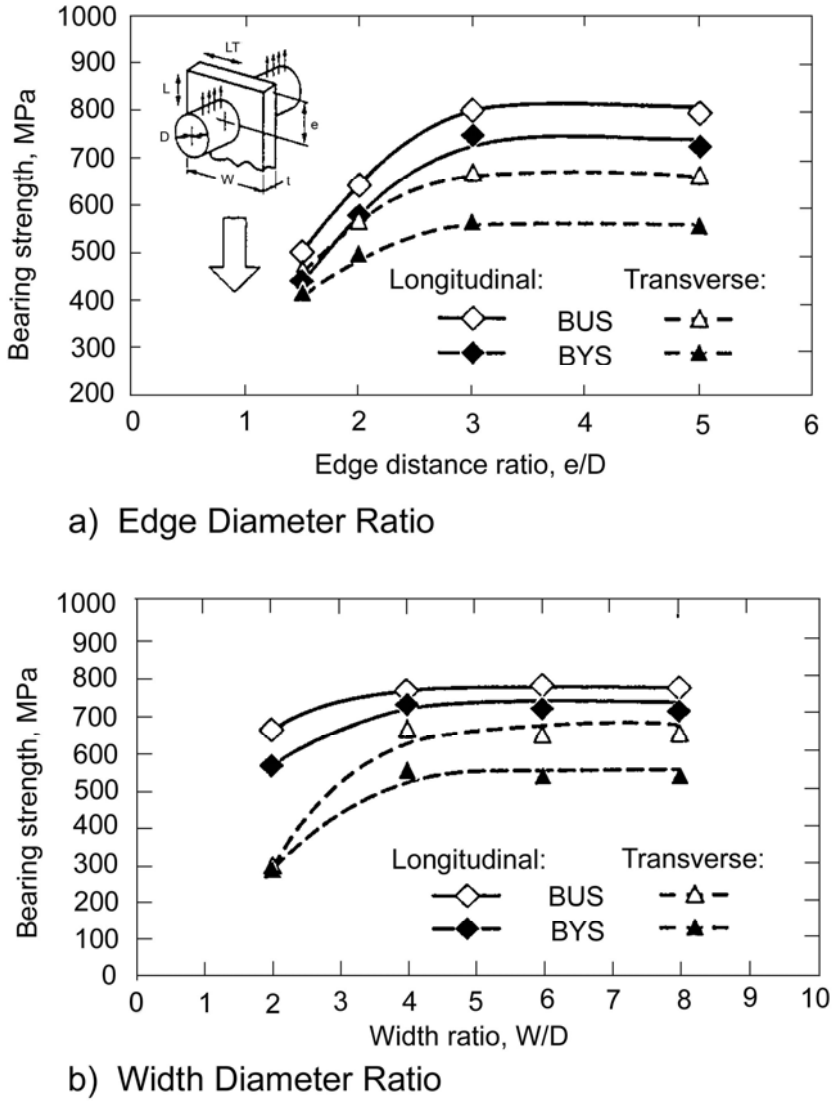

Key: BUS: Bearing ultimate strength; BYS: Bearing yield strength.

Figure 100.5-3 - FML: GLARE 2 laminate bolt-type bearing ultimate and yield strengths

The optimal efficiencies of the bolted joints can be summarised as:

- Long-transverse laminate: $D/W = 0.25$, and
- Longitudinal laminate: $D/W = 0.45$.

The values are shown in Figure 100.5.4 for GLARE 2 laminates and compared with those of ductile metal alloy, fibrous composite and brittle materials. This agrees with the Hart-Smith interpretation of bolted-joint data in various materials.

The bearing strength of a bolted-type joint can be predicted in a conservative and accurate way by a metal fraction approach, Ref. [100-15]. An increasing aluminium fraction provides increasing joint strength.

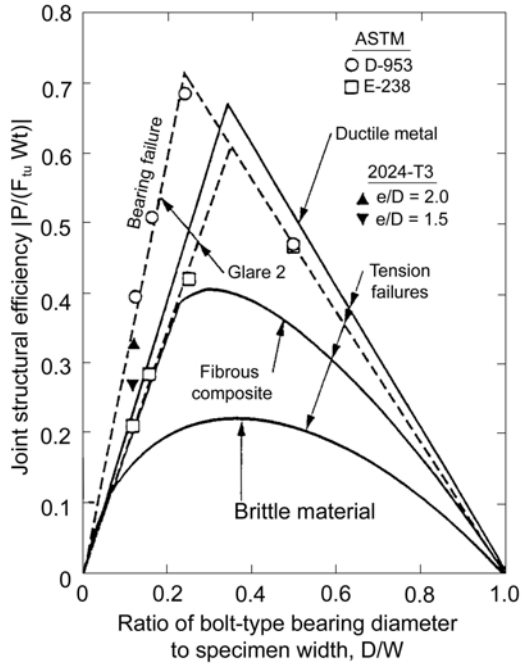

a) Long-transverse laminates

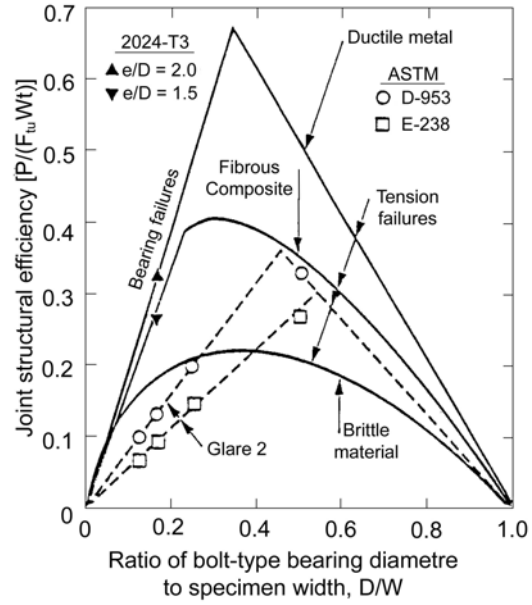

b) Longitudinal laminates

GLARE 2 laminates compared with ductile metal, fibrous composites and brittle materials

Figure 100.5-4 – FML: Comparison of the strengths of bolted joints for various materials

100.6 Manufacturing practices

100.6.1 General

Manufacturing practices for fibre metal laminates can be divided into three categories, Ref. [100-16]:

- forming.
- machining.

- joining.

[See also: 100.1 for manufacturing of FMLs]

100.6.2 Formability

100.6.2.1 General

The formability of an FML is strongly influenced by the mechanical properties of the laminate and its composition. Flow stresses and elastic moduli have their influence on the formability too, but they do not limit it. Forming processes are broadly classified by the shape of the component producible, i.e.:

- single-curved,
- double-curved.

100.6.2.2 Single-curved parts

The material is bent along straight bend lines. The radius of the bend can be:

- large, e.g. cylindrical shells.
- small, e.g. stringers.

Bending with large bend radii is easy but the fibre direction is important for small bend radii:

- parallel to the fibre direction results in minimum bend radii and springback angles, comparable to the aluminium constituents used in the laminate, e.g. 2024-T3 or 7475-T76.
- perpendicular to the fibres results in somewhat larger (20%) minimum bend radii and springback angles.

Examples of practical forming processes are:

- roll forming, using three or four rolls.
- brake-press bending.
- rubber-backed bending.

100.6.2.3 Double-curved parts

Strain is applied in two dimensions, therefore, only smoothly double-curved shells and stringers are feasible. Straining in the fibre direction results in considerable springback and an increase in internal stresses in the laminate.

Examples of practical forming processes are:

- stretch forming, and
- rubber pad forming.

100.6.3 Machinability

100.6.3.1 General

The machinability of FML is barely influenced by the mechanical properties of the laminate. In general, the machinability of FML is comparable to that of aluminium alloys. All machining processes need sharp tools with hardened surfaces, e.g. carbide tipped tools.

Examples of standard machining processes for FML are:

- drilling.
- routing.
- abrasive waterjet cutting.
- shearing.
- grinding.

100.6.3.2 Drilling and Routing

During machining, forces perpendicular to the sheet are avoided because these can result in edge delaminations. Therefore, during routing the helix angle is kept as small as possible. The feed rate is controlled carefully during drilling, especially for unsupported laminates.

100.6.3.3 Cutting laminates

Cutting by shearing is possible for laminates with 2/1, 3/2 or 4/3 lay-ups. For larger lay-ups, sawing or abrasive waterjet cutting is preferred. Cut edges can be ground to obtain the desired quality.

100.6.4 Joining

FMLs cannot be welded, but can be joined by mechanical fasteners (rivets and bolts) or by adhesive bonding, [See also: 100.5].

Conventional aluminium working equipment and processes are applied to FMLs.

100.6.5 Splice laminates

To reduce part counts, the use of splice laminates is a possibility. The seams in the individual aluminium sheets are at different locations such that they are bridged by fibre layers and by the adjacent non-spliced aluminium layers.

Spliced laminates have an improved performance parallel to the direction of the splice lines and a slightly decreased performance perpendicular to it.

100.7 Cost and availability

Commercial FML grades of ARALL and GLARE are manufactured and marketed by Structural Laminates Company; part of Alcoa. Stork Fokker, Papendrecht, NL, manufactures the GLARE grade used in the Airbus A380.

Before embarking on a design using FML, always contact the supplier for up-to-date information on products available and prices.

The price of FML as stock sheet is higher than for conventional sheet aluminium alloys. The actual price depends greatly on both the quantity and quality purchased.

As an indication only, FMLs are generally about six to eight times the price of monolithic aluminium sheet. Delivery lead times vary for standard FML grades and non-standard products:

100.8 Potential space applications

FMLs were primarily developed for aircraft applications needing improved resistance to cyclic loading compared with conventional aircraft grade alloys. Several FML grades have gained acceptance and are used for some aircraft structures, [See: 100.1].

The use of FML materials for space applications has been widely discussed, Ref. [100-17], [100-18], [100-19], [100-20].

Other than in spaceplanes or long-life structures, the demand for fatigue-resistant materials is not widespread in space structures. This removes the major reason for considering the use of ARALL or GLARE.

A study conducted for ESTEC concluded that, Ref. [100-20]:

- CARE grades of FML with carbon fibre-reinforcement, when available, were of potential interest because of their expected good compressive and shear performance.
- FML materials can be applicable in shear panels and fire walls.
- If single curvature structures are needed, then the cold-forming capabilities of FML panels can be attractive.
- FML panels have good acoustic damping characteristics.

In general, categorising FML materials in terms of their advantages and deficiencies is difficult; in some ways they behave like metals and in others as composites.

100.9 References

100.9.1 General

[100-1] MMPDS-01
Previously MIL-HDBK-5 ‘ Metallic Materials and Elements for Aerospace Vehicle Structures’: 'Aluminium Alloy Sheet Laminates', MIL HDBK-5F (Chapter 7.5), Change Notice 2, 15 December 1992

[100-2] C.A.J.R. Vermeeren: T.U. Delft, NL
'Application of Carbon Fibres in ARALL Laminates
T.U. Delft, Report LR-658, September 1991

[100-3] H.F. Wu et al
'A Pilot Study of Metal Fraction Approach for Fibre Metal Laminates'.
ALCOA Technical Center, ATC report 57-92-17
SLC report SL-020-B, December 1992

[100-4] C.A.J.R. Vermeeren et al
'New Developments in Fibre Metal Laminates'
Proceedings of Symposium 'Space Applications of Advanced Structural Materials', ESTEC, Noordwijk, 21-23 March 1990
ESA SP-303, p313- 318

[100-5] H.F. Wu & J.F. Dalton
'Effect of Elevated and Cryogenic Temperatures on the Tensile Properties of ARALL Laminates'

36th SAMPE Symposium and Exhibition, San Diego, 1991

[100-6] H.F. Wu
'Effect of Temperature and Strain Rate on Tensile Mechanical Properties of ARALL-1 Laminates'
Journal of Materials Science, Vol. 26 (1991) 3721-3729

[100-7] J.W. Gunnink
'Design Studies of Primary Aircraft Structures in ARALL Laminates'
Journal of Aircraft, Vol. 25, No. 11, November 1988

[100-8] J. Cook & M. Donnellan
'Flexural Fatigue Behaviour of ARALL Laminates'
N.A.D.C. Report NADC-90073-60, August 1990

[100-9] AKZO: Technical Information on GLARE, 1993
'Advanced Structural Materials for the Aerospace Industry'
Structural Laminates Company, leaflet 1993

[100-10] G.C. Salivar & C.A. Gardini
'The Influence of Stress Ratio and Temperature on the Fatigue Crack Growth Rate Behaviour of ARALL'
J. of Composites Technology & Research, vol. 15, no. 1, 1993

[100-11] L. Mueller: ALCOA
'ARALL - An Update'
ALCOA Aerospace Engineering, December 1987, p.33-40

[100-12] A. Vlot & R.S. Fredell
'Impact Damage Resistance and Damage Tolerance of Fibre Metal Laminates'. Proceedings of ICCM9, Madrid, 1993

[100-13] R.S. Long
'Static Strength of Adhesively Bonded ARALL-1 Joints'
Journal of Composite Materials, vol. 25, April 1991

[100-14] H.F. Wu & W.J. Slagter: ALCOA
'Parametric Studies of Bearing Strength for Fibre Metal Laminates'.
ALCOA Technical Center, ATC report 57-92-16
SLC report SL-019-E, November 1992

[100-15] W.J. Slagter
'On the Bearing Strength of Fibre Metal Laminates'
Journal of Composite Materials, Vol. 26, No. 17/1992

[100-16] J. Sinke: T.U. Delft, NL
'Manufacturing of Components of Fibre Metal Laminates: An Overview'. T.U. Delft, Dept. Aerospace, report LR-670

[100-17] A.I. Pendus et al
'Design Evaluation of GLARE Laminate Lay-ups'
Symposium. 'Advanced Materials for Lightweight Structures' ESTEC, Noordwijk, 25-27 March 1992
ESA SP-336, p301- 306

[100-18] C.A.J.R. Vermeeren et al
'Hybrid Materials for Use at Elevated Temperatures'
Symposium. 'Advanced Materials for Lightweight Structures' ESTEC, Noordwijk, 25-27 March 1992
ESA SP-336, p71- 78

[100-19] J.L. Verolme : T.U. Delft, NL
'The Compressive Properties of GLARE'

T.U. Delft, report LR-666, November 1991

[100-20] Stork Product Engineering, NL
'Possibilities for FML Applications in Space Vehicles'
ESTEC Contract 7090/87/NL/PP - Work Order No. 27

[100-21] B. Hussey & J. Wilson: RJ Technical Consultants, UK
'Light Alloys Directory & Databook'
Chapman & Hall (1998). ISBN 0 412 80410 7

[100-22] 'A380-800 Materials Overview'
Flight International (website),
Reed Business Publishing, 2005

[100-23] Stork Fokker, Papendrecht, NL, 2006

101 Hybrid laminates

101.1 Introduction

101.1.1 General

A hybrid composite is one that that consists of at least three constituent materials, i.e. distinct phases or combinations of phases, which are bonded together, e.g. thin metal sheet, polymer resin and reinforcement fibre.

In addition to the family of FML (fibre metal laminates), pioneered in the 1970s by Delft University of Technology, NL in collaboration with Fokker, [See: Chapter 100], another type of hybrid material is commonly-known as either HTCL (hybrid titanium composite laminates) or TiGr (titanium graphite laminates). Both terms refer to the same type of material, [See: 101.2].

Although the overall construction of HTCL is similar to FML, the composite phase is a carbon fibre-reinforced polymer prepreg rather than a fibre-reinforced adhesive layer, which was proposed for some development CARE® grades of FML having titanium alloy sheets, [See: Chapter 100].

The use of titanium alloy rather than an aluminium alloy is to improve the high-temperature performance. To achieve this, a high-temperature resin is used in the prepreg layer.

101.1.2 Development status

Development of HTCL or TiGr began in the late 1990s largely in response to aircraft designs needing higher-temperature performance from FMLs. United States Patents, assigned to The Boeing Company, describe titanium-polymer hybrid laminates, Ref. [101-1], [101-5].

As with the family of FMLs, the main perceived structural applications of HTCL or TiGr are the fatigue-sensitive areas of aircraft.

DLR, (Braunschweig, D), Ref. [101-2], [101-19], conducted a review of HTCL materials and have developed a concept for locally-reinforcing CFRP composites with titanium foils to increase the performance of mechanically-fastened joints in high load-carrying space structures, [See: 101.2].

101.2 HTCL hybrid titanium composite laminates

101.2.1 General

Aluminum-based materials are deemed unsuitable to meet the high temperatures anticipated for future military and commercial supersonic aircraft Ref. [101-5], [101-6], [101-7]. The development of HTCL hybrid titanium composite laminates was aimed at maintaining the advantageous characteristics of hybrid metal and fibre-reinforced plastics, already established for the aluminum-based family of FMLs, but for other applications that need structural integrity at temperatures of about 170°C; as experienced during supersonic flight, Ref. [101-2].

101.2.2 Construction

101.2.2.1 Laminate

HTCL hybrid titanium composite laminates are structural materials composed of thin sheets of titanium alloy bonded together by carbon fibre-reinforced high-temperature polymer prepregs; as shown in Figure 101.2.1, Ref. [101-2].

An HTCL laminate comprises:

- titanium alloy sheets,
- prepreg layer, containing the carbon-fibre reinforcement combined with a polymer resin,
- optional additional adhesive layers, to ensure bonding between the prepreg and the titanium sheets, Ref.[101-9].

101.2.2.2 Characteristics

In general, HTCL is more isotropic than conventional anisotropic composite laminates due to the transverse contribution of the metal sheets, Ref. [101-6].

The overall laminate mechanical properties are controlled by the titanium content and the composite ply orientation, as well as by the individual properties of the constituents. Titanium sheets are usually placed on the outer laminate surfaces to protect the inner composite plies.

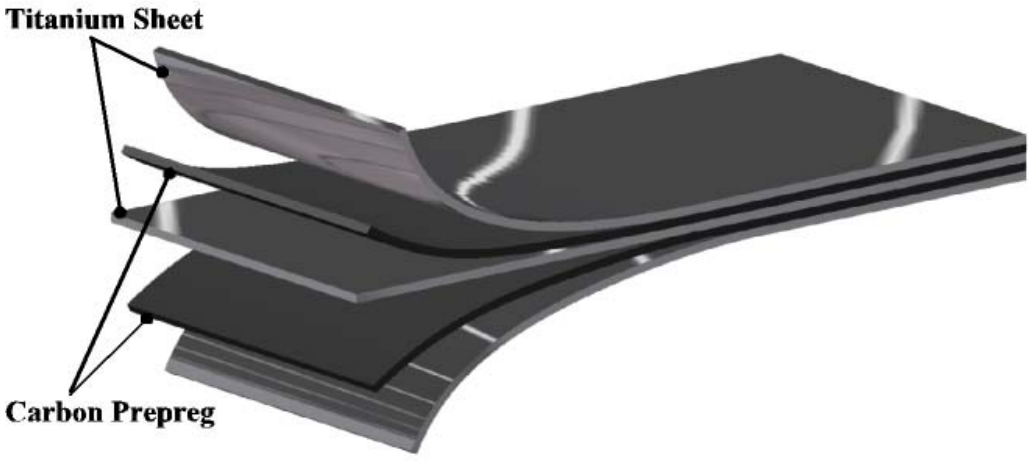

Figure 101.2-1 – HTCL hybrid titanium composite laminate: Schematic

101.2.2.3 Prepreg layers

The reinforcing fibres in the prepreg material are continuous and parallel. They are oriented in a single direction matching the cold-rolling direction of the titanium sheets, or in both the 0° and 90° directions. ±45°-plies are not necessary beacuse the shear strength and stiffness of the hybrid laminate are provided by the isotropic titanium material. The exclusion of ±45°plies also leads to better weight-efficiency because ±45° plies are always included as pairs to maintain a balanced and symmetric laminate, Ref. [101-8].

101.2.3 Constituent materials

101.2.3.1 General

The mechanical properties of a hybrid laminate are strongly dependant on the individual properties of the titanium alloy, fibre, matrix resin and the surface pretreatment of the titanium sheets.

The ultimate strength of a hybrid laminate is limited by the ultimate elongation of the brittle carbon fibres, which is of the order of 1.5% whereas the laminate yield strength is dictated by the yield strain of the titanium sheets.

101.2.3.2 Titanium alloys

During the initial period of HTCL development, the α+β-alloy Ti-6-4 (Ti-6Al-4V) was used, Ref. [101-10].

Ti-6-4 was replaced by the metastable β-alloy Ti-15-3 (Titanium 15V-3Cr-3Al-3Sn) as development continued. This alloy has good cold formability and high-temperature properties, [See also: Chapter 47].

The titanium sheets undergo a solution treatment, a cold-rolling process and a heat treatment in order to adjust the characteristics, Ref. [101-15]. The aim is to have a suitable microstructure and strength in order to achieve optimal yield strains and maximise the efficiency of the hybrid laminate, Ref. [101-9].

The thickness of titanium alloy foil layers is typically between 70µm and 250µm, Ref. [101-1], or at least 0.125mm, Ref. [101-16].

101.2.3.3 Prepreg plies

Carbon fibre-reinforced prepreg is placed between each titanium foil. The polymer composite layer can contain one or more plies, but is. typically 125 µm to 760 µm thick, Ref. [101-1].

101.2.3.4 Reinforcing fibres

The carbon fibres used are primarily intermediate modulus IM7, which have a elongation to failure of 1.5%, Ref. [101-2].

Both boron filaments and mixtures of carbon and boron reinforcements (HYBOR®, Textron Specialty Materials, USA) have also been considered, Ref. [101-1].

101.2.3.5 Resin systems

The choice of resin is largely determined by the temperature regime of the intended application, i.e.:

- high temperature applications, e.g. supersonic flight, have considered a number of high-temperature curing resin systems (up to 370°C), including:
  - thermoplastic polyimides, e.g. PIXA (Mitsu Toatsu, Japan), LARC-IA, PEEK, Ref. [101-8], [101-16], [101-17], [101-18].
  - pseudo-thermoset polyimides, e.g.PETI-5 (Fiberite Inc, USA), Ref. [101-8].
- 'normal' temperature applications have considered the use of toughened epoxies, which cure at 180°C, Ref. [101-9].

The strength and stiffness contribution of the resin to the overall laminate strength and stiffness is almost negligible. However, the resin contributes to the impact behavior, influences the

delamination growth rates and microcracking due to thermal cycling, so effectively determines the upper operating temperature of the hybrid laminate, Ref. [101-8].

The high curing temperatures result in residual stresses after curing due to the CTE-mismatch between the prepreg material and the titanium foils. In the 0° direction, the prepreg plies are under compression and the titanium sheets under tension. Post-cure residual stresses are deemed to be responsible for lower fatigue strengths of the hybrid material at lower temperatures, whereas higher operational temperatures reduce the residual stresses, Ref [101-6]. Residual stresses also affect stress concentrations at free edges and holes and can be a potential source of delamination.

101.2.4 Performance

101.2.4.1 Mechanical characteristics

Conventional titanium alloys are not considered the optimum material choice for long-life, weight-efficient aerospace structures, despite their higher thermal stability. Titanium alloys are expensive, the panel sizes are limited and they have a relatively low fatigue strength, which decreases as service temperatures increase, Ref. [101-10].

Compared with conventional alloys, laminates made of adhesively-bonded titanium sheets exhibit a considerable improvement in fracture toughness of 40%, increased fatigue life by an order of magnitude and reduced through-the-thickness crack growth rates of 20%, Ref. [101-11].

The inclusion of carbon fibres in the adhesive layers further improves the mechanical performance in terms of strength and crack grow resistance, Ref. [101-7]. The advantages of HTCL or TiGr over conventional titanium alloys include, Ref. [101-12]:

- higher specific strength and stiffness,
- superior fatigue performance,
- higher crack growth resistance.

HTCL offer advantages over CFRP composite materials, Ref. [101-2], e.g.:

- improved damage tolerance,
- easier damage detection,
- better thermo-mechanical endurance,
- lightning strike protection,
- better bearing and mechanical fastening capabilities, which are provided by the external titanium alloy sheets.

101.2.4.2 Crack propagation

The fibre bridging phenomenon, which is well known for FML materials, Ref. [101-13], is shared by HTCL. This means that the stresses at a crack in a metal sheet are transferred to the adjacent fibre layers through interlaminar shear. This results in a reduction of the stress intensity at the crack tip and an attenuation of fatigue crack propagation, Ref. [101-7], thereby shielding adjacent titanium sheets from the cracked sheet. Fatigue life improvements of two orders of mag-nitude have been reported, Ref. [101-10].

The presence of fatigue cracks does not threaten the structural integrity; even a laminate showing considerable fatigue deterioration is still capable of carrying loads. Complete laminate failure is expected to occur after failure of a sufficient number of composite layers, Ref. [101-4].

In contrast to the fatigue behavior of most homogeneous materials, cracks in titanium layers initiate and grow in an erratic and unpredictable way independent of one another. This means a precise definition of fatigue life does not exist, so stiffness reduction has been evaluated as a failure criterion, Ref. [101-14].

The bond strength between the titanium layers and the prepreg resin is deemed to be crucial in terms of an optimal structural performance and durability: whilst a high interface bond strength is optimal for load transfer and damage tolerance, a lower bond strength results in better fatigue behaviour by enabling controlled delamination and fatigue stress absorption, Ref. [101-7], [101-15], [101-10].

101.2.4.3 Environmental resistance

The outer surfaces of the hybrid material are usually chosen to be made of titanium. Consequently, the internal carbon fibre plies are protected from environmental effects such as moisture ingress, ultraviolet light and oxidation, as well as from attack by solvents, Ref. [101-5]. Owing to the electrochemical compatibility of both constituents, no galvanic corrosion is anticipated.

101.2.5 Processes

101.2.5.1 General

The choice of a manufacturing process and its process parameters has an important influence on the performance of the final product, Ref. [101-15], [101-16].

101.2.5.2 Surface preparation

Prior to manufacturing a hybrid laminate, the titanium surfaces are subjected to a pretreatment process to ensure a strong and durable bond is created between the titanium sheets and the prepreg resin. The bond is acheived by both mechanical interlocking through micro- and macro-roughness and by chemical bonds. A variety of pretreatment techniques have been used, e.g. TURCO® 5578 (Atochem, USA), Pasa-Jell 107 and SolGel. Of these, the TURCO surface treatment was preferred, Ref. [101-1]. The CAA chromic acid anodising process was also used, but processes using heavy metals are now limited by environmental restrictions.

101.2.5.3 Automated lay-up

A production technique for TiGr panels involves automated fibre placement of thermoplastic plies, with in-situ consolidation, Ref. [101-18]. A continuous carbon ply is produced from the successive lay-up of strips of prepreg tape directly onto the treated titanium surface using a thermoplastic fibre placement head. Heat and pressure are applied during the lay-up stage.

Titanium foils are then rolled out over the consolidated composite layer and co-bonded by the application of heat. Further prepreg tape is then applied to this foil, so the hybrid laminate is built-up layer by layer.

101.2.5.4 Consolidation

The consolidation process for hybrid laminates involves curing temperatures under pressure. This is usually conducted in conventional autoclaves or hot presses, Ref. [101-15].

Induction bonding has shown good potential in terms of low-cost fabrication of aircraft structures, Ref. [101-16].

101.2.5.5 Cylinders

To produce closed cylindrical skins, the ends of titanium foils are arranged as butt joints without overlapping but with minimal gaps. The butt joints are preferably offset and equally distributed around the circumference.

101.2.5.6 Inspection

The quality of the hybrid laminates can be determined using C-scan ultrasonic inspection techniques, Ref. [101-8].

101.2.6 Potential applications

101.2.6.1 General

The constituents materials, laminate configuration and the manufacturing processes should be be chosen for each application, taking into account the operational design stipulations, as well as manufacturing-related costs, Ref. [101-2].

101.2.6.2 Supersonic aircraft structures

HTCL material was originally developed as a structural material for supersonic aircraft structures, e.g. fuselage, wings, empennage, Ref. [101-5]. Both thin-gauge laminates and facings for honeycomb sandwich panels have been produced in HTCL, Ref. [101-18].

101.2.6.3 Lightweight structures

HTCL is also considered suitable for other applications that demand good lightweight performance, Ref. [101-9].

For space structures, where mass-efficiency is often important, once proven, the combination of mechanical and thermal performance offered by HTCL materials makes them a potential candidate for some reusable structures; either as entire assemblies or for local areas. One concern is the long-term fatigue performance of HTCL in structures experiencing large thermal excursions.

101.2.6.4 Local reinforcement

HTCL have been considered for attachment areas of highly-loaded composite structures; mainly to improve the efficiency of bolted joints, Ref. [101-19].

The incorporation of titanium foils locally using a ply substitution approach avoids the usual thickening of laminate and so provides weight-efficient joint design, [See: 101.2.7].

101.2.7 Example: Araine 5 composite booster root joints

101.2.7.1 General considerations

The move from steel booster cases to wound polymer composite was considered to meet the demands of mass-saving, increased operating pressure and reduced manufacturing costs. Although composite technology provides a number of benefits for large mass-sensitive structures, the practicalities of creating, inspecting, transporting and using such large structures means that joints remain a neccesity, Ref. [101-19].

Mechanically-fastened joints are widely used to assemble space structures because they provide a number of advantages over bonded or riveted joints, e.g. load-carrying capability and disassembly

for inspection. Whilst the design principles are known and proven for joints between metal components using threaded fasteners, [See: ECSS-E-HB-32-23], there are problems when designing mechanically-fastened joints in composites, [See: Chapter 22], e.g. notch sensitivity, shear and bearing strengths, dependence on composite lay-up, Ref. [101-19]. Such problems are often overcome by increasing the amount of composite present in the 'joint zone' in order to increase the load-bearing capacity.

For highly-loaded structural load-bearing joints, known as 'root joints', the increase in material can be considerable and impose mass-penalties arising from the extra material, associated metal parts and number of fasteners. Depending on where the extra material is applied, the geometry of the part itself and its adjacent component can have complex geometries that cause additional stresses, Ref. [101-19].

101.2.7.2 Concept

To improve joint efficiency in high load-bearing composite materials, an approach was to substitute composite plies for metal foils in the joint zone. The metal foils are embedded in the composite to form a locally hybrid material; as shown in Figure 101.2.2, Ref. [101-19].

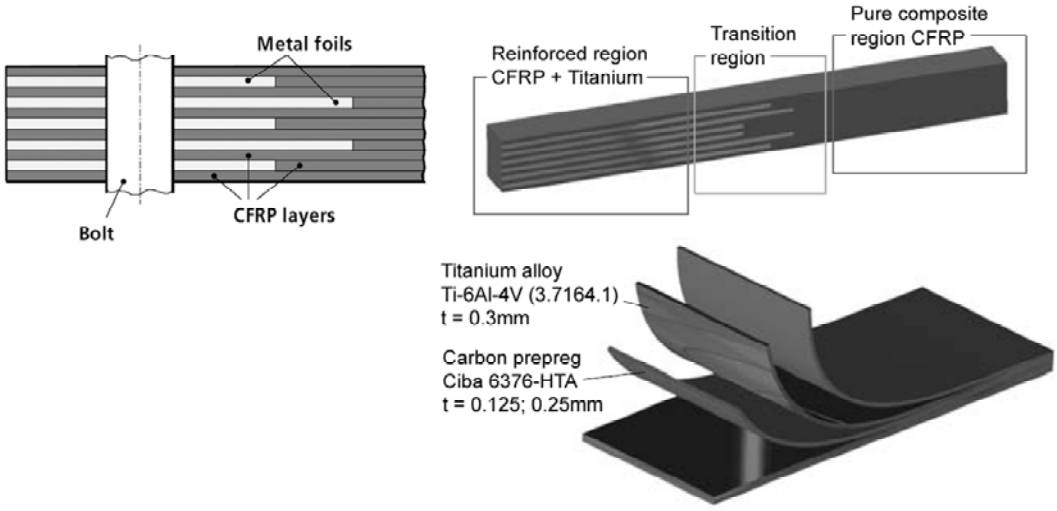

Titanium alloy: Ti6Al4V, 0.3 mm thick foils
CFRP: Ciba 6376C-HTA/HTS, 0.125mm and 0.25 mm thick plies
No additional adhesive used.

Figure 101.2-2 – Hybrid material: Schematic of locally-reinforced composite

The main features of the concept can be summarised as, Ref. [101-19]:

- no thickening of the joint zone, so avoids secondary stresses occuring due to changes in geometry.
- composite plies, carrying the majority of the load, are not interupted and load is transferred from 'all composite' to 'locally reinforced' regions.
- the metal foil thickness is determined by the thickness of the composite ply it replaces, so enabling a smooth transistion. A further consideration is the commercial availability and cost of the foils along with the manufacturing effort involved to locally reinforce the zone.

101.2.7.3 Conventional composite and hybrid joint designs

Figure 101.2.3 compares the 'conventional' all-composite joint design with a hybrid joint concept based on the advanced CFRP Ariane 5 booster case, Ref. [101-19].

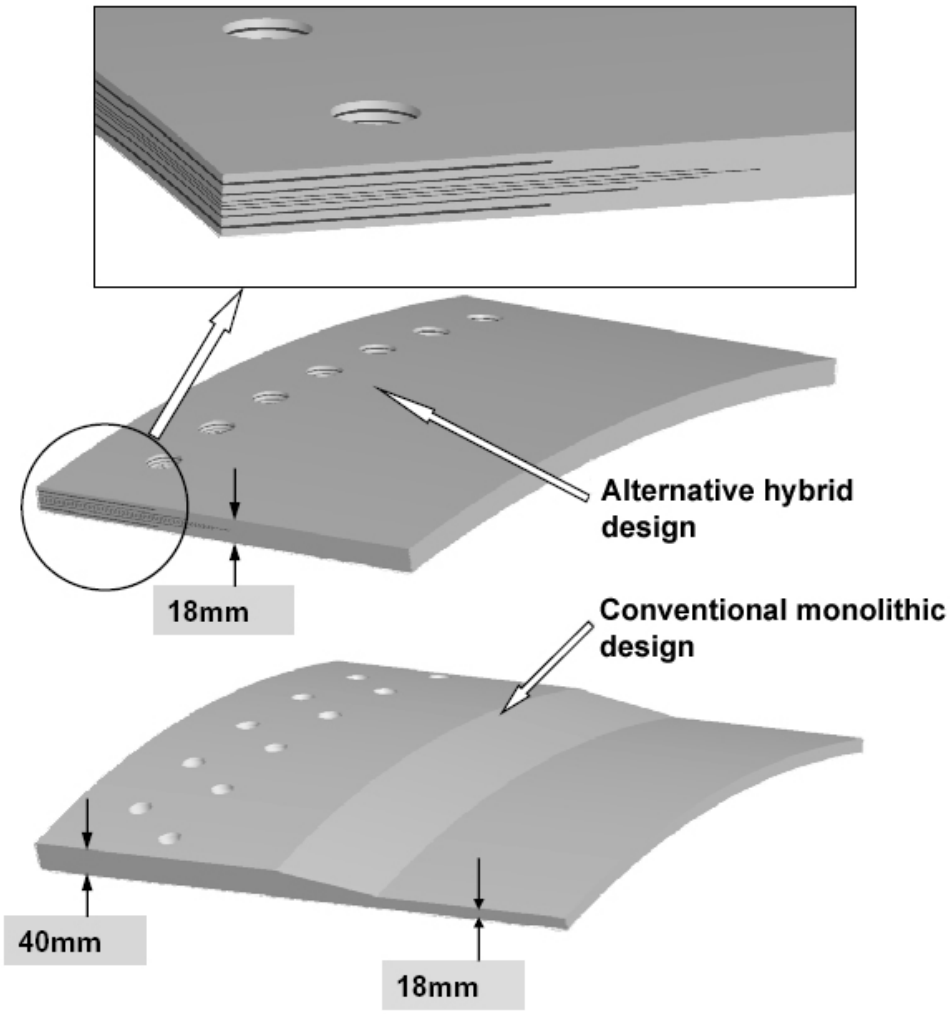

Figure 101.2-3 – Hybrid material: Ariane 5 composite boosters - Root joint concepts

Compared with the 'conventional' all composite joint, the advantages offered by the hybrid approach include, Ref. [101-19]:

- mass reduction of 35% for hybrid design.
- single row of holes due to improved joint strength, which provided mass-savings and reduced assembly costs.
- no overall increase in laminate thickness in the joint zone:
  - no load eccentricity due to geometry.
  - reduced through-the-thickness stress gradients (bolt bending reduced).
  - reduced thermal gradients during cure due to the presence of metal foils.
  - reduced post-cure residual stresses.

The main disadvantage highlighted was the potential increase in manufacturing effort needed to produce a locally-reinforced hybrid joint zone, Ref. [101-19].

101.3 References

101.3.1 General

[101-1] 'Titanium-polymer hybrid laminates'
United States Patent No. 5,866,272 (February 2, 1999)
The Boeing Company, US Patents Office website

[101-2] Axel Fink: DLR - Braunschweig (D)
'Hybrid Titanium Composite Material: Performance, Process and Applications'
Provided by DLR Institute of Composite Structures and Adaptive Systems, September 2005.

[101-3] C.A.J.R Vermeeren
'An Historical Overview of the Development of Fibre Metal Laminates'
Applied Composite Materials 10: 189-205, 2003.

[101-4] G. Lawcock, G
'Novel Fibre Reinforced Metal Laminates for Aerospace Applications - A Review'
SAMPE Journal, Vol.31, No.1, Jan/Feb 1995.

[101-5] U.S. Pat. No.6,114,050: Titanium Polymer Hybrid Laminates. Sep. 5, 2000: US Patents Office website

[101-6] WS Johnson & T Cobb
'Hybrid Titanium Composite Laminates: a new Aerospace Material'
NASA-Langley Research Center, 21st Annual Adhesion Society Meeting, February 22-25, 1998.

[101-7] DW Rhymer & WS Johnson
'Damage Fatigue Mechanisms in Advanced Hybrid Titanium Composite Laminates'.
Society for Composites, Technical Conference, 14th, Fairborn, Sept. 27-29, 1999.

[101-8] M Rommel et al
'The effect of Matrix Resins on the mechanical properties of Titanium/Composite Hybrid Laminates'
44th International SAMPE Symposium. May 23-27, 1999.

[101-9] U.S. Pat. No.5,578,384: Beta Titanium-Fibre Reinforced Composite Laminates. Nov. 26, 1996.

[101-10] JL Miller et al.
'Preliminary Evaluation of Hybrid Titanium Composite Laminates'
NASA Technical Memorandum 109095, April 1994.

[101-11] WS Johnson
'Damage Tolerance Evaluation of Adhesively Laminated Titanium'
Journal of Engineering Materials and Technology,
ASME 105, 182-187, 1983.

[101-12] E Li
'Residual Tension Strength of Fatigued Open-Hole Titanium-Graphite Hybrid Composite Laminates'
AIAA/ASME /ASCE/AHS pp. 2089-2105, 1998.

[101-13] A. Vlot & JW Gunnik
Fibre Metal Laminates - an Introduction'
Kluwer Academic Publishers, 2001.

[101-14] A Burianeck & M Spearing
'Fatigue Damage in Titanium-Graphite Hybrid Laminates'
Composites Science and Technology 62, 607-617, 2002.

[101-15] E. Li. et al
'An Evaluation of two Fabrication Methods for Hybrid Titanium Composite Material'
Composite Materials: testing and design, Vol. 13
ASTM STP 1242, p 202-214, 1997.

[101-16] JA Hinkley & NJ Johnston
'Utilization of Induction Bonding for Automated Fabrication of TIGR'
NASA/TM-1999-209123, April 1999.

[101-17] WS Johnson & E Li
'High temperature Hybrid Titanium Composite Laminates: An early Analytical Assessment'
Applied Composite Materials 3, 379-390, 1996.

[101-18] MA Lamontia et al
'Stringer-, Honeycomb Core-, and TiGr-Stiffened Skins, and Ring-Stiffened Cylinders Fabricated from Automated Thermoplastic Fibre Placement and Filament Winding'

[101-19] A Fink & B Kolesnikov: DLR - Braunschweig (D)
'Hybrid Titanium Composite Material Improving Composite Structure Coupling'
Proceedings of European Conference on Spacecraft Structures, Materials and Mechanical Testing, ESTEC, Noordwijk 10-12 May, 2005; SP-581 (CDROM)

101.3.2 ECSS documents

[See: ECSS website]
ECSS-E-HB-32-23 Threaded fasteners handbook

102 Carbon nanotechnology

102.1 Introduction

102.1.1 General

102.1.1.1 Technology review

In 2006, EADS-Astrium GmbH conducted a review of worldwide research activities into nano-composite materials with potential applications in space. This study involved screening a large number of publications and also considered internally-funded nano-technology program activities, together with contributions to ESA TRP- and Triangle Programs dedicated to nano materials, Ref. [102-1].

102.1.1.2 Demonstrator study

As part of ESA's ongoing nano-material evaluation programme, one study, Ref. [102-3], targets composite materials employed in spacecraft platforms and payloads and how developments in carbon fibres and nano-technologies can be applied, e.g. new generation pitch-based carbon fibres, [See: 3.3]; nano-species, mainly CNT carbon nano-tubes and nano-fibres for modified polymer resin systems; (nano-) carbon foams, [See: 103.2]. The aim is to assess and demonstrate improvements in performance offered by these materials in specific spacecraft elements, e.g. thermal radiators, antenna reflectors, deployable arms, low-CTE waveguides, [See: 102.3].

102.1.2 Nano material technology status

102.1.2.1 Types of nano fillers

The field of nano materials is wide, complex, and because of its tremendous variety, not easy to assess. General research into nano composites has produced numerous publications. Researchers have used many different micro and nano fillers for mechanical and thermal improvement of matrix materials, e.g. soot, organo-clay, ceramic powders, diamond powder and many others. Owing to the large number of publications concerning such materials with 'classical' nano-fillers, the review focused only on composites modified with carbon nano tubes (CNTs) because of their potential for space applications, [See: Chapter 103; See also: 43.10].

The term nano-technology applies not only to engineering material developments, but also electronics, including smart technologies (sensors and actuators). Some nano-materials are promoted for both engineering and electronics.

102.1.2.2 Material characteristics

Since the field of research is new and rapidly evolving, it is difficult to predict the achievable targets in terms of the features and material properties of nano composites. A number of contemporary publications provide enthusiastic, very optimistic and sometimes exaggerated claims, such as 'a break-through in material development'.

102.1.2.3 Potential space applications

Nano composites appear attractive for space applications, but because the technology is rapidly evolving, results need to be regularly assessed and actual progress monitored with regard to potential space applications.

102.1.3 CNT-modified composite materials

102.1.3.1 Technology review

CNT-modified composites appear generally attractive for space applications. The 2006 technology review, Ref. [102-1], provided a realistic estimate of the technological readiness of different types of CNT-modified composite materials:

- CFRP and polymer matrix materials, [See: Chapter 104].
- metallic materials, [See: Chapter 105].
- ceramic materials, [See: Chapter 106].

102.1.3.2 Demonstrator study

The demonstrator study, Ref. [102-3], evaluates the replacement of some CFRP composite parts of telecommunications satellites using CNT-modified materials, [See: 102.3].

Other ESA-studies on nano-modified MMCs and CMCs for thermal control and stability applications include, Ref. [102-10]:

- light truss structure with possible integrated health monitoring system.
- lightweight optical elements, mirrors and reflectors.
- thermal protection systems and hot structures.
- thermal control elements, heat pipes, heat sinks and improved radiators.
- components for microwave and antennas.

Nano-modified materials for applications where fire resistance or ablative characteristics are needed have also been considered.

102.2 European sources of expertise

102.2.1 Research and commercial sources

Table 102.2.1 provides an alphabetical list of European-based companies and organisations having expertise in various aspects of carbon nano technologies.

Table 102.2-1 – European sources of expertise

Centre of Expertise Contact details	Materials	Activities	
		Research	Commercial producer
Altropol Kunststoff GmbH Daimlerstraße 9, D-23617 Stockelsdorf, Germany Tel:+49 451 49960-0 http://www.altropol.de/english/portrait	Polymer nanocomposites Epoxy, Polyurethane	•	•

Centre of Expertise Contact details	Materials	Activities	
		Research	Commercial producer
site.html			
ARC Seibersdorf Research GmbH Abteilung Materials Microengineering Funktion Scientist Metal Matrix Composites, Austria Tel: +43 (0) 50550 3345 Fax +43 (0) 50550 3366 http://www.werkstofftechnik.at/default.asp?mode=jumplang&id=141&lid=2 Email: Erich.Neubauer@arcs.ac.at	Metal nanocomposites Metal Matrix Composites, Composites based onCarbon Nanotubes	•	
BOOSTEC S.A Zone Industrielle F-65460 BAZET, France Tel: +33 (0)5 62 33 45 00 Fax: +33 (0)5 62 33 45 05 http://www.boostec.com/contact.htm	Ceramic nanocomposites based on SiC	•	
Chemical Research Center, Hungarian Academy of Science, Institute of Materials and Environmental Chemistry, H-1025 Budapest, Pusztaszeri út 59-67; P.O. Box: H-1525 Budapest, Pf. 17. Hungary Tel: +36-1 438-1130 http://www.chemres.hu/MENU/ENG/research/imec.htm Email: szepvol@chemres.hu	Polymer, Metal & Ceramic nanocomposites micro- and nanostructured monolithic and composite materials, metallic structural materials, and also micro- and nanosized ceramic powders and ceramics produced from them.	•	
Degussa AG Business Unit High Performance Polymers(HPP) Degussa GmbH, Postfach 30 20 43, D-40402 Düsseldorf, Germany Tel: +49-211-65 041-341 Fax +49-211-65 041-523 http://www.degussa-hpp.de/ http://www.degussa.de/degussa/de/unternehmen/unternehmensstruktur/specialty_materials/high_performance_polymers/ Email innovation-info@degussa.com	Polymer nanocomposites High performance polymers: Polyamides Polybutylenterephthalate Polyphenylenether Polyvinylidenfluoride Polyetheretherketone	•	•
Fachhochschule Nürnberg Fachbereich WT Postfach D-90121 Nürnberg, Germany Tel: +49 (0) 911 / 5880 - 1372 Fax: +49 (0) 911 / 5880 - 5177 http://www.fh-nuernberg.de/index.php?id=3988 Email: thomas.frey@fh-nuernberg.de	Ceramic nanocomposites based on SiC	•	
Future Carbon GmbH Gottlieb-Keim-Straße 60 D-95448 Bayreuth, Germany	Carbon Nanotubes Carbon nanofelts, Carbon nano tube-modified	•	•

Centre of Expertise Contact details	Materials	Activities	
		Research	Commercial producer
Tel: +49 921 50736 158 Fax +49 921 50736 159 http://www.future-carbon.de/englisch Email: info@future-carbon.de	polymer resins		
IFW Institut für Festkörperforschung Dresden Helmholtzstraße 20 D-01069 Dresden, Germany Tel: +49 (0) 351 4659 388 http://www.ifw-dresden.de/institutes/iff/org/members/taeschner/?set_language=de Email: C.Taeschner@ifw-dresden.de	Fullerenes Nanotubes and peapods (synthesis and evaluation)	•	
Institut National des Sciences Appliquées de Lyon Physique et Physique des Matériaux Groupe d´Etudes de Métallurgie 20, avenue Albert Einstein F-69621 Villeurbanne cedex Tel: +33 (0)4 72 43 88 03 - http://www.cge.asso.fr/ecoles/ECOLE155.phtml Email. : Jean-yves.cavaille@insa-lyon.fr	Polymer nanocomposites	•	
Neue Materialien Würzburg GmbH Friedrich Bergius Ring 22a D-97076 Würzburg, Germany Tel:+49 (0)9 31 / 23 00 96 21 Fax +49 (0)9 31 / 23 00 96 18 http://www.nmwgmbh.de/wuerzburg/testframe.htm.htm Email: info@nmwgmbh.de	Polymer nanocomposites Carbon nanotube modified polymer resins	•	•
Technical University Hamburg-Harburg **TU Hamburg-Harburg** AB 5-09 Denickestraße 15 D-21073 Hamburg, Germany Tel.: +49-40-42878-3238 http://cgi.tu-harburg.de/~kvwww/	Polymer nanocomposites, Thermoplastics modified by CNTs	•	
University of Cambridge Department of Materials Science and Metallurgy University of Cambridge Pembroke Street Cambridge CB2 3QZ, UK. Tel: +44 1223 334300 http://www.msm.cam.ac.uk/Department/DeptInfo/StaffProfiles/Windle.html Email: web-responses@msm.cam.ac.uk	Polymer nanocomposites Carbon nanotubes Modelling/Analysis	•	

Centre of Expertise Contact details	Materials	Activities	
		Research	Commercial producer
University of Dublin Materials Ireland Polymer Research Centre Physics Department Trinity College Dublin, Eire Tel: +353-1-608 1708 Fax: +353-1-671 1759; http://www.tcd.ie/Physics/Molecular_Electronics/ Email: wblau@tcd.ie	Polymer nanocomposites	•	
University of Manchester Polymer Science and Technology, Oxford Road Manchester, M13 9PL, UK Tel: +44 (0) 161 306 6000 http://www.materials.manchester.ac.uk/content2/research/groups/nanostructured.html	Polymer nanocomposites	•	
University of Sussex Fullernence Science Centre School of Chemistry Physics and Environmental Science, Sussex House, Brighton, BN1 9RH, UK Tel: +44 (0)1273 606755 http://www.sussex.ac.uk/Users/kroto/FullereneCentre/people/index.html Email: information@sussex.ac.uk	Fullerenes	•	
Vienna University of Technology, Institute of Chemical Technologies and Analytics Division Chemical Technologies 164-CT Research Group Nano-Materials Getreidemarkt 9 A-1060 Vienna, Austria Tel: +43/1/58801-16135 Fax: +43/1/58801-16199 http://www.cta.tuwien.ac.at cedtmaie@mail.zserv.tuwien.ac.at	Metal nanocomposites Nanocomposites, Metal Matrix Composites (aluminium-, magnesium-, silver)	•	

102.2.2 General information sources

European CNT network: http://www.cnt-net.com/

European ExtreMat project: http://www.extremat.org/

102.3 Demonstrator study CNT-modified CFRP

102.3.1 General

The demonstrator study, Ref. [102-3], evaluates the replacement of some CFRP composite parts of telecommunications satellites with CNT-modified materials. The study aims to assess and demonstrate the improvements in performance offered by using these materials in specific spacecraft elements, e.g. thermal radiators, antenna reflectors, deployable arms, low-CTE waveguides.

102.3.2 Approach

The study combines research, selection and application of the candidate materials with the design, manufacture and testing of a breadboard. The work concludes with an evaluation of the feasibility of the concept including the performance and potential cost advantages of introducing these materials.

The main objectives of the study are summarised as:

- identify the structural elements and payload components of telecommunications spacecraft which can be selected for study of the performance improvement and cost reduction potential offered by nano-materials.
- establish the reference materials for comparison purposes and propose candidate new materials.
- trade-off, design, analyses and test an 'Elegant Breadboard Model' constructed on the basis of nano-materials developed by European companies. In principle, the new materials use carbon nano-tubes (CNT) and nano-fibres for modified composites and carbon foams.
- provide preliminary procurement specifications, manufacturing procedures, testing procedures and reference data with the purpose of establishing reliable and repeatable processes.

102.3.3 Composite element characteristics for spacecraft and payloads

Current CFRP structural elements that have a significant effect the structure sub-system (primary, secondary and tertiary structures) and payload performance are of interest as 'candidate applications'.

The mechanical, thermal and electrical properties of current CFRP structural elements used in spacecraft platforms and payloads are the means of comparison between candidate nano-materials, including:

- mechanical properties (stiffness, strength and dimensional stability): including central cylinders, shear panels, equipment supporting panels, external panels, tubes, deployable booms, structural adhesives, fittings, brackets, inserts.
- thermal properties (glass transition, service temperature limits, thermal conductivity, heat capacity): including thermal radiators, antenna reflectors, deployable booms and spacecraft external panels. In the case of antenna reflectors, improvements in thermal stability and glass transition temperature can enhance the performance and simplify designs. In the latter case, the interest is in accommodating heat pipes, replacing the aluminium face-sheets of sandwich panels with CFRP skins by improving the transverse thermal conductance and correctly accommodating the CTE mismatch.

- electrical properties (electrical conductivity, RF depolarisation, reflection and ohmic losses up to Ka band): including CFRP waveguides, feed horns, equipment housings and antenna reflectors. These components and equipment, when made of CFRP, need better EMC, ESD and RF performances. A clear case is the conductivity transverse to the fibres and the impact of anisotropic material properties in electrical performances.

102.3.4 Materials and process aspects

102.3.4.1 Conventional materials

The materials and processes used to produce flight-approved, conventional, CFRP structural elements are well established and documented, hence they form the baseline for performance comparison against nano-materials.

Generally the conventional CFRP composites consist of a commercial grade of PAN carbon fibre, e.g. M55J, combined with a thermosetting resin, usually epoxy but possibly cyanate ester, to form a prepreg (unidirectional or fabric) which is then used to produce a laminate or combined with a core material to make a sandwich panel. Cores are usually metal or composite honeycombs.

102.3.4.2 New materials

Potential new materials, and the associated processes, for 'replacing' conventional CFRP components can be summarised as:

- Nano-species
- pitch-based carbon reinforcement fibres: Some commercially-available grades of pitch-based carbon fibres offer higher stiffness and thermal conductivity than traditional PAN fibres that, for structural and thermal components, can provide better performances, [See: 3.3].
- carbon foams made from nano-species, [See: 103.2], can offer better properties than commercially-available carbon foams, [See also: 43.10], e.g. better thermal stability; increased thermal conductivity; less brittle. These characteristics make them of interest for stable core materials for antenna reflectors.
- other materials, e.g. thermoplastics, MMCs and CMCs have been the subject of other ESA-studies, Ref. [102-10], for thermal control and stability applications, [See also: Chapter 105 for MMC; Chapter 106 for CMCs].

102.3.5 Nano-species

The modification of resin systems for structural components by adding CNTs has beneficial effects even at low-to-moderate volume fractions. Electrical and thermal conductivity are enhanced, glass transition temperature is increased, behaviour at low temperature is improved and lower thermal expansion is achieved. Also stiffness, strength, toughness and damping of composite structures can be improved. Therefore, this approach can be seen as a straightforward way of extending the service range of established resin systems used in space.

Nano-species of diverse types, forms and quantities have been combined with various thermosetting resins producing various modifications to the properties of the base resin, [See: 104.2]. Published research also describes the effects of adding different types of nano-species to the same base resin, Ref. [102-12]. More recent studies have adopted an engineering approach to measure the properties of CFRP with different amounts of the same nano-species. For example, a Japanese project on composite for airframes considered a nano-modified CFRP: T700CS carbon fibre, EP827 epoxy resin, containing CSCNT 'cup-stacked carbon nanotube' dispersions with additions of 0%, 5% and 10% by weight, Ref. [102-11]. Although most modifications are beneficial to some extent, it is equally important to establish that no deleterious effects occur.

102.3.6 Manufacturing processes

It is unlikely that nano-modified thermoset resins can be used in existing manufacturing processes without some modifications, e.g. prepregging, lay-up (manual or fibre placement), filament winding, [See: Chapter 38]. New processes, or modifications of conventional ones, will probably be required. Not only does resin viscosity increases significantly with small additions of nano-materials, but the nano-fillers can agglomerate during conventional processing steps, e.g. degassing of resins or vacuum-assisted impregnation techniques.

Calandering-type techniques have been found to give even dispersions in thermoset resins, Ref. [102-8], as have combinations of mixing and wet-milling, Ref. [102-11].

Fibre reinforcements can tend to act as filtering media, disrupting the dispersion of nano-fillers within resins during composite manufacture. Although they are common industrial practices for composites, resin injection processes, such as RTM (and its derivatives) and pultrusion, are not widely used for space structures, mainly because their advantages are in the production of numerous identical parts, [See: 38.7].

102.3.7 Specification of nano-materials and processes

Basic materials procurement specification, manufacturing process specification and testing to known standards or accepted analysis techniques are essential for enabling new materials and processes to achieve space approval. This also applies to materials having a known history in space that have been subsequently modified, e.g. conventional space-approved epoxy-resin matrix material with additions of carbon-based nano material.

Materials and process specifications include very precise details of all aspects that can vary and so affect the final performance of the composite, including:

- nano-material (base material, form, shape, supplier code, supplier details, second source, chemical analysis (purity - impurities), surface condition, nano-material size distribution and all associated accept / reject criteria), Ref. [102-13].
- health and safety aspects, including manufacturer's materials safety sheet, toxicology, measurement and conformance with workplace exposure levels, Ref. [102-9], [102-14].
- base resin specification and all associated accept / reject criteria, including volume of specified nano-material present, expressed as volume or weight percent and tolerances), [See: 36.3].
- fibre reinforcement, [See 36.4].
- nano-modified thermosetting resin, [See also: 36.3]:
  - uncured: e.g. rheological characterisation (by testing), nano-material content and dispersion,
  - cured: analytical techniques, e.g. for thermal and dynamic analysis (DSC, TMA, TGA and DMA as needed) to measure residual curing, rate of curing, exothermic behaviour, glass transition temperature, volatile content, porosity and thermal stability.
- mixing and dispersion of carbon nano particles in the fluid matrix or film. Microscopic characterisation employing e.g. SEM and XRD (also in the presence of carbon fibres).
- process specification for methods used to combine nano-modified resin and fibre reinforcement, and tolerances on process conditions, e.g. times, temperatures, pressures.
- cure process (cure cycle) determined on the final composite.

102.3.8 Testing

102.3.8.1 Standards

The test standards for conventional aerospace CFRP composites can be considered for use with nano-modified materials. This also aids direct comparison between conventional and new materials, [See: Chapter 7].

The anisotropy in mechanical, electrical and thermal properties of composites needs to be taken into account during testing programmes.

102.3.8.2 Laminate test samples

For unidirectional laminates, properties are needed for both the 0° and 90° directions.

For multilayer and multidirectional laminates, through-the-thickness properties are of interest because nano-modification is seen as a means of improving the through-thickness 'weaknesses' of conventional laminated composites:

- mechanical properties, including tensile strength and Young's modulus, compressive strength and Young's modulus, 3-point bending, CTE coefficient of thermal expansion (in-plane), CME coefficient of moisture expansion (in-plane).
- thermal properties, including verification of thermal limits (maximum and minimum service temperatures), Tg - glass transition of composite, thermal conductivity (in 3 directions), thermal heat capacity.
- electrical properties, including electrical conductivity (both along and across the fibre directions), RF reflection loss in Ku, Ka and Q bands, depolarisation in Ku, Ka and Q bands.

102.3.8.3 Sandwich panels

- mechanical properties, including 3- and 4-point bending, CTE coefficient of thermal expansion (in 3 directions), CME coefficient of moisture expansion.
- thermal properties, including verification of thermal limits (maximum and minimum service temperatures), Tg glass transition of composite, thermal conductivity (in transverse direction).
- electrical properties, including electrical conductivity (in transverse direction).

102.3.9 Demonstrator structures

To date (2009), nano-materials are expected to provide some performance improvements for specific applications, e.g.:

- antenna reflector shells based on CFRP-CNT and carbon foam technology with improved thermal, thermo-elastic and electrical performances (thermal cycling and thermal distortion test, reflection loss and depolarisation in Ku, Ka and Q bands).
- low-CTE waveguides and feed horns in Ku, Ka and Q bands, based on CFRP-CNT technology (thermal cycling and S parameters at extreme temperatures, with emphasis on phase stability).
- CFRP heat pipe panel and thermal radiators based on CFRP-CNT composite sandwich plates with improved skins and core technology for spacecraft secondary structure support panel (thermal balance and thermal cycling).
- solar panel substrate based on CFRP-CNT technology (thermal cycling, thermal distortion, modal and acoustic behaviour).

Design, manufacturing and testing of demonstrator structures aims to follow the approach used for similar flight hardware qualification. The verification plan is somewhat reduced for the evaluation study, but the objective is to compare the responses of the nano-modified demonstrator with the predicted behaviour of conventional materials.

Success is measured in terms of performance in relation to the additional cost in materials and processes as well as cost reduction by simplified design. This also takes into account near-future projections of cost and performance improvements.

102.4 References

102.4.1 General

[102-1] H.G. Wulz: EADS Astrium GmbH (D)
'Nano Composites for Potential Application in Space'
Doc. No. ECSS-E-30-40/NBCM/TR001/06
Issue 1; Date: 17/08/2006
Work Order on ESTEC Contract No. 15865/01/NL/MV/CCN5

[102-2] 'SoW: Composite Materials for Payload and Platform Elements. Item 4E.026 - ARTES–5 Workplan 2007', ESA Directorate of Telecommunication and Navigation
31 October 2007 DRAFT

[102-3] EMITS ITT AO 'Nanotechnologies' (2009)

[102-4] F. Helm, F. Thurecht: HPS GmbH (D)
'Organic/ Inorganic Materials and CFRP Structures Reinforced with Carbon Nanotubes for Space Applications'
6th ESA Round Table on Micro & Nano Technologies for Space Applications (8 - 12 October 2007), p.355-361

[102-5] V. Kostopoulos et al: University of Patras (Greece)
'CNT Epoxy Modified CFRP: Towards Improved Mechanical and Sensing Properties for Multifunctional Space Structures'
6th ESA Round Table on Micro & Nano Technologies for Space Applications (8 - 12 October 2007)

[102-6] C. Pereira et al: INEG and LCM Universities of Porto (Portugal)
'Developing Advanced Composites for Spatial Structures: the Effect of Carbon Nanotubes and Fibres on Resin Flammability'
6th ESA Round Table on Micro & Nano Technologies for Space Applications (8 - 12 October 2007)

[102-7] S. Forero: FutureCarbon GmbH (D)
'Carbon Nanotubes for Applications in Space'
6th ESA Round Table on Micro & Nano Technologies for Space Applications (8 - 12 October 2007)

[102-8] H. Florian et al: University of Hamburg-Harburg (D)
'Influence of nano-modification on the mechanical and electrical proprties of conventional fibre-reinforced composites'
Composites: Part A – Applied Science and Manufacturing, 2005 Vol. 36 No. 11 p. 1525-1535

[102-9] R.H. Hurt et al: Brown University (USA)/ CEMES-CNRS Toulouse (France)
'Toxicology of Carbon Nanaomaterials'

Carbon, Vol. 44 No. 6 (2006), p.1028-1033

[102-10] L. Pambaguian et al: ESTEC TEC-QMM, with contributors from European acedemia and industry.
'Non-orgainc matrix materials reinforced with carbon nanotubes for space applications'
Proceeding of Viennano '07, Vienna, Austria, March 14-16, 2007

[102-11] Tomohiro Yokozekia et al: Uni. of Tokyo (Japan)
'Mechanical properties of CFRP laminates manufactured from unidirectional prepregs using CSCNT-dispersed epoxy'
Composites. Part A. Applied Science and Manufacture, Vol. 38 No. 10, (2007), p.2121-2130

[102-12] F.H. Gojny et al: Technical University Hamburg-Harburg (D)
'Influence of different carbon nanotubes on the mechanical properties of epoxy matrix composites – A comparative study'
Composites Science and Technology 65 (2005) p.2300–2313

[102-13] S.J. Schneider Jnr: Chair ISO/TC 206 – Fine ceramics
'Assessment of international standardisation needs for ceramic materials – Status of ISO/TC 206 Fine ceramics'
ISO Bulletin (Feb 2003)

[102-14] Paul Marks, New Scientist magazine website
'Is nanotechnology a health timebomb?'
12 November 2008
http://www.newscientist.com/article/dn16020-is-nanotechnology-a-health-timebomb.html?DCMP=NLC-nletter&nsref=dn16020

103 Carbon nanotubes and nanofibres

103.1 CNT - carbon nanotubes

103.1.1 General

CNTs possess superior strength, mechanical flexibility and electrical conductivity. The basic features of CNTs include:

- exceptional theoretical mechanical properties, Ref. [103-1], [103-2], [103-3], [103-4], [103-5], [103-6],
- electrical conductivity,
- small size in the nanometre range, i.e. diameter ~ 1nm to 50nm,
- high specific surface areas up to 1300 m2/g, Ref. [103-7].

Used as a nano filler in composites, CNTs have a high potential for enhancing the characteristics of the matrix phase, be it polymer, metal, ceramic or glasses.

There is also a high possibility that functional properties can be conferred on composites by the inclusion of CNT materials.

103.1.2 Types of CNTs

In general, CNTs are of nano dimensions, with diameters in the range of 10nm to 20nm. CNF are submicron-fibres, with diameters in the range of 150nm to 300nm, [See also: 43.10 for carbon black].

There are many different forms of CNTs, generally described as:

- SWCNT - single-wall CNTs
- DWCNT - double-wall CNTs
- MWCNT - multi-wall CNTs
- CNF – carbon nanofibres and derivative product forms, e.g. networks, foams, papers, [See: 103.3].

Questions remain concerning the appropriate types of CNTs to use.

Figure 103.1.1 shows an example of a commercially-available MWCNT, along with a summary of its characteristics, Ref. [103-15].

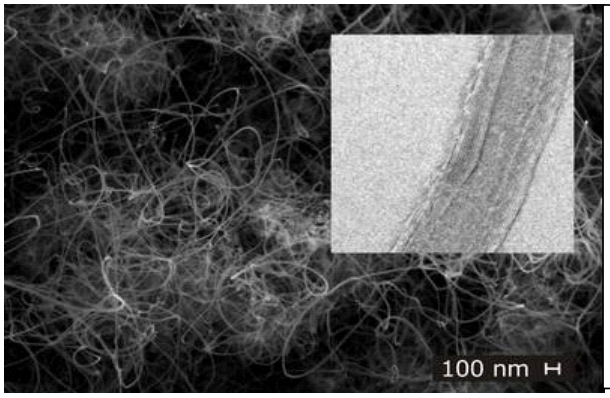

MWCNT – multi-wall carbon nanotubes

Dimensions: 15 nm
BET surface: ~ 200 m²
Purity: > 98%

Applications: Composite materials based on polymers, resins, glass and ceramics to enhance the mechanical, electrical and thermal properties; to improve rheological and wear properties. Catalyst supports.

Figure 103.1-1 – Carbon nanotubes: Example of MWCNT commercially-available product

103.1.3 Surface functionalisation

Surface functionalisation describes chemical surface treatment processes used to make the surface of CNTs chemically compatible with the physical nature of the matrix material.

Although the relevance of surface functionalisation remains an essential subject of research, it is plausible that good chemical compatibility of the partner materials occurs when the chemical nature of CNT surface is similar to that of the matrix material.

103.1.4 Development activities

103.1.4.1 Property transfer

A crucial factor in nano material development is finding the most effective means to transfer the superior physical properties of CNTs via chemical interfacial interactions between the nanotubes and the matrix material. This can be achieved firstly by suitable surface treatment, or functionalisation, of CNTs and secondly, by ensuring homogenous dispersion of CNTs within the matrix material.

103.1.4.2 Host materials

It has been demonstrated that CNTs can enhance the mechanical properties of polymers, monolithic ceramic materials, glasses and glass-ceramics. The fracture toughness of ceramic materials can be considerably improved. Also, at relatively low CNT contents, such modified ceramic materials exhibit electrical conductivity that is orders of magnitude higher than for pure ceramic materials without nano fillers.

Much research has already been done with metal matrix materials containing dispersed CNTs. Owing to the poor chemical compatibility of CNTs with many metals, special functionalisation methods for CNTs and process techniques have been developed in order to disperse CNTs in metal matrices. It has not yet been demonstrated that CNTs can significantly improve the mechanical properties of metallic composites. However, it is speculated that higher thermal conductivity could be achieved, better than the pure metallic matrices, with the possibility of reaching the performance of metal-diamond-composites.

103.1.5 Economic aspects

103.1.5.1 General

Prices stated are as of 2006 and vary depending on the particular supplier and product specification. The quantity purchased can also affect the price per unit mass or area. In general, the price depends on CNT structure, CNT content, purity and surface treatment.

Using large reactor vessels, the production capacity of CNTs and CNFs can reach kgs per day.

103.1.5.2 CNTs

The price of 'as-processed' CNTs is of the order of:

- SWCNTs: 250 € per gram
- DWCNTs: 175 € per gram
- MWCNTs: 25 € to 40 € per gram.

Most 'as-processed' CNTs undergo further treatments (mechanical and chemical). Any chemical surface treatment applied increases the price to about 100 € to 450 € per gram.

103.1.5.3 CNFs

Depending on the structure, the price of CNFs is about 20 € to 30 € per gram. CNF-based products, such as papers, foams and non-wovens, tend to be of the order of 15 € per cm2 to about 40 € per gram for foams, [See also: 103.3].

103.2 3D CNT networks and CNFs

103.2.1 General

In addition to nanotubes of various constructions, [See: 103.1], nano fillers can be produced as networks. An example is the 3-D networks manufactured by FutureCarbon GmbH (D) using CVD processes, Ref. [103-15].

Other solid MWCNT products are also available, e.g.:

- 100% CNT-paper
- nonwovens, based on polymeric fibres,
- carbon-carbon composite, based on PAN, PF and MF.

Some of the various product forms available are described, along with some potential space applications.

103.2.2 CNF foams

Figure 103.2.1 shows examples of CNF foams, along with a summary of the characteristics of available materials (as of 2006).

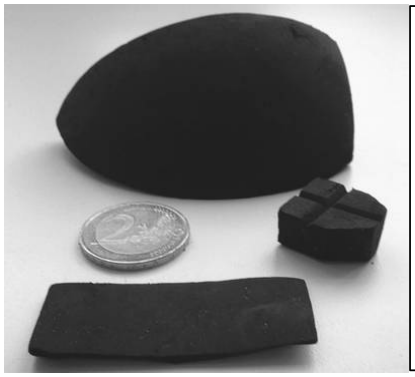

CNF-HB Foam

Diameter of fibres: 300 nm
BET-surface: ~ 60 m²
Porosity: 95% to 97%
Purity: > 98 %

Dimensions: Cuboids: 80mm × 80mm × 50mm.
Disks: 115mm diameter; thickness 10mm to 50mm.
Other shapes on demand

Figure 103.2-1 – CNF foams: Examples

103.2.3 Metallised CNF and CNT

Carbon nano tubes and fibres are available with metallised coatings; as shown in the micrograph in Figure 103.2.2.

Available coatings are: Fe, Cu, Ni, Co, Pd, Pt, Pt/Ru (as of 2006).

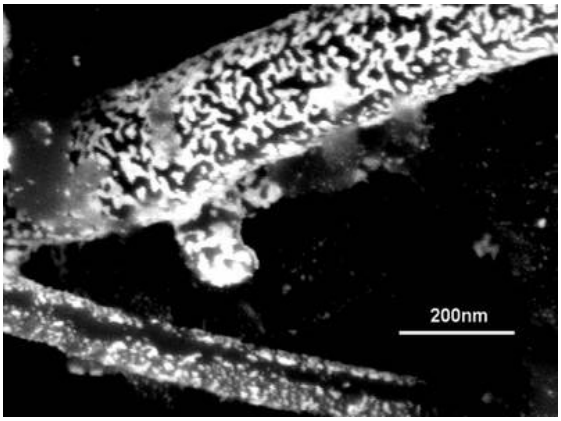

Figure 103.2-2 – Metallised CNTs and CNFs: Micrograph

103.2.4 Bucky paper

'Bucky Paper' is described as being produced from 100% MWCNT, consolidated into flexible sheets, with and without binders or other additives. These light, flexible sheets of pure carbon nanotubes offer enhanced electrical and thermal conductivity.

Figure 103.2.3 shows examples of bucky paper, which is available. in dimensions 50 mm × 50 mm (as of 2006).

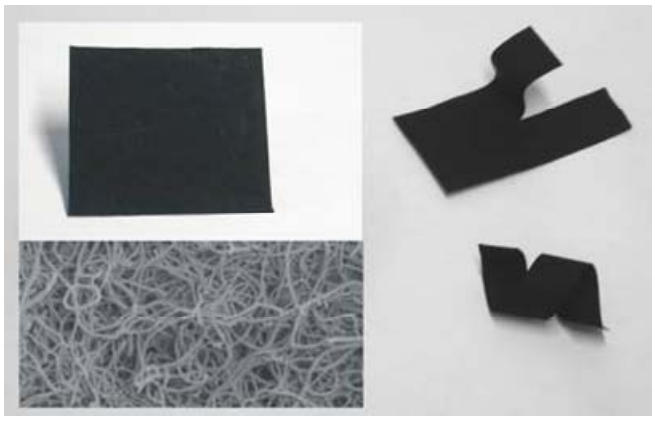

Figure 103.2-3 – Bucky paper: Examples

103.2.5 Non-wovens

Figure 103.2.1 shows examples of nano non-wovens produced from cellulose, PE, PAN or aramid. The CNT-content is 30% by weight. The light, flexible composite sheets (50 mm × 50 mm) have enhanced electrical and thermal conductivity.

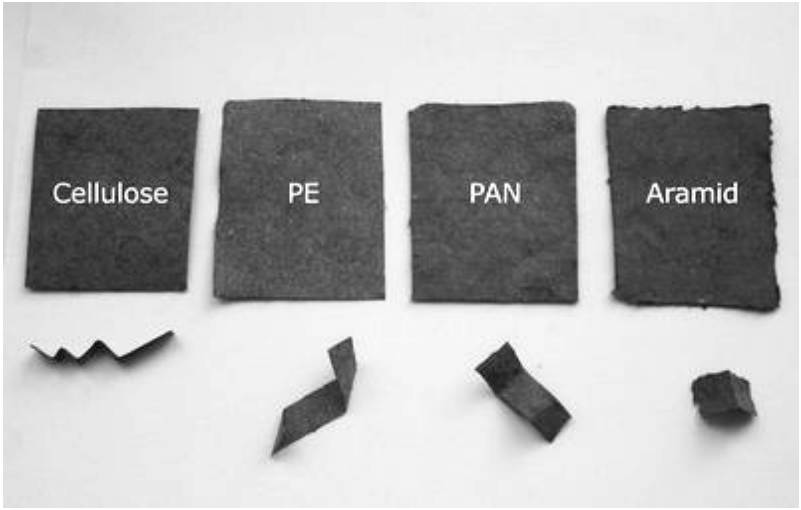

Figure 103.2-4 – Non-wovens: Examples produced from polymers, having 30 wt.% CNT content

103.2.6 Potential space applications

103.2.6.1 ESA '3D CNF-networks' study

Within the ESA Triangle Project '3D CNF networks', the potential benefits of CNF composites for use in space are being evaluated:

- CNF foams, where potential applications are:
  - Micro-mechanical damping elements, where highly elastic and solid carbon nano foams are being considered. Currently, other applications for space also are under investigation, e.g. micro-mechanical damping elements for highly mechanically sensible missions such as LISA and DARWIN.

  - Green bodies for infiltration of polymeric and metallic matrices, where CNF foams appear suitable as open-pore carbon tissues (or networks) for infiltration.
- Metallised CNFs and CNTs, where applications under evaluation include:
  - Catalysts for reactors of regenerative processes, e.g. fuel cell, Sabatier reactor.
  - Increase of electrical and thermal conductivity in highly conductive composite materials.
- Bucky paper.

As of 2006, this study is on-going.

103.3 CNT and CNF production processes

103.3.1 General

Processes are described for:

- synthesis of various types of CNTs and CNFs;
- processes for incorporation and dispersion of CNTs into the matrix phase.

103.3.2 Synthesis processes

Different processes are used to synthesise the various types (species) of CNTs and CNFs, i.e. SWCNTs, DWCNTs, MWCNTs, tubular type, platelet type, herringbone type.

The synthesis processes, include:

- CVD - chemical vapour deposition and derivative processes, e.g.
  - plasma enhanced CVD,
  - thermal CVD,
  - alcohol catalytic CVD,
  - vapour phase growth,
  - aero gel supported CVI,
  - laser-assisted CVI.
- Laser ablation.
- Arc discharge.
- Flame synthesis.
- HIPCO - high-pressure carbon monoxide conversion.

An overview of the different synthesis processes for CNTs is given in a technology report by Eindhoven University of Technology, Ref. [103-8].

Table 103.3-1 provides a summary of the three most common techniques used, Ref. [103-8].

Table 103.3-1 – Carbon nanotubes: Summary of major synthesis processes and their efficiency

Process	Arc discharge	CVD - chemical vapour deposition	Laser ablation (vaporisation)
Source Ref. [103-8]	Ebbesen and Ajayan, NEC, Japan, 1992	Endo, Shinsu University, Nagano, Japan	Smalley, Rice, 1995
Method	Connect two graphite rods to an electrical power supply; place them a few millimetres apart. At 100 amps, carbon vaporises and forms hot plasma.	Place substrate in oven, heat to 600°C and slowly add a carbon-bearing gas, such as methane. As gas decomposes it releases carbon atoms which recombine in the form of NTs.	Submit graphite to intense laser pulses (rather than electricity) to generate carbon gas from which the NTs form. By varying the conditions, prodigious amounts of SWNTs can be produced.
Typical yield	30% to 90%	20% to 100%	Up to 70%
SWNT	Short tubes with diameters of 0.6 nm to 1.4 nm.	Long tubes with diameters ranging from 0.6 nm to 4 nm.	Long bundles of tubes (5 microns to 20 microns) with individual diameters 1 nm to 2 nm.
MWNT	Short tubes with inner diameter of 1 nm to 3 nm and outer diameter of approximately 10 nm.	Long tubes with diameters ranging from 10 nm to 240 nm.	Not much interest in this technique because it is too expensive, but MWNT synthesis is possible.
Advantages	Can easily produce SWNT and MWNT. SWNTs have few structural defects; MWNTs without catalyst, not too expensive, open-air synthesis possible.	Easiest to scale up to industrial production. SWNT diameter controllable, quite pure.	Primarily SWNTs with good diameter control and few defects. The reaction product is quite pure.
Disadvantages	Tubes tend to be short with random sizes and directions. Often need a lot of purification.	NTs are usually MWNTs and often have high defect populations.	Costly technique because it needs expensive lasers and high power, but is improving.
Key:	NT – nanotubes; SWNT - single-wall nanotubes; DWNT - double-wall nanotubes; MWNT - multi-wall nanotubes.		

Ref. [103-8] provides details on CNT surface treatment, dispersion (incorporation), control processes and (nano-) inspection and diagnostics. Also described are disentanglement, purification, milling, surface treatment, functionalisation, dispersion and incorporation into host material, dispersion control and quality inspection.

Enhanced process routes for the production of CNTs are necessary to overcome the problem of their tangling during synthesis. In a CVD reactor, CNTs form in different orientations from powdery catalyst substrates. Consequently, the final product is highly tangled.

Disentanglement and homogenous dispersion within a viscous polymer matrix is not very effective. The goal is to manufacture straighter, less tangled CNTs.

103.3.3 Incorporation of CNT into matrix material

103.3.3.1 General

The key point is to transfer the excellent potential mechanical, thermal and electrical properties of the CNTs to the matrix material of the composite. Two main issues are addressed in order to improve the material properties of polymer matrices by adding carbon nanotubes as filler, Ref. [103-9], [103-10]. These are:

- good interfacial bonding,
- proper dispersion (incorporation) of the individual CNTs in the polymeric matrix.

103.3.3.2 Interfacial bonding

Experience with different kinds of CNT polymer composite showed ambivalent improvements in performance. Generally, it has been seen that carbon nanotubes provide a 'tendency' to improve mechanical properties. This effect is significantly higher with soft, aliphatic polymers, because of their better chemical compatibility with CNTs, compared with relatively hard aromatic-type polymeric matrix materials. It seems plausible that chain-like polymer types such as polyamides have higher improvement potential compared with cyclo-polymerized high-performance thermoset materials, such as cyanate esters.

Chemical compatibility can only be improved by modification of the surface characteristics of the nano filler because the chemical composition and morphology of any selected polymeric matrix system is fixed.

The chemical compatibility can be affected by:

- the selection of species of CNTs, i.e. SWCNT, DWCNT or MWCNT, platelet or herringbone type,
- the aspect ratio (ratio of tube diameter to tube length)
- modification of the surface morphology and interactions, which can be influenced by so-called functionalisation surface treatment processes.

Functionalisation is a collective term for a sequence of chemical treatment steps made to CNTs. The expression 'functionalisation' comprises complex processes such as disentanglement of CNTs, cleaning and purification, milling, surface modification by adding of reactive molecular groups and dissolution in a solvent. This topic is central focus of interest in processing of every kind of nano composites. More details can be found in Ref. [103-8], [103-9], [103-10], [103-11], [103-12], [103-13], [103-14], [103-16], [103-17], [103-18].

103.3.3.3 Dispersion (incorporation)

The dispersion of the CNTs in the matrix system is another challenge to overcome for nanotube-reinforced polymers. Nano-scaled particles exhibit an enormous surface area, being several orders of magnitude larger than the surfaces of conventional fillers. This surface area acts as the interface for load transfer, but is also responsible for the strong tendency of the CNTs to agglomerate.

Efficient use of CNT properties in polymers therefore depends on their homogeneous dispersion in the matrix, breaking up of the agglomerates and good wetting by the polymer.

The properties of conventional composites are controlled by the constitutive mechanical, electrical and optical properties of fibre, matrix and interface. In high performance nano-composites, a variety of further complex interactions need to be understood, i.e. nano-particle properties, matrix and manufacturing processes.

Given that CNTs have an extremely high surface area, a relatively low filler content of about 0.7 volume % causes an exceptional increase in viscosity. In order to distribute CNTs homogeneously in a polymer matrix, five variables need to be controlled:

- length of the tubes,
- their entanglement,
- volume fraction,
- high matrix viscosity,
- nanotube-to-nanotube attraction; mainly for SWCNT, DWCNT.

With increasing CNT length, the interactive forces increasingly hinder the separation of tubes; in a similar way to the influence of the molecular weight (chain length) in polymers. Shear forces introduced into the suspension in order to separate the agglomerates and to disperse the individual CNTs is controlled by the manufacturing process. Various methods can be used to disperse the tubes:

- Sonication.
- Stirring.
- Calendering.

Dispersion methods are explained in Ref. [103-9], [103-10], [103-16], along with application cases, advantages and disadvantages.

103.4 References

103.4.1 General

[103-1] E.T. Thostenson, T.W. Chou
'On the elastic properties of carbon nanotube-based composites: modelling and characterization',
J. Phys. D: Appl. Phys. 2003; 36: p573-582

[103-2] C. Li, T.W. Chou
'Elastic moduli of multi-walled carbon nanotubes and the effect of van der Waals forces',
Composites Science and Technology 2003;63:p1517-1524

[103-3] M.F. Yu, O.Lourie, M.J Dyer et al.
'Strength and breaking mechanism of multiwalled carbon nanotubes under tensile load',
Science 2000;287, p637-640

[103-4] M.F. Yu, B.S.Files, S. Arepalli., R.S Ruoff
'Tensile loading of ropes of single wall carbon nanotubes and their mechanical properties',
Phys. Rev. Lett. 2000; 84: p5552-5555

[103-5] X.Sun, W. Zhao
'Prediction of stiffness and strength of single-walled carbon nanotubes by molecular-mechanics based finite element approach'.
Mater. Sci. Eng. A 2005; 390: p366-371

[103-6] E.Hernández, C Goze, P. Bernier, A Rubio
'Elastic properties of C and BxCyNz composite nanotubes'. Phys. Rev. Lett. 1998; 80: p4502-4505

[103-7] A.Peigney, Ch Laurent., E. Flahaut., R.R. Bacsa, A. Rousset
'Specific surface area of carbon nanotubes and bundles of carbon nanotubes',
Carbon 2001; 39: p507-514

[103-8] Eindhoven University of Technology
'The Wondrous World of Carbon Nanotubes: A review of current carbon nanotube technologies',
27 February 2003, http://students.chem.tue.nl/ifp03/

[103-9] B. Fiedler, F.H. Gojny, M.H.G. Wichmann, K. Schulte.
'Fundamental aspects of nano-reinforced composites'
Composites Science and Technology (2005, accepted).

[103-10] F.H. Gojny, J. Nastalczyk, Z. Roslaniec, K. Schulte
'Surface modified multi-walled carbon nanotubes in CNT/epoxy-composites',
Chemical Physics Letters 370 (2003) p820-824

[103-11] F.H. Gojny, K. Schulte.
'Functionalisation Effect on the Thermo Mechanical Behaviour of Multi-Wall Carbon Nanotube/Epoxy-Composites',
Composites Science and Technology 64 (2004) p2303-2308

[103-12] S.J.V. Frankland et al.,
'Molecular simulation of the influence of chemical cross-links on the shear strength of carbon nanotube-polymer interfaces'
J Phys Chem B 2002, 106, 3046

[103-13] A. Eitan et al.,
'Surface Modification of Multiwalled Carbon Nanotubes: Toward the Tailoring of the Interface in Polymer Composites'
Chem. Mater. 2003 15 (16), p3198-3201

[103-14] A.H. Barber, S.R. Cohen, H.D.Wagner.
'Measurement of carbon nano tube-polymer interfacial strength'
Appl Phys Lett 2003; 82: p4140-4142

[103-15] FutureCarbon GmbH, Bayreuthhttp, Germany
website: http://www.future-carbon.de/englisch/doc/FC-products_prices_e.htm

[103-16] J.N.Coleman, U. Khan, W.J.Blau, Y.K.Gun´ko
'Small but Strong: A Review of the Mechanical Properties of Carbon Nanotube-Polymer Composites,
Carbon 44 (2006) p1624-1652

[103-17] F.H. Gojny, M.H.G. Wichmann, B. Fiedler & K. Schulte 'Influence of different carbon nanotubes on the mechanical properties of epoxy matrix composites: A comparative study'.
Composites Science and Technology (2005)

[103-18] F.H. Gojny, M.H.G. Wichmann, B. Fiedler & K. Schulte.'Influence of nano-reinforcement on the mechanical and electrical properties of conventional fibre-reinforced composites'.
Composites A - Applied Science & Manufacturing 2005; 36: p1525-1535

104 CNT-modified polymeric composites

104.1 Technology status

104.1.1 Polymer types

The nature of chemical bonding differs between polymeric material families, due to their chemical composition and morphology. As a result of this, the effects on properties produced by the addition of CNTs vary considerably depending on the polymer matrix and are not easy to predict. Consequently, for each type of polymer an individual incorporation route for CNTs should be found in order to optimise the performance of the nano composite, Ref. [104-1].

104.1.2 Epoxy matrix composites

The applicability of nanotube-epoxy-systems has been demonstrated as a matrix for fibre-reinforced plastics. However, preparation of resins with nanotube contents greater than 0.5 wt% remains difficult because of the very high specific surface areas of CNTs and the resulting increase in viscosity, [See: 104.2].

104.1.3 Mechanical properties

Nano-modification of epoxies leads to novel fibre-reinforced plastics with enhanced matrix-dominated mechanical properties and anisotropic electrical conductivity. The nanocomposites, reinforced by carbon nanotubes, have improved mechanical performance and a positive influence on fracture toughness has also been observed.

The combination of conventional reinforcement fibres, e.g. glass, carbon, aramid, and additional nano-modification of the polymer matrix material, e.g. with carbon nanotubes, has good potential for structural applications. Minute amounts of carbon nanotubes (0.3wt% DWCNT-NH2) have shown a significant increase of about 20% in the matrix-dominated ILSS, whilst tensile properties were not affected as they remain fibre dominated. The addition of a similar amount of carbon black gave less mechanical improvement of the matrix material.

Some evidence of an increase in glass transition temperature with DWCNT-NH2 additions have been seen from DMTA measurements on neat nanocomposites, [See: 104.3].

104.1.4 Electrical properties

Electrical properties show anisotropic behaviour. The electrical conductivity in plane was more than an order of magnitude higher than in the z-direction. A ‘tuning’ of CNT-content in nanotube-modified, epoxy-matrix FRPs has the potential of creating materials with multi-functional properties, e.g. a combination of electrical and thermal conductivity together with improved mechanical performance, [See: 104.5].

104.1.5 Summary

The current characterisation status of CNT-modified epoxy polymers provides a sound knowledge base that can be applied to the nano modification of other thermoset polymers, such as cyanate esters.

[See: 104.4]

104.2 CNT-modified epoxy materials

104.2.1 Introduction

Epoxy is a widely-established CFRP composite matrix material for structural space applications. It is proven for the manufacture of support structures, thermal components, radiators, solar generators and also for optical components such as large reflectors.

Since epoxy resin is one of the most widely investigated and reported CNT polymeric composite materials, it was selected to be representative of a CNT-modified polymeric material system for potential space applications.

104.2.2 Evaluation study

104.2.2.1 General

Epoxy is often used within material science to investigate and to study incorporation processes of CNTs into thermoset polymer matrices. Among other researchers, the Technical University of Hamburg-Harburg (TUHH), Institute for Polymer Composites have accumulated expertise that can be applied in developing advanced high-performance carbon fibre-reinforced CNT polymer composites for aerospace applications, Ref. [104-2], [104-3], [104-4], [104-5], [104-6], [104-7], [104-8], [104-9], [104-10], [104-11], [104-19], [104-20], [104-21].

Obtaining an effective dispersion of nanoparticles in a particular polymer matrix material is challenging. A high energy input is applied to overcome the nanotube-to-nanotube adhesion (Van der Waals forces), disperse nanoparticles homogeneously within the epoxy matrix and to properly impregnate the high surface area of the nano filler.

Sonication, a local introduction of vibrational energy, leads to damage of the nanotube structure and a reduction of the effective length.

A kneading process applied to a ‘paste’ resin using mini-calanders was found to be effective in dispersing CNTs and CB carbon black in epoxy matrix systems. The material characteristics described here were measured on samples prepared by this method.

104.2.2.2 Epoxy matrix

The epoxy matrix used for sample preparation was a modified epoxy resin (Ll35i) with an amine hardener (H137i), supplied by Bakelite. This epoxy system is a conventional resin for infusion processes, e.g. RTM - resin transfer moulding.

104.2.2.3 Carbon nanotubes

All CNTs used for samples were produced via the CVD-route:

- SWCNTs – single-wall carbon nanotubes, with an average diameter of d < 2 nm and a length of some micrometers.

- DWCNT (-NH2) – double-wall carbon nanotubes, purified and amino-functionalised, which appear in a tangled cotton-like form. These nanotubes consist of two graphitic shells and have an average outer diameter of 2.8 nm and a length of several micrometers. The amino-functionalisation was accomplished by ball-milling purified DWCNTs in ammonia.
- MWCNTs – multi-wall carbon nanotubes, purified and amino-functionalised, which have an average outer diameter of about 15 nm and a length of up to 50 µm. The functionalisation process was similar to that for DWCNTs.

104.2.2.4 CB - carbon black

Highly-conductive carbon black was used as a reference material. CB is highly graphitised and commonly used as conductive fillers for antistatic applications or a pigment in printing ink, [See also: 43.10]. It is usually used to increase the electrical and thermal conductivity of polymers, but also to enhance the stiffness.

CB was used as reference in order to evaluate the effect of the particle-shape on the improvements achieved for mechanical properties and, therefore, to gain information on the real potential of CNTs as mechanical reinforcement for epoxy matrices.

104.2.2.5 Sample processing parameters

All composite samples were prepared in the same way. In order to disperse the nanofillers in the epoxy resin, the CNTs and CB were manually mixed with the epoxy base resin (without hardener). Then a batch was added to a mini-calander for the final high shear mixing. The suspension was then mixed vigorously with the hardener for 10 minutes, cured for 24 h at room temperature and finally post-cured at 60 °C for 24 h.

104.2.3 Properties

104.2.3.1 Mechanical properties

Nano composites consisting of an epoxy matrix system and different types of carbon nanotubes were produced by calandering. The composites were investigated regarding dispersibility of the CNTs in the matrix and mechanical reinforcement effects.

Dispersion of the CNTs and interfacial adhesion to the epoxy matrix are key issues in the development of nano composites. Chemical functionalisation of the CNT surface is an important step in improving both interfacial bonding and dispersion.

Table 104.2-1 compares the mechanical properties of the control epoxy with composites having different filler types and contents and the effects of surface functionalisation, Ref. [104-2].

Table 104.2-1 – CNT-modified epoxy: Mechanical properties

Filler type	Filler content (wt. %)	Young's modulus (MPa)	Ultimate tensile strength (MPa)	Fracture toughness K_{1C} (MPa $m^{-3/2}$)
None	0.0	2599 (± 81)	63.80 (± 1.09)	0.65 (± 0.062)
CB	0.1	2752 (± 144)	63.28 (± 0.85)	0.76 (± 0.030)
	0.3	2796 (± 34)	63.13 (± 0.59)	0.86 (± 0.063)
	0.5	2830 (± 60)	65.34 (± 0.82)	0.85 (± 0.034)
SWCNT	0.05	2681 (± 80)	65.84 (± 0.64)	0.72 (± 0.014)
	0.1	2691 (± 31)	66.34 (± 1.11)	0.80 (± 0.041)
	0.3	2812 (± 90)	67.28 (± 0.63)	0.73 (± 0.028)
DWCNT	0.1	2785 (± 23)	62.43 (± 1.08)	0.76 (± 0.043)
	0.3	2885 (± 88)	67.77 (± 0.40)	0.85 (± 0.031)
	0.5	2790 (± 29)	67.66 (± 0.50)	0.85 (± 0.064)
DWCNT-NH_2	0.1	2610 (± 104)	63.62 (± 0.68)	0.77 (± 0.024)
	0.3	2944 (± 50)	67.02 (± 0.19)	0.92 (± 0.017)
	0.5	2978 (± 24)	69.13 (± 0.61)	0.93 (± 0.030)
MWCNT	0.1	2780 (± 40)	62.97 (± 0.25)	0.79 (± 0.048)
	0.3	2765 (± 53)	63.17 (± 0.13)	0.80 (± 0.028)
	0.5	2609 (± 13)[a]	61.52 (0.19)[a]	[a]
MWCNT-NH_2	0.1	2884 (± 32)	64.67 (± 0.13)	0.81 (± 0.029)
	0.3	2819 (± 45)	63.64 (0.21)	0.85 (± 0.013)
	0.5	2820 (± 15)	64.27 (± 0.32)	0.84 (± 0.028)

Key: [a] High viscosity disabled degassing – composite contained numerous voids, Ref. [104-2]

Small amounts of carbon nanotubes in epoxies lead to increased mechanical properties. The most significant improvements of strength (+10%), stiffness (+15%) and especially fracture toughness (+43%) were attained with amino-functionalised DWCNTs at 0.5wt% filler content.

104.2.3.2 Fracture toughness

The fracture toughness of polymers, corresponding to an improved resistance to crack propagation, thus a higher damage tolerance, is a crucial and limiting factor for the design of structural components, especially with regard to the long-term behaviour (fatigue). Therefore, improvement of epoxy fracture toughness is a desirable research goal.

Nanoparticles in general, and CNTs in particular, have potential in improving the fracture toughness of epoxies due to their:

- high mechanical properties,
- fibrous structure (high aspect ratio),
- large interface (specific surface area).

Figure 104.3.1 shows some results of fracture-toughness tests. The fracture toughness for neat epoxy resin is shown by a dashed line, Ref. [104-2].

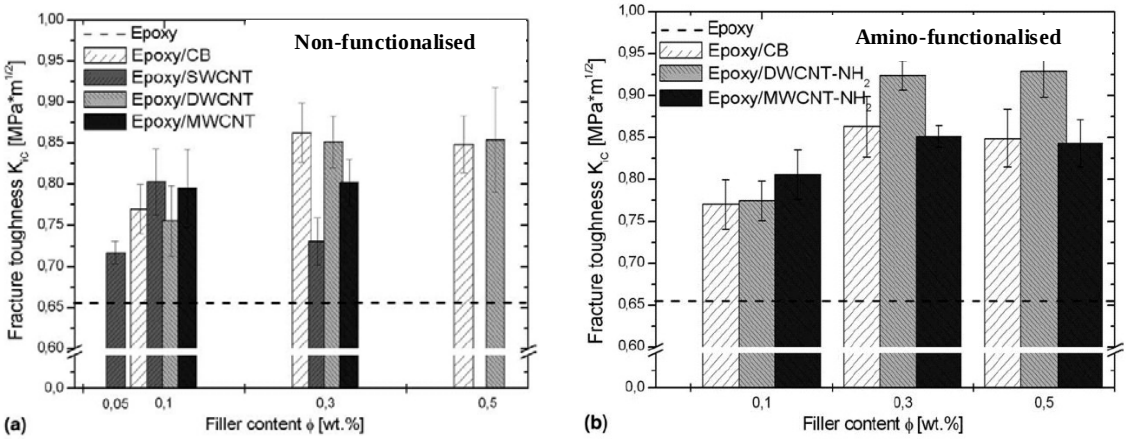

Experimentally obtained fracture toughness of epoxy-based composites containing (a) non-functionalised and (b) amino-functionalised nanoparticles, Ref. [104-2]

Figure 104.2-1 – CNT-modified epoxy: Fracture toughness

The findings can be summarised as:

- Non-functionalised nanoparticles generally increase the fracture toughness of the epoxy matrix significantly at very low filler contents; as shown in Figure 104.2.1 (a).
- The relative improvement of the KIC-value is not dependent on the particle-shape, therefore the main fracture mechanism leading to the enhanced fracture toughness could be a surface area effect of the nanoparticles. A dependency between surface area of the nanofillers and toughening capability was seen. In general, large surface areas tend to give greater improvement in fracture toughness.
- Amino-functionalisation of CNTs improves dispersion and increases the interfacial adhesion, leading to a higher effective interfacial area in the composite. As seen in Figure 104.2.1 (b), there is a positive influence of amino-functionalisation on the fracture toughness. The measured fracture toughness of the composite containing 0.3 wt% DWCNT-NH2 is 42% higher than the neat epoxy.
- Comparison between CNT and carbon black-containing epoxy underlines the advantage of fibrous over spherical particles.

104.2.3.3 Elastic properties

Figure 104.3.2 shows the Young's modulii of CNT-modified epoxy, Ref. [104-2].

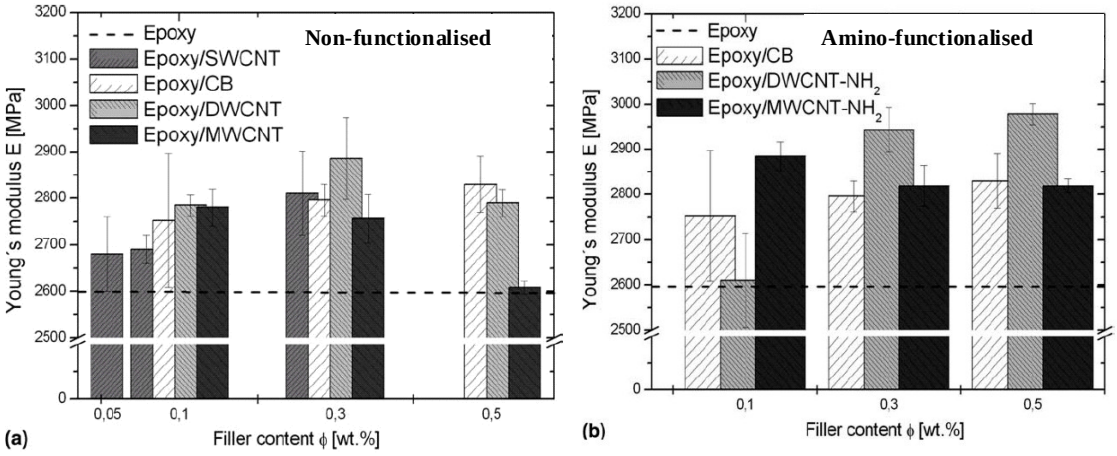

Young´s Modulus of epoxy-based composites containing (a) non-functionalised and (b) amino-functionalised nanoparticles, Ref. [104-2]

Figure 104.2-2 – CNT-modified epoxy: Young's modulus

The findings can be summarised as:

- The addition of any type of nanofiller increases the stiffness of the matrix material, given proper impregnation and sufficient adhesion. In Figure 104.3.2 the Young's modulus of the neat epoxy matrix is shown by the dashed line.
- SWCNT/epoxy composites show almost linear increases in Young's modulus with filler content; to a maximum at 0.3 wt%.
- Young's modulus of MWCNT/epoxy composites increases at a content of 0.1 wt%, but decrease at higher MWCNT loadings.
- Increasing agglomeration was seen in cured composites with CNT contents higher than 0.1 wt%; possibly caused by reagglomeration. This reduces Young's modulus more for MWCNTs owing to the smaller number of particles in MWCNT/epoxy composites, compared with SWCNTs.
- DWCNT showed better improvement in mechanical properties, giving a maximum increase in Young's modulus of +11% at 0.3 wt% DWCNT, but again decreasing for higher filler contents. This can again be attributed to reagglomeration.
- The amino-functionalised nanotubes were more efficient in improving Young's modulus; showing again the value of surface functionalisation. Amine groups on the CNT surface produce covalent bonding with the epoxy, giving significantly improved interfacial adhesion.
- DWCNT-NH2 reinforced epoxy shows the largest improvements in strength and stiffness for the given processing conditions. A maximum increase of +15% in Young's modulus is seen for a composite containing 0.5 wt% DWCNT-NH2, compared with neat epoxy resin. However, the reduced improvements at higher filler contents can be attributed to increasing levels of agglomeration, demonstrating the need to correctly impregnate the matrix.
- When compared with non-functionalised MWCNTs, a similar behaviour was observed for MWCNT-NH2. These composites showed a better enhancement of Young's modulus, but less so at higher filler contents. The decreasing efficiency can again be related to reagglomeration, which was less than for the non-functionalised MWCNTs.

In conclusion, the surface area of nano fillers and their aspect ratios are determinant factors for mechanical reinforcement. However, complete impregnation should be achieved in order to enable efficient load transfer between matrix and reinforcement. Chemical functionalisation of the CNT

surface improves dispersion and interfacial adhesion and, therefore, can be useful in improving impregnation.

104.2.3.4 Strength

Figure 104.3.3 shows the ultimate tensile strength of CNT-modified epoxy, compared with neat epoxy (dashed line), Ref. [104-2].

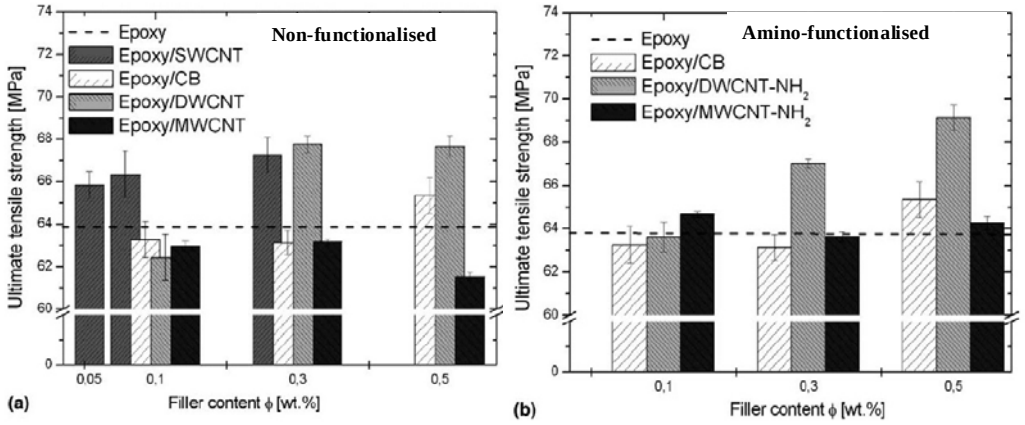

Ultimate tensile strength of epoxy-based composites containing (a) non-functionalised and (b) amino-functionalised nanoparticles, Ref. [104-2]

Figure 104.2-3 – CNT-modified epoxy: Ultimate tensile strength

The findings can be summarised as:

- in general, the addition of small amounts of SWCNTs and DWCNTs increases the UTS moderately, whereas MWCNTs lead to a slight reduction.
- carbon black, a reference material, does not significantly influence the UTS of the epoxy matrix at very low filler contents.
- the relatively large improvement in UTS by SWCNTs compared with the other nanofillers can be explained by their high specific mechanical properties and greatest aspect ratio of the CNTs under evaluation.
- combined with their high specific surface area, SWCNTs do not contain inactive internal layers, giving them the highest potential to improve the strength of materials. DWCNTs consisting of two concentric layers, exhibit a smaller specific surface area and lower aspect ratio, but do not agglomerate as much as SWCNTs. Material containing 0.3 wt% DWCNT exhibits a maximum UTS (67.8 MPa) that did not increase further at higher nanofiller contents.
- neither the addition of small amounts of MWCNT, nor MWCNT-NH2, significantly affect the UTS of the epoxy resin. This behaviour can be attributed to the concentric structure of MWCNTs, where stress transfer does not occur to internal layers. Hence, only the outermost layers of the MWCNT contribute to mechanical reinforcement.
- a 0.5 % addition of DWCNT-NH2 gave an increase in UTS of +10%, whereas the UTS of the materials containing MWCNT-NH2 remain similar to neat epoxy.
- amino-functionalisation of CNTs improves their dispersibility by increasing the surface polarity, thus resulting in generally larger improvements in UTS.

The higher UTS values attained with some species of functionalised CNTs demonstrates the importance of a chemical surface treatment to incorporate the CNTs by covalent bonding with the epoxy matrix. It is considered as an effective method to improve significantly the interfacial adhesion, so making functionalisation a key issue.

104.3 Glass fibre-reinforced CNT-modified epoxy

104.3.1 Status

Nano-particle- glass- or carbon-fibre reinforced composites with matrices containing carbon black or CNTs can be manufactured successfully by RTM resin transfer moulding, Ref. [104-3]. No filtering effect of the nano-particles by the glass fibre bundles was observed.

GFRP having a nanotube-modified epoxy matrix had improved matrix-dominated properties, e.g. interlaminar shear strength. Tensile properties were not affected by the nano-fillers because of the dominant contribution by the fibre reinforcement.

GFRP containing 0.3 wt.% amino-functionalised double-wall carbon nanotubes (DWCNT-NH2) exhibits anisotropic electrical conductivity. The in-plane conductivity is an order of magnitude higher than out-of-plane. Electrical conductivity can be enhanced by carbon nano-particles.

The fibre-orientation in structural components is usually in-plane (x-y direction), leading to fibre-dominated material properties in these directions, whereas the z-direction remains matrix dominated. The use of CNTs as a reinforcing phase is expected to increase the matrix properties, especially in the z-direction, resulting in improved interlaminar properties. Carbon nano-particles infiltrate between the micro-scale fibres.

104.3.2 Study

104.3.2.1 Sample preparation

CNT-modified epoxy GFRP samples, having 8 plies, $(0/\pm45/90/-45°)_{symm}$ lay-up, were produced by a resin transfer moulding technique using a glass fibre non-crimp fabric ('Seartex'), Ref. [104-3].

CNT-modified epoxy resin was mixed with the amine hardener and degassed for 20 minutes prior to injection. After infusion, the sample was cured in a mould. The curing conditions of were identical to those of pure resin samples (24hrs at room temperature) except that the post-cure temperature was increased to 80°C for 24 h (compared with 60°C for resin-only samples).

Despite the slight increase in viscosity, production of GFRPs with a nanotube-modified epoxy resin content of 0.3 wt.% DWCNT-NH2 was practicable. The preparation and dispersion processes were identical to those used for epoxy resin samples, [See: CNT-modified epoxy].

Calendering was an effective method for dispersing carbon-based nano-particles (nanotubes or carbon black). However, higher DWCNT filler contents (>0.5 wt.%) lead to processing problems arising from dramatically increased viscosity, which remains unresolved.

The laminates produced, 21 cm × 36 cm, are an example of nanotube-reinforced FRP at a structural component scale.

A micrograph of a manufactured FRP containing 0.1 wt.% DWCNT-NH2 confirmed that the glass fibres did not produce a filtering effect.

104.3.3 Mechanical properties

104.3.3.1 Tensile strength and stiffness

Tensile strength and Young's Modulus of composites were established by tensile testing in 0° and 90° directions, as shown in Figure 104.3.1 for GFRP having 0.1 wt.% DWCNT-NH2, Ref. [104-3].

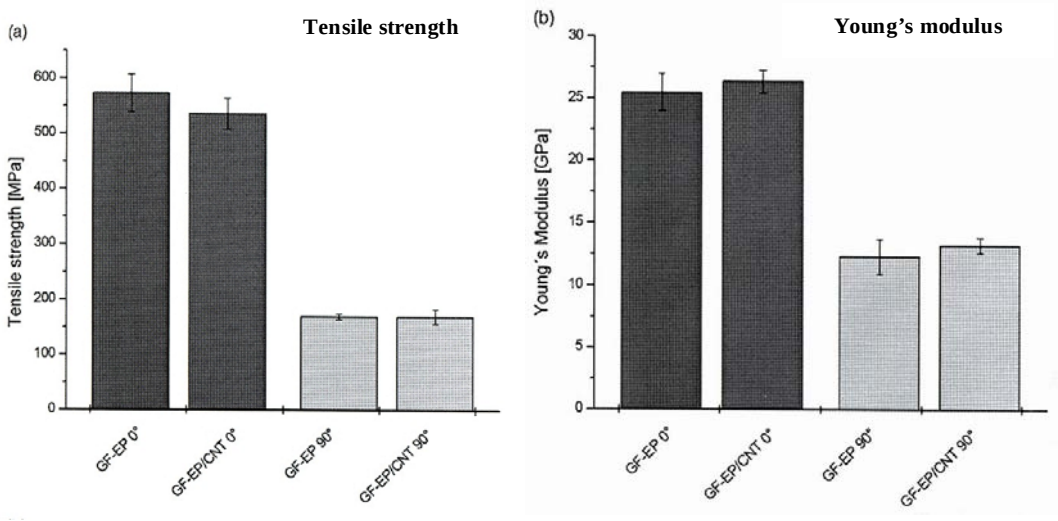

Tensile properties of the GFRPs, (a) tensile strength and (b) Young's modulus in 0°- and 90°-direction, Ref. [104-3].

Figure 104.3-1 – GFRP CNT-modified epoxy: Tensile strength and modulus

The results can be summarised as:

- incorporation of carbon nanotubes did not improve the strength of the fibre-reinforced composite samples.
- young's modulus is only marginally affected by the nanotube-reinforcement.
- fibre-dominated tensile properties in the plane of the fibre reinforcements are evident.

104.3.3.2 Interlaminar and fracture properties

ILSS tests were performed on GFRP samples with neat epoxy matrix (EP) and a nano-modified epoxy containing carbon black (EP/CB with 0.1 wt.% and 0.3 wt.%) and amino-functionalised double wall carbon nanotubes (DWCNT-NH2 with 0.1 wt.% and 0.3 wt.%). [See: Figure 104.3.3 for other ILSS results].

CNTs can improve the fracture toughness of thermosetting matrix systems, as shown in Figure 104.3.2, Ref. [104-2]. [See also: Figure 104.3.3 for interlaminar toughness (G_{IIC}) results]

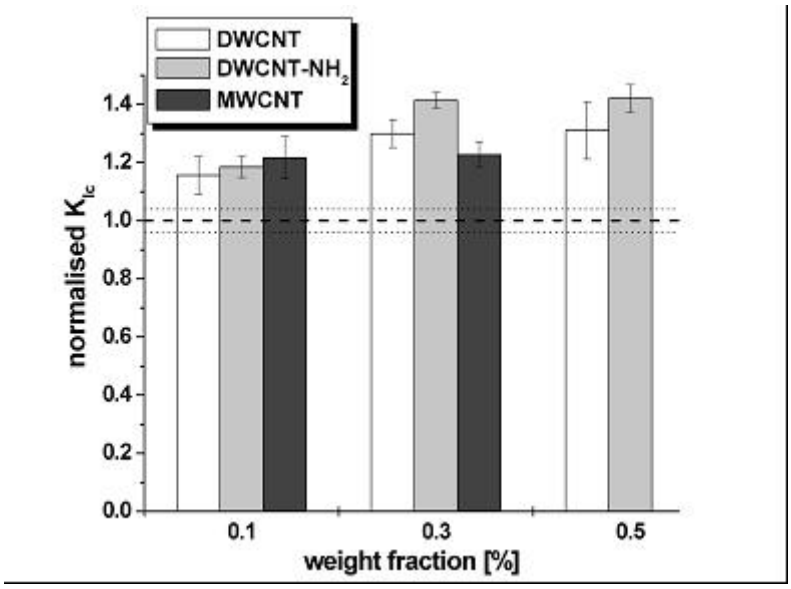

Normalised fracture toughness, Ref [104-2].

Figure 104.3-2 – GFRP CNT-modified epoxy: Fracture toughness

The GFRP used in these studies has high toughness. The failure mechanism is dominated by failure of the fibre-to-matrix interface, so limiting the influence of any improved matrix toughness. Nanoparticle-modified materials were considered as providing some benefits, e.g. a means of tailoring the interfacial strength, matrix-dominated properties.

104.3.4 Electrical properties

The application of an electrical field during the curing process enables tuning of the electrical properties of carbon-nanoparticle-modified fibre-reinforced epoxies. The anisotropic conductivity is also accompanied by improvements in mechanical properties. This is seen as a step towards the integration of functional properties into composites, Ref. [104-4].

Different types of nano fillers were used, i.e. carbon black, fumed silica and DWCNTs, both amino-functionalised and non-functionalised.

The ILSS interlaminar shear strength and interlaminar toughness (G_{IIC}) of GFRP samples with DWCNT showed the highest increase with the addition of small amounts of carbon nanotubes, as shown in Figure 104.3.3, Ref. [104-2].

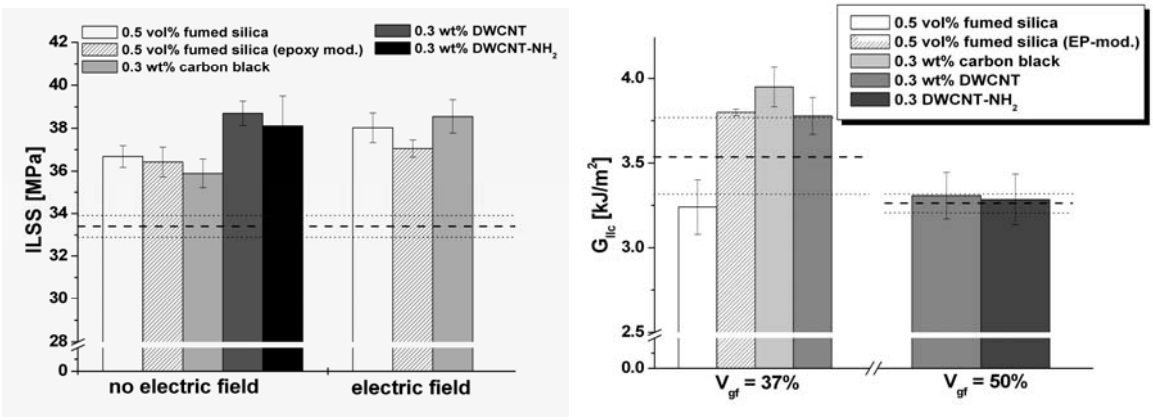

a) Interlaminar shear strength (ILSS), (b) Interlaminar toughness (GIIC) of GFRP samples with epoxy matrix modified by different nanofillers, Ref. [104-2].

Figure 104.3-3 – GFRP CNT-modified epoxy: Interlaminar properties

The incorporation of conductive nano-particles into an insulating polymer matrix is expected to produce some electrical conductivity when the volume fraction exceeds the percolation threshold (the point at which the particles form a conductive network through the bulk polymer, as shown in Figure 104.3.4).

Carbon nanotubes are very effective fillers for rendering polymeric matrices electrically conductive because of their high aspect ratio and strong tendency to reagglomerate. Percolation thresholds as low as 0.0025 wt.% are reported for MWCNTs in an epoxy matrix.

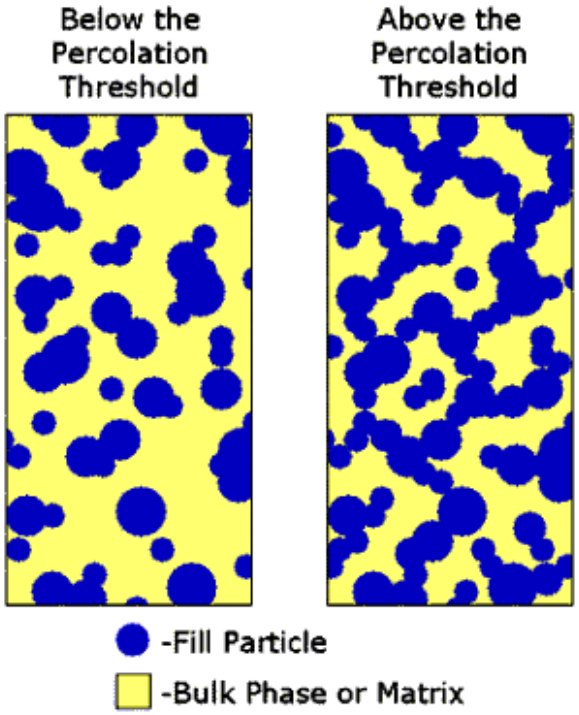

Figure 104.3-4 CNT-modified polymer: Schematic of particles forming a conductive network within a bulk polymer

Generally, the percolation threshold is considered to be lower for fibre-shaped fillers (high aspect ratio) than for spherical particles. A reagglomeration of nanotubes leads to conductive paths at lower filler contents, depending on the aspect ratio and the mobility in the matrix.

Non-functionalised DWCNTs have the highest tendency to reagglomerate. A percolation threshold below 0.1 wt.%. was determined.

Figure 104.3.5 shows the experimental results of specific conductivity of carbon nanoparticle/epoxy composites plotted against. weight percentage, Ref. [104-3].

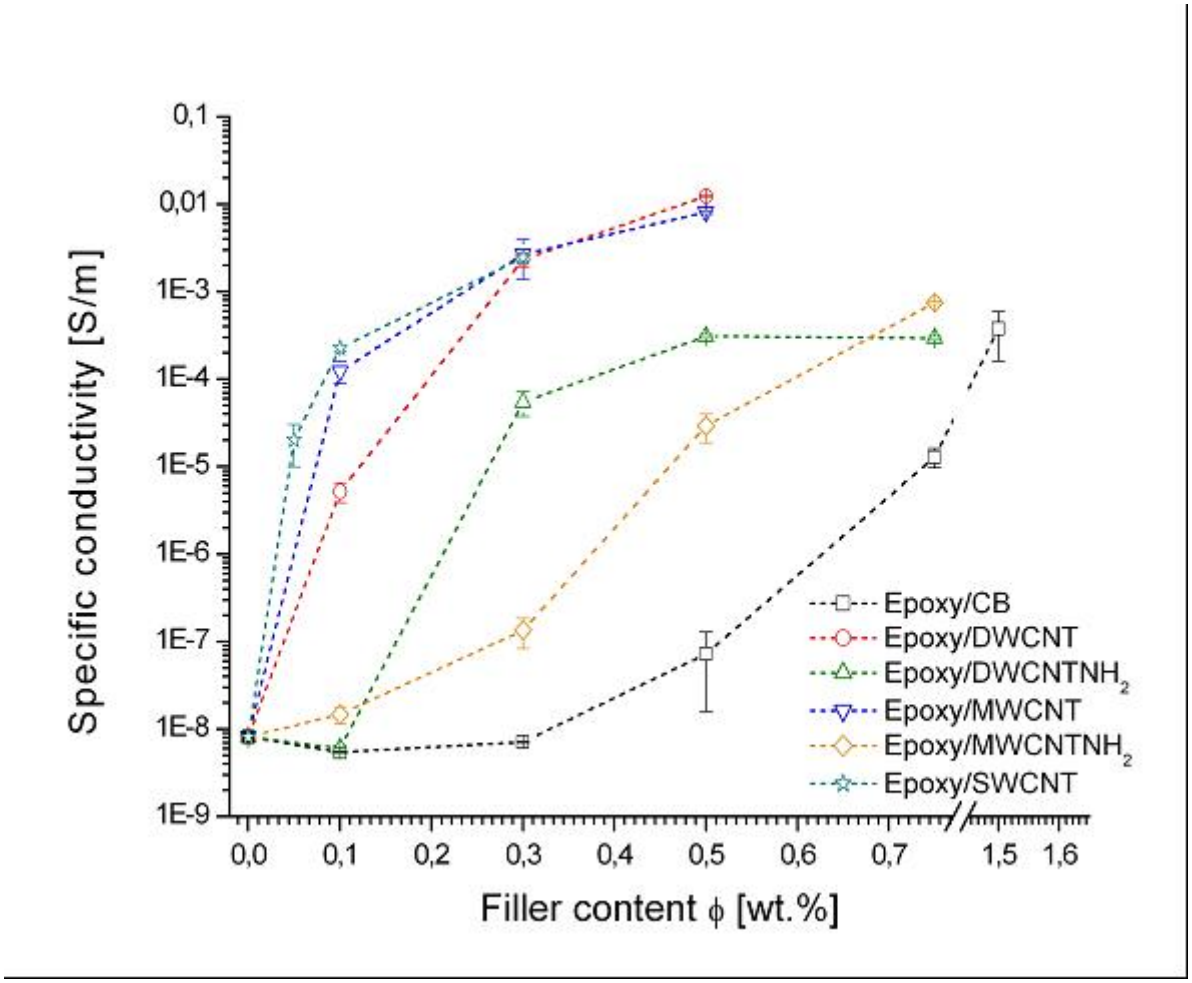

Specific conductivities of carbon nanoparticle/epoxy composites v. weight fraction, Ref. [104-3].

Figure 104.3-5 – GFRP CNT-modified epoxy: Electrical conductivity

The functionalisation of carbon nanotubes by amino-groups usually increases the percolation threshold and decreases the maximum achievable conductivity. The graphitic structure of the nanotubes becomes more defective during the functionalisation process. Also, the average nanotube length is reduced, explaining the increased percolation threshold. For carbon black, a percolation threshold of about 0.6 wt.% was achieved.

Figure 104.03.6 compares conductivity values for nano-modified composites, Ref. [104-3].

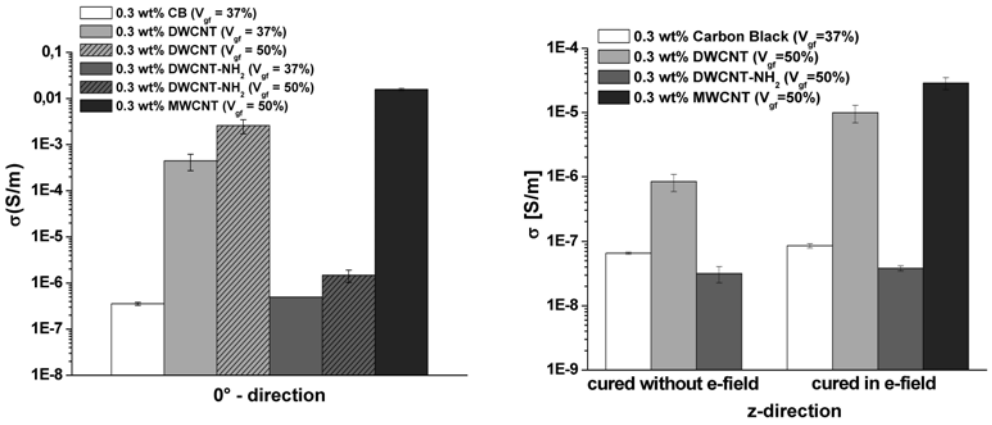

Figure 104.3-6 – GFRP CNT-modified epoxy: Comparison of electrical conductivity for 0° and z-directions

The application of an electrical field in z-direction during cure did not influence the 0°-direction conductivity. In the z-direction, for the percolated system containing 0.3 wt.% DWCNTs, the application of an electrical field during cure resulted in an increase in conductivity by more than one order of magnitude, Ref. [104-3].

The absolute conductivity values measured for the glass fibre-reinforced epoxy are very close to the reference values of the neat epoxy/CNT nanocomposites, especially for MWCNT-containing materials.

A comparison between composites containing DWCNTs and DWCNT-NH2 shows that higher glass fibre content does not reduce the overall conductivity of the composite. Indeed, the electrical conductivity is slightly increased with increasing glass fibre volume content. Ref. [104-3] provides more details and an explanation of this result.

104.4 CNT-modified cyanate ester composites

104.4.1 Introduction

Why advanced nano-composites?

Future missions demand advanced lightweight and highly thermo- and radiation-resistant materials having improved properties compared with epoxy-based systems.

As a step towards this aim, the cyanate ester family of thermoset polymers are interesting candidates for high-performance CNT-modified composites.

Cyanate ester resins cure by a cyclo-trimerisation mechanism, with or without the presence of a catalyst. Cyanate esters can be easily formulated with other industrial resins, as with epoxy resins. The different formulations can use conventional composite processing technologies, such as: filament winding, RTM resin transfer moulding, VRTM vacuum-assisted RTM, resin liquid infiltration, pultrusion, potting.

Cyanate ester resins are used for high-end applications in electronics, aerospace and in general industry because of their glass transition temperature, up to 400°C, excellent electrical and dielectric properties and thermo-mechanical stability. Furthermore, they exhibit hydrophobic behaviour, no moisture expansion, low susceptibility to microcracking and excellent resistance against particle radiation in space.

Lonza Group, CH, provide novel cyanate ester resins under the product codes Primaset® PT 15, PT 30, PT 30-S, PT 60, PT60-S and CT90, Ref. [104-22].

104.4.2 Development of CNT-cyanate ester CFRP

104.4.2.1 Space applications

For special applications in space, especially for 'hot' missions, e.g. inner planetary missions to Venus and Mercury or solar missions, there is an urgent need for novel advanced polymer composites that are resistant to high temperatures and also high levels of particle radiation. To meet this need, Astrium are developing a nano-modified cyanate-ester matrix, high-performance composite, Ref. [104-11].

The goal of the program, Ref. [104-11], is to develop structural composite materials that are thermo-mechanically stable up to 400°C and are resistant to high solar proton particle and UV fluxes. The chemical composition of cyanate ester meets these demands.

104.4.2.2 Cyanate ester chemistry

In contrast to chain-like polymer molecules, e.g. epoxy matrices, cyclo-polymerised cyanate ester molecules do not simply crack after particle impact. An impinged ring-C-atom can be replaced by a neighbour C-atom and, in this way, a molecular-scale 'self-healing effect' occurs.

A qualitative analysis of radiation effects revealed that a continuous embrittlement of cyanate ester composites is unlikely under the impact of cosmic radiation. Results of radiation experiments on cyanate ester matrices showed that very low erosion occurs, atom-layer by atom-layer is removed by forming lightly volatile hydrocarbons. Major material degradation of cyanate ester does not occur within a planned mission lifetime of several years.

104.4.2.3 Material characterisation program

The development of cyanate ester nano-composites shares some common problems with epoxies, principally how to achieve a homogenous dispersion of carbon nanotubes in the cyanate ester matrix. Consequently, the experience gained with epoxy-based materials at Technical University of Hamburg-Harburg is useful, Ref. [104-11].

The chemical composition, morphology and hardening processes of cyanate esters are different from epoxy, so new chemical pre-treatments of nano fillers, especially CNTs, are necessary to give optimum chemical compatibility between (functionalised) CNTs and the cyanate ester matrix.

Dispersion trials have been conducted with the amine-activated CNTs used for epoxy-based systems. Samples were prepared and characterised by DMA dynamical mechanical analysis and TGA thermo gravimetric analysis techniques.

104.4.2.4 Storage modulus

Figure 104.4.1 shows compares the storage modulus of Primaset® PT-30 cyanate ester matrix neat resin with 1 wt.% amine-functionalised DWCNT-NH2 modified PT-30; measured by DMA. An increase in the glass transition point was seen for the nano-modified resin; 381°C compared with 316°C for the neat resin sample.

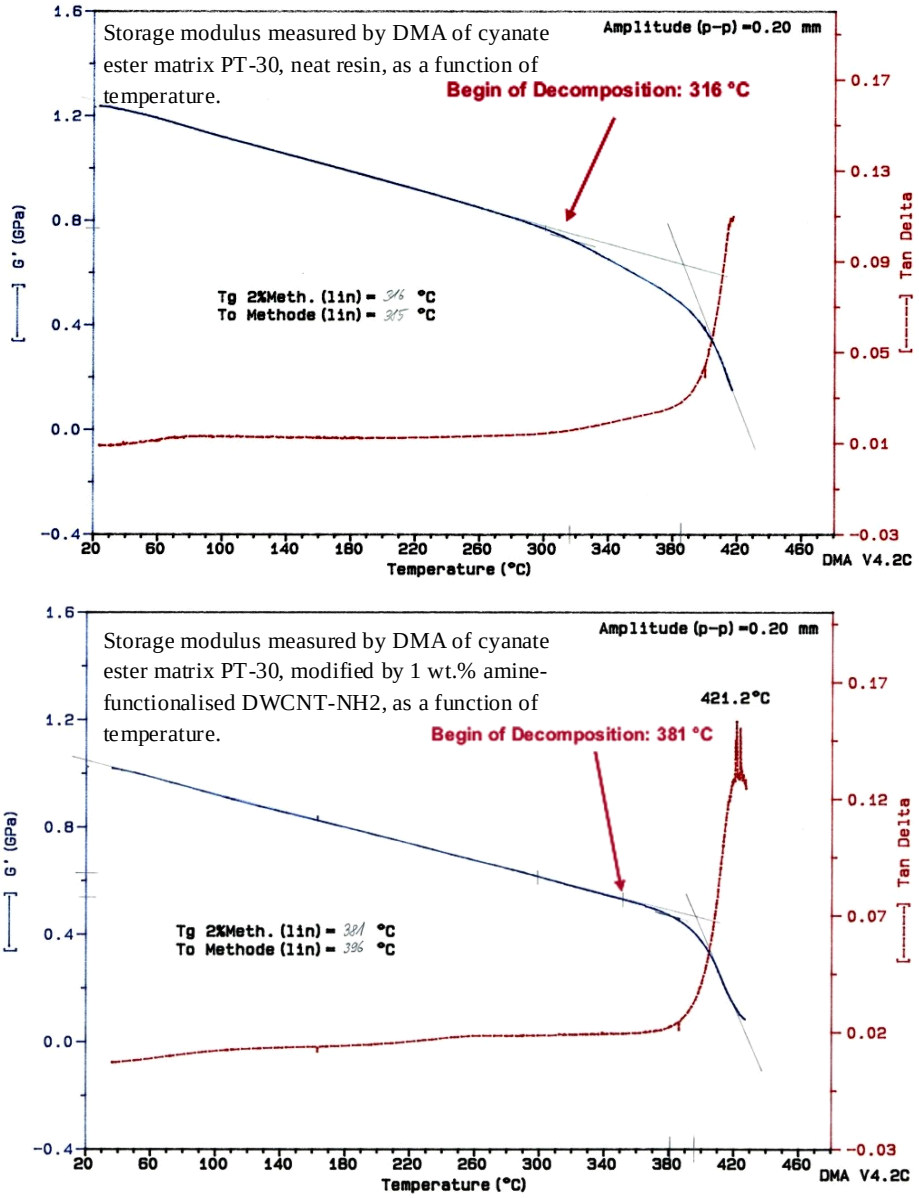

Figure 104.4-1 – CNT-modified cyanate ester: Storage modulus

Cyanate ester PT-30 resin has also been modified by incorporation of only 0.1 wt.% MWCNTs, Ref. [104-11]. Here the glass transition temperature, measured by TGA, was 426°C, which is significantly higher than 381°C for the 1 wt.% DWCNT sample or 316°C for the neat resin. Process trials are continuing.

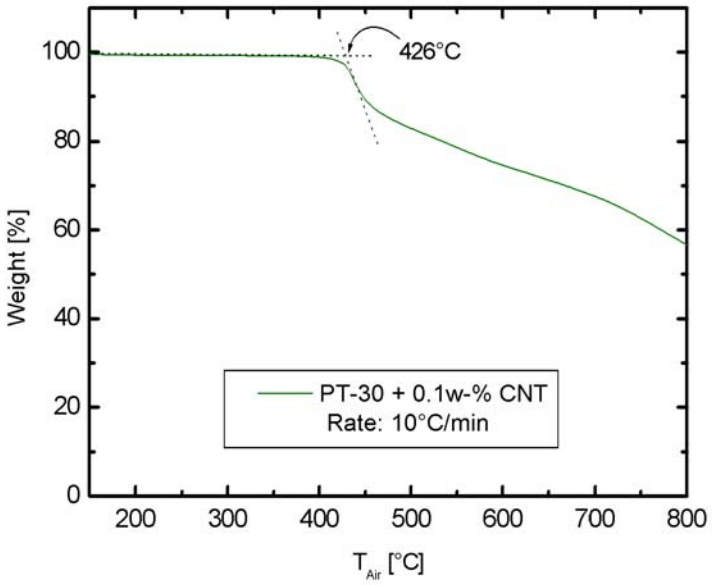

TGA measurement of cyanate ester PT-30, modified by incorporation of 0.1 wt.% MWCNTs. Glass transition temperature = 426°C compared with ~ 316°C for neat resin.

Figure 104.4-2 – CNT-modified cyanate ester: Glass transition temperature, by TGA

104.4.3 Thermal cycle tests

Thermal cycle tests on cyanate ester composite samples were performed as part of the supporting 'technology development activity' for the BepiColombo programme, Ref. [104-12].

Figure 104.4.3 shows the vacuum chamber with material samples. Testing involved 100 cycles in the temperature range □100°C to +400°C in a hydrogen-nitrogen atmosphere.

The cyanate ester composite samples survived the test without destruction, no shrinkage (accuracy of 0.01 mm) and no distortion occurred. The measured mass loss was about 5%, probably caused by chemical surface reaction between the hot hydrogen test gas with the organic material.

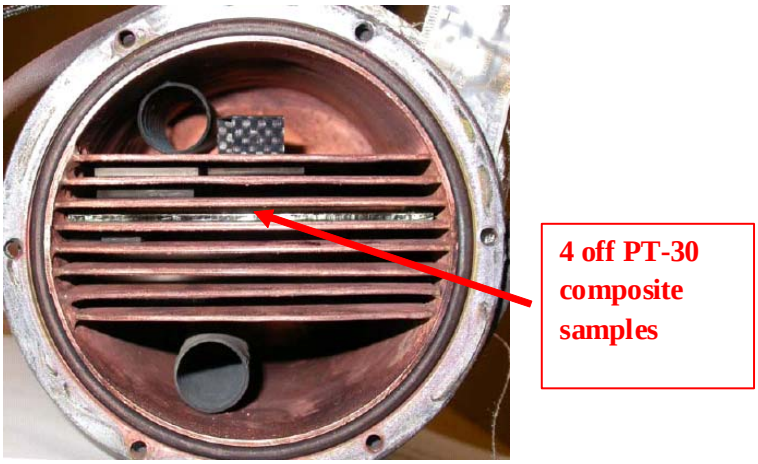

Figure 104.4-3 – CNT-modified cyanate ester: Thermal cycle test set-up from Bepi-Columbo programme

Within the initial work phase, it was demonstrated that incorporation of CNTs (DWCNTs and MWCNTs) in cyanate ester resin can enhance thermo-mechanical stability up to 400°C.

104.4.4 Characterisation of nano-modified cyanate ester composite

104.4.4.1 Manufacturing

Within the frame of the BepiColombo programme, filament winding and fibre placement manufacturing processes are envisaged for the production of composite structures made of high-performance nano-modified cyanate ester composite materials, see Figure 104.4.4.

The high viscosity of CNT-modified cyanate ester resin means that the fibre infiltration process during placement needs to be modified, e.g. by heating the resin and fibre rovings during fibre infiltration and fibre placement.

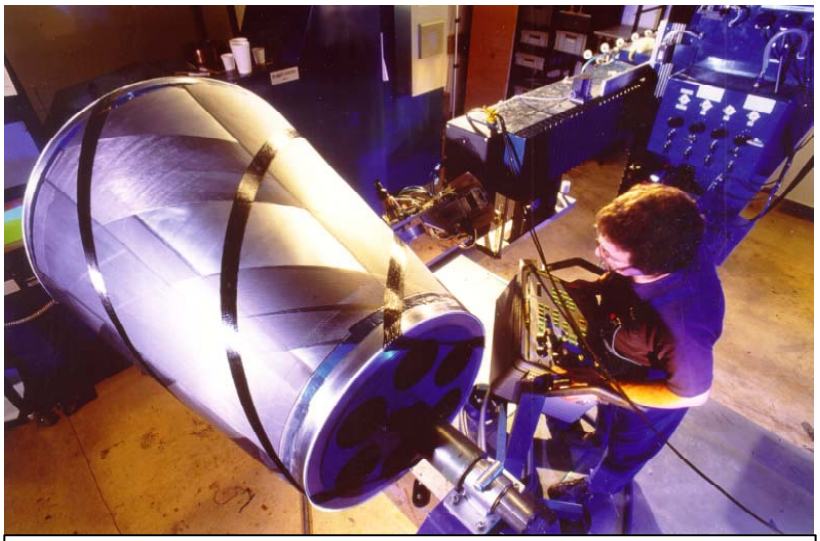

Fibre winding facility: Fibre lay-up angle is controlled by computer-controlled lay-up program

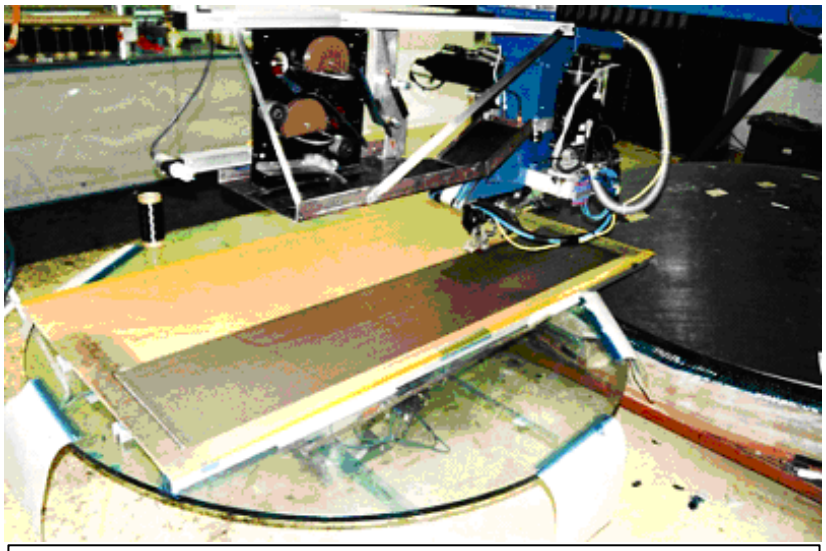

Fibre placement (5 axis): Computer-controlled lay-up program for production of carbon fibre-reinforced CNT polymer composites (samples and structures)

Figure 104.4-4 – CNT-modified cyanate ester composites: Manufacturing processes

104.4.4.2 Material characteristics

The characterisation tests for CNT-modified cyanate ester composite material include:

- mechanical tests: Bending and shear at temperatures between RT and 400°C,
- thermal tests: Measurement of thermal expansion and thermal conductivity within the temperature range $LN_2 < T < 400°C$,
- electrical conductivity measurement within the temperature range $LN_2 < T < 400°C$,
- CME coefficient of moisture expansion testing,

- outgassing tests,
- material failure investigation, using novel ultrasonic methods to detect initial occurrences of fibre-matrix-debonding at elevated temperatures.

104.5 Electrically conductive CNT polymers

104.5.1 Introduction

Electrically-conductive CNT polymer materials form two distinct groups of materials, i.e.:

- polymer surfaces coated with CNTs, known as 'surface modification'.
- CNTs incorporated into the bulk of the polymer, known as 'bulk modification'.

104.5.2 Development objectives

104.5.2.1 Conventional glass thermal control systems

Silvered borosilicate glass mirrors are currently used for thermal control applications on geostationary orbit telecom satellites. Borosilicate glass tiles backed with silver are often combined with an interference film surface coating to reflect UV energy. These mirrors have excellent thermo optical performance, but they are expensive, time consuming to apply and are easily damaged, often needing significant rework.

The improvements envisaged from an alternative design based on a metallised polymer foils include:

- significantly lower cost of materials.
- reduced production timescales.
- more robust product with reduced rework.
- flexible substrate that can conform to curved surfaces.

104.5.2.2 Conventional conductive polymer films

Silver-coated FEP polymer foils are relatively cheap but have poorer performance; they suffer from radiation-based degradation and have unacceptable electro-static discharge behaviour. The latter characteristic has meant that this material has not been used in geostationary orbit up to now.

The conventional technology for manufacturing transparent conductive films employs CVD chemical vapour deposition to synthesise ITO indium-tin-oxide films directly onto the transparent substrate. ITO-based films have several drawbacks, such as the high cost of indium, the brittleness of the resulting films and the need for expensive and cumbersome CVD equipment.

104.5.2.3 CNT-modified FEP foils

It is envisaged that the performance of FEP polymer foils can be significantly improved by modifying the polymer with CNTs to achieve the desired characteristics:

- transparency at UV and visible wavelengths.
- emissivity at IR wavelengths.
- stability to radiation, both UV and particle.

- electrical conductivity.
- temperature resistance.

104.5.3 Technology status - CNT surface modification

104.5.3.1 Conductive surface coating with SWCNT

A thin network of SWCNTs is sprayed using an air brush onto a polymer foil substrate heated to about 100°C, Ref. [104-13], [104-14], [104-15].

SWCNTs are dissolved in an aqueous suspension with the aid of ultra-sonication. Excellent adhesion of layer has been shown, even under repeated bending of the film.

The electrical and optical properties of CNT coatings are shown in Figure 104.5.1, Ref. [104-13], where the optical transmittance is plotted against the electrical resistivity.

A comparison is made between CNT-coatings and thin doped indium oxide (ITO), which is a conventional coating for transparent electrodes, Ref. [104-13].

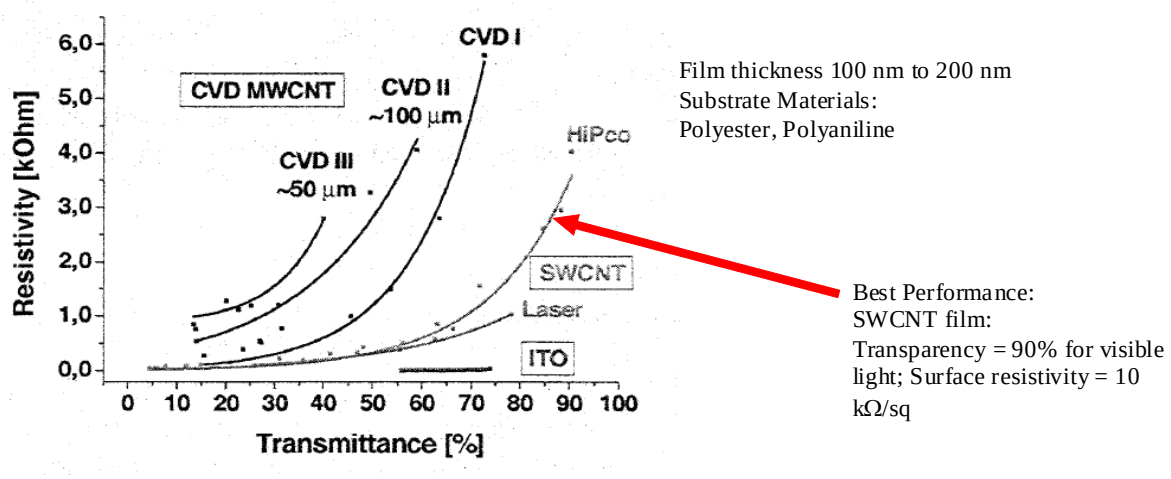

Figure 104.5-1 – CNT surface modified polymer films: Summary of electrical and optical performance

The results can be summarised as:

- SWCNTs are more suitable for transparent conductive coatings than MWCNTs.
- longer CNTs increase the conductivity for the same transparency, since they produce a decreased number of contacts between individual CNTs and the electrical transport is dominated by contact resistances between the CNTs.
- conductivity of samples with SWCNTs processed by HIPCO 'high-pressure carbon monoxide conversion' or by laser ablation is similar to that of ITO.

[See also: 104.6 – Thermal control]

104.5.3.2 CNT dispersed polymer foils

Figure 104.5.2 shows examples of commercially-available CNT-dispersed PP films, Ref. [104-18].

CNT dispersed PP film (40 ppm CNT)

CNT dispersed PP film (100 ppm CNT)

Figure 104.5-2 – CNT dispersed polymer films: Examples

104.5.3.3 Other polymer foils

For space applications, candidate materials for the production of transparent, electrically conductive polymer foils are:

- PEEK,
- PES,
- PEI,
- Fluorpolymers, such as FEP, PVD and PVF.

Typical foil thickness is of the order of 125 µm.

104.5.4 Technology status - CNT bulk modification

104.5.4.1 Nano-modified PMMA polymer

A homogeneous nanotube PMMA polymer composite was prepared by using $SOCl_2$ chemically functionalised SWCNTs, Ref [104-16]. These materials showed dramatic improvements in electrical conductivity with a very low percolation threshold below 0.2 wt.% SWCNTs, as shown in Figure 104.5.3, Ref. [104-16].

Treatment with $SOCl_2$ significantly improves the electrical conductivity of SWCNT networks in commercial polymers, like PMMA. It provides nanotube 'solubilisation' that enables an homogenous dispersion of nanotubes in the polymer matrix. Consequently only a very small amount of SWCNT produces the conductivity levels needed for several electrical applications, but without altering other polymer properties or processability.

A sharp increase of conductivity is observed between 0.1 wt.% and 0.2 wt.%, which indicates the formation of a percolating network.

Some improvement of composite mechanical characteristics, e.g. Young's modulus and tensile strength, is also observed with chemically functionalised SWCNTs. Toughness also increases by a factor of 30 compared with conventional (unmodified) PMMA films.

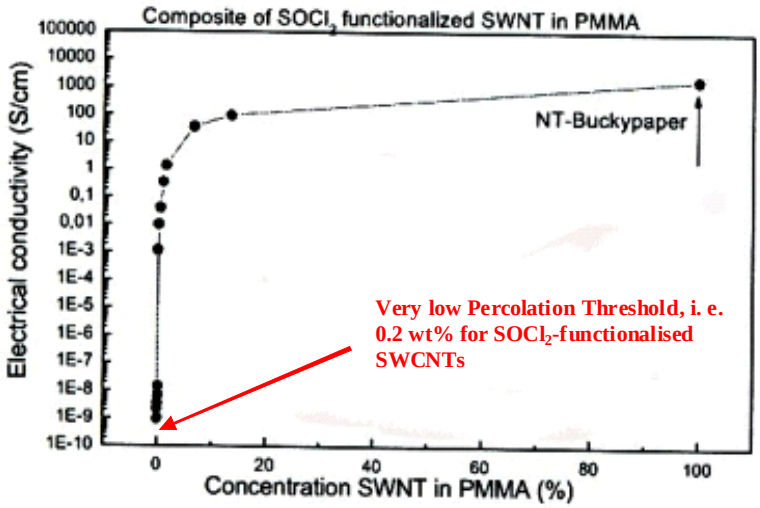

Figure 104.5-3 – CNT bulk modified polymer films: Electrical conductivity for SWCNT-modified PMMA

104.5.4.2 Nano-modified polycarbonate

To prevent electrical charging, CNT-modified polycarbonate is under development for flight vehicle windscreens, [See also: 104.6].

104.6 Potential applications

104.6.1 Introduction

104.6.1.1 CNT-modified composites

As of 2006, studies of the potential benefits of nano-modified polymer composites have been targeted at applications where either the existing materials technology cannot meet the severe service conditions of certain missions or where a significant mass-saving is considered feasible. The examples given are:

- Mercury and Sun missions: BepiColumbo, Solar Orbiter.
- reuseable vehicle primary structures: X-38.

[See also: 104.4 – cyanate ester-based nano- composites]

104.6.1.2 Electrically-conductive CNT-polymer films

As of 2006, examples of applications under consideration for electrically-conductive polymer films, made of either surface or bulk nano-modified materials, include:

- satellite thermal control: alternatives for silvered borosilicate glass mirrors.
- flight vehicle windscreens, to avoid electrical charging.

[See also: 104.5]

104.6.2 Mercury Planetary Orbiter HTHGA 'high-temperature, high-gain antenna'

The baseline HTHGA 'high-temperature, high-gain antenna' for the Mercury Planetary Orbiter, shown in Figure 104.06.1, is a Cassegrain configuration dish antenna of about 1 m diameter. It operates in X/Ka band for telecommand, telemetry and high-rate science telemetry transmission.

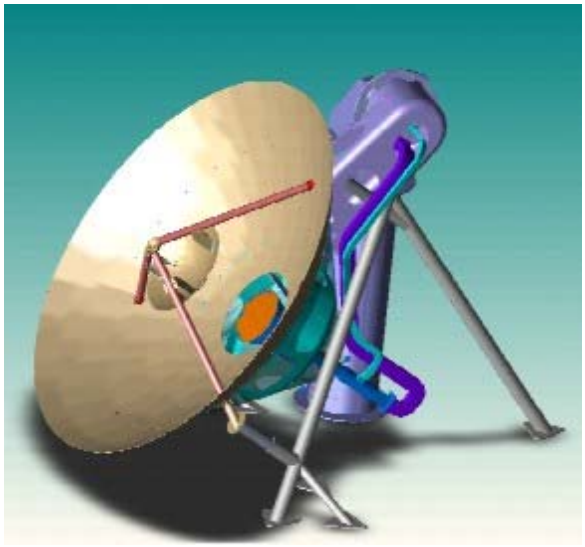

Figure 104.6-1 – Nano-modified polymer composites: Potential applications – HTHGA for Mercury Planetary Orbiter

The crucial aspects of the spacecraft design and in particular of the HTHGA system are dictated by the high radiation and high temperature environment (up to 400°C). Other design and operational factors are yet to be defined, e.g. materials, processes, components (electrical, radio frequency and mechanical).

A current study (2007) envisages the use of 400°C stable nano-modified cyanate ester composite materials to manufacture the antenna support structure and parts of the RF chain, i.e. high-temperature and radiation compatible wave guides, feeds and wave guide supports.

104.6.3 Solar arrays and solar generators

Conventional solar arrays designs are based on stiff sandwich structures made of carbon fibre-reinforced epoxy composite material. Carbon/epoxy cannot be used in the extreme environmental conditions of 'hot missions', e.g. to Mercury (BepiColombo) or to the sun (Solar Orbiter).

For the Mercury mission, the Sun intensity is up to 10 times higher than in Earth's orbit. The Solar Orbiter experiences a radiation exposure of about 25 solar constants at the closest approach to the Sun. Solar generators optimised for Earth orbits or 1 AU Sun distance cannot survive when operated under these extreme environmental conditions. Therefore special measures and design modifications are needed to ensure the safe operation of solar arrays under extreme conditions.

Assessment studies for both missions proposed a scenario using different types of solar cells with optimised designs for each special application and, by reducing the Sun incidence angle, limiting the maximum solar array and solar cell temperatures to about 250°C (hot spots up to 300°C)

Nano-modified cyanate ester composites have potential for constructing very lightweight and ultra-stiff sandwich substrates for 'hot' solar generators exposed to high temperatures and high solar radiation fluxes.

104.6.4 Re-entry and hypersonic vehicle primary structures

104.6.4.1 X-38 vehicle primary structure

An example of a possible application for cyanate ester polymer composite is for the manufacture of part of the X-38 vehicle primary structure; indicated in red in Figure 104.6.2.

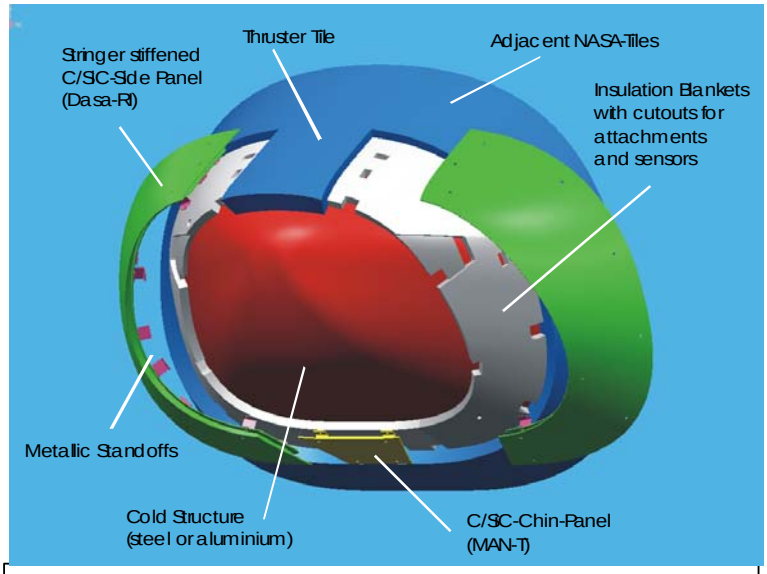

X-38 vehicle nose: CMC side panels attached to aluminum primary structure. Aluminium is a possible candidate for replacement by nano-modified cyanate ester composite.

Figure 104.6-2 – Nano-modified polymer composites: Potential applications – X-38 reusable vehicle nose structure

Aluminium is typically used for the construction of flight vehicle structures. In the case of re-entry vehicles, the temperature of the metallic walls of the primary structure is limited to 170°C in order to prevent creep.

The application of high-performance cyanate ester composites for the construction of primary structures has two perceived benefits:

- The permissible service temperature of the composite proposed is much higher, i.e. in the range of 300°C to 350°C.
- The specific stiffness (the ratio of modulus to density) is much higher compared with aluminium alloys. Consequently, a substantial mass saving is feasible by using high-performance polymer composites.

[See also: 70.24]

104.6.4.2 Hermes program

During the Hermes program, the application of high-temperature polyimide- and bismaleimide-based polymer composites was studied for primary structures by Dassault.

[See also: 6.9 – bismaleimide; 6.12 – polyimide]

104.6.5 Thermal control

Electrically-conductive FEP polymer foils having a thin SWCNT surface coating are envisaged as alternatives for silvered borosilicate glass mirrors used for thermal control on geostationary satellites. The surface resistivity needed is $\sigma s < 10^9\ \Omega/m^2$.

Bulk-modified polymer foils, with additions of SWCNTs, are also envisaged as an alternative for silvered borosilicate glass mirrors. In this case the bulk resistivity needed is $\sigma b < 10^{13}\ \Omega/m$.

104.6.6 Flight vehicle windscreens

CNT-modified polycarbonate (Plexiglass®) is under development for flight vehicle windscreens, as shown in Figure 104.6-3, Ref. [104-17]. The aim is to avoid electrical charging.

CNT-modified polycarbonate

Figure 104.6-3 – Potential applications: Flight vehicle windscreen made from CNT-modified polycarbonate

104.7 References

104.7.1 General

[104-1] J.N.Coleman, U. Khan, W.J.Blau, Y.K.Gun´ko
'Small but Strong: A Review of the Mechanical Properties of Carbon Nanotube-Polymer Composites,
'Carbon 44 (2006) p1624-1652

[104-2] F.H. Gojny, M.H.G. Wichmann, B. Fiedler and K. Schulte. 'Influence of different carbon nanotubes on the mechanical properties of epoxy matrix composites: A comparative study'.
Composites Science and Technology (2005)

[104-3] F.H. Gojny, M.H.G. Wichmann, B. Fiedler, K. Schulte'Influence of nano-reinforcement on the mechanical and electrical properties of conventional fibre reinforced composites'.
Composites A - Applied Science & Manufacturing 2005; 36: p1525-1535

[104-4] C.A. Martin, J.K.W. Sandler, A.H. Windle et al
'Electrical field-induced aligned multi-wall carbon nanotube networks in epoxy composites'.
Polymer 2005;46: p877-886

[104-5] F.H. Gojny, J. Nastalczyk, Z. Roslaniec & K. Schulte.
'Surface modified multi-walled carbon nanotubes in CNT/epoxy-composites',
Chemical Physics Letters 370 (2003) p820-824

[104-6] F.H. Gojny and K. Schulte.
'Functionalisation Effect on the Thermo Mechanical Behaviour of Multi-Wall Carbon Nanotube/Epoxy-Composites',
Composites Science and Technology 64 (2004) p2303-2308

[104-7] F.H. Gojny, M.H.G. Wichmann, U. Köpke, B. Fiedler and K. Schulte.
'Carbon Nanotube-reinforced epoxy-composites: Enhanced stiffness and fracture toughness at low nanotube content'.
Composites Science and Technology 64 (2004) p2363-2371

[104-8] F.H. Gojny, M.H.G. Wichmann, B. Fiedler and K. Schulte. 'Influence of nano-reinforcement on the ILSS of conventional fibre reinforced composites'.
Composites A Applied Science and Manufacturing (2005)

[104-9] J.D. Fidelus, F.H. Gojny, K. Schulte and H.D. Wagner. 'Thermo-mechanical properties of randomly oriented carbon/epoxy nanocomposites'
Composites A - Applied Science and Manufacturing (2005)

[104-10] F.H. Gojny, M.H.G. Wichmann, B. Fiedler, I. Kinloch, W. Bauhofer, A.H. Windle, and K. Schulte.
'Evaluation and identification of electrical and thermal conduction mechanisms in carbon nanotube/epoxy composites', 2005 (in preparation)

[104-11] H. G. Wulz et al.,
'Development of Advanced High-Performance Carbonfiber reinforced Nano modified Cyanate Ester Composite for Application in Space. Joint Development'
Report of Astrium GmbH, Technical University of Hamburg Harburg and Future Carbon GmbH. 2006 (in preparation)

[104-12] V. Liedtke, I. Huertas Olivares, D. Cabelka,
'As-Run Test Report, Thermal Cycling of HTHGA Components'
Document No: ARC-CATR-01/06, Iss 1.0, 09.05.2006

[104-13] M. Kaempgen, G .S. Duesberg, S. Roth,
'Transparent Carbon Nanotube Coatings',
Applied Surface Science 252 (2005) p425-429

[104-14] E. Artukovic et al.,
'Transparent and Flexible Carbon Nanotube Transistors'
Nano Letters, 2005, vol. 5, no. 4, p757-760.

[104-15] Paul J Glatkowski
'Carbon nanotube based conductive coatings'
Eikos Inc., 2 Master Drive, Franklin, MA. 02038 (USA)
http://www.eikos.com/

[104-16] U. Dettlaff-Weglikowska, V. Skakalova, R. Graupner, S. H. Jhang, B. H. Kim, H. J. Lee, L. Ley, Y. W. Park, Berber, D. Tomanek, and S. Roth,

Am. Chem. Soc. 2005 (accepted for publication)

[104-17] Dr. Dettlaff
Max-Planck-Institut für Festkörperforschung, Stuttgart, D
Private communications (February 2006)

[104-18] Cluster Instruments Co., Ltd,
777-97, Geomdan-dong Buk-gu, Daegu, Korea,
Tel: +82 53 382 0196, email: cluster@cluster-i.co.kr

[104-19] B. Fiedler, F.H. Gojny, M.H.G. Wichmann & K. Schulte.
'Fundamental aspects of nano-reinforced composites' Composites Science and Technology (2005) accepted.

[104-20] F.H. Gojny, J. Nastalczyk, Z. Roslaniec & K. Schulte
'Surface modified multi-walled carbon nanotubes in CNT/epoxy-composites'
Chemical Physics Letters 370 (2003) p820-824

[104-21] F.H. Gojny & K. Schulte.
'Functionalisation effect on the thermo mechanical behaviour of multi-wall carbon nanotube/epoxy-composites'
Composites Science and Technology 64 (2004) p2303-2308

[104-22] Lonza Group – Primaset® Cyanate esters
website: http://www.high-performance-materials.com/highperf/en/cyanate.html

105 MMC and CNT metal composites

105.1 MMC technology status

105.1.1 Introduction

105.1.1.1 Background

Metal matrix composites, MMCs, are generally described by:

- matrix alloy composition,
- reinforcement material,
- form of reinforcement. i.e. continuous, particulate, whisker.

Processing methods are usually by powder metallurgy routes or by casting or semi-solid processes.

Numerous variants of MMCs, produced by equally diverse methods have, over the years, been invented and evaluated. Some materials have reached commercial availability and have found use in high-performance applications, including space structures.

[See: Section XI – Advanced metallic materials]

105.1.1.2 Limitations of discontinuously-reinforced MMCs

Throughout the development of discontinuously reinforced MMCs, a number of problems have been highlighted, including:

- non-uniform distribution of particles that can occur because of::
  - Segregation, such as density differences between particles and matrix; insufficient wetting (casting processes); differences in particle size (powder metallurgy).
  - Agglomeration of particles by adhesive forces.
- porosity in castings (foam stabilisation).
- insufficient bonding between matrix and reinforcement (insufficient wetting).
- reactions, resulting in undesirable phases at high temperatures and long processing times.

One objective of the development of nano-modified metal composites, in particular CNT-modified metals, is to overcome the known deficiencies of conventional MMCs, whilst retaining their beneficial material characteristics.

105.1.2 MMC space structural applications

105.1.2.1 Al- and Mg- MMCs

MMCs, such as continuous carbon or boron fibre-reinforced aluminium and magnesium and silicon carbide reinforced aluminium are used for aerospace applications due to their lightweight and tailorable properties.

In US technology-development programs, carbon fibre-reinforced magnesium tubes for truss structures have been successfully produced by a filament-winding, vacuum-assisted casting process.

Of the short carbon fibre-reinforced aluminium composites, both particulate and whisker reinforcements in aluminium (SiCp/Al and SiCw/Al) were extensively characterised and evaluated during the 1980s. Potential applications included joints and attachment fittings for truss structures, longerons, electronic packages, thermal planes, mechanism housings, and bushings.

As of 2006, a considerable number of applications exist for MMCs in space. The need for high-precision, dimensionally-stable spacecraft structures has driven the development of MMCs in the USA.

[See: Chapter 44 – magnesium; Chapter 46 – aluminium]

105.1.2.2 Space Shuttle Orbiter

The first successful application of continuous fibre-reinforced MMC was the application of short tubular struts made of boron fibre-reinforced aluminium. These were used as the frame and rib truss members in the mid-fuselage section, and as the landing gear drag link of the Space Shuttle Orbiter.

Several hundred boron fibre-reinforced aluminium tube assemblies with titanium collars and end fittings were produced for each Orbiter. In this application, the boron fibre-reinforced aluminium tubes provided a 45% weight saving over the baseline aluminium design, Ref. [105-1].

105.1.2.3 Hubble Space Telescope – high-gain antenna boom

The major application of a carbon fibre-reinforced aluminium composite is a high-gain antenna boom for the Hubble Space Telescope. This was made from diffusion-bonded sheet comprising P100 carbon fibres in 6061 aluminium alloy. The 3.6 m long boom provided the desired stiffness and low CTE to maintain the position of the antenna during space manoeuvres. In addition, it provided the wave-guide function, with the MMCs excellent electrical conductivity enabling electrical-signal transmission between the spacecraft and the antenna dish.

The high dimensional stability of the MMC meant that the material maintains an internal dimensional tolerance of ± 0.15 mm along the entire length.

Whilst the boom currently in service has continuous carbon fibre reinforcement, replacement structures made from less expensive, carbon short fibre-reinforced aluminium have been certified.

105.1.2.4 Combined function applications

A few MMCs have been designed to serve multiple purposes, such as structural, electrical, and thermal-control functions. For example, prototype short carbon fibre-reinforced aluminium composites were developed as structural radiators to perform structural, thermal, and EMI-shielding functions.

Short carbon fibre-reinforced copper MMCs, having high thermal conductivity, were developed for high-temperature structural radiators.

A carbon short fibre-reinforced aluminium panel is used as a heat sink between two printed circuit boards to provide both thermal management and protection against flexure and vibration that could lead to premature failure of the components on the circuit board.

105.1.3 Al- and Mg- MMC characteristics

105.1.3.1 Continuous fibre-reinforced MMCs

Table 105.1.1 gives typical properties of a few (unidirectional) continuous fibre-reinforced MMCs, Ref. [105-1].

Table 105.1-1 – Continuous fibre-reinforced MMC: Typical properties

Properties	P100/6061 Al (0°)	P100/AZ91C Mg (0°)	Boron/Al (0°)
Volume percentage reinforcement	42.2	43	50
Density ρ (kg/m^3)	2500	1970	2700
Poisson's ratio η_{xy}	0.295	0.3	0.23
Specific heat Cp (J/kg K)	812	795	801
Longitudinal (*x*-direction):			
Young's modulus (GPa)	342.5	323.8	235
Ultimate tensile strength (MPa)	905	710	1100
Thermal conductivity (W/m K)	320.0	189	-
CTE (10^{-6} /K)*	–0.49	0.54	5.8
Transverse (*y*-direction):			
Young's modulus (GPa)	35.4	20.7	138
Ultimate tensile strength (MPa)	25.0	22.0	110
Thermal conductivity (W/m K)	72.0	32.0	-

* Slope of a line joining extreme points (at –100°C and +100°C) of the thermal strain curve (first cycle)

In general, the measured properties of as-fabricated MMCs are consistent with the composite properties predicted by analysis.

The primary advantage of MMCs in comparison with organic-matrix composites is the maximum operating temperature. For example: Boron fibre-reinforced aluminium offers useful mechanical properties up to 510°C, whereas an equivalent boron fibre-reinforced epoxy composite is limited to about 190°C.

MMCs such as carbon fibre-reinforced aluminium (Gr/Al), magnesium (Gr/Mg) and copper (Gr/Cu) exhibit higher thermal conductivity because of the significant contribution from the metallic matrix.

NOTE US-origin materials' data denotes the reinforcement as Gr (graphite) instead of carbon, as used in Europe.

105.1.3.2 Discontinuously-reinforced Al- MMCs

Table 105.1.2 lists typical properties of discontinuously reinforced aluminium composites for spacecraft applications, Ref. [105-1].

Discontinuously reinforced aluminium, DRA, is an isotropic MMC with specific mechanical properties superior to conventional aerospace materials.

MMCs have been produced using 6092 and 2009 matrix alloys for the best combination of strength, ductility, and fracture toughness. Matrix alloy 6063 matrix is used to obtain high thermal conductivity.

Table 105.1-2 – Discontinuously reinforced aluminium MMC: Typical properties

Properties (direction)	Graphite Al GA 7-230	Al6092/SiC/17.5p	Al/SiC/63p
Density, ρ (kg/m^3)	2450	2800	3010
Young's modulus (GPa)	88.7	100	220
Compressive yield strength (MPa)	109.6	406.5	-
Ultimate tensile strength (MPa)	76.8	461.6	253
Ultimate compressive strength (MPa)	202.6	-	-
CTE (*x*-*y*) (10^{-6} /K)	6.5 to 9.5	16.4	7.9
Thermal conductivity (*x*-*y*) (W/m K)	190	165	175
Thermal conductivity (*x*) (W/m K)	150	-	170
Electrical resistivity, (μOhm cm)	6.89	-	-

105.1.4 Discontinuously-reinforced Ti-MMC characteristics

105.1.4.1 General

Particulate-reinforced titanium alloy MMCs are commercially available. These MMCs have good ambient and elevated temperature properties, combined with wear resistance. They are considered for highly-loaded aerospace applications, and are being evaluated for a variety of potential applications, e.g. military vehicles, commercial automotive engines, sporting goods, industrial tooling, and biomedical devices, Ref. [105-2].

Whisker-reinforced titanium alloys are emerging as potential materials for space applications, Ref. [105-3].

105.1.4.2 CermeTi®

Dynamet Technology Inc. (USA) has used advanced powder-metallurgy technology to develop the CermeTi® family of titanium MMCs, Ref. [105-2]. Near-net shape CermeTi® composite components are being produced commercially and are being evaluated.

Reinforcing the titanium alloy matrix with titanium carbide (TiC) or titanium boride (TiB) particles results in improved properties. The discontinuously reinforced titanium composites have high RT and elevated temperature properties with improved wear resistance.

Particulate additives TiC and TiB_2 are used for reinforcement. The TiB_2 particles react with the titanium in-situ, transforming the particulate titanium diboride (TiB_2) to titanium monoboride (TiB) needles.

CermeTi-C MMC consists of a particulate dispersion of TiC in a matrix of Ti-6Al-4V, whereas CermeTi-B consists of TiB in a matrix of Ti-6Al-4V.

The CHIP process, described as an advanced powder metallurgy cold and hot isostatic pressing process, is used for consolidation of the material; as shown in Figure 105.1.1, Ref. [105-2].

Blended powders are cold isostatically pressed in reusable elastomeric tooling to produce a compact approximately 85% of theoretical density. This green compact is then sintered under vacuum to produce alloying and densification to about 95% of theoretical density, with closed

porosity (i.e. no interconnected pores). Hot isostatic pressing then closes residual pores to produce a fully dense material, Ref. [105-2]. Some features of the process include:

- capable of producing large parts weighing about 20 kg.
- reduced interaction and segregation of constituents because of low-temperature consolidation processing (sintering at 1232°C compared with melting at >1650°C).
- economic, because of reduced processing temperature.

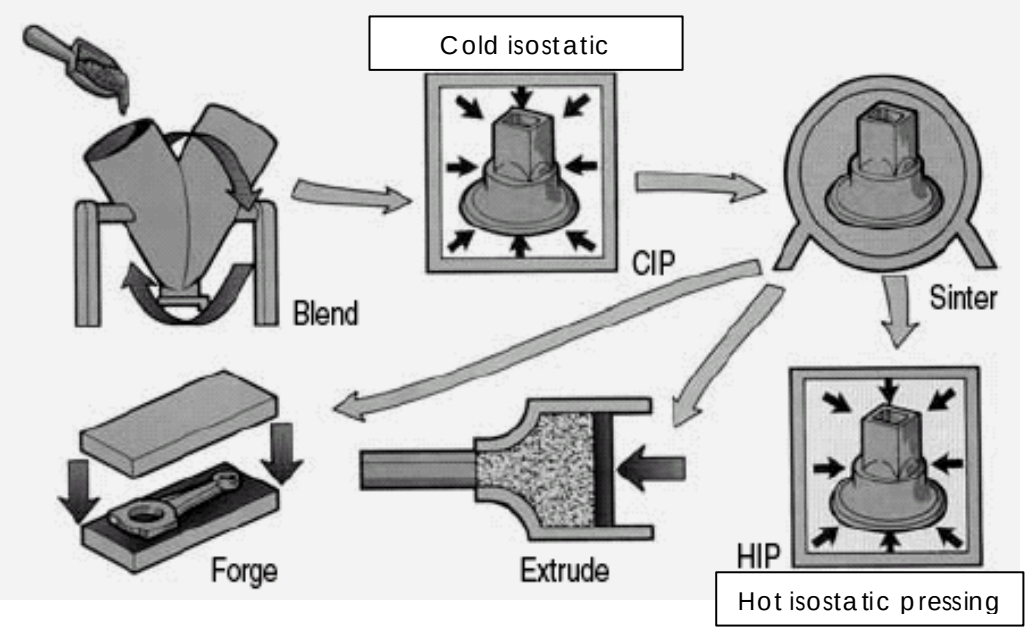

Figure 105.1-1 – Discontinuously reinforced Ti-MMC: CHIP process

Compared with Ti-6AL-4V alloy, CermeTi® Ti-MMCs has a higher modulus, better high-temperature performance and significantly superior wear resistance, whilst offering satisfactory fracture toughness; as summarised in Table 105.1.3, Ref. [105-2].

Table 105.1-3 – Discontinuously reinforced Ti-MMC: Typical properties of CermeTi® compared with Ti-6Al-4V alloy

Properties	CermeTi®-C-10 (10 wt% TiC/Ti-6Al-4V)	Ti-6Al-4V*
Yield strength (MPa)	1014	862
Tensile strength (MPa)	1082	965
Elastic modulus (GPa)	135	116
Fracture toughness (MPa $m^{-3/2}$)	40	80

Key: CermeTi® is a trademark of Dynamet Technology Inc. (USA); * CHIP processed Ref. [105-2]

105.1.4.3 TiB whisker-reinforced Ti-MMCs

Initial studies showed that some reinforcements, such as SiC, Al_2O_3, Si_3N_4, and B_4C, form one or more reaction products at the interface. This presents a major barrier to developing viable Ti-matrix MMCs. Recent research efforts have concentrated on the benefits of incorporating TiB whiskers as reinforcements in titanium or titanium alloys.

A variety of titanium alloys including α, α+β, and β alloys are already in use for diverse applications needing specific strength, creep, and corrosion resistance, Ref. [105-3]. TiBw Ti-MMCs are emerging as candidate materials for advanced applications, including space.

Table 105.1.4 gives material properties of TiB-reinforced titanium composite compared with pure Ti and other Ti compounds, Ref. [105-3].

Table 105.1-4 – Discontinuously reinforced Ti-MMC: Properties TiB compared with other Ti compounds

Properties	Ti	TiB	TiB_2	TiC	TiN
Density (kg/m^3)	4570	4560	4520	4920	5430
Elastic modulus (GPa)	110	371*	540	450	390
CTE at RT ($\times 10^{-6}$ /°C)	8.6	7.15	6.2	7.95	9.35
Vickers hardness (kg/mm^2)	150	1800†	2200	3200	2300
Melting/decomposition temperature (MPa)	1668	2200	2970	3054	3220

Key: * - Determined; † - Measured Ref. [105-3]

Table 105.1.5 shows mechanical properties at RT for various discontinuously reinforced Ti alloys containing different volume % of TiB reinforcement, Ref. [105-3].

Table 105.1-5 – Discontinuously reinforced Ti-MMC: Typical properties of TiB reinforced Ti-alloys at RT

Matrix composition (wt%)	TiB (vol%)	E (GPa)	σy (MPa)	σUTS (MPa)	Elongation (%)	Manufacturing method
Ti (ASTM Grade-4)	0	110	480	550	15.0	Wrought
Ti-6Al-4V	10	136.6	-	1000	0.25	MA + HIP
Ti-24Al-10Nb (at%)	10	-	*	695	0.0	PM + HIP
Ti-6Al-4V	11	144	1315	1470	3.1	GA + HIP/Extrusion
Ti	15	139	842	903	0.4	VAR + Hot swage
Ti-5Al-2.5Fe	15	151	*	1092	0.0	PM + HIP
Ti	20	148	*	673	0.0	PM
Ti-6Al-4V	20	154†	1170	-	2.5	MA + HIP
Ti-4.3Fe-7Mo-1.4Al-1.4V	0	110	-	1080	17.5	MM +CIP +Sinter + Hot swage
Ti-4.3Fe-7Mo-1.4Al-1.4V	10	134	-	1380	~7	MM +CIP +Sinter + Hot swage
Ti-4.3Fe-7Mo-1.4Al-1.4V	20	156	-	1640	~3	MM +CIP +Sinter + Hot swage
Ti-4.3Fe-7Mo-1.4Al-1.4V	30	180	-	1820	~1	MM +CIP +Sinter + Hot swage
Ti-6.4Fe-10.3Mo	34	163.2	*	737	0.49	PM
Ti-24.3Mo	34	171.2	*	1105	0.85	PM
Ti-53Nb	34	122.12	710	724	1.65	PM
Ti-6Al-4V	20	170	1181	1251	0.5	PM + E
Ti-6Al-4V	40	210	-	864	0	PM + E

Key: MA: Mechanical alloying; MM: Mechanical mixing; PM: Powder metallurgy; GA: Argon gas atomisation; VAR: Vacuum melting; CIP Cold isostatic pressing; E: Extrusion. * : Specimen failed before yielding; † : Data determined by extrapolation. Ref. [105-3]

105.1.5 Overview – MMC production processes

105.1.5.1 Powder metallurgy

Figure 105.1.2 shows the process flow of different powder metallurgy routes for the production of near-net shape parts made of particle-reinforced MMCs, Ref. [105-4].

[See also: Chapter 88]

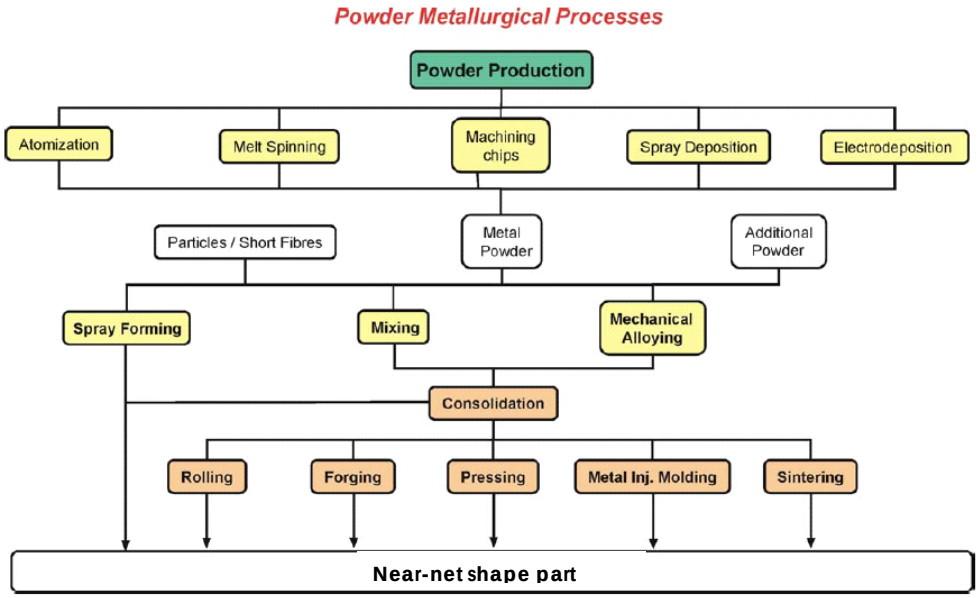

Figure 105.1-2 – Particle reinforced MMC: Powder metallurgy processes

105.1.5.2 MMC consolidation processes

Various consolidation technologies are used during the manufacture MMCs, including:

- rolling
- forging
- HIP hot isostatic pressing
- metal powder injection moulding
- new sintering technologies, e.g. Spark plasma sintering

[See also: Chapter 88]

105.1.5.3 Casting and semi-solid processes

Figure 105.1.3 shows the process flow of established casting and semi-solid-processing for the production of near-net shape parts made of particle reinforced MMCs, Ref. [105-4].

[See also: Chapter 88]

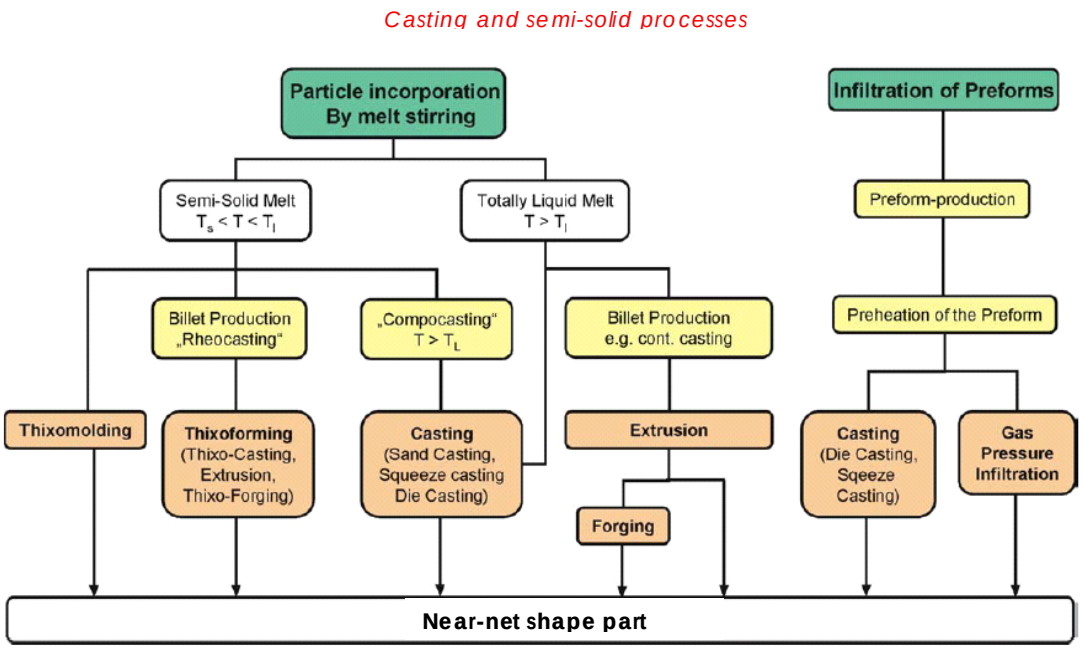

Figure 105.1-3 – Particle reinforced MMC: Casting and semi-solid processes

105.2 CNT-modified metallic materials

105.2.1 Technology status

105.2.1.1 General

CNT-modified metallic materials are sometimes denoted as CMM in literature.

There is much interest in producing metal matrix nanocomposites that incorporate nanoparticles and nanotubes for structural applications. These materials are predicted by some material scientists to offer even greater improvements in their physical, mechanical and tribology properties compared with conventional MMCs having micro-sized reinforcements. But:

'Caution! The best properties of a material that you will ever see are when you first see the properties!'

From a comprehensive literature review to establish current knowledge, conducted by Astrium in 2006, many of the enthusiastic claims made for CNT-modified metals are somewhat controversial and remain unsubstantiated.

105.2.1.2 Predicted characteristics

In particular, the incorporation of carbon nanotubes promises, in principle, higher strength, stiffness, and electrical conductivity compared with metals, and possibly offers a significant increase over these properties of MMCs.

Some, mainly theoretical, literature predicts outstanding property enhancement for CNTs added to an Al, Mg or Ti based alloy; similar to dispersion-strengthened or fibre-reinforced material, i.e. improved mechanical strength; higher E-modulus, yield strength and creep resistance. Thermo mechanical properties are also expected to improve; better heat resistance, thermal conductivity, controllable thermal expansion and low density.

Hence, CNT-materials are considered as offering a high potential for aerospace applications and are under examination regarding the replacement of magnesium and aluminium in various spacecraft and aircraft structures.

105.2.1.3 Material-based aspects

Various controversial predictions have been made regarding the range and level of benefits attainable by nano-metallic materials compared with conventional MMCs and alloys. It is very difficult to distribute CNTs homogeneously in a metallic matrix, which could explain the variations in the success claimed.

From a chemical point of view, the interfaces of CNTs (covalent bonds) and that of the metal host material (metallic bonds) are not compatible, and, further, the CNTs bundles tend to strongly agglomerate when embedded in the metallic matrix. However, it has been demonstrated that, by using a complex functionalisation treatment, CNT nano fillers can be made compatible with a metallic matrix through the development of different, complex process routes.

Some candidate materials for structural applications are described, along with their associated processing routes.

105.2.2 Overview of CMM processing routes

Table 105.2.1 provides an overview of processes available for the production of CNT-modified metallic composites, Ref [105-4]. These processes can be applied to the manufacture of bulk samples, components and structures.

Table 105.2-1 – CNT-modified metals: Overview of manufacturing processes

Matrix	Casting	Powder metallurgy		CNT (%)	Literature source
		Mixing	Consolidation and secondary operations		
Magnesium	Melt stirring			0 to 15	Li 2005
		Dry mixing	Hot pressing, HIP	2	Carreno 2004
		Dry mixing	Hot pressing	1	Yang 2005
Aluminium		Ball milling	Cold compaction, Hot extrusion	1 to 3	Edtmaier 2004
			Cold compaction, Hot extrusion	0.5 to 2	George 2005
		Ultrasonic stirring	Cold compaction, Hot pressing	5	Zhong 2003
	Nano scaled dispersion (NSD) method				Nogushi 2004
	Spray forming			?	Laha 2005
Titanium		Mechanical mixing	Hot pressing	10 to 20	Kuzumaki 2003
Copper		Ball milling	Isostatic pressing, Isothermal sintering (and rolling, annealing)	4 to 25	Chen 2003 Dong 2005
		Molecular level mixing	Cold compaction, Spark sintering	5 to 10	Cha 2005
		Electroless deposition	Hot pressing	1 to 5	Edtmaier 2004

105.2.3 CNT-modified aluminium composites

105.2.3.1 Production process

Figure 105.2.1 shows a powder metallurgy process for CNT-modified aluminium composites, Ref. [105-4].

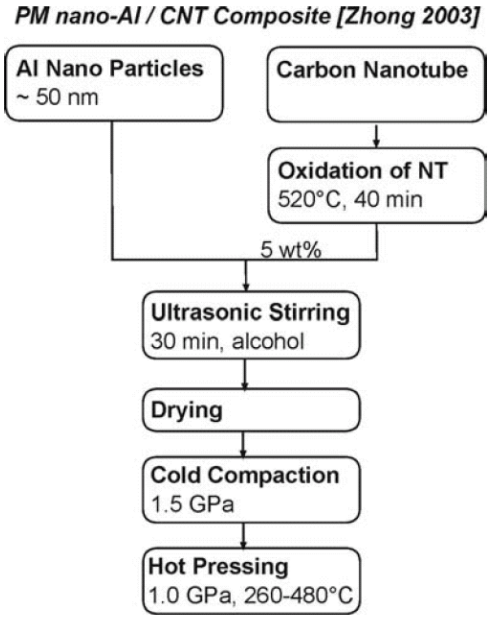

Figure 105.2-1 – CNT-modified aluminium composite: Example of powder metallurgy processing route

105.2.3.2 Mechanical properties

Table 105.2.2 compares theoretical and experimental property values for SWCNT- and MWCNT-modified aluminium composites, Ref. [105-5].

Table 105.2-2 – CNT-modified aluminium composite: Material properties

Vol.%	Shear lag Young's modulus (GPa)	Experimental Young's modulus (GPa)	Thermal mismatch yield strength (MPa)	Experimental yield strength (MPa)	Orowan looping yield strength (MPa)	Experimental ultimate tensile strength (MPa)
MWNT						
0.5	74.305	78.1	117.346	86	90.573	134
0.5 + K_2ZrF_6	74.305	75.20	117.346	93	90.573	150
2	87.376	85.85	197.346	99	101.145	138
SWNT						
1	79.167	70	471.403	79.8	184.203	141
1 + K_2ZrF_6	79.167	93.7	471.403	98.7	184.203	181
2	88.355	79.3	636.344	90.8	227.365	134

The results presented show a rather small improvement in mechanical properties for CNT-modified metal composites; stiffness (E-modulus), hardness, fatigue and yield strength, but not for ultimate strength. This indicates that CNTs act like precipitation hardening agents. Similar findings are published elsewhere, Ref [105-6], [105-7], [105-8].

However, the metallic structure is much more stable at temperatures up to 600°C; compared with a loss of 50% for the host material without CNTs.

Generally, the hardness and the stiffness also increase by about 20% when modified by CNTs.

The thermal and electrical properties of CNT-modified metallic materials show more of an improvement. The incorporation of even a small vol.% of CNT into the metallic matrix improves the thermal and electrical conductivity significantly, Ref. [105-9].

105.2.4 CNT-modified magnesium composites

105.2.4.1 Production process

For casting and semi-solid processing, Ref. [4, 16], the minor difference in density between magnesium alloy AZ91 (1.81 g/cm^3) and MWCNTs of ~1.8 g/cm^3 helps to provide good dispersion. Moreover, magnesium and carbon are chemically compatible; wetting at higher temperatures and pressures, as seen with carbon fibre-reinforced magnesium MMCs. Special coatings on CNTs, such as Ni and TiN, enhance wetting and bonding at the CNT-to-matrix interface.

A proven industrial process for the production of CNT-Mg composites is 'thixomolding'; shown schematically in Figure 105.2.2. This process provides intensive mixing by high shear forces (high viscosities), short contact times and low processing temperatures.

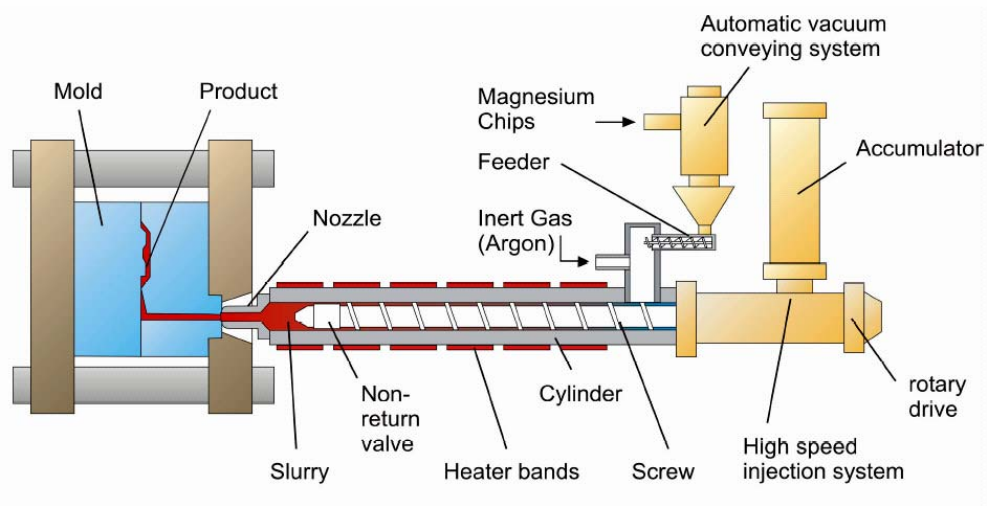

Figure 105.2-2 – CNT-modified magnesium composite: Schematic of 'thixomoulding' process

105.2.4.2 Mechanical properties

Figure 105.2.3 shows materials properties of cast CNT-magnesium composite, with respect to nano-filler content, Ref. [105-4].

The results can be summarised as:

- young's modulus and hardness increase with CNT-content
- tensile properties are influenced by the distribution of the CNTs and bonding between CNTs and matrix.

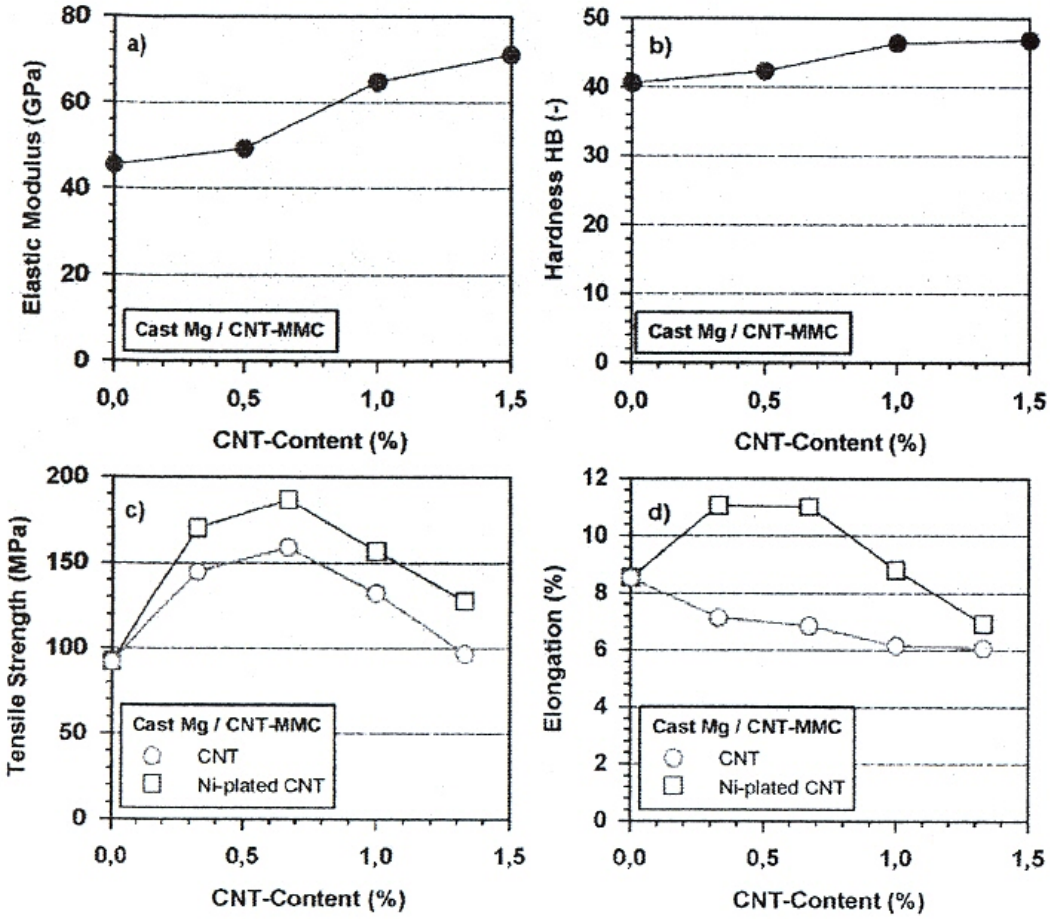

Figure 105.2-3 – CNT-modified magnesium composite: Material properties

105.2.5 CNT-modified Al and Cu - Thermal management

105.2.5.1 General

There is a crucial need for the development of novel thermally-conductive materials and structures. Advances in thermal management technologies are needed in order to accommodate the increased thermal demands of planned space missions. For example, for densely-packed electronic devices dissipating high heat flux densities in the order of tens of W/cm^2 which also demand a very accurate temperature control in the order of a tenth of a degree Kelvin.

The ability to resolve thermal management is imperative for the next-generation of IC packages, lasers and microwave generators. Accurate and reliable temperature-control of high heat

dissipating devices is vital for achieving the highest possible performance and instrument resolution.

105.2.5.2 Laser components

Laser transmitters and laser diodes are typical examples with such thermal requirements, since the accuracy of the laser wavelength strongly depends on the temperature of the laser diode. A similar temperature-dependency exists with microwave generators, e.g. klystrons.

105.2.5.3 Large-scale integrated circuits

Ultra-large-scale-integration of electronic devices demands advanced thermal management as the circuits become increasingly more dense and compact. State-of-the-art ICs for microprocessors operating at high frequencies are routinely characterised by power densities in the order of 50 W/cm^2. Such a large power density leads to highly localised heating of ICs ('hot spots').

105.2.5.4 CNT-based materials

Carbon nanotube (CNT) based systems are promoted as solutions to the problem of effective thermal management of high power devices. CNT arrays and CNT-based composite structures have shown superior thermal conductivity and therefore have a good potential for providing efficient heat transfer.

It has been shown that CNTs exhibit very high 'axial' thermal conductivity. For a discrete multiwalled nanotube (MWCNT), the thermal conductivity is expected to exceed 3000 W/mK along the tube axis. The combination of expected high thermal conductivity, tailoring of thermal strain (to match the CTE of the heat dissipating device, such as gallium arsenide or alumina) and low density make CNT metallic composites an attractive technical solution for advanced thermal management of future high heat-dissipative compact devices. Possible applications include:

- high performance power electronics,
- 3-D multi-chip packages for compact micro-electronic devices,
- laser transmitters,
- re-usable thrusters,
- heat sinks,
- battery sleeves,
- power semiconductor packages,
- microwave modules,
- black box enclosures,
- printed circuit board heat sinks,

The challenge remains to incorporate chemically compatible CNTs into metal matrices whilst conferring their outstanding thermal and mechanical properties on the host material.

105.2.6 CNT-modified copper composites

105.2.6.1 Powder metallurgy process routes

Powder metallurgy is the most commonly used technique for the production of large CNT copper composite samples, Ref. [105-10].

In a typical process method, MWCNTs are synthesised by CVD, then purified using ultrasonic cleaning in a mix of concentrated sulphuric and nitric acids at elevated temperature, followed by washing and drying. The purified CNTs, either in aggregate or bundled form, are dispersed either in an ultrasonic bath with an aqueous dispersant solution or by ball-milling, dry or in ethanol. The resultant MWCNTs are then mixed with the copper powder.

Three consolidation techniques are used:

- hot-pressing in an argon atmosphere at 900°C.
- spark-plasma sintering, followed by heating to 900°C and thermal hold for 5 minutes.
- sinter-rolling-sintering, whereby the powder mixtures are pressed at 350 MPa, sintered in vacuum at 900°C for two hours, then rolled 50 per cent, followed by a second sintering at 900°C for one hour.

These consolidation methods show a wide range of results. Sintering alone gives poor consolidated of only 50% to 60% theoretical density, due to the presence of CNT aggregates. All of the other methods show much higher densities; close to 90% theoretical density. Spark-plasma sintering results in slightly higher densities than the other methods, but combined sintering and rolling has similar results.

The dispersion of the nanotubes is again a vital factor in the production of high-performance composites. The best results have been achieved using the molecular level mixing and dispersion shown in Figure 105.2.4, Ref. [105-4].

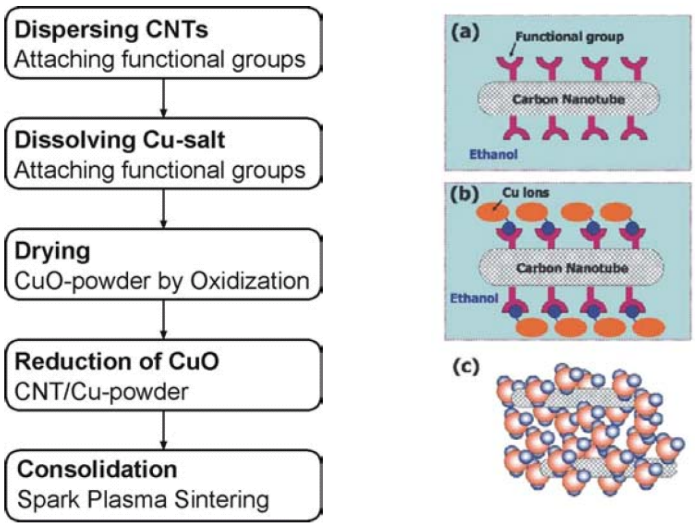

Figure 105.2-4 – CNT-modified copper composite: Molecular level mixing process

105.2.6.2 Electrochemical deposition (metal into 3D CNT network)

Electrochemical preparation of SWCNT-Cu composites uses a thick network of SWCNT (Bucky paper) as the working electrode in a $CuSO_4$ solution, at different electrochemical potentials, Ref. [105-11].

The electrical conductivity of the composites, measured at room temperature, is the same as for Cu metal. Further work is in progress.

Another approach at NASA Ames uses vertically-aligned MWNT arrays that can be fabricated on silicon wafers or copper substrates using a DC-biased plasma-enhanced chemical vapour deposition (PECVD) technique, Ref. [105-12]. NASA Ames has pilot-scale and wafer scale plasma

growth chambers for synthesising vertically aligned CNTs. After nanotube synthesis, copper filling between individual MWCNTs (so-called nanotube trenches) is accomplished using electro-deposition. Figure 105.2.5 shows a cross-section of the as-made material, Ref. [105-12]. A film of carbon nanotube/copper composite has been shown to be an effective, reusable heat sink material for integrated circuit cooling applications, Ref. [105-12].

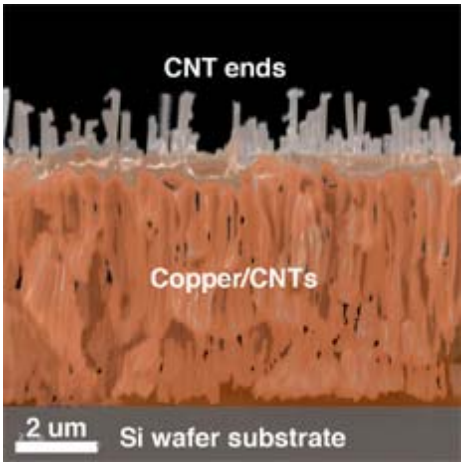

Figure 105.2-5 – CNT-modified copper composite made by NASA Ames electrodeposition method

In a three-electrode setup with a MWCNT array as the working electrode, a saturated calomel electrode was used as the reference electrode, and a platinum foil as the counter electrode, set in parallel with the MWCNT sample. Both the metal substrate and MWCNTs serve as electrodes during the electro deposition. Various additives were employed in the solution to achieve optimum gap filling into the high-aspect-ratio 'forest-like' CNT arrays.

105.2.6.3 Electrochemical deposition: Material characteristics

The preliminary property data indicate that there is a benefit in using CNTs and CNT-Cu composite films to achieve good heat conduction. Such fabricated metal composites can be used as heat-sinks for critical 'hot spots' on devices needing high heat dissipation.

It has also been shown that CNTs provide the added benefits of high mechanical stability and reusability. Consequently, this approach can be integrated into packaging processes and designs for providing highly efficient device cooling.

105.2.7 European 'ExtreMat' project

The EC-funded ExtreMat 'New Materials for Extreme Environments' is a 5-year project, started in late-2004.

A major objective of the ExtreMat project is the development of new heat sink materials, including copper-based high-temperature heat sinks, heat sinks with very high thermal conductivity and nanoscopic interface design, Ref. [105-13], [105-14]. The aim is to achieve heat flux removal up to 20 MW/m^2, with temperatures up to 1000°C using materials with tailored architecture and CTE.

A short summary of the requirements for novel heat sink materials is given, e.g. copper-based high-temperature heat sinks and heat sinks with extremely high thermal conductivity:

- thermal conductivity comparable to copper or higher (300 W/mK to 800 W/mK) with heat flux removal up to 20 MW/m^2. Such high heat fluxes are typically for high-dissipative compact instruments for space, such as densely packed electronics, laser transmitters, re-usable thrusters, power semiconductor packages or microwave modules.

- in-plane CTE matched to that of the heat transfer interface of the heat source (4 $\times 10^{-6}$ /K to 9 $\times 10^{-6}$ /K).
- reliable performance at higher temperatures (up to 1000° C).
- structural stability during thermal cycling within working temperature range (e.g. n > 5 $\times 10^{6}$).
- joinablility, e.g. brazability, control of internal stresses.
- dimensional stability.
- acceptable cost.

Figure 105.2.6 provides a summary of the thermal properties of different candidate heat sink materials. These are grouped as those currently used and those that are considered as having potential for a significant expansion of the operational range, Ref. [105-13]. Promising new systems are based on copper or silver matrices with CNTs as the included phase, Ref. [105-13].

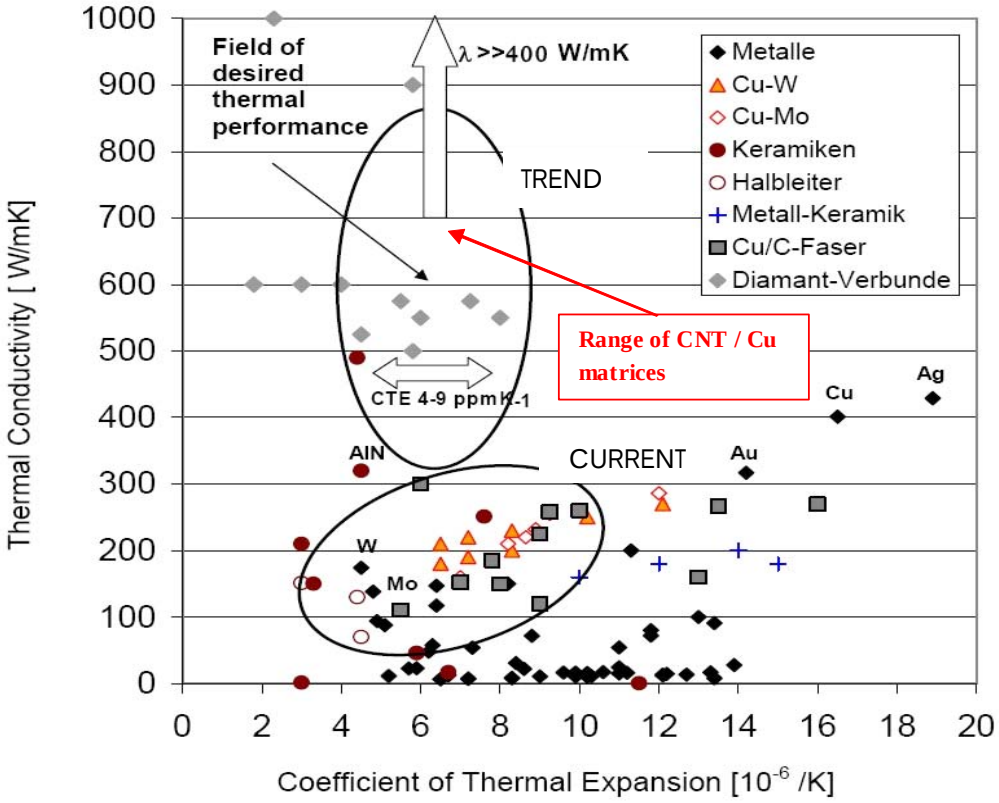

Figure 105.2-6 – Advanced heat sink applications: Potential materials

From Figure 105.2.6, it is seen that there are typical regions for pure metals, where the noble metals show high thermal conductivity but also relatively high CTEs. In the area marked 'Current', there are so-called 'state-of-the-art' heat sink materials, such as graphite-copper, molybdenum-copper and tungsten-copper. Cu/W is commonly used in US space thermal technology. A disadvantage is that this material has a very high density.

The 'Trend' zone denotes the expected thermal performance field of CNT-modified materials based on copper or silver as matrix materials. Also within this range are the currently-available metal-diamond compounds. A severe disadvantage is that in practice it is very difficult to

machine or grind metal-diamond compounds to produce a sufficiently smooth heat-transfer surface.

New CNT-modified copper materials are envisaged as meeting the high thermal conductivity requirement but be easier to machine.

105.2.8 ESA-funded studies

As of 2006, a review of worldwide research activities for CNT-modified materials, both metallic and ceramic, is being undertaken within the TRP-ESA study 'Nanotube-based Composite Materials' (Contract No. 19128/05/NL/PM).

One of the activities is to identify appropriate metallic nano CNT composites and their related processes, along with their characterisation for application in space (with the Institute for Chemical Technologies and Analytics, Technical University of Vienna).

Improved production processes with aligned CNTs are being investigated, e.g. metal infiltration processes of CNT networks. The aim is to both increase thermal conductivity and to reduce the thermal expansion of copper- or silver-based MMCs for thermal management applications.

105.3 Potential applications

105.3.1 Introduction

Given the wide range of nano-modified metals under investigation, those described are considered of interest for potential space applications and are grouped by:

- structural applications (aluminium- and magnesium-based);
- highly-loaded components (titanium-based);
- thermal applications (aluminium- and copper-based).

The example applications are perceived as targets for replacement by CNT-modified metals.

105.3.2 Structural applications

105.3.2.1 Truss structure tubes

Carbon fibre-reinforced magnesium tubes for truss-structure applications have been produced by the filament-winding, vacuum-assisted casting process, Ref. [105-1].

Figure 105.3.1 shows some cast carbon fibre-reinforced magnesium tubes (50 mm diameter; 1.2 m long) that were produced to demonstrate the reproducibility and reliability of the fabrication method, Ref. [105-1].

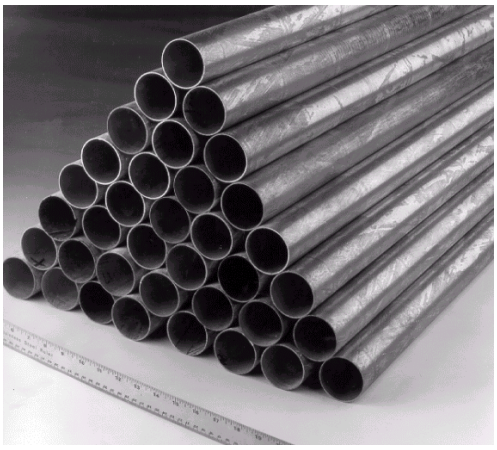

Figure 105.3-1 – Truss structures: Carbon fibre-reinforced magnesium tubes made by vacuum-assisted casting

Of the discontinuous reinforced aluminium composites, silicon carbide, both particulate (SiCp/Al) and whisker (SiCw/Al), were extensively characterised and evaluated during the 1980s.

Potential applications for nano-modified Al-, Mg- and Ti-composites could include joints and attachment fittings for truss structures, longerons, electronic packages, thermal planes, mechanism housings, and bushings.

105.3.2.2 Truss structure nodes

Figure 105.3.2 shows an example of a multi-inlet silicon carbide particulate-reinforced aluminium truss node produced by a near net-shape casting process, Ref. [105-1].

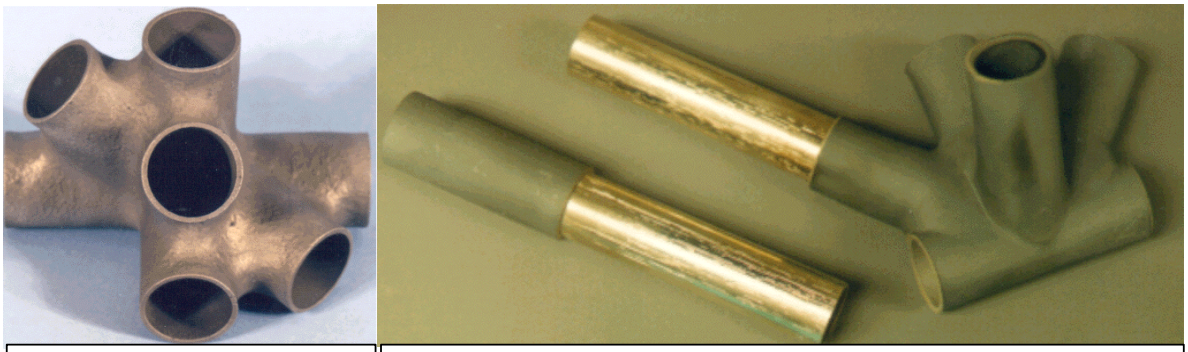

Multi-inlet fitting	Cast fitting brazed to short carbon fibre-reinforced aluminium tube

Figure 105.3-2 – Truss structure node: Silicon carbide particle-reinforced aluminium made by near net-shape casting

105.3.3 Highly-loaded components

105.3.3.1 Pressure vessels

An application for a highly-loaded component, proposed by NASA Ames, is the manufacture of pressure vessels for deep atmospheric planetary probes, Ref. [105-15].

Figure 105.3.3 shows a schematic of the powder metallurgical process for a CNT-modified titanium composite, Ref. [105-4].

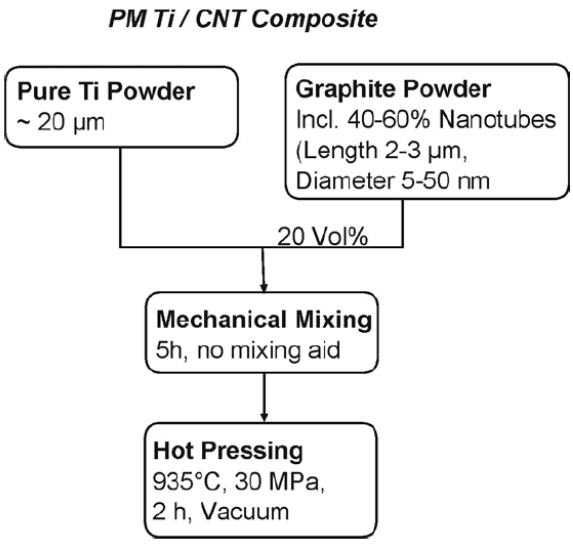

Figure 105.3-3 – CNT-modified titanium composite: Powder metallurgy process

Figure 105.3.4 shows the increase in stiffness and hardness for CNT-titanium composite compared with pure titanium, Ref. [105-4].

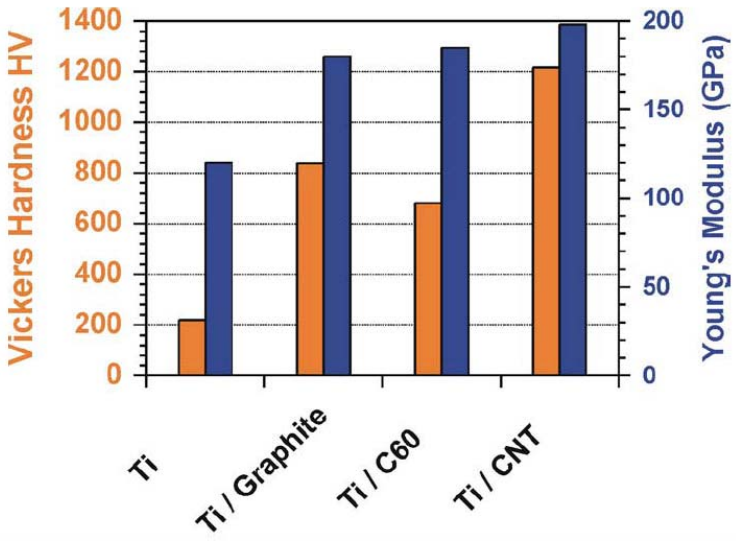

Figure 105.3-4 – CNT-modified titanium composite: Stiffness and hardness compared with pure titanium

105.3.4 Thermal applications

105.3.4.1 General

The preliminary properties show that CNT-Cu composites are efficient heat conductors, [See: 105.2]. They are potential materials for use as heat-sinks for critical 'hot spots' in high heat flux dissipating devices. CNT-Cu also has high mechanical stability and reusability and can be integrated into various packaging processes and designs for high-efficiency cooling.

105.3.4.2 Heat sinks for densely-packed electronics

An example of a fabricated CNT-Cu composite heat sink for use in integrated circuit packaging is shown in Figure 105.3.5, Ref [105-1], [105-4].

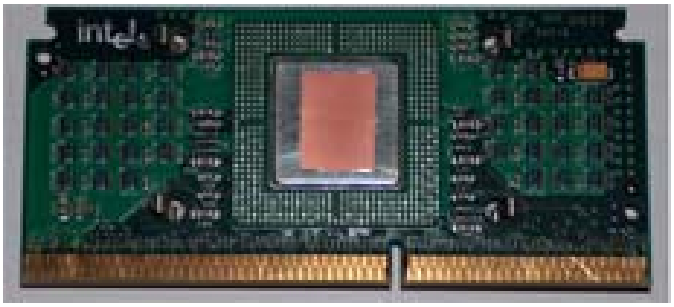

Figure 105.3-5 – Heat sink for dense-packed electronics: CNT-copper composite

105.3.4.3 Heat sinks for highly-dissipating instruments

The development of advanced aluminium and copper composites is led by the need for heat sinks with high heat flux densities (tens of Watts per cm^2) and very stable operating temperatures of ± 0.1 K in LEO.

A typical example is the ATLID Laser Transmitter Thermal Interface, shown in Figure 105.3.6.

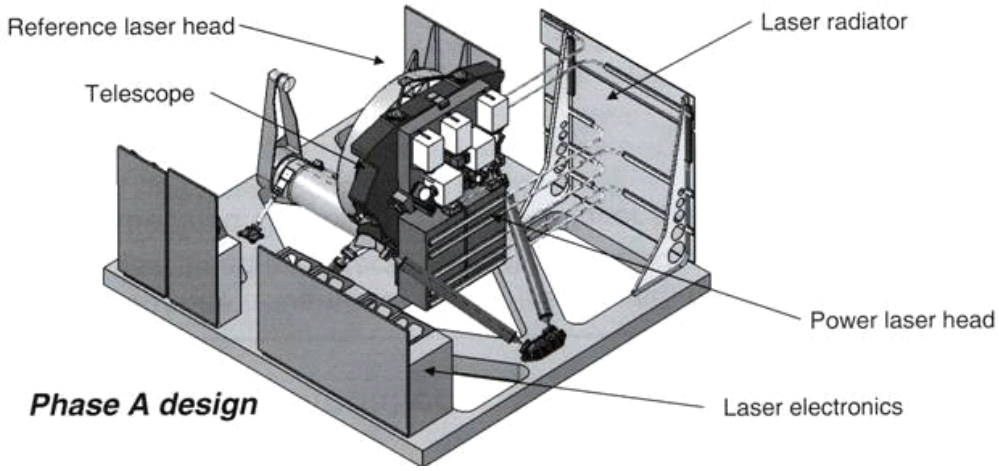

Figure 105.3-6 – Heat sink for highly-dissipating instruments: Example ALTID Laser transmitter module (Phase A concept)

105.3.4.4 High-efficiency radiators

The combined high thermal conductivity and mechanical characteristics of aluminium and copper nano composites makes them of interest for use in high-temperature structural radiators.

105.4 References

105.4.1 General

[105-1] S. Rawal
'Metal-Matrix composites for space Applications'
JOM 53 (4), 2001, p14-17

[105-2] S. Abkowitz, S. M. Abkowitz, H. Fisher, P. Schwartz, 'CermeTi Discontinously Reinforced Ti-Matrix Composites: Manufacturing, Properties, and Applications'
JOM, p.37, May 2004

[105-3] K.S.R. Chandran, K.B. Panda, S.S. Sahay,
'TiBw-Reinforced Ti Composites: Processing, Properties, Application Aspects, and Research Needs'
JOM, p. 42, May 2004

[105-4] Neue Materialien Fürth - Report
ESA TRP Project 'Nanotube Based Composite Materials'
Contract No. 19128/05/NL/PM, Route Selection Brainstorming Meeting, Munich, November 24th, 2005,

[105-5] R. George et al.
'Strengthening in carbon nanotube/alumunium (CNT/Al) composites',
Scripta Materialia 53 (2005) p1159-1163

[105-6] T. Kuzumaki et al.,
J. Mater. Res. 13 (1998), p2445

[105-7] T. Kuzumaki et al.,
Eng. Mater 2 (2000), p416

[105-8] R. Zhong et al.,
Carbon 41 (2003), p848

[105-9] C.L. Xu et al,
'Fabrication of aluminium-carbon nanotube composites and their electrical properties'
Carbon 37 (1999), p855-858

[105-10] Technical University of Vienna, Institute of Chemical Technologies - Report
ESA TRP Project 'Nanotube Based Composite Materials'
Contract No. 19128/05/NL/PM, Route Selection Brainstorming Meeting, Munich, November 24th, 2005

[105-11] N. Ferrer-Anglada, V. Gomis, Z. EI-Hachemi,
UD. Weglikovska, M. Kaempgen, S. Roth
'Carbon nanotube based composites for electronic applications: CNT-conducting polymers, CNT-Cu'
Physica Status Solidi A-Applications & Materials Science.
203(6):1082-1087, 2006 May

[105-12] NASA AMES Technology Capabilities and Facilities 'Nanoengineered Heat Sink Materials'
http://www.nasa.gov/centers/ames/research/technology-onepagers/heat_sinks.html

[105-13] C. Edtmaier
'Metall-Matrix-Verbundwerkstoffe mit Carbon Nanotubes als hochfeste und hochwärmeleitende Einlagerungsphase'

Vortrag: Hagener Symposium 2005, Hagen, D (eingeladen); 24.11.2005 - 25.11.2005; in: 'Hochleistungsprodukte der Pulvermetallurgie, Pulvermetallurgie in Wissenschaft und Praxis', Fachverband Pulvemetallurgie, ISL-Verlag Hagen, Band 21 (2005), 3-9807736-5-5; S. 115-142.

[105-14] C. Edtmaier, R. Haubner
'Copper based carbon nanotube heat-sinks'
Poster: 16th International Plansee Seminar 2005, Reutte; 30.05.2005 - 03.06.2005; in: 'High Performance PM Metals'
Plansee Holding AG, Reutte, Vol. 1 (2005), S. 277-289.

[105-15] D. Stackpoole, A. Srivastava, B. Fuentes, Cruden, J.O. Arnold
'Nano-reinforced Ti composites as candidate pressure vessel materials for deep atmospheric probes'
3rd Int. Planetary Probe Workshop, Anavyssos, Attiki, Greece, June/July 2005

[105-16] 'Tiny tubes boost for metal matrix composites', http://www.metal-powder.net/features/archive/ feature_julaug04_1.html

106 CNT ceramics

106.1 Introduction

106.1.1 Reasons for CNT-modified ceramics

106.1.1.1 Optical structures

ESA programs favour the use of high-performance ceramic-type materials, e.g. monolithic SiC, optical glass-ceramics, for future optical missions demanding geometrical accuracy from ambient to cryogenic operational temperatures.

[See also: 43.12 – silicon carbide; 43.15 – glass-ceramics]

106.1.1.2 High-performance ceramics

Ceramic materials, such as high-performance silicon carbide grades, are available for the manufacture of precision optical instruments, [See: 43.12]. The mechanical strength, elastic and thermal properties of these ceramic materials are excellent. However, toughness and reduction of microcrack propagation are areas for improvement.

Local stress concentrations in combination with microcracks can lead to catastrophic failure in crucial areas of large ceramic structures, such as optical benches. Examples of such potential failure areas include: mechanical load introduction zones, mounting points for kinetic mounts and attachment areas for mirror supports.

Pure monolithic ceramic materials are non-conductors, hence do not dissipate electrical charges. Non-conductive structures under long-term exposure to charged particle radiation in space, e.g. solar proton flux, can accumulate electrical charge, potentially leading to hazardous electrical discharges.

The low fracture toughness and low electrical conductivity of high-quality monolithic ceramic materials are seen as parameters needing improvement. For example modification of SiC using nano technology.

106.1.1.3 Hot structures

Another field of application for ceramic materials is hot structures; particularly the leading edges of hypersonic and re-entry vehicles, [See also: Chapter 70].

Very fast flight in Earth's atmosphere demands materials that are capable of withstanding temperatures between 1600°C and 3000°C, for the duration of the mission.

Ceramic materials based on hafnium and zirconium carbides and borides combined with silicon carbide are suitable materials for this type of application. However they are brittle. Reinforcement by nanotubes is a potential approach to solving this problem.

106.2 Technology status

106.2.1 General

As of 2006, developments in nano-modified ceramics can be grouped as:

- alumina-based materials, [See: 106.3].
- silicon carbide-based materials, [See: 106.4].

Both the process technologies and material characteristics are described.

106.2.2 Materials and process

As of 2006, the majority of the work has been with alumina-based ceramics. Other materials systems, such as silicon carbide, silicon nitride, silica and carbon-carbon composites have been considered to a lesser extent.

Technologies investigated for processing these CNT-ceramic matrix composites are:

- process 1: Mixing, disagglomeration and uniform distribution of CNT in a ceramic precursor, which can be either a ceramic powder, a suspension or polymeric material, then densification to a compact ceramic body.
- process 2: Formation of CNT inside a porous ceramic body and subsequent further densification.
- process 3: Synthesis of ceramic material inside of a network, composed completely or in part of CNTs, or by mixing CNTs in liquid precursors, e.g. sol-gel processing.

Process 1 is the mostly commonly applied. The CNT-ceramic precursor leads to a formation of ceramic particles which act as catalysts for the formation of CNTs on their surface, Ref. [106-1] to [106-14]. These catalyst materials are usually made of iron-containing alumina or spinell ($MgAl_2O_4$). Depending on the amount of ceramic particles present, the material can then be processed like any other ceramic material. A dispersion of alumina particles and modified CNT was demonstrated, Ref. [106-15], [106-16]. Heterocoagulation of these two particle types provide homogeneously dispersed CNTs in an alumina matrix. Consolidated ceramic bodies are formed by spark plasma sintering.

In Process 2 the ceramic catalyst support is provided within a porous ceramic body. Subsequently, CNTs form inside of the pores, Ref. [106-11], [106-12]. Then, the filled porous body is consolidated by hot-pressing. This route has many similarities to Process 1. Another template method, Ref. [106-17], [106-18], uses anodised aluminium with periodic pores, which are filled with CNTs. CNTs are also used as templates for porous silicon carbide, Ref. [106-19], [106-20].

Process 3 is described by several researchers using polymeric infiltration routes, Ref. [106-21], [106-22]. It involves the synthesis of the ceramic matrix inside a CNT-network by polymeric precursor routes or sol-gel techniques. Sol-gel technology usually produces powders, thin films or fibres, so is combined with consolidation techniques, e.g. hot-pressing.

[See also: 43.4 – monolithic ceramic processing; Chapter 88 – CMC processing]

106.3 CNT-alumina-based ceramics

106.3.1 General

CNT-alumina materials technology can be summarised as follows:

- powder processing routes appear to be the most effective for dispersing CNTs.
- several consolidation methods are feasible, especially hot pressing, spark-plasma sintering.
- CNT-contents vary from few wt.% to about 25 wt.%.
- mechanical properties increase, but so does porosity.
- significant increases are seen in electrical conductivity.

[See also: 43.6]

106.3.2 Extrusion of ceramic suspension and hot-pressing

A significant increase in some mechanical properties and electrical conductivity has been observed by incorporating CNTs in a catalyst support material, Ref. [106-3] to [106-10].

High shear forces occur during extrusion of a ceramic suspension, which is then densified at high temperature (up to 1500°C) and high pressure, Ref. [106-8]. The result is highly-aligned CNT in an oxide ceramic matrix.

The hardness of such materials increases with increasing nanotube content up to a peak value. After which, the hardness decreases; as shown in Figure 106.3.1, Ref. [106-1].

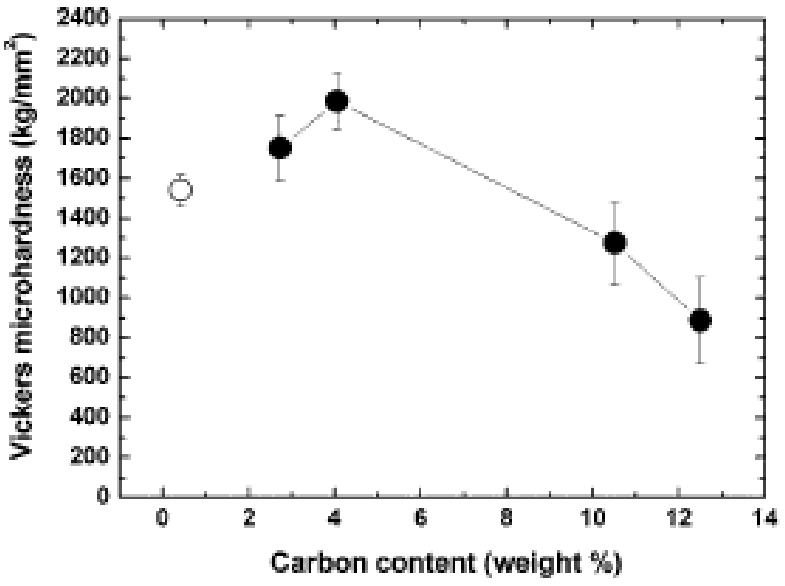

Figure 106.3-1 – Alumina-based CNT-CMCs: Hardness with increasing CNT content

106.3.3 Gel casting

106.3.3.1 Electrical conductivity

CNTs have been formed inside porous materials by gel casting, Ref. [106-11], [106-12]. These materials were then densified by hot-pressing.

Figure 106.3.2 shows the conductivity of these CNT-$MgAl_2O_4$ materials increasing to almost 9 S/cm for about 12 wt.% CNT formed inside the porous material compared with 10^{-12} S/cm for pure alumina, Ref. [106-12].

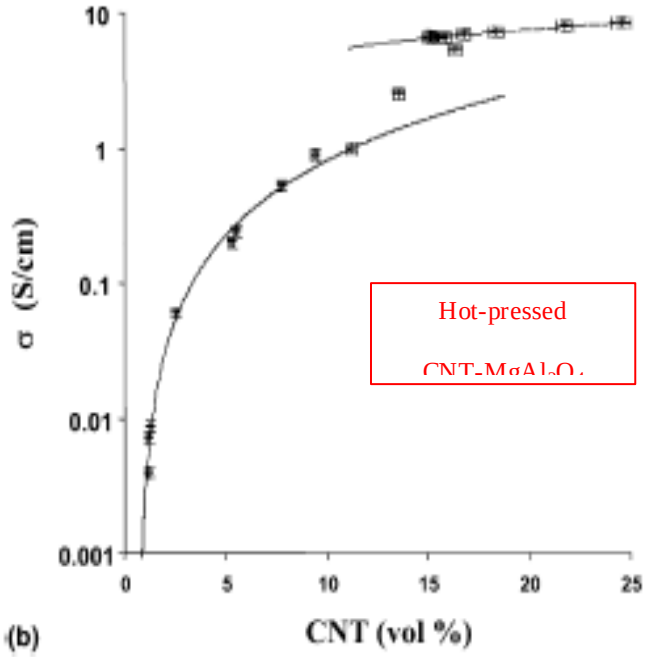

Figure 106.3-2 – Alumina-based CNT-CMCs: Electrical conductivity with increasing CNT content

Table 106.3.1 summarises the material characteristics and electrical conductivity for a variety of CNT-modified ceramic materials produced by different processes, Ref. [106-24].

Table 106.3-1 – Alumina-based CNT-CMCs: Electrical conductivity for various materials made by different processes

Materials	Processing conditions	Relative density (%TD)	Grain size (nm)	Electrical conductivity (S/m)
Pure Al_2O_3	SPS 1150°C/3 minutes	100	350	10 to 12
5.7 vol.% Carbon black/Al_2O_3	SPS 1150°C/3 minutes	100	200	15
5.7 vol.% SWCNT/Al_2O_3	SPS 1150°C/3 minutes	100	200	1050
10 vol.% SWCNT/Al_2O_3	SPS 1200°C/3 minutes	99	100	1510
15 vol.% SWCNT/Al_2O_3	SPS 1150°C/3 minutes	99	100	3345
8.5 vol.% CNT/4.3% Fe/Al_2O_3*	HP 1500°C/15 minutes	88.7	300	40 to 80
10 vol.% CNT/4.3% Fe/Al_2O_3*	HP 1500°C/15 minutes	87.5	300	280 to 400
20 vol.% MWCNT/Polymer*	-	-	-	~30
Key: * from literature; TD – Theoretical density; SPS – Spark-plasma sintering; HP – Hot pressing.				

The conductivity of CNT-alumina composites is shown to be constant over a wide range of temperature, as shown in Figure 106.3.3, Ref. [106-24].

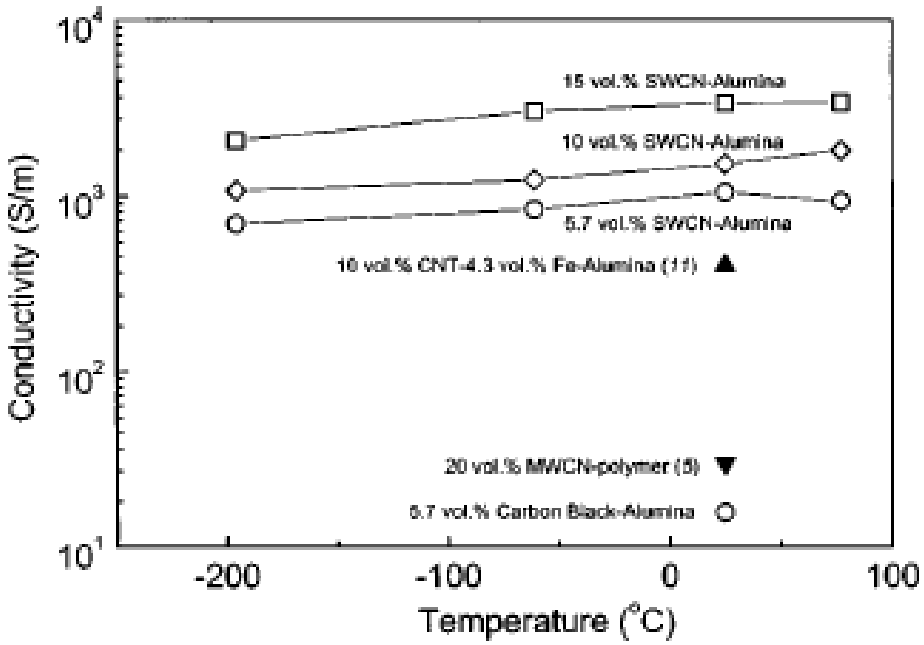

Figure 106.3-3 – Alumina-based CNT-CMCs: Electrical conductivity with temperature

106.3.3.2 Fracture resistance

Increasing CNT content also produces improved fracture behaviour, Ref. [106-15], [106-16], due to crack bridging by CNT bundles coated with the sol-gel derived alumina.

The increase in toughness with only 0.1% CNT is about 32% compared with unreinforced material. The pure alumina matrix has a toughness of about 3 MPa $m^{1/2}$, whereas that of the CNT composite is 4.7 MPa $m^{1/2}$. The fracture surfaces show the bridging effect of the CNTs, Ref. [106-23] to [106-26].

Increase in fracture toughness has also been observed for spark-plasma sintered alumina-CNT composites, Ref. [106-23] to [106-26]; as shown in Figure 106.3.4, Ref. [106-23].

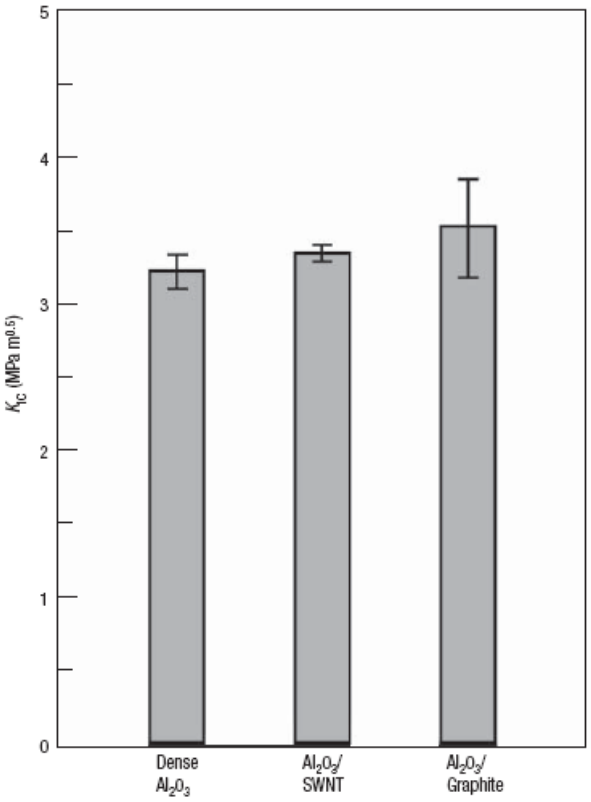

Figure 106.3-4 – Alumina-based CNT-CMCs: Fracture toughness

106.4 CNT-silicon carbide

106.4.1 NASA developments

106.4.1.1 Material processing

A summary is given of NASA's development of CNT-modified ultra-high temperature SiC composites, Ref. [106-27], [106-28].

Composite samples of a nanotube-reinforced SiC matrix were processed to verify that the tape-casting technique achieved a partial alignment of nanotubes. Two processing routes were employed:

- powder processing route, where the nanotubes are directly added to SiC powder.

- pre-ceramic polymer route, where the nanotubes are dispersed in AHPCS, which is then pyrolised to form nanocrystalline SiC.

The main advantage of the pre-ceramic route over powder processing is that processing aids are not necessary. All SiC-based systems were hot-pressed in argon at 40 MPa, at temperatures less than 2000°C.

106.4.1.2 Material properties

Table 106.4.1 compares the modulus of SiC with and without nanotube reinforcement, Ref. [106-27]. The effect on stiffness is evident; as is the anisotropy attributed to nanotube alignment during processing.

Table 106.4-1 – CNT-modified silicon carbide: Stiffness

System	E (GPa)
SiC (no additions)	290
Nano/SiC : perpendicular to alignment direction	436
Nano/SiC : parallel to alignment direction	602

Figure 106.4.1 shows that samples containing nanotubes show an improvement in toughness over the matrix material alone. The results are for samples tested perpendicular to the nanotube alignment direction, Ref. [106-27].

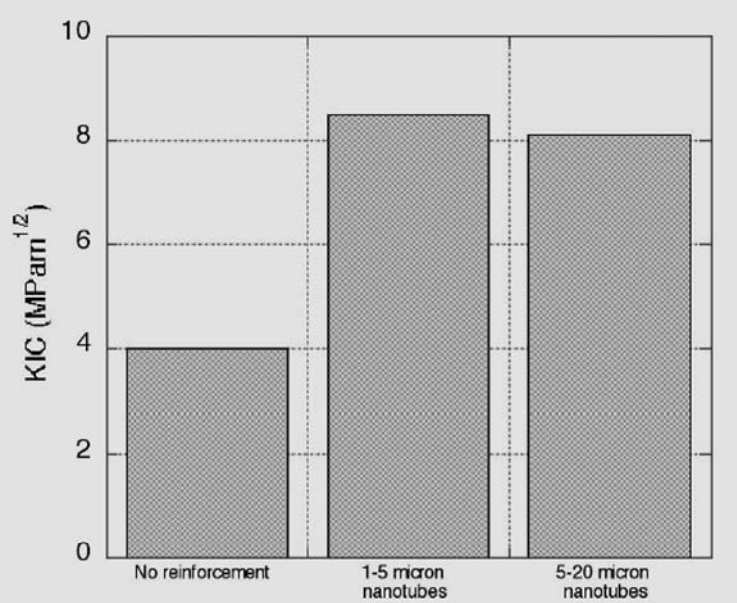

Indentation toughness tested perpendicular to nanotube alignment direction. CNT-SiC composites processed by pre-ceramic route

Figure 106.4-1 – CNT-modified silicon carbide: Fracture toughness

The CNTs survived the consolidation step and directional properties were found in preliminary mechanical tests, Ref. [106-27].

The very high thermal conductivity of CNTs in the axial direction and low thermal conductivity in the normal direction is perceived as a means of improving thermal shock resistance.

106.4.2 European developments

106.4.2.1 Material

Within the ESA TRP project 'Nanotube-based Composite Materials' (Contract No. 19128/05/NL/PM), a development program covered sintered CNT-modified SiC; based on the qualified material SiC-100, Ref. [106-29]. SiC-100 has been used to manufacture the 3.5 m diameter Herschel mirror, [See also: 43.12].

106.4.2.2 Processing

The preliminary approach involved mixing the constituents (organic binder, ceramic SiC particle, CNTs), followed by a green moulding process, isostatic pressing, slip casting, extrusion, green machining, pressureless sintering and finishing, Ref. [106-30].

Three processing routes are under investigation:

- dry process: involving raw materials: ready-to-press SiC and CNT, mixing by vibrating or rotating equipment, isostatic pressing, green machining, sintering, finishing.
- wet process: involving slurry mixing with organic aids, wet CNT feeding in SiC slurry assisted by ultrasonics, slip cast moulding process, green machining, pressureless sintering and finishing.
- plastic process: involving mixing of organic binders/CNT/SiC powder, plastic extrusion, green machining, sintering, finishing.

106.4.2.3 Characteristics

Green and sintered samples from each process should be characterised. The results are awaited from this on-going study.

106.5 Potential applications

106.5.1 Ultra-high stability structures

For space applications, CNT-modified sintered silicon carbide (SiC) is of great interest.

A number of ambitious missions are planned in the frame of the ESA 'Cosmic Vision Program', where new technologies are needed for the development of high-precision, ultra-high dimensional stability structures for the manufacture of optical and opto-mechanical instruments. Some examples of the potential applications for SiC-100 and CNT-modified SiC in space projects are listed in Table 106.5.1.

Table 106.5-1 – CNT-modified silicon carbide: Examples ultra-high stability structures for future space missions

Mission	Ultra-high stable structure	Status 2006
HERSCHEL	Large main reflector	Manufactured, in qualification phase
JWST	Optical bench, mirrors, filter- and grating wheel, mirror supports, etc.	BCD phase in progress
GAIA	Optical bench, mirrors	Technology development activity running
DARWIN	Optical bench, mirrors	Technology development activity running
LISA Pathfinder	Optical bench	Breadboard phase

Figure 106.5.1 provides some images of potential applications for SiC-based materials in (future) space optical and opto-mechanical structures, including HERSCHEL main SiC reflector; Optical benches, breadboards for JWST NIRSpec, LISA Pathfinder, mechanisms for JWST NIRSpec.

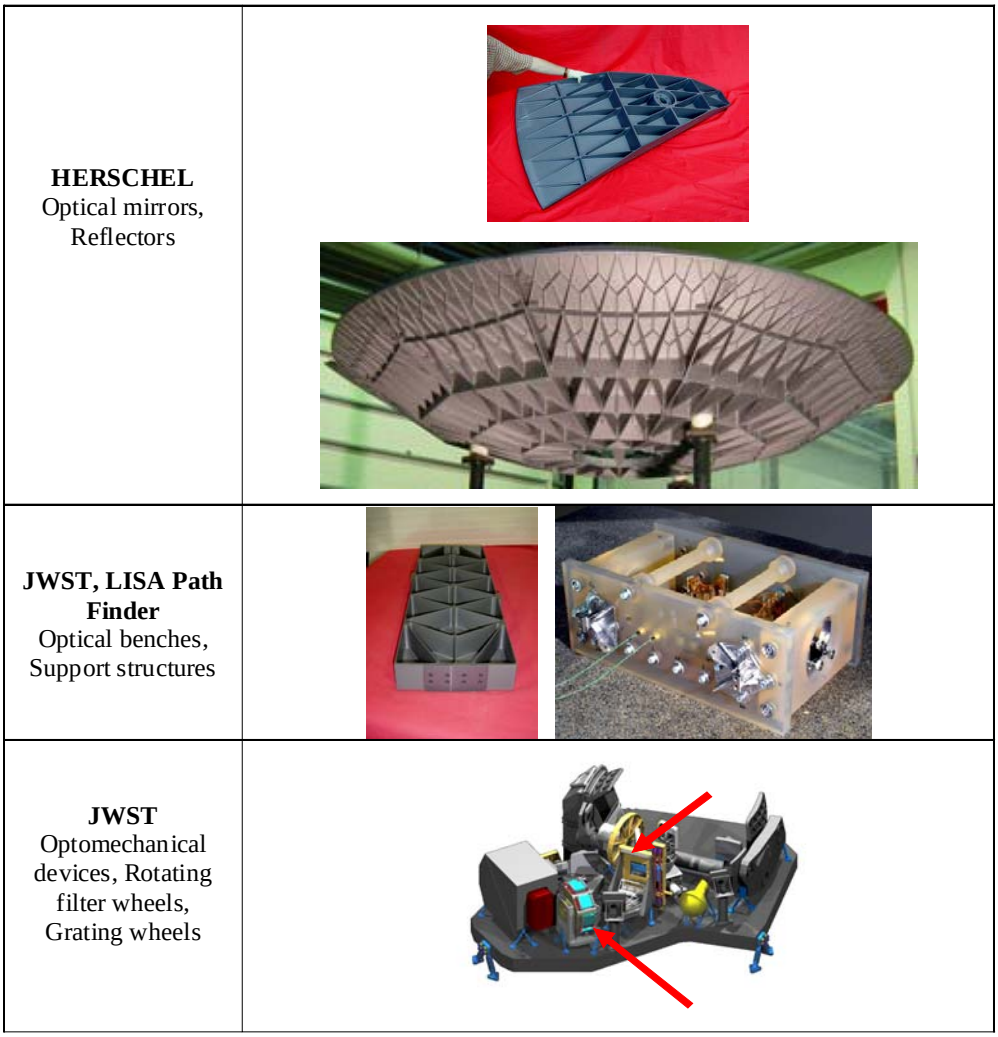

Figure 106.5-1 – CNT-modified silicon carbide: Examples of optical and opto-mechanical structures for future space missions

106.5.2 Ultra-high temperature ceramics

106.5.2.1 Hypersonic entry vehicles with sharp leading edges

Ultra high temperature ceramics (UHTCs) are candidates for use on hypersonic entry vehicles with sharp leading edges, as shown in Figure 106.5.2, Ref. [106-27].

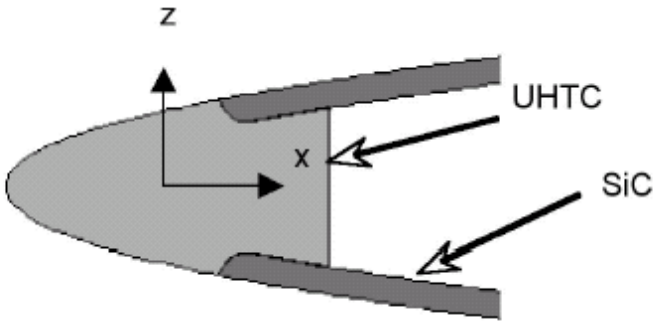

Figure 106.5-2 – CNT-modified ceramics: Potential application – leading edge of hypersonic vehicle

While a sharp leading edge geometry improves a vehicle's aerodynamic performance (a high lift-to-drag ratio and cross range capabilities 2.5 times those of blunt vehicles), it also produces more severe heating during atmospheric entry, hence needing materials with very high temperature capabilities.

The aerodynamic performance of a sharp vehicle could be of great value in future solar system missions. Manoeuvres such as aero-gravity assist to reduce travel time to distant planets need vehicles with very high lift-to-drag ratios and materials with temperature capabilities similar to those of UHTCs, Ref. [106-27].

AGA 'Aero-Gravity Assist' is a novel interplanetary transportation technology concept which would enable relatively short trip durations or use of smaller launch vehicles for solar system exploration. The manoeuvre demands a vehicle with a very high lift-to-drag (LID) ratio, of the order of 10.

Previous studies have indicated significant benefits from AGA. The 1999 baseline mission to Pluto-Kuiper Belts used a 9.5 year trajectory with a large launch vehicle (launch V_∞ = 12.3 km/sec). By comparison, the employment of AGA for a 2013 Earth-Venus-Mars-Pluto mission allows a launch $V_\infty \sim 7$ km/sec, with LID of 8.0. If the launch V_∞ were raised to 8.0 km/sec, the trip time would be reduced from 9.5 years to 6.0 years.

106.5.2.2 Role of nano-modified ceramics

While recent work has demonstrated the promising features of sharp leading edge materials, their application to missions of this kind demands an increase in their high temperature performance by increasing thermal conductivity, Ref. [106-27].

By exploitation of the high thermal conductivity of carbon nanotubes as reinforcement for UHTCs, improvements are possible in thermal conductivity, strength and modulus and also their thermal shock resistance.

106.5.2.3 CNT-modified hafnium- and zirconium diboride ceramics

NASA Ames is developing a family of UHTC materials, consisting primarily of hafnium- and zirconium diboride (HfB_2 and ZrB_2), with CNT-additions to enhance thermal conductivity and fracture toughness. The diborides have extremely high melting temperatures (>3000°C) and have relatively good resistance to oxidation in simulated reentry environments. Recent work at NASA

Ames has focussed on developing improved manufacturing methods for these materials, characterisation of mechanical and thermal properties and evaluation of the materials' performance in simulated reentry environments.

Figure 106.5.3 shows a variety of stagnation test (arc jet) models made of HfB_2-SiC, Ref. [106-27]. The wedge (wing leading edge), cone (nose tip) and quarter-sized flat face samples are of similar geometry and scale as those anticipated for use on an actual vehicle.

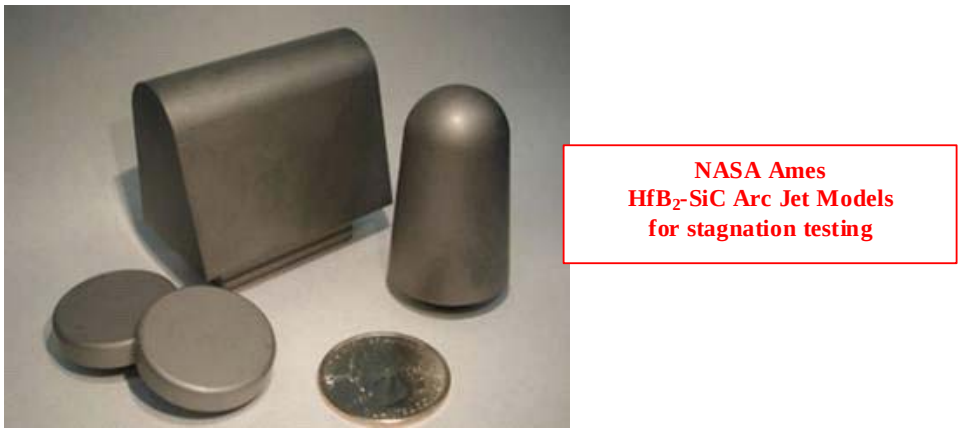

Figure 106.5-3 – CNT-modified ceramics: Potential application – NASA Ames HfB2-SiC arc-jet models of hypersonic vehicle components

Figure 106.5.4 shows a ceramic leading edge under test in a plasma wind tunnel, Ref. [106-31]. The surface temperature during testing exceeded 2000°C.

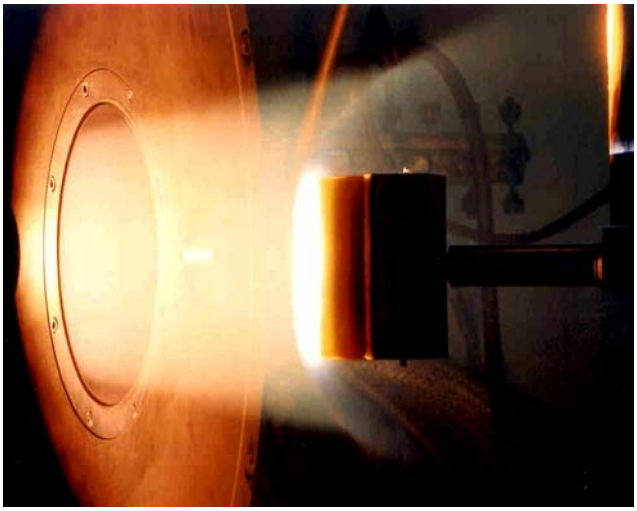

Figure 106.5-4 – CNT-modified ceramics: Plasma wind tunnel testing of ceramic leading edge

106.6 References

106.6.1 General

[106-1] J.W. An, D.S. Lim
'Effect of carbon nanotube additions on the microstructure of hot-pressed alumina'
Journal of Ceramic Processing Research, 2002 3(3) p201-204.

[106-2] J.W. An, D.H. You, D.S. Lim
'Tribological properties of hot-pressed alumina-CNT composites'
Wear, 2003. 255: p677-681.

[106-3] P. Coquay et al
'From ceramic-matrix nanocomposites to the synthesis of carbon nanotubes'
Hyperfine Interactions, 2000. 130(1-4): p275-299.

[106-4] E. Flahaut et al
'Carbon nanotube-metal-oxide nanocomposites: Microstructure, electrical conductivity and mechanical properties'
Acta Materialia, 2000. 48(14): p3803-3812.

[106-5] C. Laurent et al
'Carbon nanotubes Fe alumina nanocomposites. Part II: Microstructure and mechanical properties of the hot-pressed composites'
Journal of the European Ceramic Society, 1998. 18(14) p2005-2013

[106-6] C. Laurent, A. Peigney, A. Rousset
'Synthesis of carbon nanotube Fe-Al2O3 nanocomposite powders by selective reduction of different Al1.8Fe0.2O3 solid solutions'
Journal of Materials Chemistry, 1998. 8(5): p1263-1272.

[106-7] A. Peigney
'Composite materials: Tougher ceramics with nanotubes'
Nature Materials, 2003. 2(1): p15-16.

[106-8] A. Peigney et al
'Aligned carbon nanotubes in ceramic-matrix nanocomposites prepared by high-temperature extrusion'
Chemical Physics Letters, 2002. 352(1-2): p20-25.

[106-9] A. Peigney et al
'Carbon nanotubes Fe alumina nanocomposites. Part I: Influence of the Fe content on the synthesis of powders'
Journal of the European Ceramic Society, 1998. 18(14): p1995-2004.

[106-10] A. Peigney et al
'Carbon nanotubes in novel ceramic matrix nanocomposites'
Ceramics International, 2000. 26(6): p677-683.

[106-11] S. Rul et al
'Carbon nanotubes prepared in situ in a cellular ceramic by the gelcasting-foam method'
Journal of the European Ceramic Society, 2003. 23(8) p1233-1241.

[106-12] S. Rul et al
'Percolation of single-walled carbon nanotubes in ceramic matrix nanocomposites'

Acta Materialia, 2004. 52(4): p1061-1067.

[106-13] Q. Wei et al
'The ultrasonic assisted synthesis of nano-hydroxyapatite and MWNT/hydroxyapatite composites'
New Carbon Materials, 2005. 20(2): p164-170.

[106-14] D.S. Lim et al
'Effect of CNT distribution on tribological behavior of alumina-CNT composites'
Wear, 2005. 259(1-6): p539-544.

[106-15] J. Sun, L. Gao, X.H. Jin
'Reinforcement of alumina matrix with multi-walled carbon nanotubes'
Ceramics International, 2005. 31(6): p893-896.

[106-16] J. Sun & L. Gao
'Development of a dispersion process for carbon nanotubes in ceramic matrix by heterocoagulation'
Carbon, 2003. 41(5): p1063-1068.

[106-17] Z. Xia, W.A. Curtin, B.W. Sheldon
'Fracture toughness of highly ordered carbon nanotube/alumina nanocomposites'
Journal of Engineering Materials and Technology-Transactions of the ASME, 2004. 126(3): p238-244.

[106-18] Z. Xia et al
'Direct observation of toughening mechanisms in carbon nanotube ceramic matrix composites'
Acta Materialia, 2004. 52(4): p931-944.

[106-19] H. Wang et al
'Fabrication of porous SiC ceramics with special morphologies by sacrificing template method'
Journal of Porous Materials, 2004. 11(4): p265-271.

[106-20] Q.M. Cheng et al
'Methylene-bridged carbosilanes and polycarbosilanes as precursors to silicon carbide-from ceramic composites to SiC nanomaterials'
Journal of the European Ceramic Society, 2005.
25(2-3): p233-241

[106-21] L.N. An et al
'Carbon-nanotube-reinforeed polymer-derived ceramic composites'
Advanced Materials, 2004. 16(22): 2036 pp.

[106-22] M. Scheffler et al
'Nickel-catalyzed in situ formation of carbon nanotubes and turbostratic carbon in polymer-derived ceramics'
Materials Chemistry and Physics, 2004. 84(1): p131-139.

[106-23] G.D. Zhan, A.K. Mukherjee
'Carbon nanotube reinforced alumina-based ceramics with novel mechanical, electrical and thermal properties' International Journal of Applied Ceramic Technology,
2004. 1(2): p161-171.

[106-24] G.D. Zhan et al
'Electrical properties of nanoceramics reinforced with ropes of single-walled carbon nanotubes'
Applied Physics Letters, 2003. 83(6): p1228-1230.

[106-25] G.D. Zhan et al
'Single-wall carbon nanotubes as attractive toughening agents in alumina-based nanocomposites'
Nature Materials, 2003. 2(1): p38-42.

[106-26] G.D. Zhan et al
'Anisotropic thermal properties of single-wall-carbon-nanotube-reinforced nanoceramics'
Philosophical Magazine Letters, 2004. 84(7): p419-423.

[106-27] M. Stackpole et al
'UHTC Composites with Nanotube-Reinforcements for Advanced TPS Applications'
3rd Int. Planetary Probe Workshop, Anavyssos, Attiki, Greece, June/July 2005

[106-28] S.M. Johnson
Approach to TPS Development for Hypersonic Applications at NASA AMES Research Center'
NASA Ames Research Center, Moffett Field, CA94035 (USA), email:Sylvia.M.Johnson@nasa.gov

[106-29] Boostec SA, France
'SiC-100 Material Description and Properties'
http://www.boostec.com/sicmat.htm

[106-30] Boostec SA – Report
ESA TRP Project 'Nanotube Based Composite Materials', Contract No. 19128/05/NL/PM, Route Selection Brainstorming Meeting, Munich, November 24th, 2005,

[106-31] H.G. Wulz: Astrium GmbH (D)
'Joining, Fastening and Sealing of Hot CMC Structures'
AIAA-paper 99-3552, AIAA 33rd Thermophysics Conference, Norfolk, VA (USA), 28. June – 1 July 1999

107 CNT glass and glass-ceramics

107.1 Technology status

107.1.1 Glass-ceramic space structures

107.1.1.1 Dimensional stability

Dimensional stability needs high mechanical stiffness and thermo-mechanical stability, achieved by materials having zero thermal strain within their operational temperature range.

Figure 107.1.1 shows thermal expansion as a function of temperature for different structural materials. Zerodur® shows characteristics suitable for high thermo-mechanical stability applications around 300 K, typical of the operational temperature in LEO missions.

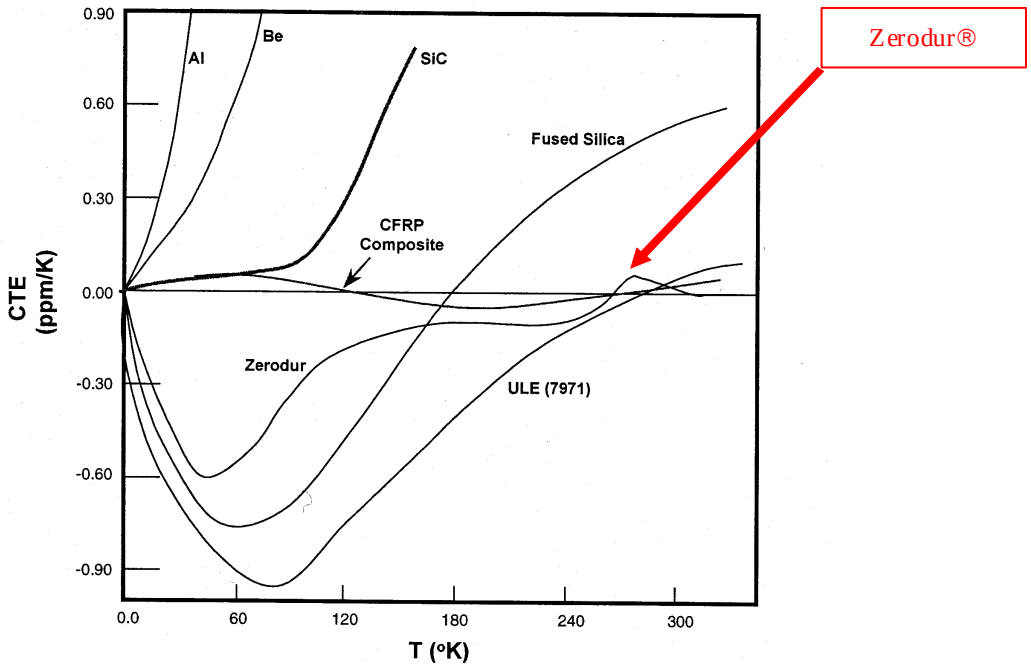

Figure 107.1-1 – Dimensionally stable structures: Thermal expansion of candidate structural materials

107.1.1.2 Zerodur® characteristics

Zerodur® is manufactured by Schott AG, Ref. [107-2]. It was selected for the construction of the optical bench of LISA Pathfinder, [See also: Potential applications].

A disadvantage of the material is its brittleness, which poses problems of low fracture toughness when mechanically joining Zerodur® components.

[See also: 43.15]

107.1.1.3 CNT-modified glasses

CNT-reinforcement of glass-type materials is considered to be a means of reducing the inherent brittleness and improving fracture toughness. Nano-modified glasses or glass-ceramics (e.g. Zerodur®) potentially have improved mechanical toughness for high-dimensionally and thermo-mechanically stable structures operating in the temperature range from 100 K to 300 K.

107.1.2 Processing

Figure 107.1.2 shows the process route for CNT-modified glasses and glass-ceramics developed by MPI Stuttgart, Ref. [107-1].

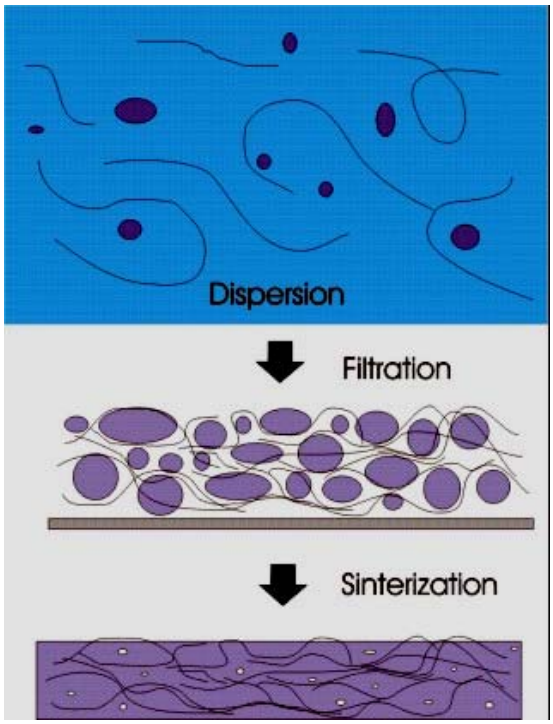

Figure 107.1-2 – CNT-modified glasses: Process

The process comprises of a sol-gel dispersion of CNTs mixed with fine boron glass powder (in the µm-range), co-filtrated, cold isostatically pressed at RT and finally sintered at 1100°C in an inert atmosphere of hydrogen and argon, Ref. [107-1].

In the resulting CNT-reinforced glass, a fine network (or tissue) of carbon is formed from carbon nanotubes, which provides cells for the glass (or glass ceramic) matrix.

107.1.3 Features of CNT-glass and glass-ceramics

Figure 107.1.3 shows a transmission electron micrograph of the consolidated and sintered CNT glass, Ref. [107-1].

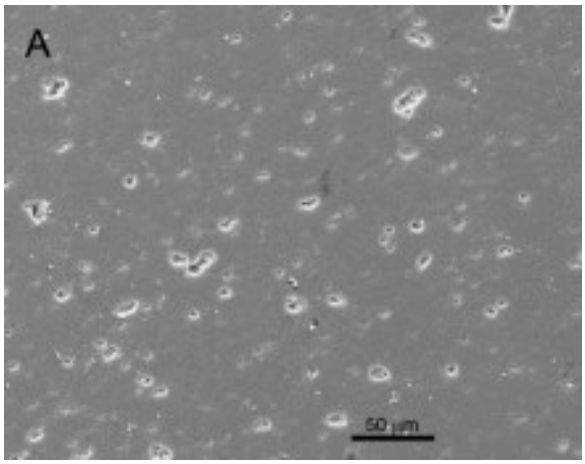

Figure 107.1-3 – CNT-modified glasses: Micrograph of consolidated and sintered material

Figure 107.1.4 shows the results of a thermal test involving placing the samples in a furnace and heating to a temperature higher than the melting point of pure glass. The sample of CNT-reinforced glass was still intact after thermal exposure, whereas the sample of pure glass was completely molten.

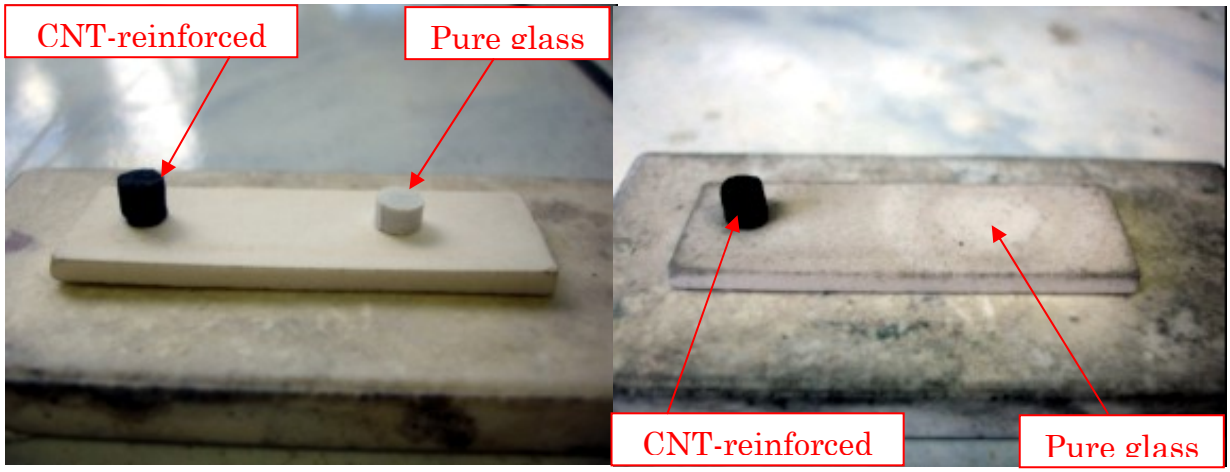

Figure 107.1-4 – CNT-modified glasses: Thermal test

107.1.4 Potential applications

107.1.4.1 High precision optical components

CNT-modified glass or glass-ceramic are considered to be potential materials for the manufacture of high precision optical components, such as reflective mirrors, RF wave guide components and RF reflectors.

The glass composition enables the thermal expansion to be adjusted by a process of controlled crystallization to obtain a glass or glass-ceramic with a controlled CTE. This depends on the amorphous phase, nature and quantity of crystals.

CNT-modified glasses or glass-ceramics offer some attractive features:

- good chemical stability from adjustment of the glass composition, e.g. additions of alumina.
- good processing behaviour.

- can be polished to a very high accuracy.
- can be easily coated.
- low helium permeability.
- non-porous.
- near-zero thermal expansion, in the range of 0°C to 50°C with 3D homogeneity.
- additions of low density CNTs decrease the mass of CNT-glass.

107.1.4.2 Highly dimensionally-stable structures

The family of CNT glasses are considered attractive candidates for the design and manufacture of highly dimensionally stable structures, such as optical benches and optical components for a wide range of electromagnetic wave lengths. The optical bench of LISA Pathfinder, shown in Figure 107.1.5, is made of Zerodur®. This is an example of a potential application for a CNT-glass ceramic, as is the construction of optical benches and optical components for LISA and DARWIN.

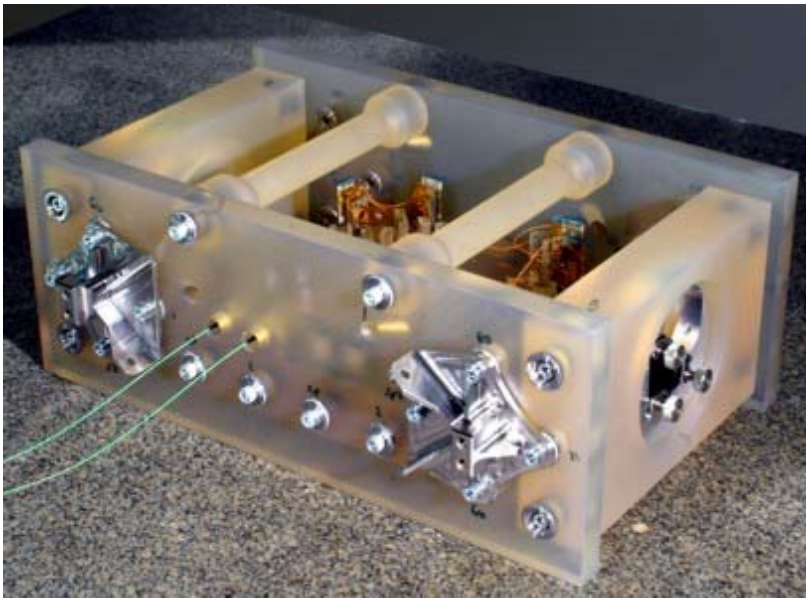

Figure 107.1-5 – LISA Path Finder optical bench: Example application of Zerodur®

107.1.4.3 European development status

An example of European development activities is the cooperation between Astrium GmbH, Max-Planck-Institute, Stuttgart and Schott AG (2006).

The goal is to develop CNT-reinforced Zerodur® glass-ceramics, having zero-expansion at room temperature and high toughness, for the construction of highly-dimensionally stable structures. The process development should be adapted from that used for making CNT-glass.

107.2 References

107.2.1 General

[107-1] M. Jung, M. Dias, U. Dettlaff, V. Skakalova, S. Roth
'CNT reinforced glasses'

Unpublished results, Max-Planck-Institute Stuttgart, 2006

[107-2] Schott AG (D) website www.schott.com

107.2.2 NASA

NASA documentation cited within materials engineering ECSS documents and relevant to the structural materials handbook include:

- NASA STD 6001: Flammability, odor, offgassing and compatibility requirements and test procedures for materials in environments that support combustion; previously NASA NHB 8060.1
- NASA MAPTIS: Materials and Processes Technical Information System
- NASA MSFC Spec. 522B: Design Criteria for Controlling Stress Corrosion Cracking
- NASA RP-1124: Outgassing data for selecting spacecraft materials
- NASA SP 8007: Space vehicle design criteria, buckling of thin walled circular cylinders
- NASA TN D 2783 (April 1965): Effect of face sheet stiffness on buckling of curved plates and cylindrical shells of sandwich construction in axial compression
- NASA TN D 3098 (January 1966): The general instability of ring stiffened corrugated cylinders under axial compression.
- NASA TN D 3454, (June 1966): Effect of face sheet stiffness on buckling of cylindrical shells of sandwich construction
- NASA CR 1457 (December 1969): Manual for structural stability analysis of sandwich plates and shells
- NASA SP–5028 (August 1965): Technical and Economic Status of Magnesium-Lithium Alloys

107.2.3 MIL

- MIL-HDBK-5: 'Metallic materials and elements for aerospace vehicle structures; superseded by MMPDS
- MIL-HDBK-17: Polymer matrix composites
- MIL-STD-1783 (Nov.1984): Including: ENSIP - Engine Structural Integrity Program
- MMPDS-01 (January 2003): 'Metallic Materials Properties Development and Standardization (MMPDS)'; DOT/FAA/AR-MMPDS-01; replaced MIL-HDBK-5
- PMP (July 2000): 'Preliminary Material Properties Handbook, Volume 2: SI Units'; AFRL-ML-WP-TR-2001-4027; destined to be integrated into MMPDS

107.2.4 Patents

- United States Patent No. 5,866,272 (February 2, 1999): Titanium-polymer hybrid laminates; The Boeing Company
- United States Patent No 6,114,050 (September 5, 2000): Titanium Polymer Hybrid Laminates